Oxidative Medicine and Cellular Longevity

Molecular Mechanisms of Natural Antioxidant Compounds with Neuroprotective Effects

Lead Guest Editor: João C. M. Barreira
Guest Editors: Isabel C. F. R. Ferreira, Beatriz P. P. Oliveira, and Rosane M. Peralta

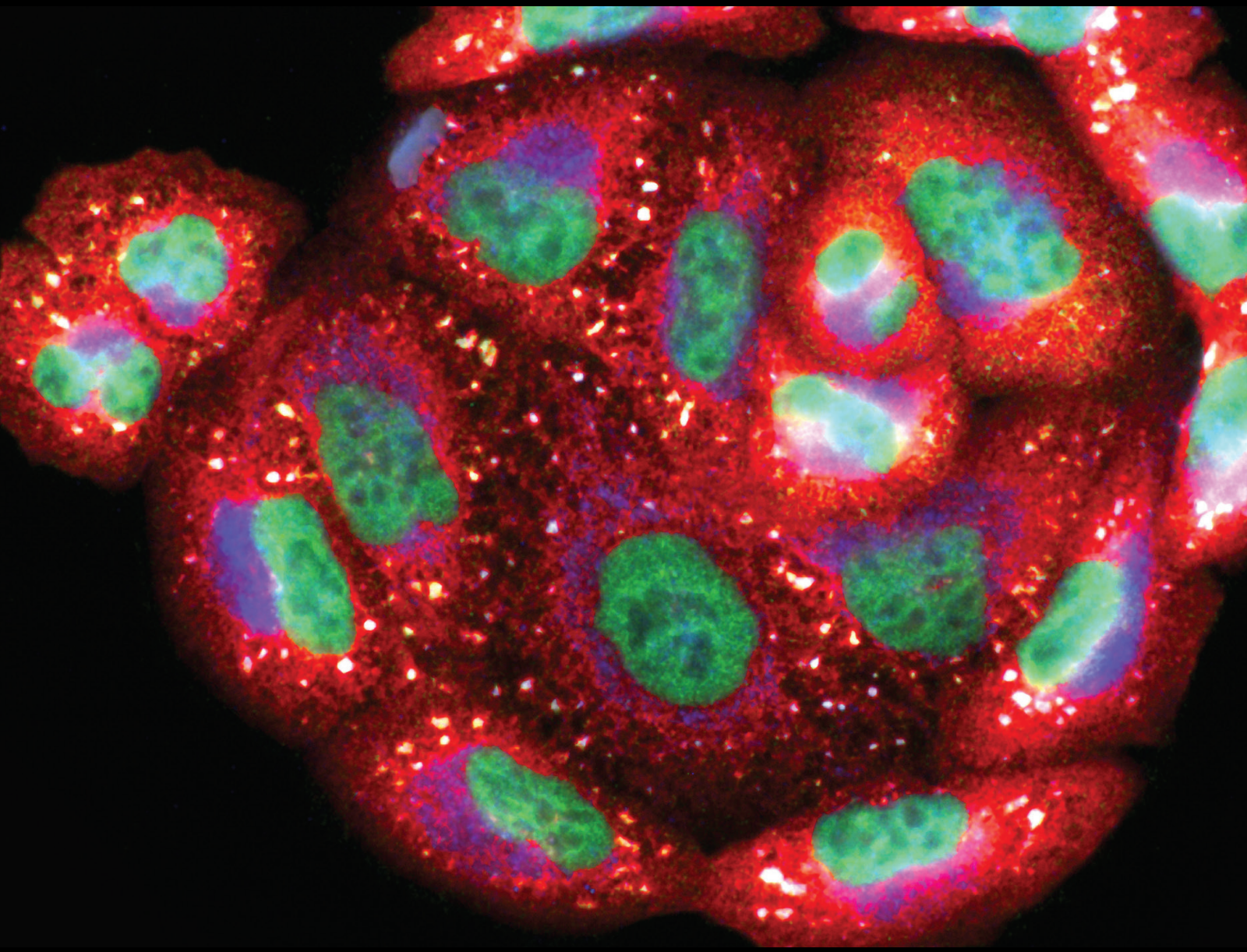

Molecular Mechanisms of Natural Antioxidant Compounds with Neuroprotective Effects

Oxidative Medicine and Cellular Longevity

Molecular Mechanisms of Natural Antioxidant Compounds with Neuroprotective Effects

Lead Guest Editor: João C. M. Barreira
Guest Editors: Isabel C. F. R. Ferreira, Beatriz P. P. Oliveira, and Rosane M. Peralta

Contents

Hindawi
Oxidative Medicine and Cellular Longevity
Volume 2020, Article ID 9741369, 20 pages
https://doi.org/10.1155/2020/9741369

Research Article

Metformin Promotes Axon Regeneration after Spinal Cord Injury through Inhibiting Oxidative Stress and Stabilizing Microtubule

Haoli Wang,[1,2] **Zhilong Zheng**,[2] **Wen Han**,[2] **Yuan Yuan**,[2] **Yao Li**,[1] **Kailiang Zhou**,[1] **Qingqing Wang**,[1] **Ling Xie**,[2] **Ke Xu**,[3] **Hongyu Zhang**,[2] **Huazi Xu**,[1] **Yanqing Wu**,[3] **and Jian Xiao**[2]

[1]*Department of Orthopaedics, The Second Affiliated Hospital and Yuying Children's Hospital of Wenzhou Medical University, Wenzhou, Zhejiang, China*
[2]*Molecular Pharmacology Research Center, School of Pharmaceutical Science, Wenzhou Medical University, Wenzhou, Zhejiang, China*
[3]*The Institute of Life Sciences, Engineering Laboratory of Zhejiang Province for Pharmaceutical Development of Growth Factors, Biomedical Collaborative Innovation Center of Wenzhou, Wenzhou University, Wenzhou, Zhejiang, China 325035*

Correspondence should be addressed to Yanqing Wu; yqwu220946@yeah.net and Jian Xiao; xjian@wzmc.edu.cn

Received 26 March 2019; Revised 7 November 2019; Accepted 13 November 2019; Published 7 January 2020

Guest Editor: João C. M. Barreira

Spinal cord injury (SCI) is a devastating disease that may lead to lifelong disability. Thus, seeking for valid drugs that are beneficial to promoting axonal regrowth and elongation after SCI has gained wide attention. Metformin, a glucose-lowering agent, has been demonstrated to play roles in various central nervous system (CNS) disorders. However, the potential protective effect of metformin on nerve regeneration after SCI is still unclear. In this study, we found that the administration of metformin improved functional recovery after SCI through reducing neuronal cell apoptosis and repairing neurites by stabilizing microtubules via PI3K/Akt signaling pathway. Inhibiting the PI3K/Akt pathway with LY294002 partly reversed the therapeutic effects of metformin on SCI in vitro and vivo. Furthermore, metformin treatment weakened the excessive activation of oxidative stress and improved the mitochondrial function by activating the nuclear factor erythroid-related factor 2 (Nrf2) transcription and binding to the antioxidant response element (ARE). Moreover, treatment with Nrf2 inhibitor ML385 partially abolished its antioxidant effect. We also found that the Nrf2 transcription was partially reduced by LY294002 in vitro. Taken together, these results revealed that the role of metformin in nerve regeneration after SCI was probably related to stabilization of microtubules and inhibition of the excessive activation of Akt-mediated Nrf2/ARE pathway-regulated oxidative stress and mitochondrial dysfunction. Overall, our present study suggests that metformin administration may provide a potential therapy for SCI.

1. Introduction

Traumatic spinal cord injury (SCI) is one of the major cause of public health problems in the world. Millions of people suffer from neurological complications related to SCI, including quadriplegia or paraplegia [1, 2]. SCI results in neurological deficits after primary and secondary injury. The primary injury causes a structural disturbance at the time of injury [3]. Then, a long-term secondary injury is considered a complicated and multifactorial stage that can cause a series of detrimental effects, including oxidative stress, inflammation, and mitochondrial dysfunction, which eventually contributes to neuronal apoptosis and inhibits axon regeneration and nerve recovery [4–6]. Therefore, effective prevention of detrimental secondary events by reduction of neuronal cell death and promotion of axon regeneration is a potential approach for improving functional recovery after SCI.

It is well known that the secondary injury caused by SCI induces neuronal cell death [7]. Furthermore, this neuronal

cell death largely results in injured axons, which is difficult for them to regenerate and reestablish connections with the other neurons during injury [8]. During axon formation, microtubule assembly is crucial for neuronal polarization and axonal growth [9, 10]. Increasing microtubule stabilization prevents swelling of the axon tip and axonal retraction after CNS injury, thus promoting the axonal growth of cultured neurons [11]. Recently, some studies have demonstrated that pharmacological treatment can boost axon growth and enhance axon regeneration by increasing microtubule stabilization [12]. Moreover, it was reported that FGF13 stabilizes microtubules and improves mitochondrial function in order to enhance axon regeneration after SCI [13]. Therefore, regulating microtubule stabilization to regenerate axons is considered as a therapeutic approach for SCI.

Oxidative stress, a highly disordered metabolic process, is the result of an imbalance between antioxidant and prooxidant [14]. Recent studies have demonstrated that oxidative stress is involved in a range of neurological diseases, including neurodegeneration disorders, cerebral ischemia, and SCI [15–17]. Previous studies have revealed that the reactive oxygen species (ROS) production, which is one of the major detrimental effects during secondary injury, showed a significant increase after SCI [18]. Once the spinal cord suffered from damage, the lesion site is accompanied with hypoxia-ischemia and inflammation and results in a redundant production of ROS. Therefore, the prevention of oxidative stress development and accumulation of ROS using antioxidants could be a helpful for SCI recovery. A previous study has suggested that antioxidant treatments can trigger the increase of stable microtubules and promote axonal regrowth [19], but the role of oxidative stress in microtubule stabilization after SCI remains unclear. In the antioxidant defensive system, the nuclear factor erythroid 2-related factor 2 (Nrf2) binds to the antioxidant response element (ARE), a cis-acting regulatory element of genes encoding antioxidant proteins and phase II detoxification enzymes, thereby regulating the expression of a large group of cytoprotective genes such as heme oxygenase-1 (HO-1) and NADH dehydrogenase quinone 1 (NQO1) that is involved in the cellular antioxidant responses [20, 21]. As one of upstream signal molecule for regulating Nrf2, the PI3K/Akt pathway is critical for the survival and growth, which participates in many biological processes such as cytoskeletal dynamics and antiapoptosis [22]. In addition, the PI3K/Akt pathway regulates the Nrf2/ARE pathway and then inhibits oxidative stress and inflammation after SCI [23]. Thus, activating the Nrf2/ARE signaling pathway is implicated as a potential therapy for the reduction of oxidative stress and promotion of functional recovery after SCI.

Metformin, as a traditional hypoglycemic agent, is widely prescribed for the treatment of type 2 diabetes and other metabolic syndromes since 1960s [24]. Metformin ameliorates hyperglycemia via inhibiting hepatic glucose production and increasing peripheral glucose utilization [25]. However, its ability is not limited to lowering glucose. Accumulating evidence suggests that metformin has benefits in various central nervous system (CNS) disorders, including ischemic brain injury, Parkinson's disease, and Huntington's disease [26–28]. In rat brain microvascular endothelial cells (RBEC), metformin increased transendothelial electrical resistance of RBEC monolayers and decreased sodium fluorescein and Evans Blue permeability via upregulating tight junction (TJ) proteins [29]. In addition, metformin has been shown to have a protective effect in improving mitochondrial homeostasis following oxidative stress-induced apoptosis in endothelial cells [30]. Recently, studies have shown that metformin treatment has improved locomotor recovery after SCI [31, 32], but the underlying mechanism of its action is still unclear, especially its role in reducing oxidative stress or promoting axonal regeneration after SCI. Moreover, the other studies have indicated that metformin can protect against hypoxic-ischemic brain injury-induced neuronal cell apoptosis [33]. However, it is unknown whether metformin protects against neuronal damage after SCI by promoting axonal regeneration. Many studies have reported that metformin is associated with the PI3K/Akt signaling pathway. Metformin was found to suppress the PI3K/Akt pathway in the treatment of esophageal cancer cell [34]. Another study have reported that the effect of metformin on ischemic heart was mediated through the PI3K/Akt pathway [35]. However, it is unclear whether the PI3K/Akt signaling pathway is involved in the role of metformin in SCI.

In the present study, we systematically investigated the role of metformin in antioxidant and neuronal regeneration after SCI. We have found some of the possible molecular mechanisms underlying SCI via the promotion of microtubule stabilization and reduction of apoptosis by activating the PI3K/Akt pathway. Moreover, this neuroprotective effect of metformin was also related to the inhibition of excessive oxidative stress and improvement of mitochondrial function by activating the Nrf2/ARE pathway. These findings have revealed that metformin administration promotes the recovery of SCI and suggested that metformin has the potential to be used in the clinical treatment of SCI.

2. Material and Methods

2.1. Spinal Cord Injury and Drug Treatment. Sprague-Dawley rats (female; 220-250 g, $N = 80$) were purchased from Animal Center of Chinese Academy of Science. The animals were housed in standard temperature conditions with a 12 h light/-dark cycle and regularly fed with food and water. After anesthetizing with 2% pentobarbital sodium (40 mg/kg, i.p.), rats were performed with a laminectomy at the T9 level exposing the cord beneath without disrupting the dura. Then, rats suffered with a compression of a vascular clip (15 g forces, Oscar, China) for 1 minute. For the sham control group, the rats received the same surgical procedure but no impact injury and received no pharmacological treatment. Metformin was diluted with normal saline, to achieve a final metformin concentration of 20 mg/mL. After surgery, rats were given metformin solution (50 mg/kg) with/without LY294002 (a specific PI3K inhibitor, 1.2 mg/kg) immediately via i.p. injection and then were injected with the same dose of metformin solution with/without LY294002 per day until the rats were sacrificed. Rats in SCI groups received equivolumetric injection of normal saline at the corresponding time

points after injury. Postoperative care included manual urinary bladder emptying twice daily until the return of bladder function and the administration of cefazolin sodium (50 mg/kg, i.p.). Following completion of the trial, rats were euthanized using an overdose of pentobarbital sodium on 7 d and 14 d, with the exception of 24 rats for locomotion recovery assessment. All surgical interventions and postoperative animal care were approved by the ethics committee of Wenzhou Medical University and performed in accordance with the *Guide for the Care and Use of Laboratory Animals*.

2.2. Locomotion Recovery Assessment. The Basso, Beattie, and Bresnahan (BBB) scores were assessed by three trained investigators who were blinded to experiment in an open-field scale at 1, 3, 5, 7, and 14 d postoperation. Briefly, the BBB scores range from 0 points (complete paralysis) to 21 points (normal locomotion). The scale was developed using the natural progression of locomotion recovery in rats with thoracic SCI [36]. Moreover, the footprint analysis was performed by dipping the rat's fore limb with blue dye and the posterior limb with red dye at 14 d after SCI. Ten rats for each group were used to assess the motor function.

2.3. Hematoxylin and Eosin Staining and Nissl Staining. The rats of each group ($n = 5$) were euthanized with an overdose of sodium pentobarbital, followed by 4% paraformaldehyde in 0.01 M phosphate-buffered saline (PBS, pH = 7.4) at 7 d after SCI. Tissue segments containing the lesion (1 cm on each side of the lesion) were paraffin embedded. Transverse paraffin sections (5 μm thick) were mounted on poly-L-lysine-coated slides for hematoxylin and eosin (H&E) staining and Nissl staining and examined under a light microscope. The cellular stain HE was used to observe the cavity, at 5 mm from the lesion site. The measurements were reported as the percentage of the preserved area in relation to the total area of each section analyzed [37]. For Nissl staining, the number of ventral motor neuron (VMN) in sections was assessed as in the previous report [38]. Transverse sections were collected at rostral, caudal 5 mm, and the lesion site and stained with cresyl violet acetate. After determination of the cells located in the lower ventral horn, cells larger than half of the sampling square (20×20 μm) were counted as a VMN. The cells above the line at 150 μm ventral from the central canal were excluded. The cells were manually counted from each field using MetaMorph software.

2.4. Cell Culture Treatment Protocols. The PC12 cells were purchased from Cell Bank of Type Culture Collection of Chinese Academy of Sciences, Shanghai Institute of Cell Biology, Chinese Academy of Sciences. PC12 cells were cultured in RPMI 1640 medium supplemented with 10% fetal bovine serum (FBS), 100 U/mL penicillin, and 100 U/mL streptomycin. Cells were incubated in a humidified atmosphere containing 5% CO_2 and 95% air at 37°C. PC12 cells were treated with metformin (1 mM), LY294002 (10 μM), ML385 (a novel and specific Nrf2 inhibitor, 2 μM), and H_2O_2 (100 μM) for 8 h. All experiments were performed at least three times.

2.5. Primary Cortical Neuron Culture. The primary cortical neurons were obtained from pregnant Sprague-Dawley rats with embryonic (E18) fetuses. Briefly, fetal rats were sacrificed by decapitation. The cerebral cortex was separated and rinsed in ice-cold Hank's buffer. After clearing up the blood vessels, the cortical tissues were cut into approximately 1 mm pieces and were then treated with 0.125% trypsin-EDTA for 20 min at 37°C. After incubation, the solution was filtered by a 100 μm cell strainer (WHB). The cell suspension was centrifuged at 1000 rpm for 5 min, and the cell pellet was resuspended in complete DMEM/F-12. Cells were incubated for 4 h in 5% CO_2 at 37°C. Then, the cells were refreshed with neuronal basal medium (Gibco, Invitrogen) containing 2% B27 and 0.5 mM L-glutamine (GlutaMAX™ Supplement, Gibco) and cultured in a humidified atmosphere of 5% CO_2 and 95% air at 37°C. The medium was replaced every 3 d.

2.6. Western Blotting Analysis. Spinal cord tissue samples were extracted 7 d and 14 d after surgery and immediately snap-frozen at -80°C for western blotting. Briefly, the tissues were lysed using RIPA buffer (1% Triton X-100, 0.5% sodium deoxycholate, 1 mM PMSF, 1 mM EDTA, 10 μg/mL leupeptin, 20 mM Tris-HCl, 150 mM NaCl, and pH 7.5). In vitro, the cells were rinsed twice with PBS and lysed in lysis buffer (1% Nonidet P-40, 0.1% SDS, 1% sodium deoxycholate, 25 mM Tris-HCl, 150 mM NaCl, and pH 7.6). Protein extraction of both the cytosolic and nuclear was performed by using the Nuclear and Cytoplasmic Protein Extraction Kit (P0027, Beyotime, China) according to the manufacturer's protocol. Tissue and cell lysates were centrifuged at 12,000 rpm for 10 min at 4°C, and the supernatant was obtained for a protein assay. Protein concentrations were quantified with the Enhanced BCA Protein Assay Kit (Beyotime, Shanghai, China). 40 μg of tissue protein was separated by SDS-PAGE and transferred to a PDGF membrane (Bio-Rad, California, USA). After blocking with 5% nonfat milk (Bio-Rad) for 2 h, the membranes were then incubated with the primary antibody against GAPDH (1 : 10000, Bioworld), phosphor-Akt (1 : 1000, Abcam), total-Akt (1 : 1000, Abcam), cleaved caspase3 (1 : 500, Abcam), Bax (1 : 1000, Cell Signaling Technology), Bcl-2 (1 : 1000, Abcam), Ace-tubulin (1 : 1000, Cell Signaling Technology), Tyr-tubulin (1 : 1000, Sigma), MAP2 (1 : 1000, Cell Signaling Technology), GAP43 (1 : 1000, Abcam), Nrf2 (1 : 1000, Abcam), NQO1 (1 : 1000, Abcam), HO-1 (1 : 10000, Abcam), and histone (1 : 1000, Abcam) at 4°C overnight. The membranes were washed with TBST (Tris-buffered saline with 0.1% Tween-20) three times and incubated with the secondary antibodies for 1 h at room temperature. Signals were visualized by a ChemiDoc XRS+ Imaging System (Bio-Rad). We analyzed the bands by using the Quantity One software.

2.7. Immunofluorescence Staining. Spinal cord tissue samples were obtained 7 d and 14 d after injury. All spinal cords were postfixed in 4% PFA, washed, and embedded in paraffin. Transverse sections of 5 μm thickness were cut, deparaffinized in xylene, and rehydrated by ethanol washes. In addition, the sections were incubated with 10% normal goat

serum for 1 h at room temperature in PBS containing 0.1% Triton X-100. They were then incubated with the appropriate primary antibodies overnight at 4°C in the same buffer. The following primary antibodies were used, based on differing targets: Ace-tubulin (1 : 500, Cell Signaling Technology), GFAP (1 : 500, Santa Cruz), NeuN (1 : 500, Abcam), GAP43 (1 : 500, Abcam), HO-1 (1 : 200, Abcam), NQO1 (1 : 1000, Abcam), and Tyr-tubulin (1 : 500, Sigma). After primary antibody incubation, sections were washed with PBST for 4×10 minutes and then incubated with Alexa Fluor 488/594 goat anti-rabbit/mouse secondary antibodies for 1 h at room temperature. Sections were rinsed three times with PBST and incubated with 4′,6-diamidino-2-phenylindole (DAPI) for 10 minutes and finally washed in PBST and sealed with a coverslip. For staining of F-actin, a rhodamine-coupled phalloidin was used (Yeasen, Shanghai). The images were captured with a confocal fluorescence microscope (Nikon, A1 PLUS, Tokyo, Japan); positive neurons in each section were counted by three observers who were blinded to the experimental groups. The rates of the corresponding protein-positive cells per section were calculated from values obtained by counting 30-40 random sections throughout the lesion site of each animal, with five animals examined per group.

2.8. TUNEL Assay. DNA fragmentation was detected using an *In Situ* Cell Death Detection Kit (Roche, South Francisco, CA, USA), and TUNEL staining was performed 7 d after SCI. The sections (5 μm thick) were deparaffinized and rehydrated. Then, these sections were treated with a 20 μg/mL proteinase K working solution for 20 min at 37°C. The sections were rinsed three times in PBS and incubated with TUNEL reaction mixture in a dark humidified box for 1 h at room temperature. Afterward, the sections were washed with PBS and treated with DAPI for 10 min at room temperature. For a positive control, spinal cord slices were treated with 10 U/mL DNase I buffer for 10 min at room temperature before incubation with the TUNEL reaction mixture. Negative control was obtained with the TUNEL reagent without the TdT enzyme. Positive cells were observed under a confocal fluorescence microscope (Nikon, A1 PLUS, Tokyo, Japan) and analyzed by using ImageJ software.

2.9. Measurement of Intracellular ROS Generation. An intracellular ROS level was detected by using the Reactive Oxygen Species Assay Kit (S0033, Beyotime, China). Briefly, according to the manufacturer's instructions, the PC12 cells were exposed to the H_2O_2 with or without metformin for 8 h and then stained with 10 mmol/L DCFH-DA for 30 min at 37°C. ROS levels were assessed through observation by a confocal fluorescence microscope in cells stained with DCFH-DA, and the intensity of fluorescence was measured and subjected to statistical analysis. For each sample, 20,000 cells were collected.

2.10. Measurement of $\Delta\Psi m$ and ATP Levels. Mitochondrial membrane potential ($\Delta\Psi m$) was detected by using the JC-1 (C2006, Beyotime, China). PC12 cells were plated in confocal dished and incubated with culture medium containing JC-1 for 20 minutes at 37°C. Then, the cells were rinsed with ice-cold PBS twice, changed by fresh medium, and detected by using a confocal fluorescence microscope (Nikon, A1 PLUS, Tokyo, Japan).

ATP levels were detected using the ATP assay Kit (S0026, Beyotime, China) according to the manufacturer's protocol.

2.11. Statistical Analysis. The results were presented as mean ± standard error of the mean (SEM) from at least three independent experiments. Data were analyzed by one-way analysis of variance (ANOVA) followed by Dunnett's *post hoc* test for comparison between control and treatment groups. $P < 0.05$ was considered to indicate statistical significance.

3. Results

3.1. Metformin Decreases Spinal Cord Tissue Damage and Improves Locomotor Function in SCI Rats. In this study, rats were given metformin solution (50 mg/kg, i.p.) immediately to determine whether the metformin has a potential to promote the recovery of SCI. A BBB rating scale were used to evaluate the therapeutic effect of metformin after SCI. As shown in Figure 1(a), the sham group performs slightly above of 20 units on the BBB locomotion score and untreated injured rats do at 1.5 (7 days) and 2 (14 days), the rescue on metformin-treated rats (score at around 3 and 4, respectively) is around 10% of the maximum achievable (Figures 1(a)–1(c)), indicating that locomotor function of the metformin group was remarkably improved when compared to the SCI group. Additionally, using H&E staining, we have further observed the damage of peripheral white matter and central gray matter after SCI. Consistent with the locomotion evaluation, the metformin-treated group showed less damage in the lesion area and preserved the motor neurons in the anterior horns (Figures 1(d) and 1(e)), indicating that metformin protected against severe damage during SCI. Meanwhile, some reports have confirmed that the PI3K/Akt signaling pathway is involved in the effect of metformin during ischemic heart [35]. Then, we have detected the phosphorylation status of Akt after SCI. The western blotting results have showed that the p-Akt was significantly upregulated after metformin treatment when compared with that in the SCI group (Figures 1(f) and 1(g)). These results suggested that the PI3K/Akt signaling pathway may be involved in the protective effect of metformin after SCI. The above findings further indicate that metformin has a neuroprotective efficacy on motor neurons during SCI.

3.2. Activation of the PI3K/Akt Signaling Pathway Is Involved in the Effect of Metformin after SCI. To further evaluate whether activating the PI3K/Akt signaling pathway is essential for metformin promoting the recovery of SCI, LY294002 (a specific PI3K inhibitor) was used to inhibit the PI3K/Akt signaling pathway. It was observed that p-Akt was significantly increased after metformin treatment when compared with that in the SCI group, and these increase was markedly inhibited by LY294002 treatment (Figures 2(a) and 2(b)). As

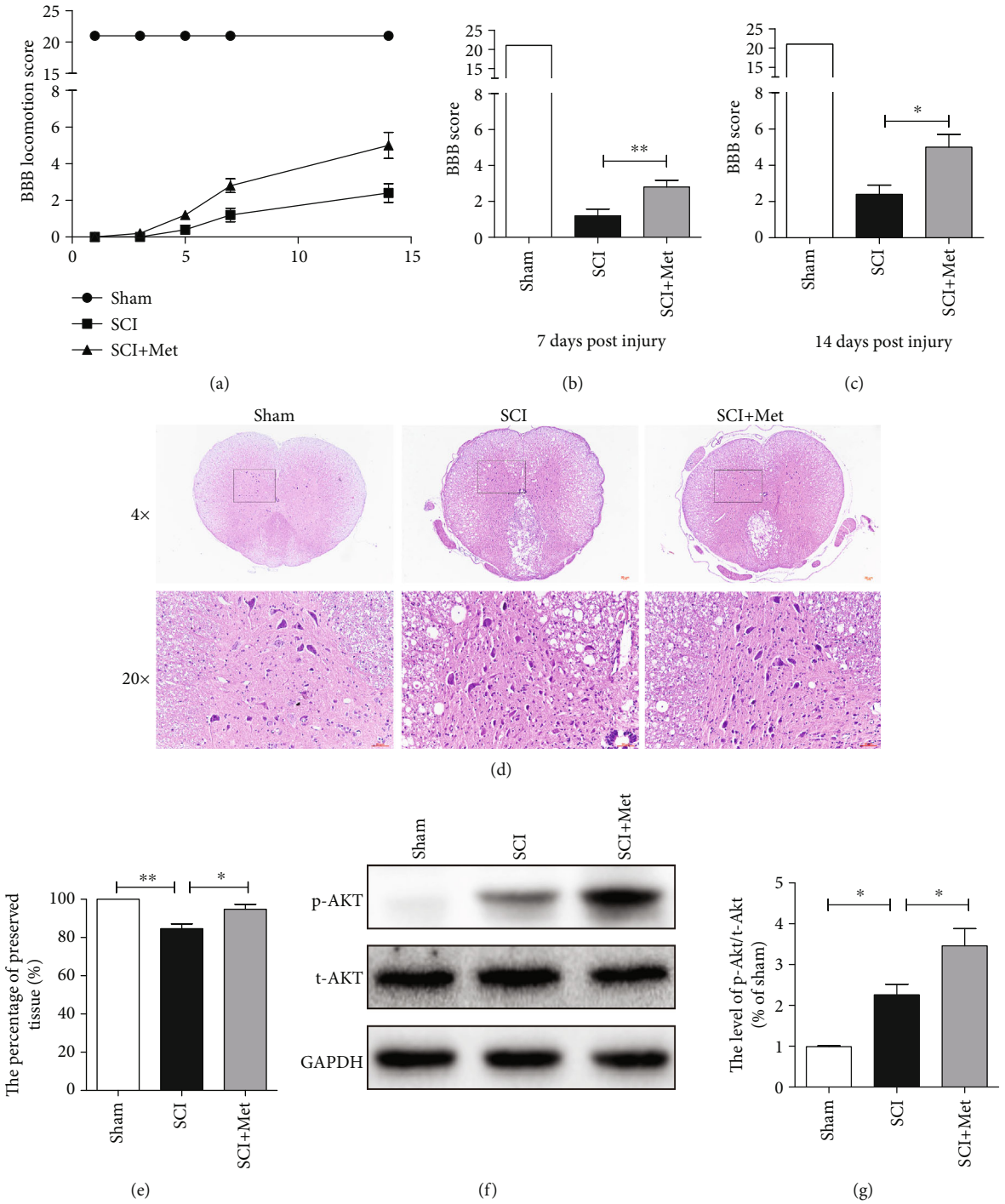

Figure 1: Metformin improved functional recovery after SCI. (a) The BBB locomotion scores of the different groups at 1, 3, 5, 7, and 14 days after SCI, $n = 10$ per group. (b, c) Quantification of the BBB locomotion scores at 7 and 14 d from (a). $n = 10$; $^{*}P < 0.05$ and $^{**}P < 0.01$ *vs.* the indicated group. (d) Representative images from H&E at 7 dpi. Scale bar: 1000 μm (4x). Scale bar: 200 μm (20x). (e) Quantification data of the percentage of the preserved tissue area from (d). $n = 5$; $^{*}P < 0.05$ and $^{**}P < 0.01$ *vs.* the indicated group. (f) Representative western blots of phosphor-Akt (p-Akt) and total-Akt (t-Akt) in each group. (g) Quantification of western blots data from (f). $n = 5$; $^{*}P < 0.05$ *vs.* the indicated group.

shown in Figures 2(c)–2(e), BBB scores have also indicated that the protective effect of metformin on functional recovery of SCI was markedly suppressed by LY294002 treatment. H&E staining has further revealed that LY294002 treatment significantly enlarged the lesion area when compared with that in metformin treatment alone group (Figures 2(f) and 2(g)). Moreover, LY294002 administration remarkably have reduced the motor neuron survival when compare to that in metformin treatment alone (Figure 2(h)). In footprint analysis, metformin-treated rats displayed coordinated

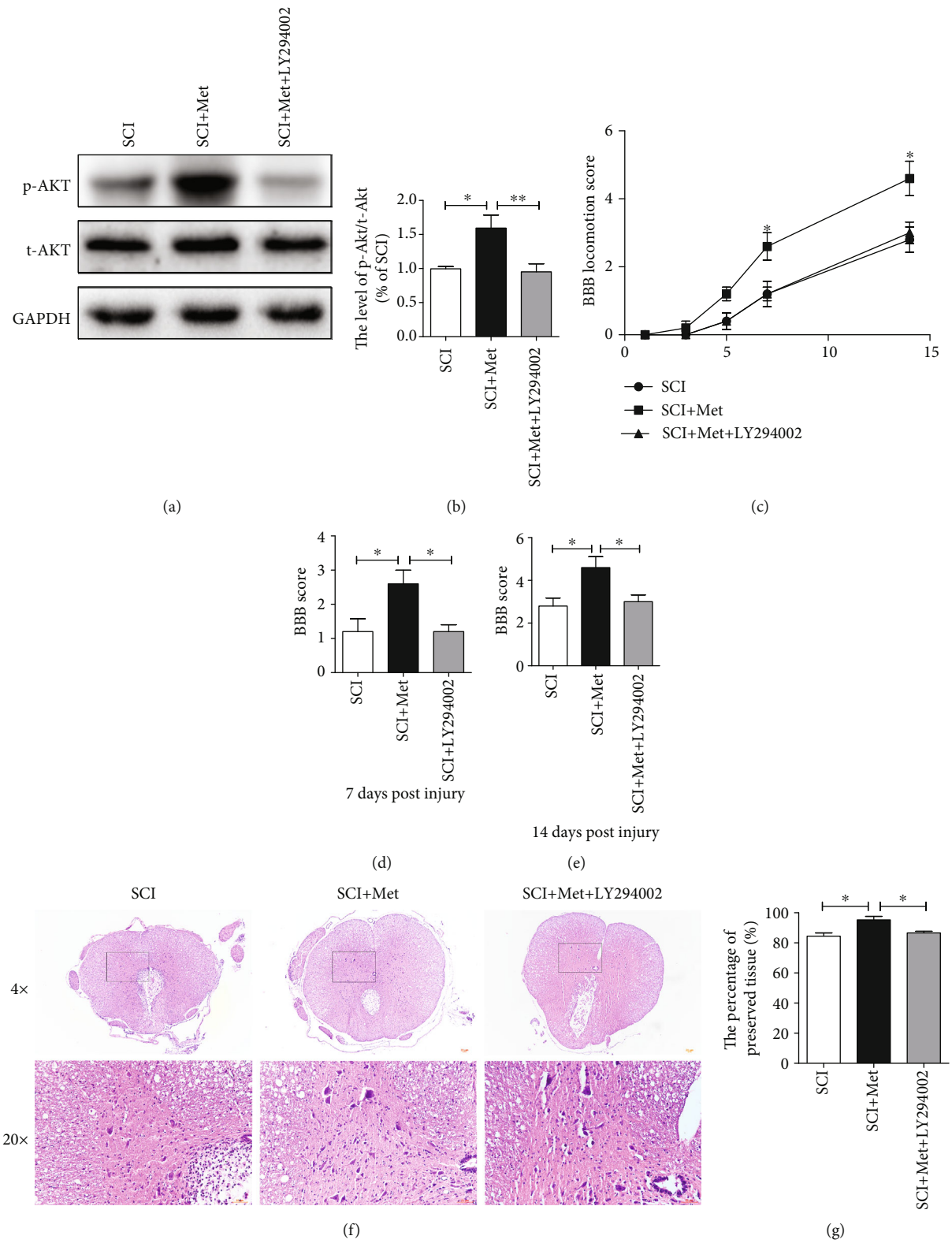

Figure 2: Continued.

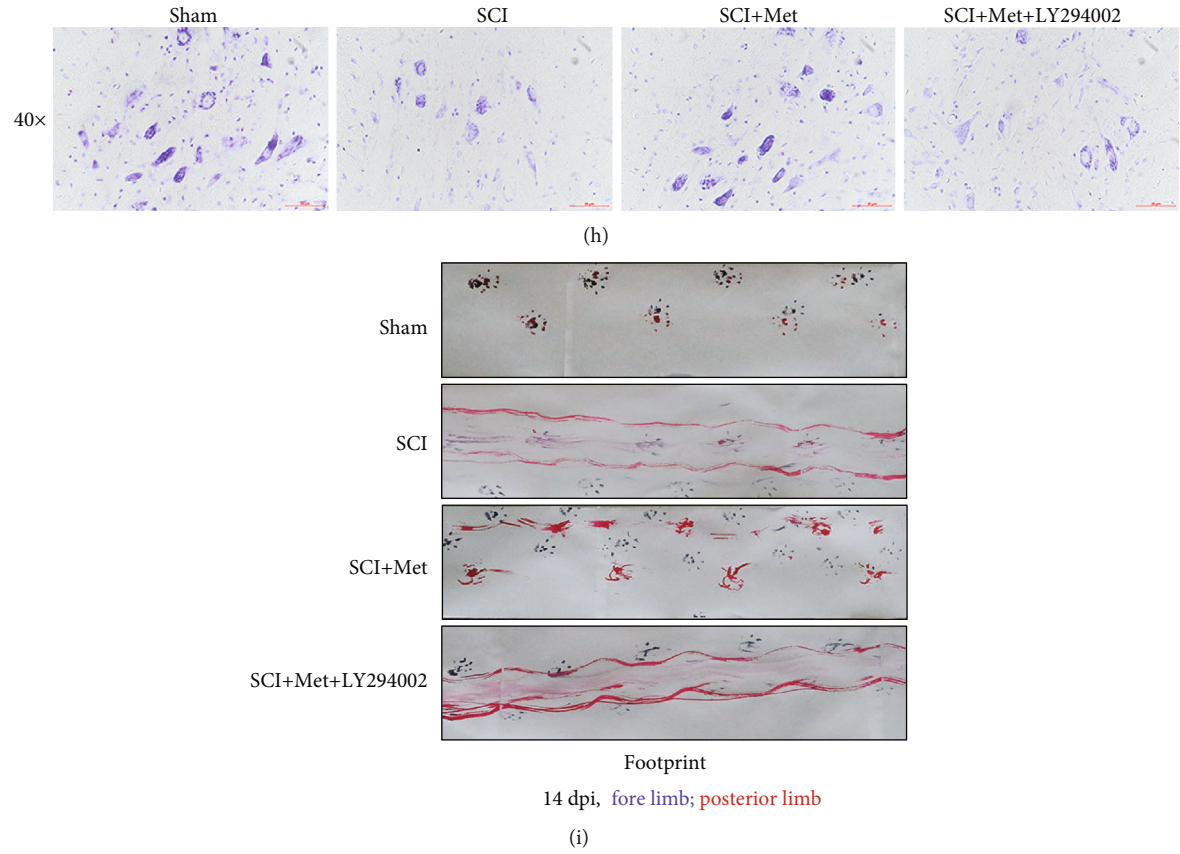

Figure 2: Metformin attenuated spinal cord tissue damage and motor neuron death and promoted functional recovery by activating the PI3K/Akt signaling pathway. (a) Representative western blots of phosphor-Akt (p-Akt) and total-Akt (t-Akt) in each group. (b) Quantification of western blots data from (a). $n = 5$; $^{*}P < 0.05$ and $^{**}P < 0.01$ *vs.* the indicated group. (c) The BBB locomotion scores of the different groups at 1, 3, 5, 7, and 14 d after SCI, $n = 10$ per group. (d, e) Quantification of the BBB locomotion scores at 7 and 14 d from (c). $n = 10$; $^{*}P < 0.05$ *vs.* the indicated group. (f) Representative images from H&E at 7 dpi. Scale bar: 1000 μm (4x). Scale bar: 200 μm (20x). (g) Quantification data of the percentage of the preserved tissue area from (f). $n = 5$; $^{*}P < 0.05$ *vs.* the indicated group. (h) Nissl staining of each group to test the surviving neurons at 14 d after SCI. (i) Footprint analysis results from the different groups.

crawling of posterior limb and very little toe dragging at 14 dpi. In contrast, the rats from SCI and LY294002 groups still showed uncoordinated crawling and extensive dragging (Figure 2(i)). The above results have demonstrated that metformin regulated the PI3K/Akt signaling pathway, increased neuronal survival, and finally promoted the functional recovery of SCI.

3.3. Metformin Reduces the Apoptosis through Activation of the PI3K/Akt Signaling Pathway. TUNEL staining was performed to evaluate whether metformin treatment reduces the apoptosis level after SCI. It was found that SCI dramatically increased the number of apoptotic cells, and metformin treatment ameliorated it. However, this protective effect of metformin was partly weakened by LY294002 treatment (Figures 3(a) and 3(b)). Moreover, consistent with TUNEL, western blot analysis has also showed that metformin treatment markedly blocked SCI-induced increases of cleaved caspase3 and Bax expression. In contrast, metformin increased the level of Bcl-2 expression compared to that in the SCI group. However, this antiapoptotic effect of metformin was significantly reversed by LY294002 treatment (Figures 3(c)–3(f)). Taken together, the above results have further confirmed the antiapoptotic effect of metformin after SCI.

3.4. Metformin Promotes Neurite Reparation after SCI. As shown above, metformin treatment exerted neuroprotective effect after SCI. Next, we have further explored whether metformin promotes axonal reparation. We examined the expression of acetylated-tubulin (Ace-tubulin; stable microtubules in axon), tyrosinated-tubulin (Tyr-tubulin; dynamic microtubules in axon), and microtubule-associated protein 2 (MAP2, a specific structural protein in neuronal dendrites) in each group at 14 dpi after SCI [39–41]. Western blotting results have revealed that Ace-tubulin and MAP2 expressions were significantly increased in the metformin group when compared to that in the SCI group. In contrast, metformin treatment dramatically attenuated the level of Tyr-tubulin when compared to that in the SCI group. Moreover, LY294002 treatment reversed the effect of metformin evidencing with decreases of Ace-tubulin and MAP2 and increases of Tyr-tubulin (Figures 4(a)–4(d)). In addition, coimmunofluorescence of GFAP-labeled astrocytes and Ace-tubulin-labeled axon was performed at 14 dpi. The results have showed that the GFAP-positive astrocytes were

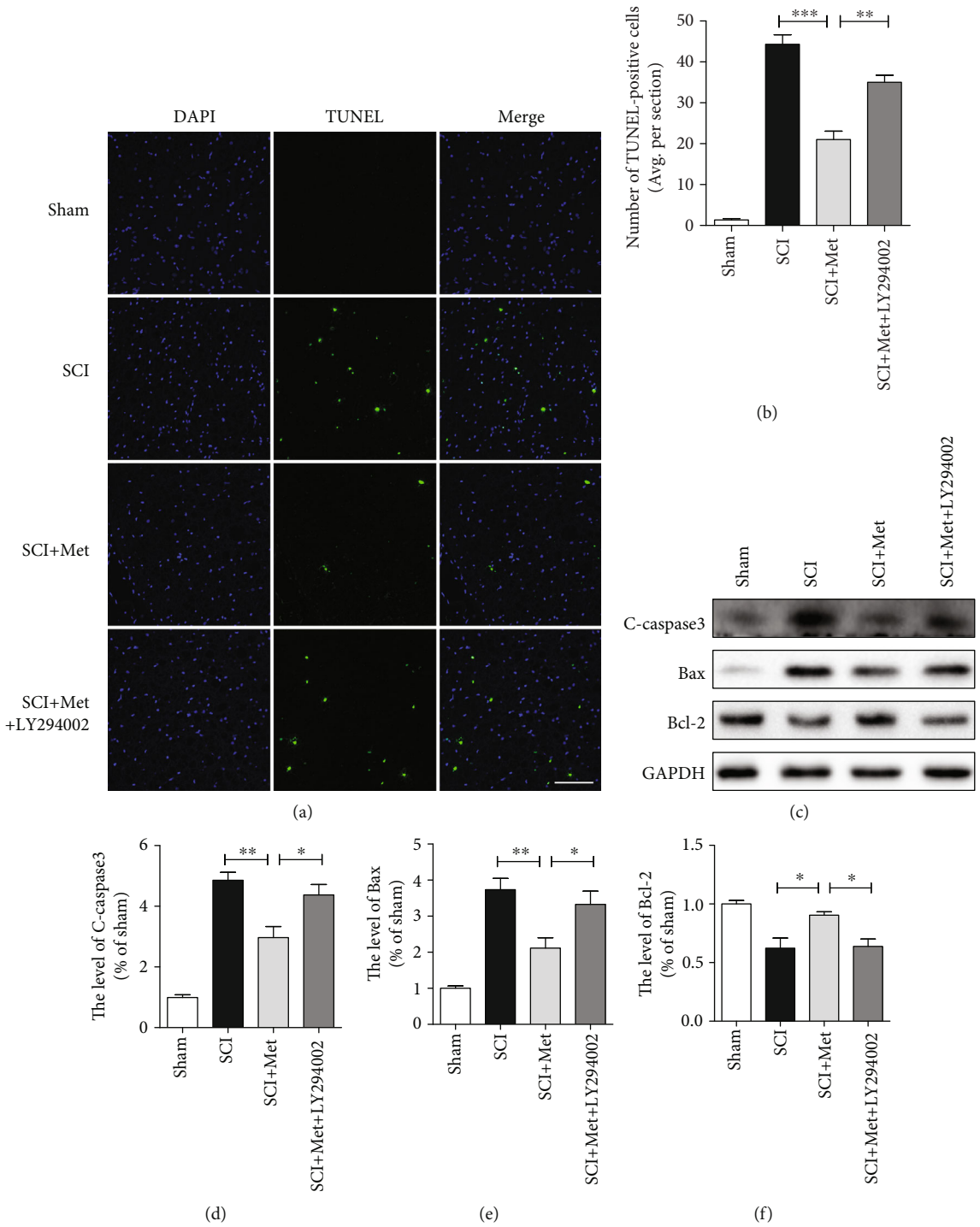

Figure 3: Metformin treatment blocked SCI-triggered apoptosis via activating the PI3K/Akt pathway after SCI. (a, b) TUNEL staining in the sham, SCI, SCI+metformin, and SCI+metformin+LY294002 group. Scale bar = 100 μm. (c) Representative western blots of cleaved caspase3 (C-caspase3), Bax, and Bcl-2 in each group. (d–f) Quantification of western blots data from (c). $n = 5$; $^{*}P < 0.05$ and $^{**}P < 0.01$ *vs.* the indicated group.

accumulated along the lesion border after SCI and metformin treatment promoted the axonal outgrowth to cross the lesion border and elongate farther into the distal area when compared with that in SCI and LY294002 treatment group (Figures 4(e) and 4(f)). To further confirm the neuroprotection effect of metformin, we have examined the expression of GAP43, which is neuronal protective protein [42]. The results indicated that the expression of GAP43 was at a very low level in the sham, SCI, and LY294002 treatment groups, which was significantly increased after metformin treatment (Figures 5(a) and 5(b)). Additionally, we have performed the coimmunofluorescence staining of GAP43 and NeuN, and

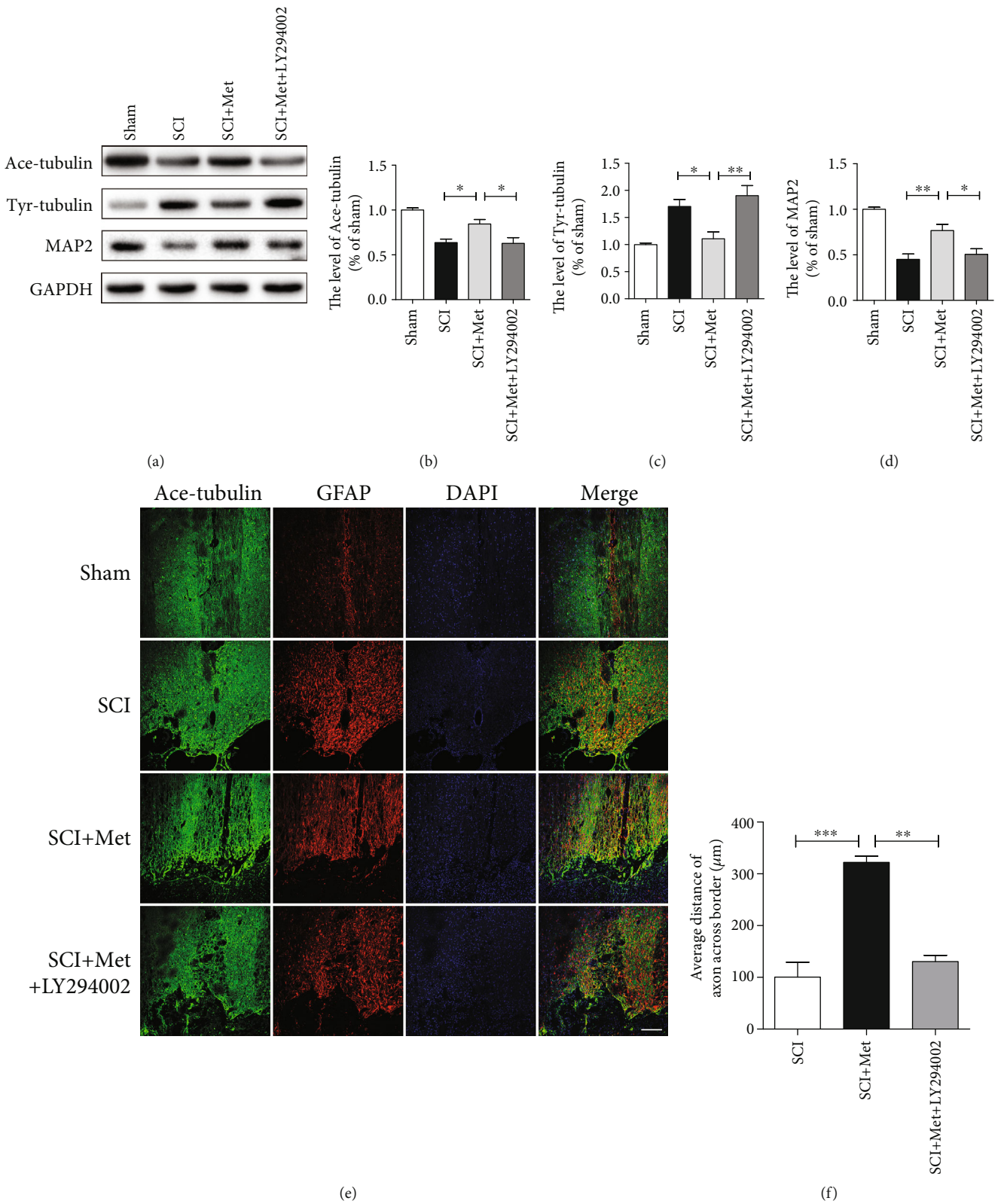

FIGURE 4: Metformin promoted neurite repair by activating the PI3K/Akt signaling pathway in acute SCI. (a) Representative western blots of Ace-tubulin, Tyr-tubulin, and MAP2 in each group. (b–d) Quantification of western blots data from (a). $n = 5$; $^{*}P < 0.05$ and $^{**}P < 0.01$ *vs.* the indicated group. (e) Coimmunofluorescence images show Ace-tubulin (green) and GFAP (red) at 14 d after SCI in each group. Scale bar = 200 μm. (f) Quantification of distance of axon across border. $n = 5$; $^{**}P < 0.01$ and $^{***}P < 0.001$ *vs.* the indicated group.

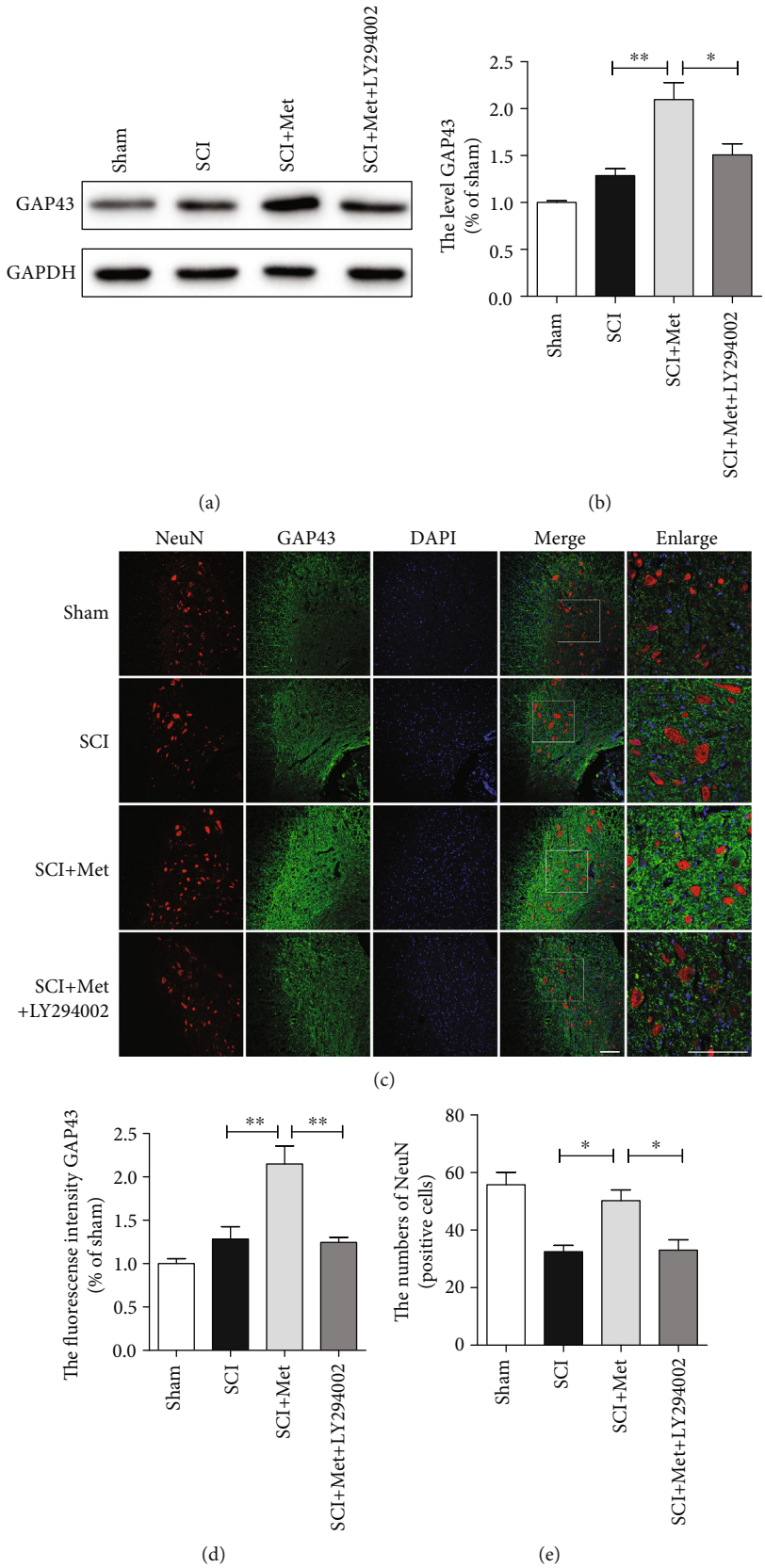

Figure 5: Metformin protects the neurons after SCI. (a) Representative western blots of GAP43 in each group. (b) Quantification of western blots data from (a). $n = 5$; $^{*}P < 0.05$ and $^{**}P < 0.01$ *vs.* the indicated group. (c) Coimmunofluorescence images show GAP43 (green) and NeuN (red) after SCI in each group. Scale bar = 100 μm. (d) Quantification of the fluorescence intensity (GAP43 level) from (c). $^{**}P < 0.01$ *vs.* indicated group. (e) Quantification of fluorescence (the number of NeuN) from (c). $n = 5$; $^{*}P < 0.05$ *vs.* the indicated group.

found that metformin markedly increased the expression of GAP43 and reduced the loss of neurons (Figures 5(c)–5(e)). These data indicate that the metformin-activated PI3K/Akt signaling pathway contributes to axon regeneration after SCI.

3.5. Metformin Reduces Oxidative Stress via Activating the Nrf2/ARE Signaling Pathways after SCI. Lots of studies have demonstrated that the Nrf2/ARE signaling pathways are essential for the anti-inflammatory and antioxidant properties of metformin [43]. To further determine the mechanism underlying the therapeutic effect of metformin for SCI, we have evaluated whether the Nrf2/ARE signaling pathway is involved in the effect of metformin on SCI. We have detected the expression levels of Nrf2, HO-1, and NQO1. As shown in Figures 6(a)–6(d), the expressions of Nrf2, HO-1, and NQO1 levels were increased after SCI when compared with that in the sham group, suggesting that SCI activated the Nrf2/ARE signaling pathway. Compared with the SCI group, metformin treatment significantly induced the higher levels of Nrf2, HO-1, and NQO1. Additionally, immunofluorescence staining has also showed that the expressions of HO-1 and NQO1 in the metformin group was remarkably increased (Figures 6(e) and 6(f)). The above results have demonstrated that metformin treatment promotes the antioxidant level through activating the Nrf2/ARE signaling pathway after SCI.

3.6. Metformin Promotes Axon Regeneration and Migration in Neurons via Affecting Microtubule Stabilization. To further determine the effect of metformin, we have examined the expression levels of Ace-tubulin, Tyr-tubulin, and MAP2 in primary cortical neurons. In vitro, H_2O_2 treatment was used to stimulate the microcirculation of acute SCI. As shown in Figures 7(a)–7(d), western blotting results revealed that Ace-tubulin and MAP2 expressions were remarkably increased in neurons after metformin treatment when compared with those in the H_2O_2 group. In contrast, metformin significantly attenuated the level of Tyr-tubulin when compared to that in the H_2O_2 group. However, LY294002 treatment markedly blocked the effect of metformin on microtubule stabilization after SCI. Additionally, we have further evaluated the effect of metformin on microtubule stabilization in primary cortical neurons. The primary cortical neurons at DIV7 were provoked to H_2O_2 with and without metformin administration. Then, immunofluorescence staining was used to detect the expressions of Ace-tubulin and Tyr-tubulin. The results have indicated that the neurons without metformin treatment after H_2O_2 had a shorter axon than that of the control group. However, the axonal length in the metformin treatment group was remarkably longer than those in the H_2O_2 and LY294002 groups (Figures 7(e) and 7(f)). The ratio of Ace-tubulin to Tyr-tubulin was performed to evaluate the relative ratio of stable to dynamic microtubules [44]. We found that metformin administration caused a significant increase in the Ace-tubulin/Tyr-tubulin ratio compared to those in the H_2O_2 and LY294002 group (Figure 7(g)). We also used the primary cortical neurons at DIV3 to detect the shape of growth cone (white frame) by immunostaining. As shown in Figure 7(h), the mean size of growth cone was significantly increased in the metformin group when compared with those in the H_2O_2 and LY294002 groups. Therefore, above results have demonstrated that metformin can regulate microtubule stabilization and consequently increase the intrinsic growth ability of axon via activating the PI3K/Akt signaling pathway.

3.7. Metformin Alleviates Mitochondrial Dysfunction and Reduces ROS by Activating the Akt/Nrf2/ARE Signaling Pathway In Vitro. Here, using H_2O_2-treated PC12 cells, we had further evaluated the effect of metformin treatment on antioxidant in vitro. We firstly detected the expression of Nrf2 protein. As shown in Figures 8(a) and 8(b), western blots of nuclear extracts with the anti-Nrf2 antibody showed that the level of translocated Nrf2 was increased after H_2O_2-treated and metformin significantly increased Nrf2 translocation. A previous study showed that Nrf2 is positively regulated by PI3K/Akt significantly and leads to the suppression of oxidative stress [23]. We used LY294002 and ML385 (a novel and specific Nrf2 inhibitor) [45, 46] to further confirm the role of Nrf2. The results showed that LY294002 treatment not only suppressed the p-Akt/t-Akt ratio, but also inhibited Nrf2 to translocate into the nucleus. However, ML385 only suppressed Nrf2 to the translocated nucleus with no obvious effect on the p-Akt expression (Figures 8(a)–8(d)). Similarly, we had found higher expressions of HO-1 and NQO1 in the metformin-treated group when compared to those in the untreated group, which was significantly reversed by ML385 treatment (Figures 8(d)–8(f)). These findings have indicated that Nrf2 activation significantly induces the expression HO-1 and NQO1 under H_2O_2 condition and metformin further increases HO-1 and NQO1 expressions via activating the Akt/Nrf2/ARE pathway. Next, to verify that the protective effect of metformin was due to the amelioration of mitochondrial function, we detected the mitochondrial membrane potential ($\Delta\psi$m) in PC12 cells using the JC-1 staining assay. Changes in the ratio of aggregate-to-monomer fluorescence were indicated as $\Delta\psi$m. As shown in Figures 9(a) and 9(b), metformin treatment significantly increased the $\Delta\psi$m of PC12 cells following exposure to H_2O_2 for 2 h when compared with those in the H_2O_2 group, ML385 group, and positive control group (CCCP group). These results revealed that metformin can restore the mitochondrial activity. The production of ROS is correlated with mitochondrial dysfunction and causes major adverse effect during secondary injury. Thus, we tried to understand whether metformin affects the level of intracellular ROS using a specific probe for hydrogen peroxide, 2′,7′-dichlorodihydrofluorescein diacetate (DCFH-DA). The fluorescence images had showed a markedly low density of fluorescence in the metformin group when compared with those in the H_2O_2 group, ML385 group, and ROSUP group (positive control group) (Figures 9(c) and 9(d)), indicating that metformin has a remarkable effect on the reduction of ROS. Additionally, we had further monitored the cellular ATP level. We found that the ATP levels were reduced after H_2O_2 and metformin treatment rescued it, whereas ML385 reversed the effect of metformin as shown by the ATP level (Figure 9(e)). Based on these results, metformin may restore mitochondrial

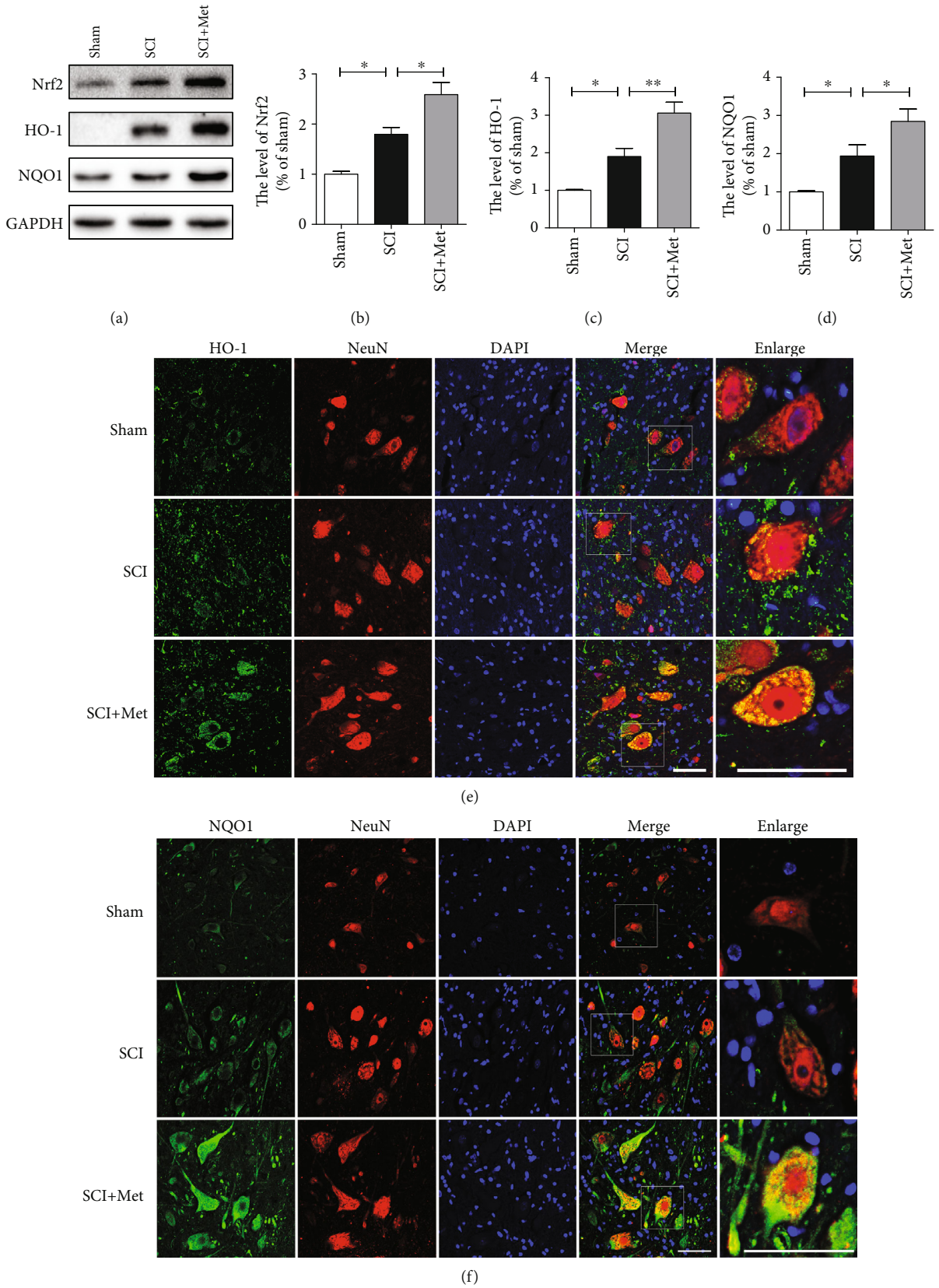

Figure 6: Metformin increased the expression of antioxidant proteins by activating the Nrf2/ARE signaling pathway after SCI. (a) Representative western blots of Nrf2, HO-1, and NQO1 in each group. (b–d) Quantification of western blots data from (a). $n = 3$; $^{*}P < 0.05$ and $^{**}P < 0.01$ *vs.* the indicated group. (e) Coimmunofluorescence images show HO-1 (green) and NeuN (red) after SCI in each group. Scale bar = 50 μm. (f) Coimmunofluorescence images show NQO1 (green) and NeuN (red) after SCI in each group. Scale bar = 50 μm.

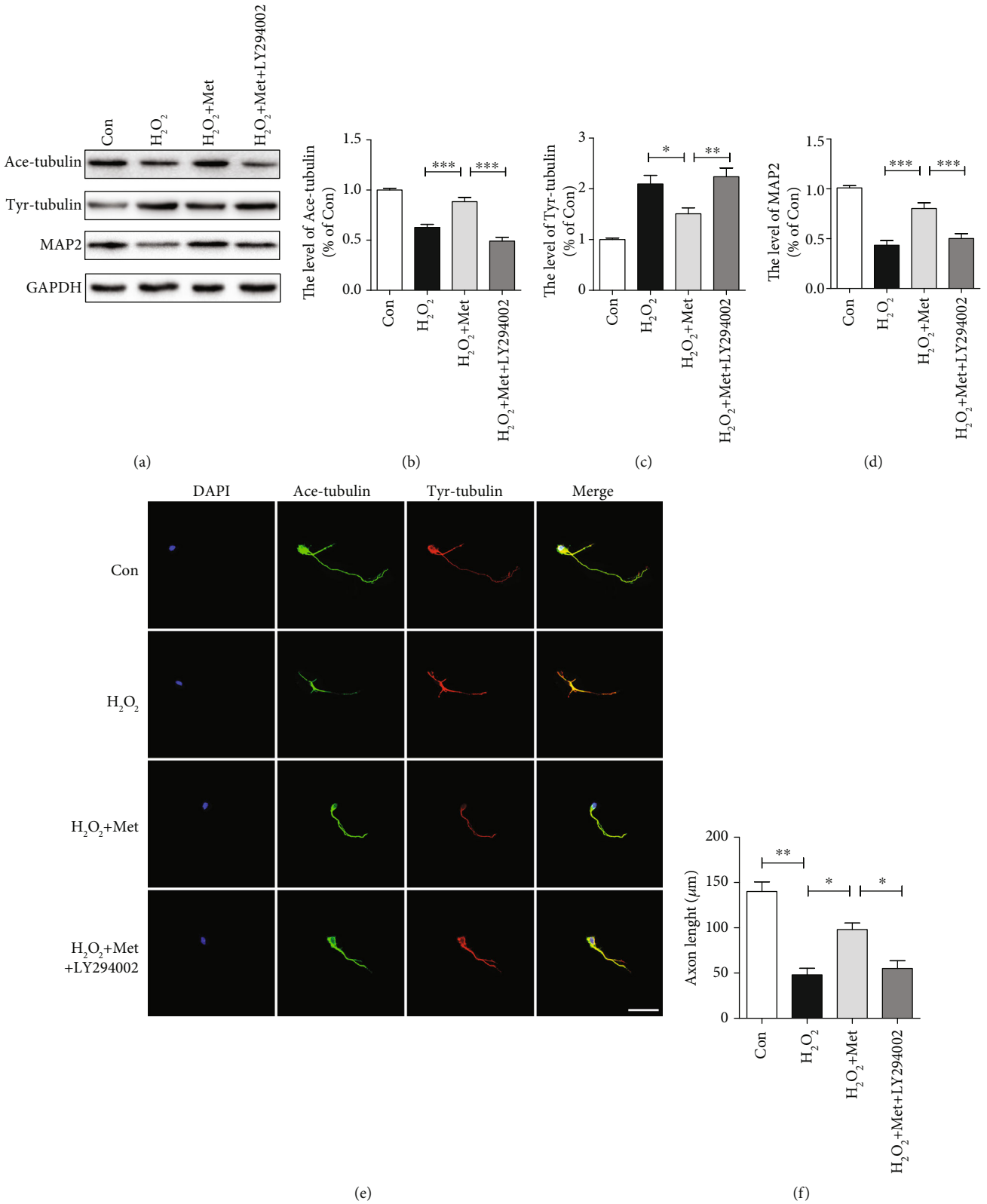

Figure 7: Continued.

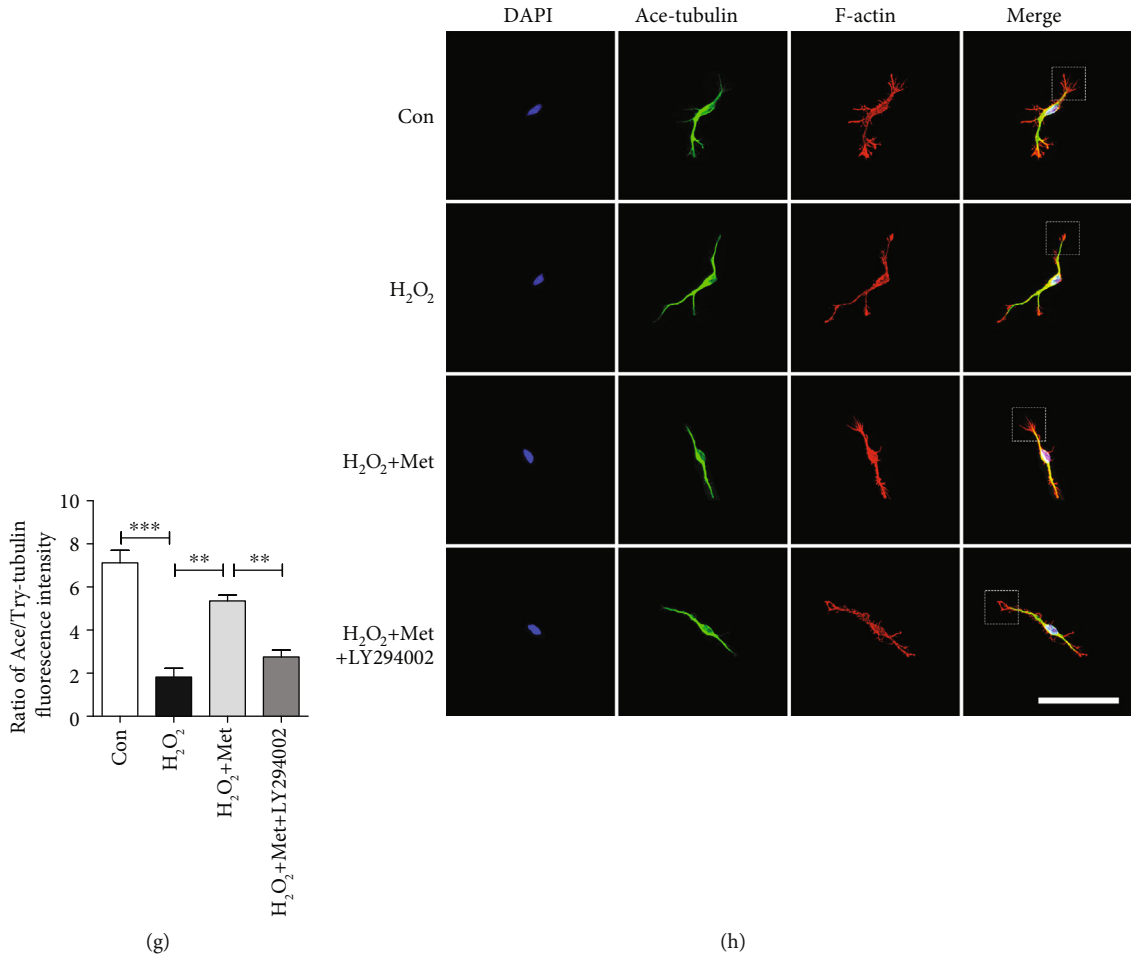

Figure 7: Metformin promote axonal regeneration by stabilizing microtubule in vitro. (a) Representative western blots of Ace-tubulin, Tyr-tubulin, and MAP2 in each group. (b–d) Quantification of western blots data from (a). $^{*}P < 0.05$, $^{**}P < 0.01$, and $^{***}P < 0.001$ *vs.* the indicated group. (e) Coimmunofluorescence images show Tyr-tubulin (green) and Ace-tubulin (red) in primary cortical neurons. Scale bar = 50 μm. (f) Quantification of axonal length from (e). $n = 4$; $^{*}P < 0.05$ and $^{**}P < 0.01$*vs.* the indicated group. (g) Quantification of Ace-tubulin/Tyr-tubulin from (e). $n = 4$; $^{**}P < 0.01$ and $^{***}P < 0.001$*vs.* the indicated group. (h) Coimmunofluorescence images show growth cone (white frame) in primary cortical neurons. Scale bar = 100 μm.

dysfunction and then reduce the ROS level, resulting in neuron protection and regeneration.

4. Discussion

SCI is a serious neurological disease that can induce neurological dysfunction and permanent damage. Series of secondary injuries, including oxidative stress, mitochondrial dysfunction, and neuronal cell apoptosis, are considered as the major factor for disability [47]. Thus, new effective therapeutic treatments for reducing SCI-induced neurological disorders and tissue damages are urgently needed. Metformin, a glucose-lowering agent, is wildly used as the treatment of type II diabetes mellitus [48]. Our previous reports had also showed that metformin treatment improves functional recovery after SCI, in part by inhibiting the neuronal apoptosis and attenuating blood-spinal cord barrier disruption [32, 49]. However, it remains unclear whether metformin has a therapeutic effect in the recovery of axonal regeneration. In a present study, we found that metformin treatment significantly reduced spinal cord damage, decreased the neuronal apoptosis, inhibited oxidative stress, promoted axonal regeneration by stabilizing microtubules, and finally improved functional recovery after SCI in rat. The activation of the PI3K/Akt and Nrf2/ARE pathway were the potential mechanisms underlying metformin treatment for SCI.

As is known, injured axon has poor ability to regenerate after SCI [50]. Therefore, it is meaningful to explore the approaches to promote axonal regeneration after. Recently, various neuroregenerative researches have focused on dendritic and axonal repair to improve functional recovery after CNS injury [51]. Previous studies have shown that metformin exerts neuroprotective effect and promotes functional recovery of memory deficits via anti-inflammation and triggering neurogenesis [52]. In addition, recent researches have confirmed that metformin has a beneficial effect in promoting the nerve regeneration after peripheral nerve injury (PNI) [53]. These studies have suggested that

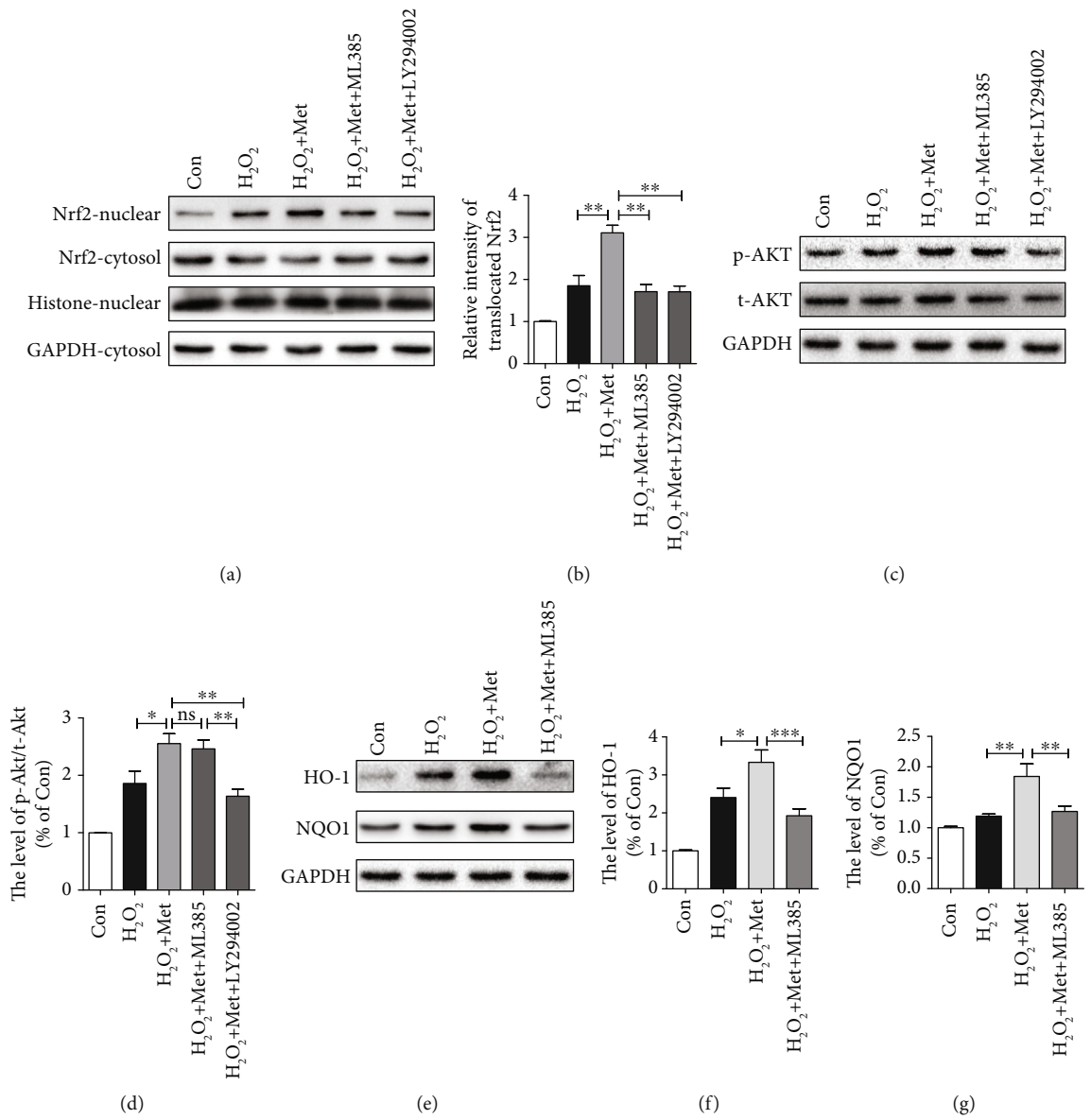

Figure 8: Metformin inhibited oxidative stress via activating the Akt/Nrf2/ARE signaling pathway. (a) Representative western blots of Nrf2-nuclear and Nrf2-cytosol in each group. (b) Quantification of western blots data from (a). $^{**}P < 0.01$ *vs.* the indicated group. (c) Representative western blots of p-Akt and t-Akt in each group. (d) Quantification of western blots data from (c). $^{*}P < 0.05$ and $^{***}P < 0.001$ *vs.* the indicated group. (e) Representative western blots of HO-1 and NQO1 in each group. (f, g) Quantification of western blots data from (e). $^{*}P < 0.05$, $^{**}P < 0.01$, and $^{***}P < 0.001$ *vs.* the indicated group.

metformin has a protective role in axonal regeneration. However, whether metformin has a therapeutic effect on axonal regeneration after SCI has not been reported. Based on these studies, we hypothesized that metformin can promote axonal regeneration after SCI. In our study, we found that metformin improved outgrowth of Ace-tubulin-labeled neurites, suggesting that metformin can promote axonal regeneration. Previous studies have demonstrated that remodeling of cytoskeleton structures, such as microtubules stabilization, is pivotal for the regrowth of injured axons and growth cone initiation [54]. We had found that metformin upregulated the expression of Ace-tubulin surrounding a lesion and increased the ratio of Ace-tubulin/Tyr-tubulin in primary cortical neurons under H_2O_2 condition, indicating that the effect of metformin on axonal regeneration was related to microtubule stabilization. Our present study has also revealed that the PI3K/Akt signaling pathway has neuroprotective effects on the central nervous system. Meanwhile, another study has further verified that the PI3K/Akt signaling pathway is involved in the protective effect of metformin on ischemic heart [35]. Moreover, PI3K/Akt have also played an important role in stabilizing microtubule structure to repair neurites after SCI [22]. These studies have demonstrated that metformin can activate the PI3K/Akt signaling pathway after SCI. Thus, we hypothesized that the PI3K/Akt pathway is essential for the effect of metformin on microtubule stabilization. In this study, we found that LY294002, a specific PI3K inhibitor, significantly reversed the effect of

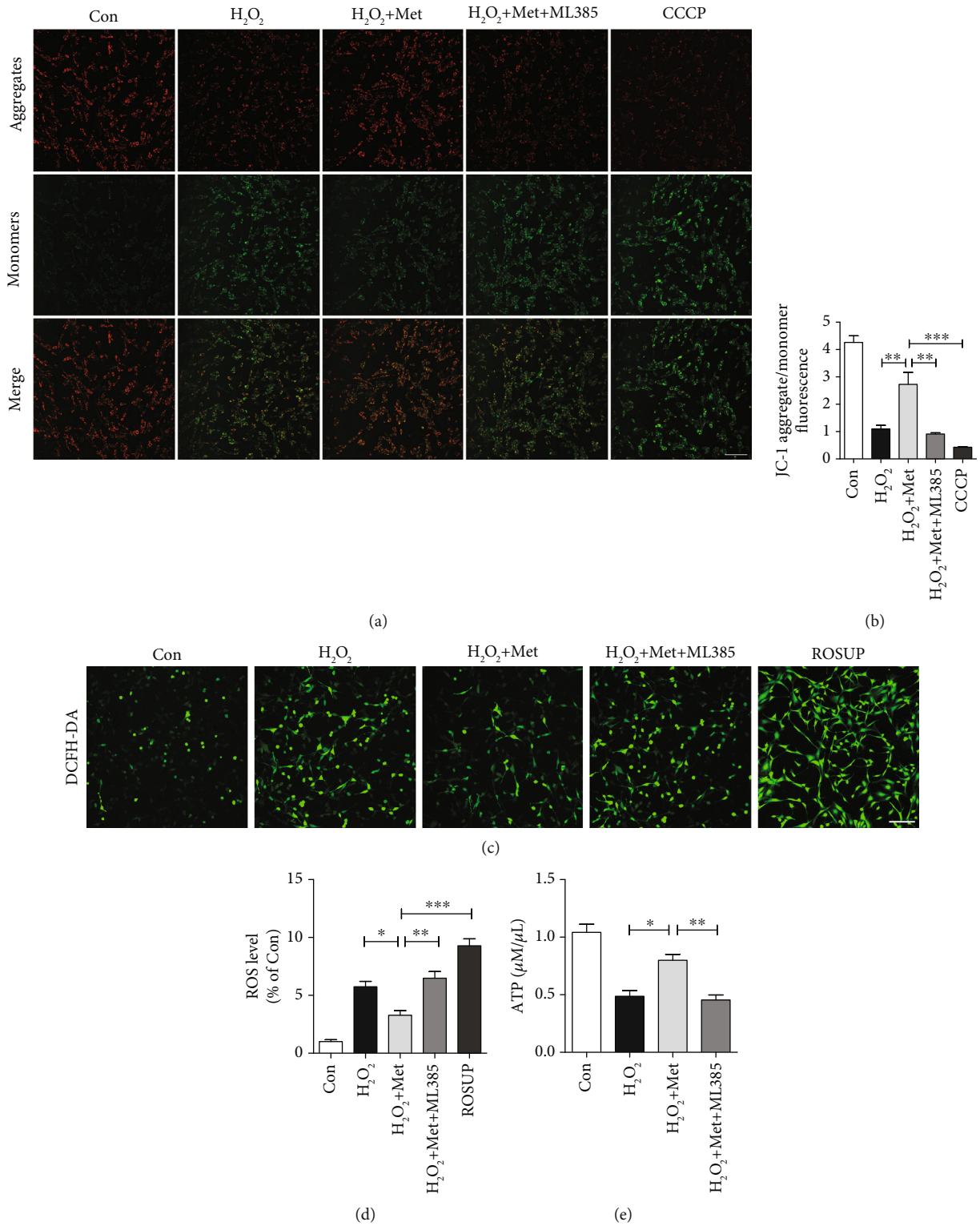

Figure 9: Metformin plays a protective role in mitochondrial function in vitro. (a) PC12 cells incubated with JC-1 represented the mitochondrial membrane potential in each group. Scale bar = 100 μm. (b) Quantification of aggregate/monomer fluorescence ratio from (a). $^{**}P < 0.01$ and $^{***}P < 0.001$ vs. the indicated group. (c) The fluorescence images of the DCFH-DA probe for hydrogen peroxide of PC12 in each group. Scale bar = 100 μm. (d) Quantification of fluorescence density from (c). $^{*}P < 0.05$, $^{**}P < 0.01$, and $^{***}P < 0.001$ vs. the indicated group. (e) The levels of total ATP in each group. $^{*}P < 0.05$ and $^{**}P < 0.01$ vs. the indicated group.

metformin on microtubule stabilization, suggesting that metformin has a potential to repair neurites by stabilizing microtubule structure after SCI.

Previous studies have showed that oxidative stress exerts a destructive role during SCI and diabetic neuropathy [55, 56]. Excessive oxidative stress with ROS accumulation can lead to neuronal apoptosis, which is not beneficial for nerve regeneration [57]. Many studies have reported that the Akt pathway plays an important role in the antiapoptosis process [58]. In this study, we found that metformin enhanced the number of Nissl bodies and maintained their normal morphology by activating the PI3K/Akt pathway, indicating that metformin treatment can protect neurons from SCI-induced apoptosis through the PI3K/Akt signaling pathway. In addition, Lu et al. had verified that fibroblast growth factor 21 improved functional recovery and axonal regeneration through regulating oxidative stress after PNI [59]. Reducing excessive oxidative stress improves the locomotor functional recovery after SCI [60]. One previous study has also demonstrated that metformin restores mitochondrial biogenesis by inhibiting of the PDK4/oxidative stress-mediated apoptosis pathway [61]. Based on these studies, we hypothesized that metformin has an important role in preventing excessive oxidative stress after SCI. To verify this hypothesis, we had exposed the PC12 cells to H_2O_2 to induce oxidative stress and treated it with 1 mM metformin. The results showed that massive accumulation of ROS was elicited in PC12 cells, which were markedly ameliorated with the treatment of metformin. Moreover, we had also found that metformin has a great antioxidative capability in vitro and in vivo, manifesting in marked increase levels of NQO1 and HO-1. In the antioxidant defensive system, Nrf2 is a pivotal antioxidative defender that binds to the ARE to maintain a normal oxidative level [62]. Moreover, many studies have shown that the Nrf2/ARE pathway plays an important role during oxidative stress [63]. Consistent with a prior study, our findings had also shown that the antioxidative capability of metformin was partially reversed by ML385 (a novel and specific Nrf2 inhibitor), suggesting that the Nrf2/ARE signaling pathway may be a potential mechanism underlying metformin protecting against oxidative stress after SCI.

It is well known that mitochondria are the principal power place of eukaryotic cell organelles and lead to ATP generation through the electron transport chain of oxidative phosphorylation reaction. Additionally, Singh et al. have demonstrated that mitochondrial dysfunction plays a significant role in secondary injury after neuronal injury, which induces the accumulation of ROS, neuronal cell death, and impairment of energy transduction [64]. On the other hand, axonal regeneration is a complex process and requires normal mitochondrial function in providing energy [65]. Thus, maintaining the normal mitochondrial function is crucial for axonal regeneration. Pintana et al. had reported that metformin can prevent brain mitochondrial dysfunction and restore learning behavior in high-fat diet-induced insulin-resistant rats [66]. Based on these studies, we hypothesized that metformin has a critical role in mitochondrial function in neuronal cells. We have found that metformin protected mitochondrial membrane potential and ATP levels from H_2O_2 condition in vitro. This result has indicated that the effect of metformin for SCI recovery is partly accomplished by protecting mitochondrial function.

Numerous studies have demonstrated that Akt exerts potent antioxidant effects via augmenting the transcriptional activity of Nrf2 [67]. Nrf2 is a key transcription factor that binds to the antioxidant response element (ARE) and then preserves a normal oxidative stress level [62]. In addition, Akt/Nrf2 signaling is regarded as the crucial molecular regulatory mechanism for alleviating oxidative stress-induced neuronal damage [68–70]. However, there is no clear evidence verified whether the role of metformin on antioxidative stress was closely related to Akt/Nrf2/ARE signaling after SCI. In this study, metformin markedly upregulated the expression levels of total Nrf2, nuclear Nrf2, NQO1, and HO-1 in vivo and in vitro. We had also found that metformin increased the expression of phosphorylation Akt. These results have indicated that the neuroprotective effect of metformin might be attributable to its antioxidant capacity through activating the Akt/Nrf2/ARE pathway.

Our study has identified that metformin exerts a great neuroprotection role after SCI and clarifies the related mechanisms underlying metformin treatment for SCI. However, there were several issues that need further research to be done. Firstly, as a more practical and less invasive route, oral administration of metformin is more beneficial for clinical application, but this might exhibit a different dose response curve when comparing with i.p. injection. Thus, it is necessary to further determine the efficacy of oral administration of metformin on the prevention of SCI. Secondly, it is well known that diabetes aggravates the prognosis of SCI [71], but the rats subjected to SCI were normal SD rats in our current study. Hence, as a traditional antidiabetic drug, the efficacy of metformin on SCI prevention in diabetic rats needs to be validated in the future study.

5. Conclusion

Our current study has demonstrated that metformin treatment significantly reduces spinal cord damage and subsequently improves the functional recovery after SCI. Additionally, we have firstly demonstrated that the protective effect of metformin on SCI is related to the reduction of neuronal cell apoptosis and the promotion of axonal regeneration by stabilizing microtubules. Moreover, suppressing excessive oxidative stress and restoring mitochondrial function are essential for the positive role of metformin with the involvement of the Akt/Nrf2/ARE signaling pathway. Our study suggested that metformin may be suitable as the potential therapeutic strategies for SCI recovery.

Data Availability

The data used to support the findings of this study are available from the corresponding authors upon request.

Conflicts of Interest

The authors confirm that there are no conflicts of interest.

Acknowledgments

This study is supported by the National Natural Science Foundation of China (81722028, 81801233, and 81802251), and Zhejiang Provincial Natural Science Foundation (R18H50001, LQ18H090008, and LQ18H150003).

References

[1] N. A. Silva, N. Sousa, R. L. Reis, and A. J. Salgado, "From basics to clinical: a comprehensive review on spinal cord injury," *Progress in Neurobiology*, vol. 114, pp. 25–57, 2014.

[2] S. K. Ray, S. Samantaray, J. A. Smith, D. D. Matzelle, A. Das, and N. L. Banik, "Inhibition of cysteine proteases in acute and chronic spinal cord injury," *Neurotherapeutics*, vol. 8, no. 2, pp. 180–186, 2011.

[3] P. F. Stahel, T. VanderHeiden, and M. A. Finn, "Management strategies for acute spinal cord injury: current options and future perspectives," *Current Opinion in Critical Care*, vol. 18, no. 6, pp. 651–660, 2012.

[4] X. Yang, S. Chen, Z. Shao et al., "Apolipoprotein E deficiency exacerbates spinal cord injury in mice: inflammatory response and oxidative stress mediated by NF-κB signaling pathway," *Frontiers in Cellular Neuroscience*, vol. 12, p. 142, 2018.

[5] A. D. Greenhalgh, J. G. Zarruk, L. M. Healy et al., "Peripherally derived macrophages modulate microglial function to reduce inflammation after CNS injury," *PLoS Biology*, vol. 16, no. 10, p. e2005264, 2018.

[6] S. P. Patel, P. G. Sullivan, J. D. Pandya et al., "N-Acetylcysteine amide preserves mitochondrial bioenergetics and improves functional recovery following spinal trauma," *Experimental Neurology*, vol. 257, pp. 95–105, 2014.

[7] J. Wang, H. Li, Y. Ren et al., "Local delivery of β-elemene improves locomotor functional recovery by alleviating endoplasmic reticulum stress and reducing neuronal apoptosis in rats with spinal cord injury," *Cellular Physiology and Biochemistry*, vol. 49, no. 2, pp. 595–609, 2018.

[8] J. C. Koch, L. Tönges, E. Barski, U. Michel, M. Bähr, and P. Lingor, "ROCK2 is a major regulator of axonal degeneration, neuronal death and axonal regeneration in the CNS," *Cell Death & Disease*, vol. 5, no. 5, p. e1225, 2014.

[9] Z. He and Y. Jin, "Intrinsic control of axon regeneration," *Neuron*, vol. 90, no. 3, pp. 437–451, 2016.

[10] E. M. Hur, Saijilafu, and F. Q. Zhou, "Growing the growth cone: remodeling the cytoskeleton to promote axon regeneration," *Trends in Neurosciences*, vol. 35, no. 3, pp. 164–174, 2012.

[11] F. Hellal, A. Hurtado, J. Ruschel et al., "Microtubule stabilization reduces scarring and causes axon regeneration after spinal cord injury," *Science*, vol. 331, no. 6019, pp. 928–931, 2011.

[12] V. Sengottuvel, M. Leibinger, M. Pfreimer, A. Andreadaki, and D. Fischer, "Taxol facilitates axon regeneration in the mature CNS," *The Journal of Neuroscience*, vol. 31, no. 7, pp. 2688–2699, 2011.

[13] J. Li, Q. Wang, H. Wang et al., "Lentivirus mediating FGF13 enhances axon regeneration after spinal cord injury by stabilizing microtubule and improving mitochondrial function," *Journal of Neurotrauma*, vol. 35, no. 3, pp. 548–559, 2018.

[14] P. Cheng, F. Kuang, and G. Ju, "Aescin reduces oxidative stress and provides neuroprotection in experimental traumatic spinal cord injury," *Free Radical Biology & Medicine*, vol. 99, pp. 405–417, 2016.

[15] P. Kurian, T. O. Obisesan, and T. J. A. Craddock, "Oxidative species-induced excitonic transport in tubulin aromatic networks: potential implications for neurodegenerative disease," *Journal of Photochemistry and Photobiology B: Biology*, vol. 175, pp. 109–124, 2017.

[16] A. K. Rana and D. Singh, "Targeting glycogen synthase kinase-3 for oxidative stress and neuroinflammation: opportunities, challenges and future directions for cerebral stroke management," *Neuropharmacology*, vol. 139, pp. 124–136, 2018.

[17] U. S. Ozdemir, M. Naziroglu, N. Senol, and V. Ghazizadeh, "Hypericum perforatum attenuates spinal cord injury-induced oxidative stress and apoptosis in the dorsal root ganglion of rats: involvement of TRPM2 and TRPV1 channels," *Molecular Neurobiology*, vol. 53, no. 6, pp. 3540–3551, 2016.

[18] X. Chen, J. Cui, X. Zhai et al., "Inhalation of hydrogen of different concentrations ameliorates spinal cord injury in mice by protecting spinal cord neurons from apoptosis, oxidative injury and mitochondrial structure damages," *Cellular Physiology and Biochemistry*, vol. 47, no. 1, pp. 176–190, 2018.

[19] E. Piermarini, D. Cartelli, A. Pastore et al., "Frataxin silencing alters microtubule stability in motor neurons: implications for Friedreich's ataxia," *Human Molecular Genetics*, vol. 25, no. 19, pp. 4288–4301, 2016.

[20] J. M. Lee and J. A. Johnson, "An important role of Nrf2-ARE pathway in the cellular defense mechanism," *Journal of Biochemistry and Molecular Biology*, vol. 37, no. 2, pp. 139–143, 2004.

[21] F. Mohagheghi, L. Khalaj, A. Ahmadiani, and B. Rahmani, "Gemfibrozil pretreatment affecting antioxidant defense system and inflammatory, but not Nrf-2 signaling pathways resulted in female neuroprotection and male neurotoxicity in the rat models of global cerebral ischemia-reperfusion," *Neurotoxicity Research*, vol. 23, no. 3, pp. 225–237, 2013.

[22] J. Chen, Z. Wang, Z. Zheng et al., "Neuron and microglia/macrophage-derived FGF10 activate neuronal FGFR2/PI3K/Akt signaling and inhibit microglia/macrophages TLR4/NF-κB-dependent neuroinflammation to improve functional recovery after spinal cord injury," *Cell Death & Disease*, vol. 8, no. 10, p. e3090, 2017.

[23] Z. Zhou, C. Liu, S. Chen et al., "Activation of the Nrf2/ARE signaling pathway by probucol contributes to inhibiting inflammation and neuronal apoptosis after spinal cord injury," *Oncotarget*, vol. 8, no. 32, pp. 52078–52093, 2017.

[24] A. Martin-Montalvo, E. M. Mercken, S. J. Mitchell et al., "Metformin improves healthspan and lifespan in mice," *Nature Communications*, vol. 4, no. 1, 2013.

[25] J. W. Calvert, S. Gundewar, S. Jha et al., "Acute metformin therapy confers cardioprotection against myocardial infarction via AMPK-eNOS-mediated signaling," *Diabetes*, vol. 57, no. 3, pp. 696–705, 2008.

[26] Y. Liu, G. Tang, Y. Li et al., "Metformin attenuates blood-brain barrier disruption in mice following middle cerebral artery occlusion," *Journal of Neuroinflammation*, vol. 11, no. 1, p. 177, 2014.

[27] S. P. Patil, P. D. Jain, P. J. Ghumatkar, R. Tambe, and S. Sathaye, "Neuroprotective effect of metformin in MPTP-induced Parkinson's disease in mice," *Neuroscience*, vol. 277, pp. 747–754, 2014.

[28] R. P. Vázquez-Manrique, F. Farina, K. Cambon et al., "AMPK activation protects from neuronal dysfunction and vulnerability across nematode, cellular and mouse models of Huntington's disease," *Human Molecular Genetics*, vol. 25, no. 6, pp. 1043–1058, 2016.

[29] F. Takata, S. Dohgu, J. Matsumoto et al., "Metformin induces up-regulation of blood-brain barrier functions by activating AMP-activated protein kinase in rat brain microvascular endothelial cells," *Biochemical and Biophysical Research Communications*, vol. 433, no. 4, pp. 586–590, 2013.

[30] A. I. Morales, D. Detaille, M. Prieto et al., "Metformin prevents experimental gentamicin-induced nephropathy by a mitochondria-dependent pathway," *Kidney International*, vol. 77, no. 10, pp. 861–869, 2010.

[31] C. Wang, C. Liu, K. Gao et al., "Metformin preconditioning provide neuroprotection through enhancement of autophagy and suppression of inflammation and apoptosis after spinal cord injury," *Biochemical and Biophysical Research Communications*, vol. 477, no. 4, pp. 534–540, 2016.

[32] D. Zhang, J. Xuan, B. B. Zheng et al., "Metformin improves functional recovery after spinal cord injury via autophagy flux stimulation," *Molecular Neurobiology*, vol. 54, no. 5, pp. 3327–3341, 2017.

[33] M. Fang, H. Jiang, L. Ye et al., "Metformin treatment after the hypoxia-ischemia attenuates brain injury in newborn rats," *Oncotarget*, vol. 8, no. 43, pp. 75308–75325, 2017.

[34] J. C. Tang, R. An, Y. Q. Jiang, and J. Yang, "Effects and mechanisms of metformin on the proliferation of esophageal Cancer cells *in vitro* and *in vivo*," *Cancer Research and Treatment*, vol. 49, no. 3, pp. 778–789, 2017.

[35] G. S. Bhamra, D. J. Hausenloy, S. M. Davidson et al., "Metformin protects the ischemic heart by the Akt-mediated inhibition of mitochondrial permeability transition pore opening," *Basic Research in Cardiology*, vol. 103, no. 3, pp. 274–284, 2008.

[36] H. Y. Zhang, Z. G. Wang, F. Z. Wu et al., "Regulation of autophagy and ubiquitinated protein accumulation by bFGF promotes functional recovery and neural protection in a rat model of spinal cord injury," *Molecular Neurobiology*, vol. 48, no. 3, pp. 452–464, 2013.

[37] T. Sugawara, A. Lewén, Y. Gasche, F. Yu, and P. H. Chan, "Overexpression of SOD1 protects vulnerable motor neurons after spinal cord injury by attenuating mitochondrial cytochrome c release," *The FASEB Journal*, vol. 16, no. 14, pp. 1997–1999, 2002.

[38] T. Mitsuhara, M. Takeda, S. Yamaguchi et al., "Simulated microgravity facilitates cell migration and neuroprotection after bone marrow stromal cell transplantation in spinal cord injury," *Stem Cell Research & Therapy*, vol. 4, no. 2, p. 35, 2013.

[39] S. Westermann and K. Weber, "Post-translational modifications regulate microtubule function," *Nature Reviews Molecular Cell Biology*, vol. 4, no. 12, pp. 938–947, 2003.

[40] V. K. Godena, N. Brookes-Hocking, A. Moller et al., "Increasing microtubule acetylation rescues axonal transport and locomotor deficits caused by LRRK2 Roc-COR domain mutations," *Nature Communications*, vol. 5, no. 1, 2014.

[41] M. H. Soltani, R. Pichardo, Z. Song et al., "Microtubule-associated protein 2, a marker of neuronal differentiation, induces mitotic defects, inhibits growth of melanoma cells, and predicts metastatic potential of cutaneous melanoma," *The American Journal of Pathology*, vol. 166, no. 6, pp. 1841–1850, 2005.

[42] N. Abe, S. H. Borson, M. J. Gambello, F. Wang, and V. Cavalli, "Mammalian target of rapamycin (mTOR) activation increases axonal growth capacity of injured peripheral nerves," *The Journal of Biological Chemistry*, vol. 285, no. 36, pp. 28034–28043, 2010.

[43] D. Colle, D. B. Santos, J. M. Hartwig et al., "Succinobucol, a lipid-lowering drug, protects against 3-nitropropionic acid-induced mitochondrial dysfunction and oxidative stress in SH-SY5Y cells via upregulation of glutathione levels and glutamate cysteine ligase activity," *Molecular Neurobiology*, vol. 53, no. 2, pp. 1280–1295, 2016.

[44] H. Witte, D. Neukirchen, and F. Bradke, "Microtubule stabilization specifies initial neuronal polarization," *The Journal of Cell Biology*, vol. 180, no. 3, pp. 619–632, 2008.

[45] A. Singh, S. Venkannagari, K. H. Oh et al., "Small molecule inhibitor of NRF2 selectively intervenes therapeutic resistance in KEAP1-deficient NSCLC tumors," *ACS Chemical Biology*, vol. 11, no. 11, pp. 3214–3225, 2016.

[46] X. Liu, Q. Zhu, M. Zhang et al., "Isoliquiritigenin ameliorates acute pancreatitis in mice via inhibition of oxidative stress and modulation of the Nrf2/HO-1 pathway," *Oxidative Medicine and Cellular Longevity*, vol. 2018, Article ID 7161592, 12 pages, 2018.

[47] W. Wang, X. Huang, J. Li et al., "Methane suppresses microglial activation related to oxidative, inflammatory, and apoptotic injury during spinal cord injury in rats," *Oxidative Medicine and Cellular Longevity*, vol. 2017, Article ID 2190897, 11 pages, 2017.

[48] IDF Clinical Guidelines Task Force, "Global guideline for type 2 diabetes: recommendations for standard, comprehensive, and minimal care," *Diabetic Medicine*, vol. 23, no. 6, pp. 579–593, 2006.

[49] D. Zhang, Q. Tang, G. Zheng et al., "Metformin ameliorates BSCB disruption by inhibiting neutrophil infiltration and MMP-9 expression but not direct TJ proteins expression regulation," *Journal of Cellular and Molecular Medicine*, vol. 21, no. 12, pp. 3322–3336, 2017.

[50] A. Kaplan, S. Ong Tone, and A. E. Fournier, "Extrinsic and intrinsic regulation of axon regeneration at a crossroads," *Frontiers in Molecular Neuroscience*, vol. 8, 2015.

[51] A. Beckers, A. van Dyck, I. Bollaerts et al., "An antagonistic axon-dendrite interplay enables efficient neuronal repair in the adult zebrafish central nervous system," *Molecular Neurobiology*, vol. 56, no. 5, pp. 3175–3192, 2019.

[52] Z. Ou, X. Kong, X. Sun et al., "Metformin treatment prevents amyloid plaque deposition and memory impairment in APP/PS1 mice," *Brain, Behavior, and Immunity*, vol. 69, pp. 351–363, 2018.

[53] J. Ma, J. Liu, H. Yu, Y. Chen, Q. Wang, and L. Xiang, "Beneficial effect of metformin on nerve regeneration and functional recovery after sciatic nerve crush injury in diabetic rats," *Neurochemical Research*, vol. 41, no. 5, pp. 1130–1137, 2016.

[54] M. He, Y. Ding, C. Chu, J. Tang, Q. Xiao, and Z. G. Luo, "Autophagy induction stabilizes microtubules and promotes axon regeneration after spinal cord injury," *Proceedings of the National Academy of Sciences of the United States of America*, vol. 113, no. 40, pp. 11324–11329, 2016.

[55] G. Kong, Z. Huang, W. Ji et al., "The ketone metabolite β-hydroxybutyrate attenuates oxidative stress in spinal cord injury by suppression of class I histone deacetylases," *Journal of Neurotrauma*, vol. 34, no. 18, pp. 2645–2655, 2017.

[56] S. Mrakic-Sposta, A. Vezzoli, L. Maderna et al., "R(+)-Thioctic acid effects on oxidative stress and peripheral neuropathy in type II diabetic patients: preliminary results by electron paramagnetic resonance and electroneurography," *Oxidative Medicine and Cellular Longevity*, vol. 2018, Article ID 1767265, 15 pages, 2018.

[57] K. Dasuri, L. Zhang, and J. N. Keller, "Oxidative stress, neurodegeneration, and the balance of protein degradation and protein synthesis," *Free Radical Biology & Medicine*, vol. 62, pp. 170–185, 2013.

[58] J. A. Romashkova and S. S. Makarov, "NF-κB is a target of AKT in anti-apoptotic PDGF signalling," *Nature*, vol. 401, no. 6748, pp. 86–90, 1999.

[59] Y. Lu, R. Li, J. Zhu et al., "Fibroblast growth factor 21 facilitates peripheral nerve regeneration through suppressing oxidative damage and autophagic cell death," *Journal of Cellular and Molecular Medicine*, vol. 23, no. 1, pp. 497–511, 2019.

[60] J. Guo, H. Wang, L. Li, Y. Yuan, X. Shi, and S. Hou, "Treatment with IL-19 improves locomotor functional recovery after contusion trauma to the spinal cord," *British Journal of Pharmacology*, vol. 175, no. 13, pp. 2611–2621, 2018.

[61] W. Q. Ma, X. J. Sun, Y. Wang, Y. Zhu, X. Q. Han, and N. F. Liu, "Restoring mitochondrial biogenesis with metformin attenuates β-GP-induced phenotypic transformation of VSMCs into an osteogenic phenotype via inhibition of PDK4/oxidative stress-mediated apoptosis," *Molecular and Cellular Endocrinology*, vol. 479, pp. 39–53, 2019.

[62] A. Giudice, C. Arra, and M. C. Turco, "Review of molecular mechanisms involved in the activation of the Nrf2-ARE signaling pathway by chemopreventive agents," *Methods in Molecular Biology*, vol. 647, pp. 37–74, 2010.

[63] I. Buendia, P. Michalska, E. Navarro, I. Gameiro, J. Egea, and R. León, "Nrf2-ARE pathway: an emerging target against oxidative stress and neuroinflammation in neurodegenerative diseases," *Pharmacology & Therapeutics*, vol. 157, pp. 84–104, 2016.

[64] I. N. Singh, P. G. Sullivan, Y. Deng, L. H. Mbye, and E. D. Hall, "Time course of post-traumatic mitochondrial oxidative damage and dysfunction in a mouse model of focal traumatic brain injury: implications for neuroprotective therapy," *Journal of Cerebral Blood Flow and Metabolism*, vol. 26, no. 11, pp. 1407–1418, 2006.

[65] S. M. Han, H. S. Baig, and M. Hammarlund, "Mitochondria localize to injured axons to support regeneration," *Neuron*, vol. 92, no. 6, pp. 1308–1323, 2016.

[66] H. Pintana, N. Apaijai, W. Pratchayasakul, N. Chattipakorn, and S. C. Chattipakorn, "Effects of metformin on learning and memory behaviors and brain mitochondrial functions in high fat diet induced insulin resistant rats," *Life Sciences*, vol. 91, no. 11-12, pp. 409–414, 2012.

[67] B. Zhang, Y. Chen, Q. Shen et al., "Myricitrin attenuates high glucose-induced apoptosis through activating Akt-Nrf2 signaling in H9c2 cardiomyocytes," *Molecules*, vol. 21, no. 7, p. 880, 2016.

[68] D. S. Lee and G. S. Jeong, "Butein provides neuroprotective and anti-neuroinflammatory effects through Nrf2/ARE-dependent haem oxygenase 1 expression by activating the PI3K/Akt pathway," *British Journal of Pharmacology*, vol. 173, no. 19, pp. 2894–2909, 2016.

[69] H. Liu, C. Yu, T. Xu, X. Zhang, and M. Dong, "Synergistic protective effect of paeoniflorin and β-ecdysterone against rotenone-induced neurotoxicity in PC12 cells," *Apoptosis*, vol. 21, no. 12, pp. 1354–1365, 2016.

[70] Y. Zhang, J. Zhang, C. Wu et al., "Higenamine protects neuronal cells from oxygen-glucose deprivation/reoxygenation-induced injury," *Journal of Cellular Biochemistry*, vol. 120, no. 3, pp. 3757–3764, 2018.

[71] K. L. Zhou, Y. F. Zhou, K. Wu et al., "Stimulation of autophagy promotes functional recovery in diabetic rats with spinal cord injury," *Scientific Reports*, vol. 5, no. 1, 2015.

Hindawi
Oxidative Medicine and Cellular Longevity
Volume 2019, Article ID 8409329, 14 pages
https://doi.org/10.1155/2019/8409329

Review Article

Mitochondrial Dysfunction and Alpha-Lipoic Acid: Beneficial or Harmful in Alzheimer's Disease?

Sávio Monteiro dos Santos[1], **Camila Fernanda Rodrigues Romeiro**[1], **Caroline Azulay Rodrigues**[1], **Alícia Renata Lima Cerqueira**[2], **and Marta Chagas Monteiro**[1,3]

[1]*Pharmaceutical Sciences Graduate Program, Institute of Health Sciences, Federal University of Pará, Belém, Pará, Brazil*
[2]*Faculty of Pharmacy, Institute of Health Sciences, Federal University of Pará, Belém, Pará, Brazil*
[3]*Neuroscience and Cell Biology Graduate Program, Institute of Biological Sciences, Federal University of Pará, Belém, Pará, Brazil*

Correspondence should be addressed to Marta Chagas Monteiro; martachagas2@yahoo.com.br

Received 26 June 2019; Accepted 30 September 2019; Published 30 November 2019

Guest Editor: João C. M. Barreira

Alzheimer's disease (AD) is a neurodegenerative disorder characterised by impairments in the cognitive domains associated with orientation, recording, and memory. This pathology results from an abnormal deposition of the β-amyloid (Aβ) peptide and the intracellular accumulation of neurofibrillary tangles. Mitochondrial dysfunctions play an important role in the pathogenesis of AD, due to disturbances in the bioenergetic properties of cells. To date, the usual therapeutic drugs are limited because of the diversity of cellular routes in AD and the toxic potential of these agents. In this context, alpha-lipoic acid (α-LA) is a well-known fatty acid used as a supplement in several health conditions and diseases, such as periphery neuropathies and neurodegenerative disorders. It is produced in several cell types, eukaryotes, and prokaryotes, showing antioxidant and anti-inflammatory properties. α-LA acts as an enzymatic cofactor able to regulate metabolism, energy production, and mitochondrial biogenesis. In addition, the antioxidant capacity of α-LA is associated with two thiol groups that can be oxidised or reduced, prevent excess free radical formation, and act on improvement of mitochondrial performance. Moreover, α-LA has mechanisms of epigenetic regulation in genes related to the expression of various inflammatory mediators, such PGE2, COX-2, iNOS, TNF-α, IL-1β, and IL-6. Regarding the pharmacokinetic profile, α-LA has rapid uptake and low bioavailability and the metabolism is primarily hepatic. However, α-LA has low risk in prolonged use, although its therapeutic potential, interactions with other substances, and adverse reactions have not been well established in clinical trials with populations at higher risk for diseases of aging. Thus, this review aimed to describe the pharmacokinetic profile, bioavailability, therapeutic efficacy, safety, and effects of combined use with centrally acting drugs, as well as report in vitro and in vivo studies that demonstrate the mitochondrial mechanisms of α-LA involved in AD protection.

1. Introduction

Alzheimer's disease (AD) is a chronic and progressive neurodegenerative disorder, impairing brain functions such as memory, thinking, and personality [1, 2]. AD is characterised by several neuropathological changes, which include cerebral atrophy, intense synaptic loss, and neuronal death, in regions of the prefrontal cortex and hippocampus that are responsible for cognitive functions [3, 4]. The mechanism that explains the pathogenesis of AD has yet to be fully elucidated [5, 6], but several hypotheses have been explored to explain this origin—hyperphosphorylation of the tau protein and β-amyloid peptide deposits (Aβ) are among those accepted in the scientific milieu [6, 7]. The accumulation of Aβ activates cells of the immune system, such as astrocytes, activated microglia, and macrophages. In turn, the activated cells promote the loss of regulation of the inflammatory response, inflammation, and oxidative stress state, as well as increase the production of Aβ, creating a vicious cycle that continues during the life of the person with AD [8, 9].

Oxidative stress in AD can be validated by changes in the brain, blood cells, and biological fluids, associated with increased malondialdehyde (MDA), lipid hydroperoxides and isoprostanes, thiobarbituric acid reactive substances (TBARS), nitric oxide synthase, and reactive oxygen species (ROS) in AD patient samples, suggesting a systemic imbalance of redox status [10–12]. Oxidative damage to brain tissue can be explained by the fact that this tissue is more susceptible to oxidative stress due to high oxygen consumption and low regenerative capacity, high polyunsaturated fat content, and low antioxidant concentration [13, 14]. In this sense, several studies show that high levels of biomarkers of oxidative damage, such as MDA, 4-hydroxynonenal (HNE), and F2-isoprostanes detected not only in brain tissues but also in fluids and peripheral tissues, are associated with worse AD prognosis [13, 15, 16]. Then, the evaluation of these oxidative stress and tissue damage markers could serve as an indicator of progression and severity of this pathology [10, 17–19].

Biomarkers of oxidative stress and antioxidants could help in the prediction of clinical outcomes and possible benefits in therapy. However, available data do not show sufficient evidence for the use of biomarkers so far described as predictors of severity or clinical outcomes in AD [20]. On the other hand, the balance of antioxidant capacity reflects cognitive function [19], reaffirming the crucial role of antioxidant defence pathways against ROS-induced damage. The main source of ROS is mitochondria, and the dysfunction of this organelle in neurons may be one of the initiating processes of neurodegeneration [13]. Mitochondrial damage, such as mitochondrial disruption, can cause astrocytes to increase matrix production due to calcium or ROS release, consequently activating caspases and generating cell death [21]. Mitochondrial dysfunction may be key in the process of AD pathogenesis, as this organelle has a fundamental role in bioenergetic modulation in the cell. Conversely, current studies are still unable to confirm this hypothesis; knowing the mechanisms of AD may direct a treatment to delay or prevent this process.

Overall, recent reviews also report that other natural products, such as flavonoids, polyphenols, alkaloids, and glycosides, exhibit neuroprotective mechanisms, due to changes in the expression of transcription factors, in signalling pathways, as well as the activation of autophagy mechanisms, among others [17, 22–24]. In this context, alpha-lipoic acid (α-LA) is a naturally occurring molecule, with antioxidant and anti-inflammatory properties [25, 26], which plays several roles in the pathogenesis of neurodegenerative diseases, such as AD, and acts as a neuroprotective agent [27]. Alpha-lipoic acid has been largely used in some diseases that have oxidative stress as the main cause in pathological processes. The antioxidants properties of α-LA have shown benefits in peripheral neuropathies, as well as in nerve injuries and diabetic neuropathy [28, 29]. Moreover, α-LA increases the production of acetylcholine [30], inhibits the production of free radicals [31], and promotes the downregulation of inflammatory processes [32]. Studies have shown that patients with mild AD who were treated with α-LA showed a slower progression of cognitive impairment [27, 32, 33], though current drug therapy is only aimed at controlling the symptoms, modulating neurotransmitter levels, and is not effective in delaying the production of the disease [34]. Therefore, this review provides an overview of molecular mechanisms in mitochondrial function in the AD context, as well as pharmacokinetic and therapeutic safety parameters of α-LA.

2. Role of the Mitochondria on the Pathophysiology of AD

Studies have suggested for a while that mitochondria are involved in primary and secondary cascades of AD pathogenesis. In the primary cascade, changes in energy metabolism are believed to be the beginning for changes in the Aβ precursor protein (Aβpp) homeostasis, as some classical studies and current reviews reported that bioenergetic disturbances (such as glucose deprivation) would shift the processing of Aβpp to the amyloidogenic route [35]. Regarding the secondary cascade, there are hypotheses concerning the interference of Aβ in calcium homeostasis, because the protein reduces the cell's ability to lower cytoplasmic calcium levels, leading to synaptic mitochondrial impairment and a reduction in ATP production [36]. In addition, another well-elucidated pathway is related to the aggregation of the mitochondrial protein amyloid beta-binding alcohol dehydrogenase (ABAD) to Aβ. This complex is already understood as a potential pathogenic pathway, because in a pathophysiological context, this aggregation seems to have induced the production of ROS and led to neuronal death [37]. Thus, more recent studies have mentioned the inhibition of ABAD as a therapeutic target in AD to reduce the toxicity mediated by the ABAD-Aβ complex [38].

Mitochondrial damage in the neurons of individuals with AD has been known for 25 years [39], and a classic study proposed the mitochondrial cascade for the origin of AD, where a person's mitochondrial DNA (mtDNA) determines basal mitochondrial function and mitochondrial durability. This could be the cause of AD being more frequent in the elderly, an epigenetic mechanism with mutations in specific mtDNA fragments, due to aging [40]. A recent study attributed mitochondrial dysfunction and consequent accumulation of ROS to increased insulin resistance in neurons of the cortex and hippocampus, thus favouring the progression of oxidative lesions in DNA—namely, 8-oxoguanine (8-oxoG)—as an accumulation of this DNA lesion has been found in the brain of patients with AD [41]. The accumulation of 8-oxoG in mitochondrial DNA induces dysfunction and impairs neuritogenesis [42].

Post-mortem investigations of the brains of AD patients showed a reduced number of mitochondria, with a simultaneous increase of mtDNA and mitochondrial proteins in the cytosol [43]. These changes expressed in AD may be related to oxidative damage in mtDNA, a genetic material that is poorly protected by stabilizing proteins and is associated with mitochondrial dysfunction and aging. Accordingly, mitochondrial dysfunction caused by oxidative damage in mtDNA is associated with changes in the number of oxidative phosphorylation subunits and abnormalities in the

fission and fusion processes of mitochondria, as well as damage in carrier proteins. These mechanisms are suggested as initiators in the early AD process [44]. The main mechanism of oxidative damage repair in DNA is defined as the base excision repair (BER) pathway, which has decreased activity in brain tissue, both in the genetic material of the nucleus and in mitochondria. These evidences, based on the analysis of cortex and cerebellum samples from individuals with AD, point to the possibility of a relationship between low BER activity and a higher level of neuronal death induced by Aβ toxicity and neurofibrillary plaques. However, due to conflicting results in the literature, it is not clear whether reduced BER activity leads to the accumulation of mutations in mtDNA [45].

Another altered mitochondrial pathway in AD is related to the sirt3 protein, a member of the sirtuin family of proteins responsible for epigenetic regulation, chromatin integrity, regulation of metabolism, and longevity, as well as playing a role in aging [17]. Sirt3, the subtype present in neuronal mitochondria and in several other cell types, is localised in the internal membrane and mitochondrial matrix and nucleus, participates in regulation of ROS production, and modulates the phosphorylation of CREB and fatty acid metabolism [46]. Modifications in electron transport chain dynamics, as well as increased ROS production and an unbalance in mitochondrial fusion and fission processes, cause mitochondrial damage; these mechanisms are cyclically propagated with high levels of ROS causing damage to proteins and DNA, increased lipid peroxidation, and consequent tissue damage. The production of ROS is one of the mechanisms that leads to the accumulation of Aβ, which is one of the characteristics of AD [47]. In the pathology of AD, aggregates of both Aβ and tau protein affect mitochondrial function and contribute to increased ROS production. In contrast, a recent study concluded that mitochondrial alterations are not dependent on high levels of Aβ and tau in the early stages of the disease, although they contribute significantly to neurodegeneration caused by mitochondrial dysfunction in more advanced stages of AD [48].

Several mechanisms, pathways, and processes in AD have yet to be elucidated, while much has been evidenced in relation to neuronal damage caused by mitochondrial dysfunction. Processes, such as mitophagy and biogenesis of mitochondria, are impaired due to mitochondrial dysfunction [43]. In addition, dysfunctional mitochondria regulate inflammatory responses through the activation of inflammasomes, a multicomplex protein that comprises nucleotide-binding domain activation, leucine-rich-containing family, pyrin domain-containing-3 (NLRP3) and sites where pro-IL-1β and pro-IL-18 processing take place, generating the activation of IL-1β and caspase-1, which is a crucial mechanism in the pathology of AD [49]. From this knowledge, specific therapeutic targets for the improvement of mitochondrial dynamics in central nervous system (CNS) cells are under investigation, aiming to use these new agents as effective treatments for AD and other neurodegenerative diseases [50]. In this sense, molecules with antioxidant, anti-inflammatory, and neuroprotective potential, such as alpha-lipoic acid, with action characteristics on mitochondrial machinery, are promising strategies in the treatment of AD.

3. Pharmacokinetics and Effects of α-LA in AD

Alpha-lipoic acid (α-LA) has been widely used in pharmaceuticals and nutraceuticals, precisely because it has antioxidant and anti-inflammatory properties [51, 52]. The chemical activity of α-LA is mainly due to the dithiolane ring, whose sulphur atoms confer a high electron density to α-LA. These effects, along with the hydrophilic and lipophilic characteristics of the molecule [53], as well as its status as the most efficient agent among all antioxidants [54], support studies with supplementation models for metabolic diseases and neurodegenerative diseases, such as AD. α-LA is classified as an ideal neuroprotective antioxidant because of its ability to cross the blood-brain barrier and its uniform uptake profile throughout the central and peripheral nervous systems [33, 55]. Synthesised in the mitochondria of animal and vegetable cells, as well as in microorganisms, α-LA can also be obtained from the diet through the consumption of dark green leafy vegetables and meats [56].

Biosynthesis of α-LA occurs in small amounts in the mitochondria from octanoic acid [52, 57], a natural cellular process during the metabolism of fatty acids. In contrast, the industrial production of α-LA results from chemical synthesis, and this process requires toxic catalysts in addition to sulphur atoms [58]. Therefore, α-LA can be found as a dietary supplement, a racemic mixture composed of its R-α-LA and S-α-LA isomers, whose main doses are 50, 100, 200, 300, or 600 mg per day. [59]. Other studies show beneficial effects of α-LA at doses of 1200 and 2400 mg in humans and interestingly no side effects [60]. In addition, the isolated R-α-LA isomer is used at doses of 200 and 300 mg [61].

The R-α-LA isomer is unstable at temperatures above 49°C, while the racemic mixture remains stable at temperatures between 60 and 62°C. Pharmacokinetic studies conducted in healthy subjects found that the R-α-LA isomer has a higher level of absorption, while the isomer S-α-LA assists in this percentage, preventing the polymerisation of the R-α-LA form [62]. In this sense, the use of supplements with the racemic mixture is more viable with respect to the R-α-LA isomer [63].

For oral supplementation of α-LA, the compound is rapidly absorbed and eliminated by the renal route. Because of its amphiphilic character, α-LA is widely distributed throughout all body compartments, including the CNS [52]. α-LA presented a mean time to reach the maximum plasma concentration (t_{max}) of 15 minutes and a mean plasma half-life ($t_{1/2}$) of 14 minutes [63]. These pharmacokinetic values differ among from other studies, where t_{max} was reported to occur within 30 minutes after oral administration [63] (10 minutes in rats) and $t_{1/2}$ was approximately 30 minutes. The short half-life of α-LA is a result of extensive extraction and hepatic metabolism, which reduces the bioavailability of the ingested dose to 30%, on average [64]. Multiple factors influence the bioavailability of α-LA, including food intake, which interferes with the absorption of α-LA, either as the racemic mixture or the isolated isomers. Thus, α-LA consumption is recommended 30 minutes before or 2 hours after food intake [62]. The high variation in pharmacokinetic parameters of α-LA has been reported in several

studies [51, 52, 61–64] but has not been fully explained. Changes in physiological conditions, such as gastric absorption and hepatic perfusion, or drug-drug interaction and drug delivery system mechanisms, are some justifications for the variation but have yet to be fully elucidated [46].

Absorption of at least 93% of the administered dose of α-LA, demonstrated in a rat study, occurred in the gastrointestinal tract, including the stomach [65]. In the gut, α-LA is internalised by the cells through receptors called the Na^+/-multivitamin transporter (SMVT). In humans, the present human Na^+/multivitamin transporter (hSMVT) is responsible for the transport of biotin and pantothenic acid, iodine ions, and racemic α-LA. However, *in vitro* evidence suggests the existence of more than one cellular transport mechanism involving other fatty acid transporters, such as the monocarboxylic acid transporter (MCT) [57]. In fact, the α-LA intestinal absorption seems to be quite variable due to the existence of α-LA transport means still not completely explained. This complex system of absorption and distribution to the tissues suggests the existence of several factors involved, for example, substrate competition and transcriptional, translational, and posttranslational regulatory mechanisms [65].

After its internalisation into the cell, α-LA is catabolised through β-oxidation or enzymatic reduction to dihydrolipoic acid (DHLA), which together with α-LA forms two molecules with a high antioxidant capacity [56], generating a potential of reduction of -0.32 V [65]. The reduction of α-LA to DHLA occurs under the action of enzymes, such as mitochondrial dihydrolipoamide dehydrogenase, cytoplasmic or extracellular glutathione reductase, and cytoplasmic thioredoxin reductase [66]. β-Oxidation is the main metabolic pathway of α-LA, resulting from oxidation of the carbon side chain, generating several metabolites [67]. In addition, α-LA is alkylated by S-methyltransferases, and thus, only 0.2% of the administered dose is excreted unchanged in the urine [46]. In different species, 12 α-LA metabolites were identified [68], with at least five in the human species. 4,6-Bismethylthiohexanoic acid (BMHA) was identified as the major metabolite in urine samples from healthy volunteers after oral administration of α-LA, followed by lower concentrations of 6,8-bismethyl octanoic acid (BMOA) and 2,4-butyric acid (BMBA) [52]. To date, there are no studies demonstrating other routes of elimination of α-LA and its metabolites after supplementation.

In vitro studies, animal studies, and clinical trials have already demonstrated the pharmacokinetic and safety profiles of α-LA [61], interesting characteristics of the molecule, whether in its racemic form or the isomers. However, there are still few available data from studies in elderly individuals. Thus, this represents an inconvenient lack of accurate information in groups notably afflicted by diseases associated with aging, such as AD. Pharmacokinetic parameters of α-LA in individuals with AD are still scarce, considering the need for these types of studies related to the beneficial effects of α-LA in CNS pathologies. However, advances in the investigation of α-LA mechanisms linked to the processes associated with mitochondrial disorders and other cellular pathways associated with neurodegenerative disorders have been achieved in studies of all levels in recent years.

3.1. In Vitro Studies. Park and colleagues [69] reported the protective action of α-LA in glioma cells (C6) in a model of glutamate-induced cytotoxicity. In this work, cell cultures were incubated with α-LA—at a dose of 200 μM—in a pretreatment scheme, one hour before the induction of glutamate cytotoxicity. As a result, the authors observed the suppression of apoptotic events, such as alteration of nuclear morphology and activation of caspase-3, and attenuation of stress markers in the endoplasmic reticulum. Glutamate-induced cytotoxicity is one of the possible causes of mitochondrial dysfunction, as it increases intracellular levels of calcium and thus activates several pathways, including apoptosis. Glutamate raises oxidative stress by increasing ROS production and glutathione (GSH) depletion *per se*, leading to cellular damage. In this sense, α-LA was effectively able to suppress cytotoxic effects in astroglial cells.

Dinicola and colleagues [53] performed a study on human neuroblastoma SK-N-BE cells treated with α-LA at a concentration of 0.5 mM for 24 hours. This work demonstrated the epigenetic regulatory activity of α-LA on the expression of the IL-1B and IL-6 genes responsible for the coding of interleukins IL-1β and IL-6, respectively. The authors investigated DNA methylation as a possible mechanism for the regulation that α-LA exerts on the gene regions. In this sense, they found lower mRNA levels of both genes in the α-LA group compared to the untreated group. The detection and quantification of IL-1β and IL-6, performed by an Enzyme-Linked Immunosorbent Assay (ELISA), also revealed lower levels in the culture supernatant of α-LA-treated cells compared to the supernatant untreated cells. Additionally, in treated cells, DNA methylation levels were inversely correlated to the levels of mRNA encoded for IL-1β and IL-6. This same group conducted another study on the treatment of ovarian cells with α-LA and obtained similar results on the downregulation of IL-1β and IL-6. The data obtained in this study suggest that α-LA modulates these proinflammatory cytokines (directly or indirectly) related to several pathological processes, including neurodegeneration [70].

Baeeri et al. [71] used rat embryonic fibroblast cells to evaluate the antioxidant effects of α-LA on senescence and cell cycle, oxidative stress, and inflammatory stimuli. These cells were submitted to α-LA concentrations of 1 to 1000 μM for 24 hours, and subsequently, oxidative stress, cell viability, cellular senescence biomarkers, and inflammatory markers were evaluated. The authors described the EC50 of α-LA, defined in this study at 947 μM, even though the highest dose evaluated (1000 μM) did not cause a toxic effect. α-LA reduced the levels of oxidative stress parameters, such as lipid peroxidation, ROS, ferric reducing antioxidant power (FRAP), and total thiol molecules (TTS). Senescence markers were also reduced with α-LA treatment, with lower levels of β-galactosidase, as well as reduced levels of apoptosis and necrosis, which presented values of 36% and 15.7%, respectively. Additionally, α-LA had an effect on caspases-3 and -9, reducing the activity of these apoptosis-promoting molecules to basal levels. The inflammatory parameters TNF-α, IL-1β, IL-6, and NF-κB showed reduced levels in cells treated with α-LA, maintaining levels similar to those of control cells.

These results point out the benefits of α-LA on cellular senescence, in addition to oxidative stress and inflammatory processes. Thus, *in vivo* studies are required to verify the interaction of α-LA with endogenous enzymes and biochemical pathways of cellular senescence.

3.2. Animal Studies. Mahboob et al. [72] demonstrated α-LA activity on the cholinergic system in an animal model of aluminium-induced neurotoxicity, associating memory, and learning effects dependent on the hippocampus and the amygdala. The BALB/c mice from this study were divided into control, aluminium, and aluminium+α-LA groups. An α-LA dose of 25 mg/kg/day was administered intraperitoneally for 12 days. After this period, the authors verified the expression of muscarinic (M1–M5) and choline acetyltransferase (ChaT) receptors in these regions of the brain using RT-PCR, PCR, and tissue histopathology and complemented their investigation with an *in silico* docking model of α-LA in two types of these receptors (M1 and M2). The results of this study showed positive effects of α-LA on applied behavioural tests, as well as the reversal of neurodegeneration evidenced by histopathology. α-LA increased the expression of M2 muscarinic receptors in the hippocampus and M1 and M2 in the amygdala, in addition to ChaT expression in both regions. In the *in silico* assays, α-LA showed a high affinity for M1 and M2 receptors compared to acetylcholine, a muscarinic receptor agonist. In this evaluation, the R-α-LA and S-α-LA isomers were coupled to the M1 and M2 receptors, where the R-α-LA isomer showed a higher mean binding affinity for both receptors. Together, these results showed the effects of α-LA on memory and learning, improving these conditions in a neurodegeneration model. However, these data should be carefully analysed, since one of the characteristics of α-LA involves chelating metals. Therefore, such effects could be the result of a direct α-LA mechanism on the agent used to simulate the disease model, which does not represent a natural physiological mechanism or part of the pathological process evaluated in a real situation.

An animal study conducted by Zhang et al. [73] aimed to verify whether α-LA could improve the state of tauopathy by investigating if the inhibition of ferroptosis, a mechanism associated with pathology, could reverse cognitive impairment in the AD model. P301S transgenic mice received α-LA treatment at doses of 3 and 10 mg/kg/day intraperitoneally for 10 weeks. In this work, behavioural parameters, immunohistochemistry, fluorescence, and expression of factors essential for the metabolism of iron and cell pathways involved in tau protein dysfunction, as well as synaptic loss and apoptosis, inflammation, and oxidative stress, were evaluated. The authors reported positive effects of α-LA on several key points in the pathophysiology of tauopathy, one of the disorders associated with AD. In this sense, α-LA could protect neurons from toxicity caused by hyperphosphorylation of tau, acting through mechanisms such as inhibition of ferroptosis. In addition, α-LA decreased the high expression of calpain 1, cleaved caspase-3, and increased levels of neuronal nuclear protein (NeuN) and synaptophysin (SYP), inhibiting neuronal loss and synaptic dysfunction. These results suggest that α-LA acts on these apoptotic signalling pathways, leading to improved cognitive function and attenuation of neurodegeneration.

Tzvetanova and colleagues [74] tested the neuroprotective potential of α-LA in an animal model of scopolamine-induced dementia. Male Wistar rats were treated with an intraperitoneal 30 mg/kg/day dose of α-LA, intraperitoneally, for 11 days. After the end of the treatment, the authors evaluated the memory and learning of the animals, as well as parameters of oxidative stress in the collected brain tissue. The experimental model with scopolamine followed dementia-like results similar to AD in the groups treated with this drug, evidenced in the behavioural tests, with impairment in memory and learning. Thus, increased oxidative stress was observed throughout the brain tissue, including in areas responsible for memory and learning, such as the cortex, hippocampus, and striatum. In these tissues, lipid peroxidation levels increased, as did GSH, catalase (CAT), and superoxide dismutase (SOD) levels. Conversely, supplementation with α-LA reversed this oxidative profile, with GSH valuesin the cortex close to the values of the control group and reduced GPx in all tissues analysed. In the α-LA group, the levels of catalase were kept close to the values of the control group, different from the scopolamine group. In addition, the authors observed a slight reduction in SOD values in the animals treated with α-LA, compared to the scopolamine group. These findings reaffirm the α-LA profile on oxidative stress in a dementia model, suggesting benefits in this aspect for other diseases associated with neurodegenerative processes.

3.3. Human Studies. Spain and colleagues [75] showed the benefits of α-LA supplementation as a racemic mixture in multiple sclerosis in people aged 40 to 70 years. In this double-blind, randomised, placebo-controlled study, α-LA was used by 27 patients at a dose of 1200 mg/day given orally for two years. The comparison between the α-LA and placebo groups showed differences in the percentage change brain volume (PCBV) where 68% less cerebral volume loss was observed in α-LA patients. Despite the PCBV benefits, some patients had altered biochemical parameters (increased alkaline phosphatase), renal failure, and glomerulonephritis. These findings, although not clearly attributed to α-LA, suggest caution with this dose in future investigations.

Fiedler and colleagues [76] carried out a study comparing the pharmacokinetic parameters in a group of healthy individuals and a group of individuals with multiple sclerosis. A single 1200 mg dose of α-LA was administered to the subjects, and blood samples from individuals were collected at 1, 2, 3, 4, 24, and 48 hours after α-LA administration. In this study, the age of the subjects ranged from 50 to 58 years and the mean α-LA plasma concentrations (C_{max}) in the healthy and multiple sclerosis groups were 1985.74 and 1894.52 ng/mL, respectively. These authors confirmed that α-LA metabolism does not change, and they did not observe differences between the groups, indicating that the bioavailability of α-LA was maintained even in individuals affected by multiple sclerosis compared to healthy subjects.

Shinto et al. [77] conducted a randomised placebo-controlled clinical study in patients diagnosed with AD,

where they assessed the benefits of α-LA combined with omega-3 fatty acids. In this evaluation, the authors reported a delay in the progression of cognitive and functional decline in patients who received α-LA and omega-3 fatty acids. Thirty-four patients received 600 mg/day of α-LA, in addition to omega-3 fatty acids, for one year. Unfortunately, the experimental design of this study did not evaluate an α-LA-only group, as little was illuminated about the additive or isolated effects of the combined treatment. Therefore, the exclusive evaluation of α-LA supplementation in patients with AD, which could provide pharmacokinetic data or molecular mechanisms of the drug in relation to the physiology of individuals with neurodegenerative processes, has yet to be described in clinical trials.

In contrast, a 12-month open label study with nine individuals (eight men and one woman) diagnosed with AD, who received standard treatment with cholinesterase inhibitors, was performed in Germany by Hager et al. [59] Based on their results, the authors suggest that treatment with α-LA would be a successful neuroprotective option in AD, at least as an adjuvant to standard treatment with acetylcholinesterase inhibitors. This work was the first to highlight the benefits of α-LA in the treatment of AD, despite a small number of patients and a nonrandomised design. However, there are no data on pharmacokinetic parameters described in this study, demonstrating only positive α-LA results in neuropsychological parameters, such as mini-mental state examination (MMSE) and an AD assessment scale, cognitive subscale (ADAS-cog).

A large number of *in vitro* and *in vivo* studies, as well as some clinical studies, have been carried out in recent years with the aim of evaluating the effects of α-LA on neurodegenerative processes. Several cellular pathways have been mentioned and even tested for the involvement of antioxidants, such as α-LA. However, most of these studies are limited to the use of combinations of two or more antioxidants, such as the study by Shinto et al. [77], which evaluated the effects of two antioxidants (α-LA omega-3) on individuals with AD. Sharman et al. [78] evaluated the effects of curcumin associated with several other antioxidants, among them, α-LA, in an AD animal model. These studies contribute to the limited knowledge on the action of α-LA as an antioxidant and an anti-inflammatory agent, but they do not elucidate the mechanisms of action involved in these processes, since they do not verify isolated α-LA activity in these disease models. The actions of α-LA seem to go deeper than scavenging ROS, reestablishing the reduced form of other antioxidants, and chelating metals. Thus, studies are needed to apply α-LA in specific models of AD aimed at elucidating molecular mechanisms related to treatment and reversal of damage in neurodegenerative disorders.

4. Molecular Mechanisms of α-LA in Neurodegeneration

In recent years, the effects of α-LA on the pathogenesis and/or progression of neurodegenerative diseases, such as Parkinson's disease, multiple sclerosis, and AD, have been reported [51, 57]. In AD, the neurodegeneration process seems to start from mitochondrial dysfunction and consequent energy deficiency in neurons, in the early stages of the disease [79]. Additionally, α-LA reduces the migration of T lymphocytes and monocytes into the central nervous system [76], a mechanism that contributes to a microenvironment with fewer inflammatory factors. Thus, the effects of α-LA are described in several recently published studies, which present it as a molecule associated with the genomic regulation of antioxidant and anti-inflammatory pathways [62]. The mechanisms of α-LA on the cellular machinery include several activities attributed to its oxidised and reduced forms (dihydrolipoic acid (DHLA)), both being active as antioxidants and anti-inflammatory agents [57, 62]. In the reduced form, DHLA exerts its antioxidant effect by donating electrons to prooxidants or oxidised molecules [54]. In fact, α-LA's main antioxidant defence activity is its ability to reestablish the reduced forms of other endogenous antioxidants, such as vitamins C and E, in addition to elevating the intracellular levels of glutathione and ubiquinone [56, 62]. However, more and more α-LA studies show the complexity of the mechanisms of action attributed to this molecule, in addition to mechanisms already extensively described in the literature. Current findings on α-LA mechanisms show that it acts indirectly on the activation of signal transduction pathways [80] through interactions with second messengers, such as cyclic adenosine monophosphate (cAMP). The increase of cAMP caused by α-LA inhibits the release of proinflammatory cytokines, such as IL-2, IFN-γ, and TNF-α. Moreover, cAMP induces IL-10 production [76], an anti-inflammatory cytokine responsible for inhibiting the production of various inflammatory mediators induced by lipopolysaccharide (LPS). In addition, IL-10 is responsible for inhibiting the expression of cytokine receptors and histocompatibility complex II (MHC-II) receptors, chemokines, and microglial adhesion molecules [81].

The ability of α-LA to regulate certain genes, such as genes that encode nuclear factors (nuclear factor erythroid 2-related factor-2 (Nrf2) and NF-κB) [53], has been reported previously; thus, α-LA is considered a pleiotropic molecule. The action of α-LA on NF-κB affected the expression of several inflammatory mediators, such as PGE2, COX-2, iNOS, TNF-α, IL-1β, and IL-6 [82]. NF-κB activation involves phosphorylation and ubiquitination under conditions of stress and inflammatory response. One of the mechanisms of regulating NF-κB involves its repression, which is carried out by SIRT1 via deacetylation. In this sense, the action of α-LA on SIRT1 may be one of the means of regulation in posttransduction control pathways [71]. Alternatively, the molecular mechanisms of gene regulation appear to result from hypermethylation of DNA in the region of gene promoters, as in the case of the 5′ flanking regions of IL-1β and IL-6. Thus, mRNA is downregulated, and consequently, synthesised protein levels decrease [70]. However, detailed α-LA mechanisms on direct or indirect pathways of epigenetic regulation have not been elucidated yet. Thus, a better understanding this action of α-LA could leverage research for more effective therapies in AD. Epigenetic mechanisms, such as DNA methylation dysfunction, histone acetylation, and

regulation of miRNAs, play a crucial role in the pathology of AD [83]. In this sense, epigenetic interventions could also be useful in preventing the disease, because in this case, factors in the microenvironment of the brain would be corrected through epigenomic modification [84].

The effects of α-LA on mitochondrial performance have already been described in previous studies to occur through several protective mechanisms. α-LA can act directly to prevent ROS production using the thiol group for redox regulation [85] and to stimulate enzymatic synthesis, such as frataxin which plays a role in the biosynthesis and assembly of the haem group in mitochondrial matrix proteins [86]. Indirectly, α-LA acts by improving the antioxidant system and stimulating mitochondrial biogenesis. Moreover, R-α-lipoic acid acts as a cofactor of mitochondrial enzymatic complexes and is therefore essential for energy production and metabolic regulation [87]. These protective routes make α-LA a substance classified in studies as a "mitochondrial nutraceutical."

Among the pathophysiological processes of AD, some mechanisms of α-LA action on tau protein hyperphosphorylation and amyloidogenesis inhibition are known and described in the current literature [73, 88]. Treatment with α-LA promotes the control of kinases such as CDK5, GSK3β, and MAPK that, together with changes in iron metabolism, lead to protein hyperphosphorylation and other effects such as free radical increase and macromolecule oxidation [73, 89]. In P301S transgenic mice with alteration to tauopathy, the α-LA reduced tau protein levels by modulating activity of calpain 1 and possibly other kinases. Furthermore, in this study, inhibition of neuronal loss and ferroptosis attributed to α-LA action was also observed. These data show possible pathways of beneficial action of α-LA in AD, such as improvements in iron loading, lipid peroxidation, and inflammation in the CNS [73]. In inhibiting amyloid tangles, α-LA demonstrated direct activity on Aβ protein aggregates, destabilizing as interactions between lipoyl groups and through covalent connections with Aβ lysine residues. The action of α-LA is associated with the reduction of Aβ deposits and the destabilizing aggregate preforming of this protein [88].

An animal model of tauopathy provided evidence that mitochondrial function is affected in this condition of tau protein dysregulation and consequent formation of fibrillar aggregates in the CNS. This state influences ATP production in mitochondria, causing imbalance of energy metabolism and ROS formation, thus making the neuron more susceptible to increased oxidative stress. [90]. In this sense, α-LA could act directly on the restoration of mitochondrial function, promoting increased synthesis of mitochondrial enzymes such as frataxin [86] or as an enzymatic cofactor, restoring mitochondrial energy metabolism [87]. Furthermore, just as tau may influence mitochondrial function, oxidative stress caused by mitochondrial dysfunction may influence abnormal tau protein function. This mechanism seems to be deeply associated with the pathogenesis of AD [90]. In addition to the effects on tauopathies, α-LA in its reduced form (DHLA) showed significant protection against neurotoxicity to amyloid β-peptide and iron and hydrogen peroxide in a study of neuronal cell culture [91]. This evidence points to the benefits of α-LA over these mechanisms in the pathogenesis of AD, acting as a potential therapeutic agent in multiple cell pathways.

4.1. In Vitro Studies. An important *in vitro* study evaluated the effects of the association between coenzyme Q-10 and α-LA on human lymphocytes. The parameters analysed were DNA damage using the comet assay, mitochondrial membrane potential using flow cytometric readings of a cyanine dye capable of penetrating the mitochondria, and an intracellular ROS assay using flow cytometric analysis of intracellular DCFH-DA oxidation. The fluorescence reading indicated that the mitochondrial membrane potential was enhanced by the decreased ratio between the green monomers of JC-1 and red fluorescence of the J-aggregates at baseline. Regarding ROS analysis, the combination of coenzyme Q-10+α-LA significantly enhanced the oxidant-mediated increase in intracellular ROS, contrarily suggesting a prooxidant activity of these supplements [92]. α-LA also plays an important role in the metabolic performance of mitochondrial activity, as α-LA acts as a cofactor of pyruvate dehydrogenase (PDH), α-ketoglutarate dehydrogenase (KGDH), and branched chain α-ketoglutarate dehydrogenase (BCKDH) mitochondrial complexes. In addition, α-LA is reduced to dihydrolipoic acid by PDH and KGDH. These direct activities have already been reviewed from previous *in vitro* studies, as can be seen in Figure 1 [87]. In addition to the direct actions, the α-LA has presented in several studies the potential to improve the activity and recovery in mitochondrial dysfunction through indirect mechanisms, such as modulation of signalling and transcription. A study evaluated the expression of NAD-dependent protein deacetylase sirtuin-1 (SIRT1), NAD-dependent protein deacetylase sirtuin-3 (SIRT3), and coactivator of the peroxisome proliferator-activated receptor 1α (PGC-1α) in liver and bovine muscle cultures treated with resveratrol and α-LA. Cell cultures were treated for 60 minutes with 40 or 80 μM of resveratrol and 30, 100, 300, or 1000 μM of α-LA. In one group, a basal medium was used to mimic restricted nutritional conditions, and glucagon and epinephrine were used in the others to mimic the glycogenic state. Real-time PCR was performed to quantify the expression of mRNA for sirtuins and PGC-1α. α-LA, at the doses used, did not affect the expression of sirt1, whereas Forkhead box protein O3 (FoxO3) and isocitrate dehydrogenase mitochondrial (IDH2) in bovine liver cells were downregulated. The effects of α-LA on the expression of NAD-dependent protein deacetylase sirtuin-3 (SIRT3), Forkhead box protein O1 (FOXO1), 5′-AMP-activated protein kinase catalytic subunit alpha-1 (PRKAA1), glucose-6-phosphatase catalytic subunit (G6PC), and PGC-1α genes were dose-dependent. On the other hand, α-LA showed a positive effect on the expression of SIRT1 and SIRT3 in bovine muscle cells. Protein expression encoded by SIRT1 showed higher levels after α-LA treatment, especially in liver cells. The results allowed for the conclusion that the conditions induced in both cell types and the treatment with resveratrol and α-LA led to the positive expression of genes involved in the antioxidant response [93].

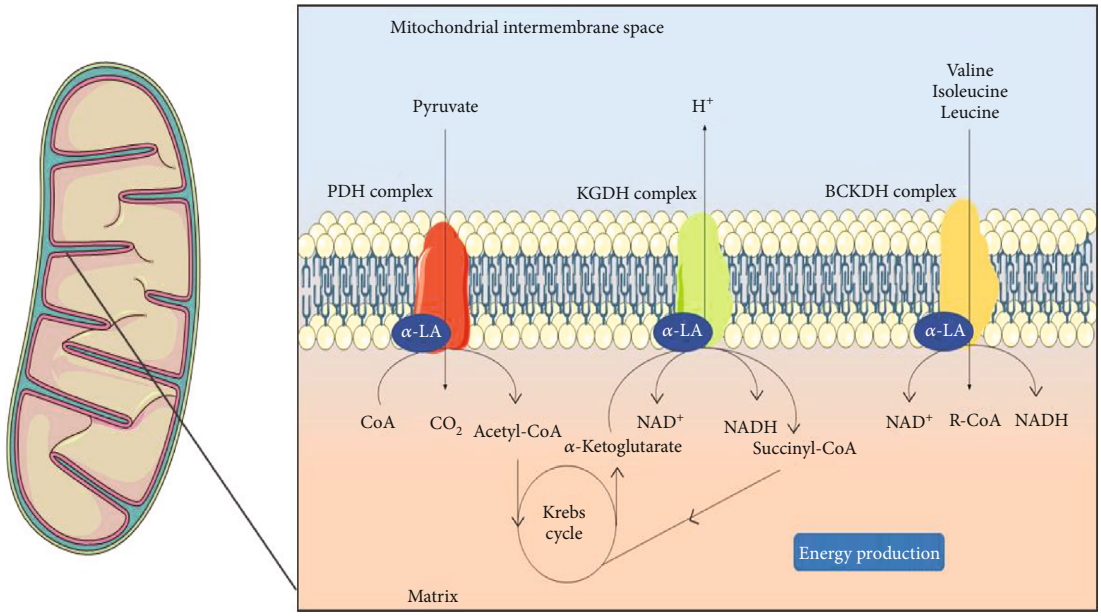

Figure 1: Physiologically, α-LA acts as a cofactor for enzymatic complexes during the oxidative phosphorylation process, such as pyruvate dehydrogenase (PDH), where α-LA residues are found in the dihydrofolipoamide acetyltransferase (E2) chain. Similarly activities occur with α-ketoglutarate dehydrogenase (KGDH) and branched chain α-ketoglutarate dehydrogenase (BCKDH) mitochondrial complexes. Thus, α-LA plays an important role in normal metabolic performance. This figure used elements from Servier Medical Art (https://www.servier.com).

4.2. Animal Studies. The expression of SIRT1 was investigated in a study in rats that evaluated the neuroprotective potential of α-LA in a focal ischemia model. The groups were divided into sham-operated, permanent mean cerebral artery occlusion (pMCAO), and the group treated with α-LA (50 mg/kg) intraperitoneally 30 minutes before surgery. The parameters evaluated were neurological deficits from a blinded examiner's test to analyse the impairment of motor motion injury, infarct volume, cerebral oedema, immunohistochemistry of cells labelled for SIRT1 and PGC-1α over five regions of the induced injury, western blot, and qPCR to analyse the mRNA levels of SIRT1 and PGC-1α at 24 h after pMCAO. In the results of neurological deficit assessment, after 24 hours of pMCAO, a significantly reduced score was observed in the group treated with α-LA. In addition, the water content measured to assess cerebral oedema was reduced in this group, compared with the pMCAO group. Infarct volume was also lower in the α-LA group. Immunohistochemistry indicated a significant increase in the expression of SIRT1 and PGC-1α on the ischemic cortex, which corroborated with the western blot results. These data demonstrate the ability of α-LA to attenuate the lesions induced by cerebral ischemia [33]. It has been known that overexpression of SIRT1 activates the transcriptional activity of PGC-1α that also activates several transcriptional factors and increases mitochondrial activity [1]. A most recent study also investigated the neuroprotective effects of α-LA on an ischemic model and assessed the role of mitochondria via activation of Nrf2. The rats were randomly divided into a sham group, control group (MCAO+saline), α-LA-20 mg/kg MCAO group, and α-LA-40 mg/kg+MCAO group. Initially, parameters of infarct behaviour and volume were evaluated. Again, it was observed that α-LA reduces cerebral oedema and improves the neurological outcome in the MCAO model. In addition, antioxidant enzymes (SOD and GSH-Px) and malondialdehyde (MDA) were analysed by ELISA after 24 h of MCAO, which showed that the enzymatic activities were recovered and MDA was reduced in the α-LA-treated groups in a dose-dependent manner. These results signified the ability of α-LA to reverse the suppression of ischemia-induced antioxidant activity. Nuclear translocation of Nrf2 was assessed by immunofluorescence in primary cortical neurons. The cells were pretreated with the control and α-LA (at concentrations of 1 μM, 10 μM, or 100 μM), and after 1 h, they were subjected to oxygen glucose deprivation (OGD) for 24 h. The results indicated that α-LA was able to modulate the activation and nuclear position of Nrf2 after the damage caused by MCAO. The ratio of nucleus/cytoplasmic Nrf2 was higher in the α-LA group 40 mg/kg, indicating that the activation of this factor also occurred in a dose-dependent manner [94]. The role of Nrf2 in mitochondrial function has been described in the context of neurodegeneration due to its role on the pathogenic processes in diseases [95]. NrF2 acts on redox homeostasis due to the regulation of target genes involved in the expression of antioxidant enzymes and on the expression of mitochondrial repair factors [96]. A recent study reported the activation of Nrf2 and subsequent binding to antioxidant response elements (ARE), in addition to decreased oxidative stress, β-amyloid (Aβ), and improved cognitive function in a mouse model of AD [97]. Therefore, this study suggests possible ways that α-LA could be inducing the overexpression of Nrf2 and promoting improved mitochondrial function in neurons. Mitochondria are also involved in the apoptosis

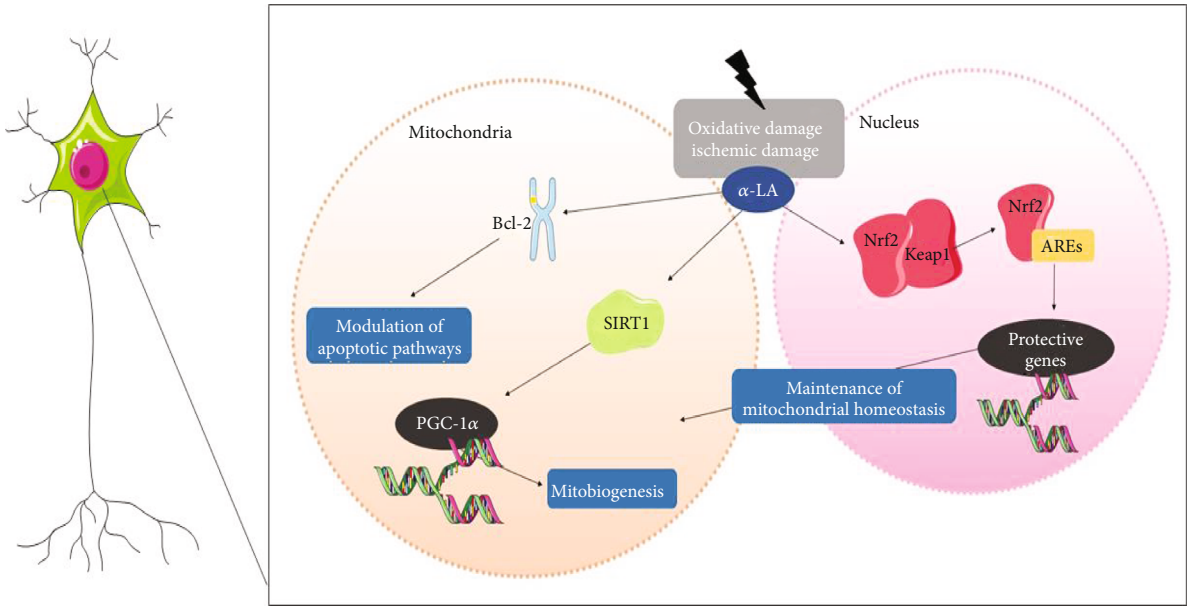

Figure 2: Cells treated with α-LA when subjected to oxidative or ischemic damage present higher expression of Blc-2 genes, modulating apoptotic pathways; sirt1 which induces peroxisome proliferator-activated receptor 1α (PGC-1α) and, therefore, mitochondrial biogenesis in the nucleus, positively regulates the nuclear factor erythroid 2-related factor-2 (Nrf2) pathway, improving the Nrf2 complex and antioxidant response elements (ARE), inducing the expression of genes that participate in mitochondrial homeostasis. This figure used elements from Servier Medical Art (https://www.servier.com).

process, especially in the context of neuronal damage. In this perspective, a study evaluated the influence of α-LA on the expression of the Bcl-2 apoptosis regulator (Bcl-2) in hippocampal subregions of rats submitted to inorganic arsenic. The animals were divided into three groups: the control group, the group that only received $NaAsO_2$ (1.5 and 2.0 mg/kg bw), and the group that received $NaAsO_2$ +α-LA (1.5 mg and 70 mg/kg bw) and $NaAsO_2$+α-LA (2.0 mg and 70 mg/kg bw). The TUNEL assay was performed to detect DNA fragmentation in cells; free floating immunohistochemistry, where apoptotic proteins were labelled, was used for cryocut coronal sections of the hippocampus; and western blot was used to determine the levels of apoptotic proteins in fresh hippocampal tissue. The results showed that the nuclei of the pyramidal and granular cells in the CA1 and CA2 regions (cornu ammonis), which received α-LA concomitantly, presented lower DNA fragmentation, compared to the control. Immunohistochemistry evidenced an intense expression of Bcl-2 in the hippocampus region of animals cotreated with α-LA and inorganic arsenic, similar to quantitative western blot results that enhanced the α-LA-inducing role in Bcl-2 expression, which was not dose-dependent [98]. Similarly, a most recent study investigated the protective role of α-LA against chlorpyrifos-induced toxicity, which rescued cells by modulating apoptotic pathways [99]. Another study investigated the protection of α-LA, through mitochondrial pathways, against cadmium-induced toxicity [100]. These studies conducted their investigation in the liver and kidney, respectively, thus lacking current mitochondrial investigations in neuronal rescue after toxicity. These processes are summarised in Figure 2.

5. Effects of α-LA When Combined with Central-Acting Agents

The effects of the association of α-LA with other substances acting on the CNS require a more in-depth description of the mechanisms observed in vitro, animal models, and human studies for a safe relation to be established, thus establishing the real clinical relevance of these findings.

5.1. Animal Studies. There is evidence that α-LA contributes to several treatments conducted with central-acting agents and in peripheral nerve cells. A study in mice evaluated the combination of α-LA and clozapine in the reversal of ketamine-induced symptoms similar to schizophrenia. Symptoms were induced for seven days, and from the eighth day, the ketamine group and the control group received α-LA (100 mg/kg), clozapine 2.5 or 5 mg/kg, or α-LA+clozapine 2.5 mg or 5 mg. The parameters evaluated regarding the symptoms were prepulse inhibition (PPI) of the startle locomotor activity, social preference, and Y-maze. In addition, oxidative stress parameters were evaluated in the prefrontal cortex (PFC), hippocampus, and striatum. In the PFC, brain-derived neurotrophic factor (BDNF) was determined. The results showed that the concentration of α-LA+clozapine 2.5 mg was able to revert the behavioural and oxidative stress parameters without causing harm. However, the concentration of α-LA+clozapine 5 mg induced motor impairment in the animals. Both concentrations significantly reversed the BDNF deficiency promoted by ketamine. Another relevant result was the reduction of ketamine-induced hyperlocomotion that was promoted by the association of α-LA and clozapine [101]. In another animal model

study, α-LA was combined with chlorpromazine to observe its effects on schizophrenia induced by ketamine. Rats were treated for 10 days with saline, α-LA 100 mg/kg or chlorpromazine (1 mg/kg, 5 mg/kg), or a combination of α-LA+chlorpromazine after ketamine treatment. The behavioural and oxidative stress parameters evaluated were the same as those of the study by Vasconcelos et al. [101]. The authors observed that the combination of α-LA+chlorpromazine elevated the locomotor activity of the animals to the levels of the control, possibly by reducing the inhibitory effect of ketamine on N-methyl-D-aspartate (NMDA) cortical receptors [102]. The improvement in the oxidative profile was described by an earlier study in humans that evaluated the effects of α-LA on the antioxidant defence of patients on drug therapy for schizophrenia. However, these drugs used by participants were not mentioned by the authors, and specific interactions between α-LA and these antipsychotic medications have not been described [103]. Desvenlafaxine is a serotonin-norepinephrine reuptake inhibitor (SNRI) used for the treatment of depression [104]. In a study conducted in a neuroendocrine model of depression in animals, female rats were treated with corticosterone, corticosterone+desvenlafaxine (10 or 20 mg/kg), α-LA (100 or 200 mg/kg), α-LA (100 mg/kg)+desvenlafaxine α-LA (200 mg/kg), desvenlafaxine (100 mg/kg), or α-LA (200 mg/kg)+desvenlafaxine (20 mg/kg). The cognitive evaluation was performed using the tail suspension test (TST), social interaction (SIT), new object recognition (NOR), and Y-maze. In addition, the activity of the enzyme acetylcholinesterase (AChE) was measured in the prefrontal cortex, hippocampus, and striatum. The results demonstrated that the associated schemes were able to reverse short-term and long-term memory deficits and control the increase of AChE in PFC, HC, and ST, effectively with the same or more than isolated substances, thus suggesting a neuroprotective effect of the combination between α-LA and desvenlafaxine, given that AChE is a marker for degenerative diseases [105].

5.2. Human Studies. Regarding drugs for the treatment of AD, a clinical trial was performed in which a clinical and neuropsychological evaluation was conducted to assess the effects of α-LA combined conventional treatments. Participants were separated into two groups: the first group (A) were patients with AD and with type 2 diabetes mellitus (T2-DM2) and the second group (B) were patients with AD without T2-DM2. Patients received 600 mg/day of α-LA, and all maintained their treatments with acetylcholinesterase inhibitors, donepezil (5 to 10 mg/day), rivastigmine (6 to 12 mg/day), and galantamine (8 to 16 mg/day), as well as an NMDA receptor antagonist, memantine (10 to 20 mg/day). The results of the study showed that 44% of the first group and 41% of the second reported adverse reactions after the association of α-LA and the conventional treatment, including muscle cramps and gastrointestinal and sleep disorders. The findings of the neuropsychological evaluation showed that the general levels of dementia improved in the group of patients who had AD and T2-DM2 compared to the group with only AD at any moment of evaluation, which was performed three times: at the beginning of treatment, after 8 months, and after 16 months of follow-up [30].

6. Conclusions

Mitochondrial damage in the neurons of individuals with AD has been known for 25 years [39], and currently, more and more evidence points to mitochondria as a strong therapeutic target in several diseases associated with aging, including AD [43]. Oxidative damage caused by increased ROS in neurons is a consequence of a number of mechanisms associated with senescence, and the role of mitochondria seems to be crucial in the cascade of AD pathology events. Interventions for mitochondrial dysfunction have the potential to reduce cognitive decline in AD as a consequence of reestablishing glucose and lipid metabolism, calcium homeostasis, and the regulation of cell death signalling pathways [50]. In this sense, antioxidants, such as α-LA, are potential candidates in the strategy of restoring mitochondrial function, with evident benefits on mitobiogenesis, besides acting as a cofactor of mitochondrial enzymatic complexes—an essential pathway for energy production and metabolic regulation [87]—and directly scavenging ROS. In addition, α-LA shows effects on inflammasomes, on the one hand by reducing pro-inflammatory mediators such as IL-2, IFN-γ, and TNF-α, and on the other hand by increasing anti-inflammatory cytokines, such as IL-10. Additionally, the effects of α-LA show high coverage of sites of action, being considered a regulator of the expression of some genes, for example, the genes that code for nuclear factors Nrf2 and NF-κB. Thus, α-LA is an agent with multiple actions on the cellular machinery, acting in several mechanisms that are involved in the pathology of AD. A large number of studies show the benefits of α-LA on symptoms of AD, but the amount of information about which pathways undergo direct or indirect interference of this antioxidant, now also considered neuroprotective, is still incipient. Clinical studies investigating α-LA in AD—limited to clinical parameters—focused primarily on brain areas associated with the symptoms of AD and did not investigate interactions, which occurred, at the molecular level. In contrast, studies that aimed to clarify the molecular mechanisms of interactions between α-LA and key molecules in the pathophysiology of AD have been conducted without having experimental groups treated with α-LA only, which is always associated with another antioxidant, to contrast with control groups. Another relevant aspect, but still considered very little in the current study of α-LA in AD, is the interaction between the drugs used in the treatment of AD and the supplementation of α-LA. Most studies that apply α-LA in parallel to treatment with standard drugs for AD do not present data on the possibility of pharmacokinetic or pharmacodynamic interactions, leaving a mechanism gap in the association response between these agents in the central nervous system. Even if the α-LA safety profile is well established, further studies should be conducted to precisely explain the effects, mainly in the brain. Additionally, isomers or a racemic mixture in AD models necessitate focus and investment in the development of improvements in molecular aspects of α-LA. These efforts could improve their pharmacokinetic

profile once its low bioavailability and short half-life characteristics are widely known problems about α-LA. However, α-LA presents a neuroprotective and anti-inflammatory molecule profile with the ability to revert cellular damage in the central nervous system; thus, it is considered an epigenetic modulator in mechanisms associated with oxidative stress and inflammation. Therefore, α-LA protects against the progression or even the establishment of the toxic tissue environment resulting from the pathogenesis of AD. These characteristics make α-LA a nutraceutical with great potential for the treatment of this disease, as well as an agent with potential benefits for mitochondrial dysfunction. The ability to act on the reestablishment of mitochondrial function could block the progression or even reverse the damage to the brain tissue that occurs in AD.

Conflicts of Interest

The authors declare that the research was conducted in the absence of any commercial or financial relationships that could be construed as a potential conflict of interest.

Authors' Contributions

All the authors wrote the paper, CFRR prepared the figures, and MCM revised the manuscript. All authors reviewed and approved the manuscript.

Acknowledgments

The authors were supported by the following Brazilian agencies: Conselho Nacional de Desenvolvimento Científico e Tecnológico (CNPq) and Federal University of Pará. This study was financed in part by the Coordenação de Aperfeiçoamento de Pessoal de Nível Superior-Brasil (CAPES) Finance Code 001 and the Federal University of Pará, and MCM is thankful for the fellowship from CNPq.

References

[1] W.-J. Huang, X. Zhang, and W.-W. Chen, "Role of oxidative stress in Alzheimer's disease," *Biomedical Reports*, vol. 4, no. 5, pp. 519–522, 2016.

[2] P. D. Ray, B.-W. Huang, and Y. Tsuji, "Reactive oxygen species (ROS) homeostasis and redox regulation in cellular signaling," *Cellular Signalling*, vol. 24, no. 5, pp. 981–990, 2012.

[3] T. Arendt, "Cell cycle activation and aneuploid neurons in Alzheimer's disease," *Molecular Neurobiology*, vol. 46, no. 1, pp. 125–135, 2012.

[4] A. Serrano-Pozo, M. P. Frosch, E. Masliah, and B. T. Hyman, "Neuropathological alterations in Alzheimer disease," *Cold Spring Harbor Perspectives in Medicine*, vol. 1, no. 1, article a006189, 2011.

[5] Y. Feng and X. Wang, "Antioxidant therapies for Alzheimer's disease," *Oxidative Medicine and Cellular Longevity*, vol. 2012, Article ID 472932, 17 pages, 2012.

[6] K. B. Magalingam, A. Radhakrishnan, N. S. Ping, and N. Haleagrahara, "Current concepts of neurodegenerative mechanisms in Alzheimer's disease," *BioMed Research International*, vol. 2018, Article ID 3740461, 12 pages, 2018.

[7] J. Hardy and D. J. Selkoe, "The amyloid hypothesis of Alzheimer's disease: progress and problems on the road to therapeutics," *Science*, vol. 297, no. 5580, pp. 353–356, 2002.

[8] G. K. Gouras, T. T. Olsson, and O. Hansson, "β-Amyloid peptides and amyloid plaques in Alzheimer's disease," *Neurotherapeutics*, vol. 12, no. 1, pp. 3–11, 2015.

[9] A. B. Reiss, H. A. Arain, M. M. Stecker, N. M. Siegart, and L. J. Kasselman, "Amyloid toxicity in Alzheimer's disease," *Reviews in the Neurosciences*, vol. 29, no. 6, pp. 613–627, 2018.

[10] M. Luca, A. Luca, and C. Calandra, "The role of oxidative damage in the pathogenesis and progression of Alzheimer's disease and vascular dementia," *Oxidative Medicine and Cellular Longevity*, vol. 2015, Article ID 504678, 8 pages, 2015.

[11] C. Venkateshappa, G. Harish, A. Mahadevan, M. M. Srinivas Bharath, and S. K. Shankar, "Elevated oxidative stress and decreased antioxidant function in the human hippocampus and frontal cortex with increasing age: implications for neurodegeneration in Alzheimer's disease," *Neurochemical Research*, vol. 37, no. 8, article 755, pp. 1601–1614, 2012.

[12] X. Zhu, B. Su, X. Wang, M. A. Smith, and G. Perry, "Causes of oxidative stress in Alzheimer disease," *Cellular and Molecular Life Sciences*, vol. 64, no. 17, pp. 2202–2210, 2007.

[13] M. Mancuso, F. Coppede, L. Migliore, G. Siciliano, and L. Murri, "Mitochondrial dysfunction, oxidative stress and neurodegeneration," *Journal of Alzheimer's Disease*, vol. 10, no. 1, pp. 59–73, 2006.

[14] C. Vida, I. Martinez de Toda, A. Garrido, E. Carro, J. A. Molina, and M. de la Fuente, "Impairment of several immune functions and redox state in blood cells of Alzheimer's disease patients. Relevant role of neutrophils in oxidative stress," *Frontiers in Immunology*, vol. 8, p. 1974, 2018.

[15] M. A. Lovell, W. D. Ehmann, M. P. Mattson, and W. R. Markesbery, "Elevated 4-hydroxynonenal in ventricular fluid in Alzheimer's disease," *Neurobiology of Aging*, vol. 18, no. 5, pp. 457–461, 1997.

[16] L. T. McGrath, B. McGleenon, S. Brennan, D. McColl, S. McILroy, and A. P. Passmore, "Increased oxidative stress in Alzheimer's disease as assessed with 4-hydroxynonenal but not malondialdehyde," *QJM*, vol. 94, no. 9, pp. 485–490, 2001.

[17] B. A. Q. Gomes, J. P. B. Silva, C. F. R. Romeiro et al., "Neuroprotective mechanisms of resveratrol in Alzheimer's disease: role of SIRT1," *Oxidative Medicine and Cellular Longevity*, vol. 2018, Article ID 8152373, 15 pages, 2018.

[18] A. Moslemnezhad, S. Mahjoub, and M. Moghadasi, "Altered plasma marker of oxidative DNA damage and Total antioxidant capacity in patients with Alzheimer's disease," *Caspian Journal of Internal Medicine*, vol. 7, no. 2, pp. 88–92, 2016.

[19] T. Persson, B. O. Popescu, and A. Cedazo-Minguez, "Oxidative stress in Alzheimer's disease: why did antioxidant therapy fail?," *Oxidative Medicine and Cellular Longevity*, vol. 2014, Article ID 427318, 11 pages, 2014.

[20] Y.-T. Chang, W. N. Chang, N. W. Tsai et al., "The roles of biomarkers of oxidative stress and antioxidant in Alzheimer's disease: a systematic review," *BioMed Research International*, vol. 2014, Article ID 182303, 14 pages, 2014.

[21] J. J. Palop and L. Mucke, "Network abnormalities and interneuron dysfunction in Alzheimer disease," *Nature Reviews Neuroscience*, vol. 17, no. 12, pp. 777–792, 2016.

[22] A. L. B. Oliveira, V. Monteiro, K. Navegantes-Lima et al., "Resveratrol role in autoimmune disease—a mini-review," *Nutrients*, vol. 9, no. 12, p. 1306, 2017.

[23] S. S. Panda and N. Jhanji, "Natural products as potential anti-Alzheimer agents," *Current Medicinal Chemistry*, vol. 26, 2019.

[24] X. Wu, H. Cai, L. Pan et al., "Small molecule natural products and Alzheimer's disease," *Current Topics in Medicinal Chemistry*, vol. 19, no. 3, pp. 187–204, 2019.

[25] E. Akbari, Z. Asemi, R. Daneshvar Kakhaki et al., "Effect of probiotic supplementation on cognitive function and metabolic status in Alzheimer's disease: a randomized, double-blind and controlled trial," *Frontiers in Aging Neuroscience*, vol. 8, p. 256, 2016.

[26] M. Shi, A. Kovac, A. Korff et al., "CNS tau efflux via exosomes is likely increased in Parkinson's disease but not in Alzheimer's disease," *Alzheimer's & Dementia*, vol. 12, no. 11, pp. 1125–1131, 2016.

[27] P. Molz and N. Schroder, "Potential therapeutic effects of lipoic acid on memory deficits related to aging and neurodegeneration," *Frontiers in Pharmacology*, vol. 8, p. 849, 2017.

[28] S. Mrakic-Sposta, A. Vezzoli, L. Maderna et al., "R(+)-thioctic acid effects on oxidative stress and peripheral neuropathy in type II diabetic patients: preliminary results by electron paramagnetic resonance and electroneurography," *Oxidative Medicine and Cellular Longevity*, vol. 2018, Article ID 1767265, 15 pages, 2018.

[29] D. Tomassoni, F. Amenta, L. di Cesare Mannelli et al., "Neuroprotective activity of thioctic acid in central nervous system lesions consequent to peripheral nerve injury," *BioMed Research International*, vol. 2013, Article ID 985093, 14 pages, 2013.

[30] A. Fava, D. Pirritano, M. Plastino et al., "The effect of lipoic acid therapy on cognitive functioning in patients with Alzheimer's disease," *Journal of Neurodegenerative Diseases*, vol. 2013, Article ID 454253, 7 pages, 2013.

[31] Q.-F. Zhao, L. Tan, H. F. Wang et al., "The prevalence of neuropsychiatric symptoms in Alzheimer's disease: systematic review and meta-analysis," *Journal of Affective Disorders*, vol. 190, pp. 264–271, 2016.

[32] M. Heneka and M. Obanion, "Inflammatory processes in Alzheimer's disease," *Journal of Neuroimmunology*, vol. 184, no. 1–2, article S016557280600470X, pp. 69–91, 2007.

[33] B. Fu, J. Zhang, X. Zhang et al., "Alpha-lipoic acid upregulates SIRT1-dependent PGC-1α expression and protects mouse brain against focal ischemia," *Neuroscience*, vol. 281, pp. 251–257, 2014.

[34] L. F. Hernandez-Zimbron and S. Rivas-Arancibia, "Deciphering an interplay of proteins associated with amyloid β 1-42 peptide and molecular mechanisms of Alzheimer's disease," *Reviews in the Neurosciences*, vol. 25, no. 6, pp. 773–783, 2014.

[35] H. M. Wilkins and R. H. Swerdlow, "Amyloid precursor protein processing and bioenergetics," *Brain Research Bulletin*, vol. 133, pp. 71–79, 2017.

[36] C. Overk and E. Masliah, "Perspective on the calcium dyshomeostasis hypothesis in the pathogenesis of selective neuronal degeneration in animal models of Alzheimer's disease," *Alzheimer's & Dementia*, vol. 13, no. 2, pp. 183–185, 2017.

[37] S. Du Yan and D. M. Stern, "Mitochondrial dysfunction and Alzheimer's disease: role of amyloid-β peptide alcohol dehydrogenase (ABAD)," *International Journal of Experimental Pathology*, vol. 86, no. 3, pp. 161–171, 2005.

[38] A. Morsy and P. C. Trippier, "Amyloid-binding alcohol dehydrogenase (ABAD) inhibitors for the treatment of Alzheimer's disease," *Journal of Medicinal Chemistry*, vol. 62, no. 9, pp. 4252–4264, 2019.

[39] P. Mecocci, U. MacGarvey, and M. F. Beal, "Oxidative damage to mitochondrial DNA is increased in Alzheimer's disease," *Annals of Neurology*, vol. 36, no. 5, pp. 747–751, 1994.

[40] R. H. Swerdlow and S. M. Khan, "A "mitochondrial cascade hypothesis" for sporadic Alzheimer's disease," *Medical Hypotheses*, vol. 63, no. 1, pp. 8–20, 2004.

[41] N. Abolhassani, J. Leon, Z. Sheng et al., "Molecular pathophysiology of impaired glucose metabolism, mitochondrial dysfunction, and oxidative DNA damage in Alzheimer's disease brain," *Mechanisms of Ageing and Development*, vol. 161, Part A, pp. 95–104, 2017.

[42] J. Leon, K. Sakumi, E. Castillo, Z. Sheng, S. Oka, and Y. Nakabeppu, "8-Oxoguanine accumulation in mitochondrial DNA causes mitochondrial dysfunction and impairs neuritogenesis in cultured adult mouse cortical neurons under oxidative conditions," *Scientific Reports*, vol. 6, no. 1, article BFsrep22086, 2016.

[43] I. G. Onyango, S. M. Khan, and J. P. Bennett Jr., "Mitochondria in the pathophysiology of Alzheimer's and Parkinson's diseases," *Frontiers in Bioscience*, vol. 22, no. 5, pp. 854–872, 2017.

[44] T. Džinić and N. A. Dencher, "Oxygen concentration and oxidative stress modulate the influence of Alzheimer's disease Aβ_{1-42} peptide on human cells," *Oxidative Medicine and Cellular Longevity*, vol. 2018, Article ID 7567959, 16 pages, 2018.

[45] D. T. Soltys, C. P. M. Pereira, F. T. Rowies et al., "Lower mitochondrial DNA content but not increased mutagenesis associates with decreased base excision repair activity in brains of AD subjects," *Neurobiology of Aging*, vol. 73, pp. 161–170, 2019.

[46] S.-j. Rhee, H. Lee, L. Y. Ahn, K. S. Lim, and K. S. Yu, "Lack of a clinically significant pharmacokinetic interaction between pregabalin and thioctic acid in healthy volunteers," *Clinical Therapeutics*, vol. 40, no. 10, pp. 1720–1728.e2, 2018.

[47] G. A. Panza, B. A. Taylor, H. V. MacDonald et al., "Can exercise improve cognitive symptoms of Alzheimer's disease?," *Journal of the American Geriatrics Society*, vol. 66, no. 3, pp. 487–495, 2018.

[48] J. H. Birnbaum, D. Wanner, A. F. Gietl et al., "Oxidative stress and altered mitochondrial protein expression in the absence of amyloid-β and tau pathology in iPSC-derived neurons from sporadic Alzheimer's disease patients," *Stem Cell Research*, vol. 27, pp. 121–130, 2018.

[49] T. Saco, P. T. Parthasarathy, Y. Cho, R. F. Lockey, and N. Kolliputi, "Inflammasome: a new trigger of Alzheimer's disease," *Frontiers in Aging Neuroscience*, vol. 6, p. 80, 2014.

[50] V. van Giau, S. S. A. An, and J. P. Hulme, "Mitochondrial therapeutic interventions in Alzheimer's disease," *Journal of the Neurological Sciences*, vol. 395, pp. 62–70, 2018.

[51] F. Bittner, C. Murchison, D. Koop, D. Bourdette, and R. Spain, "Lipoic acid pharmacokinetics at baseline and 1 year in secondary progressive MS," *Neurology - Neuroimmunology Neuroinflammation*, vol. 4, no. 5, article e380, 2017.

[52] N. Ikuta, K. Chikamoto, Y. Asano et al., "Time course effect of R-alpha-lipoic acid on cellular metabolomics in cultured

hepatoma cells," *Journal of Medicinal Food*, vol. 20, no. 3, pp. 211–222, 2017.

[53] S. Dinicola, S. Proietti, A. Cucina, M. Bizzarri, and A. Fuso, "Alpha-lipoic acid downregulates IL-1β and IL-6 by DNA hypermethylation in SK-N-BE neuroblastoma cells," *Antioxidants*, vol. 6, no. 4, p. 74, 2017.

[54] D. Tibullo, G. Li Volti, C. Giallongo et al., "Biochemical and clinical relevance of alpha lipoic acid: antioxidant and anti-inflammatory activity, molecular pathways and therapeutic potential," *Inflammation Research*, vol. 66, no. 11, article 1079, pp. 947–959, 2017.

[55] N. S. Galeshkalami, M. Abdollahi, R. Najafi et al., "Alpha-lipoic acid and coenzyme Q10 combination ameliorates experimental diabetic neuropathy by modulating oxidative stress and apoptosis," *Life Sciences*, vol. 216, no. 18, pp. 101–110, 2019.

[56] J. L. Roberts and R. Moreau, "Emerging role of alpha-lipoic acid in the prevention and treatment of bone loss," *Nutrition Reviews*, vol. 73, no. 2, pp. 116–125, 2015.

[57] B. Zehnpfennig, P. Wiriyasermkul, D. A. Carlson, and M. Quick, "Interaction of α-lipoic acid with the human Na^+/-multivitamin transporter (HSMVT)," *Journal of Biological Chemistry*, vol. 290, no. 26, pp. 16372–16382, 2015.

[58] D. Sun, G. Wei, and Q. Liu, "Clinical observation of epalrestat combined with lipoic acid in the treatment of diabetic peripheral neuropathy," *China Pharmacy*, vol. 28, no. 23, pp. 3226–3229, 2017.

[59] K. Hager, A. Marahrens, M. Kenklies, P. Riederer, and G. Münch, "Alpha-lipoic acid as a new treatment option for Azheimer type dementia," *Archives of Gerontology and Geriatrics*, vol. 32, no. 3, pp. 275–282, 2001.

[60] B. Dörsam, A. Göder, N. Seiwert, B. Kaina, and J. Fahrer, "Lipoic acid induces P53-independent cell death in colorectal cancer cells and potentiates the cytotoxicity of 5-fluorouracil," *Archives of Toxicology*, vol. 89, no. 10, pp. 1829–1846, 2015.

[61] J. Yoon, S. J. Moon, K.-O. Lee et al., "Comparison of R(+)-α-lipoic acid exposure after R(+)-α-lipoic acid 200 mg and 300 mg and thioctic acid 600 mg in healthy Korean male subjects," *Translational and Clinical Pharmacology*, vol. 24, no. 3, pp. 137–142, 2016.

[62] F. Seifar, M. Khalili, H. Khaledyan et al., "α-Lipoic acid, functional fatty acid, as a novel therapeutic alternative for central nervous system diseases: a review," *Nutritional Neuroscience*, vol. 22, no. 5, pp. 306–316, 2019.

[63] N. Ikuta, H. Okamoto, T. Furune et al., "Bioavailability of an R-α-lipoic acid/γ-cyclodextrin complex in healthy volunteers," *International Journal of Molecular Sciences*, vol. 17, no. 6, p. 949, 2016.

[64] R. Pignatello, T. M. G. Pecora, G. G. Cutuli et al., "Antioxidant activity and photostability assessment of trans-resveratrol acrylate microspheres," *Pharmaceutical Development and Technology*, vol. 24, no. 2, pp. 222–234, 2019.

[65] K. P. Shay, R. F. Moreau, E. J. Smith, A. R. Smith, and T. M. Hagen, "Alpha-lipoic acid as a dietary supplement: molecular mechanisms and therapeutic potential," *Biochimica et Biophysica Acta (BBA) - General Subjects*, vol. 1790, no. 10, pp. 1149–1160, 2009.

[66] D. Fratantonio, A. Speciale, M. S. Molonia et al., "Alpha-lipoic acid, but not di-hydrolipoic acid, activates Nrf2 response in primary human umbilical-vein endothelial cells and protects against TNF-α induced endothelium dysfunction," *Archives of Biochemistry and Biophysics*, vol. 655, pp. 18–25, 2018.

[67] J. Teichert, R. Hermann, P. Ruus, and R. Preiss, "Plasma kinetics, metabolism, and urinary excretion of alpha-lipoic acid following oral administration in healthy volunteers," *The Journal of Clinical Pharmacology*, vol. 43, no. 11, pp. 1257–1267, 2003.

[68] S. Reich-Schupke and M. Stucker, "Nomenclature of the veins of the lower limbs – current standards," *Journal der Deutschen Dermatologischen Gesellschaft*, vol. 9, no. 3, pp. 189–194, 2011.

[69] E. Park, J. Gim, D. K. Kim, C. S. Kim, and H. S. Chun, "Protective effects of alpha-lipoic acid on glutamate-induced cytotoxicity in C6 glioma cells," *Biological and Pharmaceutical Bulletin*, vol. 42, no. 1, pp. 94–102, 2019.

[70] S. Dinicola, M. Santiago-Reyes, R. Canipari, A. Cucina, M. Bizzarri, and A. Fuso, "Alpha-Lipoic acid represses IL-1B and IL-6 through DNA methylation in ovarian cells," *PharmaNutrition*, vol. 5, no. 3, pp. 77–83, 2017.

[71] M. Baeeri, H. Bahadar, M. Rahimifard et al., "α-Lipoic acid prevents senescence, cell cycle arrest, and inflammatory cues in fibroblasts by inhibiting oxidative stress," *Pharmacological Research*, vol. 141, pp. 214–223, 2019.

[72] A. Mahboob, S. M. Farhat, G. Iqbal et al., "Alpha-lipoic acid-mediated activation of muscarinic receptors improves hippocampus- and amygdala-dependent memory," *Brain Research Bulletin*, vol. 122, pp. 19–28, 2016.

[73] Y.-H. Zhang, D.-W. Wang, S.-F. Xu et al., "α-Lipoic acid improves abnormal behavior by mitigation of oxidative stress, inflammation, ferroptosis, and tauopathy in P301S tau transgenic mice," *Redox Biology*, vol. 14, pp. 535–548, 2018.

[74] E. R. Tzvetanova, A. P. Georgieva, A. V. Alexandrova et al., "Antioxidant mechanisms in neuroprotective action of lipoic acid on learning and memory of rats with experimental dementia," vol. 50, pp. 52–57, 2018.

[75] R. Spain, K. Powers, C. Murchison et al., "Lipoic acid in secondary progressive MS a randomized controlled pilot trial," *Neurology - Neuroimmunology Neuroinflammation*, vol. 4, no. 5, article e374, 2017.

[76] S. E. Fiedler, V. Yadav, A. R. Kerns et al., "Lipoic acid stimulates CAMP production in healthy control and secondary progressive MS subjects," *Molecular Neurobiology*, vol. 55, no. 7, pp. 6037–6049, 2018.

[77] L. Shinto, J. Quinn, T. Montine et al., "A randomized placebo-controlled pilot trial of omega-3 fatty acids and alpha lipoic acid in Alzheimer's disease," *Journal of Alzheimer's Disease*, vol. 38, no. 1, pp. 111–120, 2014.

[78] M. J. Sharman, E. Gyengesi, H. Liang et al., "Assessment of diets containing curcumin, epigallocatechin-3-gallate, docosahexaenoic acid and α-lipoic acid on amyloid load and inflammation in a male transgenic mouse model of Alzheimer's disease: are combinations more effective?," *Neurobiology of Disease*, vol. 124, pp. 505–519, 2019.

[79] S. Ramesh, M. Govindarajulu, E. Jones, V. Suppiramaniam, T. Moore, and M. Dhanasekaran, "Mitochondrial dysfunction and the role of mitophagy in Alzheimer's disease," *Alzheimer's Disease & Treatment, MedDocs Publishers LLC*, 2018.

[80] E. Bozhokina, S. Khaitlina, and I. Gamaley, "Dihydrolipoic but not alpha-lipoic acid affects susceptibility of eukaryotic

cells to bacterial invasion," *Biochemical and Biophysical Research Communications*, vol. 460, no. 3, pp. 697–702, 2015.

[81] J. Meng, J. Ni, Z. Wu et al., "The critical role of IL-10 in the antineuroinflammatory and antioxidative effects of *Rheum tanguticum* on activated microglia," *Oxidative Medicine and Cellular Longevity*, vol. 2018, Article ID 1083596, 12 pages, 2018.

[82] G. Li, J. Fu, Y. Zhao, K. Ji, T. Luan, and B. Zang, "Alpha-lipoic acid exerts anti-inflammatory effects on lipopolysaccharide-stimulated rat mesangial cells via inhibition of nuclear factor kappa B (NF-κB) signaling pathway," *Inflammation*, vol. 38, no. 2, pp. 510–519, 2015.

[83] X. Li, X. Bao, and R. Wang, "Neurogenesis-based epigenetic therapeutics for Alzheimer's disease (review)," *Molecular Medicine Reports*, vol. 14, no. 2, pp. 1043–1053, 2016.

[84] A. Fuso, "The involvement of the brain microenvironment in Alzheimer's disease," *Organisms Journal of Biological Sciences*, vol. 2, no. 1, pp. 105–112, 2018.

[85] T. Nietzel, J. Mostertz, F. Hochgräfe, and M. Schwarzländer, "Redox regulation of mitochondrial proteins and proteomes by cysteine thiol switches," *Mitochondrion*, vol. 33, pp. 72–83, 2017.

[86] S. Chiang, Z. Kovacevic, S. Sahni et al., "Frataxin and the molecular mechanism of mitochondrial iron-loading in Friedreich's ataxia," *Clinical Science*, vol. 130, no. 11, pp. 853–870, 2016.

[87] L. Packer and E. Cadenas, "Lipoic acid: energy metabolism and redox regulation of transcription and cell signaling," *Journal of Clinical Biochemistry and Nutrition*, vol. 48, no. 1, pp. 26–32, 2010.

[88] K. Ono, M. Hirohata, and M. Yamada, "α-Lipoic acid exhibits anti-amyloidogenicity for β-amyloid fibrils in vitro," *Biochemical and Biophysical Research Communications*, vol. 341, no. 4, pp. 1046–1052, 2006.

[89] S. Salinthone, V. Yadav, R. V. Schillace, D. N. Bourdette, and D. W. Carr, "Lipoic acid attenuates inflammation via cAMP and protein kinase A signaling," *PLoS One*, vol. 5, no. 9, article e13058, 2010.

[90] P. K. Kamat, A. Kalani, S. Rai et al., "Mechanism of oxidative stress and synapse dysfunction in the pathogenesis of Alzheimer's disease: understanding the therapeutics strategies," *Molecular Neurobiology*, vol. 53, no. 1, pp. 648–661, 2014.

[91] M. A. Lovell, C. Xie, S. Xiong, and W. R. Markesbery, "Protection against amyloid beta peptide and iron/hydrogen peroxide toxicity by alpha lipoic acid," *Journal of Alzheimer's Disease*, vol. 5, no. 3, pp. 229–239, 2003.

[92] S. Silvestri, P. Orlando, T. Armeni et al., "Coenzyme Q_{10} and α-lipoic acid: antioxidant and pro-oxidant effects in plasma and peripheral blood lymphocytes of supplemented subjects," *Journal of Clinical Biochemistry and Nutrition*, vol. 57, no. 1, pp. 21–26, 2015.

[93] Y. Ghinis-Hozumi, L. González-Dávalos, A. Antaramian et al., "Effect of resveratrol and lipoic acid on sirtuin-regulated expression of metabolic genes in bovine liver and muscle slice cultures," *Journal of Animal Science*, vol. 93, no. 8, pp. 3820–3831, 2015.

[94] C. Lv, S. Maharjan, Q. Wang et al., "α-Lipoic acid promotes neurological recovery after ischemic stroke by activating the Nrf2/HO-1 pathway to attenuate oxidative damage," *Cellular Physiology and Biochemistry*, vol. 43, no. 3, pp. 1273–1287, 2017.

[95] A. T. Dinkova-Kostova, R. V. Kostov, and A. G. Kazantsev, "The role of Nrf2 signaling in counteracting neurodegenerative diseases," *The FEBS Journal*, vol. 285, no. 19, pp. 3576–3590, 2018.

[96] K. M. Holmström, R. V. Kostov, and A. T. Dinkova-Kostova, "The multifaceted role of Nrf2 in mitochondrial function," *Current Opinion in Toxicology*, vol. 1, no. 1, pp. 80–91, 2016.

[97] Y. Tian, W. Wang, L. Xu et al., "Activation of Nrf2/ARE pathway alleviates the cognitive deficits in PS1V97L-Tg mouse model of Alzheimer's disease through modulation of oxidative stress," *Journal of Neuroscience Research*, vol. 97, no. 4, pp. 492–505, 2019.

[98] S. Dixit, P. Dhar, and R. D. Mehra, "Alpha lipoic acid (ALA) modulates expression of apoptosis associated proteins in hippocampus of rats exposed during postnatal period to sodium arsenite ($NaAsO_2$)," *Toxicology Reports*, vol. 2, pp. 78–87, 2015.

[99] W. R. Mohamed, A. B. M. Mehany, and R. M. Hussein, "Alpha lipoic acid protects against chlorpyrifos-induced toxicity in Wistar rats via modulating the apoptotic pathway," *Environmental Toxicology and Pharmacology*, vol. 59, pp. 17–23, 2018.

[100] S. Chen, G. Liu, M. Long, H. Zou, and H. Cui, "Alpha lipoic acid attenuates cadmium-induced nephrotoxicity via the mitochondrial apoptotic pathways in rat," *Journal of Inorganic Biochemistry*, vol. 184, pp. 19–26, 2018.

[101] G. S. Vasconcelos, N. C. Ximenes, C. N. de Sousa et al., "Alpha-lipoic acid alone and combined with clozapine reverses schizophrenia-like symptoms induced by ketamine in mice: participation of antioxidant, nitrergic and neurotrophic mechanisms," *Schizophrenia Research*, vol. 165, no. 2–3, pp. 163–170, 2015.

[102] L. R. L. Sampaio, F. M. S. Cysne Filho, J. C. de Almeida et al., "Advantages of the alpha-lipoic acid association with chlorpromazine in a model of schizophrenia induced by ketamine in rats: behavioral and oxidative stress evidences," *Neuroscience*, vol. 373, no. 373, pp. 72–81, 2018.

[103] B. Vidovi, S. Milovanović, B. Đorđević et al., "Effect of alpha-lipoic acid supplementation on oxidative stress and oxidative defense in patients with schizophrenia," *Psychiatria Danubina*, vol. 26, no. 3, pp. 205–213, 2014.

[104] M. R. Liebowitz and K. A. Tourian, "Efficacy, safety, and tolerability of desvenlafaxine 50 mg/d for the treatment of major depressive disorder:a systematic review of clinical trials," *Primary Care Companion to the Journal of Clinical Psychiatry*, vol. 12, no. 3, 2010.

[105] D. P. de Araújo, T. G. M. Camboim, A. P. M. Silva et al., "Behavioral and neurochemical effects of alpha lipoic acid associated with omega-3 in tardive dyskinesia induced by chronic haloperidol in rats," *Canadian Journal of Physiology and Pharmacology*, vol. 95, no. 7, pp. 837–843, 2017.

Hindawi
Oxidative Medicine and Cellular Longevity
Volume 2019, Article ID 2053149, 9 pages
https://doi.org/10.1155/2019/2053149

Research Article

CGRP Reduces Apoptosis of DRG Cells Induced by High-Glucose Oxidative Stress Injury through PI3K/AKT Induction of Heme Oxygenase-1 and Nrf-2 Expression

YaDong Liu,[1,2] **SiCong Zhang**,[1] **Jun Xue**,[1] **ZhongQing Wei**,[1] **Ping Ao**,[1] **BaiXin Shen**,[1] **and LiuCheng Ding**[1]

[1]*Department of Urology, The Second Affiliated Hospital of Nanjing Medical University, Nanjing, Jiangsu Province, China*
[2]*Department of Urology, The Third People's Hospital of Yancheng, Yancheng, Jiangsu Province, China*

Correspondence should be addressed to ZhongQing Wei; weizq1@163.com

Received 2 March 2019; Accepted 22 October 2019; Published 25 November 2019

Guest Editor: João C. M. Barreira

Dorsal root ganglion (DRG) neurons, which are sensitive to oxidative stress due to their anatomical and structural characteristics, play a complex role in the initiation and progression of diabetic bladder neuropathy. We investigated the hypothesis that the antioxidant and antiapoptotic effects of CGRP may be partly related to the expression of Nrf2 and HO-1, via the phosphatidylinositol 3-kinase (PI3K)/AKT pathway, thus reducing apoptosis and oxidative stress responses. This study shows that CGRP activates the PI3K/AKT pathway, thereby inducing increased expression of Nrf2 and HO-1 and resulting in the decrease of reactive oxygen species and malondialdehyde levels and reduced neuronal apoptosis. These effects were suppressed by LY294002, an inhibitor of the PI3K/AKT pathway. Therefore, regulation of Nrf2 and HO-1 expression by the PI3K/AKT pathway plays an important role in the regulation of the antioxidant and antiapoptotic responses in DRG cells in a high-glucose culture model.

1. Introduction

The prevalence of diabetes mellitus (DM) has significantly increased worldwide, accompanied by an increase in the incidence of obesity. Diabetic cystopathy (DCP) is one of the primary complications of DM in the lower urinary tract (LUT), and subjects often experience a series of symptoms, characterized by decreased bladder sensation, increased bladder capacity, impaired bladder contractility, and increased residual urine [1].

Multiple factors, including neuronal dysfunction, detrusor dysfunction, urothelial or urethral dysfunction, and polyuria, all contribute to the development of DCP [2, 3]. Dorsal root ganglia (DRGs) as a primary neuron had been confirmed to participate in the pathogenesis of diabetic bladder dysfunction [4]. However, the molecular mechanism leading to DCP in neuronal dysfunction remains largely unclear, although accumulating evidence shows that it is related to oxidative stress injury [5–7]. This has been confirmed by previous studies in diabetic rats treated with antioxidants [8, 9]. Meanwhile, various aspects of bladder function, including maximal bladder volume, bladder pressure, and maximal bladder pressure, measured by urodynamics, were partly improved. Bladder dysfunction due to neuronal dysfunction involves complex and sophisticated interactions among the somatic and autonomic afferent and efferent pathways. Some studies have reported a close relationship between diabetes-induced peripheral neuropathy and bladder dysfunction [10]. This has been further confirmed by neuromodulation in the treatment of voiding dysfunction in diabetic rats [11].

Nuclear factor-erythroid 2-related factor 2 (Nrf2) is a key transcription factor that regulates cellular redox homeostasis and has been confirmed to play a neuroprotective role in cerebral ischemia-reperfusion injury (CIRI) [12]. Heme oxygenase-1 (HO-1) is believed to participate in the process of heme catabolism, directly affecting the antioxidative balance in the body, and is also regulated by Nrf2 [13]. The PI3-kinase/AKT-mediated pathway is involved in

antioxidant and antiapoptotic activities through Nrf2/HO-1 in mouse β-cells [14]. Recently, it has been reported that neurotrophic factors and neurotransmitters may be associated with the pathogenesis of diabetic bladder dysfunction and oxidative stress [15]. Calcitonin gene-related peptide (CGRP) is a 37-amino-acid-long regulatory peptide derived from the calcitonin gene located on chromosome 11 [16, 17]. We confirmed that the expression of CGRP in the dorsal root ganglia (DRGs) of the control group was significantly higher than that in the DM group (unpublished). Some studies have demonstrated the widespread expression and protective effect of CGRP in both neurons and cardiomyocytes [16, 18]. Meanwhile, the experiment suggested that CGRP plays a pivotal role in the regulation of apoptosis and oxidative stress via the PI3K/AKT pathway [18]. Thus, we speculated that the oxidative stress damage and apoptosis in neurons play a role in the pathogenesis of diabetic bladder dysfunction. However, the related mechanism of DRG injury in high-glucose conditions remains largely elusive.

The main objectives of our study were to demonstrate (1) the oxidative stress injury of DRGs under high-glucose conditions and (2) the neuroprotective effect of CGRP associated with increased expression of HO-1 and Nrf2 mediated by the PI3-kinase/AKT signaling pathway.

2. Materials and Methods

2.1. Animals and Treatment. Female Sprague-Dawley rats (4–5 weeks old; Nanjing Medical University Animal Laboratory, Nanjing, China) weighing 110 ± 10 g were provided by the Animal Laboratory of Nanjing Medical University and fed a standard rodent diet with access to water ad libitum. All protocols were performed in accordance with the guidelines of Jiangsu Province Animal Research Advisory Committee for the Care and Use of Laboratory Animals. The experiments were approved by the Ethics Committee of Nanjing Medical University. The rats were killed at the same hour of the day.

2.2. Isolation of DRG Cells. Sprague-Dawley rats were euthanized by cervical dislocation, and DRGs were aseptically collected from L3 to S3 spinal levels. All DRGs were minced into small pieces and digested with 0.25% trypsin (Sigma-Aldrich) (10 min) and 0.1% collagenase (Sigma-Aldrich) (3–5 min) in DMEM/Nutrient Mixture F12 (Gibco) at 37°C. After centrifugation, the cells were resuspended in DMEM/-Nutrient Mixture F12 medium containing 2% B27 (Invitrogen, Carlsbad, CA) and 10 ng/mL NGF (Sigma-Aldrich, St. Louis, MO). The cells were seeded in 96-well plates (200 μL per well), yielding a density of 5×10^4 cells/well. The cells were cultured in a humid incubator at 37°C and 5% CO_2.

2.3. Establishment of a DRG Cell Model. Cultured cells were exposed to 25, 45, 50, 100, 200, and 400 mmol/L of glucose following seeding for 24 h and 48 h. For the cell viability assays, the concentration of glucose was determined to be 45 mmol/L at 48 h. The DRGs were exposed to 45 mmol/L of glucose and treated with CGRP alone or CGRP+ LY294002 (PI3K/AKT inhibitor, 10 μM). All the above cultures were incubated at 37°C in a humidified 5% CO_2 incubator. The oxidative stress index, which includes a measure of the reactive oxygen species (ROS), malondialdehyde (MDA), and superoxide dismutase (SOD) levels, was determined for the cultured cells.

2.4. Cell Viability Assay. The viability of DRG cells was determined using the CCK-8 assay (a common method for a cell viability assay). The CCK-8 kit was purchased from Beyotime Company (number C0040) and was strictly in accordance with the manufacturer's instructions mentioned. Briefly, 4×10^3 DRG cells were plated in each well of a 96-well plate. Media (100 μL) were added to each well. At 48 h after incubation, 10 μL of the CCK-8 solution was added to each well and the plate was incubated for another 2 h. The optical density of each well was measured at 450 nm using a microplate reader.

2.5. Apoptosis Assay. Flow cytometric analysis was performed after annexin V-FITC labeling to evaluate cell apoptosis.

The cells pretreated with CGRP for 48 hours were trypsinized and centrifuged at 12,000 g for 3 min at 4°C, followed by washing with staining buffer, and resuspension in binding buffer. Cells were stained with annexin V-FITC, followed by the addition of propidium iodide. Samples were then analyzed for apoptotic cells using a FACScan instrument.

2.6. Biochemical Assessment. All the SOD (MM-0385R1, purchased from Shanghai Huyu Biotechnology Company) and MDA (MM-0386R1, purchased from Shanghai Huyu Biotechnology Company) experimental procedures were strictly in accordance with the manufacturer's instructions mentioned in the kits. The disrupted cell or tissue lysate was centrifuged at 12,000 g for 5 min, and the supernatant was mixed with the detection solution and incubated for 40 min at 95°C in a water bath. After cooling, the samples were centrifuged at 4,000 g for 10 min. The optical density values of each group were measured and recorded at 450 nm with a 1 cm light path.

2.7. Measurement of ROS Production. DRG cells were loaded with 5 μmol/L DCFH-DA at 37°C for 30 min. The culture medium was removed, and the plates were washed three times with 0.1 mmol/L PBS (pH 7.4, Invitrogen) to remove the excess DCFH-DA. The fluorescence intensity of the oxidized derivative was analyzed using flow cytometry. The ROS values of the various treatment groups were calculated relative to the control cells.

2.8. Western Blotting. Western blotting was used to examine the expression of AKT, phosphorylated AKT (p-AKT), Nrf2, and HO-1. Total proteins (20 μg) from each sample were electrophoresed on a 12% SDS-polyacrylamide gradient gel and transferred to nitrocellulose membranes (Millipore). The membrane was blocked with 5% fat-free milk in rinse buffer for 30 min and incubated for 2 h with the following primary antibodies: AKT antibody (1 : 1000, Proteintech), p-AKT antibody (1 : 1000, Santa Cruz Biotechnology), Nrf-2 (1 : 1000 Proteintech), HO-1 (1 : 500 Proteintech), and anti-β-catenin (1 : 1000, Abcam). Next, they were incubated with an HRP-conjugated secondary antibody (goat anti-

rabbit IgG 1 : 5000, Beijing Zhongshan Golden Bridge Biotechnology Co. Ltd.) and visualized using the enhanced chemiluminescence (ECL) system (Pierce, Rockford, IL, USA). β-Actin was used as a reference protein.

2.9. Statistical Analysis. All data are presented as the mean ± standard error of the mean (SEM). The difference among groups was analyzed using one-way ANOVA, followed by two independent sample tests to compare the differences between the two groups, using the SPSS 22.0 software. Figures were constructed using GraphPad Prism 5 (GraphPad Software, San Diego, CA). $p < 0.05$ and $p < 0.01$ were considered to indicate statistically significant differences.

3. Results

3.1. Effect of Glucose Concentration on Cell Viability. The CCK-8 assay was performed to determine the concentration range of glucose to be used. A glucose concentration lower than 200 mmol/L did not affect cell viability in 24 h. Next, we incubated the cells in the same condition and performed the CCK-8 assay after 48 h of incubation. Cell viability was reduced up to a glucose concentration of 45 mmol/L. The cell viability of DRG cells was reduced in a dose-dependent manner with increasing glucose (Figure 1(a)). Thus, we selected the moderate glucose concentration (45 mmol/L) as the high-glucose (HG) culture condition. This glucose concentration was similar to that used in previous studies [19, 20]. At the indicated glucose concentration, the cell viability of DRG cells in the HG+CGRP group was significantly improved compared to the HG group ($p < 0.01$). When pretreated with LY294002, the HG+CGRP+LY294002 group showed a marked decrease in cell viability compared to the HG+CGRP group ($p < 0.01$) (Figure 1(b)).

3.2. The Effect of CGRP on DRG Cells in Apoptosis. The apoptotic cell numbers for each group are shown in Figures 2(a) and 2(b). It was observed that the apoptosis of DRG cells in a high-glucose medium was significantly increased as compared to the control group ($p < 0.01$), and then it decreased after CGRP treatment ($p < 0.01$). When pretreated with LY294002, the apoptosis of DRG cells in the HG+CGRP +LY294002 group was markedly increased compared to that in the HG+CGRP group ($p < 0.01$).

3.3. Measurement of ROS, MDA, and SOD Levels in DRG Cells. The ROS level in the DRG cells of the HG group was significantly elevated compared to the control group ($p < 0.05$), which had a reduced ROS level after CGRP treatment ($p < 0.01$). However, treatment with the inhibitor LY294002 continually increased the ROS level in cells in comparison to treatment with HG+CGRP ($p < 0.01$) (Figure 3).

The MDA levels were significantly increased in the DRG cells of the HG group compared to the control group ($p < 0.01$). After treatment with CGRP, MDA levels were significantly decreased in the HG+CGRP group as compared to the HG group ($p < 0.05$). However, treatment with LY294002 led to a further increase in the level of MDA compared to treatment with HG+CGRP ($p < 0.01$) (Figure 4(a)).

There was no difference in the SOD levels of DRG cells in the HG group and the control group. However, the SOD activity was significantly lower in the HG group than in the HG+CGRP group ($p < 0.05$). The SOD activity was also markedly reduced in the HG+CGRP+LY294002 group as compared to that in the HG+CGRP group ($p < 0.01$) (Figure 4(b)).

3.4. Effects of CGRP on HO-1 and Nrf2 Protein Expression in DRG Cells. HO-1 is considered to be a heat-shock protein that plays an important antioxidative and antiapoptotic role in diabetes [21–23]. To explore how CGRP decreases apoptosis in DRG cells in a high-glucose culture medium, we investigated whether CGRP induces the expression of HO-1. Figure 5 shows that the expression of HO-1 in the HG group was remarkably decreased compared to that of the HG +CGRP group. Pretreatment with LY294002 led to a markedly decreased expression of HO-1 compared to that of the HG+CGRP group (Figure 5(a)). Nrf2 is considered to be a regulator of HO-1 expression [24, 25]. Therefore, we next investigated the expression of Nrf2 in the different groups. Nrf2 expression in the HG group was markedly decreased compared to that in the HG+CGRP group. Nrf2 expression in the HG+CGRP+LY294002 group was markedly reduced compared to that in the HG+CGRP group (Figure 5(b)).

3.5. PI3K/AKT Signaling Is Involved in the Induction of HO-1 and Nrf2 Expression by CGRP. Finally, we wanted to elucidate the signaling pathway responsible for the induction of Nrf2 and HO-1 expression by CGRP. A previous study demonstrated that PI3K/AKT plays a crucial role in the induction of HO-1 and Nrf2 in attenuating C6, cardiomyocyte apoptosis, and renal cell damage [24, 26, 27]. Therefore, we investigated whether CGRP activates PI3 kinase and observed no difference in AKT expression among the three groups. Western blot analysis confirmed that the expression level of p-AKT was significantly increased in the HG+CGRP group as compared to the HG group. The results suggested that, as compared to the HG+CGRP group, the p-AKT expression level in the HG+CGRP+LY294002 group was downregulated by pretreatment with the PI3K/AKT inhibitor LY294002 (Figure 5(c)).

4. Discussion

In our present study, we have evaluated the effects of CGRP on antioxidation and antiapoptosis in a high-glucose culture model of DRG cells. Our results revealed that CGRP attenuated the apoptosis of DRG cells induced by oxidative stress injury by increasing the expression of HO-1 and Nrf2 through the PI3K/AKT pathway. To our knowledge, this is one of the first studies to report that CGRP decreases the ROS level in DRG cells in a HG-induced oxidative stress model. In recent years, increasing evidence has indicated that CGRP counters oxidative stress, improves bladder function, and is involved in the antiapoptotic process in vitro [4, 18, 28]. It has been reported that the polyol pathway increases advanced glycation end products (AGEs), hyperglycemia-induced activation of protein kinase C (PKC),

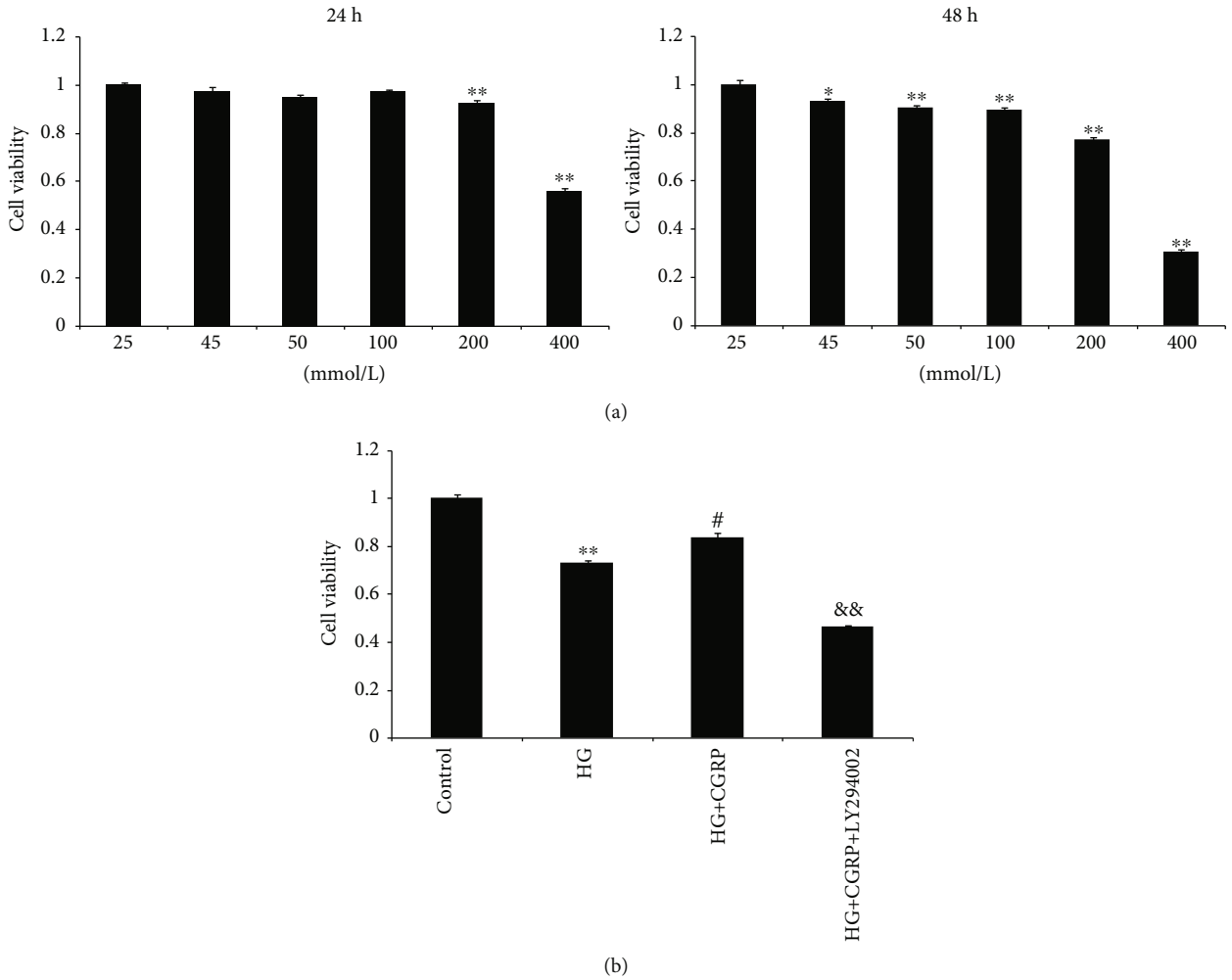

Figure 1: (a) High glucose inhibits DRG cell viability. DRG cell viability decreased in a dose-dependent manner with increasing concentrations of glucose. Dissociated rat DRG cells were cultured in different concentrations of glucose with 10 ng/mL NGF for 24 h and 48 h. The cell viability at 24 h with glucose concentrations of 200 mmol/L and 400 mmol/L was significantly decreased compared to the control (25 mmol/L). At 48 h, we found that the cell viability was significantly reduced at all glucose concentrations compared to the control. $^{*}p < 0.05$, compared to the control; $^{**}p < 0.01$, compared to the control. (b) Cell viability of DRG neurons in different groups after 48 h. Treatment with HG, HG+CGRP, and HG+CGRP+LY294002. $^{**}p < 0.01$, compared to the control; $^{\#}p < 0.05$, compared to the HG group; $^{\&\&}p < 0.01$, compared to the HG+CGRP group.

and hexosamine pathway flux, which are found to participate in the hyperglycemia-induced overproduction of superoxide [6]. In a previous study, we confirmed that transcutaneous electrical nerve stimulation (TENS) improves the diabetic cystopathy (DCP) via upregulation of CGRP and cAMP. However, the role of CGRP in the pathogenesis of DCP and the mechanism of CGRP inhibiting the apoptosis of DRG cells in high-glucose conditions remain largely unclear.

DRG cells have unique anatomical and structural characteristics that make them easily vulnerable to hyperglycemic damage [29, 30]. In the first part of our study, we provide strong evidence for the role of hyperglycemia in the development of DRG damage. Our results show that DRG damage begins when the glucose concentration is 45 mmol/L at 48 h. Meanwhile, the cell viability of DRG gradually decreased with increasing concentrations of glucose and cell culture durations. The high-glucose culture condition was selected to be 45 mmol/L in accordance with previous studies [19, 20]. However, the minimum glucose concentration required for apoptosis may be different due to different experimental conditions. Evidence suggests that DRG cells cultured in a medium containing elevated (30 mmol/L) glucose concentrations undergo apoptosis in vitro [31]. The apoptotic percentage of DRG cells was increased and neurite growth was decreased in a dose-dependent manner with an increase in the glucose concentration from 0 to 300 mmol/L above the control concentrations [31]. These results were partly consistent with ours.

The concept that oxidative stress plays a key role in nerve injury in diabetes has now been confirmed [2, 7, 32, 33]. The levels of antioxidant enzymes are considered to be an important index in oxidative stress injury. To explore the state of oxidative stress, we further measured the levels of ROS, MDA, and SOD.

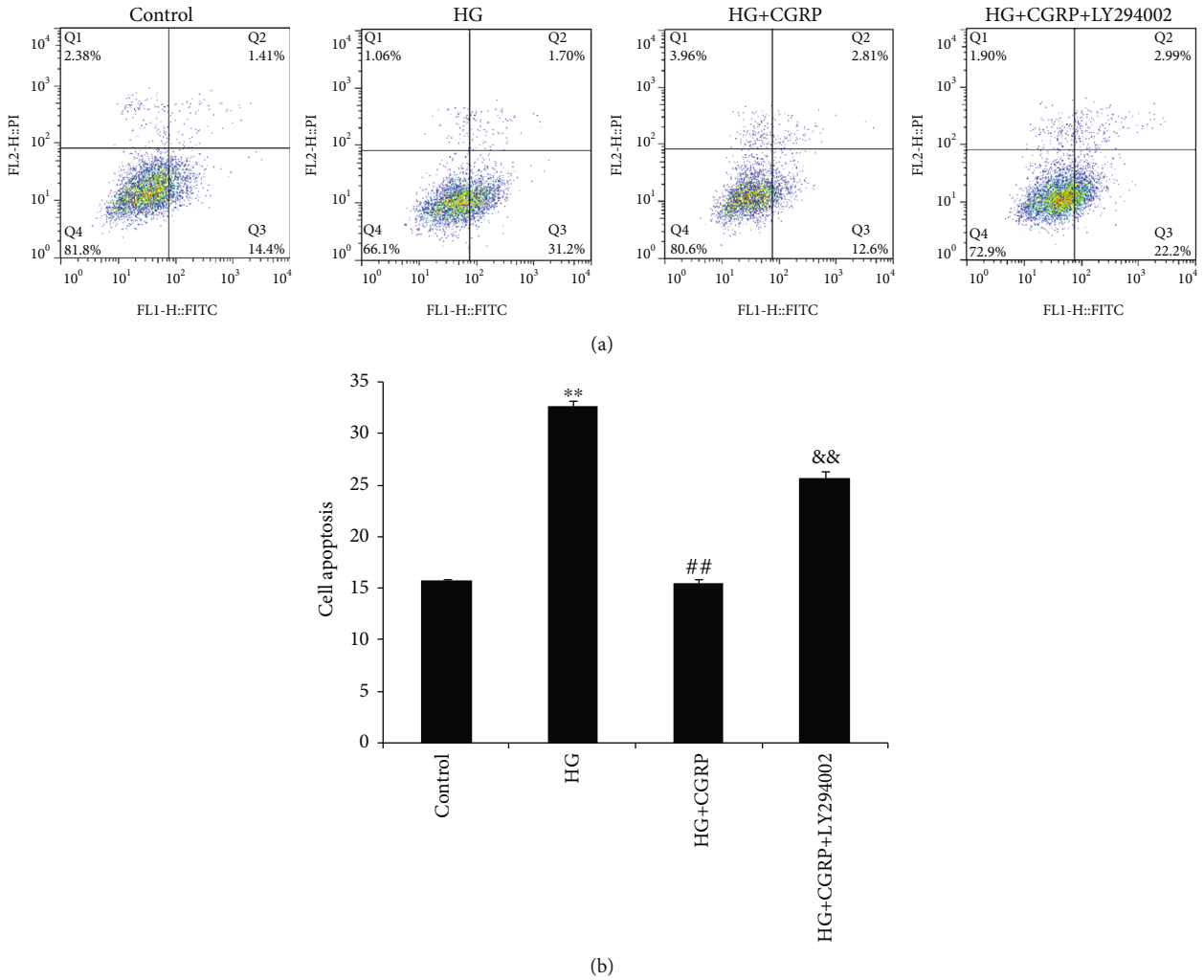

Figure 2: (a) After 48 h of treatment with HG, HG+CGRP, and HG+CGRP+LY294002, DRG cells were subjected to oxidative stress injury, and the relative number of annexin V-positive cells was determined using flow cytometry (b) Apoptosis of DRG neurons after HG, HG+CGRP, or HG+CGRP+LY294002 treatment for 48 h. $^{**}p < 0.01$, compared to the control; $^{\#\#}p < 0.01$, compared to the HG group; $^{\&\&}p < 0.01$, compared to the HG+CGRP group.

Our report indicates that the levels of ROS and MDA in DRGs in the HG group were significantly increased as compared to the control. The SOD activity was markedly decreased in the DRGs of the HG group compared to the control. Russel et al. suggested that, compared to the exposure at 45 mmol/L glucose, ROS production in DRG cells at 150 mmol/L glucose was significantly increased [34]. This might confirm that the oxidative stress injury of DRG cells induced by glucose was associated with the glucose concentration. It has been confirmed by previous studies that glucose-mediated oxidative stress leads to the injury of DRG cells [35, 36]. The other finding of this study is that the treatment of DRG cells with CGRP can inhibit the oxidative stress response. CGRP serves as an antioxidative mediator that participates in various diseases [18, 28]. This article showed that the level of ROS and MDA was reversed by CGRP in the HG+CGRP group compared to that in the HG group. Meanwhile, the apoptosis of DRG in the HG +CGRP group was reduced compared to the HG group. This was consistent with previous studies showing the application of antioxidants in preventing DRG neuronal death [19, 37]. But a previous study showed that CGRP cooperated with substance P to inhibit melanogenesis and induce the apoptosis of B16F10 cells. The expression of apoptotic protein was related to the concentration of CGRP [38]. So we speculated that the action of CGRP is related to its concentration and exposure time.

Nrf2 is a master regulator of redox homoeostasis and a key transcription factor mediating a wide array of antioxidant genes, such as HO-1. HO-1, the downstream target of Nrf2, was measured in our study to investigate antioxidative function. The dissociation of the Nrf2-Keap 1 complex, which is regulated via one or more upstream kinases, including PKC, PI3K/AKT, and MAPK, has recently been reviewed [39–41]. PI3K/AKT is considered to be one of the major pathways upregulating the activity of Nrf2 [42]. In our study, we discussed the role of Nrf2 and HO-1 expression and the antiapoptotic and antioxidative functions of the PI3K/AKT

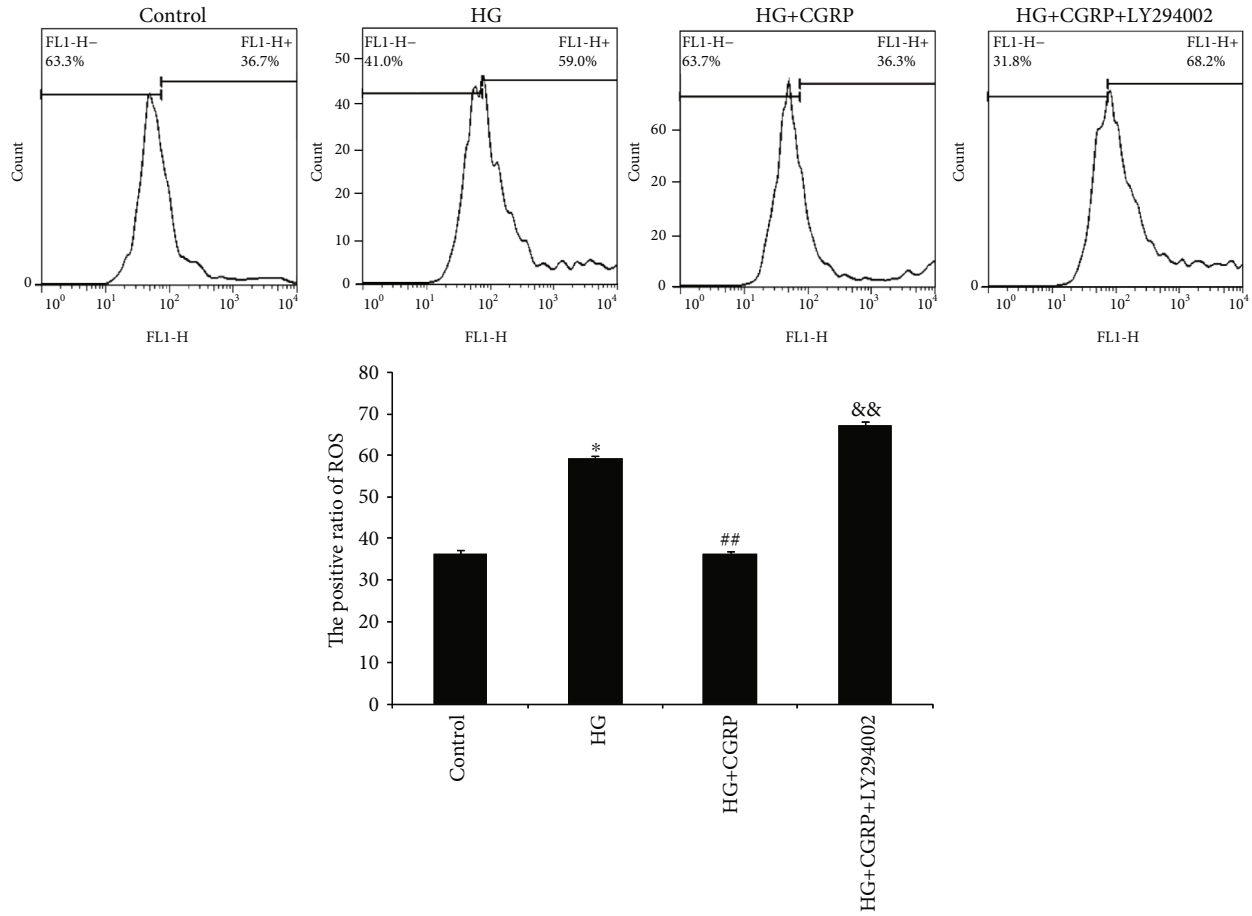

Figure 3: The production of ROS in DRG neurons after HG, HG+CGRP, or HG+CGRP+LY294002 treatment. The positive ratio of ROS shows the percent apoptosis cells of the total number. $^{*}p < 0.05$, compared with the control; $^{\#\#}p < 0.01$, compared to the HG group; $^{\&\&}p < 0.01$, compared to the HG+CGRP group (refer to the attachment for the high-definition image).

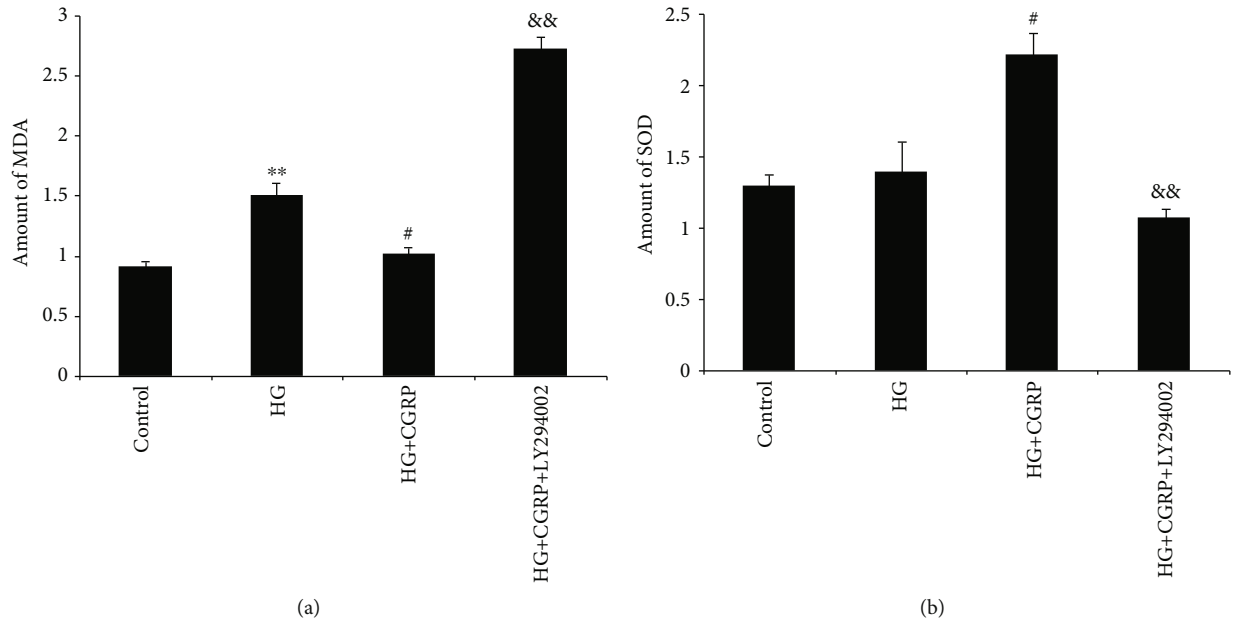

Figure 4: The MDA level (a) and SOD activity (b) in DRG neurons after HG, HG+CGRP, or HG+CGRP+LY294002 treatment for 48 h. $^{**}p < 0.01$, compared to the control; $^{\#}p < 0.05$, compared to the HG group; $^{\&\&}p < 0.01$, compared to the HG+CGRP group.

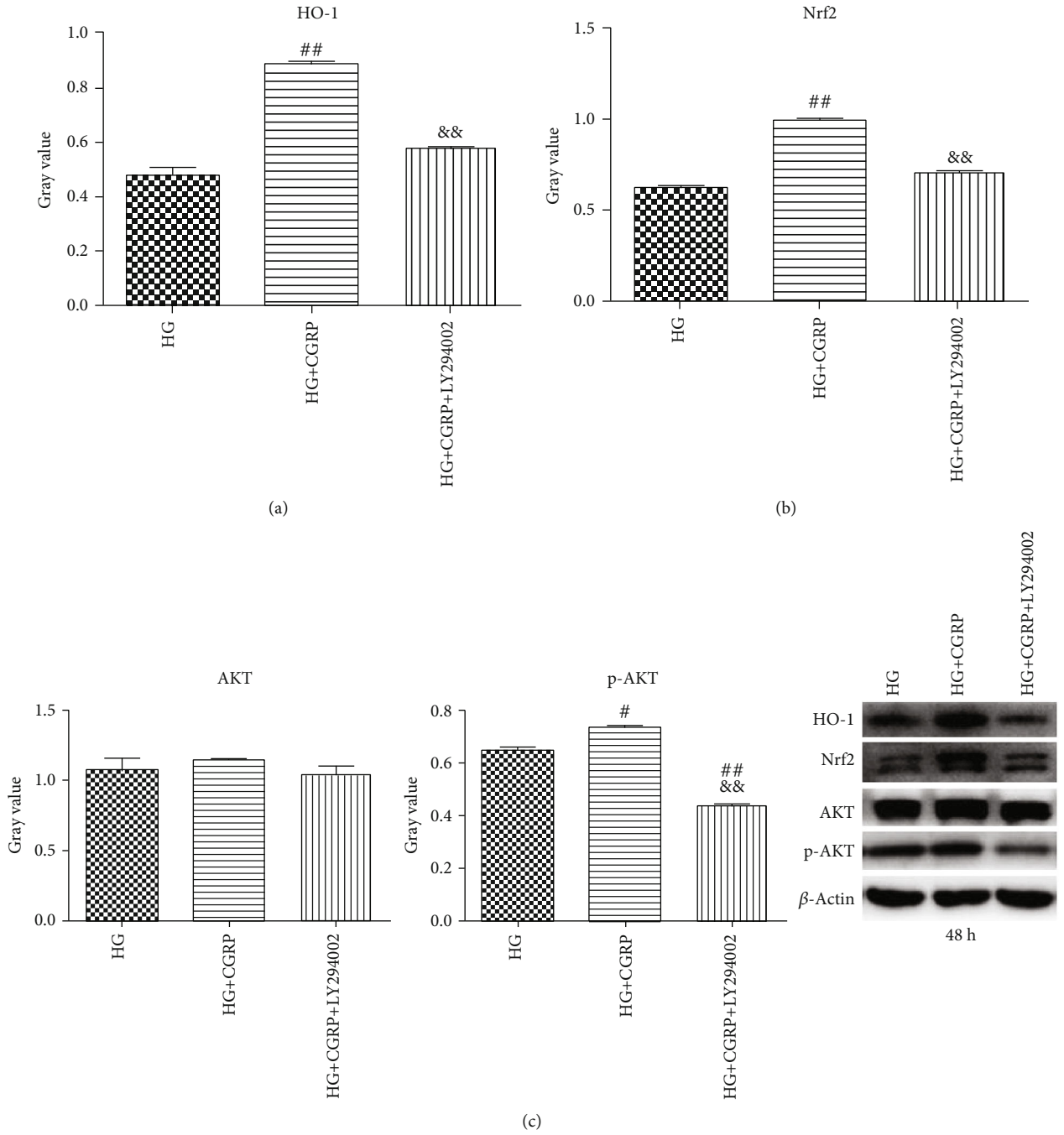

Figure 5: CGRP increases the protein expression of HO-1 and Nrf2 in DRG neurons. (a) The expression of HO-1 in DRG neurons with CGRP and CGRP+LY294002 treatment for 48 h and (b) the expression of Nrf2 in DRG neurons in each group determined by western blotting. (c) Phosphatidylinositol 3-kinase/AKT pathway-dependent Nrf-2 and HO-1 induction by CGRP. The expression level of AKT and the phosphorylation of AKT in DRG neurons with CGRP treatment for 48 h. $^{\#}p < 0.05$, compared to the HG group; $^{\#\#}p < 0.01$, compared to the HG group; $^{\&}p < 0.01$, compared to the HG+CGRP group; $^{\&\&}p < 0.05$, compared to the HG+CGRP group.

pathway in DRG cells induced by HG. We found that CGRP activated PI3K/AKT and increased the expression of Nrf2 and HO-1, thereby altering the activity of antioxidant enzymes, and finally, attenuating the apoptosis of DRG cells. This result indicated that the PI3K/AKT pathway partially regulates Nrf-2 expression, which is in accordance with a prior finding in H9c2 cardiomyocytes [43]. A similar mechanism was proposed in a study that reported the activation of the PI3K/AKT pathway by atorvastatin via AKT phosphorylation at position Ser473, which then mediated Nrf-2 activation [25]. Our study suggested that DRGs treated with high glucose show a marked increase in oxidative stress, as shown by excessive ROS and MDA production. However, cotreatment with CGRP significantly attenuated oxidative damage

induced by high glucose, as reflected in the augmentation of SOD activity and the accompanying decrease in MDA and ROS levels.

5. Conclusions

Collectively, this study is the first to demonstrate that CGRP modulates oxidative stress injury in the high-glucose-induced DRG cell model via the activation of the PI3K/AKT pathway and increases the expression of Nrf2 and HO-1. CGRP may be useful as an adjuvant therapy for diabetic neuropathy in the future, owing to its antioxidative and antiapoptotic roles.

Data Availability

The data used to support the findings of this study are available from the corresponding author upon request.

Conflicts of Interest

To authors declare that there is no conflict of interests in relation to the present paper.

Acknowledgments

This study was supported by the National Natural Science Foundation of China, Grant Nos. 81230007 and 8157041006.

References

[1] W. E. Bradley, "Diagnosis of urinary bladder dysfunction in diabetes mellitus," *Annals of Internal Medicine*, vol. 92, no. 2_Part_2, pp. 323–326, 1980.

[2] G. Liu and F. Daneshgari, "Diabetic bladder dysfunction," *Chinese Medical Journal*, vol. 127, no. 7, pp. 1357–1364, 2014.

[3] Z. Yuan, Z. Tang, C. He, and W. Tang, "Diabetic cystopathy: a review," *Journal of Diabetes*, vol. 7, no. 4, pp. 442–447, 2015.

[4] L. Ding, T. Song, C. Yi et al., "Transcutaneous electrical nerve stimulation (TENS) improves the diabetic cytopathy (DCP) via up-regulation of CGRP and cAMP," *PLoS One*, vol. 8, no. 2, article e57477, 2013.

[5] A. C. Maritim, R. A. Sanders, and J. B. Watkins 3rd., "Diabetes, oxidative stress, and antioxidants: a review," *Journal of Biochemical and Molecular Toxicology*, vol. 17, no. 1, pp. 24–38, 2003.

[6] M. Brownlee, "The pathobiology of diabetic complications: a unifying mechanism," *Diabetes*, vol. 54, no. 6, pp. 1615–1625, 2005.

[7] E. Beshay and S. Carrier, "Oxidative stress plays a role in diabetes-induced bladder dysfunction in a rat model," *Urology*, vol. 64, no. 5, pp. 1062–1067, 2004.

[8] Y. J. Jiang, D. X. Gong, H. B. Liu, C. M. Yang, Z. X. Sun, and C. Z. Kong, "Ability of alpha-lipoic acid to reverse the diabetic cystopathy in a rat model," *Acta Pharmacologica Sinica*, vol. 29, no. 6, pp. 713–719, 2008.

[9] M. C. Ustuner, S. Kabay, H. Ozden et al., "The protective effects of vitamin E on urinary bladder apoptosis and oxidative stress in streptozotocin-induced diabetic rats," *Urology*, vol. 75, no. 4, pp. 902–906, 2010.

[10] A. Z. Burakgazi, B. Alsowaity, Z. A. Burakgazi, D. Unal, and J. J. Kelly, "Bladder dysfunction in peripheral neuropathies," *Muscle & Nerve*, vol. 45, no. 1, pp. 2–8, 2012.

[11] S. C. Chen, C. H. Lai, W. J. Fan, and C. W. Peng, "Pudendal neuromodulation improves voiding efficiency in diabetic rats," *Neurourology and Urodynamics*, vol. 32, no. 3, pp. 293–300, 2013.

[12] Z. Wen, W. Hou, W. Wu et al., "6′-*O*-galloylpaeoniflorin attenuates cerebral ischemia reperfusion-induced neuroinflammation and oxidative stress via PI3K/Akt/Nrf2 activation," *Oxidative Medicine and Cellular Longevity*, vol. 2018, Article ID 8678267, 14 pages, 2018.

[13] A. Loboda, M. Damulewicz, E. Pyza, A. Jozkowicz, and J. Dulak, "Role of Nrf2/HO-1 system in development, oxidative stress response and diseases: an evolutionarily conserved mechanism," *Cellular and Molecular Life Sciences*, vol. 73, no. 17, pp. 3221–3247, 2016.

[14] S. Pugazhenthi, L. Akhov, G. Selvaraj, M. Wang, and J. Alam, "Regulation of heme oxygenase-1 expression by demethoxy curcuminoids through Nrf2 by a PI3-kinase/Akt-mediated pathway in mouse beta-cells," *American Journal of Physiology. Endocrinology and Metabolism*, vol. 293, no. 3, pp. E645–E655, 2007.

[15] C. D. Cruz, "Neurotrophins in bladder function: what do we know and where do we go from here?," *Neurourology and Urodynamics*, vol. 33, no. 1, pp. 39–45, 2014.

[16] A. V. Vega and G. Avila, "CGRP, a vasodilator neuropeptide that stimulates neuromuscular transmission and EC coupling," *Current Vascular Pharmacology*, vol. 8, no. 3, pp. 394–403, 2010.

[17] S. Sueur, M. Pesant, L. Rochette, and J. L. Connat, "Antiapoptotic effect of calcitonin gene-related peptide on oxidative stress- induced injury in H9c2 cardiomyocytes via the RAMP1/CRLR complex," *Journal of Molecular and Cellular Cardiology*, vol. 39, no. 6, pp. 955–963, 2005.

[18] N. A. Umoh, R. K. Walker, R. M. Millis, M. Al-Rubaiee, P. R. Gangula, and G. E. Haddad, "Calcitonin gene-related peptide regulates Cardiomyocyte survival through regulation of oxidative stress by PI3K/Akt and MAPK Signaling pathways," *Annal of Clinical and Experimental Hypertension*, vol. 2, p. 1007, 2014.

[19] A. M. Vincent, M. J. Stevens, C. Backus, L. L. Mclean, and E. L. Feldman, "Cell culture modeling to test therapies against hyperglycemia-mediated oxidative Stress and Injury," *Antioxidants & Redox Signaling*, vol. 7, no. 11-12, pp. 1494–1506, 2005.

[20] T. Chen, H. Li, Y. Yin, Y. Zhang, Z. Liu, and H. Liu, "Interactions of Notch1 and TLR4 signaling pathways in DRG neurons of *in vivo* and *in vitro* models of diabetic neuropathy," *Scientific Reports*, vol. 7, no. 1, p. 14923, 2017.

[21] G. Negi, V. Nakkina, P. Kamble, and S. S. Sharma, "Heme oxygenase-1, a novel target for the treatment of diabetic complications: focus on diabetic peripheral neuropathy," *Pharmacological Research*, vol. 102, pp. 158–167, 2015.

[22] K. Chen, K. Gunter, and M. D. Maines, "Neurons overexpressing heme oxygenase-1 resist oxidative stress-mediated cell death," *Journal of Neurochemistry*, vol. 75, no. 1, pp. 304–313, 2000.

[23] B. Li, S. Liu, L. Miao, and L. Cai, "Prevention of diabetic complications by activation of Nrf2: diabetic cardiomyopathy and nephropathy," *Experimental Diabetes Research*, vol. 2012, Article ID 216512, 7 pages, 2012.

[24] S. M. Zhao, H. L. Gao, Y. L. Wang, Q. Xu, and C. Y. Guo, "Attenuation of high glucose-induced rat Cardiomyocyte apoptosis by Exendin-4 via intervention of HO-1/Nrf-2 and the PI3K/AKT Signaling pathway," *The Chinese Journal of Physiology*, vol. 60, no. 2, pp. 89–96, 2017.

[25] Y. Ma, Z. Chen, Y. Zou, and J. Ge, "Atorvastatin represses the angiotensin 2-induced oxidative stress and inflammatory response in dendritic cells via the PI3K/Akt/Nrf 2 pathway," *Oxidative Medicine and Cellular Longevity*, vol. 2014, Article ID 148798, 10 pages, 2014.

[26] S. Saha, P. Sadhukhan, K. Sinha, N. Agarwal, and P. C. Sil, "Mangiferin attenuates oxidative stress induced renal cell damage through activation of PI3K induced Akt and Nrf-2 mediated signaling pathways," *Biochemistry and Biophysics Reports*, vol. 5, pp. 313–327, 2016.

[27] Y. M. Ha, M. Y. Kim, M. K. Park et al., "Higenamine reduces HMGB1 during hypoxia-induced brain injury by induction of heme oxygenase-1 through PI3K/Akt/Nrf-2 signal pathways," *Apoptosis*, vol. 17, no. 5, pp. 463–474, 2012.

[28] C. Schaeffer, D. Vandroux, L. Thomassin, P. Athias, L. Rochette, and J. L. Connat, "Calcitonin gene-related peptide partly protects cultured smooth muscle cells from apoptosis induced by an oxidative stress via activation of ERK1/2 MAPK," *Biochimica et Biophysica Acta (BBA) - Molecular Cell Research*, vol. 1643, no. 1-3, pp. 65–73, 2003.

[29] J. M. McHugh and W. B. Mchugh, "Diabetes and peripheral sensory neurons what we don't know and how it can hurt us," *AACN Clinical Issues*, vol. 15, no. 1, pp. 136–149, 2004.

[30] M. Devor, "Unexplained peculiarities of the dorsal root ganglion," *Pain*, vol. 82, Supplement 1, pp. S27–S35, 1999.

[31] J. W. Russell, K. A. Sullivan, A. J. Windebank, D. N. Herrmann, and E. L. Feldman, "Neurons undergo apoptosis in animal and cell culture models of diabetes," *Neurobiology of Disease*, vol. 6, no. 5, pp. 347–363, 1999.

[32] C. Figueroa-Romero, M. Sadidi, and E. L. Feldman, "Mechanisms of disease: the oxidative stress theory of diabetic neuropathy," *Reviews in Endocrine & Metabolic Disorders*, vol. 9, no. 4, pp. 301–314, 2008.

[33] N. D. Kanika, J. Chang, Y. Tong et al., "Oxidative stress status accompanying diabetic bladder cystopathy results in the activation of protein degradation pathways," *BJU International*, vol. 107, no. 10, pp. 1676–1684, 2011.

[34] J. W. Russell, D. Golovoy, A. M. Vincent et al., "High glucose-induced oxidative stress and mitochondrial dysfunction in neurons," *The FASEB Journal*, vol. 16, pp. 1738–1748, 2002.

[35] Z. Kiasalari, T. Rahmani, N. Mahmoudi, T. Baluchnejadmojarad, and M. Roghani, "Diosgenin ameliorates development of neuropathic pain in diabetic rats: involvement of oxidative stress and inflammation," *Biomedicine & Pharmacotherapy*, vol. 86, pp. 654–661, 2017.

[36] A. M. Vincent, L. L. McLean, C. Backus, and E. L. Feldman, "Short-term hyperglycemia produces oxidative damage and apoptosis in neurons," *The FASEB Journal*, vol. 19, no. 6, pp. 638–640, 2005.

[37] D. Yang, X. C. Liang, Y. Shi et al., "Anti-oxidative and anti-inflammatory effects of cinnamaldehyde on protecting high glucose-induced damage in cultured dorsal root ganglion neurons of rats," *Chinese Journal of Integrative Medicine*, vol. 22, no. 1, pp. 19–27, 2016.

[38] J. Zhou, J. Y. Feng, Q. Wang, and J. Shang, "Calcitonin gene-related peptide cooperates with substance P to inhibit melanogenesis and induces apoptosis of B16F10 cells," *Cytokine*, vol. 74, no. 1, pp. 137–144, 2015.

[39] Y. P. Hwang and H. G. Jeong, "Ginsenoside Rb1 protects against 6-hydroxydopamine-induced oxidative stress by increasing heme oxygenase-1 expression through an estrogen receptor-related PI3K/Akt/Nrf2-dependent pathway in human dopaminergic cells," *Toxicology and Applied Pharmacology*, vol. 242, no. 1, pp. 18–28, 2010.

[40] C. N. Nguyen, H. E. Kim, and S. G. Lee, "Caffeoylserotonin protects human keratinocyte HaCaT cells against H_2O_2-Induced Oxidative Stress and Apoptosis through Upregulation of HO-1 Expression via Activation of the PI3K/Akt/Nrf2 Pathway," *Phytotherapy Research*, vol. 27, no. 12, pp. 1810–1818, 2013.

[41] J. S. Lee and Y. J. Surh, "Nrf2 as a novel molecular target for chemoprevention," *Cancer Letters*, vol. 224, no. 2, pp. 171–184, 2005.

[42] P. Basak, P. Sadhukhan, P. Sarkar, and P. C. Sil, "Perspectives of the Nrf-2 signaling pathway in cancer progression and therapy," *Toxicology Reports*, vol. 4, pp. 306–318, 2017.

[43] S. X. Liu, Y. Zhang, Y. F. Wang et al., "Upregulation of heme oxygenase-1 expression by hydroxysafflor yellow A conferring protection from anoxia/reoxygenation-induced apoptosis in H9c2 cardiomyocytes," *International Journal of Cardiology*, vol. 160, no. 2, pp. 95–101, 2012.

Hindawi
Oxidative Medicine and Cellular Longevity
Volume 2019, Article ID 1652609, 10 pages
https://doi.org/10.1155/2019/1652609

Research Article

Differential Effects of Silibinin A on Mitochondrial Function in Neuronal PC12 and HepG2 Liver Cells

Carsten Esselun,[1] Bastian Bruns,[2] Stephanie Hagl,[2] Rekha Grewal,[1] and Gunter P. Eckert[1]

[1]*Institute for Nutritional Sciences, Justus-Liebig-University of Giessen, Giessen, Germany*
[2]*Institute of Pharmacology, Goethe-University of Frankfurt am Main, Frankfurt am Main, Germany*

Correspondence should be addressed to Gunter P. Eckert; eckert@uni-giessen.de

Received 31 May 2019; Revised 27 August 2019; Accepted 8 October 2019; Published 23 November 2019

Guest Editor: João C. M. Barreira

The Mediterranean plant *Silybum marianum* L., commonly known as milk thistle, has been used for centuries to treat liver disorders. The flavonolignan silibinin represents a natural antioxidant and the main bioactive ingredient of silymarin (silybin), a standard extract of its seeds. Mitochondrial dysfunction and the associated generation of reactive oxygen/nitrogen species (ROS/RNS) are involved in the development of chronic liver and age-related neurodegenerative diseases. Silibinin A (SIL A) is one of two diastereomers found in silymarin and was used to evaluate the effects of silymarin on mitochondrial parameters including mitochondrial membrane potential and ATP production with and without sodium nitroprusside- (SNP-) induced nitrosative stress, oxidative phosphorylation, and citrate synthase activity in HepG2 and PC12 cells. Both cell lines were influenced by SIL A, but at different concentrations. SIL A significantly weakened nitrosative stress in both cell lines. Low concentrations not only maintained protective properties but also increased basal mitochondrial membrane potential (MMP) and adenosine triphosphate (ATP) levels. However, these effects could not be associated with oxidative phosphorylation. On the other side, high concentrations of SIL A significantly decreased MMP and ATP levels. Although SIL A did not provide a general improvement of the mitochondrial function, our findings show that SIL A protects against SNP-induced nitrosative stress at the level of mitochondria making it potentially beneficial against neurological disorders.

1. Introduction

The Mediterranean plant *Silybum marianum* L. (Gaertn.; (Compositae)), commonly known as milk thistle, has been used for centuries to treat disorders of the liver. The flavonolignan silibinin (Figure 1) represents the main bioactive ingredient of silymarin (silybin), a standard extract of its seeds [1]. Silibinin A (SIL A), which was used in this study, is one of two diastereomers found in silybin [2]. Mitochondrial dysfunction and the associated generation of reactive oxygen species (ROS) are involved in the development of chronic liver diseases, including nonalcoholic fatty, alcohol-associated, and drug-associated liver diseases, as well as hepatitis B and C [3, 4]. Silybin reduced respiration and adenosine triphosphate (ATP) production but increased mitochondrial size and improved mitochondrial cristae organization in cellular models of steatosis and steatohepatitis [5]. In rats with secondary biliary cirrhosis, silybin was found to exert antioxidant effects and induces mitochondrial biogenesis [6]. Furthermore, SIL A was shown to decrease lipotoxicity by attenuating oxidative stress and NFκB activation in nonalcoholic steatohepatitis (NASH) [7, 8].

Functioning as a scavenger for ROS, SIL A is able to reduce lipid peroxidation, resulting in improved protection against apoptosis [2]. It was also proposed that SIL A shows an effect on the permeability of mitochondrial membranes in liver cells, affecting the integration of cholesterol into the lipid bilayer [2]. Furthermore, it has also been shown that SIL A can regulate the Ca^{2+} influx into mitochondria [9]. HepG2 cells are widely used to study the mechanisms of drug actions, and it has already been reported that SIL A reduced oxidative stress in HepG2 cells [10].

Beside hepatic diseases, mitochondrial dysfunction is also involved in the development of noncommunicable diseases

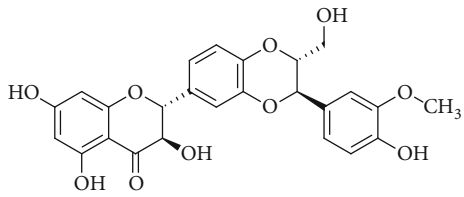

Figure 1: Chemical structure of SIL A ($C_{25}H_{22}O_{10}$) ((2R,3R)-3,5,7-trihydroxy-2-[(2R,3R)-3-(4-hydroxy-3-methoxyphenyl)-2-(hydroxymethyl)-2,3-dihydro-1,4-benzodioxin-6-yl]-2,3-dihydrochromen-4-one).

of the brain, including Alzheimer's disease (AD) and Parkinson's disease (PD), as well as amyotrophic lateral sclerosis [11–13]. SIL A prevents dopaminergic neuronal loss in cellular and animal models of PD, and it was suggested that its neuroprotective effect might be mediated by the stabilization of the mitochondrial membrane potential (MMP) [14]. In PC12 cells, silybin and SIL A were found to attenuate oxidative and nitrosative stress [15, 16]. Another study demonstrated the effects of neuroprotective hybrid compounds consisting of SIL A conjugated with phenolic acids on PC12 cell differentiation [17].

PC12 cells originate from the pheochromocytoma of the rat adrenal medulla and are widely established as a neuronal model [18, 19] in differentiated [20, 21] or undifferentiated [22, 23] form.

Recently, it has been reported that SIL A-induced ROS generation protects PC12 cells from sodium nitroprusside-(SNP-) induced nitrosative stress [15]. Nitrosative stress in the form of nitric oxide radicals plays a role in the aging process and in neurodegenerative diseases by contributing to inflammation, neuronal loss, and oxidative stress [24, 25]. SNP is a source widely used to introduce nitrosative stress into cellular models [15, 26].

An improvement of mitochondrial energy metabolism might be a mechanism contributing to the hepatic or neuroprotective action of SIL A, a hypothesis that has not yet been studied in detail. Thus, in this work, we evaluated the effects of SIL A on oxidative phosphorylation, MMP, ATP levels, and citrate synthase activity in PC12 cells and HepG2 cells, both subjected to and without SNP-induced nitrosative stress.

2. Material and Methods

2.1. Chemicals. All chemicals used for this research were of the highest purity available and were purchased from either Sigma Aldrich, Merck, or VWR. Silibinin A (SIL A) (purity 97%) was ordered from LKT Laboratories. SIL A was solubilized in DMSO, and thus, DMSO (0.1%) was used as a control for all experiments. DMSO had no effect on any of the parameters measured (data not shown). Aqueous solutions were prepared with type-1 ultrapure water.

2.2. Cell Lines. Cells used for all experiments were undifferentiated PC12 [27] and HepG2 cells [28], as previously published [29, 30].

PC12 cells were cultivated in 250 mL Greiner flasks with Dulbecco's modified Eagle medium (DMEM) (Gibco, Thermo Scientific) supplemented with 10% (*v*/*v*) fetal bovine serum (FBS), 5% horse serum (HS), and 1% antibiotics (penicillin, streptomycin, and G418). Twice a week, cells were split to maintain cell health and to prevent overgrowth.

HepG2 cells were cultivated in 250 mL Greiner flasks with Dulbecco's modified Eagle medium (DMEM) (Gibco, Thermo Scientific) supplemented with 10% (*v*/*v*) FBS, 5 U/mL penicillin, and 50 μg/mL streptomycin. Twice a week, cells were split to maintain cell health and to prevent overgrowth.

For experiments, cells were harvested from Greiner flasks, counted using a Neubauer chamber, and diluted to yield a cell suspension of 10^6 cells/mL. Cells were then transferred into 24-well (MMP, 2×10^5 cells/well) or 96-well plates (ATP, 10^5 cells/well for HepG2 and 2×10^5 cells/well for PC12 cells). Cells were allowed to attach for 48 h in reduced DMEM (2% FBS, 1% HS) before being exposed to SIL A in various concentrations. To assess the effect of SIL A on nitrosative stress, cells were incubated with 0.5 mM (PC12 cells) or 5 mM (HepG2) SNP 1 hour after SIL A exposure. After 24 h, cells were harvested.

2.3. Measurement of Mitochondrial Membrane Potential (MMP). MMP was measured using the fluorescence dye rhodamine-123 (R123). Cells of either cell line were incubated at 37°C and 5% CO_2 for 15 min with 0.4 μM R123. Cells were centrifuged at $750 \times g$ for 5 min before being washed with Hank's Balanced Salt Solution (HBSS) buffer (supplemented with Mg^{2+}, Ca^{2+}, and HEPES; pH 7.4; 37°C). Cells were suspended in fresh HBSS buffer before being assessed by the measurement of R123 fluorescence. The excitation wavelength was set to 490 nm and the emission wavelength to 535 nm (Victor X3 2030 multilabel counter, Perkin Elmer). The fluorescence was measured four times and normalized to the cell count or displayed relative to the control groups.

2.4. Measurement of ATP Concentrations. To assess the ATP concentrations, a bioluminescence kit ViaLight (Lonza), which is based on the production of light via the reaction of ATP with luciferin, was used. The 96-well plate was removed from the incubator and allowed to cool to room temperature for 10 min. Following incubation with lysis buffer for 10 min, cells were incubated for an additional 5 min with the monitoring reagent. The emitted light was assessed with a luminometer (Victor X3 2030 multilabel counter, Perkin Elmer). Since the emitted light is linearly related to the production of ATP, the concentration could be determined by a standard curve. The results were adjusted to the cell count or displayed relative to the control group.

2.5. High-Resolution Respirometry. The respiration of mitochondria was measured using an Oxygraph-2k respirometer (Oroboros) as described earlier [19]. For data evaluation, the software DatLab v. 4.3.2.7 was used. The protocol used to assess mitochondrial respiration was created by Gnaiger [31] and includes the addition of several substrates,

inhibitors, and uncouplers to a suspension of cells. Respiration is displayed in different stages of the experiment—(1) endogen: the endogenous respiration of cells; (2) Dig: the addition of 8 μM digitonin to disrupt cell membranes and remove naive substrates; (3) $CI_{(L)}$: respiration after the addition of 10 mM glutamate and 2 mM malate to compensate for proton leaks through the membrane; (4) $CI_{(P)}$: coupled complex I respiration after the addition of 2 mM ADP; (5) $CI\&CII_{(P)}$: maximal coupled CI and CII respiration after the addition of 10 mM succinate; (6) $CI\&CII_{(L)}$: leak respiration of CI and CII after the addition of 2 μg/mL oligomycin; (7) $CI\&CII_{(E)}$: maximal uncoupled CI and CII activity to compensate for increased proton transport into the matrix after the stepwise addition of carbonyl cyanide p-trifluoromethoxyphenylhydrazone (FCCP) up to a total concentration of 0.5 μM; (8) $CII_{(E)}$: uncoupled respiration using only CII substrates after CI inhibition via the addition of 0.5 μM rotenone; (9) $CIV_{(E)}$: maximal uncoupled respiration of CIV after the addition of 2.5 μM antimycin A, which inhibits complex III, as well as the addition of the electron-donator 0.5 mM *N,N,N′,N′*-tetramethyl-p-phenylenediamine dihydrochloride (TMPD) and 2 mM of the TMPD-regenerating agent ascorbate. The residual oxygen consumption of enzymes not part of the oxidative phosphorylation was measured after the addition of antimycin A and then subtracted from all stages of the experiment. The addition of 12 mM NaN_3 at the end of the experiment revealed the oxygen consumption due to the autoxidation of TMPD. This, as well as the residual oxygen consumption, was subtracted from $CIV_{(E)}$.

2.6. Citrate Synthase Activity. Cell samples from the respirometry measurements were frozen and stored at −80°C for the assessment of the citrate synthase activity. The samples were allowed to thaw while a reaction medium (0.1 mM 5,5′-dithio-bis-(2-nitrobenzoic acid) (DTNB), 0.5 mM oxaloacetate, 50 μM EDTA, 0.31 mM acetyl coenzyme A, 5 mM triethanolamine hydrochloride, and 0.1 M Tris-HCl) was mixed and heated to 30°C for 5 min. Afterwards, a volume of 200 μL of cells was added to the reaction medium, and the citrate synthase activity was determined spectrophotometrically at 412 nm. For statistical analysis, each sample was measured in triplicate.

2.7. Pyruvate and Lactate Contents. Frozen cells, which were previously harvested from 250 mL Greiner flasks after 4 days of growth and 1 day of incubation with 50 μM SIL A or control, were thawed to room temperature. Pyruvate and lactate concentrations were assessed using a pyruvate assay kit (MAK071, Sigma Aldrich) and a lactate assay kit (MAK064, Sigma Aldrich) according to the manufacturer's instructions. Absorbance was measured using a CLARIOstar plate reader (BMG Labtech).

2.8. Protein Content. Frozen cells were thawed, and protein contents were determined using a Pierce BCA Protein Assay Kit (Thermo Fisher Scientific) according to the manufacturer's instructions. Absorbance was measured using a CLARIOstar plate reader (BMG Labtech).

2.9. Statistics. Unless stated otherwise, data are presented as the means ± SEM. Statistical analysis was performed with either Student's *t*-test or one-way ANOVA followed by Tukey's post hoc test performed using GraphPad Prism version 8.0.1 for Windows (GraphPad Software).

3. Results

3.1. Comparison between Hepatic Cells and Neuronal Cells. Our data showed that mitochondrial parameters measured in hepatic HepG2 and in undifferentiated PC12 cells significantly differ from each other. The mitochondrial membrane potential (MMP) represents a driving force for complex V of the mitochondrial respiration chain (F_1/F_0-ATPase, CV) that produces ATP [32]. Thus, lower ATP levels in HepG2 cells (Figure 2(a)) may be explained by a reduced MMP in this cell line (Figure 2(b)). The complexes CII and CI&CII of the mitochondrial respiration chain in the coupled state were virtually identical in both cell lines (Figure 2(c)). However, HepG2 cells showed significantly increased activities of complexes CIV, CII, and CI&CII if uncoupled from the MMP using FCCP. This might be due to the significantly higher mitochondrial mass of HepG2 cells, as indicated by the increased citrate synthase activity (Figure 2(d)). Citrate synthase (CS) is an enzyme of the Krebs cycle that is located in the mitochondrial matrix. It represents a robust mitochondrial mass marker [33].

3.2. Silibinin's Effect on Adenosine Triphosphate Levels. Incubation of HepG2 cells with 25 μM and 50 μM SIL A for 24 hours showed a significant improvement on the basal ATP level (Figure 3(a)) ($p < 0.0001$). Incubation with 150 μM did not show an effect on ATP levels, and 500 μM significantly reduced ATP levels, indicating a toxic effect ($p < 0.0001$). To induce nitrosative stress, cells were incubated with 5 mM SNP 1 hour after incubation with SIL A. A concentration of 150 μM SIL A protected HepG2 cells from the SNP-induced drop in ATP levels (Figure 3(b)) ($p < 0.0001$). Lower concentrations, although beneficial to the basal ATP level, had no protective effect.

In PC12 cells, SIL A seemed to have little to no effect on basal ATP levels. Incubation of PC12 cells with 25 μM and 100 μM SIL A for 24 h showed no difference in ATP levels. However, cells treated with 50 μM SIL A showed a significant increase in ATP ($p = 0.0411$). Compared to HepG2 cells, PC12 cells seemed to be more vulnerable to SIL A, since incubation with 150 μM SIL A significantly reduced basal ATP levels ($p < 0.0298$). PC12 cells were also more vulnerable to nitrosative stress. When cells were incubated with 0.5 mM SNP, this significantly reduced ATP levels to around 20% (Figure 4(b)), similar to the result observed for 5 mM SNP in HepG2 cells. Incubation of cells with 25 μM, 50 μM ($p = 0.0003$), 100 μM ($p < 0.0001$), and 150 μM ($p < 0.0001$) SIL A 1 hour prior to SNP showed a concentration-dependent, protective effect in PC12 cells after 24 h (Figure 4(b)).

3.3. Mitochondrial Membrane Potential. Except for the concentration of 25 μM SIL A ($p = 0.0042$), basal MMP

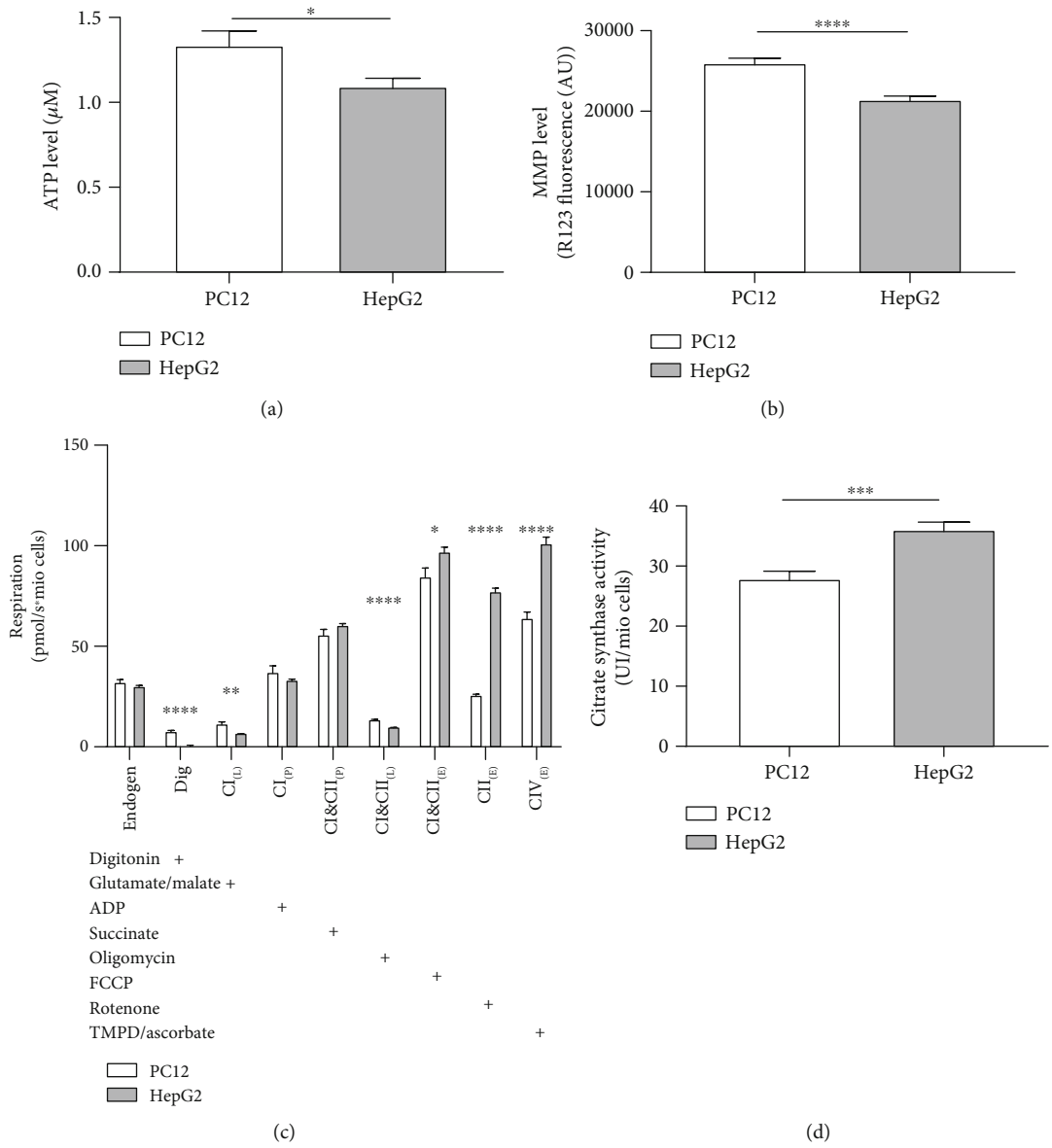

Figure 2: Comparison of mitochondrial function between untreated PC12 and untreated HepG2 cells. (a) Adenosine triphosphate (ATP) level of 10^4 cells of both cell lines. (b) Mitochondrial membrane potential (MMP) level of 2×10^4 cells of both cell lines. (c) Respiration of 10^6 cells of both cell lines. Activity of the oxidative phosphorylation (OXPHOS) complexes was assessed via the addition of several substrates, inhibitors, or uncouplers. Which substance was added in which stage of the experiment is indicated by the placement of "+." Dig = the addition of digitonin; $CI_{(L)}$ = leak respiration of complex I; $CI_{(P)}$ = coupled respiration using only complex I substrates; $CI\&CII_{(P)}$ = physiological respiration; $CI\&CII_{(L)}$ = leak respiration of complexes I and II; $CI\&CII_{(E)}$ = uncoupled respiration using maximum CI&CII activity; $CII_{(E)}$ = uncoupled respiration using complex II substrates only; $CIV_{(E)}$ = uncoupled respiration using only CIV after complex III inhibition and CIV activation using an electron donor. (d) Citrate synthase activity of 10^6 cells. The procedure for all experiments was the same as that employed for experiments treating cells with SIL A or DMSO, but instead of an effector, the cell medium was used. Data are displayed as the means ± SEM. $N = 7 - 18$. Statistical significance was tested via Student's t-test ($^{****}p < 0.0001$, $^{***}p < 0.001$, $^{**}p < 0.01$, and $^{*}p < 0.5$).

levels of HepG2 cells were unaffected by SIL A treatment (Figure 3(c)). Nitrosative stress was induced by incubation with 5 mM SNP 1 hour after incubation with SIL A. If cells were treated with 150 μM SIL A, the effect of SNP-induced stress could be significantly attenuated ($p < 0.0018$) (Figure 3(d)).

Incubation of PC12 cells with 25 μM, 50 μM, or 150 μM SIL A had no effect on the basal MMP. However, as can be seen in Figure 4(d), SIL A significantly reduced the damage caused by SNP-induced nitrosative stress (25 μM $p < 0.0487$, 50 μM $p < 0.0021$, and 150 μM $p < 0.0057$).

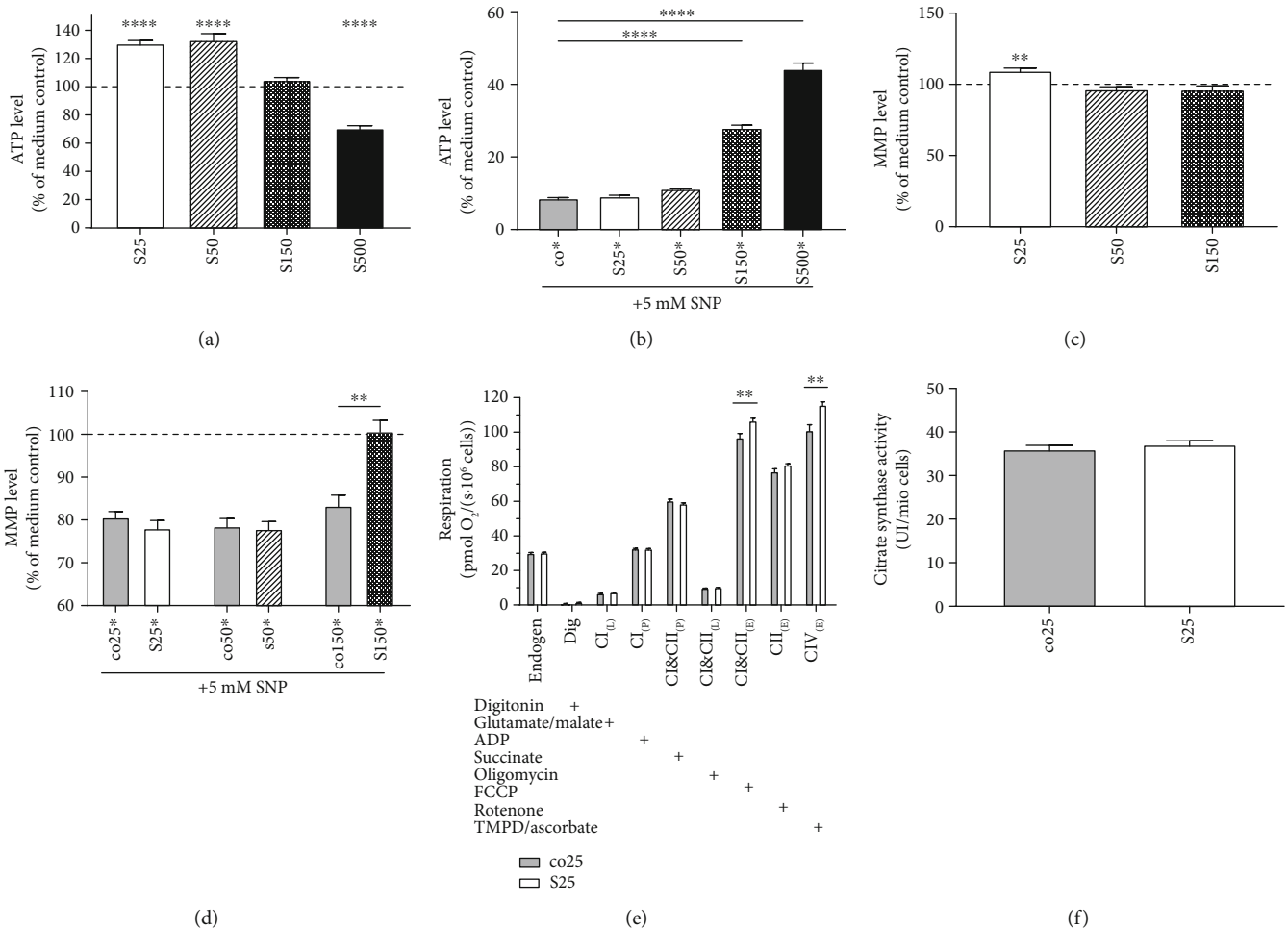

Figure 3: Effects of silibinin A (SIL A) on mitochondrial function in HepG2. (a) ATP level (% of medium control). Cells were incubated with SIL A (S) at different concentrations (25–150 μM) for 24 h and measured against control cells treated with DMSO (data not shown). DMSO results showed no significant difference compared to the medium control. (b) ATP level (% of medium control) of cells injured via the addition of 5 mM SNP 1 hour after the initial incubation with test substances. Cells were incubated for a total of 24 h. (c) MMP level (% of medium control). Cells were incubated with 50 or 150 μM SIL A for 24 h and measured against control cells treated with DMSO (data not shown). DMSO results showed no significant difference compared to the medium control. (d) MMP level (% of medium control) of cells injured via the addition of 5 mM SNP 1 hour after the initial incubation with test substances. Cells were incubated for a total of 24 h. (e) Respiration of HepG2 cells after 24 hours of incubation with the test substance or control. Measured data indicate the oxygen consumption of cells in an Oxygraph-2k (Oroboros). Cells were incubated with 25 μM SIL A (S) and compared against control cells treated with DMSO (co). Activity of OXPHOS complexes was assessed via the addition of several substrates, inhibitors, or uncouplers. Which substance was added in which stage of the experiment is indicated by the placement of "+." Dig = the addition of digitonin; $CI_{(L)}$ = leak respiration of complex I; $CI_{(P)}$ = coupled respiration using only complex I substrates; $CI\&CII_{(P)}$ = physiological respiration; $CI\&CII_{(L)}$ = leak respiration of complexes I and II; $CI\&CII_{(E)}$ = uncoupled respiration using maximum CI&CII activity; $CII_{(E)}$ = uncoupled respiration using complex II substrates only; $CIV_{(E)}$ = uncoupled respiration using only CIV after complex III inhibition and CIV activation using an electron donor. (f) Citrate synthases activity.Data are displayed as the means ± SEM. $N = 7 - 18$. Statistical significance was tested via one-way ANOVA and Tukey's post hoc test in (b). In (a, c–f), statistical significance was tested via Student's t-test of the treatment group versus the DMSO control ($^{****}p < 0.0001$, $^{***}p < 0.001$, $^{**}p < 0.01$, and $^{*}p < 0.5$).

3.4. Respiration. Incubation of HepG2 cells with 25 μM SIL A for 24 hours significantly enhanced the respiration of complexes CI&CII (in the uncoupled state) ($p = 0.0093$) and CIV (in the uncoupled state) ($p < 0.0045$) of the mitochondrial respiration chain (Figure 3(e)). In PC12 cells, SIL A had no effect on the oxygen consumption of the complexes in the oxidative phosphorylation system (Figure 4(e)).

3.5. Citrate Synthase Activity. Incubation with SIL A had no effect on HepG2 cells (Figure 3(f)) nor on PC12 cells (Figure 4(f)).

3.6. Effect of Silibinin on Glycolysis. Besides mitochondrial respiration, cells also produce ATP by glycolysis. Enhanced glycolysis might explain the enhanced ATP levels in PC12

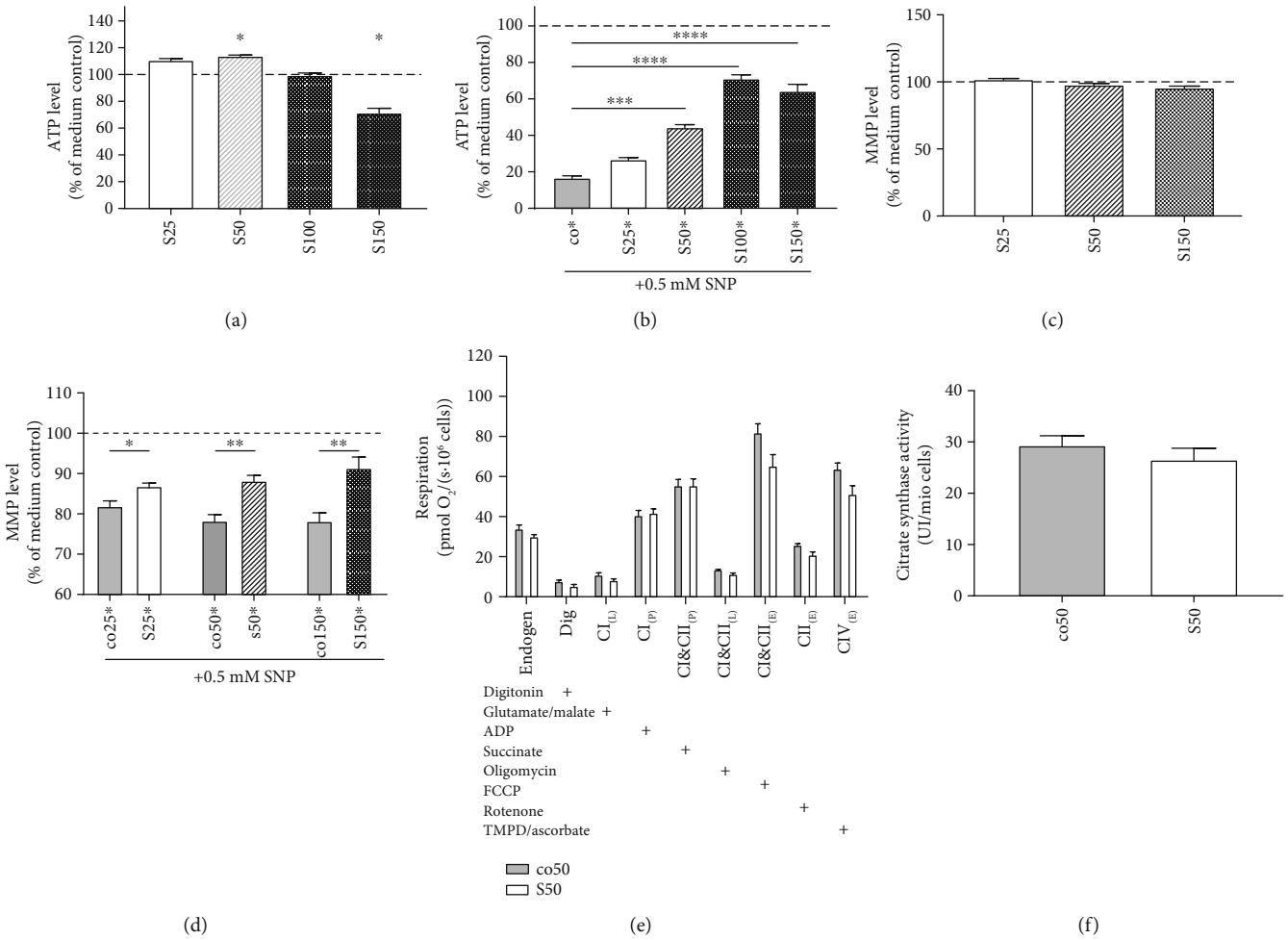

Figure 4: Effects of silibinin A (SIL A) on mitochondrial function in PC12 cells. (a) ATP level (% of medium control). Cells were incubated with SIL A (S) at different concentrations (25–150 μM) for 24 h and measured against control cells treated with DMSO (data not shown). DMSO results showed no significant difference compared to the medium control. (b) ATP level (% of medium control) of cells injured via the addition of 0.5 mM SNP 1 hour after the initial incubation with test substances. Cells were incubated for a total of 24 h. (c) MMP level (% of medium control). Cells were incubated with 25 or 150 μM SIL A for 24 h and measured against control cells treated with DMSO (data not shown). DMSO results showed no significant difference compared to the medium control. (d) MMP level (% of medium control) of cells injured via the addition of 0.5 mM SNP 1 hour after the initial incubation with test substances. Cells were incubated for a total of 24 h. (e) Respiration of PC12 cells after 24 hours of incubation with the test substance or control. Measured data show the oxygen consumption of cells in an Oxygraph-2k (Oroboros). Cells were incubated with 50 μM SIL A (S) and compared with control cells treated with DMSO (co). The activity of OXPHOS complexes was assessed via the addition of several substrates, inhibitors, or uncouplers. Which substance was added in which stage of the experiment is indicated by the placement of "+." Dig = the addition of digitonin; $CI_{(L)}$ = leak respiration of complex I; $CI_{(P)}$ = coupled respiration using only complex I substrates; $CI\&CII_{(P)}$ = physiological respiration; $CI\&CII_{(L)}$ = leak respiration of complexes I and II; $CI\&CII_{(E)}$ = uncoupled respiration using maximum CI&CII activity; $CII_{(E)}$ = uncoupled respiration using complex II substrates only; $CIV_{(E)}$ = uncoupled respiration using only CIV after complex III inhibition and CIV activation using an electron donor. (f) Citrate synthases activity. Data are displayed as the means ± SEM. $N = 6 - 12$. Statistical significance was tested via one-way ANOVA and Tukey's post hoc test in (b). In (a, c–f), statistical significance was tested via Student's t-test of the treatment group versus the DMSO control ($^{****}p < 0.0001$, $^{***}p < 0.001$, $^{**}p < 0.01$, and $^{*}p < 0.5$).

cells after SIL A incubation, although respiration was not changed (Figures 4(a) and 4(e)).

As seen in Table 1, neither pyruvate nor lactate levels were significantly affected by SIL A treatment in PC12 cells. However, in HepG2 cells, SIL A significantly reduced lactate concentrations ($p = 0.0007$) and a reducing trend of pyruvate levels was also shown. The ratio of pyruvate/lactate was not affected in either cell line.

4. Discussion

In hepatic HepG2 cells, SIL A enhanced the activity of respiratory complexes and subsequently may be responsible for an increase in the production of ATP. In PC12 cells, SIL A had no effect on respiration. However, treatment with SIL A tended to decrease the respiration of $CI\&CII_{(E)}$ and $CIV_{(E)}$ activity, whereas $CI\&CII_{(P)}$ activity was virtually identical in

Table 1: Pyruvate and lactate concentrations adjusted to the protein content of samples of either PC12 or HepG2 cells. Data are displayed as the means ± SEM. $N = 9$. Significance was tested via Student's t-test.

	Pyruvate/protein content (μmol/mg)	Lactate/protein content (μmol/mg)	Pyruvate/lactate ratio
PC12			
Control	0.4962 ± 0.05464	5.314 ± 0.8064	11.33 ± 0.6850
SIL A 50 μM	0.4883 ± 0.02037	5.056 ± 0.4885	10.91 ± 1.004
Significance	$p = 0.8942$	$p = 0.7888$	$p = 0.7420$
HepG2			
Control	0.5124 ± 0.04212	5.388 ± 0.1372	10.34 ± 0.7984
SIL A 50 μM	0.4487 ± 0.05332	4.515 ± 0.1336	10.92 ± 1.083
Significance	$p = 0.3677$	$^{***}p = 0.0007$	$p = 0.6728$

Table 2: Summary of the effects of silibinin on mitochondrial parameters in HepG2 and PC12 cells.

	Respiration	Basal MMP/+SNP	Basal ATP/+SNP	Citrate synthase activity	Glycolysis
HepG2	↑	↑/↑	↑↑/↑	↔	↓
PC12	↔	↔/↑↑	↑/↑↑	↔	↔

↑ indicates an increase, ↓ indicates a reduction, and ↔ indicates no change. SNP = sodium nitroprusside.

both groups. These findings suggest that SIL A did not affect the activity of both complexes. In HepG2 cells, on the other hand, we found a significant increase in $CI\&CII_{(E)}$ and $CIV_{(E)}$ activities. It has to be noted, however, that the uncoupling of the respiration chain from the MMP, indicating the maximum possible oxygen consumption, is an artificial state, which does not occur under normal cell conditions [34]. In an abundance of intramitochondrial ADP, $CI\&CII_{(P)}$ coupled respiration better reflects physiological respiration. This state, however, was unaffected by SIL A in both cell lines. Additionally, our results for citrate synthase activity as a marker for mitochondrial content [33, 35] showed that the increased ATP concentrations cannot be linked to increased mitochondrial mass.

Although there was no significance or trend for increased oxidative phosphorylation (OXPHOS) activity, we also did not find any indication of an impaired respiratory system. Since there have been multiple studies [36–38] showing an increased production of ROS following SIL A treatment and an impairment of respiration at high concentrations of ROS [25], our data showed that SIL A did not affect mitochondrial respiration in low concentrations. SIL A also had no influence on pyruvate or lactate concentrations, indicating that the glycolytic pathway was not affected by SIL A treatment. This is in agreement with the lack of inhibition of respiration in PC12 cells, as there is no compensatory activation of the glycolytic pathway, as found by Liemburg-Apers et al. in myoblasts with restricted respiration [39]. In HepG2 cells, we found a significant reduction in lactate levels, although pyruvate remained unchanged. This may indicate a compensatory downregulation of glycolysis induced by increased ATP levels. Our data showed that increased cellular ATP concentrations were not linked to the respiratory system. Although the underlying mechanisms are not yet identified, SIL A may affect different cellular processes linked to ATP use, as it may be mainly produced by the mitochondria, though used throughout the cell for a host of different bioenergetic processes.

As citrate synthase activity was not affected by SIL A treatment, mitochondrial biogenesis in PC12 and HepG2 cells might also not be altered by SIL A.

Table 2 shows that SNP-induced nitrosative stress caused severe damage to the mitochondria of hepatic and neuronal cells and significantly reduced MMP. Since it has been shown that higher concentrations of RNS can inhibit not only complex IV of the respiratory chain but also complexes I and III [26, 40], these results were expected. Further, these changes led to a decreased production of ATP at complex V. We used hepatic HepG2 cells due to their low expression of Cyp450 enzymes and thus their low metabolism of xenobiotics [41] to gain better insight into the effect of SIL A on the cells. However, in order to achieve similar damage, SNP concentrations differed tenfold between the two cell lines. Since the liver is characterized by a complex system eliminating ROS/RNS [42] and has increased resistance to toxins [43], it is difficult to compare both cell lines due to their metabolic differences. This is also reflected in the differences in mitochondrial parameters between the two cell lines shown in Figure 2. For example, we found a significant difference in mitochondrial mass, which was expected since hepatic mitochondria play an important role in the beta oxidation of lipids. As reported by Liu et al., we also found a strong protective effect of SIL A against nitrosative stress on both cell lines [15].

In PC12 cells, the attenuation of nitrosative stress already tended to appear at low concentrations of 25 μM, while in hepatic cells, no effect could be found below 150 μM. These significant effects could be explained by findings that silibinin is a potent scavenger for a host of free radicals *in situ* [44]. Furthermore, SIL A has been found to increase superoxide

dismutases (SOD) and glutathione peroxidase (GPx) activity in human erythrocytes [45]. Liu et al. found that treatment with SIL A generated increased levels of ROS, activating anti-apoptotic pathways and therefore protecting against SNP-induced damages [15]. Since ROS also plays a key role in the balance of free radicals and scavengers, potentially increasing oxidative stress, concentrations that are too high lead to toxic effects. Our data are in support of this assumption, as we observed toxic effects on basal ATP levels at a concentration of 150 μM in PC12 cells and a concentration of 500 μM in HepG2 cells. This agrees with the results of Matsuo et al., who also found toxic levels of ROS due to the application of high flavonoid concentrations in human cells [46, 47]. It should be noted, however, that although 500 μM SIL A had a toxic effect on basal ATP, the protective effects against SNP-induced damage still increased compared to 150 μM SIL A.

Lower concentrations of 25 μM and 50 μM SIL A attenuated nitrosative damages as well as increased basal levels of ATP. These concentrations are similar to the unconjugated SIL A concentrations found in the plasma of rats (18 μM) after the oral administration of 500 mg/kg SIL A [48]. In humans, however, SIL A is best administered as silibinin-phosphatidylcholine complex, resulting in a mean plasma concentration of 75 μM in human cancer patients [49].

In conclusion, we report that effective concentrations of SIL A attenuated nitrosative stress in both PC12 and HepG2 cells. Furthermore, low concentrations of SIL A improved basal MMP and ATP levels in HepG2 cells, though less so in PC12 cells. SIL A enhanced uncoupled mitochondrial respiration in HepG2 cells but did not affect the mitochondrial content of either cell line. Based on our findings that SIL A protects against SNP-induced nitrosative stress at the level of mitochondria, we conclude that SIL A might be beneficial against neurological disorders although it did not provide a general improvement of the mitochondrial function.

Data Availability

The dataset generated during this study is available from the corresponding author upon reasonable request.

Conflicts of Interest

The authors declare no conflict of interest.

References

[1] N. D. Scott Luper, "A review of plants used in the treatment of liver disease: part 1," *Alternative Medicine Review*, vol. 3, no. 6, pp. 410–421, 1998.

[2] F. Fraschini, G. Demartini, and D. Esposti, "Pharmacology of silymarin," *Clinical Drug Investigation*, vol. 22, no. 1, pp. 51–65, 2002.

[3] A. Mansouri, C.-H. Gattolliat, and T. Asselah, "Mitochondrial dysfunction and signaling in chronic liver diseases," *Gastroenterology*, vol. 155, no. 3, pp. 629–647, 2018.

[4] C. García-Ruiz, A. Baulies, M. Mari, P. M. García-Rovés, and J. C. Fernandez-Checa, "Mitochondrial dysfunction in non-alcoholic fatty liver disease and insulin resistance: cause or consequence?," *Free Radical Research*, vol. 47, no. 11, pp. 854–868, 2013.

[5] G. Vecchione, E. Grasselli, F. Cioffi et al., "The nutraceutic silybin counteracts excess lipid accumulation and ongoing oxidative stress in an in vitro model of non-alcoholic fatty liver disease progression," *Frontiers in Nutrition*, vol. 4, p. 42, 2017.

[6] G. Serviddio, F. Bellanti, E. Stanca et al., "Silybin exerts antioxidant effects and induces mitochondrial biogenesis in liver of rat with secondary biliary cirrhosis," *Free Radical Biology & Medicine*, vol. 73, pp. 117–126, 2014.

[7] F. Salamone, F. Galvano, F. Cappello, A. Mangiameli, I. Barbagallo, and G. L. Volti, "Silibinin modulates lipid homeostasis and inhibits nuclear factor kappa B activation in experimental nonalcoholic steatohepatitis," *Translational Research*, vol. 159, no. 6, pp. 477–486, 2012.

[8] Q. Ou, Y. Weng, S. Wang et al., "Silybin alleviates hepatic steatosis and fibrosis in NASH mice by inhibiting oxidative stress and involvement with the Nf-κB pathway," *Digestive Diseases and Sciences*, vol. 63, no. 12, pp. 3398–3408, 2018.

[9] H. Farghali, L. Kameniková, S. Hynie, and E. Kmonicková, "Silymarin effects on intracellular calcuim and cytotoxicity: a study in perfused rat hepatocytes after oxidative stress injury," *Pharmacological Research*, vol. 41, no. 2, pp. 231–237, 2000.

[10] S. Lama, D. Vanacore, N. Diano et al., "Ameliorative effect of silybin on bisphenol A induced oxidative stress, cell proliferation and steroid hormones oxidation in HepG2 cell cultures," *Scientific Reports*, vol. 9, no. 1, p. 3228, 2019.

[11] C. Stockburger, S. Eckert, G. P. Eckert, K. Friedland, and W. E. Müller, "Mitochondrial function, dynamics, and permeability transition: a complex love triangle as a possible target for the treatment of brain aging and Alzheimer's disease," *Journal of Alzheimer's Disease*, vol. 64, no. s1, pp. S455–S467, 2018.

[12] K. Friedland-Leuner, C. Stockburger, I. Denzer, G. P. Eckert, and W. E. Müller, "Mitochondrial dysfunction: cause and consequence of Alzheimer's disease," *Progress in Molecular Biology and Translational Science*, vol. 127, pp. 183–210, 2014.

[13] T. Briston and A. R. Hicks, "Mitochondrial dysfunction and neurodegenerative proteinopathies: mechanisms and prospects for therapeutic intervention," *Biochemical Society Transactions*, vol. 46, no. 4, pp. 829–842, 2018.

[14] Y. Lee, H. R. Park, H. J. Chun, and J. Lee, "Silibinin prevents dopaminergic neuronal loss in a mouse model of Parkinson's disease via mitochondrial stabilization," *Journal of Neuroscience Research*, vol. 93, no. 5, pp. 755–765, 2015.

[15] B. Liu, P. Yang, Y. Ye et al., "Role of ROS in the protective effect of silibinin on sodium nitroprusside-induced apoptosis in rat pheochromocytoma PC12 cells," *Free Radical Research*, vol. 45, no. 7, pp. 835–847, 2011.

[16] H.-H. Jiang, F.-S. Yan, L. Shen, and H.-F. Ji, "Silymarin versus silibinin: differential antioxidant and neuroprotective effects against H2O2-induced oxidative stress in PC12 cells," *Natural Product Communications*, vol. 11, no. 5, p. 1934578X1601100, 2016.

[17] S. Schramm, G. Huang, S. Gunesch et al., "Regioselective synthesis of 7- _O_ -esters of the flavonolignan silibinin and SARs lead to compounds with overadditive neuroprotective effects," *European Journal of Medicinal Chemistry*, vol. 146, pp. 93–107, 2018.

[18] D.-H. Bak, H. D. Kim, Y. O. Kim, C. G. Park, S.-Y. Han, and J.-J. Kim, "Neuroprotective effects of 20(S)-protopanaxadiol against glutamate-induced mitochondrial dysfunction in

PC12 cells," *International Journal of Molecular Medicine*, vol. 37, no. 2, pp. 378–386, 2016.

[19] S. Hagl, D. Berressem, B. Bruns, N. Sus, J. Frank, and G. P. Eckert, "Beneficial effects of ethanolic and hexanic rice bran extract on mitochondrial function in PC12 cells and the search for bioactive components," *Molecules*, vol. 20, no. 9, pp. 16524–16539, 2015.

[20] V. Waetzig, J. Riffert, J. Cordt et al., "Neurodegenerative effects of azithromycin in differentiated PC12 cells," *European Journal of Pharmacology*, vol. 809, pp. 1–12, 2017.

[21] C.-W. Phan, V. Sabaratnam, P. Bovicelli, G. Righi, and L. Saso, "Negletein as a neuroprotectant enhances the action of nerve growth factor and induces neurite outgrowth in PC12 cells," *BioFactors*, vol. 42, no. 6, pp. 591–599, 2016.

[22] W. Liu, S. Kong, Q. Xie et al., "Protective effects of apigenin against 1-methyl-4-phenylpyridinium ion-induced neurotoxicity in PC12 cells," *International Journal of Molecular Medicine*, vol. 35, no. 3, pp. 739–746, 2015.

[23] Y.-C. Shen, C.-W. Juan, C.-S. Lin, C.-C. Chen, and C.-L. Chang, "Neuroprotective effects of terminalia chebubal extracts and ellagic acid in PC12 cells," *African Journal of Traditional, Complementary and Alternative medicines*, vol. 14, no. 4, pp. 22–30, 2017.

[24] F. Jiménez-Jiménez, H. Alonso-Navarro, M. Herrero, E. García-Martín, and J. Agúndez, "An update on the role of nitric oxide in the neurodegenerative processes of Parkinson's disease," *Current Medicinal Chemistry*, vol. 23, no. 24, pp. 2666–2679, 2016.

[25] D. C. Liemburg-Apers, P. H. G. M. Willems, W. J. H. Koopman, and S. Grefte, "Interactions between mitochondrial reactive oxygen species and cellular glucose metabolism," *Archives of Toxicology*, vol. 89, no. 8, pp. 1209–1226, 2015.

[26] A. M. Lenkiewicz, G. A. Czapski, H. Jęsko et al., "Potent effects of alkaloid-rich extract from Huperzia selago against sodium nitroprusside-evoked PC12 cells damage via attenuation of oxidative stress and apoptosis," *Folia Neuropathologica*, vol. 2, pp. 156–166, 2016.

[27] L. A. Greene and A. S. Tischler, "Establishment of a noradrenergic clonal line of rat adrenal pheochromocytoma cells which respond to nerve growth factor," *Proceedings of the National Academy of Sciences*, vol. 73, no. 7, pp. 2424–2428, 1976.

[28] D. P. Aden, A. Fogel, S. Plotkin, I. Damjanov, and B. B. Knowles, "Controlled synthesis of HBsAg in a differentiated human liver carcinoma- derived cell line," *Nature*, vol. 282, no. 5739, pp. 615-616, 1979.

[29] S. Hagl, A. Kocher, C. Schiborr, N. Kolesova, J. Frank, and G. P. Eckert, "Curcumin micelles improve mitochondrial function in neuronal PC12 cells and brains of NMRI mice - impact on bioavailability," *Neurochemistry International*, vol. 89, pp. 234–242, 2015.

[30] A. Irías-Mata, N. Sus, S. Flory et al., "α-Tocopherol transfer protein does not regulate the cellular uptake and intracellular distribution of α\- and γ-tocopherols and -tocotrienols in cultured liver cells," *Redox Biology*, vol. 19, pp. 28–36, 2018.

[31] E. Gnaiger, *Mitochondrial pathways and respiratory control: an introduction to OXPHOS analysis*, Mitochondr Physiol Network 19.12. OROBOROS MiPNet Publications, Innsbruck, 2014.

[32] M. Pohland, M. Pellowska, H. Asseburg et al., "MH84 improves mitochondrial dysfunction in a mouse model of early Alzheimer's disease," *Alzheimer's Research & Therapy*, vol. 10, no. 1, p. 18, 2018.

[33] S. Larsen, J. Nielsen, C. N. Hansen et al., "Biomarkers of mitochondrial content in skeletal muscle of healthy young human subjects," *The Journal of Physiology*, vol. 590, no. 14, pp. 3349–3360, 2012.

[34] L. G. J. Nijtmans, C. Ugalde, and L. P. van den Heuvel, "Smeitink JAM. Function and dysfunction of the oxidative phosphorylation system," in *Mitochondrial Function and Biogenesis*, C. M. Koehler and M. F. Bauer, Eds., vol. 8, pp. 149–176, Springer, Berlin, 2004.

[35] S. D. Hughes, M. Kanabus, G. Anderson et al., "The ketogenic diet component decanoic acid increases mitochondrial citrate synthase and complex I activity in neuronal cells," *Journal of Neurochemistry*, vol. 129, no. 3, pp. 426–433, 2014.

[36] S. Fan, M. Qi, Y. Yu et al., "P53 activation plays a crucial role in silibinin induced ROS generation via PUMA and JNK," *Free Radical Research*, vol. 46, no. 3, pp. 310–319, 2012.

[37] J. Ham, W. Lim, F. W. Bazer, and G. Song, "Silibinin stimluates apoptosis by inducing generation of ROS and ER stress in human choriocarcinoma cells," *Journal of Cellular Physiology*, vol. 233, no. 2, pp. 1638–1649, 2018.

[38] N. Zheng, L. Liu, W. W. Liu et al., "Crosstalk of ROS/RNS and autophagy in silibinin-induced apoptosis of MCF-7 human breast cancer cells _in vitro_," *Acta Pharmacologica Sinica*, vol. 38, no. 2, pp. 277–289, 2017.

[39] D. C. Liemburg-Apers, T. J. J. Schirris, F. G. M. Russel, P. H. G. M. Willems, and W. J. H. Koopman, "Mitoenergetic dysfunction triggers a rapid compensatory increase in steady- state glucose flux," *Biophysical Journal*, vol. 109, no. 7, pp. 1372–1386, 2015.

[40] T. R. Figueira, M. H. Barros, A. A. Camargo et al., "Mitochondria as a source of reactive oxygen and nitrogen species: from molecular mechanisms to human health," *Antioxidants & Redox Signaling*, vol. 18, no. 16, pp. 2029–2074, 2013.

[41] M. Gomez-Lechon, M. Donato, A. Lahoz, and J. Castell, "Cell lines: a tool for in vitro drug metabolism studies," *Current Drug Metabolism*, vol. 9, no. 1, pp. 1–11, 2008.

[42] S. Li, H.-Y. Tan, N. Wang et al., "The role of oxidative stress and antioxidants in liver diseases," *International Journal of Molecular Sciences*, vol. 16, no. 11, pp. 26087–26124, 2015.

[43] A. Rowland, J. O. Miners, and P. I. Mackenzie, "The UDP-glucuronosyltransferases: their role in drug metabolism and detoxification," *The International Journal of Biochemistry & Cell Biology*, vol. 45, no. 6, pp. 1121–1132, 2013.

[44] H. Fu, M. Lin, Y. Muroya et al., "Free radical scavenging reactions and antioxidant activities of silybin: mechanistic aspects and pulse radiolytic studies," *Free Radical Research*, vol. 43, no. 9, pp. 887–897, 2009.

[45] I. Altorjay, L. Dalmi, B. Sári, S. Imre, and G. Balla, "The effect of silibinin (Legalon) on the the free radical scavenger mechanisms of human erythrocytes in vitro," *Acta Physiologica Hungarica*, vol. 80, no. 1-4, pp. 375–380, 1992.

[46] M. Matsuo, N. Sasaki, K. Saga, and T. Kaneko, "Cytotoxicity of flavonoids toward cultured normal human cells," *Biological & Pharmaceutical Bulletin*, vol. 28, no. 2, pp. 253–259, 2005.

[47] D. Procházková, I. Boušová, and N. Wilhelmová, "Antioxidant and prooxidant properties of flavonoids," *Fitoterapia*, vol. 82, no. 4, pp. 513–523, 2011.

[48] J.-W. Wu, L.-C. Lin, S.-C. Hung, C.-W. Chi, and T.-H. Tsai, "Analysis of silibinin in rat plasma and bile for hepatobiliary excretion and oral bioavailability application," *Journal of Pharmaceutical and Biomedical Analysis*, vol. 45, no. 4, pp. 635–641, 2007.

[49] T. W. Flaig, D. L. Gustafson, L.-J. Su et al., "A phase I and pharmacokinetic study of silybin-phytosome in prostate cancer patients," *Investigational New Drugs*, vol. 25, no. 2, pp. 139–146, 2007.

Hindawi
Oxidative Medicine and Cellular Longevity
Volume 2019, Article ID 3642491, 22 pages
https://doi.org/10.1155/2019/3642491

Review Article

The Importance of Natural Antioxidants in the Treatment of Spinal Cord Injury in Animal Models: An Overview

Angélica Coyoy-Salgado,[1] **Julia J. Segura-Uribe**,[2] **Christian Guerra-Araiza**,[3] **Sandra Orozco-Suárez**,[2] **Hermelinda Salgado-Ceballos**,[2] **Iris A. Feria-Romero**,[2] **Juan Manuel Gallardo**,[4] **and Carlos E. Orozco-Barrios**[1]

[1]*CONACyT-Unidad de Investigación Médica en Enfermedades Neurológicas, Hospital de Especialidades Dr. Bernardo Sepúlveda, Centro Médico Nacional Siglo XXI, Instituto Mexicano del Seguro Social, Mexico City, Mexico*
[2]*Unidad de Investigación Médica en Enfermedades Neurológicas, Hospital de Especialidades Dr. Bernardo Sepúlveda, Centro Médico Nacional Siglo XXI, Instituto Mexicano del Seguro Social, Mexico City, Mexico*
[3]*Unidad de Investigación Médica en Farmacología, Hospital de Especialidades Dr. Bernardo Sepúlveda, Centro Médico Nacional Siglo XXI, Instituto Mexicano del Seguro Social, Mexico City, Mexico*
[4]*Unidad de Investigación Médica en Enfermedades Nefrológicas, Hospital de Especialidades Dr. Bernardo Sepúlveda, Centro Médico Nacional Siglo XXI, Instituto Mexicano del Seguro Social, Mexico City, Mexico*

Correspondence should be addressed to Angélica Coyoy-Salgado; acoyoys@gmail.com
and Carlos E. Orozco-Barrios; crls2878@gmail.com

Received 31 May 2019; Accepted 4 October 2019; Published 12 November 2019

Guest Editor: João C. M. Barreira

Patients with spinal cord injury (SCI) face devastating health, social, and financial consequences, as well as their families and caregivers. Reducing the levels of reactive oxygen species (ROS) and oxidative stress are essential strategies for SCI treatment. Some compounds from traditional medicine could be useful to decrease ROS generated after SCI. This review is aimed at highlighting the importance of some natural compounds with antioxidant capacity used in traditional medicine to treat traumatic SCI. An electronic search of published articles describing animal models of SCI treated with natural compounds from traditional medicine was conducted using the following terms: Spinal Cord Injuries (MeSH terms) AND Models, Animal (MeSH terms) AND [Reactive Oxygen Species (MeSH terms) AND/OR Oxidative Stress (MeSH term)] AND Medicine, Traditional (MeSH terms). Articles reported from 2010 to 2018 were included. The results were further screened by title and abstract for studies performed in rats, mice, and nonhuman primates. The effects of these natural compounds are discussed, including their antioxidant, anti-inflammatory, and antiapoptotic properties. Moreover, the antioxidant properties of natural compounds were emphasized since oxidative stress has a fundamental role in the generation and progression of several pathologies of the nervous system. The use of these compounds diminishes toxic effects due to their high antioxidant capacity. These compounds have been tested in animal models with promising results; however, no clinical studies have been conducted in humans. Further research of these natural compounds is crucial to a better understanding of their effects in patients with SCI.

1. Introduction

Spinal cord injury (SCI) is a life-disrupting condition associated with high mortality and long-term morbidity, which may provoke severe consequences to patients, such as paraplegia or quadriplegia, and frequently continues as a terminal condition. According to the National SCI Statistical Center, an annual incidence of 17,500 new SCI cases is estimated. Since it is a frequent and severe motor injury, it becomes a potential economic, social, and family burden. In 2017, between 245,000 and 353,000 patients with SCI were alive in the United States, with an estimated lifetime cost of $1.6-$4.8M per patient [1].

Among the leading causes of SCI are traffic and sports accidents, as well as falls and violence. Traumatic SCI

occurrence shows a peak between the ages of 15 and 29 years and another peak over the age of 65 years, with an incidence rate of 3–4 times higher in males [2, 3]. Depending on the severity of the lesion, patients show neurological deficits, which can range from loss of sensation to death, including paralysis, impaired bowel, bladder, and sexual function, as well as autonomic dysfunction [4–7].

Natural antioxidants are used as an alternative treatment for some neuropathologies, including SCI. This review is aimed at providing an overview of various natural compounds that produce beneficial effects for the treatment of SCI in animal models. Furthermore, the differences between animal responses to these various compounds are addressed to establish a better understanding of the cellular and molecular mechanisms occurring in the spinal cord following injury.

2. Pathophysiology of SCI

SCI can be divided into primary, secondary, and chronic phases [8, 9]. The first phase is the result of the physical forces involved in the initial traumatic event, which commonly are the most critical elements of injury severity. These forces include compression, shearing, laceration, and acute stretch/distraction [10]. After the initial injury, a cascade of subsequent events is initiated. In this second phase, the injury expands and neurological deficits and outcomes are exacerbated [11, 12]. Secondary SCI is a delayed and progressive injury following the first damage. Finally, a chronic phase, begins days to years after the injury, leading to neurological impairments in both orthograde and retrograde directions, including some brain regions [13, 14].

During the secondary cascade, some vascular changes are observed [15]. Furthermore, neutrophils and macrophages release superoxide anion and hydrogen peroxide as a means to sterilize the injury site. Infiltrating activated hematogenous phagocytic cells and tissue macrophages generate massive quantities of superoxide anion by nicotinamide adenine dinucleotide phosphate (NADPH) oxidase as its primary source [16].

In addition, phagocytic inflammatory cells release reactive oxygen species (ROS). Free radicals react with polyunsaturated fatty acids leading to peroxidation and disruption of the typical phospholipid architecture of cellular and subcellular organelle membranes. Moreover, lipid peroxidation generates aldehyde products that impair the function of key metabolic enzymes, such as Na^+/K^+-ATPase [17].

SCI is generally characterized by an increase in cytokines, such as TNF-α, IL-1β, and IL-6 that lead to upregulation of inflammatory and apoptotic agents, including NF-κB, AP-1, JNK, p38 MAPK, and PGE2 [3].

After SCI, an upregulated liberation of excitatory amino acids, such as glutamate and aspartate, is observed due to the release from disrupted cells [18–20].

Finally, in the chronic phase, the glial scar, which is integrated by reactive astrocytes, microglia/macrophages, and extracellular matrix molecules—chondroitin sulfate proteoglycans in particular—prevents axon growth through it by acting as a physical barrier [21–25].

Consequently, it becomes necessary to develop reliable strategies and treatments for SCI patients. An essential strategy for SCI treatment is the reduction of ROS levels, which could be carried out using antioxidants or compounds that regulate ROS or modify their signaling pathways [26, 27].

3. ROS Production and Spinal Cord Injury

3.1. Oxidative and Nitrosative Stress. The homeostasis of redox mechanisms in the spinal cord is maintained in balance. However, under adverse conditions such as neurodegenerative diseases or traumas, this balance is altered. The group of biochemical and molecular reactions following SCI is called secondary damage. The most extensively studied and accepted mechanism of secondary damage is the injury produced by oxidative and nitrosative stress [28].

The essential molecule within oxidative stress is the superoxide ($O_2^{\cdot-}$) radical, which is produced by the reduction of an electron in an O_2 molecule. This radical has ambivalent functions: it can act as an oxidizing or reducing agent. Despite being considered a modestly reactive free radical, it can react with other molecules to generate more reactive free radicals (Figure 1(a)). For example, the nitric oxide ($^{\cdot}NO$) radicals produce peroxynitrite ($ONOO^-$), which has a higher oxidation potencial. Consecutively, the $ONOO^-$ radical can be protonated to form peroxynitrous acid (ONOOH), which in turn can be decomposed into two highly reactive molecules, nitrogen oxide and hydroxyl radical ($^{\cdot}NO_2$ and $^{\cdot}OH$). Furthermore, the $ONOO^-$ radical interacts with carbon dioxide (CO_2) as well, to produce nitrosoperoxycarbonate ($ONOOCO_2$), which decomposes into nitrogen oxide and carbonate ($^{\cdot}CO_3$) radical (Figure 1(b)) [29].

Moreover, $O_2^{\cdot-}$ can be dismuted by the superoxide dismutase (SOD) enzyme to form hydrogen peroxide (H_2O_2) in the presence of Fe^{2+}, which is later oxidized to Fe^{3+}, $^{\cdot}OH$ and OH^- (Fenton reaction). Fe^{3+} is released from its transporter and storage proteins (transferrin and ferritin, respectively) by pH acidification due to the traumatic impact (Figure 1(a)). Additionally, Fe is also released by the hemoglobin resulting from trauma [30].

3.2. Lipid Peroxidation. Lipid peroxidation (LP) is the oxidative degradation of unsaturated fatty acids, such as arachidonic acid, linoleic acid, eicosapentaenoic acid, and docosahexaenoic acid, by the action of oxygen-free radicals, which causes disruptions in the integrity of the cell membrane [31].

This process is carried out in three stages: initiation, propagation, and termination. The initiation phase occurs when a free radical ($^{\cdot}R$) attacks and removes hydrogen along with its single electron from an allylic carbon of the fatty acid (LH), generating an alkyl radical ($^{\cdot}L$). The propagation phase starts with the participation of O_2 to form the peroxyl radical ($^{\cdot}LOO$). Subsequently, the radical $^{\cdot}LOO$ reacts with another fatty acid converting it into another alkyl radical $^{\cdot}L$ and LOOH, propagating the oxidative state in a series of chain reactions leading to the destabilization of the membrane

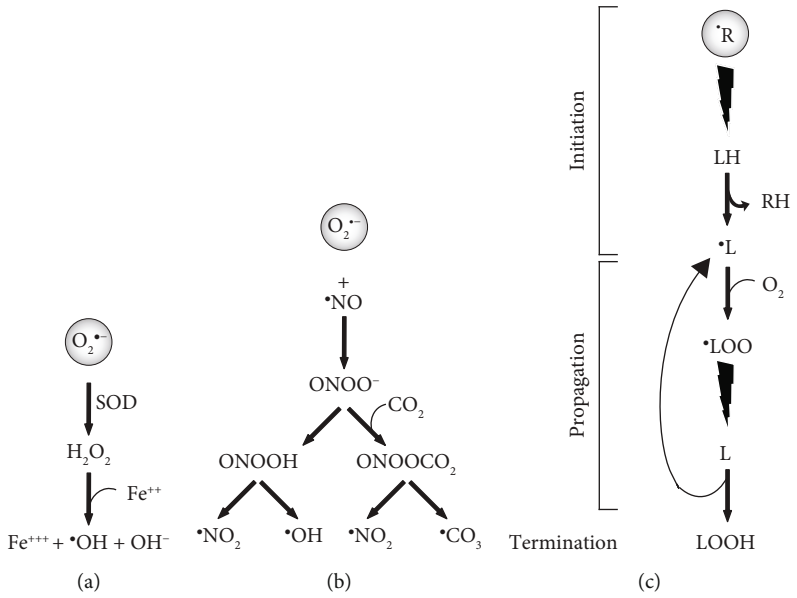

Figure 1: Main pathways of ROS and NOS in the central nervous system. (a) Fenton reaction; (b) peroxynitrite reaction; (c) lipid peroxidation. $O_2^{\bullet-}$: superoxide radical; SOD: superoxide dismutase; H_2O_2: hydrogen peroxide; Fe^{++}: ferrous iron; Fe^{+++}: ferric iron; ${}^{\bullet}OH$: hydroxyl radical; OH-: hydroxyl anion; ${}^{\bullet}NO$: nitric oxide or nitrogen monoxide; ${}^{\bullet}NO_2$: nitrogen dioxide; ONOO-: peroxynitrite anion; CO_2: carbon dioxide; ONOOH: peroxynitrous acid; $ONOOCO_2$: nitrosoperoxocarbonate; ${}^{\bullet}CO_3$: carbonate radical; ${}^{\bullet}R$: free radical; RH: neutralized radical; LH: polyunsaturated fatty acid; ${}^{\bullet}L$: alkyl radical; O_2: molecular oxygen; ${}^{\bullet}LOO$: peroxyl radical; LOOH: lipid hydroperoxide.

(Figure 1(c)). These reactions are terminated by the depletion of substrates, encountering another radical or a scavenger and ending with nonradical molecules. Within this group of reactions, a couple of toxic aldehyde products, 4-hydroxynonenal (4-HNE) and 2-propenal (acrolein), are generated. The toxicity of 4-HNE and acrolein lies in their ability to bind to protein amino acids, altering their structure and function.

In contrast, another nontoxic product, malondialdehyde (MDA), together with the quantification of 4-HNE and acrolein, is widely used to measure LP levels. These markers have allowed the characterization of the LP in SCI models [32–34].

LP is an event that appears within the first 30 minutes after SCI and increases considerably from the first hour to a maximum point three hours after the SCI in a contusion model [35].

Another type of damage is caused by the ${}^{\bullet}NO$ radical which, as mentioned above, reacts with the radical $O_2^{\bullet-}$ producing the $ONOO^-$ radical. This radical produces the nitration of proteins when interacting with the amino acid tyrosine, generating posttranslational modifications by converting tyrosine into 3-nitrotyrosine (3-NT). 3-NT is used as a biological marker of the action of $ONOO^-$ [36] and has been detected within the first hour after the injury and for several days. Nitric oxide synthase (NOS) in all its isoforms, including a mitochondrial variant, is responsible for the production of the radical ${}^{\bullet}NO$. The expression of nNOS increases in the CNS after a traumatic injury [37].

4. Effects of Natural Antioxidant Compounds on SCI

Medicinal plants have been used for thousands of years. Herbs, roots, bulbs, and fruits contain different compounds which act as therapeutic ingredients [38]. Recently, traditional medicine has been the focus of attention in the treatment of some diseases, including SCI [39].

Due to their antioxidant characteristics and ROS modulation properties, many natural compounds could be useful to reduce ROS generated in the SCI (Table 1). For that reason, it is vital to study the mechanisms of action through which they perform their effects. Therefore, some examples of antioxidant compounds found in several plant species used as SCI treatment are described and discussed as follows.

4.1. Extracts from Leaves

4.1.1. Asiatic Acid. Traditional Chinese medicine has offered many proposals, including asiatic acid (AA) and other compounds. AA is extracted from the Chinese herb *Centella asiatica*. It is a pentacyclic triterpenoid compound with anti-inflammatory, hepatoprotective, cardioprotective, neuroprotective, gastroprotective, and anticancer properties [40].

AA was proposed as SCI treatment for its therapeutic potential. Promising results were observed in the model used, in which Sprague-Dawley rats with induced SCI responded to the treatment: scores increased in the tests evaluated, Basso, Beattie, and Bresnahan (BBB) and inclined plane. Also, AA reduced myeloperoxidase activity, as well as interleukin-1β (IL-1β), interleukin-18 (IL-18), interleukin-6 (IL-6), tumor necrosis factor-α (TNF-α), ROS, H_2O_2, and MDA levels. Moreover, the activity of superoxide dismutase (SOD) and the content of glutathione (GSH) increased with AA [41].

The mechanism of AA involves the activation of the nuclear factor- (erythroid-derived 2-) like-2 factor (Nrf2), a cytoprotective factor that regulates the expression of genes

Table 1: Antioxidant mechanisms and effects of natural compounds or extracts on SCI models.

Compound or extract	Plant species	Origin	Effects on SCI models	Antioxidant mechanisms	References
From leaves					
Asiatic acid (AA)	*Centella asiatica*	China	Improves scores in locomotion tests Anti-inflammatory and antioxidant properties	Increases SOD activity and GSH content	[41–44]
Ligustilide (LIG)	*Radix angelicae sinensis Ligusticum chuanxiong*	China	Neuroprotective, cardiovascular, anti-inflammatory, and antioxidant effects	Scavenger, significantly suppresses iROS and iNOS expression Inhibits PLCγ and increases PI levels	[49, 50]
Tetramethylpyrazine (TMP)	*Ligusticum wallichii Franchat*	China	Neuroprotective effects Anti-inflammatory properties	Increases GSH levels and SOD activity, activates the Akt/Nrf2/HO-1 pathway	[55–60]
Epigallocatechin-3-gallate (EGCG)	*Camellia sinensis* (green tea)	China Japan Korea	Improves motor function Relieves neuropathic pain Anti-inflammatory and antioxidant properties	Increases GR and MDA levels and reduces myeloperoxidase and iNOS activity	[67, 68, 70, 77]
Ginsenosides	*Panax ginseng* C.A. Meyer	Asia	Neuroprotective effects Antioxidant properties	Enhances the Nrf2/Ho-1 pathway and antioxidant proteins, decreases COX-2 and iNOS expression	[80–85]
Panax notoginsenoside (PNS)	*Panax notoginseng* (sachi ginseng)	China Burma Nepal	Anti-inflammatory, antioxidant, neuroprotective, and antiapoptotic effects	Activation of Nrf2 and upregulation of downstream antioxidant systems, including HO-1 and GSTP1	[93, 96, 99, 100]
Ginkgo biloba extract 761 (EGb-761)	*Ginkgo biloba*	China	Neuroprotective effects Anti-inflammatory and antioxidant properties	Scavenger, inhibits xanthine oxidase and iNOS activity, reduces superoxide anion with SOD activity	[112–129]
Hyperforin	*Hypericum perforatum* (St. John's wort)	Europe Asia Africa	Antioxidant properties Antiapoptotic effects	Decreases G-Px values, inhibits NADPH-dependent lipid peroxidation, and attenuates nonenzymatic Fe^{2+}/ascorbate-dependent lipid peroxidation	[133–139]
Rosmarinic acid (RA)	*Lamiaceae* family (rosemary, sage, lemon balm, and thyme)	India	Anti-inflammatory and antioxidant properties	Scavenger, upregulation in Nrf-2 levels with the concomitant increase in antioxidant enzymes (SOD, CAT, G-Px, GST, and GSH)	[140–143]

Table 1: Continued.

Compound or extract	Plant species	Origin	Effects on SCI models	Antioxidant mechanisms	References
Carnosol	*Rosmarinus officinalis* L	Worldwide	Anti-inflammatory and antioxidant properties	Upregulates p-AKT and Nrf-2 expression	[144]
Silymarin (SM), silybin	*Silybum marianum* (milk thistle)	Mediterranean diet North Africa	Induce effective functional, recovery Antioxidant properties	Scavenger, inhibits ROS production enzymes, activates antioxidant enzymes via transcription factors (Nrf2 and NF-κB)	[146, 147]
From roots or bulbs					
Plumbagin	*Plumbago zeylanica* L	India and Ceylon	Anti-inflammatory and antioxidant properties	Activates the Nrf2/ARE pathway by which antioxidant enzymes are increased	[150, 151]
Tetrandrine (TET)	*Stephania tetrandrae* S	China	Protection against hypoxic/ischemic injury	Scavenger, blocks iNOS and COX-2 expression	[154–157]
Puerarin	*Radix Puerariae lobata*	China Worldwide	Anti-inflammation and antiapoptotic properties	Increases TRX-1/TRX-2 mRNA levels and the activity of the PI3K/Akt signaling pathway	[159–164]
Allicin	*Allium sativum* (garlic)	Asia	Improves scores in locomotion tests Inhibition of oxidative stress	Reduces iNOS protein expression levels, enhances NADH levels	[167–170]
Curcumin	*Curcuma longa* (turmeric)	India China Southeast Asia	Antioxidant and anti-inflammatory properties	Scavenger, restores mitochondrial membrane potential, upregulates Cu-Zn SOD, improves GSH levels, inhibits iNOS expression by suppressing NF-κB signaling pathway, and activates transcription factors AP-1 and Nrf2	[171–173]
From fruits					
Quercetin	Apples, berries, onions, broccoli, red grapes, and caper	America Europe Asia Africa	Exerts neuroprotection Promotes locomotor function recovery Axonal regeneration	Scavenger of ROS and reactive nitrogen species	[177–184]
Tocotrienols	Certain cereals, palm oil, rice bran oil, coconut oil, barley germ, wheat germ and annatto, grape seed oil, oat, hazelnuts, maize, olive oil	America Europe Asia Africa Oceania	Improves scores in locomotion tests Anti-inflammatory and antioxidant properties	Scavenger, inhibits iNOS protein expression and activity	[38, 193, 194]

Table 1: Continued.

Compound or extract	Plant species	Origin	Effects on SCI models	Antioxidant mechanisms	References
Resveratrol	*Polygonum cuspidatum*, red wine, red grape skins, berries, blueberries, and peanuts	China Japan Korea America Europe Africa	Improved scores in locomotion tests Increased number of neurons Antioxidant properties Antiapoptotic effects	Increases activation of antioxidant enzymes such as SOD and antioxidant compounds such as GSH, induces HO-1 expression	[196–199]
Other extracts					
Sesquiterpenoids, flavonoids, phenols	*Tithonia diversifolia*	Africa Asia	Neuroprotection Antioxidant properties	Scavenger	[216]
Salvianolic acid B (Sal B), 3,4-dihydroxyphenyl lactic acid (DLA), tanshinone IIA (TIIA)	*Salvia miltiorrhiza Bunge* (Danshen)	China	Neuroprotection Antioxidant properties Antiapoptotic effects BSCB integrity regulation	Increases SOD expression, upregulates the expression of HO-1, decreases myeloperoxidase activity	[220–227]

SOD: superoxide dismutase; GSH: glutathione; iROS: intracellular reactive oxygen species; iNOS: inducible nitric oxide synthase; PLCγ: phospholipase Cγ; PI: phosphoinositol; GR: glutathione reductase; MDA: malondialdehyde; HO-1: heme oxygenase-1; GSTP1: glutathione S-transferase P1; G-Px: glutathione peroxidase; CAT: catalase; GST: glutathione transferase; TRX: thioredoxin; BSCB: blood-spinal cord barrier.

encoding antioxidant, anti-inflammatory, and detoxifying proteins, as well as heme oxygenase-1 (HO-1), a protein coded by a Nrf2-dependent gene, which degrades toxic heme groups; produces biliverdin, iron ions, and carbon monoxide; and contributes to angiogenesis [42]. The effects of AA can also be attributed to the inhibition of ROS and the nucleotide-binding domain and leucine-rich repeat- (LRR-) containing (NLR) family pyrin domain-containing 3 (NLRP3) inflammasome pathway. The NLRP3 inflammasome is a multiprotein complex that activates caspase-1, leading to the secretion of proinflammatory molecules such as IL-1β and IL-18. Under normal conditions, NLRP3 remains autorepressed, but this changes with increasing concentrations of damage-associated and pathogen-associated molecular patterns as well as ROS, which are crucial elements for NLRP3 activation [43].

SCI can lead to secondary acute lung injury (ALI). AA administration significantly attenuates pulmonary permeability index and pulmonary histologic conditions and exhibits a protective effect on SCI-induced ALI by alleviating the inflammatory response through inhibiting NLRP3 inflammasome activation and oxidative stress with the upregulation of Nrf2 protein levels [44]. The use of AA may be a potential efficient therapeutic strategy for the treatment of SCI and SCI-induced ALI [41, 44].

4.1.2. Ligustilide. Ligustilide (3-butylidene-4,5-dihydrophthalide) is the main lipophilic constituent of the *Umbelliferae* family of medicinal plants, including *Radix angelicae sinensis* and *Ligusticum chuanxiong* [45]. As it crosses the blood-brain barrier, ligustilide (LIG) exerts marked neuroprotective effects against several CNS pathologies, including forebrain ischemic injury in mice, permanent forebrain ischemia and focal cerebral ischemia/reperfusion in rats [46–48]. In addition, LIG exhibited a wide range of pharmacologic effects *in vitro* and *in vivo*: cardioprotective, antioxidant, anti-inflammatory, and neuroprotective activities [49]. Xiao et al. demonstrated that LIG promotes functional recovery in rats with SCI by preventing the production of ROS. Treatment with LIG significantly increased BBB scores and reduced the time for recovery of coordination in rats with SCI. Furthermore, LIG suppressed SCI-induced production of ROS, inducible nitric oxide synthase (iNOS), inflammation, and JNK signaling. However, further studies are needed to identify the mechanisms by which LIG regulates neuroprotection and mediates locomotor recovery following SCI [50].

4.1.3. Tetramethylpyrazine. Tetramethylpyrazine (TMP), an alkaloid extracted from the Chinese medicinal herb *Ligusticum wallichii Franchat* (chuanxiong), is widely used in the treatment of ischemic stroke and cardiovascular disease [51–53] and has shown anti-inflammatory and neuroprotective effects against SCI as well [54, 55]. In different models of SCI, TMP improved locomotor functions when compared with control animals [52, 56–60]. This improvement in motor activity correlated positively with a decreased area of the injury-induced lesion and increased tissue sparing [51, 58, 59]. Furthermore, a decreased permeability of the blood-spinal cord barrier was also observed [55]. TMP promoted angiogenesis increasing vessel number, vessel volume fraction, and connectivity as well [58, 60]. A mechanism proposed for these effects is the overexpression of PGC-1, a transcriptional coactivator linked to energy metabolism in the mitochondria. This protein is involved in a variety of neurological disorders and apoptosis [57]. Additionally, TMP prevents the reduction of HO-1 and Akt phosphorylation produced in SCI [55].

Regarding neuropathic pain produced in SCI, TMP treatment increased both mechanical withdrawal thresholds and thermal withdrawal latencies [53, 61]. The effect of TMP on neuropathic pain relies on neuronal survival in the dorsal horn and the inhibition of astrocyte activation [62]. In the case of neuronal survival, TMP can modulate mediators of apoptosis such as Bcl-2 and caspase-3 [61], whereas, in the case of the inhibition of astrocyte activation, TMP releases matrix metalloproteinase-2/9 (MMP-2/9) to induce central sensitization and maintain neuropathic pain [62]. Moreover, TMP treatment decreased the expression of pSTAT3. Therefore, TMP could attenuate neuropathic pain by the inhibition of the JAK/STAT3 pathway [53].

TMP shows anti-inflammatory effects in SCI: TMP treatment reduced the expression of proinflammatory cytokines TNF-α, IL-1β, macrophage migration inhibitory factor positive (MIF), IL-18, IL-2, and COX-2 [51–56]; upregulated the expression of anti-inflammatory cytokines IL-10, I-κB, and IL10; inhibited the activation of NF-κB [51, 52]; alleviated neutrophil infiltration; and attenuated microglia activation [51, 52, 54]. Matrix metalloproteinases 2 (MMP2) and 9 (MMP9) are implicated in neuropathic pain by mediating inflammatory pathways. TMP administration induces downregulation of both metalloproteases [60]. Thus, TMP prevents inflammation in spinal cord injury in rats.

TMP reduced neuronal apoptosis by increasing Bcl-2 and reducing Bax, as well as reduced TUNEL-positive cells and caspase-3 and caspase-9 activities [55, 57, 59–61]. Furthermore, TMP increases miR-21 expression, thus decreasing the expression of its targets FasL, PDCD4, and PTEN [59]. In addition to miR-21, TMP decreased the expression of miR-214-3p by increasing the expression of Bcl2L2, suggesting that TMP can modulate apoptosis in SCI [63].

Finally, TMP can decrease ROS in SCI. In rats, TMP treatment decreased lipid peroxidation and increased glutathione levels and superoxide dismutase activity. Also, TMP regulated the expression of Nrf2 mRNA and its binding in HO-1 promoter positively. Thus, TMP showed effects against ROS through the activation of the Akt/Nrf2/HO-1 pathway [55, 56].

4.1.4. Epigallocatechin-3-Gallate. Epigallocatechin-3-gallate (EGCG) is the most abundant polyphenol found in green tea, for which multiple benefits have been described: anticholesterolemic, antioxidant, and anti-inflammatory functions, as well as a modulator of apoptosis. In the CNS, a neuroprotective effect has been shown in a wide range of neurodegenerative diseases in various animal models. In the case of SCI, the administration of EGCG improves both motor and sensory (allodynia, nociception, and hyperalgesia) functions in

acute and chronic models. EGCG administration (100 mg/kg weight) produces the recovery of motor function [64–68] accompanied by a decrease of the injury area and an increase in the number of neurons [64]. The main mechanisms underlying the effects of EGCG range from the induction of the expression of neurotrophic factors, such as BDNF, GDNF [66, 69], and NT3, and their receptors, Trk-B, Trk-C, and NGFR-p75 [69], to the expression of growth factors, such as FGF2 and VEGF [70], accompanied by an increase of GAP43 [64], and the attenuation of myelin degradation [65, 66]. *In vitro* models have shown that EGCG decreases the inhibitory activity of neuritic growth and the collapse of the growth cone induced by NOGO-66. This effect was observed through the 67 kDa laminin receptor to which EGCG binds with high affinity [71]. Also, EGCG attenuates axon repulsion mediated by semaphorin [72]. Evidence shows that EGCG has protective effects for the modulation of neurotrophic factors and their receptors, as well as axonal sprouting. EGCG relieves the neuropathic pain produced in SCI and constriction of the sciatic nerve models [67, 68, 73–75], allowing the recovery of sensory functions by improving tactile allodynia and mechanical nociception. EGCG also increases the latency of paw withdrawal and tail-flick tests [67, 68]. Within the molecular mechanisms of EGCG to alleviate neuropathic pain is the reduction of the expression of CX3CL1, a fractalkine chemokine that has been shown to play an essential role in the development of neuropathic pain. The administration of EGCG reduced thermal hyperalgesia, as an effect of the reduction of CX3CL1 protein expression but not its RNA. Therefore, EGCG is suggested to act as a mediator of nociceptive signaling between neurons and glial cells [75].

Another mechanism that has been studied is the suppression of TLR4 expression. Several studies have demonstrated the involvement of TLRs and inflammation in the development of neuropathic pain. Although EGCG can inhibit other effector molecules of inflammation, the sole inhibition of TLR4 can inhibit the TLR4/NF-κB pathway. Also, EGCG induces the decrease of HMGB1, which has been implicated in chronic neuropathic pain by joining to TLR4 and activating the immune response [73].

EGCG has a more significant action on neuropathic pain than on motor recovery. In the short term, the administration of EGCG only affects sensory recovery but not on motor recovery [76].

EGCG can inhibit the expression of RhoA, FASN, and TNF-α. In addition to limiting axonal regeneration, Álvarez-Pérez et al. demonstrated that RhoA participates in the generation of neuropathic pain. In the case of FASN, which is an enzyme that synthesizes palmitate, a lipid that is capable of activating the synthesis and release of proinflammatory agents, EGCG induces the decrease of FASN and the activation of the inflammatory pathways involved in neuropathic pain [74].

In addition to the mediators of inflammation described in neuropathic pain and a potent anti-inflammatory effect, EGCG is able to attenuate the activity of myeloperoxidase and attenuate the expression of inflammatory cytokines, such as TNF-α, IL-1β, IL-6, IL-2, MIP1, RANTES, nitrotyrosine, iNOs, COX, PARP, NF-κB, and HMGB1 [65, 73], accompanied by an increase in the anti-inflammatory cytokine IL-10 as well [73].

EGCG also modified the expression of IL-4, IL-12p70, and TNF-α1. The mechanism depends on the nuclear translocation of the p65 subunit of NF-κB, consequently inhibiting its activity along with the inflammatory pathways that it regulates. EGCG can modulate the expression of macrophages type M1 and M2. Both macrophage populations have different actions in the mechanisms of inflammation, allowing opposed states [70]. Therefore, EGCG modulates the expression of inflammatory cytokines that affect the expression and activity of its inductors.

EGCG also has antioxidant effects. In SCI, EGCG significantly reduces MDA levels [64] and increases glutathione reductase. This overexpression is accompanied by the decrease of isoprostanes in urine and the suppression of HO-1 [77].

As survival mechanisms, on the one hand, EGCG increases the expression of Bcl-2 and survivin and, on the other hand, it decreases the expression of Bax [64–66, 68]. These effects are reflected by the TUNEL assay low positivity in treated spinal cords [64]. Furthermore, PARP is a protein that is capable of inducing death by the depletion of NAD and ATP. EGCG decreases the expression of PARP, which could contribute to the reduction of Bax and the increase of Bcl2 [65].

4.1.5. Ginsenosides. Ginsenosides are steroid-like molecules which have a four trans-ring structure with sugar residues attached [78]. Ginsenosides Rb1, Rg1, and Rg3 show multiple pharmacological activities on the cardiovascular and immune systems, as well as neuroprotective effects [79, 80].

Ginsenosides can act as antioxidants or scavengers for free radicals [81], increase the activity of superoxide dismutase, and reduce lipid peroxidation [82, 83].

Rb1 protects neurons against oxidative injury, enhancing the Nrf2/HO-1 pathway since the activation of Nrf2 upregulates the transcription of multiple antioxidant response element-controlled genes [84, 85]. Also, ginsenoside Rb1 protects the ischemic brain through upregulation of the expression of Bcl-xL *in vitro* and *in vivo* [86].

Panax ginseng C.A. Meyer (*P. ginseng*) is an herb commonly known as Asian or Korean ginseng [87], which contains ginsenoside saponins that account for the pharmacological efficacy [88].

P. ginseng has 150 different types of ginsenoside saponins, but Rb1, Rb2, Rc, Rd, Re, and Rg1 constitute more than 90% of the total ginsenosides [89].

Regarding the effects on SCI, the ginsenosides Rb1 and Rg1, extracted from *Panax ginseng* C.A. Meyer, were efficient neuroprotective agents for spinal cord neurons *in vitro* survival assays. These compounds protected spinal neurons from excitotoxicity induced by glutamate and kainic acid, as well as oxidative stress induced by H_2O_2. The neuroprotective effects are dose dependent, which optimal doses were 20-40 mM for both Rb1 and Rg1 [81].

Other authors demonstrated *in vitro* that dgRb1 (dihydroginsenoside Rb1), a stable chemical derivative of gRb1, upregulated VEGF and Bcl-xL expression and facilitated neuronal survival through the hypoxia response element (HRE) and signal transducers and activators of transcription 5 (Stat5) response element [90]. Consistently, Sakanaka et al. showed that an intravenous infusion of dgRb1 improved SCI in rats, as well as ischemic brain damage in MCA-occluded rats. The dgRb1-treated groups showed significant improvement of motor activity and behavioral abnormalities concerning locomotor and rearing activities and BBB score in a dose-dependent manner after SCI [90].

Kim et al. reported that ginseng extracts injected intraperitoneally improved recovery after contusive SCI in rats [91]. Additionally, Zhu et al. showed that the oral administration of red ginseng extract promoted the recovery from the motor and behavioral abnormalities in rats with SCI. Furthermore, this extract also stimulated neuronal restoration in the injured spinal cord by inhibiting the inflammatory processes and upregulating the expression of neuroprotective factors (VEGF and Bcl-xL) [92].

Wang et al. showed that ginseng treatment significantly downregulated oxidative stress on spinal injury in rats by enhancing antioxidant proteins and decreasing inflammatory proteins and proinflammatory cytokines [93].

Moreover, different doses of *P. ginseng* showed a significant improvement in locomotor function after spinal injury in rats. *P. ginseng* treatments decreased the expression of COX-2 and iNOS at the lesion site and the cavity area. These results suggest that *P. ginseng* may improve the recovery of motor function after SCI [91].

4.1.6. Panax Notoginsenoside. Unlike many other herbal medicines with a highly variable range of applications, *Panax notoginseng*, which is classified as a warm, sweet, slightly bitter, and nontoxic in Chinese medicine, has protective actions against cardiovascular diseases and diabetes [94, 95]. Moreover, many pharmacological activities of *P. notoginseng*, such as antioxidant, anti-inflammatory, hypoglycemic, antihyperlipidemic, anticoagulation, neuroprotective, and hepatoprotective effects, as well as antitumor and estrogen-like activities, have been reviewed [96].

Over 200 chemical constituents, including saponins, flavonoids, phytosterols, saccharides, polysaccharides, amino acids, fatty acids, dencichine, cyclopeptides, volatile oils, aliphatic acetylene hydrocarbons, and trace elements, have been isolated from *P. notoginseng* [97].

Panax notoginsenoside (PNS) is the principal active ingredient extracted from *P. notoginseng*, which main components are ginsenoside Rb1 (29.86%), Rg1 (20.46%), Rd (7.96%), Re (6.83%), and notoginsenoside R1 (2.74%) [98]. PNS shows many beneficial effects, including anti-inflammation, antiedema, antioxidation, and antiapoptosis [96, 99], as well as neuroprotection in animal models of cerebral ischemia/reperfusion injury [100].

Compelling neuroprotective effects of PNS were demonstrated in a spinal cord ischemia-reperfusion injury model. SCI was induced in rats previously treated with PNS, in which the BBB scores significantly increased, as well as the number of neurons and a restored neuronal morphology observed by a histopathological examination. Furthermore, PNS decreased cytokine levels, as well as the expression of AQP-4 after the injury, suggesting an antiedema effect. An antiapoptotic mechanism of PNS was also verified since the treatment reduced the expression of Fas and FasL and inhibited injury-induced apoptosis [101].

4.1.7. Ginkgo biloba Extract 761 (EGb-761). Ginkgo biloba (Ginkgoaceae) is an ancient Chinese tree which has been cultivated and held sacred for its health-promoting properties [102]. EGb-761 is a patented extract from the leaves of the Ginkgo biloba tree composed of flavonoids (24%), ginkgolide (3.1%), bilobalides (2.9%), and organic acids (5-10%), particularly a ginkgo glycoside [103].

As one of the EGb-761 major constituents, ginkgolide B can improve hemorrhage, edema, necrosis, and inflammatory cell infiltrates in the injured spinal cord [39].

EGb-761 decreases blood viscosity, thereby increasing microcirculation [104], and modifies neurotransmission [105] and neuroplasticity as well [106]. Ginkgo biloba extracts have been used for the treatment of diseases related to the CNS, including brain injury, neurodegenerative disorders, and degenerative dementia [107–109].

EGb-761 also enhances cognition, reduces the detrimental effects of ischemia [110], shows neuroprotective effects, and enhances neurogenesis after ischemic stroke [111].

EGb-761 possesses antioxidant and free radical-scavenging activities [112, 113]. In neurons treated with hydrogen peroxide, EGb-761 reduced oxidative stress and increased the viability of neurons [114, 115]. EGb-761 inhibits xanthine oxidase activity [116], reduces the production of superoxide anion, and inhibits SOD in human postmortem brain tissue [117]. By using electron spin resonance spectrometry, it was demonstrated that EGb-761 is a potent superoxide anion scavenger with SOD activity [118]. Also, EGb-761 can scavenge peroxyl radicals [119].

In spinal cord ischemic injury, EGb-761 protected spinal cord neurons *in vivo*, as well as hydrogen peroxide-induced spinal cord neuronal death *in vitro* [120]. During the acute phase after SCI, EGb-761 administration significantly reduced secondary injury-induced tissue necrosis and cell apoptosis and improved functional performance in rats [121].

EGb-761 performs its neuroprotective effects through scavenging free radicals, lowering oxidative stress, reducing neural damage, and preventing platelet aggregation, as well as its anti-inflammatory properties [122–124].

EGb-761 protects against ischemic SCI via their antioxidant effects in a rat model [125]. Furthermore, EGb-761 decreases SOD downregulation and significantly reduces MDA levels in spinal cord ischemia/reperfusion in rabbits [126, 127]. In another study, EGb-761 was not able to demonstrate a uniform effect on the biochemical markers of spinal cord ischemia/reperfusion in rats. However, histopathologic data appear to show a protective effect of EGb-761 on the spinal cord tissue [128].

Research has demonstrated that iNOS expression is upregulated after SCI. In contrast, EGb761 can suppress

iNOS expression and prevent neuronal death in SCI rats: in the treated group, the area of cavities was smaller, and the demyelinated zones were limited at and around the site of the SCI in comparison to the control group [129].

In acute spinal cord contusion in rats, cell apoptosis increased until day 14 after the injury. Furthermore, seven days after the injury, the number of apoptotic cells significantly decreased in the EGb761-treated group [121].

4.1.8. Hyperforin

Hypericum perforatum, also known as St. John's wort, hypericum, or millepertuis, is a member of the family *Hypericaceae*. Native from Europe, western Asia, and northern Africa, this herbaceous perennial plant currently can be found worldwide. The crude drug, known as *Hyperici herba*, is collected from the upper part of the aerial parts of the plant before or during the flowering period [130–132].

H. perforatum has demonstrated neuroprotective activities. Neuroprotection can be achieved by a direct action on one or several mechanisms, such as an antiapoptotic effect, or indirectly, through antioxidant properties. Chemically, structure-activity relationships suggest that a sugar side chain of flavonoids might be essential for neuroprotective activities [133] and multiple hydroxyl groups confer substantial antioxidant properties [134].

The active component of *H. perforatum* is hyperforin [135, 136], which reduces the overload of $[Ca^{2+}]$ through NMDA receptor modulation in neurons [136, 137]. *H. perforatum* standardized extract protects against enzymatic and nonenzymatic lipid peroxidation of rat brain, inhibiting NADPH-dependent lipid peroxidation and attenuating nonenzymatic Fe^{2+}/ascorbate-dependent lipid peroxidation in cerebral cortex mitochondria [138].

After SCI in rats, *H. perforatum* showed a reduction in oxidative stress, apoptosis, and intracellular Ca^{2+} influx values through the regulation of the TRPM2 (transient receptor potential melastatin 2) and TRPV1 (transient receptor potential vanilloid 1) channels in dorsal root ganglion (DRG) neurons. Additionally, *H. perforatum* induced protective effects on lipid peroxidation and decreased GSH-Px values in the DRG neurons [139].

4.1.9. Rosmarinic Acid and Carnosol. Rosmarinic acid (RA) is a polyphenol found in the *Lamiaceae* family, abundantly present in rosemary, sage, lemon balm, and thyme. RA is a natural antioxidant with free radical scavenging and potential biological effects against oxidative stress and inflammation [140–142].

Shang et al. showed that RA treatment significantly decreased oxidative stress and enhanced the antioxidant status in post-SCI rats. Treatment with RA regulated redox homeostasis and oxidative stress markers, such as ROS, lipid peroxides, and sulfhydryl and carbonyl groups in proteins. RA treatment also caused the upregulation in Nrf-2 levels with the concomitant increase in antioxidant enzymes, such as SOD, CAT, GPx, GST, and GSH, and exerted anti-inflammatory effects through the downregulation of NF-κB and proinflammatory cytokine levels (IL-6, IL-1β, TNF-α, and MCP-1) after SCI [143].

Carnosol, an orthodiphenolic diterpene with excellent antioxidant potential, is also found in rosemary. Wang et al. showed the protective role of carnosol against SCI-induced oxidative stress and inflammation through modulating NF-κB, COX-2, and Nrf-2 levels in Wistar rats. After the significant increase in ROS generation, oxidant levels, lipid peroxide content, protein carbonyl and sulfhydryl levels, and the reduction of the antioxidant status generated by induced SCI, carnosol treatment regulated inflammation key proteins and redox status through the significant downregulation of NF-κB and COX-2 levels and the upregulation of p-AKT and Nrf-2 expression [144].

4.1.10. Silymarin and Silybin. Silymarin (SM) is a mixture of flavonoids extracted from *Silybum marianum* (milk thistle) plant, including flavonolignans (silybin A and silybin B, isosilybin A, isosilybin B, silychristin, and silydianin), as well as fatty acids and polyphenols [145]. SM can contribute to antioxidant defenses as a scavenger of free radicals and by inhibiting specific free radical production enzymes. It also maintains an appropriate redox status by activating some enzymes and nonenzymatic antioxidants via transcription factors, including Nrf2 and NF-κB. Furthermore, SM activates the synthesis of protective molecules, such as thioredoxin (Trx), heat shock proteins, and sirtuins [146].

SM and silybin inhibited cell proliferation in cultures of glial cells in a concentration-dependent manner, as well as mixed cortical and spinal neuronal/glial cells against peroxide toxicity, and protected spinal cord neuronal/glial, glial and microglial cell cultures from LPS stimulation or peroxide toxicity. SM and silybin attenuated peroxide-induced ROS formation, with SM being more effective than silybin. Moreover, intrathecal administration of SM immediately after SCI effectively improved hindlimb locomotor behavior in the rats. These findings showed that SM and silybin exhibit general neuroprotective actions in the CNS [147].

Silybin elicits neuroprotection by the inhibition of peroxide-induced ROS through neuroinflammation and activation of glial cells, by modulating NF-κB or protein kinase C (PKC), as well as apoptosis, through inhibiting p53 and caspase-9, among other signaling pathways [147, 148].

4.2. Extracts from Roots or Bulbs

4.2.1. Plumbagin. Plumbagin, an analog of vitamin K3 isolated from the root of *Plumbago zeylanica L*, activates the Nrf2/ARE pathway resulting in the upregulation of target genes and increased resistance to oxidative and metabolic insults of neurons in culture and to ischemic stroke *in vivo* [149]. In a rat model, post-SCI treatment with plumbagin reduced SCI-induced oxidative stress and proinflammatory mediators [150]. SCI decreased the antioxidant levels of both nonenzymatic (GSH) and enzymatic antioxidants (NQO1, GST, GPx, SOD, and CAT) in sham rats. However, a significant increase in the antioxidant pool was observed in SCI rats treated with plumbagin.

Moreover, it is well-known that Nrf2 activates the antioxidant machinery of cells [151]. Interestingly, plumbagin showed a significant upregulation of Nrf-2 in SCI, which suggests an essential role of plumbagin in cytoprotection as a potent Nrf-2 inducer [150].

4.2.2. Tetrandrine. Tetrandrine (TET), a bis-benzylisoquinoline alkaloid extracted from the roots of the Chinese medicinal herb *Stephania tetrandrae* S Moore, is a potential therapeutic candidate against cancer [152, 153], inflammation [154], and brain ischemia/reperfusion injury [155].

TET is a calcium channel blocker that can protect the liver, heart, small bowel, and brain from ischemia/reperfusion injury by inhibiting damaging factors, such as lipid peroxidation, generation of reactive oxygen species, production of cytokines and inflammatory mediators, neutrophil recruitment, and platelet aggregation [156].

Bao et al. studied the protective effect of TET on rat spinal cord astrocytes with oxygen-glucose-serum deprivation/-reoxygenation-induced injury [157]. As expected, this intentional insult which mimics hypoxic/ischemic conditions *in vivo* caused considerable oxidative stress: an increase in ROS and MDA content, as well as a decreased SOD activity. Also, it increased the expression of proapoptotic Bax and caspase-3 proteins, as well as the reduction of the antiapoptotic protein Bcl-2 [158]. The results of TET as a pretreatment to oxygen-glucose-serum deprivation/reoxygenation injury showed a dose-dependent suppression of Akt phosphorylation and NF-κB activity and inhibition of the elevated caspase-3 activity. Additionally, TNF-α, IL-1β, and IL-6 accumulation induced by hypoxic/ischemic conditions were diminished. Overall, these results show a protective effect of TET against hypoxic/ischemic injury in spinal cord astrocytes through the PI3K/AKT/NF-κB signaling pathway attributable to its antioxidant and anti-inflammatory properties [157].

4.2.3. Puerarin. Puerarin, a natural isoflavone, is the main constituent of *Radix Puerariae lobata*. In SCI, puerarin has shown neuroprotective effects by improving motor function, mainly in ischemia-reperfusion [159–161] as well as in traumatic injury models [162]. Some mechanisms of neuroprotection have been described. As SCI causes the elevation of glutamate levels and mGluRs mRNA expression, which lead to neuronal injury, it has been shown that puerarin administration decreases both the excessive delivery of glutamate and the activation of mGluRs [160]. Also, puerarin upregulates the expression of GAP43, promoting the regeneration of nerve fibers [163]. Another mechanism of protection by puerarin is the inhibition of Cdk5 and p25. Cdk25 causes neuronal death and often is accompanied by the accumulation of p35 and p25, which in turn activates Cdk5, inducing feedback for the stimulus of the injury [161].

Moreover, puerarin can attenuate histological damage, decrease neuron death, and inhibit glial cell activation. These effects can be promoted by increasing the activity of the PI3K/Akt signaling pathway, which is involved in axonal outgrowth and the promotion of antioxidant and antiapoptosis effects [162].

Puerarin diminishes neuroinflammation [162, 164] by decreasing the activity of NF-κB and proinflammatory cytokines, such as IL-6, IL-1β, and TNF-α [164]. Regarding apoptosis, puerarin reduces ROS by increasing thioredoxin- (TRX-) 1/TRX-2 mRNA levels, which are known to regulate apoptosis by modulating the redox ratio of the cell [159].

4.2.4. Allicin. Allium sativum (garlic) is a common and tasty ingredient found all over the world, which also has been used for medicinal purposes. In ancient Chinese and Indian medicine, it was used to treat several conditions, including leprosy, infections, and snake bites. Throughout history, garlic has been used to treat cardiovascular diseases and reduce high blood glucose concentration, blood pressure, and cholesterol levels. More recently, its antitumor, anti-inflammatory, antifungal, and antimicrobial effects have been studied [165, 166].

Garlic contains many substances, from which allicin is the principal chemical component responsible for its biological activity [167].

Allicin is formed during the chopping, crushing, or chewing of garlic cloves through a chemical interaction between alliin, a sulfur-containing amino acid, and the enzyme alliinase [168] and has been reported to prevent arteriosclerosis, stenocardia, cerebral infarction, arrhythmia, and hydrargyria, as well as to enhance the immune system and reduce oxidation [166, 169].

Liu et al. found that allicin treatment for glutamate-induced oxidative stress in spinal cord neurons significantly reduced LDH release, loss of cell viability, and apoptotic neuronal death. Allicin effects were associated with reduced oxidative stress, as evidenced by decreased ROS generation, reduced lipid peroxidation, and preservation of antioxidant enzyme activities. Also, allicin diminished the expression of iNOS and significantly increased the expression of heat shock protein 70 (HSP70) at both mRNA and protein levels. Knockdown of HSP70 by specific targeted small interfering RNA (siRNA) not only mitigated allicin-induced protective activity but also partially nullified its effects on the regulation of iNOS [167]. Furthermore, when the beneficial effects of allicin on SCI in mice were investigated, the results showed that allicin significantly increased BBB scores, which was associated with the inhibition of oxidative stress and inflammatory responses. It was also demonstrated that allicin increased the levels of HSP70, increased the phosphorylation of Akt, and reduced the iNOS protein expression levels. Additionally, treatment with allicin significantly reduced ROS and enhanced NADH levels [170]. Liu et al. and Wang and Ren results agreed and collectively demonstrated that the beneficial effects of allicin are mediated by the HSP70/Akt/i-NOS pathway and recognized its potential use for SCI treatment [167, 170].

4.2.5. Curcumin. Curcumin (1,7-bis(4-hydroxy-3-methoxyphenyl)-1,6-heptadiene-3,5-dione) is a nonsteroidal, naturally occurring compound found in an Indian spice

commonly used as a dietary pigment known as turmeric. Curcumin exhibits a variety of pharmacologic effects, including anti-inflammatory, anticarcinogenic, anti-infectious, antioxidant, and hypocholesterolemic activities. Diets containing curcumin have shown to stimulate NGF, BDNF, GDNF, and PDGF levels *in vivo* [171, 172]. Curcumin also enhances neurogenesis and synaptogenesis and improves cognition in rats, as well as in clinical trials for different neurodegenerative diseases [173], probably through promoting these neurotrophic factors.

After spinal cord hemisection, curcumin treatment provides neuroprotection against SCI-induced disability in rats by the attenuation of neuron loss, prevention of neuronal apoptosis, and decreasing astrocyte activation. Curcumin can attenuate astrocyte reactivation *in vitro* by downregulating GFAP expression, which may improve neuronal survival [174].

4.3. Extracts from Fruits or Derivatives

4.3.1. Quercetin. Many fruits and vegetables contain quercetin (3,3′,4′,5,7-pentahydroxyflavone), a common flavonol [175]. Together with flavones, anthocyanidins, and other compounds, flavonols belong to the class of flavonoids, which in turn represent a major class of polyphenols [176].

Like other polyphenols, quercetin is a scavenger of ROS and reactive nitrogen species such as NO and ONOO [177]. As well as its metabolites, quercetin acts by modulating the antioxidant defense mechanisms in the cell [178, 179].

The beneficial effects of quercetin on cardiovascular diseases, cancer, infections, inflammatory processes, gastrointestinal tract function, and diabetes have been reported [177, 180, 181]. Moreover, quercetin can exert neuroprotection [182] and antagonize oxidative stress when orally administered *in vivo*. At a dose of 0.5-50 mg/kg, quercetin protected rodents from oxidative stress and neurotoxicity induced by different insults [183, 184]. Also, quercetin reduces the immunoreactivity of degenerating neurons [185] and promotes neuronal recovery through the inhibition of inflammatory responses [186].

In a recent study, it was observed that quercetin treatment following acute SCI in rats promoted electrophysiological and locomotor recovery, reduced cavity formation, and contributed to astrocyte activation and axonal regeneration. Additionally, quercetin increased the expression of the brain-derived neurotrophic factor (BDNF), although it reduced p-JNK2 and p-STAT3 expression [187, 188]. It has been reported that BDNF activates tropomyosin-related kinase B (Trk-B) through several downstream signaling pathways, such as AKT, CaMK, and Ras/Raf/MEK/ERK, leading to cell survival, growth, and neuroplasticity [189], while the JAK2/STAT3 pathway depends on the binding of erythropoietin (EPO) to a receptor that results in the dimerization of JAK2. This dimerization leads to STAT3 and STAT5 phosphorylation and the formation of stable homodimers and heterodimers, which subsequently induce the transcription of genes that regulate cell proliferation and survival [190]. Consequently, it was proposed that quercetin effects possibly worked through BDNF and JAK2/STAT3 signaling pathways [188].

4.3.2. Tocotrienols. Tocotrienols, isomers of vitamin E, are found in some cereal and vegetable derivatives, such as palm oil, rice bran oil, coconut oil, barley germ, wheat germ, and annatto. Other sources of tocotrienols include grape seed oil, oat, hazelnuts, maize, olive oil, Buckthorn berry, rye, flaxseed oil, poppy seed oil, and sunflower oil [191, 192].

Tocotrienols exhibit strong neuroprotective, antioxidant, and anticancer effects and cholesterol-lowering properties, which are not observed in tocopherols [193]. Due to a better distribution in the lipid layers of the cell membrane, experimental evidence has found that tocotrienols function as better antioxidants and free radical scavengers when compared to tocopherols [194].

In a rat model, tocotrienol protected against SCI by reducing oxidative stress and inflammation and inhibiting iNOS protein expression and activity, as well as plasma NO production. Also, treatment with tocotrienols suppressed TGF-β, collagen type IV, and fibronectin protein expression levels. Furthermore, the BBB scores in rats treated with 120 mg/kg/day tocotrienol were significantly higher when compared with the group administered with MPS sodium succinate [38].

4.3.3. Resveratrol. Resveratrol is a naturally occurring stilbene class of polyphenol produced in the skin of many edible plants as a response to fungal infection [195].

The resveratrol-mediated decrease in neuronal MDA levels is often associated with increased activation of antioxidant enzymes such as SOD [196] and antioxidant compounds such as glutathione (GSH) [197].

The antioxidant enzyme HO-1 is implicated particularly as a significant effector of resveratrol-mediated neuroprotection after postischemic reperfusion [198, 199]. Furthermore, resveratrol treatment induces HO-1 expression in cultured mouse cortical neurons [200].

Resveratrol ameliorates kainate-induced excitotoxicity [201]. Subsequently, resveratrol has been shown to improve histopathological and behavioral outcomes after various types of acute CNS injuries, including stroke [202–204], traumatic brain injury [205, 206], subarachnoid hemorrhage [207], and SCI [208–210].

In moderate damage to the spinal cord, Liu et al. showed that injured animals treated with resveratrol showed a significant increase in BBB scores. Furthermore, after resveratrol administration, the histopathological analysis showed a restored neuronal morphology and increased the number of neurons. Concerning the antioxidation effects of resveratrol, the treatment overturned the decreased SOD activity and the increased MDA levels caused by SCI, which suggests an antioxidation effect after the injury. Resveratrol treatment also showed an anti-inflammation effect after SCI by inhibiting immunoreactivity and the expression of inflammatory cytokines, such as IL-1β, IL-10, TNF-α, and myeloperoxidase (MPO). Finally, an antiapoptosis role of resveratrol was observed by the inhibition of injury-induced apoptosis and

the modulation of the expression of apoptosis-related genes Bax, Bcl-2, and caspase-3 [210].

4.4. Other Extracts

4.4.1. Tithonia diversifolia Extracts. As mentioned above, Chinese and European traditional medicine is vast. However, it is not the only option to offer proposals for future acute SCI treatments. An example of African traditional medicine is *Tithonia diversifolia*, which proved to possess anti-inflammatory properties to treat diabetes mellitus, diarrhea, fever, hematomas, hepatitis, hepatomas, malaria, and wounds [211, 212]. *T. diversifolia* is a bushy perennial weed that can be found in Nigerian fields, as well as in wastelands and roadsides in Taiwan.

Phytochemical investigations have identified the existence of some bioactive compounds, such as chromene, flavone, cadinene, germacrene, eudesmane, and rearranged eudesmane derivatives in *T. diversifolia* [213–215].

Juang et al. obtained *T. diversifolia* ethanolic extracts (TDE) and used it to treat rats with T5 static compression as a model of SCI. First, these researchers noticed that SCI increased the water apparent diffusion coefficient (ADC)—a measurement of the diffusion of water molecules within the central nervous system—after six hours. A low value of ADC indicates that the nerve fiber tracts are well organized, while a high value means that the tracts are damaged and disorganized. TDE treatment slightly decreased the ADC level after one week in the SCI model. Therefore, it was proposed that TDE protects cells against hydrogen peroxide or radical scavenging-induced toxicity through an antioxidant mechanism, which might be responsible for cell neuroprotection [216].

4.4.2. Danshen Extracts. Danshen (*Salvia miltiorrhiza Bunge*) is a traditional Chinese herb used for the treatment of heart, liver, and skin diseases, among others. Danshen crude extracts (DCE) attenuate edema and bleeding. Furthermore, DCE treatment improved spinal cord microcirculation, as well as motor function by elevating GDNF mRNA expression in the gray matter of acute SCI in rats [217]. Moreover, DCE increased the expression of the antiapoptotic gene Bcl-2, decreased the number of TUNEL-positive cells, decreased MDA levels, and increased the expression of superoxide dismutase as well [218], which demonstrated that DCE treatment decreased apoptosis and showed beneficial effects over oxidative stress in SCI.

Several chemical components, such as salvianolic acid B (Sal B), 3,4-dihydroxyphenyl lactic acid (DLA), and tanshinone IIA (TIIA), are obtained from Danshen extracts.

Salvianolic acid B (Sal B) is commonly used for the prevention and treatment of cardiovascular disease and shows neuroprotective effects in animal models.

Sal B improves motor function [219, 220]. One probable mechanism of Sal B is through the oligodendrocyte precursor cell differentiation due to the increase of the myelin sheath and the number of regenerating axons. These observations indicate that Sal B can protect axons and the myelin sheath [221].

Furthermore, Sal B has shown anti-inflammatory effects by attenuating the upregulation of TNF-α and NF-κB [219]. Moreover, Sal B activates proapoptotic mediators as caspase-3 [220, 221].

Interestingly, Sal B regulates the blood-spinal cord barrier (BSCB) permeability and can reduce spinal edema [220]. In this case, Sal B upregulated the expression of ZO-1 and occludin mediated by HO-1, and p-caveolin was significantly decreased as well [219, 220]. Additionally, Sal A induced the expression of miR-101, which regulates BSCB integrity via the miR-101/Cul3/Nrf2/HO-1 signaling pathway [220].

DLA is obtained by water extraction and improves motor function and tissue damage in SCI. Moreover, it shows its effects on the inflammatory response by reducing IκB-α degradation and the nuclear translocation of NF-κB p65 subunit, as well as polymorphonuclear cell infiltration and IL-6 production [222].

TIIA is one of the principal components of Danshen, which has shown anti-inflammatory and antiapoptotic effects on several diseases: activates blood circulation and exerts neuroprotective effects. In SCI, TIIA improves motor function and reduces tissue injury [223–225]. A possible mechanism for TIIA is the low activation of astrocytes and upregulated expression of Nestin, NeuN, and NF200, indicating that TIIA can promote cell differentiation [225]. The anti-inflammatory mechanisms are carried out by the inhibition of the activation of NF-κB, MAPK, and JNK pathways and the downregulation of proinflammatory cytokines TNF-α, IL-1β, IL-6, and iNOS. TIIA decreases neutrophil and monocyte infiltration by decreasing the myeloperoxidase activity [223, 226]. Also, the anti-inflammation induced by TIIA has shown positive responses to neuropathic pain [226].

TIIA reduces apoptosis by decreasing caspase-3 activation and upregulating Bcl-2 [223, 224, 227]. Finally, TIIA increases the expression of heat-shock protein 70 and inhibits Bax expression [224] and shows effects on redox state imbalance and antiedema [223, 227].

5. Discussion

Different cellular and molecular targets are currently under investigation to improve the outcome after SCI. However, no strategies that effectively improve the secondary damage underlying SCI are currently approved by the FDA. Due to the complexity of SCI—in which secondary posttraumatic mechanisms produce neuronal degeneration associated with increased oxidative stress and inflammation—and the lack of therapeutic options, further investigation of other treatments becomes necessary to improve the quality of life of patients with this lesion.

This review describes several compounds derived from plants, vegetables, and fruits that have been tested in SCI models, in which they exhibit antioxidant, anti-inflammatory, and antiapoptotic therapeutic potential. These properties come from compounds such as the asiatic acid, obtained from *Centella asiatica*, and plumbagin, an analog of vitamin K3 isolated from *Plumbago zeylanica* L, which increase the levels of antioxidant enzymes. Ligustilide is a

bioactive ingredient that reduces oxidative stress and inflammation. Tetrandrine, which is extracted from the root of *Stephania tetrandrae*, is a compound with neuroprotective effects through blocking calcium canals. Consequently, it reduces the molecules associated with oxidative stress damage. *Danshen* extracts decreased apoptosis and oxidative stress and improved motor function in acute SCI. Ginsenosides extracted from *P. ginseng* promote neuronal restoration, inhibit inflammatory processes, and downregulate oxidative stress.

Puerarin, the main constituent of *Radix Puerariae lobata*, and tetramethylpyrazine, extracted from *Ligusticum wallichii Franchat*, showed neuroprotective, as well as antioxidant and antiapoptosis effects, and also reduced neuroinflammation against SCI.

EGb-761, an extract from *Ginkgo biloba*, improved functional performance after SCI, due to its antioxidant, free radical scavenging, and antiapoptosis properties.

Some polyphenols, including quercetin, rosmarinic acid, silymarin, epigallocatechin-3-gallate, and resveratrol, are ROS and reactive nitrogen species scavengers. Therefore, they contribute to regulating oxidative stress. Lastly, curcumin is a nonsteroidal compound with a variety of pharmacological effects.

Some limitations of this review were the lack of information about the use of other natural compounds from Mexican and Latin American countries—which are known to possess an impactful millennial tradition in the use of medicinal plants—to treat SCI. However, this opens up the possibility of future research for new American natural compounds with antioxidant properties, which could be used as a potential treatment for SCI as well. Due to the heterogeneity between the beginning, the duration, and the routes of administration of the treatments, it is impossible to compare their efficiency and strength. Therefore, another limitation could be the lack of standard procedures that allow the comparison of the effectiveness of these compounds.

Although many natural compounds have been used in SCI, little is known about their effectiveness as natural antioxidants, the mechanisms through which these compounds exert their antioxidant activities or their ability to cross the BBB in preclinical models.

As a conclusion, 21 compounds commonly used in SCI models with beneficial properties were described in this review. These compounds are potential therapeutic candidates with neuroprotective effects such as reducing the levels of ROS and diminishing oxidative stress.

Even though these compounds have been tested in animal models with promising results, no clinical studies have been conducted in humans. Therefore, it is crucial to design some strategies to study the effects of these natural compounds in patients with SCI, given that most of these plants are available worldwide at a much lower cost than some synthetic drugs used for SCI therapy.

Conflicts of Interest

The authors declare no conflicts of interest regarding the publication of this paper.

Acknowledgments

The authors wish to thank the Programa Cátedras CONACYT and the Hospital de Especialidades Bernardo Sepúlveda, Centro Médico Nacional SXXI, Instituto Mexicano del Seguro Social. The authors financed this review with resources of their own.

References

[1] National SCI Statistical Centerhttps://www.nscisc.uab.edu.

[2] M. J. DeVivo, "Epidemiology of traumatic spinal cord injury: trends and future implications," *Spinal Cord*, vol. 50, no. 5, pp. 365–372, 2012.

[3] P. E. Ludwig, A. A. Patil, A. J. Chamczuk, and D. K. Agrawal, "Hormonal therapy in traumatic spinal cord injury," *American Journal of Translational Research*, vol. 9, no. 9, pp. 3881–3895, 2017.

[4] S. Samantaray, A. Das, D. C. Matzelle et al., "Administration of low dose estrogen attenuates gliosis and protects neurons in acute spinal cord injury in rats," *Journal of Neurochemistry*, vol. 136, no. 5, pp. 1064–1073, 2016.

[5] H. Q. Cao and E. D. Dong, "An update on spinal cord injury research," *Neuroscience Bulletin*, vol. 29, no. 1, pp. 94–102, 2013.

[6] W. H. Donovan, "Spinal cord injury-past, present, and future," *The Journal of Spinal Cord Medicine*, vol. 30, no. 2, pp. 85–100, 2007.

[7] E. Pickelsimer, E. J. Shiroma, and D. A. Wilson, "Statewide investigation of medically attended adverse health conditions of persons with spinal cord injury," *The Journal of Spinal Cord Medicine*, vol. 33, no. 3, pp. 221–231, 2010.

[8] M. G. Fehlings and C. H. Tator, "The relationships among the severity of spinal cord injury, residual neurological function, axon counts, and counts of retrogradely labeled neurons after experimental spinal cord injury," *Experimental Neurology*, vol. 132, no. 2, pp. 220–228, 1995.

[9] J. W. McDonald and C. Sadowsky, "Spinal-cord injury," *The Lancet*, vol. 359, no. 9304, pp. 417–425, 2002.

[10] A. Ackery, C. Tator, and A. Krassioukov, "A global perspective on spinal cord injury epidemiology," *Journal of Neurotrauma*, vol. 21, no. 10, pp. 1355–1370, 2004.

[11] P. K. Yip and A. Malaspina, "Spinal cord trauma and the molecular point of no return," *Molecular Neurodegeneration*, vol. 7, no. 1, p. 6, 2012.

[12] M. D. Norenberg, J. Smith, and A. Marcillo, "The pathology of human spinal cord injury: defining the problems," *Journal of Neurotrauma*, vol. 21, no. 4, pp. 429–440, 2004.

[13] S. C. Cramer, L. Lastra, M. G. Lacourse, and M. J. Cohen, "Brain motor system function after chronic, complete spinal cord injury," *Brain*, vol. 128, Part 12, pp. 2941–2950, 2005.

[14] G. Yiu and Z. He, "Glial inhibition of CNS axon regeneration," *Nature Reviews Neuroscience*, vol. 7, no. 8, pp. 617–627, 2006.

[15] A. Ulndreaj, J. C. Chio, C. S. Ahuja, and M. G. Fehlings, "Modulating the immune response in spinal cord injury," *Expert Review of Neurotherapeutics*, vol. 16, no. 10, pp. 1127–1129, 2016.

[16] S. J. Cooney, Y. Zhao, and K. R. Byrnes, "Characterization of the expression and inflammatory activity of NADPH oxidase

after spinal cord injury," *Free Radical Research*, vol. 48, no. 8, pp. 929–939, 2014.

[17] I. Jamme, E. Petit, D. Divoux, A. Gerbi, J. M. Maixent, and A. Nouvelot, "Modulation of mouse cerebral Na+, K(+)-ATPase activity by oxygen free radicals," *NeuroReport*, vol. 7, no. 1, pp. 333–337, 1995.

[18] M. Liu, W. Wu, H. Li et al., "Necroptosis, a novel type of programmed cell death, contributes to early neural cells damage after spinal cord injury in adult mice," *The Journal of Spinal Cord Medicine*, vol. 38, no. 6, pp. 745–753, 2015.

[19] Y. Wang, H. Wang, Y. Tao, S. Zhang, J. Wang, and X. Feng, "Necroptosis inhibitor necrostatin-1 promotes cell protection and physiological function in traumatic spinal cord injury," *Neuroscience*, vol. 266, pp. 91–101, 2014.

[20] S. Li and P. K. Stys, "Mechanisms of ionotropic glutamate receptor-mediated excitotoxicity in isolated spinal cord white matter," *The Journal of Neuroscience*, vol. 20, no. 3, pp. 1190–1198, 2000.

[21] V. Gallo, A. Bertolotto, and G. Levi, "The proteoglycan chondroitin sulfate is present in a subpopulation of cultured astrocytes and in their precursors," *Developmental Biology*, vol. 123, no. 1, pp. 282–285, 1987.

[22] L. L. Jones, R. U. Margolis, and M. H. Tuszynski, "The chondroitin sulfate proteoglycans neurocan, brevican, phosphacan, and versican are differentially regulated following spinal cord injury," *Experimental Neurology*, vol. 182, no. 2, pp. 399–411, 2003.

[23] R. Katoh-Semba, M. Matsuda, K. Kato, and A. Oohira, "Chondroitin Sulphate Proteoglycans in the Rat Brain: Candidates for Axon Barriers of Sensory Neurons and the Possible Modification by Laminin of their Actions," *The European Journal of Neuroscience*, vol. 7, no. 4, pp. 613–621, 1995.

[24] M. B. Bracken and T. R. Holford, "Neurological and functional status 1 year after acute spinal cord injury: estimates of functional recovery in National Acute Spinal Cord Injury Study II from results modeled in National Acute Spinal Cord Injury Study III," *Journal of Neurosurgery*, vol. 96, 3 Supplement, pp. 259–266, 2002.

[25] N. A. Silva, N. Sousa, R. L. Reis, and A. J. Salgado, "From basics to clinical: a comprehensive review on spinal cord injury," *Progress in Neurobiology*, vol. 114, pp. 25–57, 2014.

[26] D. R. Sengelaub and X. M. Xu, "Protective effects of gonadal hormones on spinal motoneurons following spinal cord injury," *Neural Regeneration Research*, vol. 13, no. 6, pp. 971–976, 2018.

[27] O. H. Bedreag, A. F. Rogobete, M. Sărăndan et al., "Oxidative stress and antioxidant therapy in traumatic spinal cord injuries," *Romanian Journal of Anaesthesia and Intensive Care*, vol. 21, no. 2, pp. 123–129, 2014.

[28] M. Bains and E. D. Hall, "Antioxidant therapies in traumatic brain and spinal cord injury," *Biochimica et Biophysica Acta*, vol. 1822, no. 5, pp. 675–684, 2012.

[29] E. D. Hall, "Antioxidant therapies for acute spinal cord injury," *Neurotherapeutics*, vol. 8, no. 2, pp. 152–167, 2011.

[30] E. D. Hall, J. A. Wang, D. M. Miller, J. E. Cebak, and R. L. Hill, "Newer pharmacological approaches for antioxidant neuroprotection in traumatic brain injury," *Neuropharmacology*, vol. 145, Part B, pp. 247–258, 2019.

[31] J. M. Gutteridge, "Lipid peroxidation and antioxidants as biomarkers of tissue damage," *Clinical Chemistry*, vol. 41, no. 12, Part 2, pp. 1819–1828, 1995.

[32] M. L. Seligman, E. S. Flamm, B. D. Goldstein, R. G. Poser, H. B. Demopoulos, and J. Ransohoff, "Spectrofluorescent detection of malonaldehyde as a measure of lipid free radical damage in response to ethanol potentiation of spinal cord trauma," *Lipids*, vol. 12, no. 11, pp. 945–950, 1977.

[33] S. A. Baldwin, R. Broderick, D. Osbourne, G. Waeg, D. A. Blades, and S. W. Scheff, "The presence of 4-hydroxynonenal/protein complex as an indicator of oxidative stress after experimental spinal cord contusion in a rat model," *Journal of Neurosurgery*, vol. 88, no. 5, pp. 874–883, 1998.

[34] J. Luo, K. Uchida, and R. Shi, "Accumulation of acrolein-protein adducts after traumatic spinal cord injury," *Neurochemical Research*, vol. 30, no. 3, pp. 291–295, 2005.

[35] A. T. Michael-Titus, "Omega-3 fatty acids and neurological injury," *Prostaglandins, Leukotrienes, and Essential Fatty Acids*, vol. 77, no. 5-6, pp. 295–300, 2007.

[36] H. Ahsan, "3-Nitrotyrosine: A biomarker of nitrogen free radical species modified proteins in systemic autoimmunogenic conditions," *Human Immunology*, vol. 74, no. 10, pp. 1392–1399, 2013.

[37] Y. Xiong, A. G. Rabchevsky, and E. D. Hall, "Role of peroxynitrite in secondary oxidative damage after spinal cord injury," *Journal of Neurochemistry*, vol. 100, no. 3, pp. 639–649, 2007.

[38] C. Xun, M. Mamat, H. Guo et al., "Tocotrienol alleviates inflammation and oxidative stress in a rat model of spinal cord injury via suppression of transforming growth factor-β," *Experimental and Therapeutic Medicine*, vol. 14, no. 1, pp. 431–438, 2017.

[39] Q. Zhang, H. Yang, J. An, R. Zhang, B. Chen, and D. J. Hao, "Therapeutic Effects of Traditional Chinese Medicine on Spinal Cord Injury: A Promising Supplementary Treatment in Future," *Evidence-based Complementary and Alternative Medicine*, vol. 2016, Article ID 8958721, 18 pages, 2016.

[40] M. F. Nagoor Meeran, S. N. Goyal, K. Suchal, C. Sharma, C. R. Patil, and S. K. Ojha, "Pharmacological properties, molecular mechanisms, and pharmaceutical development of asiatic acid: a pentacyclic triterpenoid of therapeutic promise," *Frontiers in Pharmacology*, vol. 9, p. 892, 2018.

[41] W. Jiang, M. Li, F. He et al., "Neuroprotective effect of asiatic acid against spinal cord injury in rats," *Life Sciences*, vol. 157, pp. 45–51, 2016.

[42] A. Loboda, M. Damulewicz, E. Pyza, A. Jozkowicz, and J. Dulak, "Role of Nrf2/HO-1 system in development, oxidative stress response and diseases: an evolutionarily conserved mechanism," *Cellular and Molecular Life Sciences*, vol. 73, no. 17, pp. 3221–3247, 2016.

[43] J. Tschopp and K. Schroder, "NLRP3 inflammasome activation: the convergence of multiple signalling pathways on ROS production?," *Nature Reviews Immunology*, vol. 10, no. 3, pp. 210–215, 2010.

[44] W. Jiang, M. Li, F. He et al., "Protective effects of asiatic acid against spinal cord injury-induced acute lung injury in rats," *Inflammation*, vol. 39, no. 6, pp. 1853–1861, 2016.

[45] Y. Chen, Y. Yu, C. Chen, W. Yang, C. Wang, and J. R. Du, "Pharmacokinetic profile of Z-ligustilide in rat plasma and brain following oral administration," *Natural Product Research and Development*, vol. 22, pp. 126–131, 2010.

[46] X. Kuang, Y. Yao, J. R. Du, Y. X. Liu, C. Y. Wang, and Z. M. Qian, "Neuroprotective role of Z-ligustilide against forebrain

ischemic injury in ICR mice," *Brain Research*, vol. 1102, no. 1, pp. 145–153, 2006.

[47] X. Kuang, J. Du, Y. Liu, G. Zhang, and H. Peng, "Postischemic administration of Z-Ligustilide ameliorates cognitive dysfunction and brain damage induced by permanent forebrain ischemia in rats," *Pharmacology, Biochemistry, and Behavior*, vol. 88, no. 3, pp. 213–221, 2008.

[48] X. Kuang, L. F. Wang, L. Yu et al., "Ligustilide ameliorates neuroinflammation and brain injury in focal cerebral ischemia/reperfusion rats: involvement of inhibition of TLR4/peroxiredoxin 6 signaling," *Free Radical Biology & Medicine*, vol. 71, pp. 165–175, 2014.

[49] P. O. Donkor, Y. Chen, L. Ding, and F. Qiu, "Locally and traditionally used *Ligusticum* species - A review of their phytochemistry, pharmacology and pharmacokinetics," *Journal of Ethnopharmacology*, vol. 194, pp. 530–548, 2016.

[50] W. Xiao, A. Yu, D. Liu, J. Shen, and Z. Xu, "Ligustilide treatment promotes functional recovery in a rat model of spinal cord injury via preventing ROS production," *International Journal of Clinical and Experimental Pathology*, vol. 8, no. 10, pp. 12005–12013, 2015.

[51] L. Fan, K. Wang, Z. Shi, J. Die, C. Wang, and X. Dang, "Tetramethylpyrazine protects spinal cord and reduces inflammation in a rat model of spinal cord ischemia-reperfusion injury," *Journal of Vascular Surgery*, vol. 54, no. 1, pp. 192–200, 2011.

[52] J. Z. Hu, J. H. Huang, Z. M. Xiao, J. H. Li, X. M. Li, and H. B. Lu, "Tetramethylpyrazine accelerates the function recovery of traumatic spinal cord in rat model by attenuating inflammation," *Journal of the Neurological Sciences*, vol. 324, no. 1-2, pp. 94–99, 2013.

[53] S. Wang, A. Li, and S. Guo, "Ligustrazine attenuates neuropathic pain by inhibition of JAK/STAT3 pathway in a rat model of chronic constriction injury," *Pharmazie*, vol. 71, no. 7, pp. 408–412, 2016.

[54] J. W. Shin, J. Y. Moon, J. W. Seong et al., "Effects of tetramethylpyrazine on microglia activation in spinal cord compression injury of mice," *The American Journal of Chinese Medicine*, vol. 41, no. 6, pp. 1361–1376, 2013.

[55] C. Wang, P. Wang, W. Zeng, and W. Li, "Tetramethylpyrazine improves the recovery of spinal cord injury via Akt/Nrf2/HO-1 pathway," *Bioorganic & Medicinal Chemistry Letters*, vol. 26, no. 4, pp. 1287–1291, 2016.

[56] J. Yang, S. Yang, and Y. J. Yuan, "Integrated investigation of lipidome and related signaling pathways uncovers molecular mechanisms of tetramethylpyrazine and butylidenephthalide protecting endothelial cells under oxidative stress," *Molecular BioSystems*, vol. 8, no. 6, pp. 1789–1797, 2012.

[57] J. Hu, Y. Lang, Y. Cao, T. Zhang, and H. Lu, "The neuroprotective effect of tetramethylpyrazine against contusive spinal cord injury by activating PGC-1α in rats," *Neurochemical Research*, vol. 40, no. 7, pp. 1393–1401, 2015.

[58] J. Hu, Y. Cao, T. Wu, D. Li, and H. Lu, "Micro-CT as a tool to investigate the efficacy of tetramethylpyrazine in a rat spinal cord injury model," *Spine*, vol. 41, no. 16, pp. 1272–1278, 2016.

[59] J. H. Huang, Y. Cao, L. Zeng et al., "Tetramethylpyrazine enhances functional recovery after contusion spinal cord injury by modulation of microRNA-21, FasL, PDCD4 and PTEN expression," *Brain Research*, vol. 1648, Part A, pp. 35–45, 2016.

[60] J. Z. Hu, X. K. Wang, Y. Cao et al., "Tetramethylpyrazine facilitates functional recovery after spinal cord injury by inhibiting MMP2, MMP9, and vascular endothelial cell apoptosis," *Current Neurovascular Research*, vol. 14, no. 2, pp. 110–116, 2017.

[61] Y. F. Leng, X. M. Gao, S. X. Wang, and Y. H. Xing, "Effects of tetramethylpyrazine on neuronal apoptosis in the superficial dorsal horn in a rat model of neuropathic pain," *The American Journal of Chinese Medicine*, vol. 40, no. 6, pp. 1229–1239, 2012.

[62] L. Jiang, C. L. Pan, C. Y. Wang et al., "Selective suppression of the JNK-MMP2/9 signal pathway by tetramethylpyrazine attenuates neuropathic pain in rats," *Journal of Neuroinflammation*, vol. 14, no. 1, p. 174, 2017.

[63] Y. Fan and Y. Wu, "Tetramethylpyrazine alleviates neural apoptosis in injured spinal cord via the downregulation of miR-214-3p," *Biomedicine & Pharmacotherapy*, vol. 94, pp. 827–833, 2017.

[64] A. R. Khalatbary, T. Tiraihi, M. B. Boroujeni, H. Ahmadvand, M. Tavafi, and A. Tamjidipoor, "Effects of epigallocatechin gallate on tissue protection and functional recovery after contusive spinal cord injury in rats," *Brain Research*, vol. 1306, pp. 168–175, 2010.

[65] A. R. Khalatbary and H. Ahmadvand, "Anti-inflammatory effect of the epigallocatechin gallate following spinal cord trauma in rat," *Iranian Biomedical Journal*, vol. 15, no. 1-2, pp. 31–37, 2011.

[66] W. Tian, X. G. Han, Y. J. Liu et al., "Intrathecal epigallocatechin gallate treatment improves functional recovery after spinal cord injury by upregulating the expression of BDNF and GDNF," *Neurochemical Research*, vol. 38, no. 4, pp. 772–779, 2013.

[67] W. M. Renno, G. Al-Khaledi, A. Mousa, S. M. Karam, H. Abul, and S. Asfar, "(−)-Epigallocatechin-3-gallate (EGCG) modulates neurological function when intravenously infused in acute and, chronically injured spinal cord of adult rats," *Neuropharmacology*, vol. 77, pp. 100–119, 2014.

[68] W. M. Renno, M. Al-Maghrebi, M. S. Rao, and H. Khraishah, "(-)-Epigallocatechin-3-gallate modulates spinal cord neuronal degeneration by enhancing growth-associated protein 43, B-cell lymphoma 2, and decreasing B-cell lymphoma 2-associated x protein expression after sciatic nerve crush injury," *Journal of Neurotrauma*, vol. 32, no. 3, pp. 170–184, 2015.

[69] W. M. Renno, K. M. Khan, and L. Benov, "Is there a role for neurotrophic factors and their receptors in augmenting the neuroprotective effect of (−)-epigallocatechin-3-gallate treatment of sciatic nerve crush injury?," *Neuropharmacology*, vol. 102, pp. 1–20, 2016.

[70] L. Machova Urdzikova, J. Ruzicka, K. Karova et al., "A green tea polyphenol epigallocatechin-3-gallate enhances neuroregeneration after spinal cord injury by altering levels of inflammatory cytokines," *Neuropharmacology*, vol. 126, pp. 213–223, 2017.

[71] U. Gundimeda, T. H. McNeill, B. A. Barseghian et al., "Polyphenols from green tea prevent antineuritogenic action of Nogo-A via 67-kDa laminin receptor and hydrogen peroxide," *Journal of Neurochemistry*, vol. 132, no. 1, pp. 70–84, 2015.

[72] R. J. Pasterkamp and J. Verhaagen, "Semaphorins in axon regeneration: developmental guidance molecules gone

wrong?," *Philosophical Transactions of the Royal Society of London. Series B, Biological Sciences*, vol. 361, no. 1473, pp. 1499–1511, 2006.

[73] X. Kuang, Y. Huang, H. F. Gu et al., "Effects of intrathecal epigallocatechin gallate, an inhibitor of Toll-like receptor 4, on chronic neuropathic pain in rats," *European Journal of Pharmacology*, vol. 676, no. 1-3, pp. 51–56, 2012.

[74] B. Álvarez-Pérez, J. Homs, M. Bosch-Mola et al., "Epigallocatechin-3-gallate treatment reduces thermal hyperalgesia after spinal cord injury by down-regulating RhoA expression in mice," *European Journal of Pain*, vol. 20, no. 3, pp. 341–352, 2016.

[75] M. Bosch-Mola, J. Homs, B. Álvarez-Pérez et al., "(-)-Epigallocatechin-3-Gallate Antihyperalgesic Effect Associates With Reduced CX3CL1 Chemokine Expression in Spinal Cord," *Phytotherapy Research*, vol. 31, no. 2, pp. 340–344, 2017.

[76] X. Xifró, L. Vidal-Sancho, P. Boadas-Vaello et al., "Novel epigallocatechin-3-gallate (EGCG) derivative as a new therapeutic strategy for reducing neuropathic pain after chronic constriction nerve injury in mice," *PLoS One*, vol. 10, no. 4, article e0123122, 2015.

[77] W. M. Renno, L. Benov, and K. M. Khan, "Possible role of antioxidative capacity of (-)-epigallocatechin-3-gallate treatment in morphological and neurobehavioral recovery after sciatic nerve crush injury," *Journal of Neurosurgery. Spine*, vol. 27, no. 5, pp. 593–613, 2017.

[78] T. Kaku, T. Miyata, T. Uruno, I. Sako, and Y. Kinoshita, "Chemico-pharmacological studies on saponins of Panax ginseng C. A. Meyer," *Arzneimittel-Forschung*, vol. 25, pp. 539–547, 1975.

[79] T. H. Lan, Z. W. Xu, Z. Wang, Y. L. Wu, W. K. Wu, and H. M. Tan, "Ginsenoside Rb1 prevents homocysteine-induced endothelial dysfunction via PI3K/Akt activation and PKC inhibition," *Biochemical Pharmacology*, vol. 82, no. 2, pp. 148–155, 2011.

[80] T. Ahmed, S. H. Raza, A. Maryam et al., "Ginsenoside Rb1 as a neuroprotective agent: a review," *Brain Research Bulletin*, vol. 125, pp. 30–43, 2016.

[81] B. Liao, H. Newmark, and R. Zhou, "Neuroprotective Effects of Ginseng Total Saponin and Ginsenosides Rb1 and Rg1 on Spinal Cord Neurons *in Vitro*," *Experimental Neurology*, vol. 173, no. 2, pp. 224–234, 2002.

[82] G. X. Chu and X. Chen, "Anti-lipid peroxidation and protection of ginsenosides against cerebral ischemia-reperfusion injuries in rats," *Zhongguo Yao Li Xue Bao*, vol. 11, no. 2, pp. 119–123, 1990.

[83] Y. C. Kim, S. R. Kim, G. J. Markelonis, and T. H. Oh, "Ginsenosides Rb1 and Rg3 protect cultured rat cortical cells from glutamate-induced neurodegeneration," *Journal of Neuroscience Research*, vol. 53, no. 4, pp. 426–432, 1998.

[84] J. Ye, J. P. Yao, X. Wang et al., "Neuroprotective effects of ginsenosides on neural progenitor cells against oxidative injury," *Molecular Medicine Reports*, vol. 13, no. 4, pp. 3083–3091, 2016.

[85] N. Ni, Q. Liu, H. Ren et al., "Ginsenoside Rb1 protects rat neural progenitor cells against oxidative injury," *Molecules*, vol. 19, no. 3, pp. 3012–3024, 2014.

[86] B. Zhang, R. Hata, P. Zhu et al., "Prevention of ischemic neuronal death by intravenous infusion of a ginseng saponin, ginsenoside Rb(1), that upregulates Bcl-x(L) expression," *Journal of Cerebral Blood Flow and Metabolism*, vol. 26, no. 5, pp. 708–721, 2006.

[87] R. Collins, "A ten-year audit of traditional Chinese medicine and other natural product research published in the Chinese Medical Journal (2000–2009)," *Chinese Medical Journal*, vol. 124, no. 9, pp. 1401–1408, 2011.

[88] Y. J. Kim, D. Zhang, and D. C. Yang, "Biosynthesis and biotechnological production of ginsenosides," *Biotechnology Advances*, vol. 33, no. 6, Part 1, pp. 717–735, 2015.

[89] C. H. Lee and J. H. Kim, "A review on the medicinal potentials of ginseng and ginsenosides on cardiovascular diseases," *Journal of Ginseng Research*, vol. 38, no. 3, pp. 161–166, 2014.

[90] M. Sakanaka, P. Zhu, B. Zhang et al., "Intravenous infusion of dihydroginsenoside Rb1 prevents compressive spinal cord injury and ischemic brain damage through upregulation of VEGF and Bcl-XL," *Journal of Neurotrauma*, vol. 24, no. 6, pp. 1037–1054, 2007.

[91] Y. O. Kim, Y. Kim, K. Lee et al., "*Panax ginseng* Improves Functional Recovery after Contusive Spinal Cord Injury by Regulating the Inflammatory Response in Rats: An *In Vivo* Study," *Evidence-based Complementary and Alternative Medicine*, vol. 2015, Article ID 817096, 7 pages, 2015.

[92] P. Zhu, K. Samukawa, H. Fujita, H. Kato, and M. Sakanaka, "Oral administration of red ginseng extract promotes neurorestoration after compressive spinal cord injury in rats," *Evidence-based Complementary and Alternative Medicine*, vol. 2017, Article ID 1265464, 10 pages, 2017.

[93] W. Wang, H. Shen, J. J. Xie, J. Ling, and H. Lu, "Neuroprotective effect of ginseng against spinal cord injury-induced oxidative stress and inflammatory responses," *International Journal of Clinical and Experimental Medicine*, vol. 8, no. 3, pp. 3514–3521, 2015.

[94] R. Uzayisenga, P. A. Ayeka, and Y. Wang, "Anti-Diabetic Potential of Panax Notoginseng Saponins (PNS): A Review," *Phytotherapy Research*, vol. 28, no. 4, pp. 510–516, 2014.

[95] X. Yang, X. Xiong, H. Wang, and J. Wang, "Protective effects of *Panax notoginseng* saponins on cardiovascular diseases: a comprehensive overview of experimental studies," *Evidence-based Complementary and Alternative Medicine*, vol. 2014, Article ID 204840, 13 pages, 2014.

[96] N. Zhou, Y. Tang, R. F. Keep, X. Ma, and J. Xiang, "Antioxidative effects of *Panax notoginseng* saponins in brain cells," *Phytomedicine*, vol. 21, no. 10, pp. 1189–1195, 2014.

[97] T. Wang, R. Guo, G. Zhou et al., "Traditional uses, botany, phytochemistry, pharmacology and toxicology of *Panax notoginseng* (Burk.) F.H. Chen: A review," *Journal of Ethnopharmacology*, vol. 188, pp. 234–258, 2016.

[98] Z. H. Chen, J. Li, J. Liu et al., "Saponins isolated from the root of *Panax notoginseng* showed significant anti-diabetic effects in KK-Ay mice," *The American Journal of Chinese Medicine*, vol. 36, no. 5, pp. 939–951, 2008.

[99] M. Zheng, L. Qu, and Y. Lou, "Effects of icariin combined with Panax notoginseng saponins on ischemia reperfusion-induced cognitive impairments related with oxidative stress and CA1 of hippocampal neurons in rat," *Phytotherapy Research*, vol. 22, no. 5, pp. 597–604, 2008.

[100] H. Li, C. Q. Deng, B. Y. Chen, S. P. Zhang, Y. Liang, and X. G. Luo, "Total saponins of *Panax Notoginseng* modulate the expression of caspases and attenuate apoptosis in rats following focal cerebral ischemia-reperfusion," *Journal of Ethnopharmacology*, vol. 121, no. 3, pp. 412–418, 2009.

[101] N. Ning, X. Dang, C. Bai, C. Zhang, and K. Wang, "Panax notoginsenoside produces neuroprotective effects in rat model of acute spinal cord ischemia-reperfusion injury," *Journal of Ethnopharmacology*, vol. 139, no. 2, pp. 504–512, 2012.

[102] B. P. Jacobs and W. S. Browner, "*Ginkgo biloba*: a living fossil," *The American Journal of Medicine*, vol. 108, no. 4, pp. 341-342, 2000.

[103] J. V. Smith and Y. Luo, "Studies on molecular mechanisms of Ginkgo biloba extract," *Applied Microbiology and Biotechnology*, vol. 64, no. 4, pp. 465–472, 2004.

[104] A. J. Kellermann and C. Kloft, "Is There a Risk of Bleeding Associated with Standardized Ginkgo bilobaExtract Therapy? A Systematic Review and Meta-analysis," *Pharmacotherapy*, vol. 31, no. 5, pp. 490–502, 2011.

[105] T. Yoshitake, S. Yoshitake, and J. Kehr, "The Ginkgo biloba extract EGb 761® and its main constituent flavonoids and ginkgolides increase extracellular dopamine levels in the rat prefrontal cortex," *British Journal of Pharmacology*, vol. 159, no. 3, pp. 659–668, 2010.

[106] F. Tchantchou, P. N. Lacor, Z. Cao et al., "Stimulation of neurogenesis and synaptogenesis by bilobalide and quercetin via common final pathway in hippocampal neurons," *Journal of Alzheimer's Disease*, vol. 18, no. 4, pp. 787–798, 2009.

[107] P. Montes, E. Ruiz-Sanchez, C. Rojas, and P. Rojas, "Ginkgo biloba extract 761: a review of basic studies and potential clinical use in psychiatric disorders," *CNS & Neurological Disorders Drug Targets*, vol. 14, no. 1, pp. 132–149, 2015.

[108] C. Shi, S. Xiao, J. Liu et al., "Ginkgo biloba extract EGb761 protects against aging-associated mitochondrial dysfunction in platelets and hippocampi of SAMP8 mice," *Platelets*, vol. 21, no. 5, pp. 373–379, 2010.

[109] J. H. Cho, J. H. Sung, E. H. Cho et al., "Gingko biloba extract (EGb 761) prevents ischemic brain injury by activation of the Akt signaling pathway," *The American Journal of Chinese Medicine*, vol. 37, no. 3, pp. 547–555, 2009.

[110] F. DeFeudis and K. Drieu, "Ginkgo biloba extract (EGb 761) and CNS functions: basic studies and clinical applications," *Current Drug Targets*, vol. 1, no. 1, pp. 25–58, 2000.

[111] S. E. Nada, J. Tulsulkar, and Z. A. Shah, "Heme oxygenase 1-mediated neurogenesis is enhanced by Ginkgo biloba (EGb 761®) after permanent ischemic stroke in mice," *Molecular Neurobiology*, vol. 49, no. 2, pp. 945–956, 2014.

[112] L. Brunetti, B. Michelotto, G. Orlando et al., "Aging increases amyloid β-peptide-induced 8-iso-prostaglandin $F_{2\alpha}$ release from rat brain," *Neurobiology of Aging*, vol. 25, no. 1, pp. 125–129, 2004.

[113] N. E. Mohamed and A. E. Abd El-Moneim, "Ginkgo biloba extract alleviates oxidative stress and some neurotransmitters changes induced by aluminum chloride in rats," *Nutrition*, vol. 35, pp. 93–99, 2017.

[114] Y. Oyama, P. A. Fuchs, N. Katayama, and K. Noda, "Myricetin and quercetin, the flavonoid constituents of *Ginkgo biloba* extract, greatly reduce oxidative metabolism in both resting and Ca^{2+}-loaded brain neurons," *Brain Research*, vol. 635, no. 1-2, pp. 125–129, 1994.

[115] Y. Oyama, L. Chikahisa, T. Ueha, K. Kanemaru, and K. Noda, "*Ginkgo biloba* extract protects brain neurons against oxidative stress induced by hydrogen peroxide," *Brain Research*, vol. 712, no. 2, pp. 349–352, 1996.

[116] L. Marcocci, L. Packer, M. T. Droy-Lefaix, A. Sekaki, and M. Gardès-Albert, "Antioxidant action of Ginkgo biloba extract EGb-761," *Methods in Enzymology*, vol. 46, pp. 462–475, 1994.

[117] W. Gsell, N. Reichert, M. B. Youdim, and P. Riederer, "Interaction of neuroprotective substances with human brain superoxide dismutase. An in vitro study," *Journal of Neural Transmission*, vol. 45, pp. 271–279, 1995.

[118] J. Pincemail, M. Dupuis, C. Nasr et al., "Superoxide anion scavenging effect and superoxide dismutase activity of Ginkgo biloba extract," *Experientia*, vol. 45, no. 8, pp. 708–712, 1989.

[119] I. Maitra, L. Marcocci, M. T. Droy-Lefaix, and L. Packer, "Peroxyl radical scavenging activity of *Ginkgo biloba* extract EGb 761," *Biochemical Pharmacology*, vol. 49, no. 11, pp. 1649–1655, 1995.

[120] E. Mechirova, I. Domorakova, M. Dankova, V. Danielisova, and J. Burda, "Effect of Noradrenalin and EGb 761 pretreatment on the ischemia-reperfusion injured spinal cord neurons in rabbits," *Cellular and Molecular Neurobiology*, vol. 29, no. 6-7, pp. 991–998, 2009.

[121] M. Yan, Y. W. Liu, W. Shao et al., "EGb761 improves histological and functional recovery in rats with acute spinal cord contusion injury," *Spinal Cord*, vol. 54, no. 4, pp. 259–265, 2016.

[122] V. S. Kotakadi, Y. Jin, A. B. Hofseth et al., "Ginkgo biloba extract EGb 761 has anti-inflammatory properties and ameliorates colitis in mice by driving effector T cell apoptosis," *Carcinogenesis*, vol. 29, no. 9, pp. 1799–1806, 2008.

[123] X. Jiang, B. Nie, S. Fu et al., "EGb761 protects hydrogen peroxide-induced death of spinal cord neurons through inhibition of intracellular ROS production and modulation of apoptotic regulating genes," *Journal of Molecular Neuroscience*, vol. 38, no. 2, pp. 103–113, 2009.

[124] J. Wang, C. Ma, W. Rong et al., "Bog bilberry anthocyanin extract improves motor functional recovery by multifaceted effects in spinal cord injury," *Neurochemical Research*, vol. 37, no. 12, pp. 2814–2825, 2012.

[125] R. K. Koc, H. Akdemir, A. Kurtsoy et al., "Lipid peroxidation in experimental spinal cord injury. Comparison of treatment with *Ginkgo biloba*, TRH and methylprednisolone," *Research in Experimental Medicine*, vol. 195, no. 2, pp. 117–123, 1995.

[126] L. H. Fan, K. Z. Wang, and B. Cheng, "Effects of Ginkgo biloba extract on lipid peroxidation and apoptosis after spinal cord ischemia/reperfusion in rabbits," *Chinese Journal of Traumatology*, vol. 9, no. 2, pp. 77–81, 2006.

[127] Z. Zhao, N. Liu, J. Huang, P. H. Lu, and X. M. Xu, "Inhibition of $cPLA_2$ activation by *Ginkgo biloba* extract protects spinal cord neurons from glutamate excitotoxicity and oxidative stress-induced cell death," *Journal of Neurochemistry*, vol. 116, no. 6, pp. 1057–1065, 2011.

[128] S. Badem, M. Ugurlucan, H. El et al., "Effects of *Ginkgo biloba* Extract on Spinal Cord Ischemia -Reperfusion Injury in Rats," *Annals of Vascular Surgery*, vol. 28, no. 5, pp. 1296–1305, 2014.

[129] Q. Ao, X. H. Sun, A. J. Wang et al., "Protective effects of extract of *Ginkgo biloba* (EGb 761) on nerve cells after spinal cord injury in rats," *Spinal Cord*, vol. 44, no. 11, pp. 662–667, 2006.

[130] J. Barnes, L. A. Anderson, and J. D. Phillipson, "St John's wort (Hypericum perforatum L.): a review of its chemistry,

pharmacology and clinical properties," *The Journal of Pharmacy and Pharmacology*, vol. 53, no. 5, pp. 583–600, 2001.

[131] J. M. Greeson, B. Sanford, and D. A. Monti, "St. John's wort (*Hypericum perforatum*): a review of the current pharmacological, toxicological, and clinical literature," *Psychopharmacology*, vol. 153, no. 4, pp. 402–414, 2001.

[132] J. Patočka, "The chemistry, pharmacology, and toxicology of the biologically active constituents of the herb *Hypericum perforatum* L," *Journal of Applied Biomedicine*, vol. 1, no. 2, pp. 61–70, 2003.

[133] M. Nakayama, M. Aihara, Y. N. Chen, M. Araie, K. Tomita-Yokotani, and T. Iwashina, "Neuroprotective effects of flavonoids on hypoxia-, glutamate-, and oxidative stress-induced retinal ganglion cell death," *Molecular Vision*, vol. 17, pp. 1784–1793, 2011.

[134] K. E. Heim, A. R. Tagliaferro, and D. J. Bobilya, "Flavonoid antioxidants: chemistry, metabolism and structure-activity relationships," *The Journal of Nutritional Biochemistry*, vol. 13, no. 10, pp. 572–584, 2002.

[135] O. Krishtal, N. Lozovaya, A. Fisunov et al., "Modulation of ion channels in rat neurons by the constituents of *Hypericum perforatum*," *Pharmacopsychiatry*, vol. 34, Supplement 1, pp. 74–82, 2001.

[136] V. Kumar, A. Mdzinarishvili, C. Kiewert et al., "NMDA receptor-antagonistic properties of hyperforin, a constituent of St John's Wort," *Journal of Pharmacological Sciences*, vol. 102, no. 1, pp. 47–54, 2006.

[137] K. M. Vance, D. M. Ribnicky, G. E. Hermann, and R. C. Rogers, "St. John's Wort enhances the synaptic activity of the nucleus of the solitary tract," *Nutrition*, vol. 30, 7–8 Supplement, pp. S37–S42, 2014.

[138] J. Benedi, R. Arroyo, C. Romero, S. Martín-Aragón, and A. M. Villar, "Antioxidant properties and protective effects of a standardized extract of *Hypericum perforatum* on hydrogen peroxide-induced oxidative damage in PC12 cells," *Life Sciences*, vol. 75, no. 10, pp. 1263–1276, 2004.

[139] Ü. S. Özdemir, M. Nazıroğlu, N. Şenol, and V. Ghazizadeh, "*Hypericum perforatum* attenuates spinal cord injury-induced oxidative stress and apoptosis in the dorsal root ganglion of rats: involvement of TRPM2 and TRPV1 channels," *Molecular Neurobiology*, vol. 53, no. 6, pp. 3540–3551, 2016.

[140] N. Osakabe, A. Yasuda, M. Natsume et al., "Rosmarinic acid, a major polyphenolic component of *Perilla frutescens*, reduces lipopolysaccharide (LPS)-induced liver injury in D-galactosamine (D-GalN)-sensitized mice," *Free Radical Biology & Medicine*, vol. 33, no. 6, pp. 798–806, 2002.

[141] W. Boonyarikpunchai, S. Sukrong, and P. Towiwat, "Antinociceptive and anti-inflammatory effects of rosmarinic acid isolated from *Thunbergia laurifolia* Lindl.," *Pharmacology, Biochemistry, and Behavior*, vol. 124, pp. 67–73, 2014.

[142] M. Petersen, "Rosmarinic acid: new aspects," *Phytochemistry Reviews*, vol. 12, no. 1, pp. 207–227, 2013.

[143] A. J. Shang, Y. Yang, H. Y. Wang et al., "Spinal cord injury effectively ameliorated by neuroprotective effects of rosmarinic acid," *Nutritional Neuroscience*, vol. 20, no. 3, pp. 172–179, 2017.

[144] Z. H. Wang, Y. X. Xie, J. W. Zhang et al., "Carnosol protects against spinal cord injury through Nrf-2 upregulation," *Journal of Receptor and Signal Transduction Research*, vol. 36, no. 1, pp. 72–78, 2016.

[145] M. C. Comelli, U. Mengs, C. Schneider, and M. Prosdocimi, "Toward the definition of the mechanism of action of silymarin: activities related to cellular protection from toxic damage induced by chemotherapy," *Integrative Cancer Therapies*, vol. 6, no. 2, pp. 120–129, 2007.

[146] P. F. Surai, "Silymarin as a natural antioxidant: an overview of the current evidence and perspectives," *Antioxidants*, vol. 4, no. 1, pp. 204–247, 2015.

[147] M. J. Tsai, J. F. Liao, D. Y. Lin et al., "Silymarin protects spinal cord and cortical cells against oxidative stress and lipopolysaccharide stimulation," *Neurochemistry International*, vol. 57, no. 8, pp. 867–875, 2010.

[148] A. Borah, R. Paul, S. Choudhury et al., "Neuroprotective potential of silymarin against CNS disorders: insight into the pathways and molecular mechanisms of action," *CNS Neuroscience & Therapeutics*, vol. 19, no. 11, pp. 847–853, 2013.

[149] T. G. Son, S. Camandola, T. V. Arumugam et al., "Plumbagin, a novel Nrf2/ARE activator, protects against cerebral ischemia," *Journal of Neurochemistry*, vol. 112, no. 5, pp. 1316–1326, 2010.

[150] W. Zhang, L. Cheng, Y. Hou, M. Si, Y. P. Zhao, and L. Nie, "Plumbagin protects against spinal cord injury-induced oxidative stress and inflammation in Wistar rats through Nrf-2 upregulation," *Drug Res (Stuttg).*, vol. 65, no. 9, pp. 495–499, 2015.

[151] W. Li, T. O. Khor, C. Xu et al., "Activation of Nrf2-antioxidant signaling attenuates NFκB-inflammatory response and elicits apoptosis," *Biochemical Pharmacology*, vol. 76, no. 11, pp. 1485–1489, 2008.

[152] C. Shi, S. Ahmad Khan, K. Wang, and M. Schneider, "Improved delivery of the natural anticancer drug tetrandrine," *International Journal of Pharmaceutics*, vol. 479, no. 1, pp. 41–51, 2015.

[153] Y. J. Chen, "Potential role of tetrandrine in cancer therapy," *Acta Pharmacologica Sinica*, vol. 23, no. 12, pp. 1102–1106, 2002.

[154] S. J. Wu and L. T. Ng, "Tetrandrine inhibits pro-inflammatory cytokines, iNOS and COX-2 expression in human monocytic cells," *Biological & Pharmaceutical Bulletin*, vol. 30, no. 1, pp. 59–62, 2007.

[155] S. J. Liu, S. W. Zhou, and C. S. Xue, "Effect of tetrandrine on neutrophilic recruitment response to brain ischemia/reperfusion," *Acta Pharmacologica Sinica*, vol. 22, no. 11, pp. 971–975, 2001.

[156] Y. Chen, Y. H. Tsai, and S. H. Tseng, "The potential of tetrandrine as a protective agent for ischemic stroke," *Molecules*, vol. 16, no. 9, pp. 8020–8032, 2011.

[157] G. Bao, C. Li, L. Qi, N. Wang, and B. He, "Tetrandrine protects against oxygen-glucose-serum deprivation/reoxygenation- induced injury via PI3K/AKT/NF-κB signaling pathway in rat spinal cord astrocytes," *Biomedicine & Pharmacotherapy*, vol. 84, pp. 925–930, 2016.

[158] X. Xia, Y. Ma, L. B. Yang et al., "Impact of heat shock protein A 12B overexpression on spinal astrocyte survival against oxygen-glucose-serum deprivation/restoration in primary cultured astrocytes," *Journal of Molecular Neuroscience*, vol. 59, no. 4, pp. 511–520, 2016.

[159] F. Tian, L. H. Xu, W. Zhao, L. J. Tian, and X. L. Ji, "The optimal therapeutic timing and mechanism of puerarin treatment of spinal cord ischemia-reperfusion injury in rats," *Journal of Ethnopharmacology*, vol. 134, no. 3, pp. 892–896, 2011.

[160] F. Tian, L. H. Xu, W. Zhao, L. J. Tian, and X. L. Ji, "The neuroprotective mechanism of puerarin treatment of acute spinal cord injury in rats," *Neuroscience Letters*, vol. 543, pp. 64–68, 2013.

[161] F. Tian, L. H. Xu, B. Wang, L. J. Tian, and X. L. Ji, "The neuroprotective mechanism of puerarin in the treatment of acute spinal ischemia-reperfusion injury is linked to cyclin-dependent kinase 5," *Neuroscience Letters*, vol. 584, pp. 50–55, 2015.

[162] D. Zhang, G. Ma, M. Hou, T. Zhang, L. Chen, and C. Zhao, "The neuroprotective effect of puerarin in acute spinal cord injury rats," *Cellular Physiology and Biochemistry*, vol. 39, no. 3, pp. 1152–1164, 2016.

[163] M. Wu, G. Zhao, X. Yang et al., "Puerarin accelerates neural regeneration after sciatic nerve injury," *Neural Regeneration Research*, vol. 9, no. 6, pp. 589–593, 2014.

[164] M. Liu, K. Liao, C. Yu, X. Li, S. Liu, and S. Yang, "Puerarin alleviates neuropathic pain by inhibiting neuroinflammation in spinal cord," *Mediators of Inflammation*, vol. 2014, Article ID 485927, 9 pages, 2014.

[165] L. Bayan, P. H. Koulivand, and A. Gorji, "Garlic: a review of potential therapeutic effects," *Avicenna Journal of Phytomedicine*, vol. 4, no. 1, pp. 1–14, 2014.

[166] K. Alam, O. Hoq, and S. Uddin, "Medicinal plant *Allium sativum*. A review," *Journal of Medicinal Plant Studies*, vol. 4, no. 6, pp. 72–79, 2016.

[167] S. G. Liu, P. Y. Ren, G. Y. Wang, S. X. Yao, and X. J. He, "Allicin protects spinal cord neurons from glutamate-induced oxidative stress through regulating the heat shock protein 70/inducible nitric oxide synthase pathway," *Food & Function*, vol. 6, no. 1, pp. 320–329, 2015.

[168] L. D. Lawson and C. D. Gardner, "Composition, stability, and bioavailability of garlic products used in a clinical trial," *Journal of Agricultural and Food Chemistry*, vol. 53, no. 16, pp. 6254–6261, 2005.

[169] W. Huang, Y. Wang, Y. G. Cao et al., "Antiarrhythmic effects and ionic mechanisms of allicin on myocardial injury of diabetic rats induced by streptozotocin," *Naunyn-Schmiedeberg's Archives of Pharmacology*, vol. 386, no. 8, pp. 697–704, 2013.

[170] S. Wang and D. Ren, "Allicin protects traumatic spinal cord injury through regulating the HSP70/Akt/iNOS pathway in mice," *Molecular Medicine Reports*, vol. 14, no. 4, pp. 3086–3092, 2016.

[171] S. C. Gupta, S. Prasad, J. H. Kim et al., "Multitargeting by curcumin as revealed by molecular interaction studies," *Natural Product Reports*, vol. 28, no. 12, pp. 1937–1955, 2011.

[172] P. Maiti and G. L. Dunbar, "Use of curcumin, a natural polyphenol for targeting molecular pathways in treating age-related neurodegenerative diseases," *International Journal of Molecular Sciences*, vol. 19, no. 6, p. 1637, 2018.

[173] A. Bhat, A. M. Mahalakshmi, B. Ray et al., "Benefits of curcumin in brain disorders," *BioFactors*, vol. 45, no. 5, pp. 666–689, 2019.

[174] M. S. Lin, Y. H. Lee, W. T. Chiu, and K. S. Hung, "Curcumin provides neuroprotection after spinal cord injury," *The Journal of Surgical Research*, vol. 166, no. 2, pp. 280–289, 2011.

[175] L. G. Costa, J. M. Garrick, P. J. Roquè, and C. Pellacani, "Mechanisms of neuroprotection by quercetin: counteracting oxidative stress and more," *Oxidative Medicine and Cellular Longevity*, vol. 2016, Article ID 2986796, 10 pages, 2016.

[176] D. Del Rio, A. Rodriguez-Mateos, J. P. Spencer, M. Tognolini, G. Borges, and A. Crozier, "Dietary (poly)phenolics in human health: structures, bioavailability, and evidence of protective effects against chronic diseases," *Antioxidants & Redox Signaling*, vol. 18, no. 14, pp. 1818–1892, 2013.

[177] A. W. Boots, G. R. Haenen, and A. Bast, "Health effects of quercetin: from antioxidant to nutraceutical," *European Journal of Pharmacology*, vol. 585, no. 2-3, pp. 325–337, 2008.

[178] B. Halliwell, J. Rafter, and A. Jenner, "Health promotion by flavonoids, tocopherols, tocotrienols, and other phenols: direct or indirect effects? Antioxidant or not?," *The American Journal of Clinical Nutrition*, vol. 81, no. 1, pp. 268S–276S, 2005.

[179] C. G. Fraga, M. Galleano, S. V. Verstraeten, and P. I. Oteiza, "Basic biochemical mechanisms behind the health benefits of polyphenols," *Molecular Aspects of Medicine*, vol. 31, no. 6, pp. 435–445, 2010.

[180] G. S. Kelly, "Quercetin. Monograph," *Alternative Medicine Review : A Journal of Clinical Therapeutic*, vol. 16, no. 2, pp. 172–194, 2011.

[181] M. Russo, C. Spagnuolo, I. Tedesco, S. Bilotto, and G. L. Russo, "The flavonoid quercetin in disease prevention and therapy: facts and fancies," *Biochemical Pharmacology*, vol. 83, no. 1, pp. 6–15, 2012.

[182] B. Ossola, T. M. Kääriäinen, and P. T. Männistö, "The multiple faces of quercetin in neuroprotection," *Expert Opinion on Drug Safety*, vol. 8, no. 4, pp. 397–409, 2009.

[183] A. Ishisaka, S. Ichikawa, H. Sakakibara et al., "Accumulation of orally administered quercetin in brain tissue and its antioxidative effects in rats," *Free Radical Biology & Medicine*, vol. 51, no. 7, pp. 1329–1336, 2011.

[184] S. Das, A. K. Mandal, A. Ghosh, S. Panda, N. Das, and S. Sarkar, "Nanoparticulated quercetin in combating age related cerebral oxidative injury," *Current Aging Science*, vol. 1, no. 3, pp. 169–174, 2008.

[185] C. Unsal, M. Kanter, C. Aktas, and M. Erboga, "Role of quercetin in cadmium-induced oxidative stress, neuronal damage, and apoptosis in rats," *Toxicology and Industrial Health*, vol. 31, no. 12, pp. 1106–1115, 2015.

[186] Y. Zhang, B. Yi, J. Ma et al., "Quercetin promotes neuronal and behavioral recovery by suppressing inflammatory response and apoptosis in a rat model of intracerebral hemorrhage," *Neurochemical Research*, vol. 40, no. 1, pp. 195–203, 2015.

[187] E. Schültke, E. Kendall, H. Kamencic, Z. Ghong, R. W. Griebel, and B. H. Juurlink, "Quercetin promotes functional recovery following acute spinal cord injury," *Journal of Neurotrauma*, vol. 20, no. 6, pp. 583–591, 2003.

[188] Y. Wang, W. Li, M. Wang et al., "Quercetin reduces neural tissue damage and promotes astrocyte activation after spinal cord injury in rats," *Journal of Cellular Biochemistry*, vol. 119, no. 2, pp. 2298–2306, 2018.

[189] M. A. Alam, V. P. Subramanyam Rallabandi, and P. K. Roy, "Systems biology of immunomodulation for post-stroke neuroplasticity: multimodal implications of pharmacotherapy and neurorehabilitation," *Frontiers in Neurology*, vol. 7, p. 94, 2016.

[190] A. Tabarroki and R. V. Tiu, "Molecular genetics of myelofibrosis and its associated disease phenotypes," *Translational medicine@ UniSa*, vol. 8, pp. 53–64, 2014.

[191] A. A. Qureshi, H. Mo, L. Packer, and D. M. Peterson, "Isolation and identification of novel tocotrienols from rice bran with hypocholesterolemic, antioxidant, and antitumor properties," *Journal of Agricultural and Food Chemistry*, vol. 48, no. 8, pp. 3130–3140, 2000.

[192] H. Ahsan, A. Ahad, J. Iqbal, and W. A. Siddiqui, "Pharmacological potential of tocotrienols: a review," *Nutrition & Metabolism*, vol. 11, no. 1, p. 52, 2014.

[193] C. K. Sen, S. Khanna, and S. Roy, "Tocotrienols: vitamin E beyond tocopherols," *Life Sciences*, vol. 78, no. 18, pp. 2088–2098, 2006.

[194] K. Hensley, E. J. Benaksas, R. Bolli et al., "New perspectives on vitamin E: γ-tocopherol and carboxyethylhydroxychroman metabolites in biology and medicine," *Free Radical Biology & Medicine*, vol. 36, no. 1, pp. 1–15, 2004.

[195] E. H. Siemann and L. L. Creasy, "Concentration of the phytoalexin resveratrol in wine," *American Journal of Enology and Viticulture*, vol. 43, pp. 49–52, 1992.

[196] S. D. Rege, S. Kumar, D. N. Wilson et al., "Resveratrol protects the brain of obese mice from oxidative damage," *Oxidative Medicine and Cellular Longevity*, vol. 2013, Article ID 419092, 7 pages, 2013.

[197] K. Sinha, G. Chaudhary, and Y. K. Gupta, "Protective effect of resveratrol against oxidative stress in middle cerebral artery occlusion model of stroke in rats," *Life Sciences*, vol. 71, no. 6, pp. 655–665, 2002.

[198] G. Cheng, X. Zhang, D. Gao, X. Jiang, and W. Dong, "Resveratrol inhibits MMP-9 expression by up-regulating PPAR α expression in an oxygen glucose deprivation-exposed neuron model," *Neuroscience Letters*, vol. 451, no. 2, pp. 105–108, 2009.

[199] H. Zhuang, Y. S. Kim, R. C. Koehler, and S. Doré, "Potential mechanism by which resveratrol, a red wine constituent, protects neurons," *Annals of the New York Academy of Sciences*, vol. 993, no. 1, pp. 276–286, 2003.

[200] J. Yang, J. Huang, C. Shen et al., "Resveratrol treatment in different time-attenuated neuronal apoptosis after oxygen and glucose deprivation/reoxygenation via enhancing the activation of Nrf-2 signaling pathway in vitro," *Cell Transplantation*, vol. 27, no. 12, pp. 1789–1797, 2018.

[201] M. Virgili and A. Contestabile, "Partial neuroprotection of in vivo excitotoxic brain damage by chronic administration of the red wine antioxidant agent, trans-resveratrol in rats," *Neuroscience Letters*, vol. 281, no. 2-3, pp. 123–126, 2000.

[202] C. Girbovan, L. Morin, and H. Plamondon, "Repeated resveratrol administration confers lasting protection against neuronal damage but induces dose-related alterations of behavioral impairments after global ischemia," *Behavioural Pharmacology*, vol. 23, no. 1, pp. 1–13, 2012.

[203] S. S. Huang, M. C. Tsai, C. L. Chih, L. M. Hung, and S. K. Tsai, "Resveratrol reduction of infarct size in Long-Evans rats subjected to focal cerebral ischemia," *Life Sciences*, vol. 69, no. 9, pp. 1057–1065, 2001.

[204] F. Karalis, V. Soubasi, T. Georgiou et al., "Resveratrol ameliorates hypoxia/ischemia-induced behavioral deficits and brain injury in the neonatal rat brain," *Brain Research*, vol. 1425, pp. 98–110, 2011.

[205] R. H. Singleton, H. Q. Yan, W. Fellows-Mayle, and C. E. Dixon, "Resveratrol attenuates behavioral impairments and reduces cortical and hippocampal loss in a rat controlled cortical impact model of traumatic brain injury," *Journal of Neurotrauma*, vol. 27, no. 6, pp. 1091–1099, 2010.

[206] U. Sönmez, A. Sönmez, G. Erbil, I. Tekmen, and B. Baykara, "Neuroprotective effects of resveratrol against traumatic brain injury in immature rats," *Neuroscience Letters*, vol. 420, no. 2, pp. 133–137, 2007.

[207] A. W. Shao, H. J. Wu, S. Chen, A. B. Ammar, J. M. Zhang, and Y. Hong, "Resveratrol Attenuates Early Brain Injury After Subarachnoid Hemorrhage Through Inhibition of NF-κB-Dependent Inflammatory/MMP-9 Pathway," *CNS Neuroscience & Therapeutics*, vol. 20, no. 2, pp. 182–185, 2014.

[208] O. Ates, S. Cayli, E. Altinoz et al., "Effects of resveratrol and methylprednisolone on biochemical, neurobehavioral and histopathological recovery after experimental spinal cord injury," *Acta Pharmacologica Sinica*, vol. 27, no. 10, pp. 1317–1325, 2006.

[209] S. Kaplan, G. Bisleri, J. A. Morgan, F. H. Cheema, and M. C. Oz, "Resveratrol, a Natural Red Wine Polyphenol, Reduces Ischemia-Reperfusion- Induced Spinal Cord Injury," *The Annals of Thoracic Surgery*, vol. 80, no. 6, pp. 2242–2249, 2005.

[210] C. Liu, Z. Shi, L. Fan, C. Zhang, K. Wang, and B. Wang, "Resveratrol improves neuron protection and functional recovery in rat model of spinal cord injury," *Brain Research*, vol. 1374, pp. 100–109, 2011.

[211] M. Takanashi, 1998, U.S. Patent 5,773,004.

[212] C. C. Lin, M. L. Lin, and J. M. Lin, "The antiinflammatory and liver protective effect of *Tithonia diversifolia* (Hemsl.) gray and *Dicliptera chinensis* Juss. Extracts in rats," *Phytotherapy Research*, vol. 7, no. 4, pp. 305–309, 1993.

[213] A. Schuster, S. Stokes, F. Papastergiou, V. Castro, L. Poveda, and J. Jakupovic, "Sesquiterpene lactones from two *Tithonia* species," *Phytochemistry*, vol. 31, no. 9, pp. 3139–3141, 1992.

[214] M. Bordoloi, N. C. Barua, and A. C. Ghosh, "An artemisinic acid analogue from *Tithonia diversifolia*," *Phytochemistry*, vol. 41, no. 2, pp. 557–559, 1996.

[215] Y. H. Kuo and C. H. Chen, "Sesquiterpenes from the leaves of *Tithonia diversifolia*," *Journal of Natural Products*, vol. 61, no. 6, pp. 827-828, 1998.

[216] C. L. Juang, F. S. Yang, M. S. Hsieh, H. Y. Tseng, S. C. Chen, and H. C. Wen, "Investigation of anti-oxidative stress *in vitro* and water apparent diffusion coefficient in MRI on rat after spinal cord injury *in vivo* with *Tithonia diversifolia* ethanolic extracts treatment," *BMC Complementary and Alternative Medicine*, vol. 14, no. 1, p. 447, 2014.

[217] L. Wei and L. Zhang, "Effects of Danshen injection on glial cell line-derived neurotrophic factor mRNA of acute spinal cord injury rats and its mechanisms," *Zhongguo Zhong Xi Yi Jie He Za Zhi*, vol. 33, no. 7, pp. 933–937, 2013.

[218] Y. G. Yu, J. Yang, X. H. Cheng et al., "The protection of acute spinal cord injury by subarachnoid space injection of Danshen in animal models," *The Journal of Spinal Cord Medicine*, vol. 42, no. 3, pp. 355–359, 2019.

[219] Z. K. Fan, G. Lv, Y. F. Wang et al., "The protective effect of salvianolic acid B on blood-spinal cord barrier after compression spinal cord injury in rats," *Journal of Molecular Neuroscience*, vol. 51, no. 3, pp. 986–993, 2013.

[220] D. S. Yu, Y. S. Wang, Y. L. Bi et al., "Salvianolic acid A ameliorates the integrity of blood-spinal cord barrier via miR-101/Cul3/Nrf2/HO-1 signaling pathway," *Brain Research*, vol. 1657, pp. 279–287, 2017.

[221] Z. Zhu, L. Ding, W. F. Qiu, H. F. Wu, and R. Li, "Salvianolic acid B protects the myelin sheath around injured spinal cord axons," *Neural Regeneration Research*, vol. 11, no. 3, pp. 487–492, 2016.

[222] X. Chen, C. Zhou, J. Guo et al., "Effects of dihydroxylphenyl lactic acid on inflammatory responses in spinal cord injury," *Brain Research*, vol. 1372, pp. 160–168, 2011.

[223] X. Yin, Y. Yin, F. L. Cao et al., "Tanshinone IIA attenuates the inflammatory response and apoptosis after traumatic injury of the spinal cord in adult rats," *PLoS One*, vol. 7, no. 6, article e38381, 2012.

[224] L. Zhang, W. Gan, and G. An, "Influence of tanshinone IIa on heat shock protein 70, Bcl-2 and Bax expression in rats with spinal ischemia/reperfusion injury," *Neural Regeneration Research*, vol. 7, no. 36, pp. 2882–2888, 2012.

[225] X. M. Zhang, J. Ma, Y. Sun et al., "Tanshinone IIA promotes the differentiation of bone marrow mesenchymal stem cells into neuronal-like cells in a spinal cord injury model," *Journal of Translational Medicine*, vol. 16, no. 1, p. 193, 2018.

[226] J. Tang, C. Zhu, Z. H. Li et al., "Inhibition of the spinal astrocytic JNK/MCP-1 pathway activation correlates with the analgesic effects of tanshinone IIA sulfonate in neuropathic pain," *Journal of Neuroinflammation*, vol. 12, p. 57, 2015.

[227] Y. D. Yang, X. Yu, X. M. Wang, X. H. Mu, and F. He, "Tanshinone IIA improves functional recovery in spinal cord injury-induced lower urinary tract dysfunction," *Neural Regeneration Research*, vol. 12, no. 2, pp. 267–275, 2017.

Hindawi
Oxidative Medicine and Cellular Longevity
Volume 2019, Article ID 7850154, 13 pages
https://doi.org/10.1155/2019/7850154

Research Article

Neuroprotective Effect of SCM-198 through Stabilizing Endothelial Cell Function

Qiu-Yan Zhang,[1,2] Zhi-Jun Wang,[2,3] Lei Miao,[4] Ying Wang,[5] Ling-Ling Chang,[2] Wei Guo,[2] and Yi-Zhun Zhu[2,3]

[1]*Yantai Institute of Materia Medica, Yantai Branch, Shanghai Institute of Materia Medica, Chinese Academy of Sciences, China*
[2]*Shanghai Key Laboratory of Bioactive Small Molecules, Department of Pharmacology, School of Pharmacy, Fudan University, 826, Zhangheng Road, Pudong New District, Shanghai 201203, China*
[3]*State Key Laboratory of Quality Research in Chinese Medicine and School of Pharmacy, Macau University of Science and Technology, Macau, China*
[4]*Department of Pediatric Surgery, Guangzhou Institute of Pediatrics, Guangzhou Women and Children's Medical Center, Guangzhou Medical University, Guangzhou, 510623 Guangdong, China*
[5]*Department of Pharmacology, University of California, Davis, USA*

Correspondence should be addressed to Wei Guo; guowei@fudan.edu.cn and Yi-Zhun Zhu; yzzhu@must.edu.mo

Received 31 May 2019; Revised 31 July 2019; Accepted 14 August 2019; Published 11 November 2019

Guest Editor: João C. M. Barreira

Leonurine, also named SCM-198, which was extracted from *Herba leonuri*, displayed a protective effect on various cardiovascular and brain diseases, like ischemic stroke. Ischemic stroke which is the leading cause of morbidity and mortality, ultimately caused irreversible neuron damage. This study is aimed at exploring the possible therapeutic potential of SCM-198 in the protection against postischemic neuronal injury and possible underlying mechanisms. A transient middle cerebral artery occlusion (tMCAO) rat model was utilized to measure the protective effect of SCM-198 on neurons. TEM was used to determine neuron ultrastructural changes. The brain slices were stained with Nissl staining solution for Nissl bodies. Fluoro-Jade B (FJB) was used for staining the degenerating neurons. In the oxygen-glucose deprivation and re-oxygenation (OGD/R) model of bEnd.3 cells treated with SCM-198 (0.1, 1, 10 μM). Then, the bEnd.3 cells were cocultured with SH-SY5Y cells. Cell viability, MDA level, CAT activity, and apoptosis were examined to evaluate the cytotoxicity of these treatments. Western blot and immunofluorescent assays were used to examine the expression of protein related to the p-STAT3/NOX4/Bcl-2 signaling pathway. Coimmunoprecipitation was performed to determine the interaction between p-STAT3 and NOX4. In the transient middle cerebral artery occlusion (tMCAO) rat model, we found that treatment with SCM-198 could ameliorate neuron morphology and reduce the degenerating cell and neuron loss. In the *in vitro* model of bEnd.3 cell oxygen-glucose deprivation and reoxygenation (OGD/R), treatment with SCM-198 restored the activity of catalase (CAT), improved the expression of Cu-Zn superoxide dismutase (SOD1), and decreased the malondialdehyde (MDA) production. SCM-198 treatment prevented OGD/R-induced cell apoptosis as indicated by increased cell viability and decreased the number of TUNEL-positive cells, accompanied with upregulation of Bcl-2 and Bcl-xl protein and downregulation Bax protein. The results were consistent with SH-SY5Y cells which coculture with bEnd.3 cells. The forthcoming study revealed that SCM-198 activated the p-STAT3/NOX4/Bcl-2 signaling pathway. All the data indicated that SCM-198 protected against oxidative stress and neuronal damage in *in vivo* and *in vitro* injury models via the p-STAT3/NOX4/Bcl-2 signaling pathway. Our results suggested that SCM-198 could be the potential drug for neuroprotective effect through stabilizing endothelial cell function.

1. Introduction

Stroke is one of the leading cause of morbidity and mortality worldwide [1], owing to its incredibly short therapeutic time window and fewer effective emergency medicines, tissue-type plasminogen activator (tPA) serving as priority therapeutic drug in ischemic stroke, with only 10% patients of which applicable to this therapy [2]. Clinically speaking, stroke could be categorized into two types: around 85% of ischemic stroke and hemorrhagic stroke which includes intracerebral bleeding and subarachnoidal bleeding accounting for 10% and 3%, respectively [3]. Meanwhile, in the ischemic stroke, secondary damage led by reperfusion will worsen prognosis including a breakdown of blood-brain barrier (BBB), inflammation, oxidative stress, excitotoxicity, and finally irreversible neuronal damage [4].

NADPH oxidases (NOX) are one kind of the main sources of ROS and the only kind of enzyme known that has ROS formation function solely [5]. In mammals, the NOX family includes seven members: NOX1 to NOX5, dual oxidase- (Duox-) 1, and Duox-2 [6–8]. Among NOX, NOX4 appears mostly as a target for ischemia-reperfusion (IR) therapy [9, 10] because it is induced under hypoxia in various cell and tissues making it seem to be the most possible key point of IR injury [11]. In addition, recent researches demonstrated that NOX4 exerted the protective effect against blood-brain barrier breakdown, oxidative stress, and neuronal apoptosis during ischemic stroke [12, 13].

Research revealed that the activated signal transducers and transcription 3 (STAT3) is involved in the protection against cerebral ischemic reperfusion injury [14–16]. Previous studies investigated that activated STAT3 in stroke model could promote numerous genes which play a protective effect on neural injury and repair [17, 18]. Further experiments revealed that the regulation of the STAT3 signaling pathway could prevent neuroapoptosis [19]. However, the further mechanism of the downstream regulators is unclear. On the contrary, there also some other different results which reveal that blocking the STAT3 pathway could improve cerebral recovery and neurological outcomes [20]. Therefore, the rigid contribution of activated STAT3 after stroke remains incompletely explored.

Herbaleonuri, also called Chinese Motherwort or Siberian Motherwort, is found in China, central Europe, Scandinavia, and Russia and has been documented for treatment of vaginal bleeding, dystocia, retained fatal membranes, bruising, metrorrhagia, metrostaxis, hemuresis, and some other diseases. Leonurine ($C_{14}H_{21}N_3O_5$), extracted from the leaves of *Herbaleonuri*, also named SCM-198, was reported to be protective in cardio cerebral vascular diseases. Our previous results firstly provide the evidence that SCM-198 could prevent cardiac fibrosis and activate cardiac fibroblasts partly through modulation of the NOX4-ROS pathway [21]. And our investigation found that SCM-198 could maintain the BBB integrity by regulating the HDAC4/-NOX4/MMP-9 tight junction pathway [22–25]. SCM-198 may directly inhibit the overactivated microglia, maintain their ramified morphology, and decrease proinflammatory cytokines via the NF-κB and JNK pathways in microglia and Aβ1-40-injected SD rats [26]. Therefore, we investigated the protective effect of SCM-198 on neuron and microvascular endothelial cells in both tMCAO rat model and OGD/R *in vitro* model and put forward new mechanisms that contribute to the protective effects of SCM-198 via the STAT3/NOX4/Bcl-2 pathways.

2. Materials and Methods

2.1. Animal Model and Treatment. All the experimental protocol was approved by the institutional ethical committee with internationally accepted ethical standards. Protocols and animal handling were performed in accordance with the guidelines of the National Institutes of Health *Guide for the Care and Use of Laboratory Animals*. Male Sprague-Dawley (SD) rats were supplied by the laboratory animal center, Fudan University. Rats weighing 180-220 g were housed with enough food and water under diurnal lighting condition.

Briefly, we performed the surgery as described previously [27]. All the animals mentioned above were randomly divided into five groups: control operation group, tMCAO group treated with saline, edaravone- (3 mg/kg/day) treated group, and SCM-198 (15 mg/kg/day in normal saline) treatment groups that were posttreated (0.5 h and 2 h after operation). All the drugs were given through tail vein injection once daily for 3 times.

2.2. Transmission Electron Microscopy (TEM). TEM was used to determine neuron ultrastructural changes. All of the ultrathin sections were examined with a Jeol JEM 1200 EX (Jeol Ltd., Tokyo, Japan) transmission electron microscope. An investigator blinded to the study protocol examined tissues [28].

2.3. Tissue Prepared. After three days of treatment, the rats ($n = 6$) were anesthetized with pentobarbital sodium (50 mg/kg), then perfused with 0.9% saline and subsequently with 4% paraformaldehyde in PBS. The brains were removed and postfixed over 12 h in the same aldehyde fixative solution, then immersed in 15% and 30% sucrose solution over 6 days at 4°C. The brains were sectioned at 20 μm which were used for the next experiments [29].

2.4. Nissl Staining. Brain slices described above were stained with Nissl staining solution (Beyotime) for 20 min. The slices were dehydrated in 70%, 95%, and 100% ethanol, cleared in xylene, then covered with neutral resin. Five sections were selected from each rat and three images for cortex and striatum, respectively. The images were analyzed by ImageJ.

2.5. Fluoro-Jade B (FJB) Staining. FJB was used for staining the degenerating neurons. Brain sections described above were stained according to Liu et al. [30].

2.6. Immunofluorescent Staining. Immunofluorescence was assessed as described earlier [31, 32]. Coronal brain slices described above were blocked and incubated in polyclonal rabbit anti-NeuN antibody (Abcam, 1 : 500) overnight in 4°C, followed by Alexa Fluor 488-conjugated goat anti-

rabbit IgG (1 : 1000, Life Technologies) and counterstaining with DAPI. Fluorescence staining was viewed with a laser scanning confocal microscope (Zeiss, Oberkochen, Germany).

2.7. bEnd.3 Cell Culture and Treatment. Mouse bEnd.3 cells were bought from the American Type Culture Collection (ATCC). Cells were cultured according to our previous method [25].

To mimic ischemic-like conditions *in vitro*, bEnd.3 cells were exposed to OGD and reperfusion as we described previously [33]. In brief, the cells were washed with PBS then replaced with glucose-free medium (Invitrogen). The cells were placed in a BioSpherix incubator chamber (ProOx C21, USA), which was flushed with 95% N_2 and 5% CO_2 for 6 h then transferred to 95% air, 5% CO_2, and continued to be cultured in the glucose-containing medium for 4 h each time. The cells were divided into five groups: control, OGD, and cells treated with SCM-198 (0.1 μM, 1 μM, and 10 μM) 2 h before OGD. The inhibitors were added 1 h before OGD until the end of the experiment.

2.8. SH-SY5Y Cell Culture and Coculture with bEnd.3 Cells. SH-SY5Y cell lines were purchased from the American Type Culture Collection. SH-SY5Y cells were cultured with Dulbecco's modified Eagle's medium (DMEM, HyClone, USA) containing 10% fetal bovine serum (FBS, Gibco, USA) and 100 μg/mL penicillin/streptomycin (Gibco) and cultured at 37°C containing 5% CO_2 and 95% O_2.

The coculture system was set up according to a previous study with some modifications [34]. After coculture for 24 h, the SH-SY5Y cells were washed with PBS then replaced with glucose-free medium (Invitrogen). The cells were placed in a BioSpherix incubator chamber (ProOx C21, USA), which was flushed with 95% N_2 and 5% CO_2 for 9 h then transferred to 95% air, 5% CO_2, and continued to be cultured in the glucose-containing medium for 2 h each time.

2.9. MTT and Lactate Dehydrogenase (LDH) Assay. Cell viability was determined by the mitochondrial-dependent reduction of MTT (3-[4,5-dimethylthiazol-2-yl]-2,5-diphenyl tetrazolium bromide) to formazan by adding 10 μL of the MTT agent (5 mg/mL; Sigma-Aldrich) to cells in the plates [35].

LDH activity was detected using the LDH activity assay kit according to the manufacturer's instructions.

2.10. The Measurement of the Level of MDA and the Activity of CAT. Lipid peroxidation is quantified by measuring the level of malondialdehyde (MDA) assay kit (Byotime). The catalase activity (CAT) was determined following the manufacturer's instructions (Beyotime).

2.11. TUNEL. To measure the cell apoptosis after OGD/R insult, we counted the TUNEL- (terminal deoxynucleotidyl transferase-mediated dUTP-biotin nick-end labeling-) positive cells which were determined by a cell death detection kit, according to the manufacturer's protocol (Biotool).

2.12. Coimmunoprecipitation. Coimmunoprecipitation was carried out as described previously [36]. Briefly, bEnd.3 cells were subjected to OGD treatment and reperfusion, then lysed on ice in RIPA buffer. After preclearing with normal IgG, cell lysates (0.5 mg of protein) were incubated overnight at 4°C with 2 μg of anti-NOX4 (Proteintech, 1 : 100) and anti-p-STAT3 (CST, 1 : 100), followed by precipitation with 20 μL of protein A/G Plus-Agarose (Santa Cruz Biotech.) for 1 h at 4°C. The precipitated complexes were used for western blot analysis, as described below.

2.13. Western Blot. Western blot analyses were performed as previously described [36, 37].

Each membrane was incubated with specific antibodies as follows: Bcl-xl (Cell Signaling Technology, 1 : 1000), Bcl-2 (Cell Signaling Technology, 1 : 1000), Bax (Cell Signaling Technology, 1 : 1000), SOD1 (Cell Signaling Technology, 1 : 1000), NOX4 (Proteintech, 1 : 1000), STAT3 (Cell Signaling Technology, 1 : 1000), p-STAT3 (Cell Signaling Technology, 1 : 1000), Akt (Cell Signaling Technology, 1 : 1000), and p-Akt (Cell Signaling Technology, 1 : 1000). To measure the expression of each protein, the relative intensity was calculated by comparing the intensity of GAPDH using densitometry.

3. Results

3.1. The Protection of SCM-198 on Neuron Morphology after Ischemic Stroke. As we know, reperfusion can cause secondary brain injury, including irreversible neuron losses, injury, and degeneration. According to a previous research, we hypothesized whether SCM-198 exerts the effect on neurons in the tMCAO model. Firstly, we investigated brain tissue ultrastructural conditions. Three days after tMCAO operation, large vacuoles and lysosomes appeared in the cytoplasm. Nearly all of the mitochondria in the model group showed ultrastructural pathological changes and most of them were swollen. We could hardly find normal neurons in this group (Figure 1(a)). SCM-198 treatment groups revealed less intercellular edema, better neuron ultrastructure, and better mitochondrial protection than the tMCAO-insulted group. Well-protected neurons and slight dendritic swelling in 0.5 h post operation treatment groups demonstrated great amelioration after SCM-198 treatment. In the 0.5 h post operation treatment with edaravone group, neurons were swelling and with less dense cytoplasm compared with normal neurons. Mitochondrial accumulation occurred which implicated oxidative stress in the insulted region. We next measured the neural cell loss in the peri-ischemic region of tMCAO cortex by Nissl staining. The results revealed that SCM-198 reduced cell shrinkage and empty spaces (Figure 1(b)).

3.2. SCM-198 Reduced Neuron Loss after I/R Insult. Fluoro-Jade B, a kind of cell death marker used for staining degenerating neurons, was chosen for further demonstration of neuroprotection. No FJB-positive cells were found in the control group. On the contrary, vast degenerating neurons were detected in the peri-ischemic regions of the

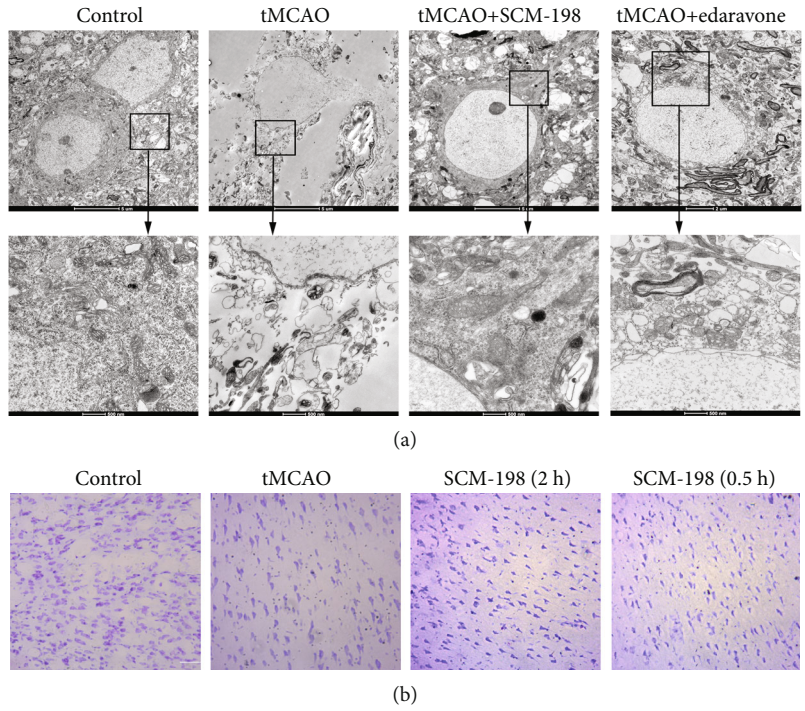

Figure 1: The protection of SCM-198 on neuron morphology after ischemic stroke. (a) The representative TEM of neurons in the peri-ischemic region in the tMCAO model. SCM-198 diminished the changes in neuron morphology after I/R injury. Scale bar = 5 μm and 500 nm, $n = 3$. (b) Representative pictures of coronal sections from the ischemic rat brain stained with Nissl staining. SCM-198 reduced cell shrinkage and empty spaces. Scale bar = 20 μm ($n = 5$).

tMCAO group. SCM-198, in the 0.5 h and 2 h post operation treatment groups, significantly reduced the number of degenerating neurons. Edaravone also decreased the degenerating neurons; the effect was a little weaker than the SCM-198 0.5 h group but there was no significant difference (Figures 2(a) and 2(b)). This result was confirmed by NeuN immunoreactivity (Figure 2(c)); from the result we found that there was a substantial amount of NeuN-positive cells in the control group. tMCAO led to more neuron loss, while SCM-198 could reduce neuron loss in the ipsilateral brain cortex. There was also no significant difference between SCM-198 and edaravone. With this, these results demonstrated that SCM-198 could significantly protect against ischemic injury and improve neuronal survival.

3.3. SCM-198 Improved bEnd.3 Cells Antioxidative Capacity In Vitro. No obvious cytotoxicity was observed at concentrations from 0.001 to 100 μM SCM-198 [26]. Possible antioxidative mechanisms of SCM-198 were studied mainly using bEnd.3 cells *in vitro*. To elucidate the involvement of SCM-198 on OGD/R-induced cellular injury, the content of MDA, activity of CAT, and SOD1 expression were measured. As shown in Figure 3(a), cell viability, evaluated by an MTT assay, was significantly reduced after exposure to OGD for 6 h and reperfusion for 2 h, while SCM-198 could increase cell viability in a concentration-dependent manner. OGD/R led to cell viability decrease to 57.56% ± 3.47; 1 and 10 μM of SCM-198 improve the viability to 76.54% ± 4.15 and 81.73% ± 5.18, respectively. The MDA level of the SCM-198 (1 and 10 μM) group was significantly decreased as compared to the OGD/R group (Figure 3(b)). The level of MDA in the OGD/R group was two- and threefold than SCM-198 (1 and 10 μM). The dose 1 and 10 μM of SCM-198 could predominantly increase intercellular antioxidative capacity by restoring the activity of CAT (Figure 3(c)) and increase the expression of SOD1 (Figure 3(d)). SCM-198, 1 and 10 μM, could enhance the activity of CAT from 0.35 U ± 0.03 to 0.47 U ± 0.07 and 0.49 U ± 0.03. OGD/R-induced cell apoptosis was determined by TUNEL staining; the result showed that OGD/R obviously increased the apoptosis ratio about 58.36% ± 2.72, whereas treatment with SCM-198 (1 and 10 μM) inhibited cell apoptosis to 19.56% ± 4.50 and 14.70% ± 3.47 (Figure 3(e)).

3.4. SCM-1 98 Protected Neurons via Modulating BMECs in BMEC/Neuron Coculture System. As SCM-198 could effectively protect against OGD/R insult in BMEC cells, we then utilized a coculture system to determine whether SCM-198 has an effect on neurons through protecting the BMECs. After 4 h reperfusion, bEnd.3 cells were cocultured with the SH-SY5Y cell line for 24 h before SH-SY5Y was subjected to OGD for 9 h and reperfusion for 2 h. bEnd.3 treatment with SCM-198 coculture with SH-SY5Y exhibited protection against OGD/R injury by improving the cell viability and antioxidant ability and reducing apoptosis. Figure 4(a) shows that conditioned medium with SCM-198, especially 1 μM and 10 μM, increased the cell viability to 77.52% ± 5.84 and 80.09% ± 5.42, respectively, when compared with the OGD/R group without SCM-198 (52.95% ± 1.85). SCM-198 could reduce the LDH leakage and the MDA level in the

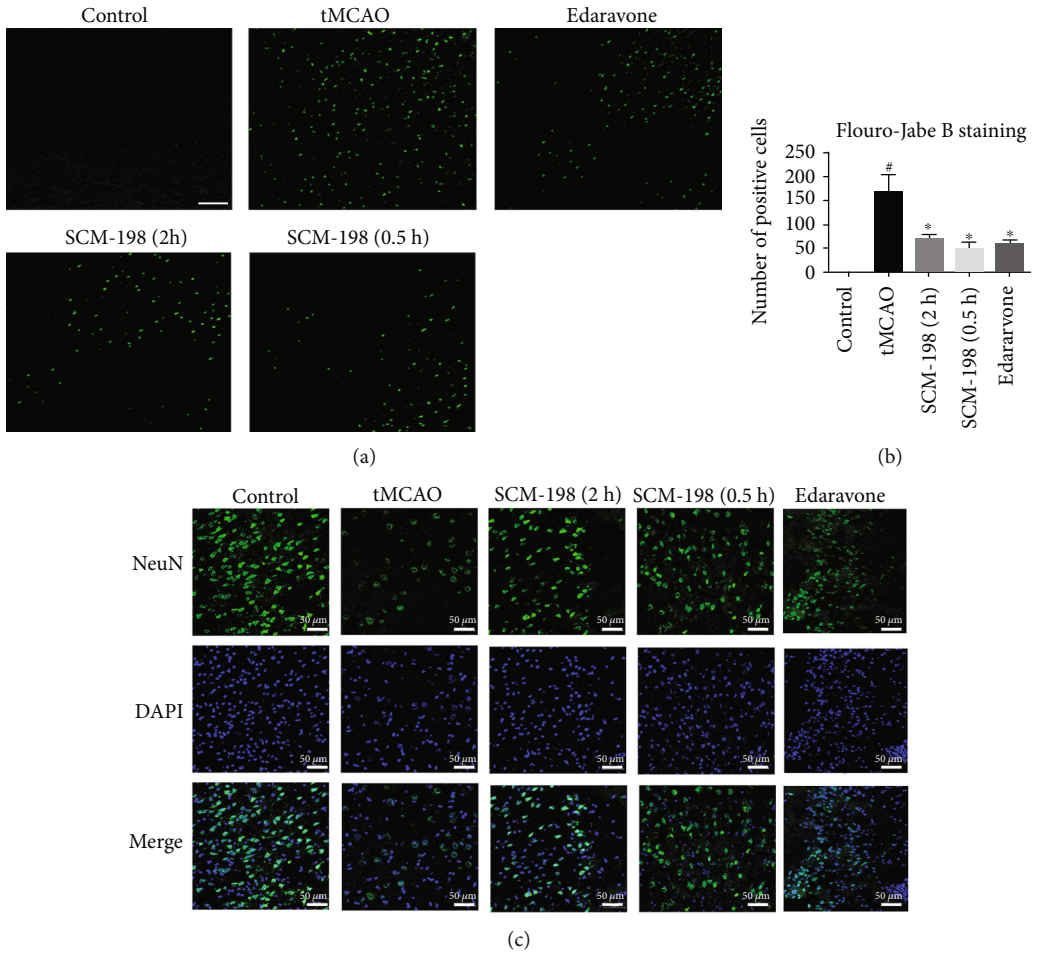

Figure 2: SCM-198 reduced neuron loss after I/R insult. (a) FJB staining of brain sections after reperfusion. Representative pictures of FJB staining of brain sections after reperfusion. No FJB-positive cells were found in the control group. Vast degenerating neurons were detected in the peri-ischemic regions of the tMCAO group. SCM-198 significantly reduced the number of degenerating neurons. (b) The quantitative analysis of the number of degenerating neurons. Scale bar = 50 μm. Values are expressed as mean ± SD. $^{\#}p < 0.05$ versus control group, $^{*}p < 0.05$ versus tMCAO group ($n = 5$). (c) Immunofluorescence staining for NeuN after ischemia reperfusion. SCM-198 could reduce neuron loss in the ipsilateral brain cortex. Scale bar = 50 μm.

SH-SY5Y cells and increase the activity of CAT (Figures 4(b)–4(d)). The leakage of LDH and MDA level in the OGD/R group was three times larger than the control group, while SCM-198 (1 μM and 10 μM) was nearly half of the OGD/R group. SCM-198, 1 μM and 10 μM, increased CAT activity by about 50% compared with the model group. SCM-198 could markedly decrease cell apoptosis, which was confirmed by TUNEL stain. Figure 4(e) shows that OGD/R increased the apoptosis ratio to 50.51% ± 3.59, whereas treatment with SCM-198 (1 and 10 μM) dropped down cell apoptosis to 23.12% ± 4.59 and 14.36% ± 6.53. Consistent with these observations, we believe that SCM-198 could exert a protective effect on neurons via modulating BMECs.

3.5. The Mechanism of SCM-198 Inhibited Apoptosis Induced by OGD/R. Apoptosis is mainly responsible for cell death after ischemia. As we mentioned above, SCM-198 could reduce neuron loss *in vivo* and cell apoptosis *in vitro*. We examined the effect of SCM-198 on the Bcl-2 family, including the antiapoptosis protein Bcl-2 and Bcl-xl and proapoptosis protein Bax. Our results showed that following OGD/R injury Bcl-2 and Bcl-xl significantly decreased, whereas they were improved with SCM-198 treatment (1 and 10 μM) (Figures 5(a)–5(c)). At the same time, the coculture results are consistent with the findings in bEnd.3 cells. BMEC treatment with SCM-198 cocultured with SH-SY5Y exerted protection against apoptosis induced by OGD/R by increasing the expression of Bcl-2 and Bcl-xl and reducing the Bax level (Figures 5(d)–5(f)).

Next, we further explored the mechanism of SCM-198 in reducing cell apoptosis caused by OGD/R in bEnd.3 cells. The results indicated that SCM-198, 1 and 10 μM, protected against apoptosis through improving the level of p-STAT3 and inhibiting the expression of NOX4, then modulated p-Akt, the proteins which were involved in cell apoptosis (Figures 5(g)–5(i)).

3.6. SCM-198 Inhibited Apoptosis through the STAT3/NOX4/Bcl-2 Pathway. As we know, STAT3 and NOX4 are both involved in regulating apoptosis by modulating

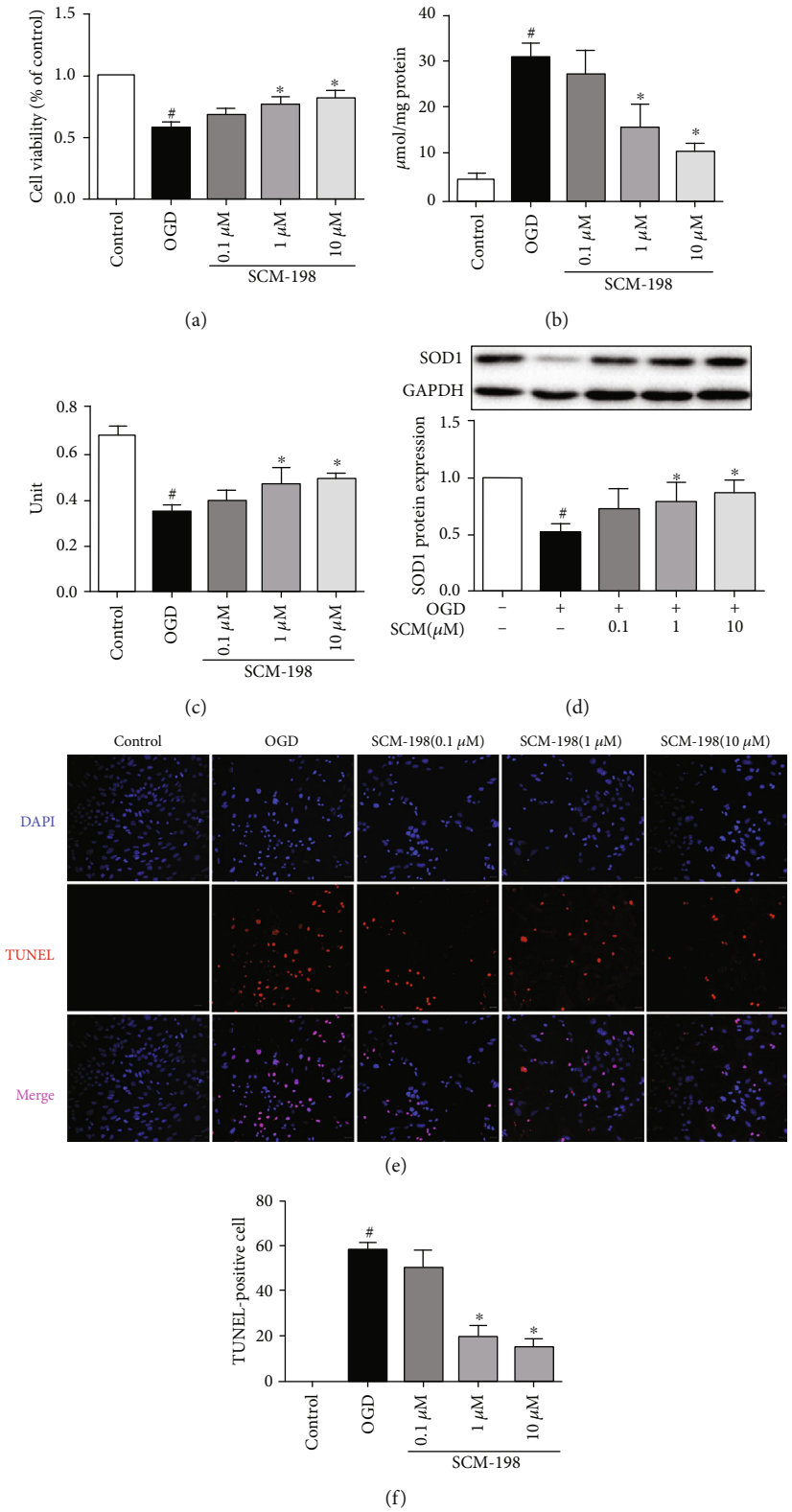

Figure 3: SCM-198 improved bEnd.3 cell antioxidative capacity *in vitro*. SCM-198 exhibited antioxidant abilities and improved the cell viability of bEnd.3. (a) Cell viability, evaluated by an MTT assay, was significantly reduced after OGD/R injury exposure, while 1 μM and 10 μM of SCM-198 could increase cell viability. (b) MDA level of the SCM-198 group was remarkably decreased as compared to the OGD/R group. (c) SCM-198 could predominantly increase intercellular antioxidative capacity by restoring the CAT activity. (d) SCM-198 obviously improved the expression of SOD1. (e) SCM-198 reduced the cell apoptosis in bEnd.3. OGD/R-induced cell apoptosis was determined by TUNEL staining. (f) The result showed that OGD/R obviously increased the apoptosis ratio, whereas treatment with SCM-198 reduced cell apoptosis. Values are expressed as mean ± SD. $^{\#}p < 0.05$ versus control group, $^{*}p < 0.05$ versus OGD group ($n = 3$).

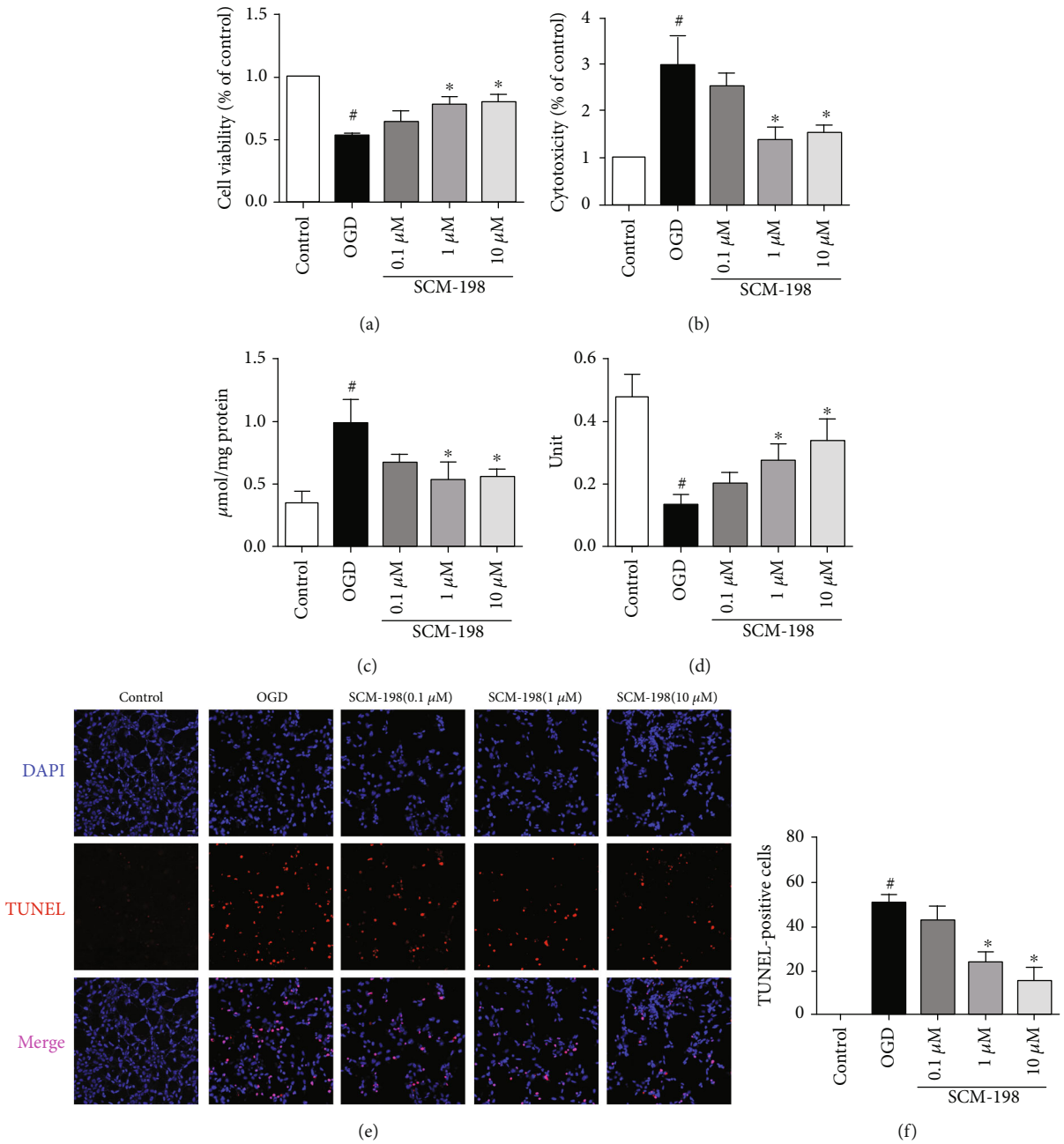

Figure 4: SCM-198 protected neurons via modulating BMECs in BMEC/neuron coculture system. bEnd.3 treated with SCM-198 and cocultured with SH-SY5Y exhibited protection against OGD/R injury by improving the cell viability and the antioxidative ability. (a) Treatment with SCM-198, especially 1 μM and 10 μM, increased bEnd.3 cell viability in OGD/R irritation. (b) SCM-198 could reduce the LDH leakage in SH-SY5Y cells. (c) SCM-198 decreased the production of MDA in SH-SY5Y cells after OGD/R injury. (d) SCM-198 increased the activity of CAT. (e) SCM-198 reduced cell apoptosis in SH-SY5Y. OGD/R-induced cell apoptosis was determined by TUNEL staining; the result showed that OGD/R obviously increased the number of apoptosis, whereas treatment with SCM-198 reduced cell apoptosis. (f) The quantitative analysis of apoptotic cells was calculated. Values are expressed as mean ± SD. $^{\#}p < 0.05$ versus control group, $^{*}p < 0.05$ versus OGD group ($n = 3$).

the PI3K/Akt pathway, but the connection between STAT3 and NOX4 remains unclear. Firstly, we used IL-6 to upregulate p-STAT3 in different concentrations or WP1066 to inhibit STAT3 1 h before OGD/R injury; western blot indicated that the level of NOX4 was inhibited by the overexpression of p-STAT3 and increased by inhibiting STAT3, respectively (Supplementary 1). But when we used DPI or GKT137831 to inhibit NOX4 before being subjected to OGD/R, the level of STAT3 was unchanged (Supplementary 2). We deemed that STAT3 could regulate the expression in ischemic stroke, so we used WP1066 for further study. The results revealed that treatment with 10 μM of SCM-198 still observably decreased the overexpression of NOX4 induced by WP1066 and improved the expression of p-Akt. Then, SCM-198 further reduced the

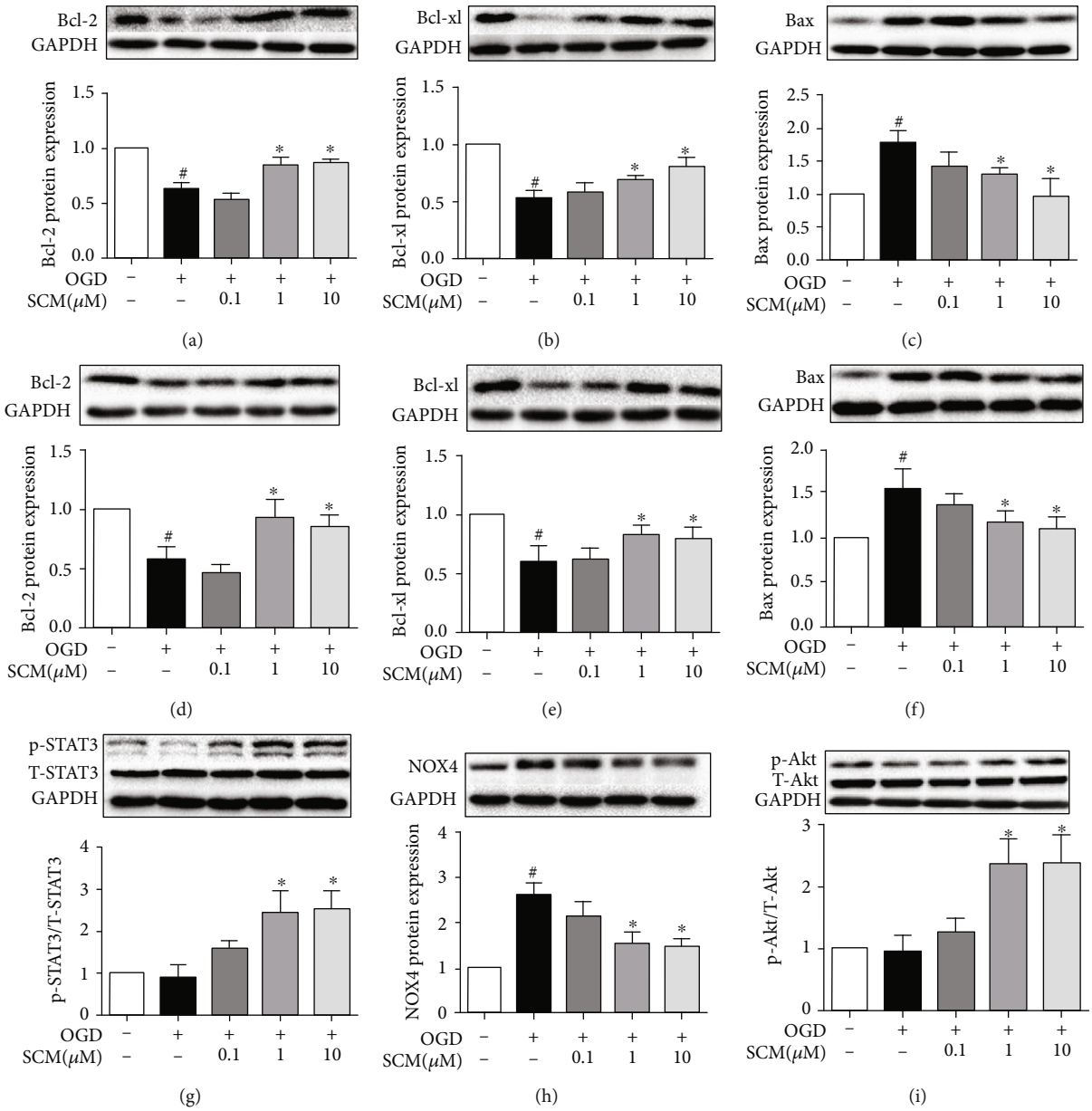

Figure 5: The mechanism of SCM-198 inhibited apoptosis induced by OGD/R. (a–c) SCM-198 regulated the expression of apoptosis-related protein in bEnd.3. OGD/R increased the expression of Bax. OGD/R also decreased the expression of Bcl-2 and Bcl-xl, while SCM-198 could markedly improve the expression of Bcl-2 and Bcl-xl and reduce Bax expression. (d, e) SCM-198 regulated the expression of apoptosis-related protein in SH-SY5Ycells. OGD/R increased the expression of Bax and decreased the expression of Bcl-2 and Bcl-xl, while SCM-198 could obviously improve the expression of Bcl-2 and Bcl-xl and reduce Bax expression. (g–i) SCM-198 regulated the expression of p-STAT3, NOX4, and p-Akt in bEnd.3. SCM-198 protected against apoptosis through improving the level of p-STAT3 and inhibiting the expression of NOX4, then modulated p-Akt. Values are expressed as mean ± SD. $^{\#}p < 0.05$ versus control group, $^{*}p < 0.05$ versus OGD group ($n = 3$).

level of Bax and increased the expression of Bcl-xl and Bcl-2 (Figure 6).

3.7. SCM-198 Upregulates Interaction between p-STAT3 and NOX4. Our previous results have indicated that p-STAT3 participated in OGD/R-mediated NOX4 expression. We speculated that SCM-198 could affect the interaction between p-STAT3 and NOX4. Coimmunoprecipitation analysis demonstrated that the interaction between p-STAT3 and NOX4 was increased by treatment with SCM-198 (Figures 7(a) and 7(b)). These data suggested that SCM-198 improved p-STAT3-NOX4 interaction, which may inhibit NOX4 activation and subsequent apoptosis.

4. Discussion

In the present study, we demonstrated that NOX4 and apoptosis pathway mediated the protective effects of SCM-198 on endothelial cells and neurons during stroke *in vivo* and *in vitro*. In addition, we newly discovered and elucidated the p-STAT3/NOX4 pathway influenced by SCM-198 during BBB breakdown. The expression of p-STAT3 serves as a

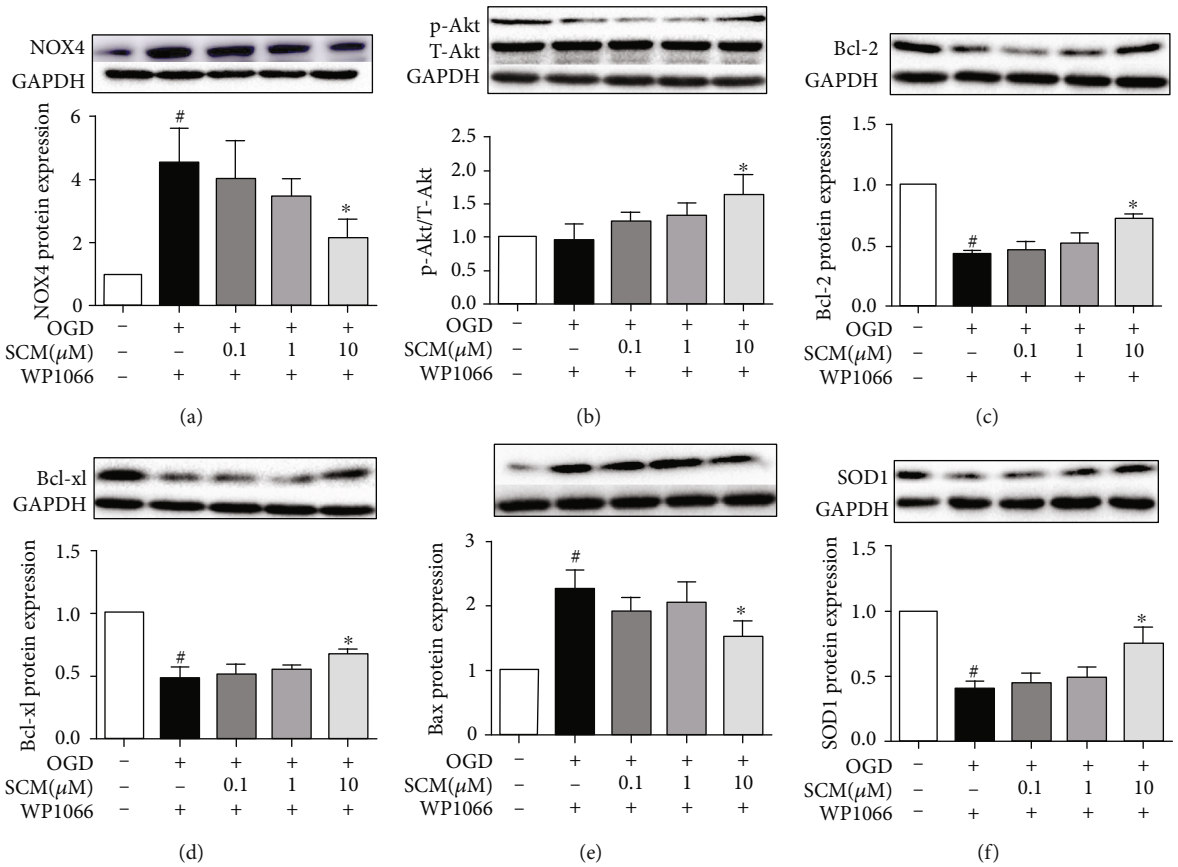

Figure 6: SCM-198 inhibited apoptosis through the STAT3/NOX4/Bcl-2 pathway. (a) SCM-198 (10 μM) still observably decreased the overexpression of NOX4 induced by WP1066. (b) SCM-198 (10 μM) improved the expression of p-Akt. (c–e) SCM-198 (10 μM) could enhance the protection against apoptosis after inhibiting the activation of p-STAT3 in bEnd.3. (f) SCM-198 (10 μM) improved the expression of SOD1 after using WP1066. Values are expressed as mean ± SD. $^{\#}p < 0.05$ versus control group, $^{*}p < 0.05$ versus OGD group ($n = 3$).

negative regulator of NOX4, and maybe it is achieved through direct binding in this hypoxia occasion affected by SCM-198. These results provide new insights into the stroke protective roles of SCM-198 apart from BBB maintenance we have reported recently [25].

In ischemic stroke, the brain firstly suffers from a vast loss of oxygen and nutrient causing tissue damage mainly in the cortex and striatum [38], and reperfusion aggravates the insult due to the fresh oxygen [3]. Conventional remedies for stroke include tPA, an enzyme that recommended for clinical use to catalyze blood clots less than 3 hours after acute ischemia occurs, and edaravone, a free radical scavenger and the only neuroprotective agent clinically approved for acute ischemic stroke in Japan [39]. However, studies have reported that treatment with tPA is frequently accompanied with a detrimental complication such as brain edema because of reperfusion pursued. Edaravone could suppress ROS production and potentially suppress the open of mitochondrial permeability transition pore (MPTP) [39]. Until now, edaravone is the only clinically approved treatment for stroke in Japan and treatment for amyotrophic lateral sclerosis (ALS) in the US and Japan. The limited availability of effective clinical medicine leads to a large unmet need in society, so the development of new approaches for acute stroke management is urgent.

SCM-198 has been reported to have cardioprotective effects against ischemic myocardial injuries through scavenging intracellular ROS and increasing antiapoptosis-associated protein levels [40]. In addition, several studies have reported that SCM-198 can ameliorate the infarction area of the cerebral cortex and improve neurological damage [24, 41]. In this study, we found that the administration of SCM-198 0.5 h post I/R in rat could preserve neuron morphology while neurons in the edaravone treatment group were still swelling and with less dense cytoplasm mass. In the meantime, SCM-198 could prevent neural cell loss in the peri-ischemic region of the cortex (Figure 1). Furthermore, this was repeatedly confirmed by FJB staining and NeuN detecting. The effect of SCM-198 was a little better than edaravone although there was no significance. But as we know, SCM-198 has fewer side effects and is easier to obtain. In the *in vitro* study, we induced bEnd.3 cells or coculture system with OGD/R model. The results reveal that SCM-198 significantly improved cell viability and inhibited cell apoptosis without obvious cytotoxicity in the OGD/R-induced cells. But the results displayed that the effect of

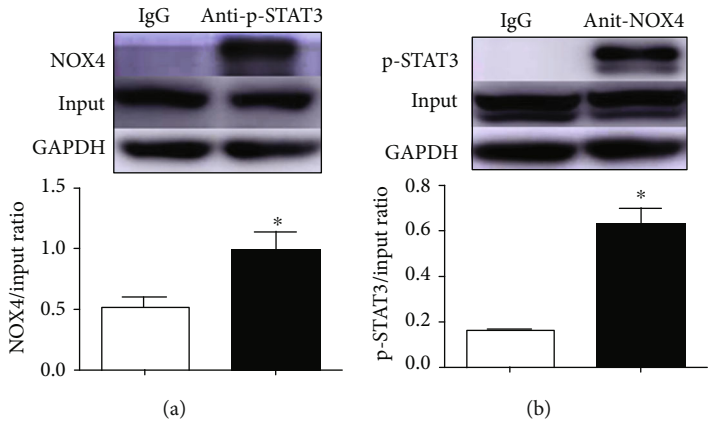

Figure 7: SCM-198 upregulates the interaction between p-STAT3 and NOX4. (a, b) The interactions between p-STAT3 and NOX4 were confirmed by immunoprecipitation. Values are expressed as mean ± SD. $^*p < 0.05$ versus IgG group ($n = 3$).

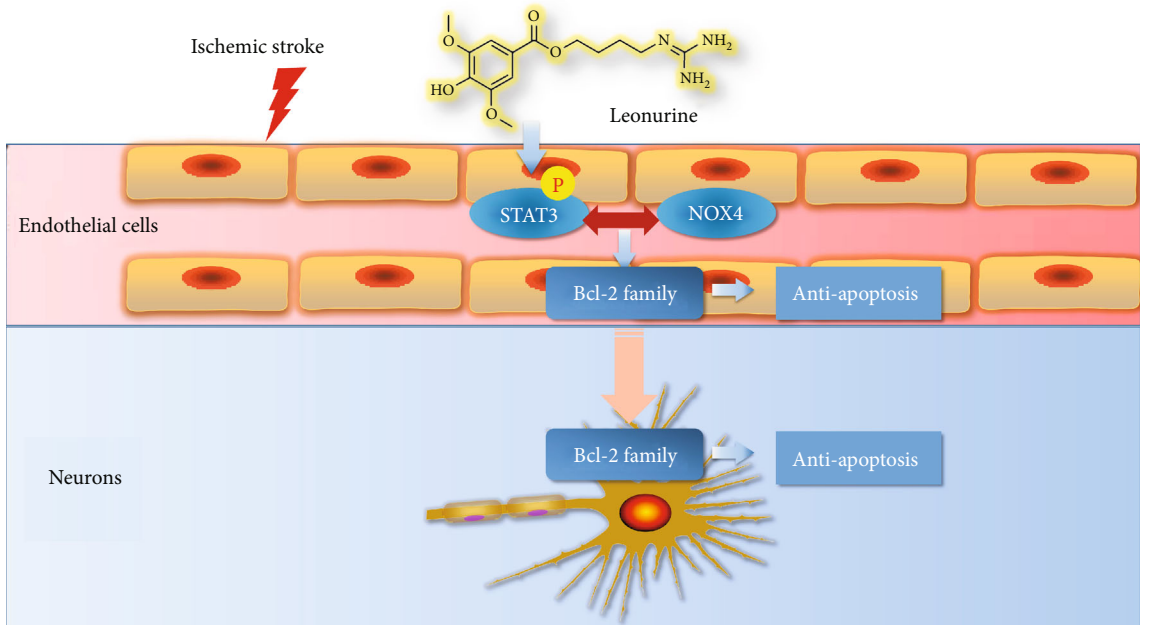

Figure 8: SCM-198 could be the potential drug for neuroprotective effect through stabilizing endothelial cell function.

SCM-198 with 1 and 10 μM sometimes showed a dose response effect between bEnd.3 cells and SH-SY5Y cells. In SH-SY5Y cells, 1 and 10 μM sometimes worked the same way; we speculated that there may be two reasons: (1) conditioned media influenced the results and (2) different experimental systems. Taken together, SCM-198 might play a neuroprotective role in I/R and OGR/R conditions.

STAT3 was reported to be a controversial contributor to cerebral ischemic reperfusion injury. The JAK2/STAT3 pathway is made up of JAK and STAT protein family. Among the STAT proteins, STAT3 is considered the most conserved, and it can be stimulated by various factors and stimuli [18], such as inflammatory cytokines and chemokines. There are contrary functional options about JAK2/STAT3 activation in cerebral ischemia [42]. Many previous studies are agree with that the activation of the JAK2/STAT3 pathway attenuates brain ischemia/reperfusion injury [43]. It is reported that estradiol or catalpol could protect against I/R injury through activating STAT3 [44], which is consistent with the results of ours. In order to make sure the relationship between STAT3 activation and the neuroprotective effects of SCM-198, WP1066, a STAT3 inhibitor, was utilized. Our results revealed that WP1066 could partially counteract the protective effect of SCM-198 (Figure 6), while the overexpression of p-STAT3 could inhibit the expression of NOX4. Co-IP experiment confirmed the direct binding of p-STAT3 and NOX4, and the binding activity could be regulated by SCM198. In addition, the inhibition of NOX4, expression of p-STAT3, was not influenced, indicating that NOX4 was regulated by p-STAT3.

NOX4, a primary source of ROS, is highly expressed in many tissues during hypoxia which suggested that NOX4 could be an important uniform therapeutic target for postischemic injuries. Furthermore, Kleinschnitz et al. reported

that NOX4 predominantly localizes in endothelial cells and neurons in the brain (rodent and human) [12]. In the meantime, the breakdown of BBB, the special structure that differentiates the brain from the heart and other organs, could be attributed to the ROS produced by the endothelial NOX4 during ischemic stroke [13]. Neuronal NOX4 also contributes majorly to neuronal cellular autotoxicity upon ischemia or hypoxia [13]. Pharmacological inhibition of NOX4 could be a promising approach to develop stroke protective drugs. Large-animal stroke models and preparation for clinical trial are ongoing (European Research Council-Proof of Concept Project 737586 SAVEBRAIN). In our study, SCM-198 could markedly reduce the upregulation of NOX4 in endothelial cells and neuronal cells suffering from ischemic condition, which was consistent with our previous studies [21, 25].

5. Conclusion

In summary, our results showed that SCM-198 could exert neuroprotective effects by stabilizing endothelial cell function through regulating the p-STAT3/NOX4/Bcl-2 pathway (Figure 8). Moreover, the regulation of NOX4 could be due to the direct binding to p-STAT3 protein, which could be affected by SCM-198. SCM-198 could be the potential drug for I/R injury.

Abbreviations

tPA: Tissue-type plasminogen activator
STAT3: Activated signal transducers and transcription 3
tMCAO: Transient middle cerebral artery occlusion
FJB: Fluoro-Jade B
TEM: Transmission electron microscopy
CBF: Cerebral blood flow
DAPI: 4′, 6-Diamidino-2-phenylindole
ATCC: American Type Culture Collection
FBS: Fetal bovine serum
DMEM: Dulbecco's modified Eagle's medium
GSH: Glutathione
MTT: 3-[4,5-Dimethylthiazol-2-yl]-2,5-diphenyl tetrazolium bromide
OGD/R: Oxygen-glucose deprivation and reoxygenation
MDA: Malondialdehyde
LDH: Lactate dehydrogenase
CAT: Catalase
TUNEL: Terminal deoxynucleotidyl transferase-mediated dUTP-biotin nick-end labeling
ALS: Amyotrophic lateral sclerosis
ECs: Endothelial cells
NOX: NADPH oxidases
BBB: Blood-brain barrier
MPTP: Mitochondrial permeability transition pore.

Data Availability

All data generated or analyzed during this work are included in this published paper.

Conflicts of Interest

The authors declare that there is no conflict of interest.

Authors' Contributions

Qiu-Yan Zhang, Zhi-Jun Wang, and Wei Guo designed and conducted the experiments, analyzed the data, and wrote the article. Lei Miao, Ying Wang, and Ling-Ling Chang performed the animal experiments. Yi-Zhun Zhu reviewed and edited the article. Qiu-Yan Zhang, Zhi-Jun Wang, and Lei Miao contributed equally to this work.

Acknowledgments

This work has been supported by the National Natural Science Foundation of China (Nos. 81402956, 81573421, 81330080, 81872864, and 81803516), the Shanghai Committee of Science and Technology of China (No. 16431902000), the Shanghai Chenguang Program (No. 14CG03), and the Shanghai Municipal Commission of Health and Family Planning (20184Y0102).

Supplementary Materials

Supplementary1: inhibition of the activity of NOX4 had no effect on the expression of pSTAT3. The inhibitors of NOX4, GKT137831 and DPI, were used before OGD/R injury. But they could not influence the expression of p-STAT3. Supplementary2: upregulation of the expression of p-STAT3 by IL6 could inhibit the level of NOX4 in bEnd.3. A: different concentrations of IL6 were used to improve the expression of p-STAT3 after 12 h incubation; B: IL6 stimulated bEnd.3 for 12 h could not inhibit the expression of NOX4 after OGD/R injury; C: 17.5 ng/mL of IL6 significantly decreased the expression of NOX4 after incubation for 24, 48, and 72 h; D:WP1066 could exacerbate the activation of NOX4 induced by OGD/R injury. *(Supplementary Materials)*

References

[1] C. F. Tsai, B. Thomas, and C. L. M. Sudlow, "Epidemiology of stroke and its subtypes in Chinese vs white populations: a systematic review," *Neurology*, vol. 81, no. 3, pp. 264–272, 2013.

[2] J. Liu, Y. Wang, Y. Akamatsu et al., "Vascular remodeling after ischemic stroke: mechanisms and therapeutic potentials," *Progress in Neurobiology*, vol. 115, pp. 138–156, 2014.

[3] K. A. Radermacher, K. Wingler, F. Langhauser et al., "Neuroprotection after stroke by targeting NOX4 as a source of oxidative stress," *Antioxidants & Redox Signaling*, vol. 18, no. 12, pp. 1418–1427, 2013.

[4] W. Ying and Z. G. Xiong, "Oxidative stress and NAD+ in ischemic brain injury: current advances and future perspectives," *Current Medicinal Chemistry*, vol. 17, no. 20, pp. 2152–2158, 2010.

[5] A. I. Casas, V. T. V. Dao, A. Daiber et al., "Reactive oxygen-related diseases: therapeutic targets and emerging clinical indications," *Antioxidants & Redox Signaling*, vol. 23, no. 14, pp. 1171–1185, 2015.

[6] M. W. Ma, J. Wang, Q. Zhang et al., "NADPH oxidase in brain injury and neurodegenerative disorders," *Molecular Neurodegeneration*, vol. 12, no. 1, 2017.

[7] B. Lassegue, A. San Martin, and K. K. Griendling, "Biochemistry, physiology, and pathophysiology of NADPH oxidases in the cardiovascular system," *Circulation Research*, vol. 110, no. 10, pp. 1364–1390, 2012.

[8] Y. Maejima, J. Kuroda, S. Matsushima, T. Ago, and J. Sadoshima, "Regulation of myocardial growth and death by NADPH oxidase," *Journal of Molecular and Cellular Cardiology*, vol. 50, no. 3, pp. 408–416, 2011.

[9] C. Doerries, K. Grote, D. Hilfiker-Kleiner et al., "Critical role of the NAD(P)H oxidase subunit p47phox for left ventricular remodeling/dysfunction and survival after myocardial infarction," *Circulation Research*, vol. 100, no. 6, pp. 894–903, 2007.

[10] S. M. Craige, K. Chen, Y. Pei et al., "NADPH oxidase 4 promotes endothelial angiogenesis through endothelial nitric oxide synthase activation," *Circulation*, vol. 124, no. 6, pp. 731–740, 2011.

[11] P. W. Kleikers, C. Hooijmans, E. Göb et al., "A combined preclinical meta-analysis and randomized confirmatory trial approach to improve data validity for therapeutic target validation," *Scientific Reports*, vol. 5, no. 1, 2015.

[12] C. Kleinschnitz, H. Grund, K. Wingler et al., "Post-stroke inhibition of induced NADPH oxidase type 4 prevents oxidative stress and neurodegeneration," *PLoS Biology*, vol. 8, no. 9, 2010.

[13] A. I. Casas, E. Geuss, P. W. M. Kleikers et al., "NOX4-dependent neuronal autotoxicity and BBB breakdown explain the superior sensitivity of the brain to ischemic damage," *Proceedings of the National Academy of Sciences of the United States of America*, vol. 114, no. 46, pp. 12315–12320, 2017.

[14] X. Liu, X. Zhang, J. Zhang et al., "Diosmin protects against cerebral ischemia/reperfusion injury through activating JAK2/STAT3 signal pathway in mice," *Neuroscience*, vol. 268, pp. 318–327, 2014.

[15] G. Chen, S. Zhang, J. Shi, J. Ai, and C. Hang, "Effects of recombinant human erythropoietin (rhEPO) on JAK2/STAT3 pathway and endothelial apoptosis in the rabbit basilar artery after subarachnoid hemorrhage," *Cytokine*, vol. 45, no. 3, pp. 162–168, 2009.

[16] H. Zhu, L. Zou, J. Tian, G. du, and Y. Gao, "SMND-309, a novel derivative of salvianolic acid B, protects rat brains ischemia and reperfusion injury by targeting the JAK2/STAT3 pathway," *European Journal of Pharmacology*, vol. 714, no. 1-3, pp. 23–31, 2013.

[17] D. J. Raible, L. C. Frey, and A. R. Brooks-Kayal, "Effects of JAK2-STAT3 signaling after cerebral insults," *JAK-STAT*, vol. 3, 2014.

[18] Z. Liang, G. Wu, C. Fan et al., "The emerging role of signal transducer and activator of transcription 3 in cerebral ischemic and hemorrhagic stroke," *Progress in Neurobiology*, vol. 137, pp. 1–16, 2016.

[19] D. Amantea, C. Tassorelli, R. Russo et al., "Neuroprotection by leptin in a rat model of permanent cerebral ischemia: effects on STAT3 phosphorylation in discrete cells of the brain," *Cell Death & Disease*, vol. 2, no. 12, 2011.

[20] I. Satriotomo, K. K. Bowen, and R. Vemuganti, "JAK2 and STAT3 activation contributes to neuronal damage following transient focal cerebral ischemia," *Journal of Neurochemistry*, vol. 98, no. 5, pp. 1353–1368, 2006.

[21] X. H. Liu, L. L. Pan, H. Y. Deng et al., "Leonurine (SCM-198) attenuates myocardial fibrotic response via inhibition of NADPH oxidase 4," *Free Radical Biology & Medicine*, vol. 54, pp. 93–104, 2013.

[22] C. X. Chen and C. Y. Kwan, "Endothelium-independent vasorelaxation by leonurine, a plant alkaloid purified from Chinese motherwort," *Life Sciences*, vol. 68, no. 8, pp. 953–960, 2001.

[23] X. H. Liu, P. F. Chen, L. L. Pan, R. D. Silva, and Y. Z. Zhu, "4-Guanidino-n-butyl syringate (Leonurine, SCM 198) protects H9c2 rat ventricular cells from hypoxia-induced apoptosis," *Journal of Cardiovascular Pharmacology*, vol. 54, no. 5, pp. 437–444, 2009.

[24] K. P. Loh, J. Qi, B. K. H. Tan, X. H. Liu, B. G. Wei, and Y. Z. Zhu, "Leonurine protects middle cerebral artery occluded rats through antioxidant effect and regulation of mitochondrial function," *Stroke*, vol. 41, no. 11, pp. 2661–2668, 2010.

[25] Q. Y. Zhang, Z. J. Wang, D. M. Sun et al., "Novel therapeutic effects of leonurine on ischemic stroke: new mechanisms of BBB integrity," *Oxidative Medicine and Cellular Longevity*, vol. 2017, Article ID 7150376, 17 pages, 2017.

[26] Z. Y. Hong, X. R. Shi, K. Zhu, T. T. Wu, and Y. Z. Zhu, "SCM-198 inhibits microglial overactivation and attenuates Aβ1-40-induced cognitive impairments in rats via JNK and NF-κB pathways," *Journal of Neuroinflammation*, vol. 11, no. 1, p. 147, 2014.

[27] F. J. Ortega, J. Jolkkonen, N. Mahy, and M. J. Rodríguez, "Glibenclamide enhances neurogenesis and improves long-term functional recovery after transient focal cerebral ischemia," *Journal of Cerebral Blood Flow and Metabolism*, vol. 33, no. 3, pp. 356–364, 2013.

[28] K. Sun, Q. Hu, C. M. Zhou et al., "Cerebralcare Granule®, a Chinese herb compound preparation, improves cerebral microcirculatory disorder and hippocampal CA1 neuron injury in gerbils after ischemia-reperfusion," *Journal of Ethnopharmacology*, vol. 130, no. 2, pp. 398–406, 2010.

[29] C. C. Wei, Y. Y. Kong, X. Hua et al., "NAD replenishment with nicotinamide mononucleotide protects blood–brain barrier integrity and attenuates delayed tissue plasminogen activator-induced haemorrhagic transformation after cerebral ischaemia," *British Journal of Pharmacology*, vol. 174, no. 21, pp. 3823–3836, 2017.

[30] F. Liu, D. P. Schafer, and L. D. McCullough, "TTC, fluoro-Jade B and NeuN staining confirm evolving phases of infarction induced by middle cerebral artery occlusion," *Journal of Neuroscience Methods*, vol. 179, no. 1, pp. 1–8, 2009.

[31] L. L. Pan, X. H. Liu, Y. Q. Shen et al., "Inhibition of NADPH oxidase 4-related signaling by sodium hydrosulfide attenuates myocardial fibrotic response," *International Journal of Cardiology*, vol. 168, no. 4, pp. 3770–3778, 2013.

[32] W. Xin, C. Huang, X. Zhang et al., "Methyl salicylate lactoside inhibits inflammatory response of fibroblast-like synoviocytes and joint destruction in collagen-induced arthritis in mice," *British Journal of Pharmacology*, vol. 171, no. 14, pp. 3526–3538, 2014.

[33] J. Liu, X. Jin, K. J. Liu, and W. Liu, "Matrix metalloproteinase-2-mediated occludin degradation and caveolin-1-mediated claudin-5 redistribution contribute to blood-brain barrier damage in early ischemic stroke stage," *The Journal of Neuroscience*, vol. 32, no. 9, pp. 3044–3057, 2012.

[34] J. Wang, Y. Chen, Y. Yang et al., "Endothelial progenitor cells and neural progenitor cells synergistically protect cerebral

endothelial cells from hypoxia/reoxygenation-induced injury via activating the PI3K/Akt pathway," *Molecular Brain*, vol. 9, no. 1, 2016.

[35] G. Lv, D. Sun, J. Zhang et al., "Lx2-32c, a novel semi-synthetic taxane, exerts antitumor activity against prostate cancer cells _in vitro_ and _in vivo_," *Acta Pharmaceutica Sinica B*, vol. 7, no. 1, pp. 52–58, 2017.

[36] X. Liu, L. Pan, X. Wang, Q. Gong, and Y. Z. Zhu, "Leonurine protects against tumor necrosis factor-α-mediated inflammation in human umbilical vein endothelial cells," *Atherosclerosis*, vol. 222, no. 1, pp. 34–42, 2012.

[37] G. Du, H. Zhu, P. Yu et al., "SMND-309 promotes angiogenesis in human umbilical vein endothelial cells through activating erythropoietin receptor/STAT3/VEGF pathways," *European Journal of Pharmacology*, vol. 700, no. 1-3, pp. 173–180, 2013.

[38] Y. Yang, E. Y. Estrada, J. F. Thompson, W. Liu, and G. A. Rosenberg, "Matrix metalloproteinase-mediated disruption of tight junction proteins in cerebral vessels is reversed by synthetic matrix metalloproteinase inhibitor in focal ischemia in rat," *Journal of Cerebral Blood Flow and Metabolism*, vol. 27, no. 4, pp. 697–709, 2007.

[39] S. Matsumoto, M. Murozono, M. Kanazawa, T. Nara, T. Ozawa, and Y. Watanabe, "Edaravone and cyclosporine A as neuroprotective agents for acute ischemic stroke," *Acute Medicine & Surgery*, vol. 5, no. 3, pp. 213–221, 2018.

[40] X. H. Liu, L. L. Pan, P. F. Chen, and Y. Z. Zhu, "Leonurine improves ischemia-induced myocardial injury through antioxidative activity," *Phytomedicine*, vol. 17, no. 10, pp. 753–759, 2010.

[41] J. Qi, Z. Y. Hong, H. Xin, and Y. Z. Zhu, "Neuroprotective effects of leonurine on ischemia/reperfusion-induced mitochondrial dysfunctions in rat cerebral cortex," *Biological & Pharmaceutical Bulletin*, vol. 33, no. 12, pp. 1958–1964, 2010.

[42] G. Hu, T. Yang, J. Zhou et al., "Mechanism of surrounding rock failure and crack evolution rules in branched pillar recovery," *Minerals*, vol. 7, no. 6, p. 96, 2017.

[43] H. Chen, W. Lin, Y. Zhang et al., "IL-10 promotes neurite outgrowth and synapse formation in cultured cortical neurons after the oxygen-glucose deprivation via JAK1/STAT3 pathway," *Scientific Reports*, vol. 6, no. 1, 2016.

[44] Y. Sehara, K. Sawicka, J. Y. Hwang, A. Latuszek-Barrantes, A. M. Etgen, and R. S. Zukin, "Survivin is a transcriptional target of STAT3 critical to estradiol neuroprotection in global ischemia," *The Journal of Neuroscience*, vol. 33, no. 30, pp. 12364–12374, 2013.

Hindawi
Oxidative Medicine and Cellular Longevity
Volume 2019, Article ID 1479571, 12 pages
https://doi.org/10.1155/2019/1479571

Research Article

A Solid Dispersion of Quercetin Shows Enhanced Nrf2 Activation and Protective Effects against Oxidative Injury in a Mouse Model of Dry Age-Related Macular Degeneration

Yan Shao,[1] **Haitao Yu**,[2] **Yan Yang**,[3] **Min Li**,[4] **Li Hang**,[1] **and Xinrong Xu**[1]

[1]*Department of Ophthalmology, The Affiliated Hospital of Nanjing University of Chinese Medicine, Nanjing 210029, China*
[2]*School of Pharmacy, Nanjing University of Chinese Medicine, Nanjing 210023, China*
[3]*Department of Ophthalmology, The Second Affiliated Hospital of Nanjing University of Chinese Medicine, Nanjing 210017, China*
[4]*Department of Ophthalmology, Liyang Branch of the Affiliated Hospital of Nanjing University of Chinese Medicine, Liyang 213300, China*

Correspondence should be addressed to Xinrong Xu; xinrong_xu@aliyun.com

Received 30 May 2019; Accepted 17 September 2019; Published 7 November 2019

Guest Editor: João C. M. Barreira

Age-related macular degeneration (AMD) represents a major reason for blindness in the elderly population. Oxidative stress is a predominant factor in the pathology of AMD. We previously evaluated the effects of phospholipid complex of quercetin (Q-PC) on oxidative injury in ARPE-19 cells, but the underlying mechanisms are not fully understood. Herein, the solid dispersion of quercetin-PC (Q-SD) was prepared with solubility being 235.54 μg/mL in water and 2.3×10^4 μg/mL in chloroform, which were significantly higher than that of quercetin (QT) and Q-PC. Q-SD also exhibited a considerably higher dissolution rate than QT and Q-PC. Additionally, Q-SD had Cmax of 4.143 μg/mL and AUC of 12.015 μg·h/mL in rats, suggesting better bioavailability than QT and Q-PC. Then, a mouse model of dry AMD (Nrf2 wild-type (WT) and Nrf2 knockout (KO)) was established for evaluating the effects of Q-SD in vivo. Q-SD more potently reduced retinal pigment epithelium sediments and Bruch's membrane thickness than QT and Q-PC at 200 mg/kg in Nrf2 WT mice and did not work in Nrf2 KO mice at the same dosage. Additionally, Q-SD significantly decreased ROS and MDA contents and restored SOD, GSH-PX, and CAT activities of serum and retinal tissues in Nrf2 WT mice, but not in Nrf2 KO mice. Furthermore, Q-SD more potently increased Nrf2 mRNA expression and stimulated its nuclear translocation in retinal tissues of Nrf2 WT mice. Q-SD significantly increased the expression of Nrf2 target genes HO-1, HQO-1, and GCL of retinal tissues in Nrf2 WT mice, not in Nrf2 KO mice. Altogether, Q-SD had improved physicochemical and pharmacokinetic properties compared to QT and Q-PC and exhibited more potent protective effects on retina oxidative injury in vivo. These effects were associated with activation of Nrf2 signaling and upregulation of antioxidant enzymes.

1. Introduction

Age-related macular degeneration (AMD) is a leading irreversible blindness in elderly people all over the world. This disease can be generally divided into two categories, namely, dry AMD and wet AMD. The former is characterized by choroidal capillary atrophy, drusen, and retinal pigment epithelium (RPE) atrophy, and geographic atrophy of the macular region commonly occurs in its advanced stage, resulting in decreased visual acuity and even wet AMD. The wet AMD is primarily featured by choroidal neovascularization (CNV), leading to retinal exudation and hemorrhage and eventually serious impairment of vision [1, 2]. Recently, much progress has been made in the management of wet AMD due to the application of anti-VEGF (vascular endothelial growth factor) agents in clinical practice [3, 4]. However, the underlying mechanism of dry AMD pathology remains largely unknown, and thus, there are no effective therapeutic options for dry AMD.

A large number of studies have highlighted a critical role for oxidative stress in the pathology of dry AMD [5].

Oxidative stress reflects an imbalance between the systemic manifestation of reactive oxygen species (ROS) and a biological system's ability to readily detoxify the reactive intermediates or to repair the resulting damage [6]. Long-term light exposure can stimulate lipofuscin-mediated oxidative stress in the macula and produce a large amount of superoxide anion, singlet oxygen, and hydrogen peroxide, leading to RPE cell injuries and aggravating the pathogenesis of dry AMD [7]. The nuclear factor erythroid 2-related factor 2 (Nrf2) is a basic leucine zipper protein that regulates the expression of antioxidant proteins that protect against oxidative damage triggered by injury and inflammation, thus serving as a pivotal regulator of redox system in mammal cells [8]. Under normal or unstressed conditions, Nrf2 is kept in the cytoplasm by a cluster of proteins that degrade it quickly. Under oxidative stress, however, Nrf2 is not degraded but instead travels to the nucleus where it binds to antioxidant response elements (AREs) and initiates transcription of antioxidant genes and their proteins [9]. Activation of Nrf2 can induce the expression of many antioxidases and phase II metabolizing enzymes, heme oxygenase-1 (HO-1), quinone oxidoreductase-1 (NQO-1), glutathione-S-transferase, glutamate cysteine ligase (GCL), superoxide dismutase (SOD), catalase (CAT), and glutathione peroxidase (GSH-PX) [10]. These enzymes can quickly scavenge ROS and protect the body from injuries caused by active substances or toxic substances. In addition, they can also regulate cell proliferation and death and enhance the ability to scavenge ROS, thus maintaining intracellular redox balance and reduce oxidative damage.

Quercetin (QT) is a naturally occurring flavonoid compound. Increasing investigations have demonstrated that QT has antioxidant, ROS-scavenging, anti-inflammatory, and antitumor effects [11]. However, QT has the disadvantages of poor water and fat solubility and low bioavailability [12]. Our previous studies showed that the phospholipid complex of quercetin (Q-PC) had a threefold increase in water solubility and 734-fold increase in fat solubility and exhibited stronger protective effects than QT against oxidative injury in ARPE-19 cells by increasing cell viability and reducing apoptosis [13]. Moreover, Q-PC was also found to have stronger protective effects against liver oxidative injury than quercetin in rats [14]. Although formation of phospholipid complex significantly increased the solubility of QT, the hydrophobicity of phospholipid complex resulted in poor dispersity of QT [15]. Therefore, the phospholipid complex had limited increase in bioavailability. Studies have indicated that preparation of solid dispersion can significantly increase the solubility and dissolution rate of drugs, which can further enhance the bioavailability of drugs [16, 17]. In the current study, we successfully prepared the solid dispersion of quercetin phospholipid complex (Q-SD), determined its bioavailability in rats, and evaluated its protective effects on retinal injury caused by oxidative stress in Nrf2 wild-type and Nrf2 knockout mice.

2. Materials and Methods

2.1. Chemicals, Reagents, and Antibodies. Quercetin was obtained from Sigma Chemical (St. Louis, MO, USA). Reagent-grade soy lecithin (purity > 97%) was purchased from Shanghai Guyan Industry Co., Ltd. (Shanghai, China). Polyvinylpyrrolidone (PVP K30) was purchased from J&K Chemical Ltd. (Shanghai, China). Hydroquinone was obtained from Alfa Aesar (Heysham, Lancashire, UK). The primary antibodies used in Western blot analyses against Nrf2, HO-1, NQO-1, GCL, GAPDH, and Lamin B, and the secondary antibody Goat Anti-Rabbit IgG/HRP were all obtained from Abcam (Cambridge, UK).

2.2. Perpetration of Q-SD. We used the solvent method to prepare Q-SD. Briefly, quercetin and soy lecithin (mass ratio 1 : 1) were dissolved in ethanol of adequate volume stirred for 1 h. Decompression distillation was carried out to remove ethanol. After 12 h vacuum drying, the resulting precipitates were grinded and sieved through 100 mesh sieve, yielding Q-PC stored in a desiccator for subsequent experiments. Next, the prepared Q-PC and PVP K30 at a mass ratio of 1 : 3 were dissolved in absolute ethanol of adequate volume with full mixing. This ratio was determined by orthogonal tests via preliminary experiments. After the mixture was evaporated in vacuo at 50°C, the Q-SD was obtained for experiments.

We then determined the standard curve of Q-SD. The chromatographic conditions were a Waters 600 C_{18} column, methanol 0.4% H_3PO_4 solution (v/v 50 : 50) as the mobile phase, 370 nm wavelength, 1.0 mL/min flow velocity, 30°C column temperature, and 20 μL sample size. The control solution was prepared according to following procedures. QT of 10 mg was dissolved in ethanol and volumed in a 50 mL volumetric flask, and thereby the QT control solution at a concentration of 200 mg/L was obtained. Anhydrous ethanol was used to dilute to the control solution to yield a series of solutions at 10, 20, 40, 60, 80, and 100 mg/L. Each solution of 20 μL was injected into a high-performance liquid chromatograph (HPLC, Waters 600, USA) for measurement of the peak area. Concentrations of QT ([C]) were marked at the horizontal ordinate and peak areas (A) at the longitudinal coordinate giving the standard curve equation $A = 4986.6 \times [C] - 10.43219$ ($R = 0.9998$), linear range 2.06 – 93.7 μg/mL.

2.3. Determination of Q-SD Solubility. QT, Q-PC, and Q-SD (all containing 20 mg pure quercetin) were precisely weighed and added into a 100 mL conical flask, and then distilled water/chloroform of 20 mL was added. The solutions were incubated in a 25°C thermostatic oscillator for 6 h. Each sample of 5 mL was filtered through 0.45 μm microporous membrane. The successive filtrate of 10 μL was subjected to HPLC analyses. Control solution of 10 μL at 40 mg/L was spontaneously analyzed by HPLC. The equilibrium solubility of the three kinds of samples in water and chloroform was measured, respectively, based on the peak area.

2.4. Determination of Dissolution Rate of Q-SD. QT, Q-PC at a mass ratio of 1 : 1, and Q-SD at a mass ratio of 1 : 1 : 3 (all containing 20 mg pure quercetin) were evenly dispersed in 200 mL distilled water at 37°C and centrifuged at 100 r/min. Each sample of 2 mL was collected at the time points of 10, 20, 30, 40, 50, and 60 min and was subjected to filtration. The successive filtrate of 1 mL was volumed in

a 10 mL volumetric flask with distilled water. HPLC analyses were used, and mass concentrations were calculated through introducing the peak area into the standard curve equation followed by calculation of the cumulative dissolution percentage.

2.5. Determination of Serum Concentrations of Q-SD. Eighteen Sprague Dawley rats obtained from the Model Animal Research Centre of Nanjing University (Nanjing, China) were randomly divided into three groups, namely, the QT treatment group, Q-PC treatment group, and Q-SD treatment group ($n = 6$). All rats in the three groups were intragastric administrated with corresponding drugs containing pure QT at 100 mg/kg. Blood samples were collected from orbit at time points of 0.25, 0.5, 0.75, 1, 1.5, 2, 4, and 8 h in each rat. After adding heparin, blood samples were centrifuged at 3000 r/min for 15 min, and the supernatants were collected for examinations. Next, each sample of 0.2 mL was added into a 10 mL centrifuge tube and incubated with 0.2 mL 25% hydrochloric acid in water bath at 80°C for 1 h. Ethyl acetate of 1 mL was added to each sample followed by vortex for 3 min and centrifugation at 3000 r/min for 10 min. The upper organic phase was collected with addition of 1 mL ethyl acetate, and the abovementioned procedures were repeated. The two upper organic phases were combined together and subjected to nitrogen drying in 50°C water bath followed by dissolution with 200 μL methanol and centrifugation at 12000 r/min for 10 min. The supernatants were analyzed by HPLC for determining drug concentrations.

2.6. Animal Experimental Procedures. Eighty-four female C57BL/6 mice (6-month old, body weight 25-33 g, Nrf2 wild genotype) were purchased from the Model Animal Research Centre of Nanjing University (Nanjing, China). Thirty-six Nrf2 knockout (Nrf2 KO) mice (C57BL/6 background) were kindly provided by Dr. Peng Cao (Jiangsu Provincial Academy of Chinese Medicine, Nanjing, China), and the mouse strain was from Johns Hopkins University Medical School (USA). All mice were maintained under a 12 h light/dark cycle at a controlled temperature (25°C) with free access to food and tap water. The Nrf2 wild-type (Nrf2 WT) mice were divided into 7 groups, namely, the aging control group, model control group, QT group (200 mg/kg), Q-PC group (200 mg/kg), and Q-SD groups (50, 100, and 200 mg/kg). The Nrf2 KO mice were divided into 3 groups, namely, the aging control group, model control group, and Q-SD group (200 mg/kg). These doses were defined as the content of pure QT in the phospholipid complex or solid dispersion and were determined by preliminary experiments.

Animals were treated according to the following procedures: (1) For the aging control mice of both Nrf2 WT and Nrf2 KO, they were fed normal diet during months 1-9. (2) For the model control mice of both Nrf2 WT and Nrf2 KO, they were fed with normal diet during months 1-3, then high-fat diet, received the intake of hydroquinone dissolved in the drinking water (0.8%) during months 4-6, and were intragastric administrated with 0.5% CMC-Na suspension daily during months 7-9. (3) For the treatment mice of both Nrf2 WT and Nrf2 KO, they were fed normal diet during months 1-3, then high-fat diet, received the intake of hydroquinone dissolved in the drinking water (0.8%) during months 4-6, and were intragastric administrated with corresponding drugs (suspended in 0.5% CMC-Na) daily during months 7-9. All experimental procedures were approved by the institutional and local committee on the care and use of animals, and all animals received humane care according to the National Institutes of Health (USA) guidelines.

2.7. Transmission Electron Microscopy. Eyeballs of three mice in each group were isolated and fixed immediately in 4% paraformaldehyde for 20 min. The cornea, crystalline lens, and vitreous body were removed from the eye tissues. Wall tissue (2 × 4 mm) was excised from the bilateral area of the optic disc and fixed with glutaral/osmic acid, coated with epoxy resins, and sectioned. After double staining with uranyl acetate and lead citrate, the sections were examined with a transmission electron microscope (Tecnai G2 Spirit Bio TWIN; FEI, Hillsboro, OR, USA), and images were taken. The semiquantitative evaluation of width of the sediment beneath the RPE and the thickness of Bruch's membrane was determined according to the methods reported by Espinosa-Heidmann et al. [18].

2.8. Measurements of ROS, MDA, and Antioxidant Enzymes. Blood was collected from the orbital cavity of three mice of each group, and serum was isolated. Meanwhile, the eyeball was extracted and the retina was isolated, and tissue homogenates were prepared via centrifugation at 4°C, 3000 r/min for 10 min. The ROS levels in the serum were determined using Fenton's reaction and Griess reagent chromogenic method, and the ROS levels in the retina tissue were determined using the DCFH-DA method. Levels of MDA in serum and retinal tissues were measured using the thiobarbituric acid method. In addition, activities of SOD, GSH-PX, and CAT in serum and retinal tissues were measured using corresponding enzyme-linked immunosorbent assay kits at the wavelength of 450, 412, and 405 nm, respectively. All the kits above were purchased from the Nanjing Jiancheng Bioengineering Institute (Nanjing, China), and experiments were performed according to the instructions provided by the manufactures.

2.9. Real-Time PCR. Total RNA was isolated from the retina and choroid of three mice of each group using a TRIzol reagent (Sigma, St. Louis, MO, USA) following the protocol provided by the manufacturer. Reverse transcription was carried out using kits according to the instructions provided by Thermo Scientific Fisher (USA). Glyceraldehyde phosphate dehydrogenase (GAPDH) was used as the invariant control. Fold changes in the mRNA levels of target genes related to GAPDH were calculated. Experiments were performed in triplicate. The primers of genes (GenScript, Nanjing, China) were as follows: Nrf2: (forward) 5′-AGTGAC TCGGAAATGGATGAG-3′, (reverse) 5′-TGTGCTGGC TGTGCGTTAGG-3′; HO-1 (forward) 5′-GCTGGTGAT GGCTGCCTTGT-3′, (reverse) 5′-ACTGGGTGCTGCTT GTTGCG-3′; HQO-1 (forward) 5′-ATGTATGACAATGG ACCCTTCC-3′, (reverse) 5′-TCCCTTGCAGAGTGTC

Table 1: Equilibrium solubility of quercetin of different dosage forms (25°C, $n = 3$).

Solvent	Concentration (μg/mL)		
	Quercetin	Quercetin-PC	Quercetin-SD
Water	20.15 ± 1.45	46.81±2.68**	235.54±4.73**##
Chloroform	2.18 ± 0.25	1.35×10^3±29.22**	2.3×10^3±102.9**#

Significance: **$p < 0.01$ versus quercetin; #$p < 0.05$ versus quercetin-PC; ##$p < 0.01$ versus quercetin-PC.

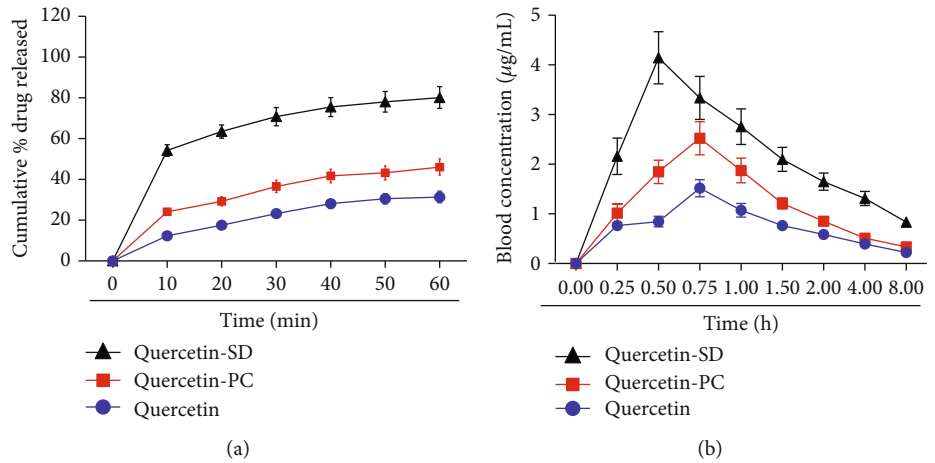

Figure 1: Quercetin-SD has better physicochemical and pharmacokinetic properties than quercetin and quercetin-PC. (a) Determination of cumulative dissolution rates of quercetin, quercetin-PC, and quercetin-SD at indicated time points. (b) Determination of blood concentrations of quercetin, quercetin-PC, and quercetin-SD at indicated time points in rats.

ATGG-3′; GCL (forward) 5′-GAAGTGGATGTGGACACTA GATG-3′, (reverse) 5′-TTGTAGTCAGGATGGTCTGCG ATAA-3′; and GAPDH (forward) 5′-ATGACATCAAGACG GTGGTG-3′, (reverse) 5′-CATACCAGGTATGAGCTTG-3′.

2.10. Western Blot Analysis. Proteins were extracted from the retina and choroid of three mice of each group using a radioimmunoprecipitation assay buffer containing 150 mM NaCl, 50 mM Tris, 0.1% sodium dodecyl sulphate, 1% Nonidet P-40, and 0.5% deoxycholate supplemented with protease inhibitor phenylmethylsulfonyl fluoride. In examining Nrf2 expression, nuclear proteins and cytoplasmic proteins were separated using a Bioepitope Nuclear and Cytoplasmic Extraction Kit (Bioworld Technology, St. Louis Park, MN, USA) according to the protocol. Proteins (50 μg/well) were separated by SDS-polyacrylamide gel, transferred to a PVDF membrane (Millipore, Burlington, MA, USA), blocked with 5% skim milk in Tris-buffered saline containing 0.1% Tween 20. Target proteins were detected by corresponding primary antibodies and subsequently by horseradish peroxidase-conjugated secondary antibodies. Protein bands were visualized using a chemiluminescence reagent (Millipore, Burlington, MA, USA). Equivalent loading was confirmed using an antibody against GAPDH for total proteins and against Lamin B for nuclear proteins. Representative blots were from three independent experiments. The levels of target protein bands were densitometrically determined using Quantity One 4.4.1. The variation in the density of bands was expressed as fold changes compared to the control in the blot after normalization to GAPDH or Lamin B.

2.11. Statistical Analysis. Data were presented as mean ± SEM, and results were analyzed using GraphPad Prism 5 software. The significance of difference was determined by Student's t-test for comparison between two groups and one-way ANOVA with post hoc Dunnett's test for comparison between multiple groups. A value of $p < 0.05$ was considered to be statistically significant.

3. Results

3.1. Q-SD Has Better Physicochemical and Pharmacokinetic Properties Than QT and Q-PC. We initially characterized several key physicochemical properties of Q-SD. The results showed that the equilibrium solubility of Q-SD in both water and chloroform was significantly higher than that of QT and Q-PC (Table 1). Determination of the dissolution rate showed that Q-SD had significantly higher cumulative dissolution rates than that of QT and Q-PC at each time point (Figure 1(a)). Next, we determined some key pharmacokinetic parameters of Q-SD in rats and obtained the serum concentration-time curve (Figure 1(b)). The maximum serum concentration of Q-SD was considerably increased to 4.143 μg/mL from 1.517 μg/mL of QT or 2.523 μg/mL of Q-PC. In addition, the area under the curve of Q-SD was remarkably increased to 12.015 μg·h/mL from 5.461 μg·h/mL of QT and 8.074 μg·h/mL of Q-SD. These results collectively

demonstrated that Q-SD had better physicochemical and pharmacokinetic properties than QT and Q-PC.

3.2. Q-SD More Potently Improves Retina Pathological Changes in Nrf2 WT Model Mice of Dry AMD. We established the disease model in both Nrf2 WT and Nrf2 KO mice to evaluate the effects of drugs, which reflects typical pathological changes of dry AMD in humans and has been widely used by investigators [18, 19]. Histopathological examinations using transmission electron microscopy showed that there was less spotted sediment and relatively normal Bruch's membrane (BrM) thickness in Nrf2 WT mice of the aging control group, obvious sediment, and thickened BrM in Nrf2 KO mice; massive successive flat sediment and thickened BrM were observed in Nrf2 WT mice of the model control group, but more severe in Nrf2 KO mice (Figure 2(a)). Q-SD at 200 mg/kg distinctly decreased RPE sediment compared to the model control in Nrf2 WT mice, not in Nrf2 KO mice (Figure 2(a)). Consistently, the scoring of sediment severity demonstrated that Q-SD at 200 mg/kg significantly reduced the deposit severity score compared to the QT and Q-PC groups at the same dosage in Nrf2 WT mice and did stronger than that of Q-SD at 100 mg/kg (Figure 2(b)). Furthermore, BrM thickness was significantly reduced by Q-SD at 200 mg/kg in Nrf2 WT mice, not in Nrf2 KO mice and did stronger than that of Q-SD at 100 mg/kg (Figure 2(c)). Collectively, these data indicated that Q-SD more potently improved retina pathological changes in Nrf2 WT, not in Nrf2 KO model mice of dry AMD.

3.3. Q-SD Exerts More Potent Antioxidant Effects in Nrf2 WT Model Mice of Dry AMD. We speculated that regulation of the redox system could be involved in the effects of Q-SD and thus subsequently examined ROS, MDA, and several antioxidant enzymes in mice. We found that the ROS and MDA levels in both serum and retinal tissues were significantly upregulated in Nrf2 WT and Nrf2 KO mice of the model control group but more obvious in Nrf2 KO mice. Q-SD at 200 mg/kg significantly decreased the ROS and MDA levels, not in Nrf2 KO mice. Q-SD at 200 mg/kg produced the strongest effect on the MDA level compared to that of Q-SD at 100 mg/kg in Nrf2 WT mice (Figures 3(a) and 3(b)). Furthermore, examinations of the three key antioxidant enzymes SOD, GSH-PX, and CAT showed that their activities in serum and retinal tissues were significantly decreased in the model group of Nrf2 WT and more remarkable in Nrf2 KO mice. Treatment with Q-SD at 200 mg/kg significantly increased their activities in serum and retinal tissues in Nrf2 WT mice, not in Nrf2 KO mice. Q-PC at 200 mg/kg and Q-SD at 100 mg/kg also increased their activities in Nrf2 WT mice; as expected, Q-SD at 200 mg/kg yielded the most significant effect (Figures 3(c)–3(e)). Taken together, these results suggested that Q-SD exerted more potent antioxidant effects in the Nrf2 WT model mice of dry AMD.

3.4. Activation of Nrf2 Is Associated with the Potent Protective Effects on Retina Injury by Q-SD in Model Mice of Dry AMD. We further explored the underlying mechanism for Q-SD effects focusing on Nrf2 signaling pathway. We observed that Nrf2 mRNA was markedly increased in retinal and choroid tissues in Nrf2 WT and Nrf2 KO mice; Nrf2 mRNA was markedly increased in Nrf2 WT mice of the model group and was nearly undetectable in Nrf2 KO mice. Q-SD at 200 mg/kg significantly increased Nrf2 mRNA level compared to the model group in Nrf2 WT mice, not in Nrf2 KO mice (Figure 4(a)) (Nrf2 KO mice data not presented in the figure). Moreover, the nuclear abundance of Nrf2 was significantly increased in the model group of Nrf2 WT mice, and Q-SD at 200 mg/kg significantly stimulated nuclear translocation of Nrf2 compared to the model group (Figure 4(b)). However, the cytoplasm abundance of Nrf2 in the model group and Q-SD treatment groups in Nrf2 WT mice was not significantly altered (Figure 4(b)). Nrf2 protein expression in neither nucleus nor cytoplasm was undetectable in Nrf2 KO mice (Figure 4(b)). Furthermore, we examined the expression of major target genes of Nrf2, which are critically involved in the antioxidant system. Real-time PCR analyses showed that the transcript levels of HO-1, NQO-1, and GCL were significantly upregulated in Nrf2 WT mice of the model group and that Q-SD at 100 mg/kg and 200 mg/kg significantly increased their mRNA levels compared to the model group. In the model group Nrf2 KO mice, the mRNA expression of HO-1, NQO-1, and GCL was not significantly enhanced compared to that of the aging control group (Figure 5). Meanwhile, in the model group Nrf2 WT mice, the protein expression of HO-1, NQO-1, and GCL was significantly increased compared to the aging control, and Q-SD at 100 mg/kg and 200 mg/kg significantly upregulated the protein expression of HO-1, NQO-1, and GCL. In Nrf2 KO mice, the protein abundance of HO-1, NQO-1, and GCL was remarkably lower than that in Nrf2 WT mice, and there was no significant difference between the aging control and model control in Nrf2 KO mice (Figure 6). Altogether, these data revealed that activation of Nrf2 was associated with the potent protective effects on retina injury by Q-SD in model mice of dry AMD.

4. Discussion

Currently, there are no promising therapeutic options for dry AMD in clinical practice. Accumulating evidence indicates that agents that are able to protect the retina against oxidative stress-induced injury can be an important direction for management of dry AMD. An early clinical research termed Age-Related Eye Disease Study (AREDS) showed that pharmacological use of antioxidants, such as β-carotene, vitamin C, vitamin E, zinc, and copper, could prevent AMD progression and reduce 25% risk in advanced AMD progression and 19% risk in moderate vision loss within 5 years [20]. *Fructus lycii* is a well-known tonic medicine frequently used for treating aging-related eye diseases in traditional Chinese medicine system and has been demonstrated to possess antioxidative and antiaging effects [21]. Our previous studies showed that Fructus lycii ethanol extract effectively reduced the RPE sediment and Bruch's membrane thickness in mice with experimental AMD, and its major components lutein and

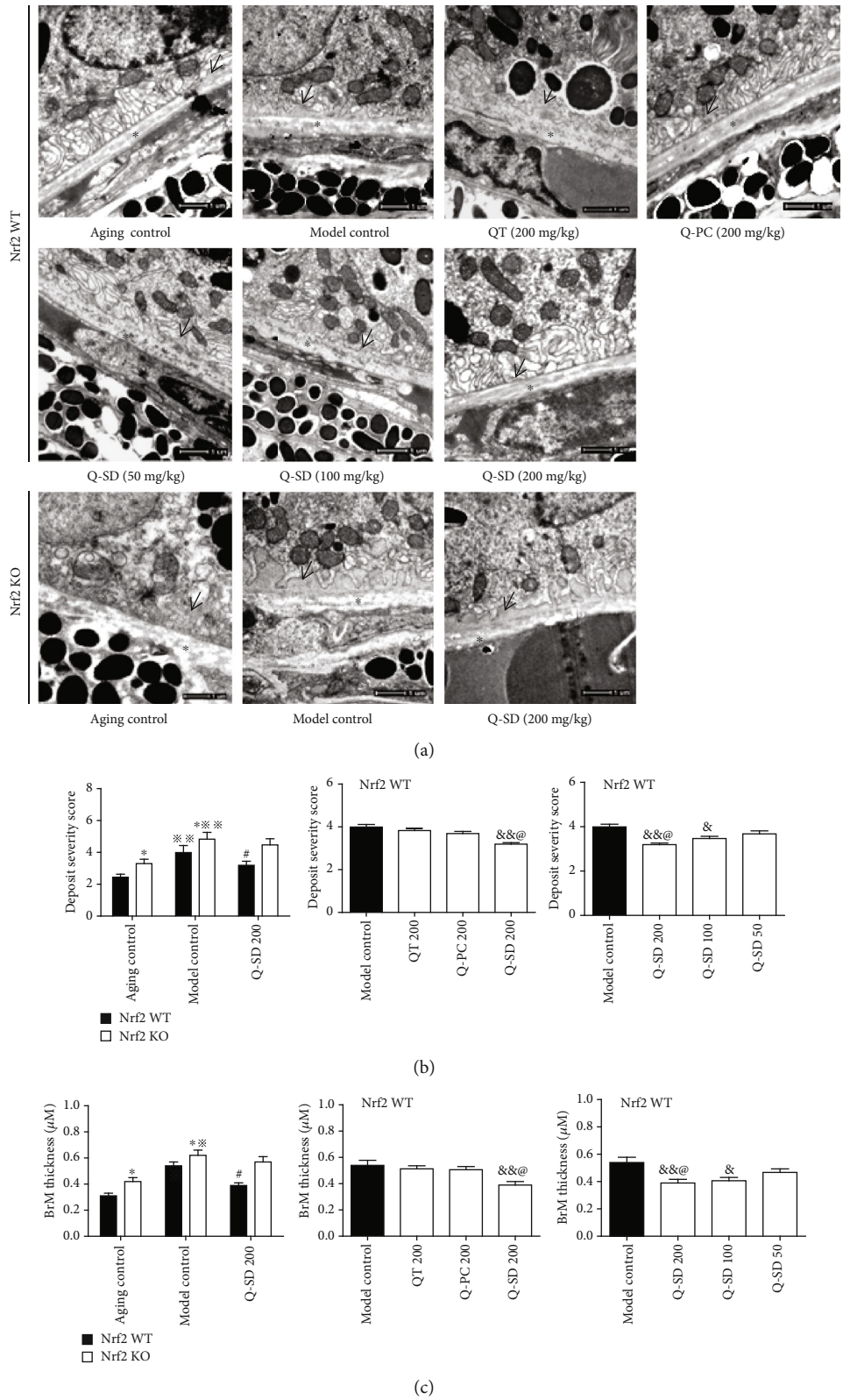

Figure 2: Quercetin-SD more potently improves retina pathological changes in Nrf2 WT mice model of dry AMD. (a) Transmission electron microscopy examination of mouse eye tissues (magnification ×25000). Arrows are used to indicate sediment, and asterisks to indicate Bruch's membrane. (b) Deposit severity score for RPE sediments. (c) Quantification of Bruch's membrane thickness. Significance: $*p < 0.05$ Nrf2 WT versus Nrf2 KO in the aging control and model control; $^{※}p < 0.05$, $^{※※}p < 0.01$ model control versus aging control; $^{\#}p < 0.05$ Q-SD 200 versus model control; $^{\&}p < 0.05$, $^{\&\&}p < 0.01$ versus model control; $^{@}p < 0.05$ Q-SD 200 versus Q-PC 200 or Q-SD 100 ($n = 3$).

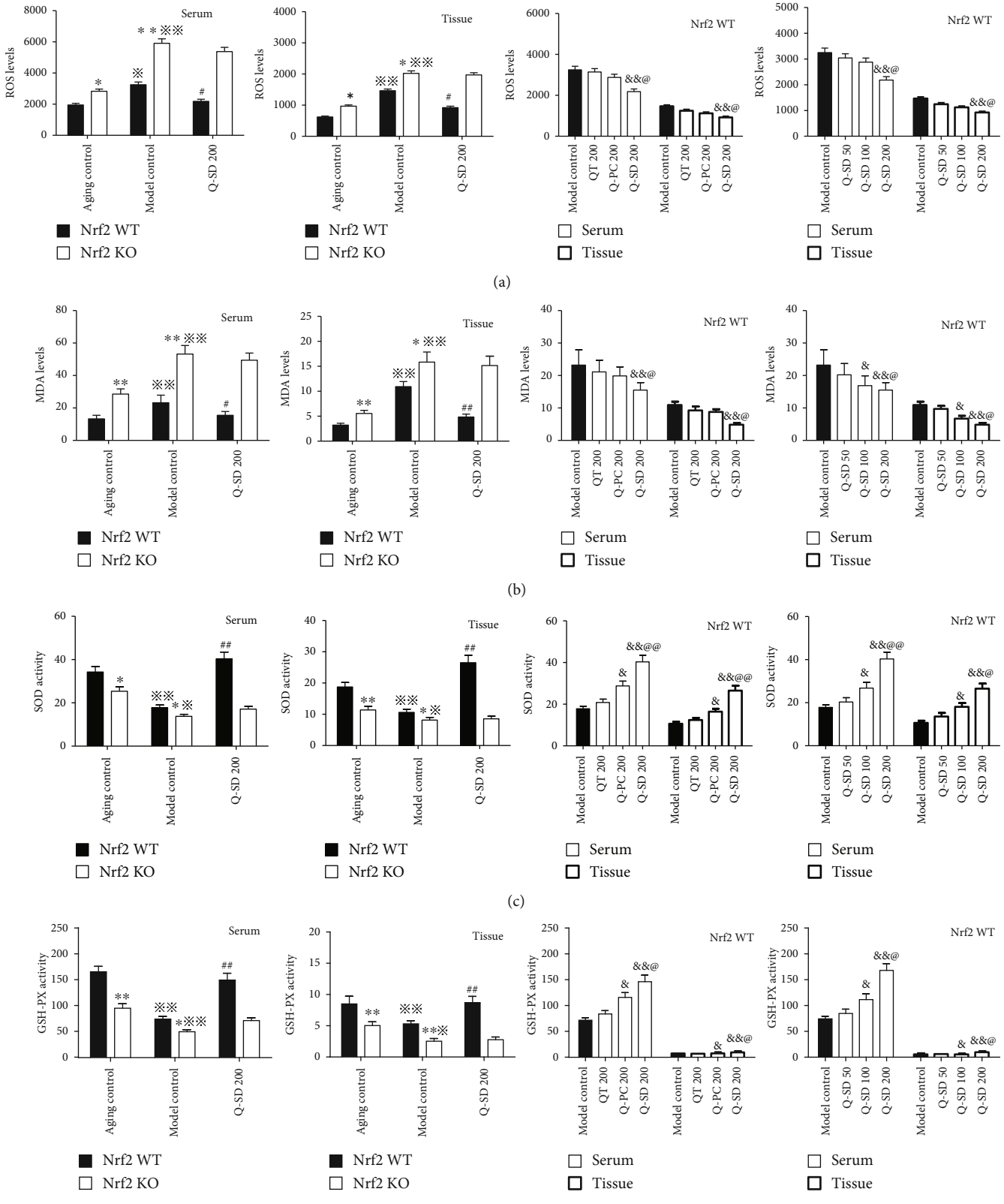

Figure 3: Continued.

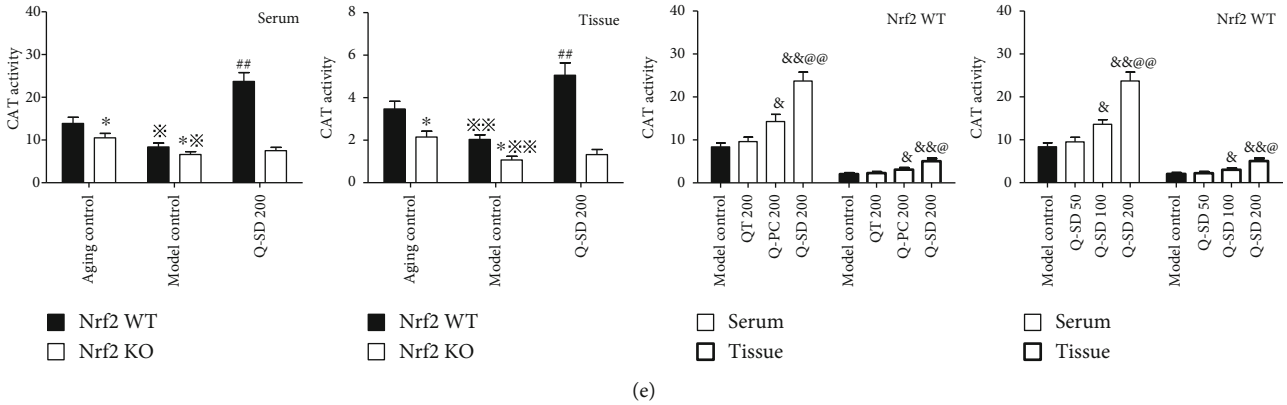

(e)

Figure 3: Quercetin-SD exerts more potent antioxidant effects in the Nrf2 WT and Nrf2 KO mice models of dry AMD. (a) Determination of ROS levels in serum and retinal tissues. (b) Determination of MDA levels in serum and retinal tissues. (c) Determination of SOD levels in serum and retinal tissues. (d) Determination of GSH-PX levels in serum and retinal tissues. (e) Determination of CAT levels in serum and retinal tissues. Significance: $*p < 0.05$, $**p < 0.01$ Nrf2 WT versus Nrf2 KO in the aging control and model control; $^{※}p < 0.05$, $^{※※}p < 0.01$ model control versus aging control; $^{\#}p < 0.05$, $^{\#\#}p < 0.01$ Q-SD 200 versus model control; $^{\&}p < 0.05$, $^{\&\&}p < 0.01$ versus model control; $^{@}p < 0.05$, $^{@@}p < 0.01$ Q-SD 200 versus Q-PC 200 or Q-SD 100 ($n = 3$).

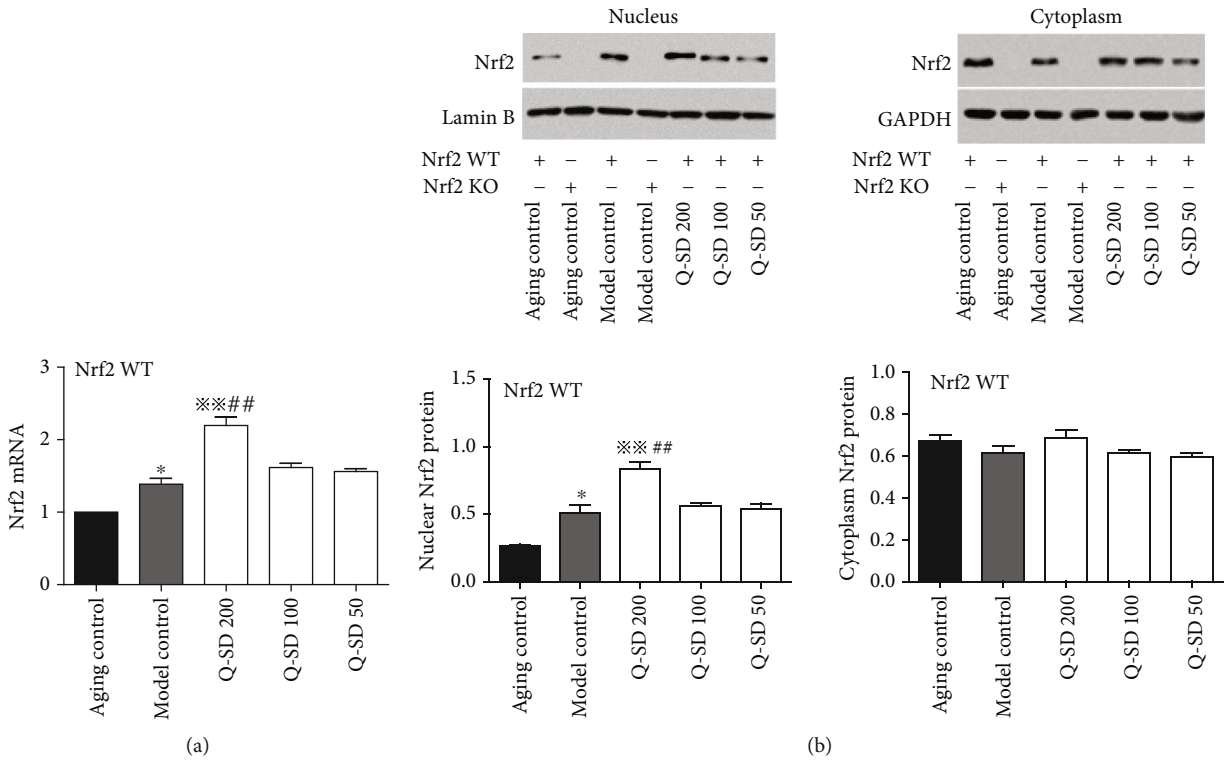

(a) (b)

Figure 4: Effects of quercetin-SD on the expression of Nrf2 in Nrf2 WT and Nrf2 KO model mice of dry AMD. (a) Real-time PCR analyses of Nrf2 mRNA expression in retina tissues. (b) Western blot analyses of Nrf2 protein abundance in the nucleus and cytoplasm with quantification. Significance: $*p < 0.05$ model control versus aging control; $^{※※}p < 0.01$ Q-SD versus model control; $^{\#\#}p < 0.01$ Q-SD 200 versus Q-SD 100 ($n = 3$).

zeaxanthin could protect ARPE-19 cells against hydrogen peroxide-induced oxidative injury [19].

It has been well-recognized that many flavonoid compounds have free radical-scavenging and antioxidant functions, including naringenin, quercetin, and apigenin. However, flavonoid compounds have the disadvantages of poor water- and fat-solubility, low absorption, and less bioavailability [22]. Pharmaceutical studies have revealed that formation of phospholipid complex can markedly improve the physicochemical properties of drugs and enhance their absorption and therapeutic effects in vivo [23]. We previously reported that Q-PC had higher solubility, especially

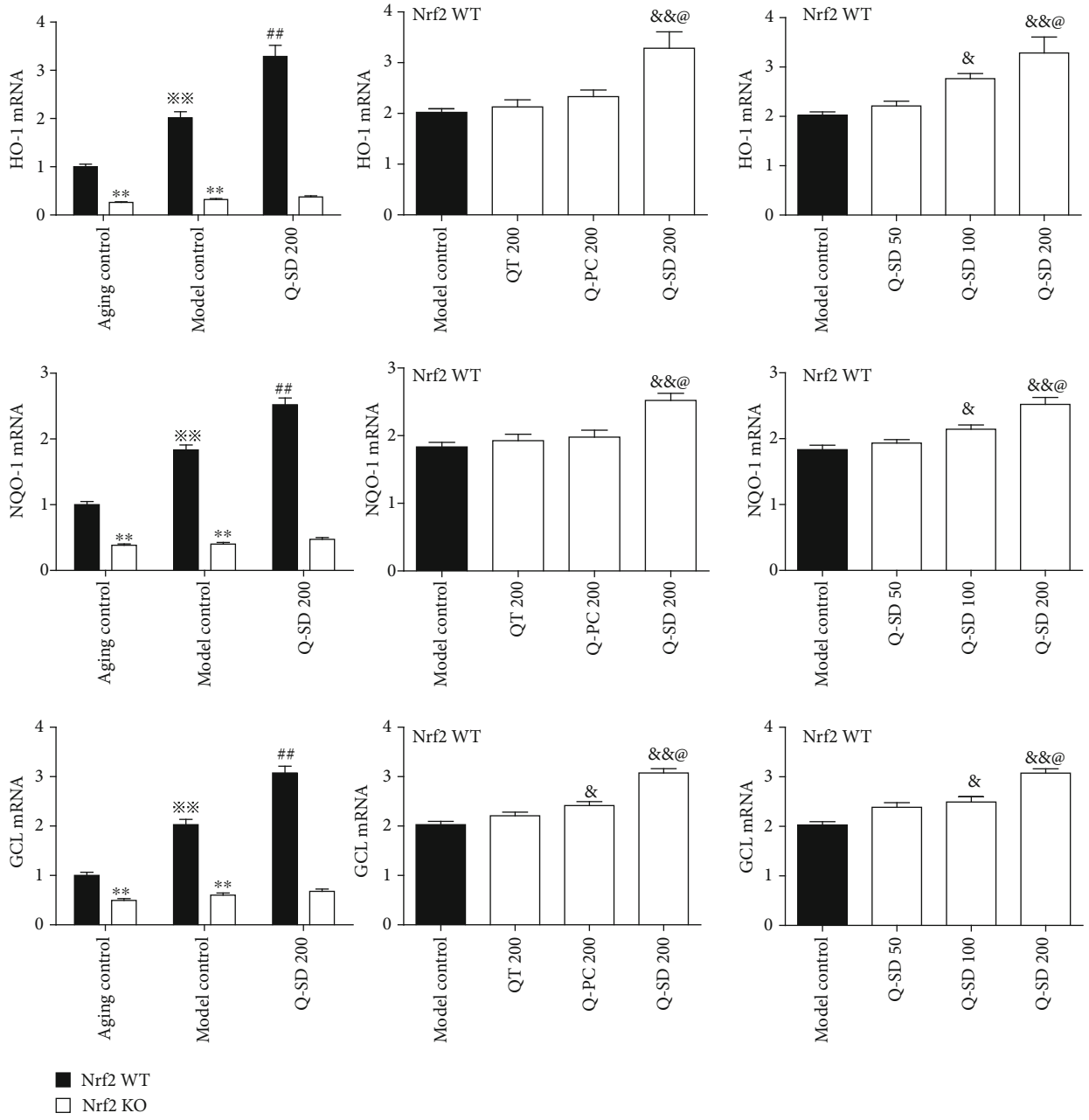

Figure 5: Effects of quercetin-SD on mRNA expression of antioxidant enzymes in Nrf2 WT and Nrf2 KO model mice of dry AMD. Real-time PCR analyses of the mRNA expression of HO-1, NQO-1, and GCL in retinal tissues. Significance: $**p < 0.01$ Nrf2 WT versus Nrf2 KO in aging control and model control; $^{※※}p < 0.01$ model control versus aging control; $^{\#\#}p < 0.01$ Q-SD 200 versus model control; $^{\&}p < 0.05$, $^{\&\&}p < 0.01$ versus model control; $^{@}p < 0.05$ Q-SD 200 versus Q-PC 200 or Q-SD 100 ($n = 3$).

the fat-solubility, than that of QT and that Q-PC thereby exhibited stronger protective effects against oxidative-induced damages in ARPE-19 cells [13]. However, we realized that Q-PC had poor dispersity due to the hydrophobicity of phospholipid complexes. Instead, further preparation of phospholipid complex into solid dispersion can improve the solubility and dissolution rate of the drug, leading to increased bioavailability. For instance, omega-3 phospholipid-based solid dispersion of fenofibrate effectively increased the oral drug exposure in rats, suggesting that this formulation should be promising for improving the oral bioavailability of fenofibrate [24]. Many studies have revealed that the hydrophilic excipient addition PVP could convert drugs to an amorphous form rather than a crystalline state and greatly enhance the solubility and dissolution of drugs [24, 25]. Therefore, we used PVP K30 to prepare Q-SD in the present study. Consistently, our current data demonstrated that formation of solid dispersion tremendously increased the water- and fat-solubility and dissolution rate of Q-PC. More importantly, Q-SD had considerably higher blood concentrations than Q-PC in rats, confirming that Q-SD had high bioavailability. Given

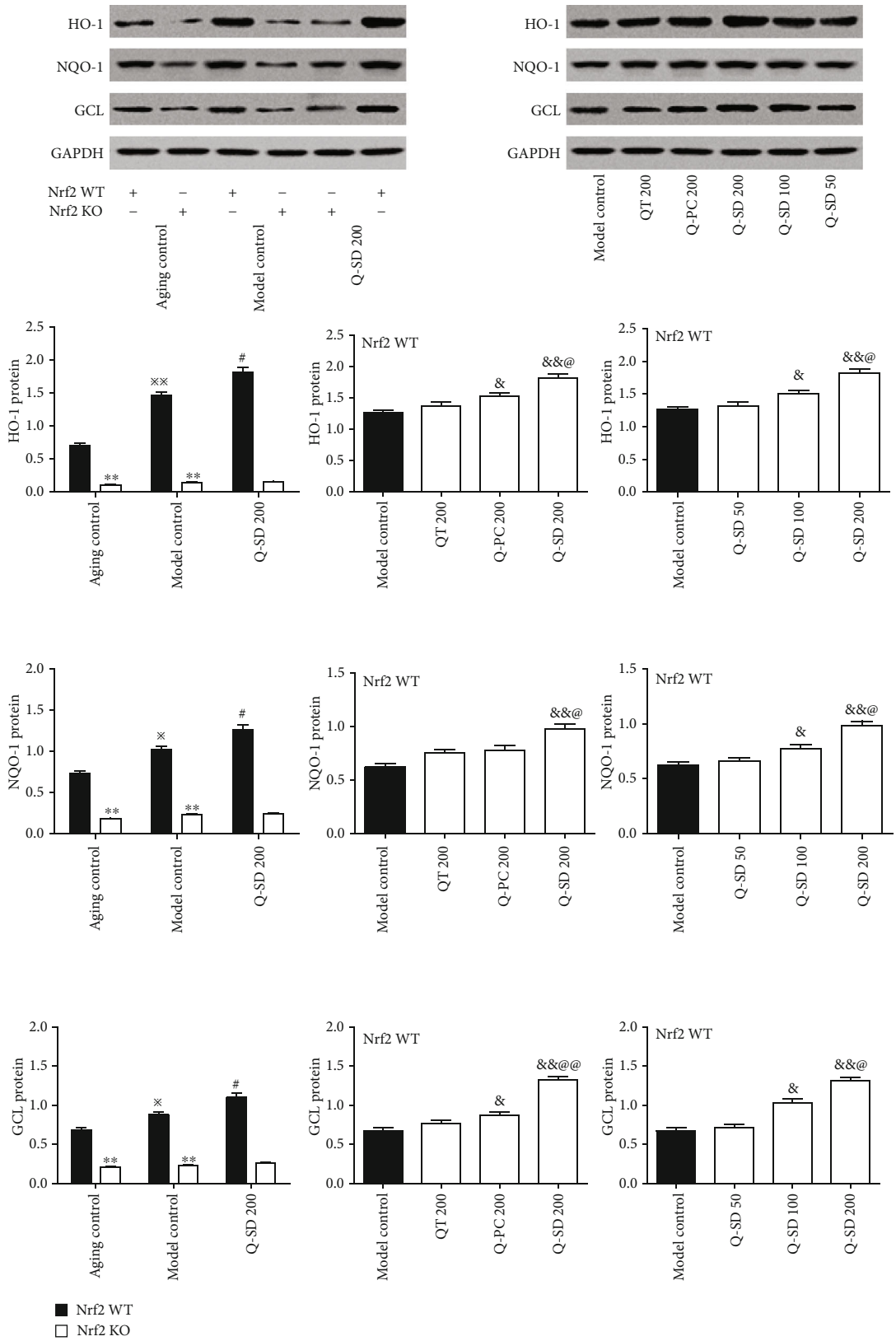

Figure 6: Effects of quercetin-SD on protein expression of antioxidant enzymes in Nrf2 WT and Nrf2 KO model mice of dry AMD. Western blot analyses of the protein expression of HO-1, NQO-1, and GCL in retina tissues with quantification. Significance: $^{**}p < 0.01$ Nrf2 WT versus Nrf2 KO in the aging control and model control; $^{※}p < 0.05$, $^{※※}p < 0.01$ model control versus aging control; $^{\#}p < 0.05$ Q-SD 200 versus model control; $^{\&}p < 0.05$, $^{\&\&}p < 0.01$ versus model control; $^{@}p < 0.05$, $^{@@}p < 0.01$ Q-SD 200 versus Q-PC 200 or Q-SD 100 ($n = 3$).

that flavonoid drugs have similar pharmacokinetic behaviors in rats and mice, we thus established an animal model of dry AMD in mice to examine the potential effects of QT, Q-PC, and Q-SD on retinal injury caused by oxidative stress. We observed that QT and Q-PC did not reduce RPE sediments and BrM thickness, Q-SD significantly did at the same dosage, and that there were dose-dependent responses in the effects of Q-SD. These data clearly supported the claim that formation of solid dispersion considerably enhanced the protective effects of QT on retinal oxidative injury in mice owing to the increased bioavailability.

Nrf2 signaling had been characterized to be a pivotal antioxidant mechanism in mammal cells. Recent evidence indicated that disruption of Nrf2 gene increased the vulnerability of the outer retina to age-related degeneration. Nrf2-deficient mice developed ocular pathology similar to cardinal features of human AMD related to oxidative injury and inflammation, suggesting that Nrf2 signaling and its downstream target genes played important roles in the pathogenesis of AMD [26]. Regulation of Nrf2 signaling could be a potential strategy for intervention of dry AMD. In line with this recognition, our previous studies demonstrated that apigenin exhibited protective effects on ARPE-19 cells against oxidative injury, which were dependent on activation of Nrf2 signaling [27]. Moreover, Hanneken and co-workers reported that QT could induce Nrf2 and related phase II metabolic enzymes and thus protect ARPE-19 cells against hydrogen peroxide-induced injury [28]. Consistent results were also recaptured by our previous studies. Our current studies used the oxidative injury model in mice to validate the *in vivo* effects. However, due to limited number of Nrf2 KO mice, we only evaluated Q-SD at 200 mg/kg in these animals, because we reasoned that Q-SD at this dose could produce significant effects. We observed increased the mRNA expression and nuclear protein abundance of Nrf2 in the Nrf2 WT mice of the model group, which was extremely low in Nrf2 KO mice. Transcription of HO-1, NQO-1, and GCL was all increased in Nrf2 WT mice, not in Nrf2 KO mice; consistently, the protein expression of these three molecules was not significantly increased in the Nrf2 KO mice of the model group. These results also indicated that the oxidative stress stimulated Nrf2 nuclear translocation and initiated the transcription of phase II metabolic enzymes.

We further found that treatment with Q-SD at 100 mg/kg and 200 mg/kg caused significant increase in the transcription and expression of Nrf2 and phase II metabolic enzymes compared to the model group, whereas QT at the same dose did not show significant effects and Q-PC at 200 mg/kg only shows certain effects on the mRNA and protein expression of GCL and protein expression of HO-1 in Nrf2 WT mice. These data indicated that QT exerted its protective effects through activating Nrf2 signaling and also confirmed that formation of solid dispersion considerably increased the bioavailability of QT *in vivo*. Moreover, QT was found to regulate the expression of antioxidant enzymes SOD, GSH-PX, and CAT via a Nrf2 pathway in HepG2 cells [29]. Our current studies demonstrated similar results showing that QT of different dosage forms could restore the serum and tissue activities of SOD, GSH-PX, and CAT and reduced ROS and MDA levels to different extents in Nrf2 WT model mice of dry AMD, and there was effect-concentration responses in Q-SD effects. Under these conditions, Q-SD at a high dose produced the strongest effect. These observations further confirmed that Q-SD had high bioavailability again. The present studies validated the *in vivo* protective effects of QT on retina injury caused by oxidative stress in mice. Next, we will examine the *in vivo* pharmacokinetic properties of Q-PC and Q-SD for further validation and development.

In summary, preparation of solid dispersion significantly improved the solubility and dissolution rate of QT and thereby increased its bioactivity. Q-SD exhibited more potent protective effects on retina oxidative injury in model mice of dry AMD, which were associated with activation of Nrf2 signaling and related antioxidant enzymes. Our studies highlighted that Q-SD could be a safe and effective therapeutic option for AMD.

Data Availability

The data used to support the findings of this study are available from the corresponding author upon request.

Conflicts of Interest

The authors declare that the research was conducted in the absence of any commercial or financial relationships that could be construed as a potential conflict of interest.

Acknowledgments

The work was supported by the Jiangsu Provincial Key Research and Development Program (Grant No. BE2018757).

References

[1] E. Buschini, A. M. Fea, C. A. Lavia et al., "Recent developments in the management of dry age-related macular degeneration," *Clinical Ophthalmology*, vol. 9, pp. 563–574, 2015.

[2] M. A. Zarbin, R. P. Casaroli-Marano, and P. J. Rosenfeld, "Age-related macular degeneration: clinical findings, histopathology and imaging techniques," *Developments in Ophthalmology*, vol. 53, pp. 1–32, 2014.

[3] S. Pershing, N. Talwar, S. T. Armenti et al., "Use of bevacizumab and ranibizumab for wet age-related macular degeneration: influence of CATT results and introduction of aflibercept," *American Journal of Ophthalmology*, vol. S0002-9394, no. 19, pp. 30231–30234, 2019.

[4] M. C. Gillies, A. P. Hunyor, J. J. Arnold et al., "Effect of ranibizumab and aflibercept on best-corrected visual acuity in treat-and-extend for neovascular age-related macular degeneration," *JAMA Ophthalmology*, vol. 137, no. 4, pp. 372–379, 2019.

[5] D. Chiras, G. Kitsos, M. B. Petersen, I. Skalidakis, and C. Kroupis, "Oxidative stress in dry age-related macular degeneration and exfoliation syndrome," *Critical Reviews in Clinical Laboratory Sciences*, vol. 52, no. 1, pp. 12–27, 2015.

[6] H. Sies, C. Berndt, and D. P. Jones, "Oxidative stress," *Annual Review of Biochemistry*, vol. 86, no. 1, pp. 715–748, 2017.

[7] S. G. Jarrett and M. E. Boulton, "Consequences of oxidative stress in age-related macular degeneration," *Molecular Aspects of Medicine*, vol. 33, no. 4, pp. 399–417, 2012.

[8] Q. Ma, "Role of nrf2 in oxidative stress and toxicity," *Annual Review of Pharmacology and Toxicology*, vol. 53, no. 1, pp. 401–426, 2013.

[9] S. Singh, S. Vrishni, B. K. Singh, I. Rahman, and P. Kakkar, "Nrf2-ARE stress response mechanism: a control point in oxidative stress-mediated dysfunctions and chronic inflammatory diseases," *Free Radical Research*, vol. 44, no. 11, pp. 1267–1288, 2010.

[10] T. Nguyen, P. Nioi, and C. B. Pickett, "The Nrf2-antioxidant response element signaling pathway and its activation by oxidative stress," *Journal of Biological Chemistry*, vol. 284, no. 20, pp. 13291–13295, 2009.

[11] M. Russo, C. Spagnuolo, I. Tedesco, S. Bilotto, and G. L. Russo, "The flavonoid quercetin in disease prevention and therapy: facts and fancies," *Biochemical Pharmacology*, vol. 83, no. 1, pp. 6–15, 2012.

[12] X. Cai, Z. Fang, J. Dou, A. Yu, and G. Zhai, "Bioavailability of quercetin: problems and promises," *Current Medicinal Chemistry*, vol. 20, no. 20, pp. 2572–2582, 2013.

[13] X. R. Xu, H. T. Yu, Y. Yang, L. Hang, X. W. Yang, and S. H. Ding, "Quercetin phospholipid complex significantly protects against oxidative injury in ARPE-19 cells associated with activation of Nrf2 pathway," *European Journal of Pharmacology*, vol. 770, pp. 1–8, 2016.

[14] K. Maiti, K. Mukherjee, A. Gantait, B. P. Saha, and P. K. Mukherjee, "Enhanced therapeutic potential of naringenin-phospholipid complex in rats," *Journal of Pharmacy and Pharmacology*, vol. 58, no. 9, pp. 1227–1233, 2006.

[15] D. Singh, M. S. M. Rawat, A. Semalty, and M. Semalty, "Quercetin-phospholipid complex: an amorphous pharmaceutical system in herbal drug delivery," *Current Drug Discovery Technologies*, vol. 9, no. 1, pp. 17–24, 2012.

[16] Y. Huang and W. G. Dai, "Fundamental aspects of solid dispersion technology for poorly soluble drugs," *Acta Pharmaceutica Sinica B*, vol. 4, no. 1, pp. 18–25, 2014.

[17] A. W. Khan, S. Kotta, S. H. Ansari, R. K. Sharma, and J. Ali, "Enhanced dissolution and bioavailability of grapefruit flavonoid naringenin by solid dispersion utilizing fourth generation carrier," *Drug Development and Industrial Pharmacy*, vol. 41, no. 5, pp. 772–779, 2015.

[18] D. G. Espinosa-Heidmann, I. J. Suner, P. Catanuto, E. P. Hernandez, M. E. Marin-Castano, and S. W. Cousins, "Cigarette smoke-related oxidants and the development of sub-RPE deposits in an experimental animal model of dry AMD," *Investigative Ophthalmology & Visual Science*, vol. 47, no. 2, pp. 729–737, 2006.

[19] X. Xu, L. Hang, B. Huang, Y. H. Wei, S. Zheng, and W. Li, "Efficacy of ethanol extract of *Fructus lycii* and its constituents lutein/zeaxanthin in protecting retinal pigment epithelium cells against oxidative stress: *in vivo* and *in vitro* models of age-related macular degeneration," *Journal of Ophthalmology*, vol. 2013, Article ID 862806, 10 pages, 2013.

[20] Age-Related Eye Disease Study Research Group, "A randomized, placebo-controlled, clinical trial of high-dose supplementation with vitamins C and E and beta carotene for age-related cataract and vision loss: AREDS report no. 9," *Archives of Ophthalmology*, vol. 119, no. 10, pp. 1439–1452, 2001.

[21] G. H. Lee, Y. Shin, and M. J. Oh, "Aroma-active components of Lycii fructus (kukija)," *Journal of Food Science*, vol. 73, no. 6, pp. C500–C505, 2008.

[22] G. B. Gonzales, "In vitrobioavailability and cellular bioactivity studies of flavonoids and flavonoid-rich plant extracts: questions, considerations and future perspectives," *Proceedings of the Nutrition Society*, vol. 76, no. 3, pp. 175–181, 2017.

[23] H. Wang, Y. Cui, Q. Fu et al., "A phospholipid complex to improve the oral bioavailability of flavonoids," *Drug Development and Industrial Pharmacy*, vol. 41, no. 10, pp. 1693–1703, 2015.

[24] L. Yang, Y. Shao, and H. K. Han, "Development of omega-3 phospholipid-based solid dispersion of fenofibrate for the enhancement of oral bioavailability," *European Journal of Pharmaceutical Sciences*, vol. 78, pp. 103–110, 2015.

[25] V. R. Shinde, M. R. Shelake, S. S. Shetty, A. B. Chavan-Patil, Y. V. Pore, and S. G. Late, "Enhanced solubility and dissolution rate of lamotrigine by inclusion complexation and solid dispersion technique," *Journal of pharmacy and pharmacology*, vol. 60, no. 9, pp. 1121–1129, 2008.

[26] Z. Zhao, Y. Chen, J. Wang et al., "Age-related retinopathy in NRF2-deficient mice," *PLoS One*, vol. 6, no. 4, article e19456, 2011.

[27] X. Xu, M. Li, W. Chen, H. Yu, Y. Yang, and L. Hang, "Apigenin attenuates oxidative injury in ARPE-19 cells through activation of Nrf2 pathway," *Oxidative Medicine and Cellular Longevity*, vol. 2016, Article ID 4378461, 9 pages, 2016.

[28] A. Hanneken, F. F. Lin, J. Johnson, and P. Maher, "Flavonoids protect human retinal pigment epithelial cells from oxidative-stress-induced death," *Investigative Ophthalmology & Visual Science*, vol. 47, no. 7, pp. 3164–3177, 2006.

[29] M. Alia, S. Ramos, R. Mateos, A. B. Granado-Serrano, L. Bravo, and L. Goya, "Quercetin protects human hepatoma HepG2 against oxidative stress induced by *tert*-butyl hydroperoxide," *Toxicology and Applied Pharmacology*, vol. 212, no. 2, pp. 110–118, 2006.

Hindawi
Oxidative Medicine and Cellular Longevity
Volume 2019, Article ID 7860650, 23 pages
https://doi.org/10.1155/2019/7860650

Research Article

Dietary Supplementation of the Antioxidant Curcumin Halts Systemic LPS-Induced Neuroinflammation-Associated Neurodegeneration and Memory/Synaptic Impairment via the JNK/NF-κB/Akt Signaling Pathway in Adult Rats

Muhammad Sohail Khan, Tahir Muhammad, Muhammad Ikram, and Myeong Ok Kim

Division of Life Science and Applied Life Science (BK 21), College of Natural Sciences, Gyeongsang National University, Jinju 52828, Republic of Korea

Correspondence should be addressed to Myeong Ok Kim; mokim@gnu.ac.kr

Received 27 March 2019; Revised 23 August 2019; Accepted 26 September 2019; Published 7 November 2019

Guest Editor: João C. M. Barreira

Curcumin is a natural polyphenolic compound widely known to have antioxidant, anti-inflammatory, and antiapoptotic properties. In the present study, we explored the neuroprotective effect of curcumin against lipopolysaccharide- (LPS-) induced reactive oxygen species- (ROS-) mediated neuroinflammation, neurodegeneration, and memory deficits in the adult rat hippocampus via regulation of the JNK/NF-κB/Akt signaling pathway. Adult rats were treated intraperitoneally with LPS at a dose of 250 μg/kg for 7 days and curcumin at a dose of 300 mg/kg for 14 days. After 14 days, the rats were sacrificed, and western blotting and ROS and lipid peroxidation assays were performed. For immunohistochemistry and confocal microscopy, the rats were perfused transcardially with 4% paraformaldehyde. In order to verify the JNK-dependent neuroprotective effect of curcumin and to confirm the in vivo results, HT-22 neuronal and BV2 microglial cells were exposed to LPS at a dose of 1 μg/ml, curcumin 100 μg/ml, and SP600125 (a specific JNK inhibitor) 20 μM. Our immunohistochemical, immunofluorescence, and biochemical results revealed that curcumin inhibited LPS-induced oxidative stress by reducing malondialdehyde and 2,7-dichlorofluorescein levels and ameliorating neuroinflammation and neuronal cell death via regulation of the JNK/NF-κB/Akt signaling pathway both in vivo (adult rat hippocampus) and in vitro (HT-22/BV2 cell lines). Moreover, curcumin markedly improved LPS-induced memory impairment in the Morris water maze and Y-maze tasks. Taken together, our results suggest that curcumin may be a potential preventive and therapeutic candidate for LPS-induced ROS-mediated neurotoxicity and memory deficits in an adult rat model.

1. Introduction

Neuroinflammation is a protective mechanism, which occurs inside the brain and is the primary response to injury. If neuroinflammatory responses are prolonged, however, this can lead to neuronal dysfunction and eventually result in neuronal apoptosis and memory impairments [1, 2]. Increasing evidence indicates that neuroinflammation caused by toxic reactions or disturbances in the homeostasis of antioxidants plays an essential role in the pathogenesis of neurodegenerative disorders such as Parkinson's and Alzheimer's disease (AD) [3–5]. Reactive oxygen species (ROS) have been previously identified as potent mediators of neurodegenerative disorders. They have been shown to affect protein, lipids, and nucleic acids, paving the way for cellular dysfunction and neuronal apoptosis. Emerging evidence has suggested that oxidative stress encourages the activation of stress kinases like phosphorylated-c-Jun N-terminal kinase 1 (p-JNK), an important mediator of neuroinflammation and neurodegeneration. Chronic oxidative stress and neuroinflammation are thus key contributors to the advancement of diseases like AD [2, 6].

Several lines of investigation have demonstrated that lipopolysaccharide (LPS) and other toxic agents such as ethanol and d-galactose activate numerous ROS-mediated neuroinflammatory and apoptotic signaling pathways that in turn lead to neurodegeneration and memory deficits [7–9]. LPS is a bacterial endotoxin which triggers neuroinflammation and is used as an inflammagen in various animal model studies to evaluate the interaction between inflammation, brain function, and memory impairments. It is well known that LPS treatment leads to an increase in the generation of ROS and cytokine production, ultimately resulting in neuronal cell death and memory impairments [1, 10, 11]. Various mechanisms have been studied and proposed for LPS-induced neuronal damage, the most well-established of which is the increased generation of ROS, subsequently augmenting oxidative stress and neuronal damage. Furthermore, an elevated level of ROS can activate other mediators like phosphorylated-nuclear factor kappa B (p-NF-κB), tumor necrosis factor-α (TNF-α), and interleukin-1β (IL-1β), affecting the function of neuronal cells in the hippocampus via neuronal apoptosis and subsequently resulting in memory impairments. Moreover, according to recent studies, LPS given intraperitoneally can activate astrocytes and microglial cells, inducing the processes of astrogliosis and microgliosis, respectively. Activation of both astrocytes and microglia induces neurotoxicity, neuroinflammation, and the production of ROS by stimulating proinflammatory mediators [7, 12–16]. Badshah et al. demonstrated the systemic administration of LPS to adult mice at a dose of 250 μg/kg for 1 week-induced neuronal cell death by increasing the expression of caspase-3 and poly [ADP-ribose] polymerase 1 (PARP-1), triggering the mitochondrial apoptotic pathway [1].

Several antioxidants are known for their effectiveness against oxidative stress-mediated neuronal cell death and memory disorders. Most of these have been reported to cross the blood-brain-barrier and reduce the deleterious effects of various toxic molecules such as oxygen and nitrogen free radicals in brain cells. Natural sources of polyphenolic compounds include plants, vegetables, fruits, green tea, olive oil, and red wine [17, 18]. Although no preventative treatments are currently available, studies into neurodegenerative disorders have suggested that lifestyle changes, exercise, and a daily intake of natural polyphenol supplements may help to prevent these diseases. Curcumin, obtained from the rhizomes of the Curcuma longa plant, is a natural yellowish compound which has been used for centuries for the treatment of neuropathological disorders because of its antioxidant and anti-inflammatory properties. Curcumin not only acts as a free radical scavenger but also improves learning and memory deficits. Studies involving curcumin have reported that it has a neuroprotective effect, and it has been shown to counteract AD, depression, and seizures [19–21]. Furthermore, curcumin has also been shown to have a protective role in other conditions such as cancer, pancreatitis, rheumatoid arthritis, liver disease, and pulmonary dysfunction [22, 23]. In addition, curcumin protects the brain from LPS toxicity by inhibiting the production of nitric oxide (NO), prostaglandin E2 (PGE2), ROS, and proinflammatory cytokines [24–26].

Although it is known that curcumin has anti-inflammatory and neuroprotective properties, there exists little evidence about its exact underlying mechanism of action, particularly in the context of ROS-mediated neuroinflammation, neurodegeneration, and memory impairments. Therefore, we conducted this study to explore the effects of curcumin against LPS-induced hippocampal microglial activation, neuroinflammation, neurodegeneration, and memory impairments. Our results confirmed that curcumin not only has potent antioxidant, anti-inflammatory, and antiapoptotic properties but also protects against LPS-induced ROS-mediated neuroinflammation, neurodegeneration, and memory impairments. Our results further confirm that natural compounds like curcumin could potentially be used as alternatives to synthetic and semisynthetic drugs for the treatment of neurodegenerative disorders.

2. Materials and Methods

2.1. Chemicals. The LPS, 2,7-dichlorodihydrofluorescein diacetate (DCFH-DA), dimethyl sulfoxide (DMSO), and JNK inhibitor (SP600125) used in the experiments were all purchased from Sigma-Aldrich Chemical Co (St. Louis, MO, USA).

2.2. Animals. Male Sprague-Dawley rats weighing 250-300 grams were purchased from Samtako Bio (Osan, Republic of Korea). All animals were kept in the university animal house on a 12/12 h light and dark cycle at room temperature and humidity for a week before the start of experimentation to allow acclimatization to the new environment. Animals were allowed to feed ad libitum. Rats were handled carefully according to the guidelines provided by the Animal Ethical Committee of the Gyeongsang National University, South Korea (Approval ID: 125).

2.3. Grouping and Treatment of Experimental Animals. Animals were randomly divided into the following three groups ($n = 15$ for each):

(i) Control (Cont.) group: injected with normal saline for 1 week

(ii) LPS-treated group: intraperitoneally injected with LPS dissolved in normal saline for 1 week at a dose of 250 μg/kg/day, as reported previously [1]

(iii) LPS+curcumin-treated group: injected with LPS as above and curcumin (300 mg/kg/day for 14 days, as reported [3]) 7 days before and after LPS treatment

Curcumin was dissolved in DMSO, and the final injectable volume was prepared using normal saline. The LPS was dissolved in the same volume of normal saline used for curcumin.

2.4. In Vivo ROS Assay. For the determination of the ROS level inside the hippocampus ($n = 5$ per group), we performed the ROS assay. This assay was performed as previously described [12] and was based on the alteration of DCFH-DA to 2,7-dichlorofluorescein (DCF). Briefly, brain

homogenates from the hippocampus were diluted with Lock's buffer at a 1 : 20 ratio, and the final concentration was adjusted to 2.5 mg tissue per 500 μl. The reaction mixture comprised Lock's buffer (pH 7.4), brain homogenates from hippocampal tissue (0.2 μl), and DCFH-DA (10 μl, 5 mM). The mixture was covered and incubated for 15 min at room temperature. After the incubation, the fluorescent product DCF was measured by a microplate reader (excitation at 484 nm and emission at 530 nm). A blank parallel was used first to evaluate background signal. Results were expressed as pmol DCF formed/min/mg of protein in the tissue homogenate.

2.5. In Vitro ROS Assay. The same procedure used in vivo was then used for the quantification of ROS in the BV2 microglial cells. The in vitro ROS assay was also based on the conversation of DCFH-DA to DCF. The microglial BV2 cells used in the in vitro studies were kindly provided as a gift from Dr. I. W. Choi (Inje University, Busan, Republic of Korea). The BV2 microglial cells were seeded in a 75 cm^2 Nunc™ EasYFlask™ with a Nunclon™ Delta surface (Thermo Fisher Scientific, Nunc A/S, Roskilde, Denmark) containing Dulbecco's modified Eagle medium (DMEM) (Life Technologies, Carlsbad, CA, US) supplemented with 10% fetal bovine serum (FBS) and 1% antibiotics (penicillin-streptomycin) at 37°C in humidified air containing 5% CO_2. The cells were grown, counted, and further subcultured in 35 mm Petri dishes (Thermo Fisher Scientific, Nunc A/S, Roskilde, Denmark) in DMEM supplemented with 10% FBS and 1% antibiotics (penicillin-streptomycin) at 37°C in humidified air containing 5% CO_2. When the cells reached 70-80% confluence, they were treated with LPS (1 μg/ml) as reported previously [1], LPS (1 μg/ml)+curcumin (100 μg/ml) as reported previously [6], and LPS+SP600125 (20 μM) as reported previously [7] for 24 hours. For ROS analysis, cells were exposed to DCFH-DA (50 μM) at 37°C for 30 min. The absorbance for ROS-positive cells was measured at 484/530 nm.

2.6. In Vivo Lipid Peroxidation (LPO) Assay. To evaluate oxidative stress, we performed the LPO assay. An LPO Assay Kit (CAS 4091-99-0, Santa Cruz Biotechnology, Dallas, TX, USA) was used for evaluating the level of free malondialdehyde (MDA) in the rat hippocampal tissue, as performed previously [12]. The LPO assay was performed as instructed by the manufacturer. In brief, the hippocampal tissues were homogenized on ice in 300 μl of the MDA lysis buffer with 3 μl BHT and centrifuged (13,000×g, 10 min). A total of 10 mg of protein was precipitated by homogenizing the sample in 150 μl dH2O+3 μl BHT, adding 1 vol of 2 N perchloric acid, vertexing, and then centrifuging to remove the precipitated protein. The final volume (200 μl) of the supernatant from each sample was then introduced into a 96-well plate, and the absorbance was measured using a microplate reader at 532 nm. The total MDA content was expressed as nmol/mg of protein in the tissue homogenate.

2.7. In Vitro LPO Assay. The LPO assay was also used for evaluating oxidative stress in BV2 cells using the LPO assay kit (BioVision, San Francisco, CA, USA; Cat#739-100). BV2 cells were grown and treated in the same way as previously mentioned in the methodology of the in vitro ROS assay. LPO analysis was performed as mentioned for in vivo experiments.

2.8. Protein Extraction. When the in vivo treatment was completed, all animals were sacrificed under anesthesia, and the brains were carefully removed to avoid any damage. The hippocampal tissues were carefully separated, kept in liquid nitrogen, and stored at -80°C for a further biochemical experimental work. When required, the hippocampal tissues were homogenized in pre-prep extraction solution (iNtRON Biotechnology, Inc., Sungnam, South Korea) and centrifuged at 13,000 rpm at 4°C for 25 min. After homogenization, the supernatant was collected and stored at −80°C.

2.9. Quantitative Analysis of Proteins by Western Blotting. Before western blotting, the optical densities (OD) of proteins were analyzed using the Bio-Rad protein assay kit (Bio-Rad Laboratories, CA, USA), as described previously [14]. Equal amounts of protein, approximately 20–30 μg, were used for electrophoresis using 4–12% Bolt™ Mini Gels (Life Technologies, Carlsbad, CA, US). Proteins were transferred to PVDF (polyvinylidene fluoride) membranes (Sigma-Aldrich Chemical Co.). The membranes were treated with 5% skim milk (w/v) for 90 min, washed with TBST (3 times, 10 min each), and treated with primary antibodies (anti-caspase-3, anti-TNF-α, anti-IL-1β, anti-p-JNK, anti-p-NF-κB65, anti-Bcl-2-associated X protein (Bax), anti-B-cell lymphoma 2 (Bcl-2), anti-cytochrome c (Cyt c), anti-PARP-1, anti-phosphorylated-glycogen synthase kinase 3 (p-GSK3β) (Ser 9), anti-phosphorylated protein kinase B (p-Akt) (Ser 473), anti-synaptosomal associated protein 25 (SNAP-25), anti-postsynaptic density protein 95 (PSD95), and anti-β-actin, all from Santa Cruz Biotechnology, Dallas, TX, USA) overnight at 4°C, followed by horseradish peroxidase-conjugated secondary antibodies for 1 h. The membranes were washed with TBST (3 times, 10 min each), treated with a chemiluminescence system (Atto Corporation Tokyo, Japan), and protein bands were then detected on an X-ray film. The protein bands were analyzed by ImageJ software (version 1.50, NIH, https://imagej.nih.gov/ij/, Bethesda, MD, USA) which was used to quantify the integrated density.

2.10. Morphological Analysis and Sample Preparation. When the drug treatment and behavioral studies were completed, the animals were perfused transcardially with 4% ice-cold paraformaldehyde, as previously described [7, 12]. In short, the brain was fixed in 4% paraformaldehyde for 72 h and then transferred to 20% sucrose and stored for another 72 h. Following this, the brains were washed with fresh PBS and immediately frozen in O.C.T. Compound (Sakura Finetek USA, Inc., Torrance, CA, USA). Upon solidification of the blocks, 14 μm coronal sections of the hippocampus were cut using a CM 3050C cryostat (Leica, Germany). The sections were thaw-mounted on ProbeOn Plus™ charged slides (Thermo Fisher Scientific, Nunc a/S, Roskilde, Denmark).

2.11. Immunofluorescence Staining. Immunofluorescence staining was performed following a previously described protocol [12, 14]. In brief, brain tissue slides were dried overnight, washed twice with PBS (0.01 M) for 10 min, and blocked with blocking serum (2% normal goat serum and 0.3% Triton X-100 in PBS) for 1 hour. The slides were then incubated with the aforementioned primary antibodies (Santa Cruz Biotechnology) overnight at 4°C. The next day, the slides were treated with secondary TRITC/FITC-labelled antibodies (1,100) (Santa Cruz Biotechnology) for 2 h. Slides were washed with PBS (twice for 5 min) and mounted with 4′,6′-diamidino-2-phenylindole (DAPI) and Prolong Antifade Reagent (Molecular Probe, Eugene, OR, USA). Finally, the stained slides were examined under a confocal laser-scanning FluoView FV 1000 MPE microscope (Olympus, Tokyo, Japan).

2.12. Fluoro-Jade B (FJB) Staining. Briefly, the tissue slides were dried overnight in a drying chamber and washed with PBS (0.01 M) twice for 5 min. Slides were dipped in a solution containing 1% sodium hydroxide and 80% ethanol for 5 min. Then the slides were kept in 70% alcohol followed by keeping in distilled water for 2 min. Following that, the tissue slides were treated with a solution containing 0.1% acetic acid and 0.06% FJB for 20 min. Slides were washed and left to dry for 10 min, mounted with DPX mounting medium, and coverslips were applied. Slides were examined under a confocal laser-scanning FluoView FV 1000 MPE microscope (Olympus, Tokyo, Japan), and images were taken. Results were analyzed with ImageJ software, and quantification of the immunohistofluorescence and FJB images was performed according to our recently published protocol [7].

2.13. TUNEL Staining. TUNEL (terminal deoxynucleotidyl transferase- (TdT-) mediated dUTP nick-end labeling) staining is used to detect dead neurons and evaluate the extent of neuronal apoptosis. The kit used in this assay was purchased from Sigma-Aldrich Chemical Co. (Cat. No. 11684809910, St. Louis, MO, USA), and the staining was performed according to the manufacturer's recommendations.

2.14. Hematoxylin and Eosin (H&E) Staining. H&E staining is used to analyze cell morphology. In brief, slides from each group ($n = 5$) were first dipped in tap water for a short time and transferred to staining solution. The slides were then transferred to the hematoxylin solution for 8-10 min. Next, the sides were washed with running water for 10-15 min and transferred to the eosin solution for 30 sec. Following this, the slides were then dehydrated with a graded series of alcohol. Finally, all the slides were mounted with mounting medium (Thermo Fisher Scientific, MA, USA) and coverslips applied. Images of the slides were taken using a simple microscope.

2.15. Cresyl Violet Staining. Cresyl violet/Nissl staining is used for the examination and determination of neuronal cell death. First, slides comprising 14 μm brain sections were washed with PBS (0.01 M) for 15 min and stained with a solution of Cresyl violet (0.5%) containing a few drops of glacial acetic acid for 10-15 min. Slides were washed with distilled water, dehydrated with a graded series of alcohol (70, 95, and 100%), retained in xylene; nonfluorescent mounting medium was used, and coverslips were applied. Images were taken using a fluorescent light microscope, and quantification of the immunohistochemical images was performed.

2.16. Morris Water Maze (MWM) and Y-Maze Tests. For the behavioral studies, a MWM test was conducted on the rats ($n = 10$/group), as described previously [12]. The MWM comprises a circular tank (100 cm in diameter, 40 cm in height) containing water (23 ± 1°C) filled to a depth of 15.5 cm. White ink was added to the water to make it look opaque. A transparent escape platform (10 cm in diameter, 14.4 cm in height) was kept at the midpoint of one quadrant, hidden 1 cm below the water level. Rats were trained for 5 days before the start of the study using a single hidden platform in one quadrant with three quadrants of rotational starting. The escape latency (the time taken to look for and locate the hidden platform) was calculated for every trial. After 24 h of the 5^{th} day, a probe test was then performed for the evaluation of memory consolidation. The platform was removed, and the rats were allowed to swim freely for 60 sec. Then, the length of time spent in the target quadrant and the number of times the rat crossed over the platform location (the platform remained hidden during the training) were recorded. The total time spent by a rat in the target quadrant was considered to be a measure of the degree of memory consolidation. SMART video-tracking software (Panlab Harvard Apparatus, Holliston, MA, USA) was used to record the movement of the rats. The Y-maze test was performed as described previously with necessary changes [14].

2.17. In Vitro Cell Culturing and Treatment for Western Blotting and Confocal Microscopy. The HT-22 neuronal cells used in the in vitro studies were kindly provided by Prof. Koh (Gyeongsang National University, South Korea). The HT-22 cells were seeded in DMEM supplemented with 10% fetal bovine serum (FBS) and 1% antibiotics in a humidified 5% CO_2 incubator at 37°C. The HT-22 cell were incubated with LPS (1 μg/ml), LPS (1 μg/ml)+Cur (100 μg/ml) and LPS (1 μg/ml)+SP600125 (20 μM) for 24 h.

2.18. Statistical Analyses. Differences between the control, LPS, and LPS+curcumin groups were analyzed using the one-way analysis of variance (ANOVA) and Student's t-test. All data are expressed as the mean ± SEM for the three independent experiments and were analyzed using GraphPad Prism 5 software (GraphPad Software, Inc., San Diego, CA, US). A P value < 0.05 was considered statistically significant. For the in vivo study, the * symbol denotes a significant difference between the control and LPS groups and the Ω symbol denotes a significant difference between the LPS and curcumin groups. Likewise, for the in vitro study, the * symbol denotes a significant difference between the control and LPS groups, the Ω symbol denotes a significant difference between the LPS and curcumin groups, and the # symbol denotes a significant difference between the LPS and JNK inhibitor SP600125 groups.

3. Results

3.1. Curcumin Ameliorated LPS-Induced Increases in ROS Generation, Oxidative Stress, and P-JNK Level in the Adult Rat Hippocampus and in LPS-Treated BV2 Cell. Recently, it has been suggested that curcumin has strong antioxidant properties and can reduce the ROS burden. It is also well known that JNK is a crucial stress kinase and is highly expressed during increased intracellular ROS generation [7, 20]. Therefore, we analyzed the expression of p-JNK through western blotting, confocal microscopy, and immunohistochemistry. Our results showed that treatment with LPS significantly increased the expression of p-JNK in the adult rat hippocampus. On the other hand, treatment with 300 mg/kg/i.p. curcumin for 2 weeks significantly reduced the expression of p-JNK, providing evidence that curcumin has potent antioxidant properties (Figures 1(f), 1(g), and 1(j)). Furthermore, to investigate if curcumin could inhibit p-JNK activation in a similar way to the JNK inhibitor SP600125, we exposed BV2 microglial cells to 1 μg/ml LPS, 100 μg/ml curcumin, and 20 μM SP600125. The in vitro immunoblot and confocal microscopy results confirmed that LPS treatment significantly increased the expression of p-JNK in BV2 cells. Curcumin significantly reduced this increase similar to SP600125 treatment (Figures 1(h) and 1(i)). Studies using animal models have shown that LPS treatment induces the generation of ROS [21–23]. We therefore carried out ROS and LPO assays on rats treated with saline, LPS, and LPS+curcumin. We found that treatment with LPS enhanced ROS generation and oxidative stress in the hippocampus of adult rats, and curcumin ameliorated both of these in the LPS+curcumin-treated group (Figures 1(b) and 1(c)). We further investigated whether curcumin could reduce ROS generation and oxidative stress in a similar way to SP600125 by performing ROS and LPO assays on BV2 cell lines. The in vitro results demonstrated that LPS treatment significantly increased the levels of DCF and MDA (markers of ROS and oxidative stress) in the BV2 cells. Curcumin treatment significantly reduced the levels of DCF and MDA in a similar way to that of the JNK inhibitor SP600125 (Figures 1(d) and 1(e).

3.2. Curcumin Attenuated LPS-Induced Proinflammatory Cytokine Production and Restored the P-Akt/P-GSK3β Survival Pathway. Recent studies have demonstrated that LPS treatment induces microglial activation and cytokine production both in vivo and in vitro, playing a significant role in neuroinflammation-induced neurodegenerative disorders. In addition, the inhibitory effects of curcumin on the release of proinflammatory cytokines are well documented [24, 25]. Therefore, to determine the inhibitory role of curcumin against LPS-induced neuroinflammation in adult rats, we evaluated the expression of p-NF-κB (a transcription factor), TNF-α and IL-1β (proinflammatory cytokines), and GFAP and Iba1 (markers of reactive microglia and astrocytes) through western blotting. We found that LPS treatment significantly increased the expression of p-NF-κB, TNF-α, IL-1β, GFAP, and Iba1. Curcumin treatment inhibited this overexpression of p-NF-κB, TNF-α, IL-1β, GFAP, and Iba-1 in the hippocampal tissue of LPS-treated adult rats (Figure 2(a)). Confocal microscopy also showed an increased immunoreactivity of p-NF-κB and TNF-α in the hippocampus of LPS-treated adult rats. Curcumin treatment significantly reduced the immunoreactivity of TNF-α and p-NF-κB, suggesting that it prevents cytokine production in LPS-treated rats (Figures 2(b) and 2(c)). To investigate if curcumin prevents neuroinflammation via a JNK-dependent mechanism, we exposed BV2 microglial cells to LPS at a dose of 1 μg/ml for 24 h. We found that curcumin (100 μg/ml) and the JNK inhibitor SP600125 (20 μM) analogously attenuated the LPS-induced elevated level of proinflammatory cytokines, providing evidence that curcumin may inhibit cytokine production via a JNK-dependent mechanism (Figures 2(d)–2(g)).

Mounting studies have reported that LPS treatment inhibited the phosphorylation of Akt and GSK3-β in rat models of Parkinson's disease [26]. Our western blot and immunofluorescent results indicated that LPS treatment disrupts the survival pathway, demonstrated by a decrease in the expression and phosphorylation of Akt and GSK3-β proteins compared to saline-treated adult rats. Treatment with curcumin at a dose of 300 mg/kg/day not only restored this survival pathway but also significantly increased the level of p-Akt and p-GSK3β in the adult rat hippocampus (Figures 2(h)–2(j)).

3.3. Curcumin Mitigated LPS-Induced Neuronal Apoptosis and Neurodegeneration in the Adult Rat Hippocampus and in HT-22 Neuronal Cells. Recently, interest has been focused on LPS-induced ROS-mediated neuroinflammation-associated neurodegeneration. Badshah et al. demonstrated that LPS could induce neuronal apoptosis by increasing the expression of apoptotic markers like caspase-3 and PARP-1 [1]. Other studies have also shown that LPS induces prolonged neuroinflammatory responses by activating microglial cells, subsequently initiating the mitochondrial apoptotic pathway and neuronal cell death [27–29]. In the present study, we validated the antiapoptotic properties of curcumin against LPS-induced neuroinflammation-associated neurodegeneration. Our immunoblot and immunofluorescence results showed that LPS at a dose of 250 μg/kg for 7 days increased the expression of the apoptotic proteins Bax, caspase-3, Cyt c, and PARP-1 and decreased the expression of the antiapoptotic protein Bcl-2 in the adult rat hippocampus. Treatment with curcumin at a dose of 300 mg/kg for 14 days significantly decreased these apoptotic markers and inhibited neuronal apoptosis (Figures 3(a)–3(d)).

There exists considerable evidence in the literature regarding the exposure of HT-22 cells to LPS-induced injury. Ji et al. reported that stimulation of hippocampal HT-22 neuronal cells with LPS remarkably upregulated the expression of the apoptotic markers Bax and caspase-3 and downregulated the expression of the antiapoptotic protein Bcl-2 [30]. Similarly, in the current study, we treated HT-22 neuronal cells with LPS in order to evaluate JNK-dependent and inflammation-associated neuronal apoptosis. Our western blot and confocal results demonstrated that LPS treatment

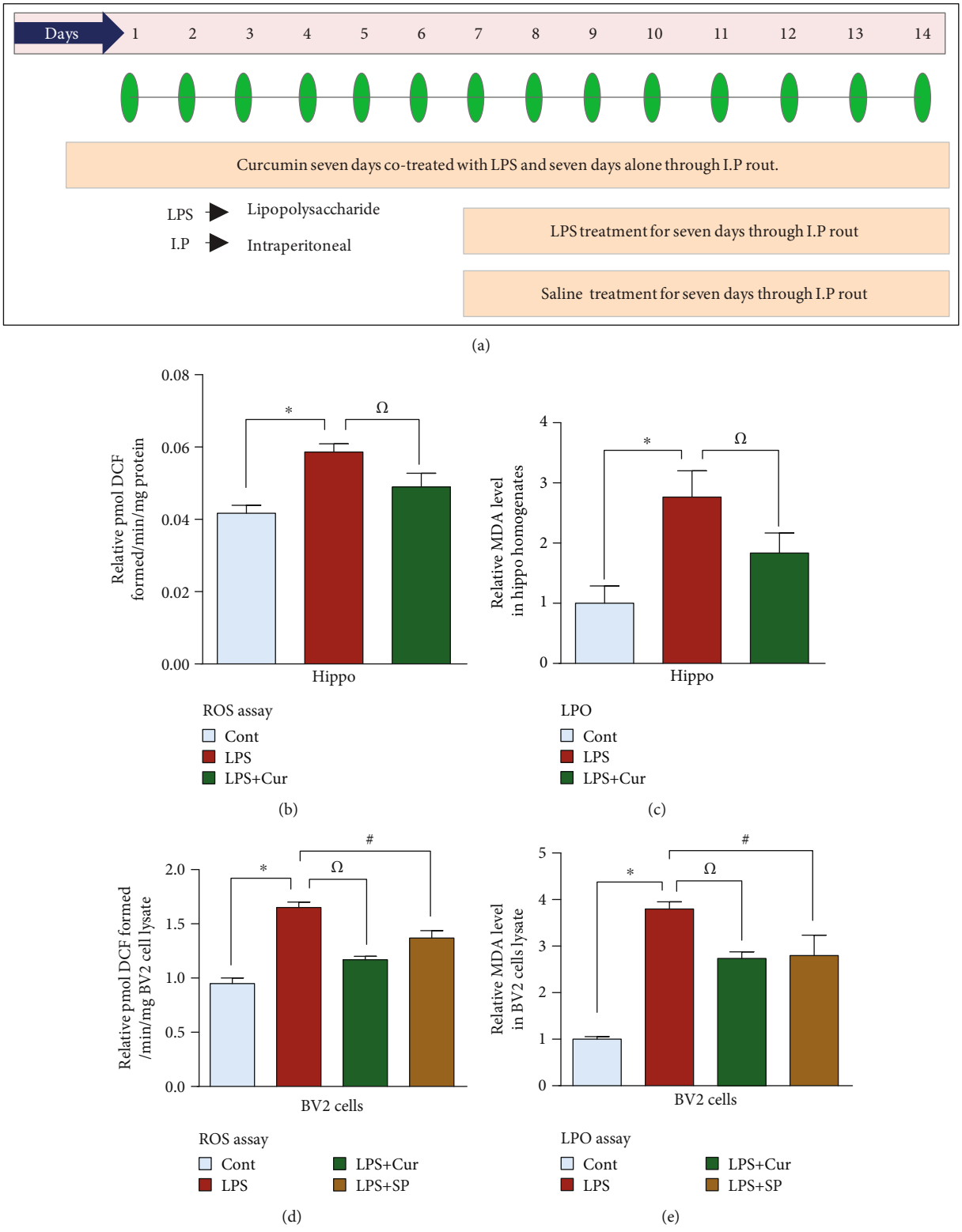

Figure 1: Continued.

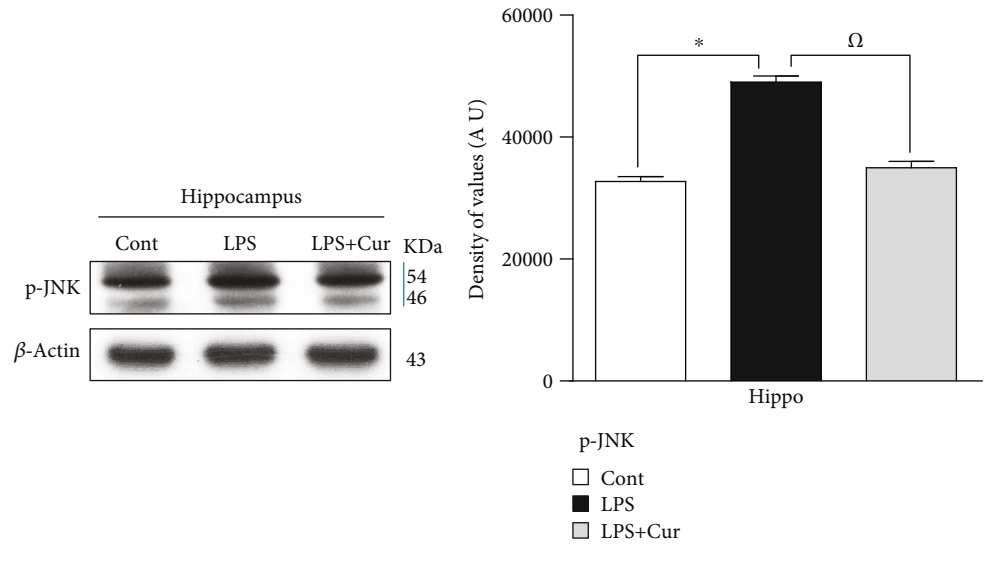

(f)

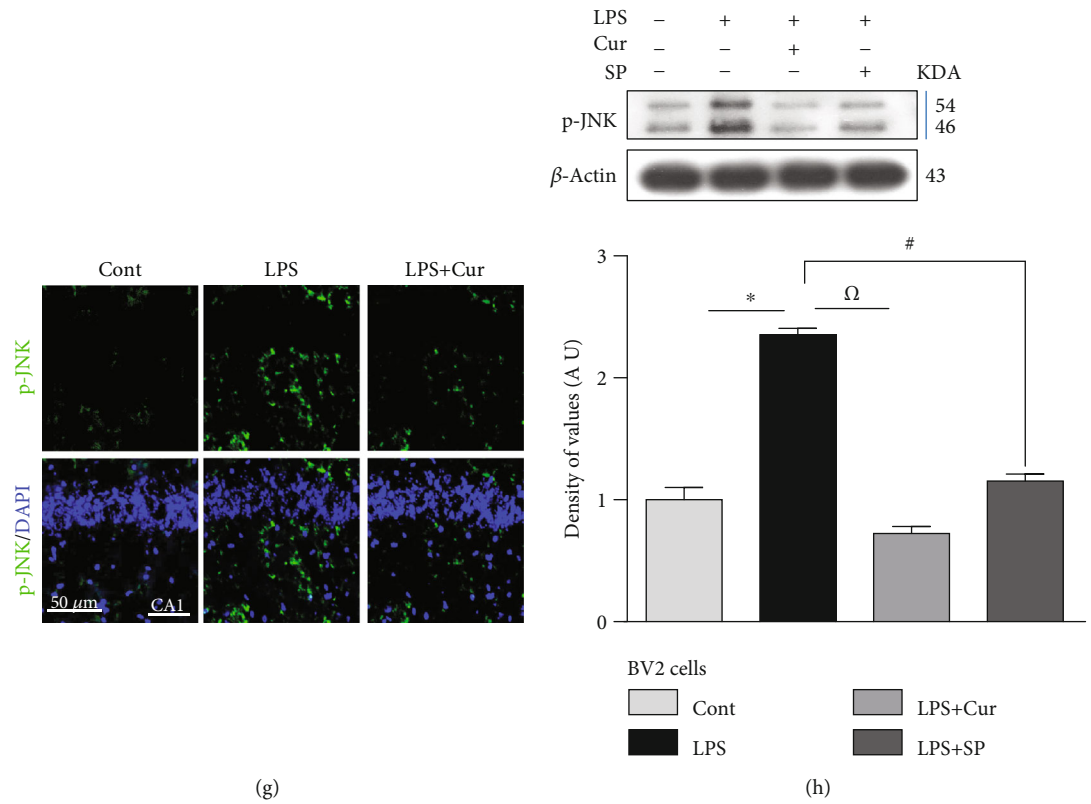

(g) (h)

Figure 1: Continued.

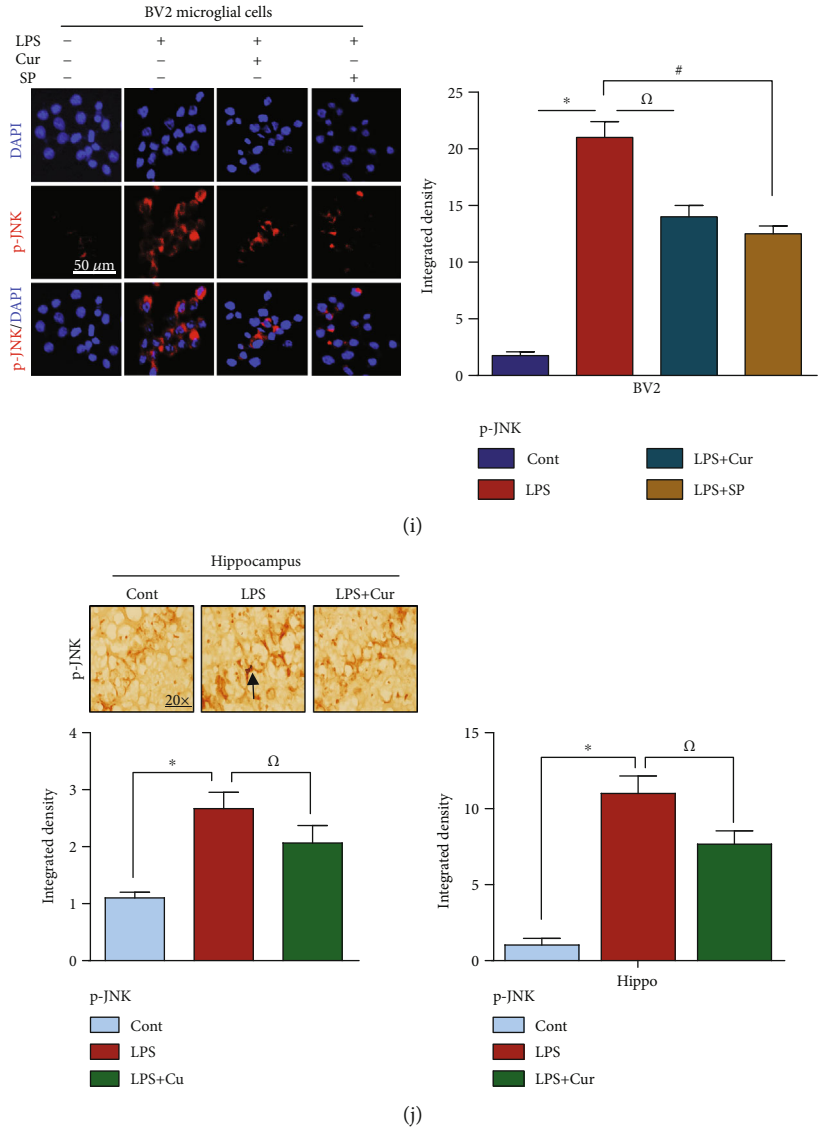

Figure 1: Curcumin mitigated the LPS-induced increase in ROS and oxidative stress and JNK activation in the adult rat hippocampus and in BV2 cells. (a) Presenting study plan for the current research work. Rats were divided into three groups: (1) control (2), LPS (3), and LPS +curcumin (b–e), representative histograms showing the ROS/LPO assays both in vivo and in vitro. Five animals were kept per group, and each experiment was repeated 3 times; i.e., $(n = 5)/(n = 3)$. (f) Identifying the western blot results of p-JNK in the hippocampus of control, LPS, and LPS+curcumin. (g) Indicating the confocal results of p-JNK in the hippocampus of the adult rat. (h) Showing the western blot results of p-JNK in BV2 microglial cells. (i) Showing the confocal microscopy results of p-JNK in BV2 cells. (j) Immunohistochemistry results of p-JNK in the CA1 region of adult rat hippocampus. In each case of western blot assay, the same immunoblot was probed using β-actin as a loading control. 15 animals were kept per group; i.e., $n = 15$. Eight animals per group for western blot ($n = 8$), while 5 animals per group were used for confocal microscopy ($n = 5$). (n) Showing numbers of animal per group. Sigma Gel software was used to quantify the western blot results whereas ImageJ software was used to analyze the immunofluorescence results of p-JNK. Green color (FITC) and blue color (DAPI) represents the confocal microscopy results of p-JNK in the hippocampus while red color indicates immunofluorescent reactivity of p-JNK in BV2 microglial cells. Magnifications: 20x. Scale bar = 50 μm. $^*P < 0.05$ shows the significant difference between the control and LPS groups while the Ω symbol shows the significance between the LPS and LPS+curcumin groups. In the in vitro study, the # symbol represents the significant difference between the LPS and LPS+SP600125 groups.

at a dose of 1 μg/ml significantly elevated the levels of caspase-3, Cyt c, and PARP-1. Curcumin at a dose of 100 μg/ml and the JNK inhibitor SP600125 at a dose of 20 μM markedly reduced their expression (Figures 3(e)–3(g)).

Additionally, to determine the extent of LPS-induced neurodegeneration, we performed FJB, TUNEL, and Nissl staining. We found that LPS treatment increased the number of FJB-positive cells in the hippocampus of adult rats. However, treatment with curcumin reduced the number of FJB-positive cells and inhibited neuronal cell death (Figure 3(h)). Next, the Nissl staining results demonstrated that LPS treatment for 7 days at a dose of 250 μg/kg significantly decreased the number of viable neurons. Curcumin treatment for 14 days at a dose of 300 mg/kg prevented

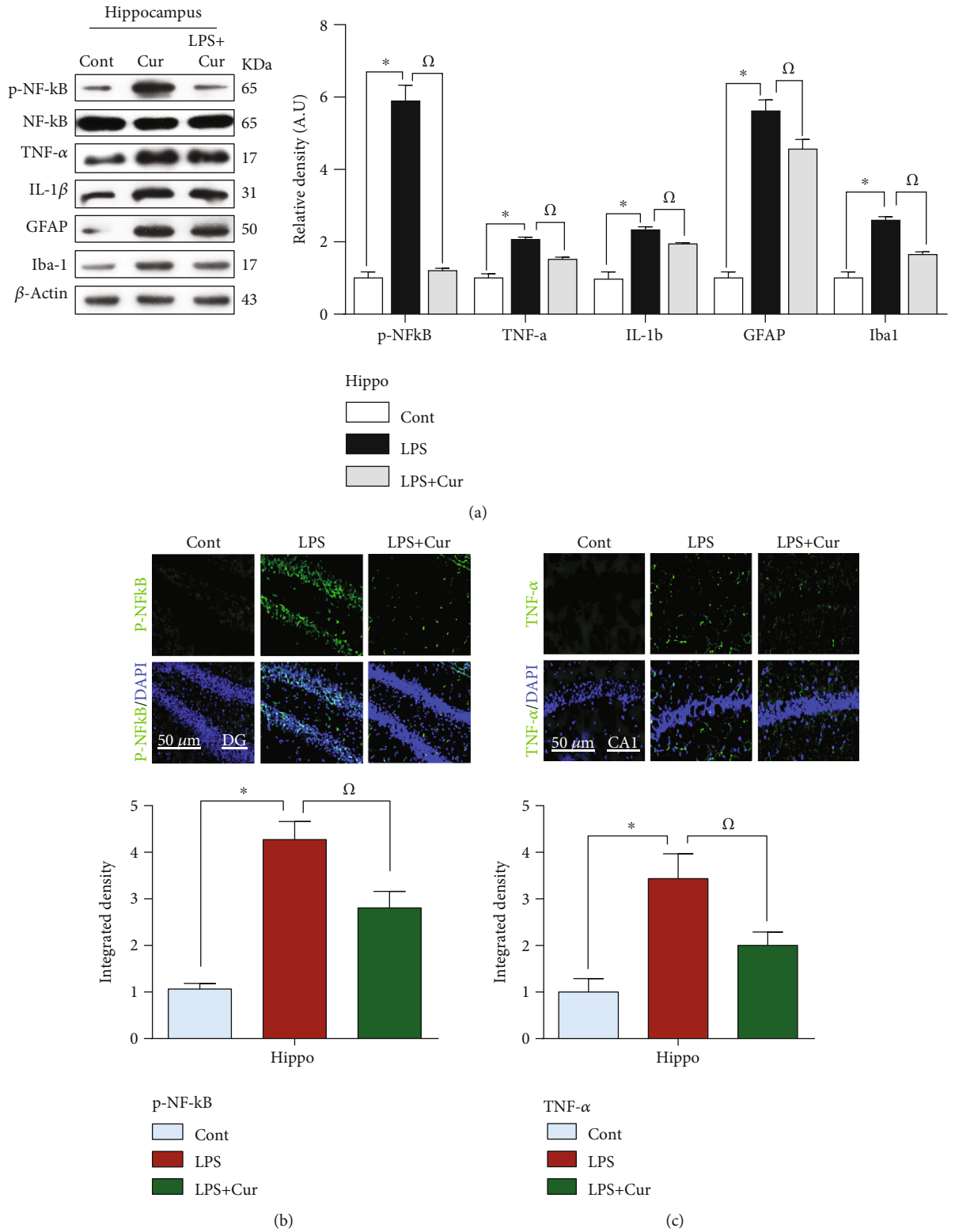

Figure 2: Continued.

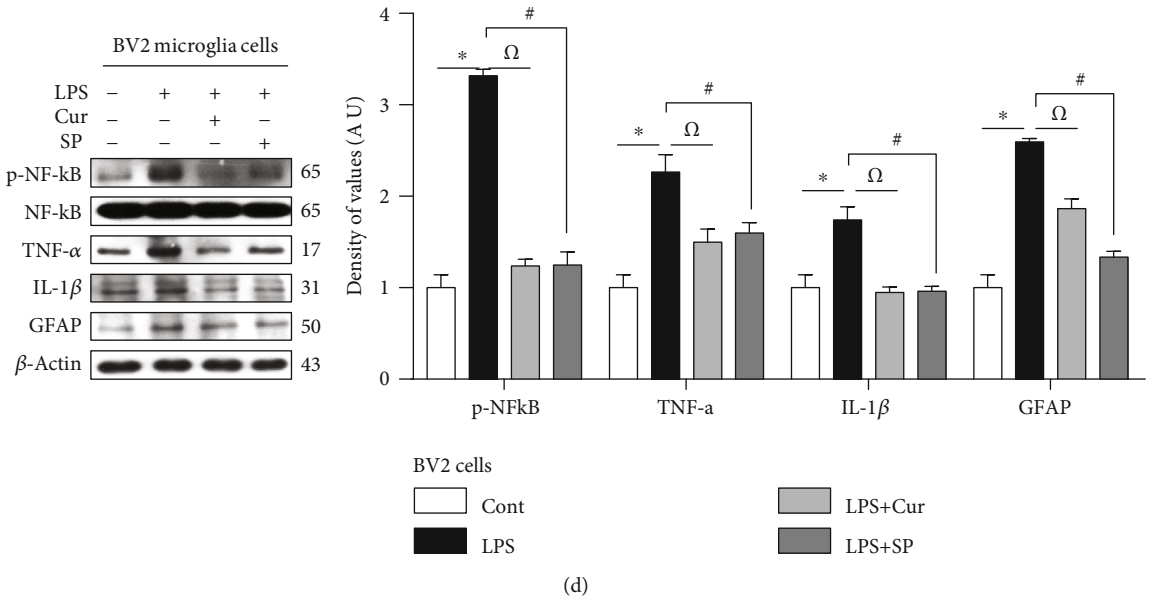

(d)

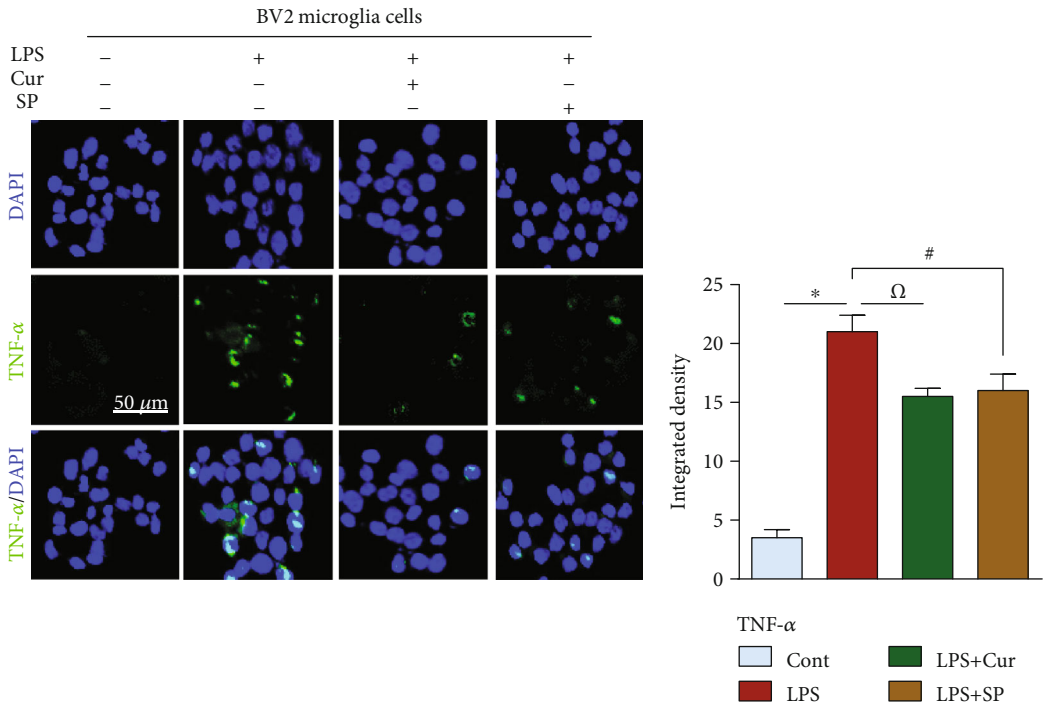

(e)

Figure 2: Continued.

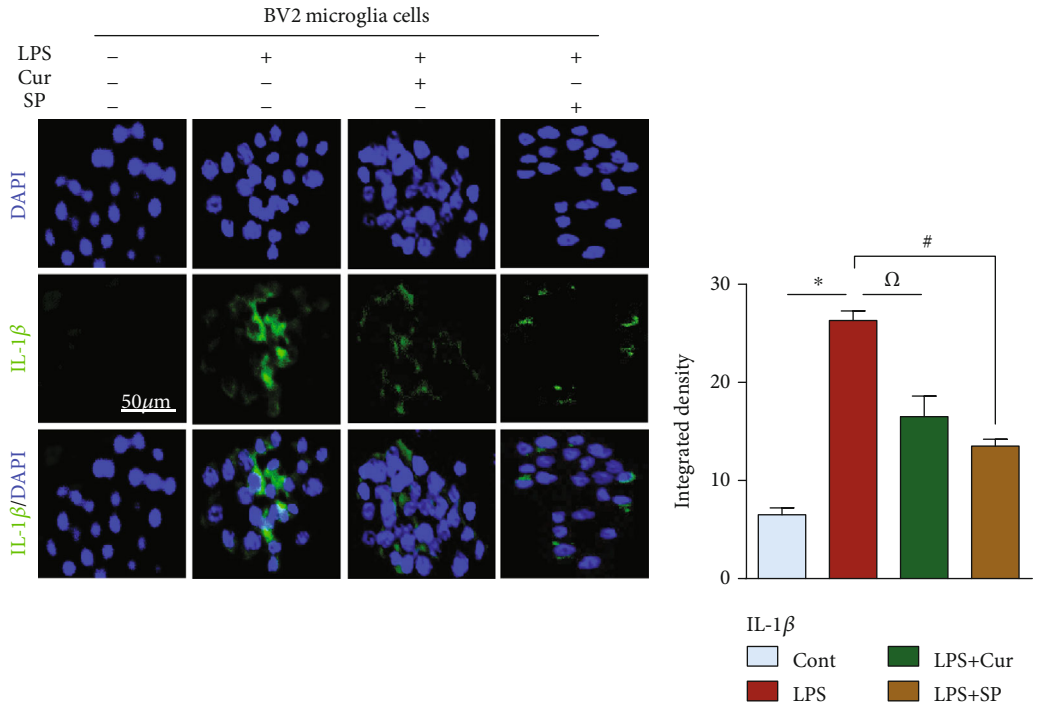

(f)

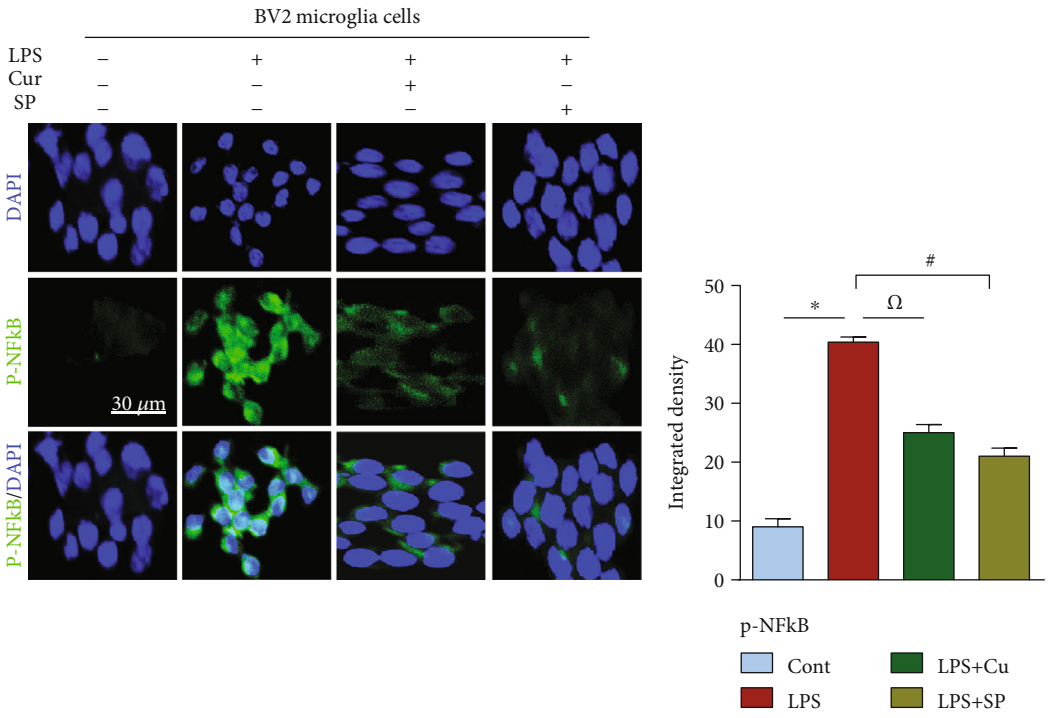

(g)

Figure 2: Continued.

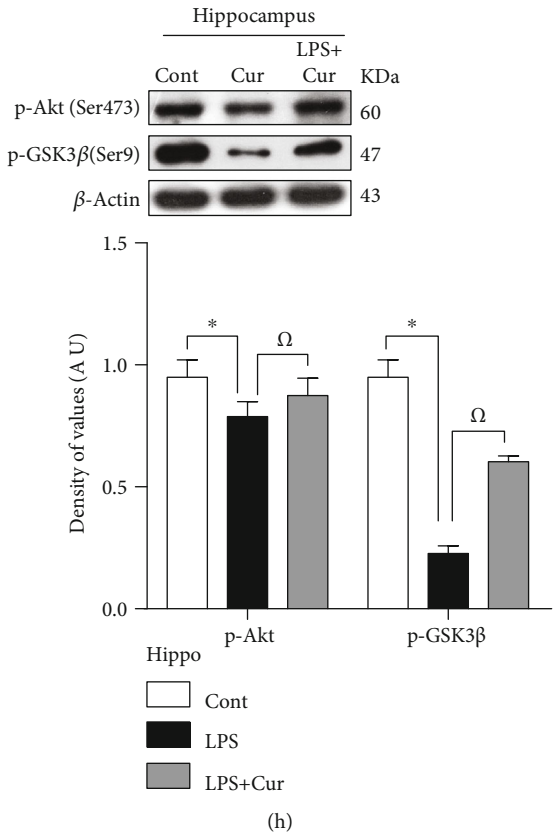

(h)

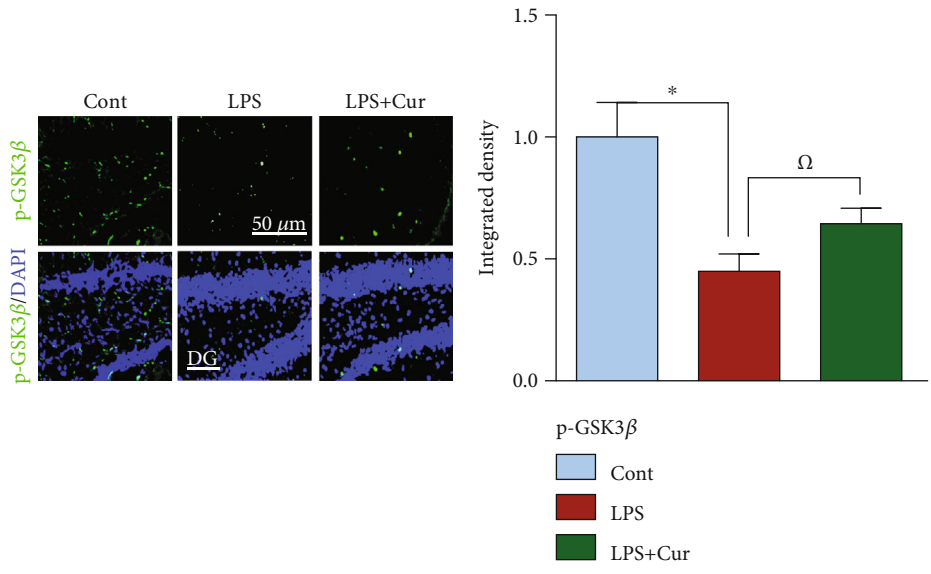

(i)

Figure 2: Continued.

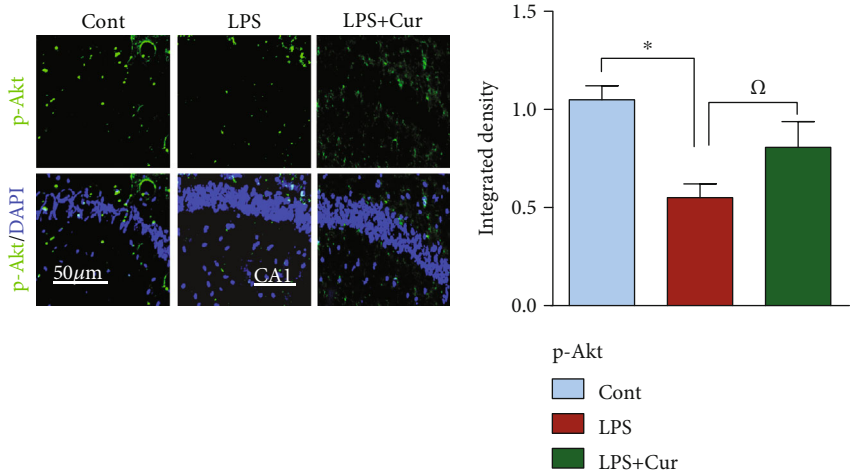

Figure 2: Curcumin treatment suppressed neuroinflammatory cytokines both in vivo/in vitro while restoring the survival pathway in adult rat hippocampus. (a) Western blot analysis of activated microglia (GFAP, Iba1), transcription factor (p-NF-κB), and inflammatory cytokines (TNF-α, IL-1β) in adult rats. (b, c) Indicating the immunofluorescent results of p-NF-κB (transcription factor) and TNF-α (inflammatory cytokines) in the CA1 region of an adult rat hippocampus. (d) Showing the western blot results of inflammatory cytokines in LPS-exposed BV2 microglial cells. (e–g) Representing the confocal results of inflammatory markers (TNF-α, IL-1β) and transcription factor (p-NF-κB) in BV2 cells. (h–j) Signifying the western blot and confocal results of survival proteins in an adult rat hippocampus. $n = 5$ for confocal microscopy, while$n = 8$ for western blot. Green: FITC, blue: DAPI, red: TRITC; $n = 3$ experiments. Magnification: 20x. Scale bar = 30/50 μ m. One-way ANOVA followed by Student's t-test was used to determine the mean ± SEM, whereas statistical analysis was evaluated by using GraphPad Prism 5 software. Sigma Gel software was used to quantify the western blot results whereas ImageJ software was used to analyze the immunofluorescence results. β-Actin was used as a loading control in western blot analysis.

neuronal apoptosis and remarkably increased the number of viable neurons (Figure 3(l)). The results of the TUNEL assay also showed that LPS increased the number of dead neurons. Curcumin significantly improved the cell viability of the affected neurons and ameliorated neurodegeneration (Figure 3(i)). To determine the effect of LPS on cell morphology, we conducted H&E staining. The results showed that LPS treatment dysregulated cell morphology, demonstrated by the appearance of shrunken neuronal cells. Curcumin treatment restored cell morphology and improved cell survival (Figure 3(k)).

3.4. Curcumin Increased the Expression of Pre- and Postsynaptic Protein Markers and Rescued Memory-Related Deficits in an Adult Rat Model of LPS Challenge. A recent study indicated that neuroinflammation and neurodegeneration in response to ROS can lead to synaptic deficits and memory impairments [31, 32]. To analyze the effect of curcumin against LPS-induced synaptic degeneration, we examined the expression level of the presynaptic protein SNAP25 and the postsynaptic protein PSD95 through western blotting and confocal microscopy. Results showed that LPS treatment, due to its toxic effects, decreased the expression of both SNAP25 and PSD95 compared to the control and curcumin-treated groups (Figures 4(a)–4(c)). Moreover, to evaluate the memory, we performed the MWM and Y-maze tests. The LPS-treated rats exhibited an increased latency time, indicative of learning and memory deficits. Conversely, a reduced latency time, indicative of memory improvements, was exhibited by the curcumin-treated group (Figure 4(d)). A probe test was also performed on the 5th day in which the hidden platform was removed. The LPS-treated rats exhibited fewer platform crossings and a reduced length of time spent in the target quadrant. Curcumin treatment increased the number of platform crossings and the length of time spent in the target quadrant (Figures 4(e) and 4(f)). Next, we performed a Y-maze test to investigate spatial working memory by assessing spontaneous alternation percentage. We found that the LPS-treated rats exhibited a lower alteration percentage than the saline-treated rats, indicating poor working memory. Curcumin significantly increased alteration percentage in LPS-challenged rats, indicating that curcumin can improve memory dysfunctions (Figure 4(g)).

4. Discussion

The aim of the present study was to evaluate the underlying antioxidant neuroprotective mechanism of the dietary polyphenolic compound curcumin in LPS-treated adult rats via regulation of the JNK/NF-κB/Akt signaling pathway. Several studies have demonstrated that LPS triggers ROS generation/oxidative stress and activates the stress kinase JNK, subsequently mediating the pathogenesis of various neurodegenerative disorders [33, 34]. Similarly, in our study, LPS treatment elevated ROS generation and enhanced LPO, demonstrated by increased levels of DCF and MDA, and upregulated the expression of p-JNK in the hippocampus of adult rats and in HT-22/BV2 cells. Dietary curcumin supplementation reduced these elevated levels of ROS/oxidative stress and p-JNK.

Many studies have reported that LPS induces JNK activation which mediates neuroinflammatory responses and LPS

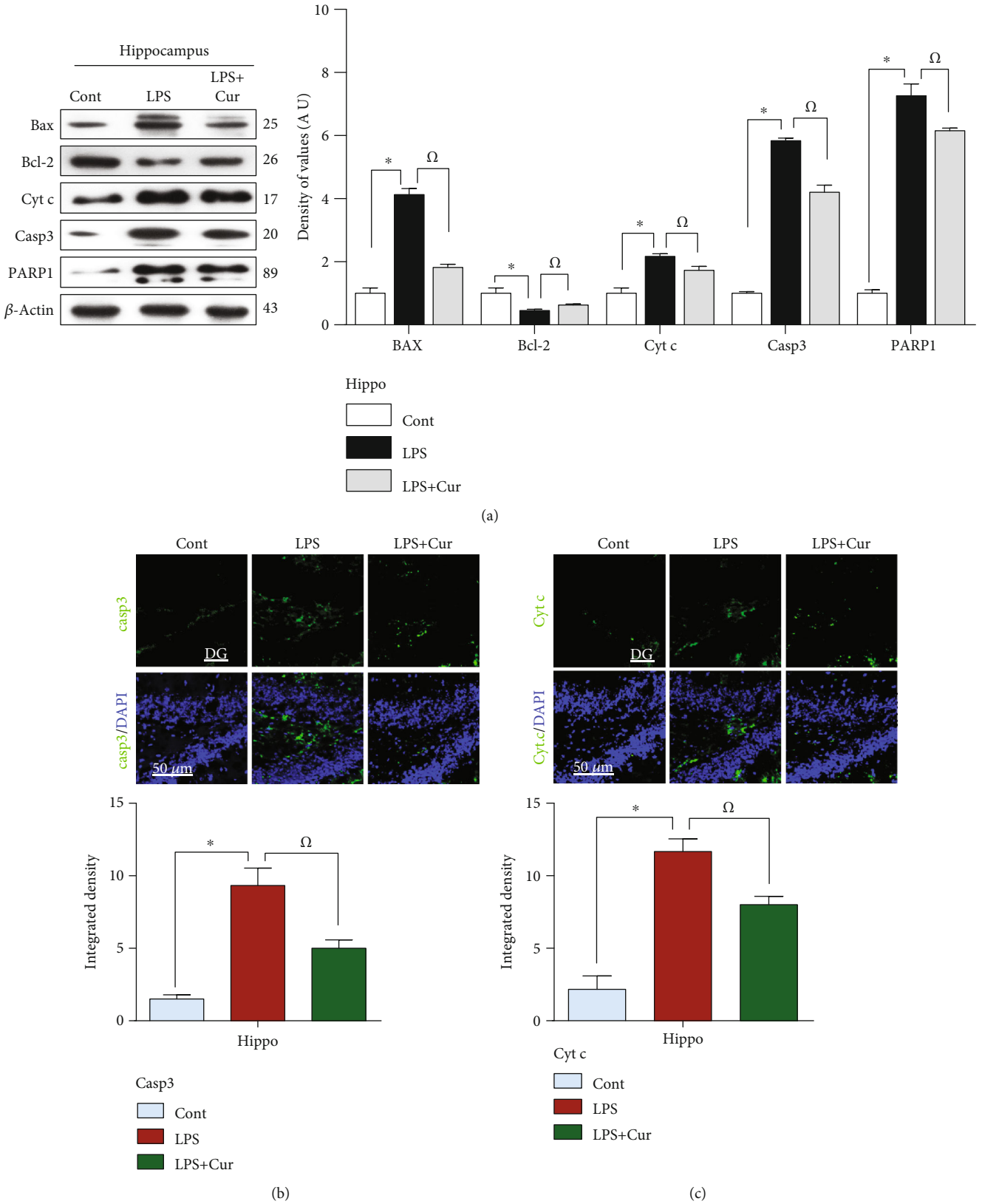

Figure 3: Continued.

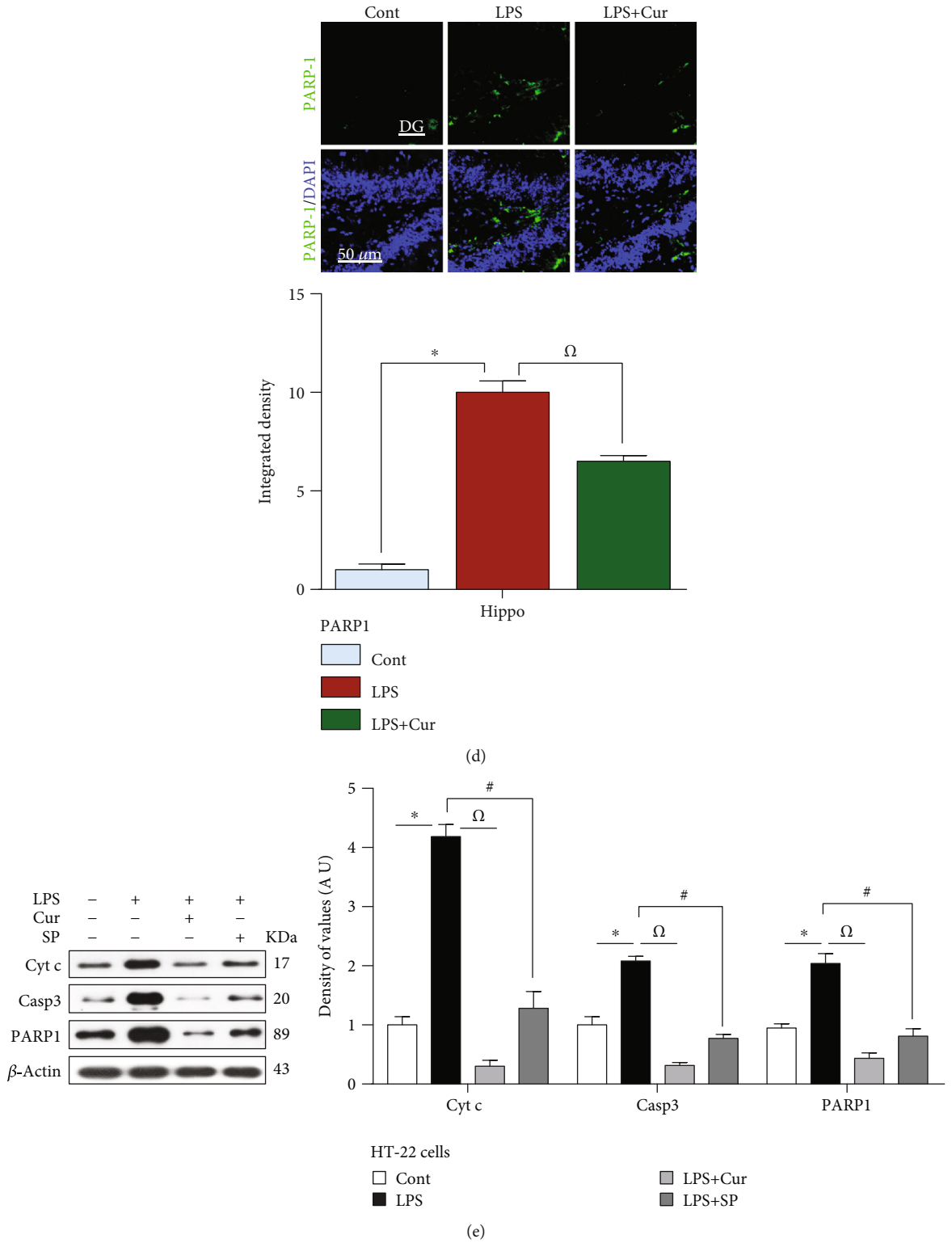

Figure 3: Continued.

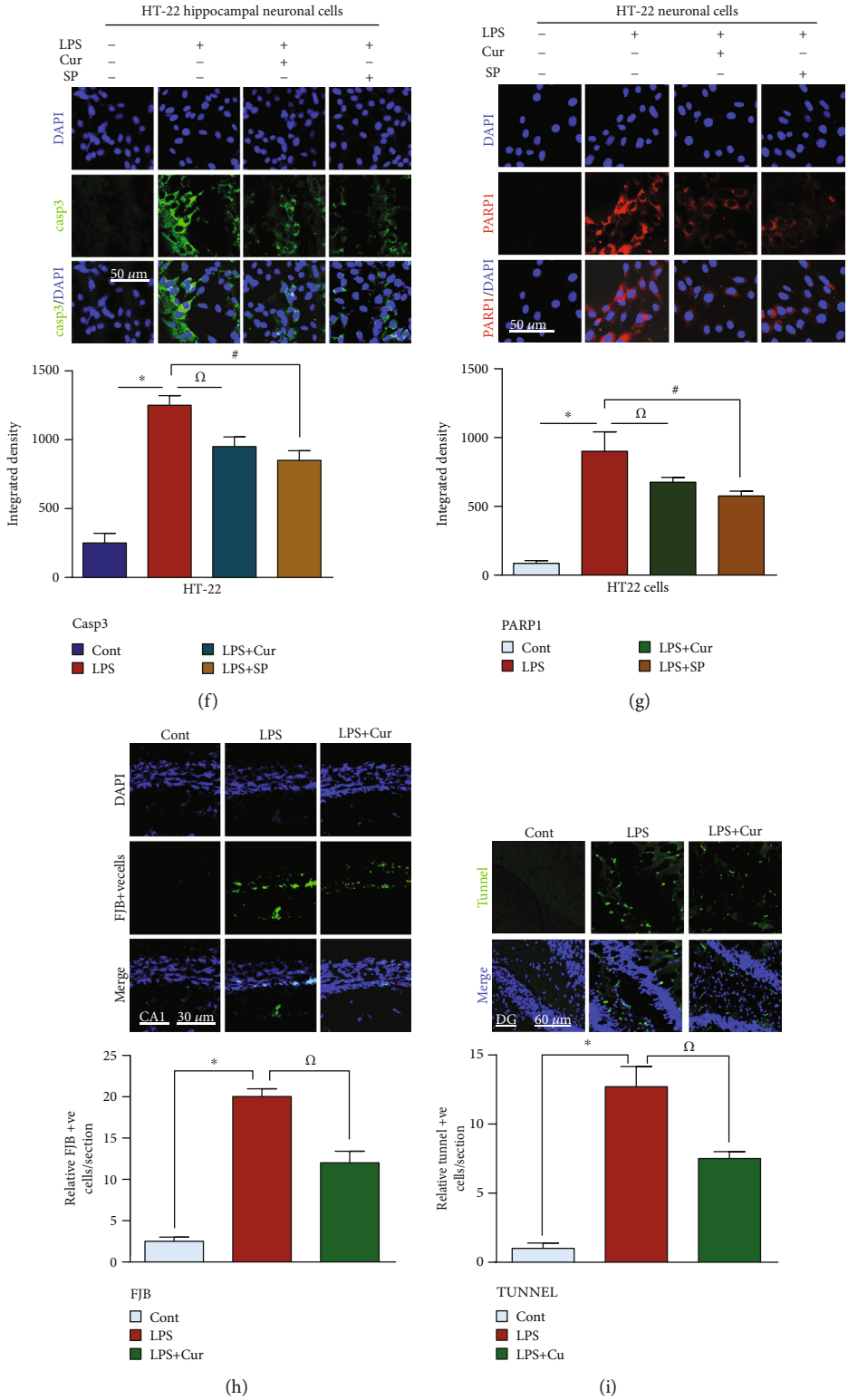

Figure 3: Continued.

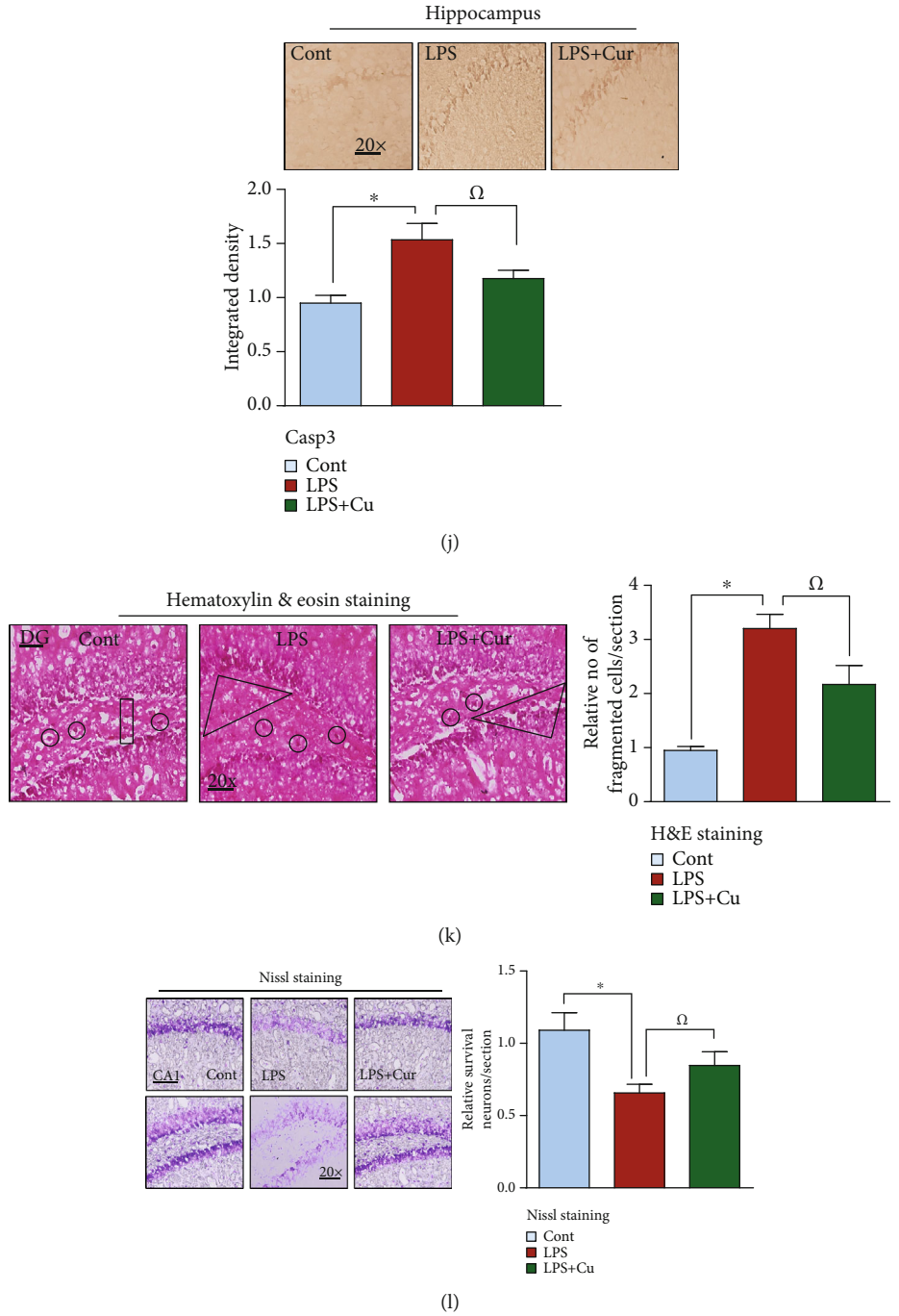

FIGURE 3: Curcumin treatment abrogated neuronal cell apoptosis in LPS-treated adult rats and in HT-22 hippocampal neuronal cells. (a–d) Representative western blot and immunofluorescent analysis of neuronal apoptotic protein markers in an adult rat hippocampus. (e–g) Showing the confocal and western blot results of apoptotic markers in LPS-exposed HT-22 neuronal cells. (h) Representing the FJB results, (i) indicating the tunnel assay results, and (j) specifying the immunohistochemistry results of caspase-3 in the hippocampus of the adult rat. (k, l) Representing the H&E and Nissl results, respectively. Sigma Gel software was used to quantify the western blot results of the related protein bands. Beta-actin was used as a loading control. ∗/#/Ω were used to show the level of significance. $^{*}P < 0.05$. One-way ANOVA followed by Student's t-test was used to determine the mean ± SEM whereas statistical analysis was evaluated by using GraphPad Prism 5 software. $n = 3$ means that the number of experiments were repeated 3 times. ($n = 5$ animals/group for confocal and histochemistry); $n = 3$ experiments. Magnification: 20x. Scale bar = 30/50 μm. The presented data are relative to the control. The number of animal used per group and the level of significance are mentioned in Materials and Methods.

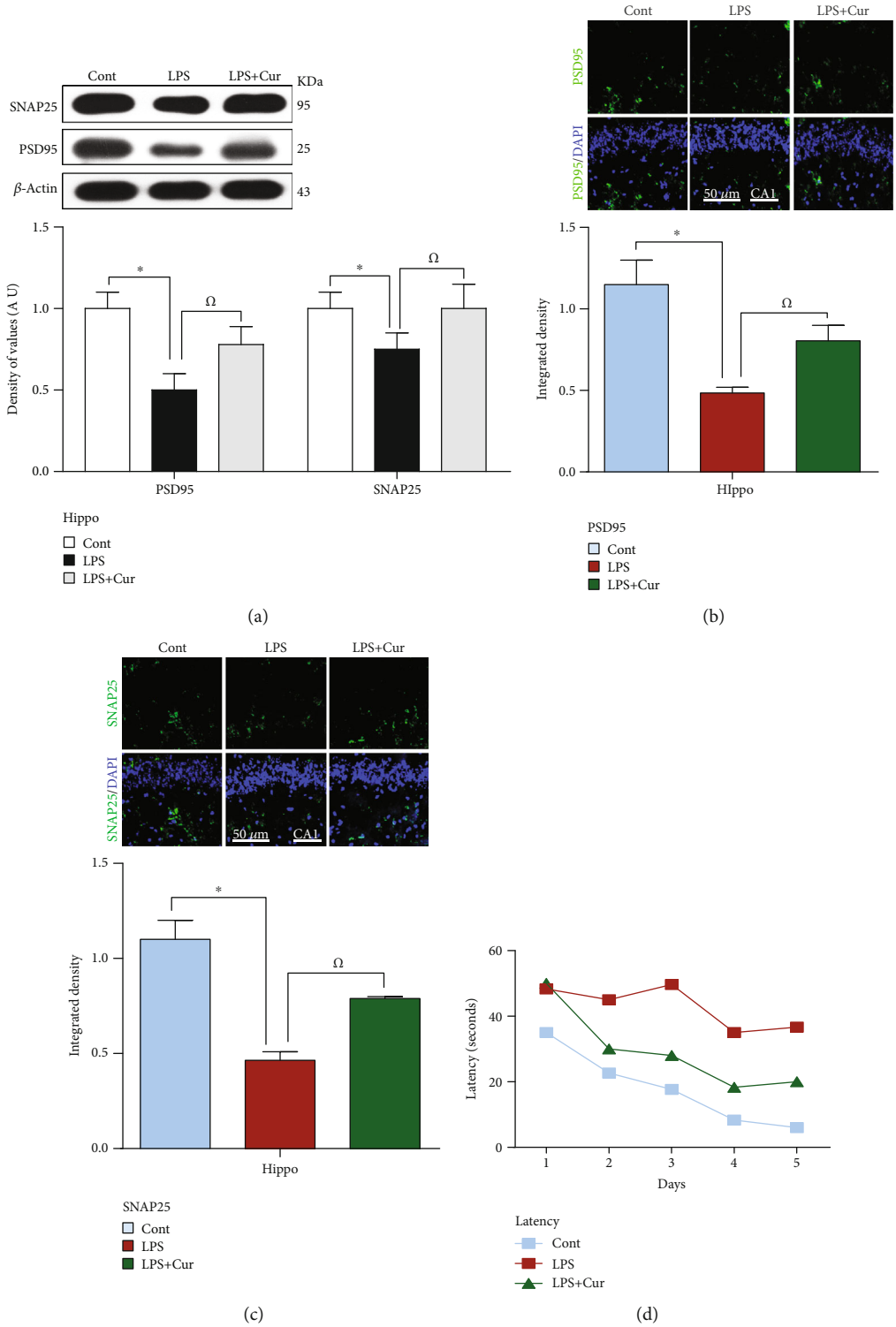

Figure 4: Continued.

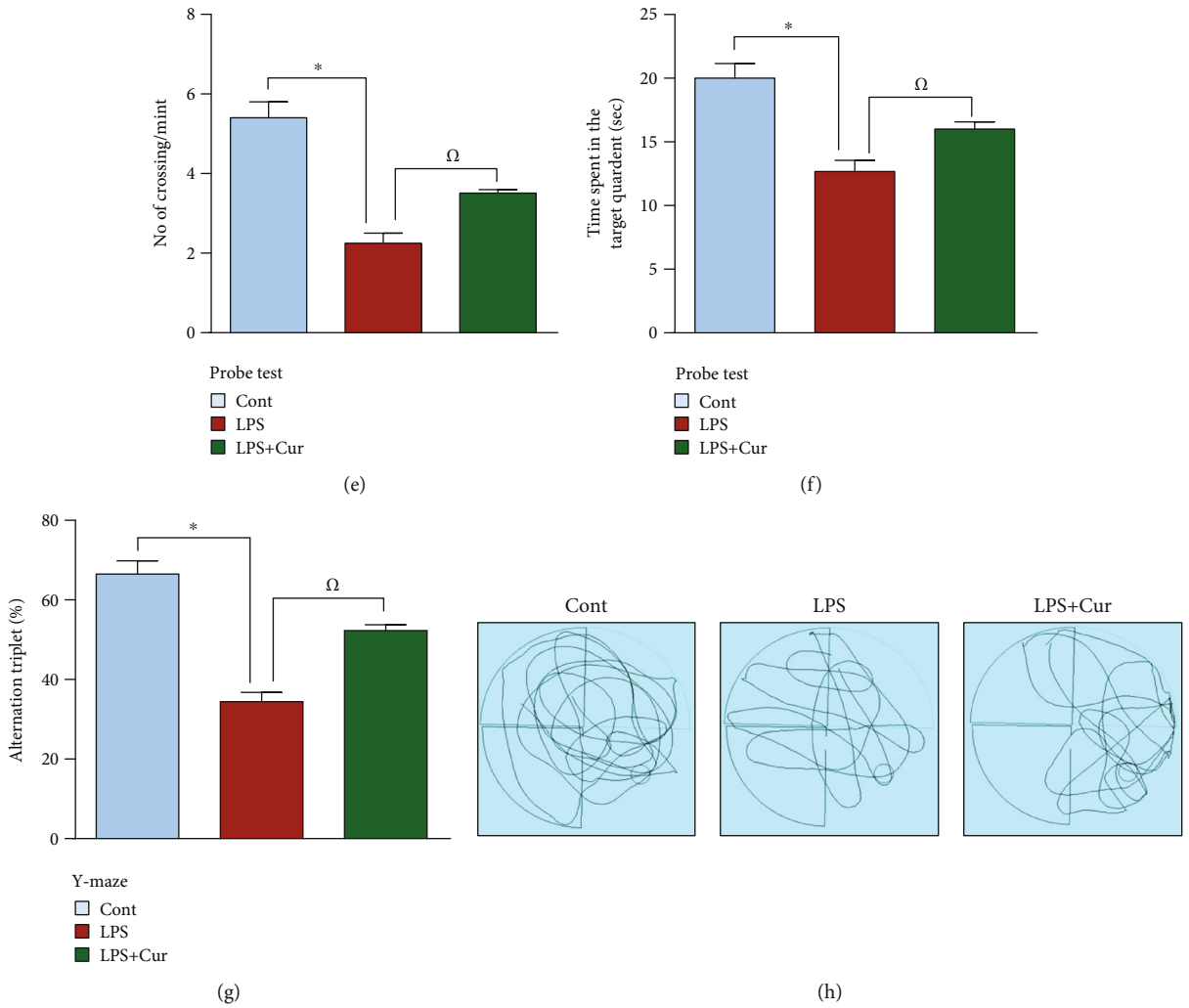

Figure 4: Curcumin treatment improves memory impairment and increases the expression level of synaptic proteins. (a–c) Immunoblot and confocal analysis indicating the expression of synaptic proteins including SNAP-25 and PSD95 in the hippocampus of the saline-treated group, LPS-treated group, and LPS+curcumin-treated group ($n = 8$ for western and $n = 5$ for confocal). Each immunoblot was probed with an anti-β-actin antibody as a loading control. Bands were quantified with Sigma gel software. FITC (green) showing the immunoreactivity of the related antibodies while DAPI (blue) showing the nucleus of the cell. The number of experiments was repeated 3 times ($n = 3$). ImageJ software was used for the quantification of confocal analysis. (d) The related histogram representing a total of 5 days of latency of the control, LPS, and LPS+curcumin groups. (e) The histogram represents the number of crossings during the probe test among the control, LPS, and LPS+curcumin groups. (f) Graphical representation showing time spent in the target quadrant by control, LPS, and LPS+curcumin. (g) The representative histogram shows the spontaneous alteration (%) in the Y-maze test. (h) Showing the trajectories of the water maze test.

has been extensively used in models studying neuroinflammation. Recently, other studies have suggested that systemic administration of LPS activates oxidative stress and JNK which initiates downstream neuroinflammatory cascades. Numerous in vivo and in vitro studies have proposed that LPS provokes microgliosis and activates a number of signaling pathways including activation of NF-κB via several mediators including ROS/oxidative stress and p-JNK, which in turn promote the release of proinflammatory cytokines such as TNF-α and IL-1β [4, 35, 36]. In agreement with earlier studies, our rat model of LPS challenge exhibited an increased expression of Iba-1, GFAP, p-NF-κB, TNF-α, and IL-1β. On the other hand, our in vivo and in vitro results demonstrated that curcumin treatment significantly diminished this ROS/JNK-mediated increased expression of NF-κB, Iba-1, GFAP, TNF-α, and IL-1β in a similar manner to the JNK inhibitor SP600125.

Several studies have supported the notion that LPS-induced ROS/JNK-mediated neuroinflammation provokes neuronal cell death and downregulates the level of survival proteins such as p-Akt/p-GSK3β via microgliosis and the production of proinflammatory cytokines. With respect to neuroinflammation, it has been suggested that several mechanisms are involved in the secretion of proinflammatory

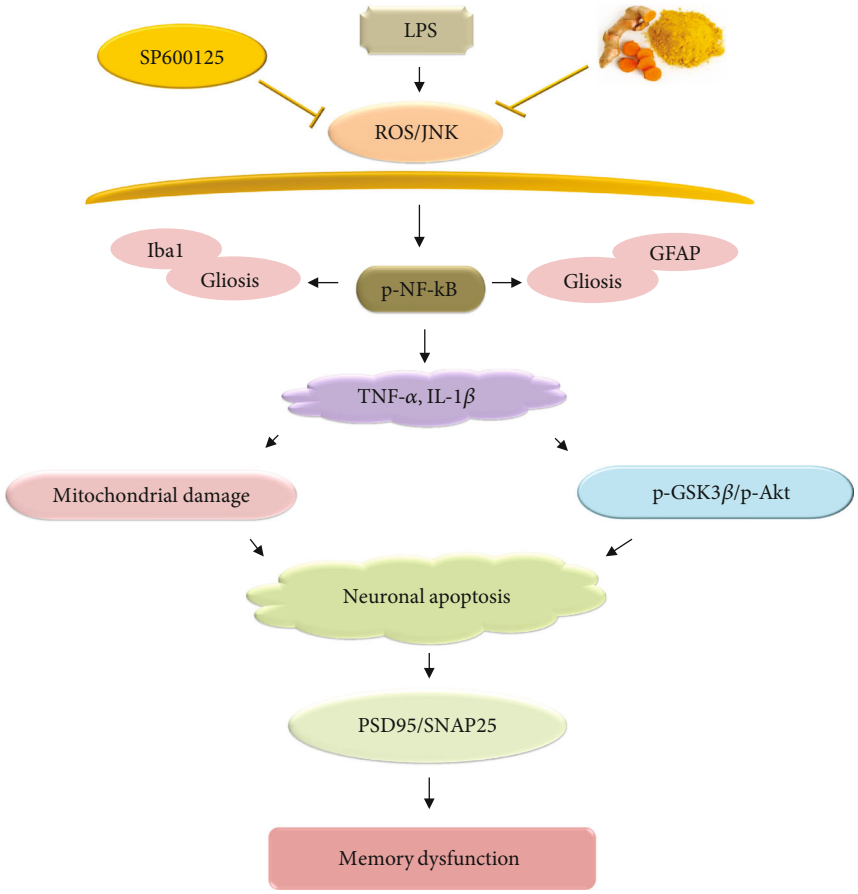

Figure 5: Proposed schematic diagram of LPS-induced ROS-mediated neuroinflammation, neurodegeneration, and memory deficits via dysregulation of the JNK/NF-κB/Akt signaling pathway.

cytokines by astrocytes and microglial cells. One such mechanism is the LPS-induced p-JNK pathway that functions as a link between ROS/oxidative stress and neuroinflammation-mediated apoptotic neurodegeneration [4, 26, 37, 38]. It is well known that dietary curcumin is a strong candidate for the prevention of ROS/oxidative stress-mediated neuroinflammation-related neurodegeneration [39]. Additionally, curcumin can inhibit the dysfunction of mitochondrial activity and suppress the apoptotic proteins Bax, caspase-3, Cyt c, and PARP-1. Curcumin also upregulates the expression of the antiapoptotic protein Bcl-2, which prevents the dysregulation of mitochondrial homeostasis [28, 40–42]. Here, our results also demonstrated that curcumin treatment markedly inhibited neuronal apoptosis in the adult rat hippocampus via the suppression of neuroinflammation, regulation of the survival proteins p-Akt and p-GSKβ, and the reduction of apoptotic protein markers. Additionally, many studies have shown that exposure of HT-22 neuronal cells to LPS activates cell death pathways and mitochondrial dysfunction [30]. Likewise, in the present study, we observed that curcumin treatment prevented neuronal apoptosis via a JNK-dependent mechanism in LPS-treated HT-22 neuronal cells. To further explore the neuroprotective effect of curcumin, we performed TUNEL, FJB, Nissl, and H&E staining. Our results demonstrated that in the adult rat hippocampus, the number of TUNEL- and FJB-positive neuronal cells was remarkably decreased in the LPS-treated group, while the number of viable neurons in the Nissl assay was greatly increased upon curcumin treatment. Moreover, consistent with previous studies, our findings demonstrated that curcumin treatment restored fragmented and shrunken neuronal cells during H&E immunohistochemistry.

Studies in animal models have shown that LPS induces detrimental physiological responses such as chronic neuroinflammation, disrupted mitochondrial function, and alteration of the homeostasis of antioxidants/oxidation, in turn resulting in memory disorders [1, 36, 43, 44]. Polyphenolic compounds with antioxidant properties, particularly curcumin, have thus been studied for their effectiveness in reducing oxidative stress/neuroinflammation-associated learning and memory deficits [17, 45, 46]. The results of this study demonstrated that curcumin, a potent scavenger of ROS, improved memory deficits by increasing the expression level of memory-related proteins, detected using western blotting and confocal microscopy. Furthermore, curcumin treatment significantly decreased latency time, increased the number of platform crossings, increased the length of time spent in the target quadrant, and enhanced alteration percentage in the Morris water maze and Y-maze tasks.

5. Conclusions

In conclusion, we obtained notable data about the underlying antioxidant neuroprotective mechanism of dietary curcumin in a rat model of LPS-induced neurotoxicity. Our results demonstrated that curcumin regulated the JNK/NF-κB/Akt signaling pathway and consequently ameliorated ROS generation, oxidative stress, and neuroinflammation-associated neurodegeneration. Curcumin also improved memory-associated pre- and postsynaptic markers, as well as cognitive functions, in LPS-treated adult rats (Figure 5). Taken together, these data suggest that dietary curcumin acts as a potent antioxidant and anti-inflammatory agent and could be beneficial as a dietary supplement for the prevention of oxidative stress/neuroinflammation-related neurological disorders.

Abbreviations

AD:	Alzheimer's disease
Cyt c:	Cytochrome c
CNS:	Central nervous system
DCFH-DA:	2′7′-Dichlorodihydrofluorescein diacetate
DCF:	2′7′-Dichlorofluorescei
DMEM:	Dulbecco's modified Eagle medium
DAPI:	4′,6′-Diamidino-2-phenylindole
DG:	Dentate gyrus
DMSO:	Dimethyl sulfoxide
FBS:	Fetal bovine serum
FITC:	Fluorescein isothiocyanate
FJB:	Fluoro-jade B
HRP:	Horseradish peroxidase
IL-1β:	Interleukin-1β
I.P.:	Intraperitoneally
LPO:	Lipid peroxidation
LPS:	Lipopolysaccharide
MDA:	Malondialdehyde
P-JNK:	Phospho-c-Jun N-terminal kinase 1
MWM:	Morris water maze
PARP-1:	Poly (ADP-ribose) polymerase-1
PD:	Parkinson's disease.

Data Availability

The data used to support the findings of this study are available from the corresponding author upon request.

Ethical Approval

The animal maintenance, treatments, behavioral studies, and surgical procedures were carried out in accordance with the animal ethics committee (IACUC) guidelines issued by the Division of Applied Life Sciences, Department of Biology at Gyeongsang National University, South Korea. The experimental methods were carried out in accordance with the approved guidelines (Approval ID: 125), and all experimental protocols were approved by the animal ethics committee (IACUC) of the Division of Applied Life Sciences, Department of Biology at Gyeongsang National University, South Korea.

Conflicts of Interest

The authors declared no competing financial interests.

Authors' Contributions

Muhammad Sohail Khan is the first author who designed and managed the experimental work, and wrote the manuscript. Tahir Muhammad is the second author who performed the Western blot analysis and other technical arrangements. Myeong Ok Kim is the corresponding author who reviewed and approved the manuscript and holds all the responsibilities related to this manuscript.

Acknowledgments

This research was supported by the Brain Research Program through the National Research Foundation of Korea (NRF) funded by the Ministry of Science, ICT and Future Planning (2016M3C7A1904391).

References

[1] H. Badshah, T. Ali, and M. O. Kim, "Osmotin attenuates LPS-induced neuroinflammation and memory impairments via the TLR4/NFκB signaling pathway," *Scientific Reports*, vol. 6, no. 1, p. 24493, 2016.

[2] L. Chen, H. Deng, H. Cui et al., "Inflammatory responses and inflammation-associated diseases in organs," *Oncotarget*, vol. 9, no. 6, pp. 7204–7218, 2018.

[3] J. Zhao, Y. Zhao, W. Zheng, Y. Lu, G. Feng, and S. Yu, "Neuroprotective effect of curcumin on transient focal cerebral ischemia in rats," *Brain Research*, vol. 1229, pp. 224–232, 2008.

[4] X. Zhan, B. Stamova, and F. R. Sharp, "Lipopolysaccharide associates with amyloid plaques, neurons and oligodendrocytes in Alzheimer's disease brain: a review," *Frontiers in Aging Neuroscience*, vol. 10, p. 42, 2018.

[5] J. W. Lee, Y. Lee, D. Yuk et al., "Neuro-inflammation induced by lipopolysaccharide causes cognitive impairment through enhancement of beta-amyloid generation," *Journal of Neuroinflammation*, vol. 5, no. 1, article 1742-2094-5-37, p. 37, 2008.

[6] L. Y. Shi, L. Zhang, H. Li et al., "Protective effects of curcumin on acrolein-induced neurotoxicity in HT22 mouse hippocampal cells," *Pharmacological Reports*, vol. 70, no. 5, pp. 1040–1046, 2018.

[7] S. U. Rehman, A. Ahmad, G. H. Yoon, M. Khan, M. N. Abid, and M. O. Kim, "Inhibition of c-Jun N-terminal kinase protects against brain damage and improves learning and memory after traumatic brain injury in adult mice," *Cerebral Cortex*, vol. 28, no. 8, pp. 2854–2872, 2018.

[8] Y. Ma, B. Ma, Y. Shang et al., "Flavonoid-rich ethanol extract from the leaves of Diospyros kaki attenuates cognitive deficits, amyloid-beta production, oxidative stress, and neuroinflammation in APP/PS1 transgenic mice," *Brain Research*, vol. 1678, pp. 85–93, 2018.

[9] N. Tajuddin, K. H. Moon, S. A. Marshall et al., "Neuroinflammation and neurodegeneration in adult rat brain from binge

ethanol exposure: abrogation by docosahexaenoic acid," *PLoS One*, vol. 9, no. 7, article e101223, 2014.

[10] B. García-Bueno, J. R. Caso, and J. C. Leza, "Stress as a neuroinflammatory condition in brain: damaging and protective mechanisms," *Neuroscience & Biobehavioral Reviews*, vol. 32, no. 6, pp. 1136–1151, 2008.

[11] C. R. A. Batista, G. F. Gomes, E. Candelario-Jalil, B. L. Fiebich, and A. C. P. de Oliveira, "Lipopolysaccharide-induced neuroinflammation as a bridge to understand neurodegeneration," *International Journal of Molecular Sciences*, vol. 20, no. 9, article 2293, 2019.

[12] T. Muhammad, T. Ali, M. Ikram, A. Khan, S. I. Alam, and M. O. Kim, "Melatonin rescue oxidative stress-mediated neuroinflammation/ neurodegeneration and memory impairment in scopolamine-induced amnesia mice model," *Journal of Neuroimmune Pharmacology*, vol. 14, no. 2, pp. 278–294, 2019.

[13] J. H. Han, Y. Lee, J. Im et al., "Astaxanthin ameliorates lipopolysaccharide-induced neuroinflammation, oxidative stress and memory dysfunction through inactivation of the signal transducer and activator of transcription 3 pathway," *Marine Drugs*, vol. 17, no. 2, article md17020123, p. 123, 2019.

[14] A. Khan, M. Ikram, T. Muhammad, J. Park, and M. O. Kim, "Caffeine modulates cadmium-induced oxidative stress, neuroinflammation, and cognitive impairments by regulating Nrf-2/HO-1 in vivo and in vitro," *Journal of Clinical Medicine*, vol. 8, no. 5, p. 680, 2019.

[15] E. S. Chung, Y. C. Chung, E. Bok et al., "Fluoxetine prevents LPS-induced degeneration of nigral dopaminergic neurons by inhibiting microglia-mediated oxidative stress," *Brain Research*, vol. 1363, pp. 143–150, 2010.

[16] B. Lee, I. Shim, and H. Lee, "Gypenosides attenuate lipopolysaccharide-induced neuroinflammation and memory impairment in rats," *Evidence-based Complementary and Alternative Medicine*, vol. 2018, Article ID 4183670, 10 pages, 2018.

[17] B. Uttara, A. Singh, P. Zamboni, and R. Mahajan, "Oxidative stress and neurodegenerative diseases: a review of upstream and downstream antioxidant therapeutic options," *Current Neuropharmacology*, vol. 7, no. 1, pp. 65–74, 2009.

[18] M. Nakayama, M. Aihara, Y.-N. Chen, M. Araie, K. Tomita-Yokotani, and T. Iwashina, "Neuroprotective effects of flavonoids on hypoxia-, glutamate-, and oxidative stress–induced retinal ganglion cell death," *Molecular Vision*, vol. 17, p. 1784, 2011.

[19] A. Wu, Z. Ying, and F. Gomez-Pinilla, "Dietary curcumin counteracts the outcome of traumatic brain injury on oxidative stress, synaptic plasticity, and cognition," *Experimental Neurology*, vol. 197, no. 2, pp. 309–317, 2006.

[20] C. Forni, F. Facchiano, M. Bartoli et al., "Beneficial role of phytochemicals on oxidative stress and age-related diseases," *BioMed Research International*, vol. 2019, Article ID 8748253, 16 pages, 2019.

[21] H.-L. Hsieh and C.-M. Yang, "Role of redox signaling in neuroinflammation and neurodegenerative diseases," *BioMed Research International*, vol. 2013, Article ID 484613, 18 pages, 2013.

[22] Y. He, Y. Yue, X. Zheng, K. Zhang, S. Chen, and Z. du, "Curcumin, inflammation, and chronic diseases: how are they linked?," *Molecules*, vol. 20, no. 5, pp. 9183–9213, 2015.

[23] A. H. Rahmani, M. A. Alsahli, S. M. Aly, M. A. Khan, and Y. H. Aldebasi, "Role of curcumin in disease prevention and treatment," *Advanced Biomedical Research*, vol. 7, no. 1, p. 38, 2018.

[24] D. K. Choi, S. Koppula, and K. Suk, "Inhibitors of microglial neurotoxicity: focus on natural products," *Molecules*, vol. 16, no. 2, pp. 1021–1043, 2011.

[25] M. Venigalla, E. Gyengesi, and G. Münch, "Curcumin and Apigenin–novel and promising therapeutics against chronic neuroinflammation in Alzheimer's disease," *Neural Regeneration Research*, vol. 10, no. 8, pp. 1181–1185, 2015.

[26] B. Huang, J. Liu, T. Meng et al., "Polydatin prevents lipopolysaccharide (LPS)-induced Parkinson's disease via regulation of the AKT/GSK3β-Nrf2/NF-κB signaling axis," *Frontiers in Immunology*, vol. 9, p. 2527, 2018.

[27] A. Keskin-Aktan, K. G. Akbulut, Ç. Yazici-Mutlu, G. Sonugur, M. Ocal, and H. Akbulut, "The effects of melatonin and curcumin on the expression of SIRT2, Bcl-2 and Bax in the hippocampus of adult rats," *Brain Research Bulletin*, vol. 137, pp. 306–310, 2018.

[28] R. Pluta, M. Ulamek-Koziol, and S. J. Czuczwar, "Neuroprotective and neurological/cognitive enhancement effects of curcumin after brain ischemia injury with Alzheimer's disease phenotype," *International Journal of Molecular Sciences*, vol. 19, no. 12, p. 4002, 2018.

[29] Y. H. Zhang, H. Chen, Y. Chen et al., "Activated microglia contribute to neuronal apoptosis in toxoplasmic encephalitis," *Parasites & Vectors*, vol. 7, no. 1, p. 372, 2014.

[30] Y. F. Ji, D. Wang, Y. R. Liu, X. R. Ma, H. Lu, and B. A. Zhang, "MicroRNA-132 attenuates LPS-induced inflammatory injury by targeting TRAF6 in neuronal cell line HT-22," *Journal of Cellular Biochemistry*, vol. 119, no. 7, pp. 5528–5537, 2018.

[31] D. M. Sama and C. M. Norris, "Calcium dysregulation and neuroinflammation: discrete and integrated mechanisms for age-related synaptic dysfunction," *Ageing Research Reviews*, vol. 12, no. 4, pp. 982–995, 2013.

[32] E. Tonnies and E. Trushina, "Oxidative stress, synaptic dysfunction, and Alzheimer's disease," *Journal of Alzheimer's Disease*, vol. 57, no. 4, pp. 1105–1121, 2017.

[33] J. Park, J. S. Min, B. Kim et al., "Mitochondrial ROS govern the LPS-induced pro-inflammatory response in microglia cells by regulating MAPK and NF-κB pathways," *Neuroscience Letters*, vol. 584, pp. 191–196, 2015.

[34] T. Wang, L. Qin, B. Liu et al., "Role of reactive oxygen species in LPS-induced production of prostaglandin E2 in microglia," *Journal of Neurochemistry*, vol. 88, no. 4, pp. 939–947, 2004.

[35] A. Zaky, M. Mahmoud, D. Awad, B. M. El Sabaa, K. M. Kandeel, and A. R. Bassiouny, "Valproic acid potentiates curcumin-mediated neuroprotection in lipopolysaccharide induced rats," *Frontiers in Cellular Neuroscience*, vol. 8, p. 337, 2014.

[36] A. Anaeigoudari, M. N. Shafei, M. Soukhtanloo et al., "Lipopolysaccharide-induced memory impairment in rats is preventable using 7-nitroindazole," *Arquivos de Neuro-Psiquiatria*, vol. 73, no. 9, pp. 784–790, 2015.

[37] M. S. Bitar, A. K. Ayed, S. M. Abdel-Halim, E. R. Isenovic, and F. al-Mulla, "Inflammation and apoptosis in aortic tissues of aged type II diabetes: amelioration with α-lipoic acid through phosphatidylinositol 3-kinase/Akt- dependent mechanism," *Life Sciences*, vol. 86, no. 23-24, pp. 844–853, 2010.

[38] D. K. Dang, E. J. Shin, Y. Nam et al., "Apocynin prevents mitochondrial burdens, microglial activation, and pro-apoptosis induced by a toxic dose of methamphetamine in the striatum of mice via inhibition of p47phox activation by ERK," *Journal of Neuroinflammation*, vol. 13, no. 1, p. 12, 2016.

[39] G. M. Cole, B. Teter, and S. A. Frautschy, "Neuroprotective effects of curcumin," *Advances in Experimental Medicine and Biology*, vol. 595, pp. 197–212, 2007.

[40] L. Zhao, Q. Gu, L. Xiang et al., "Curcumin inhibits apoptosis by modulating Bax/Bcl-2 expression and alleviates oxidative stress in testes of streptozotocin-induced diabetic rats," *Therapeutics and Clinical Risk Management*, vol. Volume 13, pp. 1099–1105, 2017.

[41] C. Fan, Q. Song, P. Wang, Y. Li, M. Yang, and S. Y. Yu, "Neuroprotective effects of curcumin on IL-1β-induced neuronal apoptosis and depression-like behaviors caused by chronic stress in rats," *Frontiers in Cellular Neuroscience*, vol. 12, p. 516, 2018.

[42] H. Ogiwara, A. Ui, B. Shiotani, L. Zou, A. Yasui, and T. Kohno, "Curcumin suppresses multiple DNA damage response pathways and has potency as a sensitizer to PARP inhibitor," *Carcinogenesis*, vol. 34, no. 11, pp. 2486–2497, 2013.

[43] R. Zakaria, W. M. Wan Yaacob, Z. Othman, I. Long, A. H. Ahmad, and B. al-Rahbi, "Lipopolysaccharide-induced memory impairment in rats: a model of Alzheimer's disease," *Physiological Research*, vol. 66, no. 4, pp. 553–565, 2017.

[44] T. Muhammad, M. Ikram, R. Ullah, S. Rehman, and M. Kim, "Hesperetin, a citrus flavonoid, attenuates LPS-induced neuroinflammation, apoptosis and memory impairments by modulating TLR4/NF-κB signaling," *Nutrients*, vol. 11, no. 3, p. 648, 2019.

[45] A. Ataie, M. Sabetkasaei, A. Haghparast, A. H. Moghaddam, and B. Kazeminejad, "Neuroprotective effects of the polyphenolic antioxidant agent, curcumin, against homocysteine-induced cognitive impairment and oxidative stress in the rat," *Pharmacology, Biochemistry, and Behavior*, vol. 96, no. 4, pp. 378–385, 2010.

[46] L. Zhang, X. Ding, Z. Wu, M. Wang, and M. Tian, "Curcumin alleviates pain and improves cognitive impairment in a rat model of cobra venom-induced trigeminal neuralgia," *Journal of Pain Research*, vol. Volume 11, pp. 1095–1104, 2018.

Hindawi
Oxidative Medicine and Cellular Longevity
Volume 2019, Article ID 8416105, 13 pages
https://doi.org/10.1155/2019/8416105

Research Article

Sailuotong Capsule Prevents the Cerebral Ischaemia-Induced Neuroinflammation and Impairment of Recognition Memory through Inhibition of LCN2 Expression

Yehao Zhang,[1] **Jianxun Liu**,[1,2] **Mingjiang Yao**,[1] **WenTing Song**,[1] **Yongqiu Zheng**,[1] **Li Xu**,[1] **Mingqian Sun**,[1] **Bin Yang**,[1] **Alan Bensoussan**,[2] **Dennis Chang**,[2] **and Hao Li**[1]

[1]*Institute of Basic Medical Sciences of Xiyuan Hospital, China Academy of Chinese Medical Sciences, Beijing Key Laboratory of Pharmacology of Chinese Materia, Beijing 100091, China*
[2]*NICM, Western Sydney University, Penrith, NSW 2751, Australia*

Correspondence should be addressed to Jianxun Liu; liujx0324@sina.com and Hao Li; xyhplihao1965@126.com

Received 29 January 2019; Revised 27 March 2019; Accepted 4 May 2019; Published 3 September 2019

Guest Editor: João C. M. Barreira

Background. Astrogliosis can result in astrocytes with hypertrophic morphology after injury, indicated by extended processes and swollen cell bodies. Lipocalin-2 (LCN2), a secreted glycoprotein belonging to the lipocalin superfamily, has been reported to play a detrimental role in ischaemic brains and neurodegenerative diseases. Sailuotong (SLT) capsule is a standardized three-herb preparation composed of ginseng, ginkgo, and saffron for the treatment of vascular dementia. Although recent clinical trials have demonstrated the beneficial effect of SLT on vascular dementia, its potential cellular mechanism has not been fully explored. *Methods*. Male adult Sprague-Dawley (SD) rats were subjected to microsphere-embolized cerebral ischaemia. Immunostaining and Western blotting were performed to assess astrocytic reaction. Human astrocytes exposed to oxygen-glucose deprivation (OGD) were used to elucidate the effects of SLT-induced inflammation and astrocytic reaction. *Results*. A memory recovery effect was found to be associated with the cerebral ischaemia-induced expression of inflammatory proteins and the suppression of LCN2 expression in the brain. Additionally, SLT reduced the astrocytic reaction, LCN2 expression, and the phosphorylation of STAT3 and JAK2. For *in vitro* experiments, OGD-induced expression of inflammation and LCN2 was also decreased in human astrocyte by the SLT treatment. Moreover, LCN2 overexpression significantly enhanced the above effects. SLT downregulated these effects that were enhanced by LCN2 overexpression. *Conclusions*. SLT mediates neuroinflammation, thereby protecting against ischaemic brain injury by inhibiting astrogliosis and suppressing neuroinflammation via the LCN2-JAK2/STAT3 pathway, providing a new idea for the treatment strategy of ischaemic stroke.

1. Introduction

The incidence of stroke around the world has reached epidemic levels. In the past two decades, there have been marked increases in strokes, the number of living stroke victims, the population-level loss of life (called disability-adjusted life years or DALYs), and the number of deaths related to strokes [1]. Lasting physical debility and cognitive deterioration are experienced by most stroke survivors [2]. Stroke patients, who endure an acute period of infarction, must then cope with ongoing neuroinflammation and the associated neurological impairment. Inflammation is a serious aspect of the disease development of ischaemic stroke and other types of ischaemic brain injury. These injuries are caused by a decrease in blood circulation, followed by the activation of intravascular leukocytes and the concomitant release of inflammatory cytokines from the ischaemic brain parenchyma and endothelium, all of which have the potential to increase the damage to central nervous system (CNS) tissues [3].

The CNS contains many resident cells that originate from nerve epithelial cells, collectively known as neuroglia. Neuroglial cell subtypes include astrocytes, oligodendrocytes, and polyglia [4]. Astrocytes actively maintain the immune

response following CNS ischaemia through the production of complement components, inflammatory mediators such as interleukin- (IL-) 6 and IL-1β, and chemokines, including C-X-C motif chemokine ligand 12 (CXCL12), CXCL1, CXCL10, monocyte chemoattractant protein (MCP)-1, and lipocalin-2 (LCN2) [5, 6]. After prolonged activation, reactive astrocytosis (also called astrogliosis) results in a structure called a glial scar, which is the demarcation line between an ischaemic core and the healthy surrounding brain tissue [7]. Activated astrocytes release the glycoprotein LCN2, which mediates certain biological processes, including cell death [8], cell migration [9], and innate immunity [10]. Recent studies have indicated that brain injury or infection can result in neuroinflammation that may encourage the release of LCN2 from astrocytes [11, 12]. Similarly, studies have also shown that continuing and disproportionate immune responses can exacerbate the secretion of inflammatory cytokines, such as LCN2, with a subsequent aggravation of neural inequity in the hippocampus, leading to long-term behavioural impairments [13, 14]. Therefore, targeting astrocytic LCN2 may be a prospective molecule-level therapy for clinicians treating inflammatory CNS impairments.

The use of herbal medicine to treat cerebrovascular diseases in Asia has persisted for centuries. The Sailuotong (SLT) capsule is a standardized herb preparation composed of *Panax ginseng* (ginseng), *Ginkgo biloba* (ginkgo), and *Crocus sativus* (saffron) in three specific doses that is used to treat vascular dementia (VaD) [15]. Each of these herbal components have been proven to avert and/or treat circulatory diseases such as hypertension and stroke. For example, a standardized extract of *G. biloba* (EGB 761) has antioxidant and antiplatelet characteristics and can reduce cerebral ischaemic injury [16–20]. Other studies have shown that the ginsenosides Rg1, Rb1, and Rg2 have neuroprotective effects [21–24].

Although the most recent clinical study showed that SLT improves cognition and surveillance in patients [25], and many preclinical studies have demonstrated a cerebrovascular protective effect of its single components, the mechanism by which SLT regulates astrocyte activities through its anti-inflammatory effects has not been previously studied. Here, we investigated two questions: does SLT treatment alleviate reactive astrocytes and, thus, mediate neuroinflammation, and if so, does the benefit of SLT treatment involve the inhibition of Janus kinase-2 (JAK2) signal transducer and activator of transcription-3- (STAT3-) mediated LCN2 expression?

2. Materials and Methods

2.1. Rat Model of Microsphere-Induced Cerebral Embolism. Adult male Sprague-Dawley rats (weighing 220–250 g) were used in this study (Beijing Vital River Laboratory Animal Technology Co. Ltd., Beijing, China). The animal protocols were carried out according to the recommendations of the Chinese Academy of Medical Sciences Committee for Experimental Animal Use and Care. The procedures used were designed to reduce or diminish the quantity and discomfort of the animals tested. All rats were kept on a 12-hour light/dark cycle in standard conditions ($23 \pm 1^{\circ}$C and $55 \pm 5\%$ humidity) with access to water and food *ad libitum*.

Forty-six adult SD rats were arbitrarily separated into four groups. Cerebral embolism was induced using the microsphere method as previously described [20]. In short, the rats were anaesthetized with chloral hydrate (40 mg/kg), and the common carotid artery, internal carotid artery, and right external carotid were separated using forceps. The common carotid artery was clipped with an artery clamp, and the distal end of the external carotid artery was ligated with a thread. Fluorescence microspheres (106–212 μm in diameter, UVPMS-BY2, Cospheric, USA) were injected into the external carotid artery with a syringe, and the artery clamp was simultaneously released, allowing the microspheres to travel to the various arteries of the brain and cause embolisms. The proximal end of the external carotid artery was then ligated with a thread, and the wound was sutured layer by layer. In the control group, rats received the same amount of serum without microspheres.

2.2. Drug Administration. SLT was supplied by the Shineway Pharmaceutical Group (Shijiazhuang, China). Extracts of ginseng (20170301, Panax ginseng C.A. Meyer), ginkgo (20170122, Ginkgo biloba L.), and saffron (20170320, Crocus sativus L.) were prepared in a Good Manufacturing Practice-certified facility (Shineway Pharmaceutical Group, Hebei, China). Ultraviolet (UV) spectroscopy or HPLC-UV was used to measure the composition of ingredients to regulate the quality of the ingredients. The readings showed that 77% of the total ginsenosides were found in the ginseng extract (UV), with ginsenoside Rg1, Re, and Rb1 present at 5.5%, 3.2%, and 13.1%, respectively (HPLC-UV); 49% of the total flavones were found in the extract (UV); 28.7% of the total glycosides were found in the extract, including aglycone of quercetin, isorhamnetin, and kaempferol (HPLC-UV); 11.6% of the total ginkgolides A, B, and C, and bilobalide, were found in the ginkgo extract, with 3.3% of ginkgolide A (HPLC-UV) among them; and 65% of the total crocins were found in the saffron extract (UV), including 27% of crocin-1 (HPLC-UV) [26]. SLT was prepared from the above three extracts to a specific formulation and was then administered intragastrically at doses of 16.5 and 33 mg/kg for 28 days. Each rat in the control group and the model group was given an identical volume of saline intragastrically every day.

2.3. Evaluation of Neurological Deficits. Neurological deficit scores were calculated 2 hours and 24 hours after ischaemia in each group using a previously published five-point system [27]. Specifically, a rat that exhibited normal spontaneous movement (without obvious neurological defects) received a 0, a rat that could not fully extend its right paw received a 1, a rat that circled clockwise received a 2, a rat that fell to the right received a 3, and a rat that could not walk received a 4. The deficit scores were assigned by an investigator who was unaware of the groups.

2.4. Morris Water Maze (MWM) Test. The MWM was used to evaluate three-dimensional spatial memory and learning

in all four groups of rats [28]. The water maze was a circular pool (330 cm in diameter and 60 cm high containing water at a depth of 45 cm at 22°C ± 1°C). A nontoxic black ink was introduced to make the water opaque. The pool was divided into equal quadrants, each containing four points (north, east, south, and west). A round platform (10 cm in diameter) was painted black and hidden by being submerged 1.5 cm in the southwest quadrant. The location of the training platform remained unchanged during the experiment. The swimming paths of the rats were recorded with digital imaging equipment.

2.5. Measurement of Cerebral Infarction. For the evaluation of the success of the cerebral ischaemia model, the rats were anaesthetized with chloral hydrate (40 mg/kg) twenty-four hours after surgery ($n = 3$ in the control and test groups). Blood was taken from the abdominal aorta before decapitation and the quick removal of the brain. The brains were stored in a cold, oxygenated physiological salt solution. Coronal slices (1 mm) were attained and fixed for 10 min in prewarmed 2% triphenyltetrazolium chloride (TTC). The slices were then fixed for 30 min in 10% paraformaldehyde.

2.6. Culture and Transfection of Human Astrocytes. Human astrocytes (ScienCell Research Laboratories, CA, USA) were cultured in astrocyte media (AM) (ScienCell, USA) in a humidified, 5% CO_2 atmosphere at 37°C. After cells reached 70% confluence, the astrocytes were stably transfected using the LCN2 gene expression vector (EX-m0282-Lv201), the control expression vector (EX-NEG-Lv201), and 7.5 μl/ml of the lentiviral vector (LPP-m0282-Lv201-100) (GeneCopoeia, Rockville, USA) for 24 hours. Following transfection, the cells were kept in fresh AM without the lentiviral vector for 48 hours.

2.7. Oxygen-Glucose Deprivation (OGD) Management and Treatment. OGD experiments were performed as based on a previous method [20]. After purification and transfection, the cells were placed in a premixed gas (94% N_2, 5% CO_2, and 1% O_2) culture box and cultured in deoxygenated DMEM without glucose and fetal bovine serum (FBS) for 6 hours. After 6 hours, normal AM with 10% FBS serum was given, and cells were transferred to an atmosphere incubator for 12 hours. The control group cells were cultured with normal AM. During OGD stimulation, cells were treated for 6 hours with 2.5, 5, or 10 mg/l SLT.

2.8. Western Blotting. Protein was extracted from the ischaemic penumbra with RIPA buffer (Beyotime Biotechnology, Shanghai, China) 28 days after cerebral ischaemia and combined with a protease and phosphatase inhibitor cocktail (MCE, New Jersey, USA). The tissue was cut into fine fragments, completely homogenized with a sonifier, and then centrifuged (10000-14000 g, 3-5 min), and the supernatant was collected for subsequent experiments. Protein of equivalent molecular weight was loaded into SDS-PAGE gel wells and transferred from the gel to polyvinylidene difluoride (PVDF) membranes. Nonspecific sites were blocked for 60 min with 5% bovine serum albumin (BSA) in TBST buffer, and the blots were then incubated overnight at 4°C with antibodies against LCN2 (Abcam, 1 : 2000 dilution), phosphorylated- (p-) JAK2 (Tyr1007/1008) (Abcam, 1 : 1000), glial fibrillary acidic protein (GFAP; Proteintech, 1 : 2000), JAK2 (Abcam, 1 : 2000), p-STAT3 (Tyr705) (Cell Signaling Technology, 1 : 2000), STAT3 (Cell Signaling Technology, 1 : 2000), and β-actin (Sigma, 1 : 5000) in TBST. Antibody binding was detected with anti-rabbit horseradish peroxidase- (HRP-) conjugated immunoglobulin G (IgG; 1 : 1000) in TBST (60 min, room temperature). The reaction bands were detected using the ECL detection reagent per the manufacturer's instructions (Thermo Fisher Scientific, MA, USA). The extraction procedure for cell protein was the same as the above steps.

2.9. Immunofluorescence Analysis and Hematoxylin-Eosin (HE) Staining. The brains were dissected and fixed in paraffin. Coronal cryostat sections (20 μm) were stained with HE and immunofluorescent dyes. Brain sections were fixed at 4°C for 24 hours in 4% paraformaldehyde in PBS (0.01 M, pH 7.4), dehydrated in a series of graded alcohol dehydrations, and fixed in paraffin. The tissues were sectioned (5 μm) with a Leica® RM1850 rotary microtome (Leica Microsystems, Germany). The paraffin sections were dried at 60°C, dewaxed, and subjected to antigen retrieval. The sections were exposed for 1 hour at 37°C to primary antibodies targeting the following proteins: LCN2 (Abcam, 1 : 200), GFAP (Proteintech, 1 : 200), p-JAK2 (Tyr1007/1008) (Abcam, 1 : 100), and p-STAT3 (Tyr705) (Cell Signaling Technology, 1 : 200). The sections were washed twice with ice-cold PBS and then saturated with fluorescent secondary antibodies (Cell Signaling Technology, 1 : 100) in the dark for 1 hour. DAPI (4′,6-diamidino-2-phenylindole) (1 : 1000) was added in the dark for 2 min. The DAPI was rinsed 3 times with PBS for 1 min. The staining procedure for the cells was the same as above. For HE staining, sections were stained with alum HE. Colour images were obtained using a 20x laser scanning confocal microscope (Olympus FV1200, Tokyo, Japan).

2.10. Determination of Chemokine/Cytokine Expression in Brain Extracts, Serum Samples, and Astrocytes. A MILLIPLEX® MAP Rat Cytokine/Chemokine Magnetic Bead kit (Millipore, USA) was used per the manufacturer's instructions to quantify the concentrations of chemokines and cytokines in the cerebral hemisphere extracts, serum samples, and astrocytes. The protein cerebral hemisphere of concentration was quantitated by the BCA protein assay (Invitrogen). The protein concentration was quantified to 16 mg/ml. The chemokines and cytokines in ischaemic penumbra tissues were collected 28 days after cerebral ischaemia in EMD Millipore's buffer. Blood serum was collected from the abdominal aorta. The chemokines and cytokines from astrocytes that had been conditioned in medium were collected after OGD induction. The following cytokines were analysed: tumor necrosis factor-α (TNF-α), IL-1α, IL-1β, IL-12, and IL-6 and the chemokine CXCL10 (IP-10). A FLEXMAP 3D™ system was used to determine the median fluorescence intensity. The cytokine and chemokine levels in brain homogenates, serum samples, and cell samples were subjected to five-parameter logistic analysis.

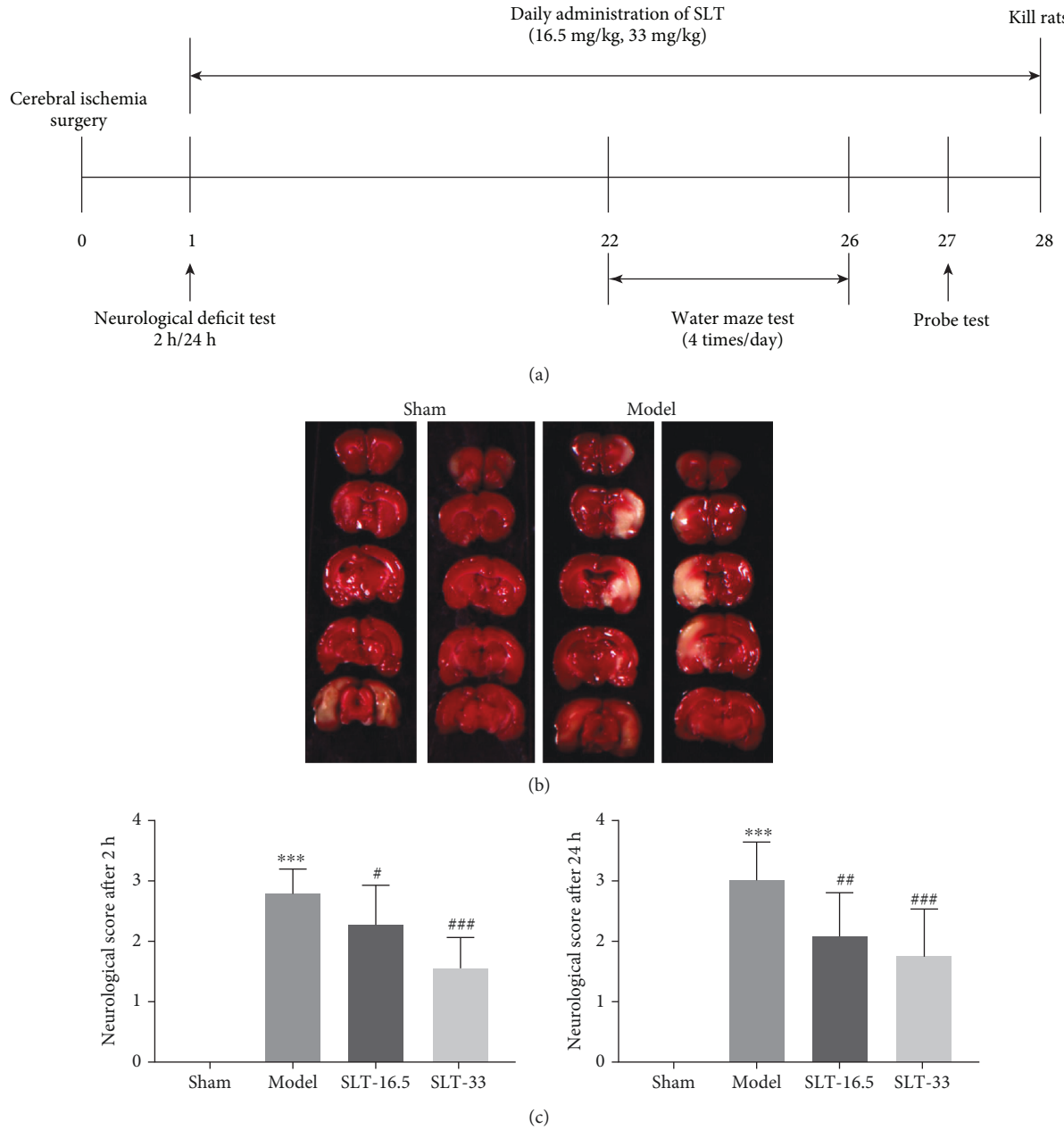

Figure 1: SLT treatment reduced ischaemic infarct volume in the cerebral ischaemia model. (a) Timeline depicts the treatment of SLT and assessments of the cognitive functions of rats. The male rats ($n = 10$) were orally treated with SLT at a daily dose of 16.5 mg/kg and 33 mg/kg for 4 weeks. After surgery for 22 days, memory tests were conducted. The training trial was performed four times a day for 5 days. (b) Cerebral infarct volume was assessed via TTC staining 24 h after cerebral ischaemia. Neurological score (c) of rats after cerebral ischaemia was assessed using a five-point scale system. Data are expressed as the mean ± SEM ($n = 10$). $^{***}P < 0.001$ vs. sham group; $^{\#}P < 0.05$, $^{\#\#}P < 0.01$, and $^{\#\#\#}P < 0.001$ vs. the model groups.

2.11. Statistical Analyses. Data management and analysis were performed using GraphPad Prism software (San Diego, CA). All data are reported as the means ± SD. Each experiment was repeated three times. Univariate analysis of variance (ANOVA) was used for multiple comparisons. Student's t-test was conducted to analyse intergroup comparisons. Two-way ANOVA was used in the neurologic study and MWM test to compare the time functions between groups. P values of <0.05 were reported as statistically significant.

3. Results

3.1. Protection from Cerebral Ischaemia-Induced Brain Injury. SLT was intragastrically administered for 28 days. Cerebral infarction volume was measured by the TTC method 24 hours after surgery. The resulting neurological deficit scores were indicative of protective capabilities of SLT. In comparison to the cerebral ischaemia group, the SLT-16.5 (16.5 mg/kg, daily) and SLT-33 (33 mg/kg, daily) groups showed significantly lower scores ($P < 0.05$).

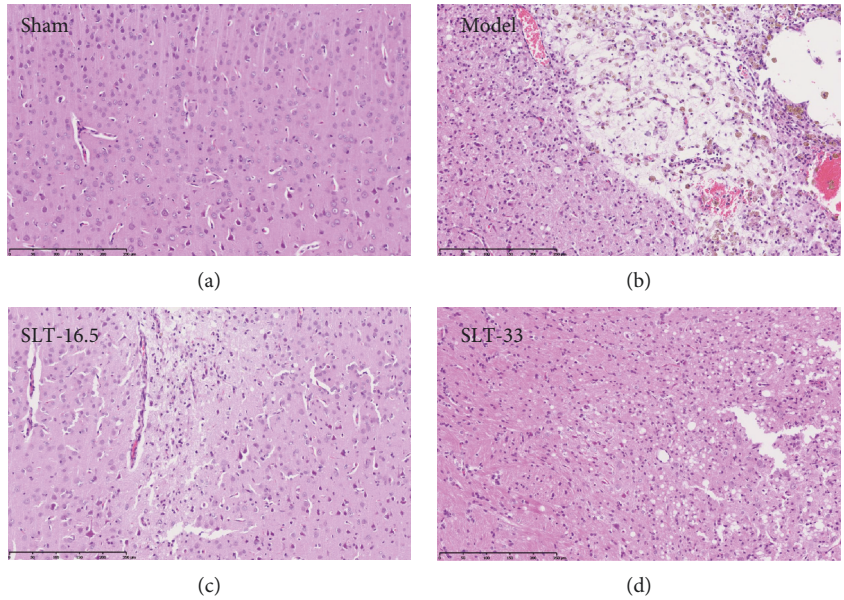

Figure 2: The ischaemic penumbra area in the box was assessed for neuronal apoptosis using HE staining. Cortex sections and hippocampal regions stained with HE presented with neuronal loss and signs of cerebral edema, and swollen cells were observed in the ipsilateral hippocampus; plentiful apoptotic neurons were observed with karyopyknosis, cell gaps, and debris. SLT (33 mg/kg, daily) significantly alleviated the symptoms of apoptosis in a dose-dependent manner.

Additionally, the score in the SLT-33 group was less than that in the SLT-16.5 group. The scores for all groups at 2 and 24 hours after surgery and the incidence of cerebral ischaemia are shown in Figure 1(c). The surgery model functioned as expected, as rats with induced cerebral ischaemia displayed obvious cerebral infarctions, whereas rats in the control group showed no signs of cerebral injury.

Figures 1(a) and 1(b) show the infarct volume of the control and test groups at 24 hours after cerebral ischaemia. The striatum, hippocampus, and cortex showed extensive lesions in the model group, whereas those brain regions in the SLT group (33 mg/kg) showed significant differences from those in the model group, in agreement with the neurological deficit scores.

3.2. SLT Reduces Brain Damage after Surgery. Twenty-eight days after surgery, HE staining identified histological deviations in brain tissues (Figure 2). The neurons in the control group were arranged in an orderly manner with round cells, pale stained nuclei, clear nuclear membranes, and clear nucleoli. No degeneration, necrosis, or other lesions were observed. In the model group, focal infarction areas were observed in the cortex, hippocampus, and white matter, with large infarction foci and no necrotic material absorption. Histiocyte (foam cell) and nerve cell degeneration were obvious. The number and size of infarcts in the SLT group were significantly lower than those in the model group. Necrosis in the infarcts of the SLT group was not obvious, and necrotic substances were absorbed. The SLT group exhibited no obvious nerve cell degeneration.

3.3. Effect of SLT on Memory Impairment Induced by Brain Ischaemia in the MWM Test. The MWM was used to measure changes in learning, memory, and strategy in rats and to determine the effects of SLT. After 5 days of training, all rats found the hidden platform. During this training, the mean swimming speed of the rats in each group was comparable, suggesting that all groups had normal sensory-motor functions and survival motivation (Figure 3(a)). With daily training, the escape latency of the SLT-16.5 group and the SLT-33 group decreased significantly more than that of the model group ($P < 0.01$, model group vs. control group; $P < 0.01$, SLT-33 group vs. model group) (Figure 3(b)). During the retrieval trial, memory retention was assessed by calculating the number of platform crossings and time spent in the target quadrant for each rat. The images of the rat trajectories showed there were fewer platform region crossings in the model group than in the control group (Figure 3(e)). However, the SLT-16.5 group and the SLT-33 group showed significantly greater retention than the model group, measured as more platform crossings ($P < 0.001$, model group vs. control group; $P < 0.001$, SLT-33 group vs. model group) (Figure 3(d)). In addition, we found that with larger doses of SLT, rats spent more time in the target quadrant. The time spent in the target quadrant of the SLT-16.5 group and the SLT-33 group was greater than that of the model group and even reached values observed in the control group ($P < 0.001$, model group vs. control group; $P < 0.001$, SLT-33 group vs. model group) (Figure 3(c)). These results suggest that SLT improved situational memory after ischaemic brain injury.

3.4. Effect of SLT on Inflammation Markers. There were significant differences in cytokine levels following surgery. After 28 days, the proinflammatory cytokines IL-6, IL-12, and IL-1α and chemokine CXCL10 (IP-10) were constant in the control group, while they increased in the ipsilateral hemispheres of the model group, with IL-6, IL-12, and CXCL10

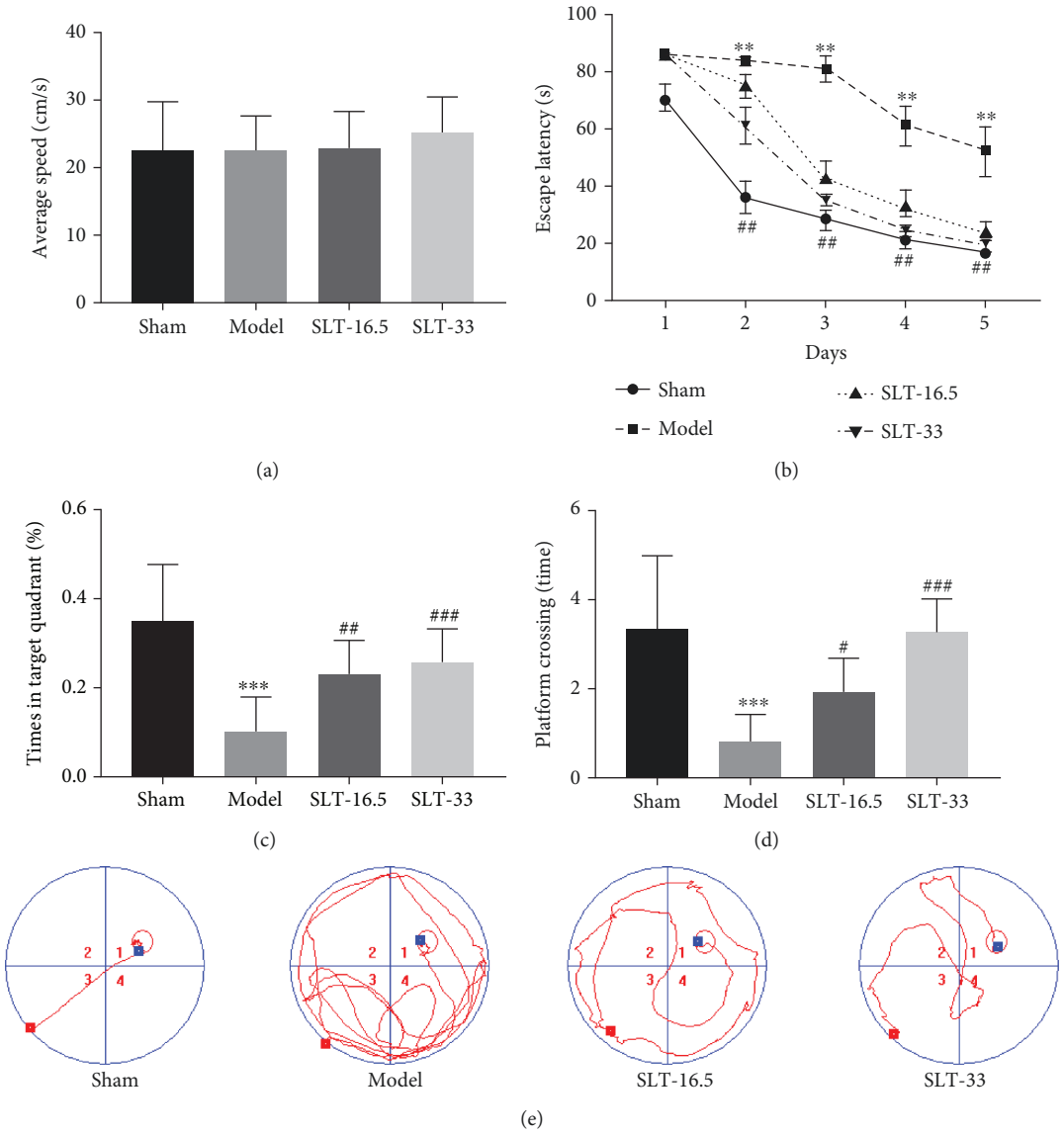

FIGURE 3: Neuroprotective effects of SLT on the Morris water maze (MWM) test: (a) average swimming speed, (b) escape latency, (c) platform crossing, (d) target quadrant time, and (e) trajectory of swimming. Data are expressed as the mean ± SEM ($n = 10$). $^{**}P < 0.01$ and $^{***}P < 0.001$ vs. sham group; $^{\#}P < 0.05$, $^{\#\#}P < 0.01$, and $^{\#\#\#}P < 0.001$ vs. model groups.

showing significant increases ($P < 0.001$). However, these cytokine levels were significantly and dose-dependently reduced by SLT treatment ($P < 0.05$, SLT-33 group vs. model group; $P < 0.01$, SLT-33 group vs. model group) (Figures 4(a)–4(c)). In addition, the same results were found in the serum. Further analysis showed that the levels of IL-1α, IL-12, and CXCL10 in the model group were above those in the control group ($P < 0.05$ for IL-1α, IL-12, and CXCL10) (Figures 4(d)–4(f)). Similarly, the cytokine levels were lower in the SLT-33 group than in the ischaemic group ($P < 0.05$, SLT-33 group vs. model group; $P < 0.01$, SLT-33 group vs. model group).

3.5. SLT Decreases LCN2 Upregulation in a Rodent Model of Cerebral Ischaemia. In an *in vivo* study, SLT was demonstrated to prevent cerebral ischaemia-induced neuroinflammation. We further investigated the anti-inflammatory effects using immunofluorescence microscopy and Western blot analysis. Intragastric administration of SLT for 28 days reduced LCN2 secretion due to cerebral ischaemia. The analyses of GFAP and LCN2 were quantified and presented in their relative ratios to β-actin expression, and the p-JAK2 and p-STAT3 were quantified in total JAK2 and STAT3 expression. LCN2 and GFAP immunofluorescence staining showed that LCN2 protein expression was induced in GFAP-positive astrocytes, and the rats with cerebral ischaemia had more cortical astrocytes than rats in the control group (Figure 5). Nevertheless, immunostaining showing that SLT (33 mg/kg) repressed astrocytes in the ischaemic hemispheres. The p-STAT3 and p-JAK2 staining

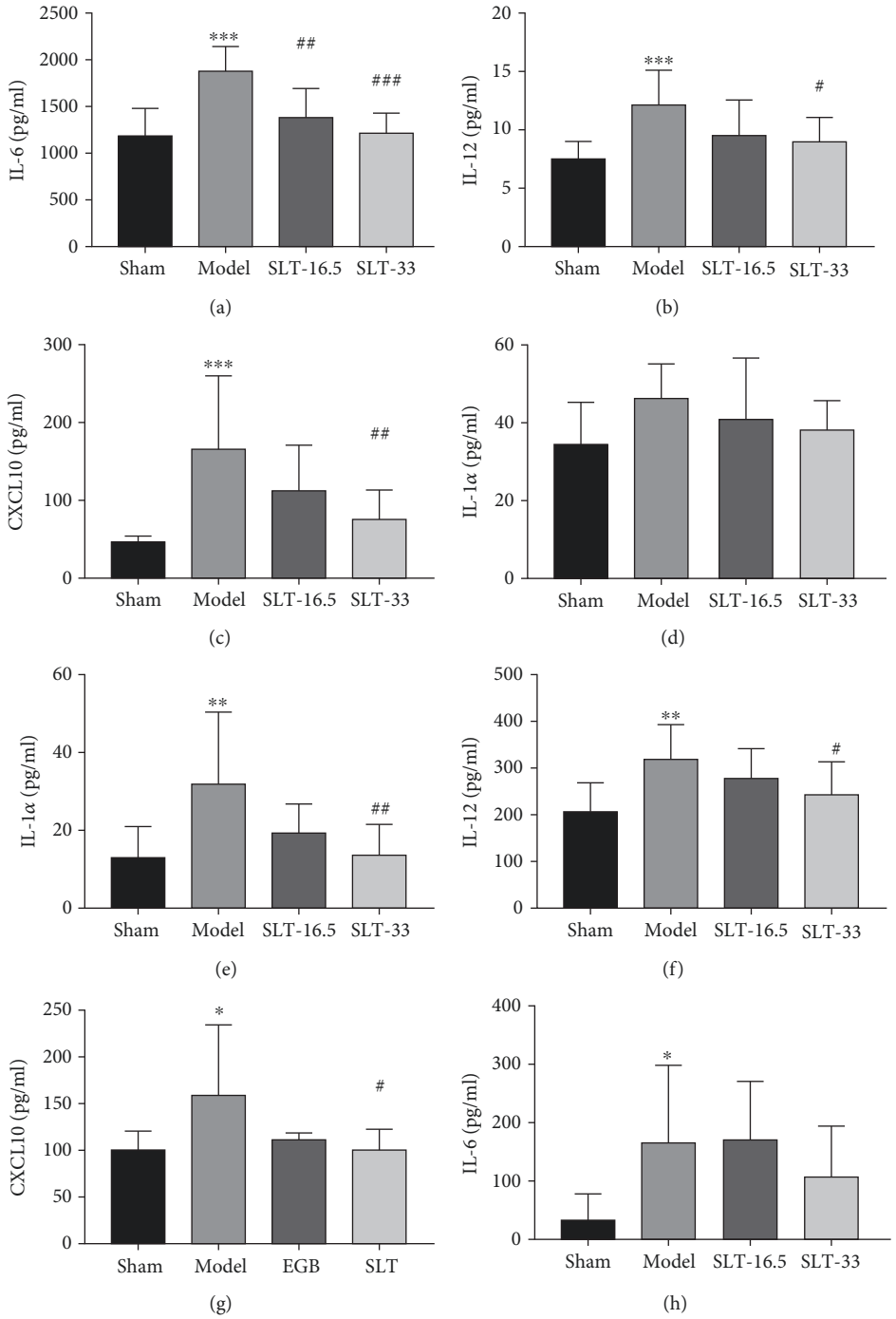

Figure 4: Effects of SLT treatment on the level of cytokines/chemokines in the brain after cerebral ischaemia. (a–f) Analysis showing the relative levels of the proinflammatory mediators IL-1α, IL-6, IL-12, and CXCL10 (IP-10) in the brain and in serum; (a–d) was in the brain; (e–h) was in serum. Data are expressed as the mean ± SEM ($n = 5$). $^{*}P < 0.05$, $^{**}P < 0.01$, and $^{***}P < 0.001$ vs. sham group; $^{\#}P < 0.05$, $^{\#\#}P < 0.01$, and $^{\#\#\#}P < 0.001$ vs. the model groups.

in astrocytes was significantly stronger after ischaemia but decreased after SLT treatment (Figures 5(a)–5(c)). The same pattern was observed for GFAP, LCN2, p-STAT3, and p-JAK2 using Western blot analysis (Figures 5(d)–5(h)). Finally, SLT dose-dependently decreased the expression of LCN2, p-STAT3, and p-JAK2 in rats exposed to ischaemia ($P < 0.01$).

3.6. SLT Decreases OGD-Induced Injury in Astrocytes. A CCK8 assay showed that OGD resulted in a significant reduction in cell viability. SLT (3.125~100 mg/l) displayed a dose-dependent toxicity to human astrocytes (CCK8 assay), yet the lower concentrations of SLT (2.5~50 mg/l) reduced the damage caused by OGD. Because the protective effect became apparent at 2.5 mg/l ($P < 0.05$, vs. OGD group), no

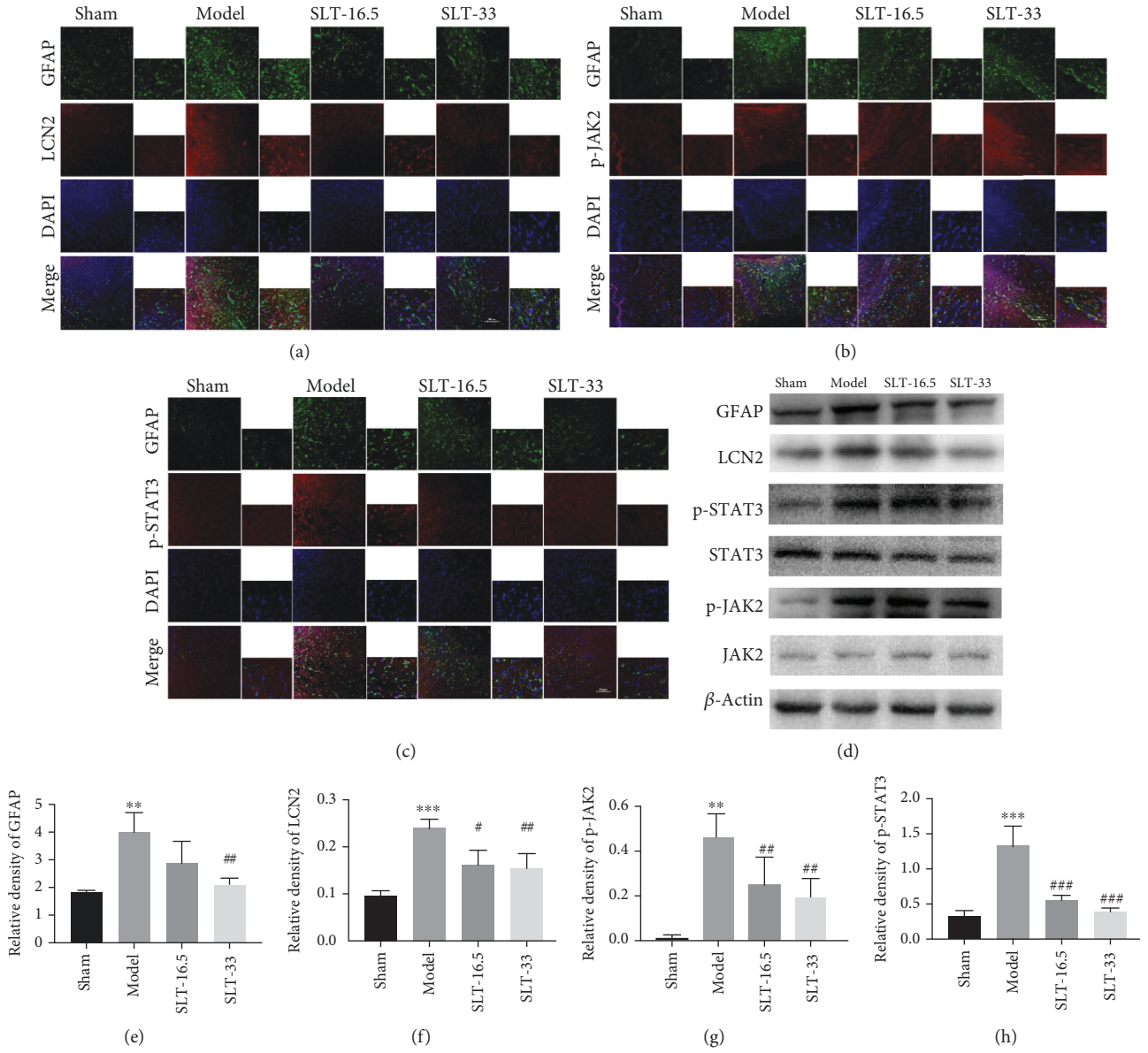

Figure 5: Effects of SLT on the activation of astrocytes and the expression of LCN2, p-JAK2, and p-STAT3, in cerebral ischaemia rats. (a–c) Double immunofluorescence staining for astrocytic LCN2, p-STAT3, p-JAK2, and GFAP expression in the ischaemic penumbra area after cerebral ischaemia. Scale bar = 20 μm. (d–h) Western blots and quantitative analysis of GFAP, LCN2, p-JAK2, and p-STAT3 expression are expressed as the mean ± SEM ($n = 4$). $^{*}P < 0.05$, $^{**}P < 0.01$, and $^{**}P < 0.001$ vs. sham group; $^{\#}P < 0.05$, $^{\#\#}P < 0.01$, and $^{\#\#\#}P < 0.001$ vs. model groups.

higher concentrations were used in the *in vitro* tests (Figure S1).

To further investigate the specific effects of LCN2, human astrocytes were subjected to the expression vector LCN2 by lentiviruses 24 hours before OGD induction. The cells were induced in an OGD environment to imitate ischaemia, and SLT treatment markedly decreased the levels of the proinflammatory cytokines IL-6, IL-1β, and CXCL10 ($P < 0.05$). LCN2 overexpression enhanced this difference ($P < 0.05$, vs. control group) (Figures 6(a)–6(c)).

The morphology of astrocytes was observed by GFAP staining (Figures 7(a)–7(c)). Prolonged cellular protuberances confirmed OGD-induced astrocyte activation, and LCN2 overexpression enhanced this effect. The OGD group showed higher levels of GFAP, LCN2, p-JAK2, and p-STAT3 than the control group ($P < 0.05$, $P < 0.01$) (Figures 7(a)–7(h)), and overexpression of LCN2 enhanced these effects (Figure 7). However, SLT negated these increases after OGD induction ($P < 0.05$, $P < 0.01$).

4. Discussion

High levels of LCN2 trigger inflammation and later reduce cognitive activity, making LCN2 a possible target in anti-inflammation therapies [29, 30]. We have confirmed the efficacy of SLT in regulating reactive astrocytes and LCN2

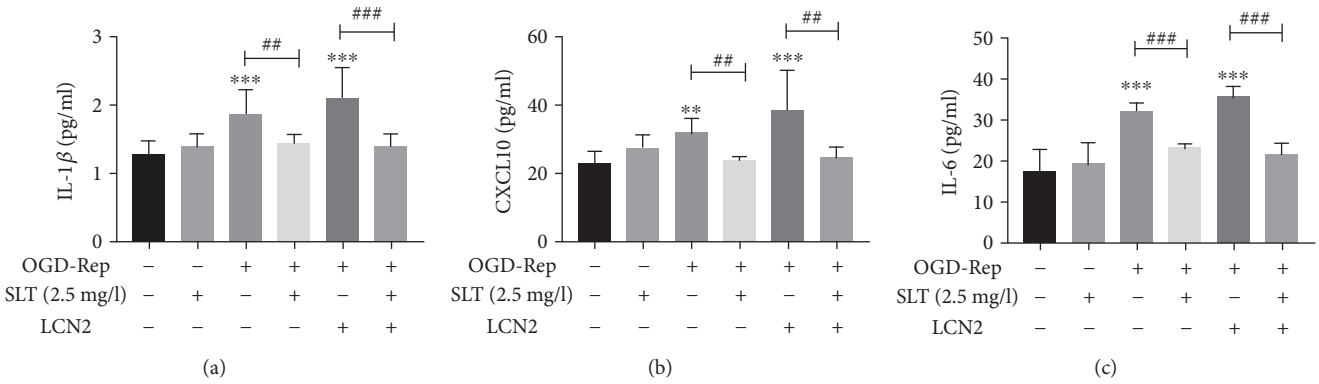

Figure 6: SLT suppressed OGD-induced inflammation in astrocytes in vitro. (a–c) Analysis showing the relative levels of the proinflammatory mediators IL-1β, IL-6, and CXCL10 (IP-10). Data are expressed as the mean ± SEM ($n = 5$). $^{*}P < 0.05$, $^{**}P < 0.01$, and $^{***}P < 0.001$ vs. control group; $^{\#}P < 0.05$, $^{\#\#}P < 0.01$, and $^{\#\#\#}P < 0.001$ vs. the indicated groups.

expression in a cerebral ischaemic model. We found that SLT can protect cognitive function, significantly reducing stroke injury and protecting the cerebral cortex from injury by reducing cerebral infarction volume in ischaemic rats. Furthermore, SLT improves astrocyte activation, reduces STAT3 and JAK2 phosphorylation, and reduces the expression of LCN2 *in vitro* and *in vivo*. These results suggest that SLT plays a powerful therapeutic role in cerebral ischaemia by reducing astrocytic LCN2 release and inhibiting neuroinflammatory injury through the JAK2/STAT3 pathway.

The neuronal inflammation has emerged as a crucial element in stroke, both in the beginning and later stages. Recent reviews have noted that lymphocytes and inflammatory mediators promulgate the development of neurological lesions and deficits, although most of these findings have been from experimental stroke models [31–34]. Other studies have shown that inflammation may also play a role in the aetiology of mild cognitive impairment (MCI) [35, 36]. As mentioned in Introduction, assorted traditional Chinese medicine formulations for the treatment of stroke, such as SLT, have been developed [15]. SLT is composed of ginseng extract (ginseng total saponins), *G. biloba* extract (*G. biloba* total flavonoids), and saffron extract (saffron total glycosides). Pharmacodynamic reports have shown that SLT meaningfully improves problems produced by cerebral ischaemia as well as learning and memory ability in experimental models of cerebral ischaemia. Neurocognitive and cardiovascular functions improved in normal adults after a one-week regime on SLT [15]. Additionally, from 2012 to 2014, an international multicentre phase II clinical trial of SLT use in patients with mild to moderate VaD showed that SLT improved cognition and daily functioning in Chinese patients [25]. SLT reportedly prevents H_2O_2-induced endothelial cell damage via a direct decrease in intracellular reactive oxygen species (ROS) generation and increase in superoxide dismutase (SOD) activity [37]. In our present study, SLT improved cognitive function of cerebral ischaemic model rats in the MWM test. Neurological deficits were also attenuated in cerebral ischaemic rats treated with SLT. Hence, these results provide the first evidence that SLT alleviates memory impairment in animal models.

Proinflammatory cytokines and chemokines are small (8–12 kDa) proteins with numerous purposes. In the CNS, proinflammatory cytokines and chemokines facilitate innate and adaptive immune responses, indicating the need for leukocyte recruitment as well as astrocyte activation during neuroinflammation [38, 39]. Although cytokines/chemokines function by starting the inflammatory response and the recruitment of peripheral immune cells to help remove harmful stimulation, chemokines are involved in certain neurological diseases involving inflammation of nerves, including neurodegenerative dementia, Alzheimer's disease, multiple sclerosis, traumatic brain injury, and certain types of meningitis [40, 41]. In the current study, SLT notably reduced the level of proinflammatory cytokines and chemokines, including IL-6, IL-12, and CXCL10, in tissues adjacent to the damage and in the serum. Additionally, SLT reduced these proinflammatory cytokines and chemokines in the astrocytic supernatant.

Astrogliosis can cause extension of cell processes and swelling of cell bodies after injury. Reactive gliosis has been shown to be sustained for up to 60 days after controlled cortical impact injury in rats, signifying a continuing response of astrocytes to brain injury [42]. However, the lack of effective treatment for astrogliosis has become a focus of clinical treatment. LCN2, a secreted glycoprotein in the lipocalin superfamily, has been reported to play a harmful role in ischaemic brains and neurodegenerative diseases [14, 43–45]. Neuroinflammation due to brain injury or neurodegenerative diseases initiates the secretion of LCN2 from astrocytes, microglia, endothelial cells, and neurons. Inflammatory mediators released by activated astrocytes play an important role in cell migration and the recruitment of glial cells to the injury site. Our data suggest that astrocytes were significantly activated after cerebral ischaemia and that LCN2 was upregulated throughout the cerebral ischaemic cortex. SLT treatment significantly inhibited astrocyte activation and decreased LCN2 expression. The same phenomenon was also found in OGD-induced astrocytes.

Over the years, research into the cellular and molecular pathways related to astrogliosis has provided a basis for future treatment options for memory disorders. LCN2 plays

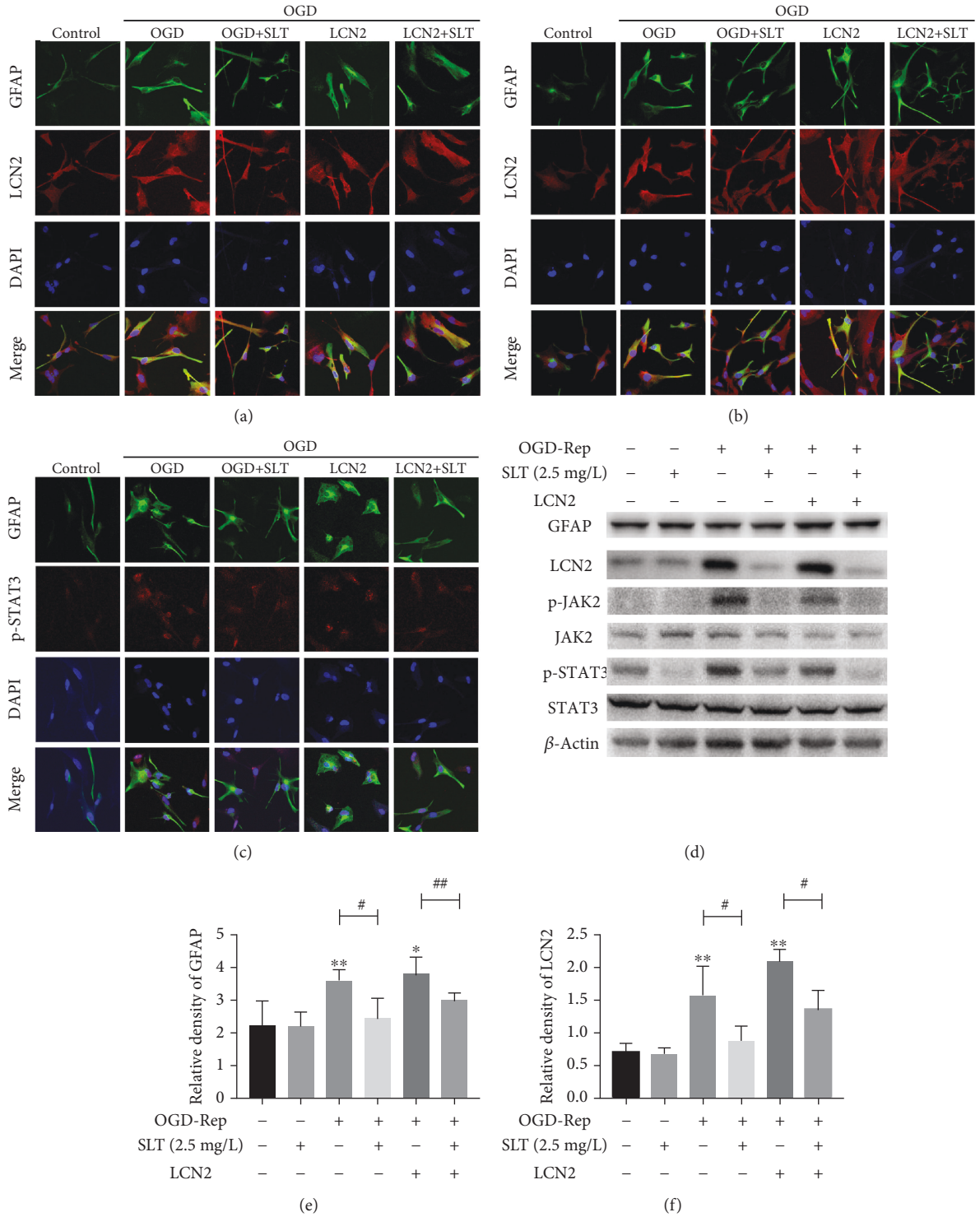

Figure 7: Continued.

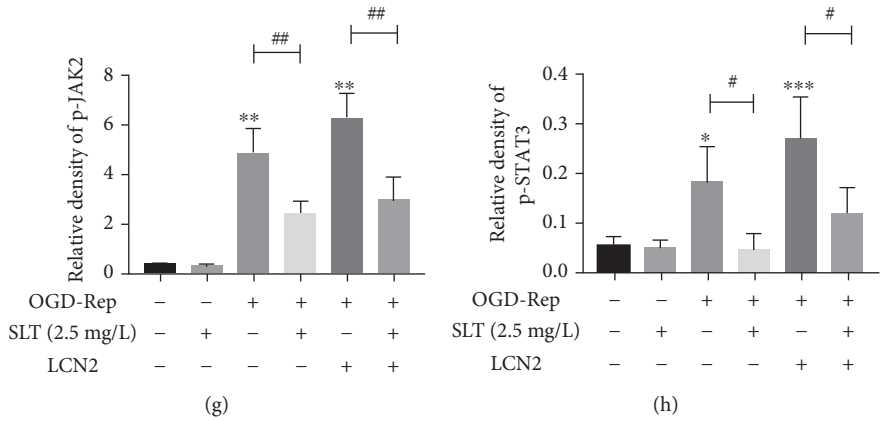

Figure 7: The effects of SLT on the activation of astrocytes and the expression of astrocytic LCN2, p-JAK2, and p-STAT3 after OGD induction in vitro. (a–h) Double immunofluorescence staining for GFAP, LCN2, p-JAK2, and p-STAT3 in astrocytes after OGD induction. Scale bar = 20 μm. Western blots and quantitative analysis of GFAP, LCN2, p-JAK2, and p-STAT3 expression are expressed as the mean ± SEM ($n = 3$). $^{*}P < 0.05$ and $^{**}P < 0.01$ vs. control group; $^{\#}P < 0.05$ and $^{\#\#}P < 0.01$ vs. the indicated groups.

a critical role in astrocytic reactions [46]. JAK2-STAT3 activation is implicated in haematopoiesis [47], immune responses [48], morphogenesis [49], gliogenesis [50], and the regulation of memory formation. Previous studies have demonstrated that JAK2/STAT3 is essential for the induction of LCN2 [51]. Specifically, upregulation of CXCL10 by the JAK2/STAT3 pathway in astrocytes plays a central role in LCN2-induced cell migration. Thus, the neuroinflammatory pathway could be regulated by inhibiting the constitutive secretion of LCN2. In these experiments, astrocytic p-STAT3 and p-JAK2 were highly activated in the ischaemic hemisphere after cerebral ischaemia *in vivo* and after OGD *in vitro*. However, SLT inhibited JAK2-STAT3 activation in the cerebral ischaemia model and OGD-related neuroinflammatory alterations. Meanwhile, p-STAT3 and p-JAK2 were upregulated by LCN2 overexpression *in vitro*, but SLT inhibited this effect. These studies indicate that the LCN2 partially mediates JAK2/STAT3 pathway upregulation of GFAP expression in astrocytes [51]. Thus, inactivation of LCN2 by SLT confers significant antineuroinflammatory and anti-astrogliotic roles in the brain. These results do not explain all the mechanisms of SLT protection, and although the reduction in LCN2 expression is considered to be a key mechanism, SLT, as a multicomponent drug, may have other indirect neuroprotective effects. Additionally, although most of the data from experiments indicated that the effects of LCN2 were largely mediated through JAK2-STAT3 inhibition, we cannot rule out the possibility of some nonspecific effects of LCN2.

5. Conclusion

Overall, this study indicates that SLT has antiastrogliosis and antineuroinflammatory effects and improves neuronal survival and memory deficiency in a cerebral ischaemia model and OGD-induced astrocytes. As a standardized herb formula, SLT has a potential application for neuroinflammatory diseases, such as VaD, through the inactivation of LCN2.

Abbreviations

CCK8: Cell counting kit-8
CNS: Central nervous system
CXCL: Chemokine (C-X-C motif) ligand
DALYs: Disability-adjusted life years
DAPI: 4′,6-Diamidino-2-phenylindole
FBS: Fetal bovine serum
GFAP: Glial fibrillary acidic protein
HE: Hematoxylin-eosin
HPLC: High-performance liquid chromatography
IL-1α: Interleukin-1α
IL-1β: Interleukin-1β
IL-6: Interleukin-6
JAK2: Janus kinase 2
LCN2: Lipocalin-2
OGD: Oxygen-glucose deprivation
POAD: Peripheral occlusive arterial disease
SLT: Sailuotong capsule
STAT3: Signal transducer and activator of transcription 3
TNF-α: Tumor necrosis factor-alpha
TTC: Triphenyltetrazolium chloride
UV: Ultraviolet
VaD: Vascular dementia.

Data Availability

All the datasets and materials supporting the conclusions of this article are provided in the manuscript, which include the article and the additional files. Some pictures of Figure 7 were reproduced from Zhang et al. [20] (under the Creative Commons Attribution License/public domain).

Conflicts of Interest

The authors declare that they have no conflicts of interest.

Authors' Contributions

Yehao Zhang performed the research study. Mingjiang Yao and Jianxun Liu designed the research study. Bin Yang, WenTing Song, and Yongqiu Zheng contributed to data analysis. Mingqian Sun, Li Xu, Dennis Chang, and Hao Li contributed to the drafting and revising of the manuscript and accepted the final manuscript.

Acknowledgments

The authors are grateful to American Journal Experts for their helpful suggestions and highly qualified English language editing. This study was supported by grants of the National Basic Research Program (973 Program, China) (No. 2015CB554405) and National Science and Technology Major Project (No. 2018ZX09737-009).

Supplementary Materials

Figure S1: the effect of SLT on cell viability in astrocytes. (A) MTT assay detecting the cell viability treated with different dosages of SLT for 24 h. (B) MTT assay detecting the cell viability treated with different dosages of SLT for 6 h during OGD induction. Data are expressed as the mean ± SEM ($n = 6$). $^{*}P < 0.05$, $^{**}P < 0.01$, and $^{**}P < 0.001$ vs. the control groups; $^{\#}P < 0.05$, $^{\#\#}P < 0.05$, and $^{\#\#\#}P < 0.001$ vs. the OGD groups. Figure S2: analysis showing the relative levels of the proinflammatory mediators IL-1β, IL-6, and CXCL10 (IP-10) in the control cell and LCN2 overexpression cell conditioned in medium without OGD deprivation. Figure S3: the expression of astrocytic LCN2 in vitro without OGD deprivation. *(Supplementary Materials)*

References

[1] G. J. Hankey, "Stroke," *The Lancet*, vol. 389, no. 10069, pp. 641–654, 2017.

[2] C. S. Ivan, S. Seshadri, A. Beiser et al., "Dementia after stroke: the Framingham Study," *Stroke*, vol. 35, no. 6, pp. 1264–1268, 2004.

[3] J. Anrather and C. Iadecola, "Inflammation and stroke: an overview," *Neurotherapeutics*, vol. 13, no. 4, pp. 661–670, 2016.

[4] D. Petrovic-Djergovic, S. N. Goonewardena, and D. J. Pinsky, "Inflammatory disequilibrium in stroke," *Circulation Research*, vol. 119, no. 1, pp. 142–158, 2016.

[5] M. Pekny, U. Wilhelmsson, Y. R. Bogestål, and M. Pekna, "The role of astrocytes and complement system in neural plasticity," *International Review of Neurobiology*, vol. 82, pp. 95–111, 2007.

[6] C. S. McKimmie and G. J. Graham, "Astrocytes modulate the chemokine network in a pathogen-specific manner," *Biochemical and Biophysical Research Communications*, vol. 394, no. 4, pp. 1006–1011, 2010.

[7] H. Li, N. Zhang, H. Y. Lin et al., "Histological, cellular and behavioral assessments of stroke outcomes after photothrombosis-induced ischemia in adult mice," *BMC Neuroscience*, vol. 15, no. 1, p. 58, 2014.

[8] J. P. Kehrer, "Lipocalin-2: pro- or anti-apoptotic," *Cell Biology and Toxicology*, vol. 26, no. 2, pp. 83–89, 2010.

[9] J. Yang, D. R. Bielenberg, S. J. Rodig et al., "Lipocalin 2 promotes breast cancer progression," *Proceedings of the National Academy of Sciences of the United States of America*, vol. 106, no. 10, pp. 3913–3918, 2009.

[10] G. J. Biessels and L. P. Reagan, "Hippocampal insulin resistance and cognitive dysfunction," *Nature Reviews Neuroscience*, vol. 16, no. 11, pp. 660–671, 2015.

[11] Z. L. Wu, J. R. Ciallella, D. G. Flood, T. M. O'Kane, D. Bozyczko-Coyne, and M. J. Savage, "Comparative analysis of cortical gene expression in mouse models of Alzheimer's disease," *Neurobiology of Aging*, vol. 27, no. 3, pp. 377–386, 2006.

[12] F. Marques, A. J. Rodrigues, J. C. Sousa et al., "Lipocalin 2 is a choroid plexus acute-phase protein," *Journal of Cerebral Blood Flow & Metabolism*, vol. 28, no. 3, pp. 450–455, 2008.

[13] P. Eikelenboom, R. Veerhuis, W. Scheper, A. J. M. Rozemuller, W. A. van Gool, and J. J. M. Hoozemans, "The significance of neuroinflammation in understanding Alzheimer's disease," *Journal of Neural Transmission*, vol. 113, no. 11, pp. 1685–1695, 2006.

[14] M. Jin, J. H. Kim, E. Jang et al., "Lipocalin-2 deficiency attenuates neuroinflammation and brain injury after transient middle cerebral artery occlusion in mice," *Journal of Cerebral Blood Flow & Metabolism*, vol. 34, no. 8, pp. 1306–1314, 2014.

[15] G. Z. Steiner, A. Yeung, J. X. Liu et al., "The effect of Sailuotong (SLT) on neurocognitive and cardiovascular function in healthy adults: a randomised, double-blind, placebo controlled crossover pilot trial," *BMC Complementary and Alternative Medicine*, vol. 16, no. 1, p. 15, 2015.

[16] R. Bridi, F. P. Crossetti, V. M. Steffen, and A. T. Henriques, "The antioxidant activity of standardized extract of *Ginkgo biloba* (EGb 761) in rats," *Phytotherapy Research*, vol. 15, no. 5, pp. 449–451, 2001.

[17] E. J. Lee, H. Y. Chen, T. S. Wu, T. Y. Chen, I. A. Ayoub, and K. I. Maynard, "Acute administration of *Ginkgo biloba* extract (EGb 761) affords neuroprotection against permanent and transient focal cerebral ischemia in Sprague-Dawley rats," *Journal of Neuroscience Research*, vol. 68, no. 5, pp. 636–645, 2002.

[18] I. Domoráková, J. Burda, E. Mechírová, and M. Feriková, "Mapping of rat hippocampal neurons with NeuN after ischemia/reperfusion and Ginkgo biloba extract (EGb 761) pretreatment," *Cellular and Molecular Neurobiology*, vol. 26, no. 7-8, pp. 1193–1204, 2006.

[19] R. A. Paganelli, A. Benetoli, and H. Milani, "Sustained neuroprotection and facilitation of behavioral recovery by the *Ginkgo biloba* extract, EGb 761, after transient forebrain ischemia in rats," *Behavioural Brain Research*, vol. 174, no. 1, pp. 70–77, 2006.

[20] Y. Zhang, J. Liu, B. Yang et al., "*Ginkgo biloba* extract inhibits astrocytic lipocalin-2 expression and alleviates neuroinflammatory injury via the JAK2/STAT3 pathway after ischemic brain stroke," *Frontiers in Pharmacology*, vol. 9, p. 518, 2018.

[21] T. F. Lee, Y. J. Shiao, C. F. Chen, and L. C. H. Wang, "Effect of ginseng saponins on β-amyloid-suppressed acetylcholine release from rat hippocampal slices," *Planta Medica*, vol. 67, no. 7, pp. 634–637, 2001.

[22] L. Shen and J. Zhang, "NMDA receptor and iNOS are involved in the effects of ginsenoside Rg1 on hippocampal neurogenesis

in ischemic gerbils," *Neurological Research*, vol. 29, no. 3, pp. 270–273, 2007.

[23] G. Zhang, A. Liu, Y. Zhou, X. San, T. Jin, and Y. Jin, "Panax ginseng ginsenoside-Rg_2 protects memory impairment via anti-apoptosis in a rat model with vascular dementia," *Journal of Ethnopharmacology*, vol. 115, no. 3, pp. 441–448, 2008.

[24] H. Zhao, Q. Li, X. Pei et al., "Long-term ginsenoside administration prevents memory impairment in aged C57BL/6J mice by up-regulating the synaptic plasticity-related proteins in hippocampus," *Behavioural Brain Research*, vol. 201, no. 2, pp. 311–317, 2009.

[25] J. Jia, C. Wei, S. Chen et al., "Efficacy and safety of the compound Chinese medicine SaiLuoTong in vascular dementia: a randomized clinical trial," *Alzheimer's & Dementia: Translational Research & Clinical Interventions*, vol. 4, pp. 108–117, 2018.

[26] Y. Zhang, L. Miao, L. Lin, C. Y. Ren, J. X. Liu, and Y. M. Cui, "Repeated administration of Sailuotong, a fixed combination of *Panax ginseng, Ginkgo biloba, and Crocus sativus* extracts for vascular dementia, alters CYP450 activities in rats," *Phytomedicine*, vol. 38, pp. 125–134, 2018.

[27] J. B. Bederson, L. H. Pitts, M. Tsuji, M. C. Nishimura, R. L. Davis, and H. Bartkowski, "Rat middle cerebral artery occlusion: evaluation of the model and development of a neurologic examination," *Stroke*, vol. 17, no. 3, pp. 472–476, 1986.

[28] R. Morris, "Developments of a water-maze procedure for studying spatial learning in the rat," *Journal of Neuroscience Methods*, vol. 11, no. 1, pp. 47–60, 1984.

[29] J. Choi, H. W. Lee, and K. Suk, "Increased plasma levels of lipocalin 2 in mild cognitive impairment," *Journal of the Neurological Sciences*, vol. 305, no. 1-2, pp. 28–33, 2011.

[30] E. Jang, S. Lee, J. H. Kim et al., "Secreted protein lipocalin-2 promotes microglial M1 polarization," *The FASEB Journal*, vol. 27, no. 3, pp. 1176–1190, 2013.

[31] J. Wang, "Preclinical and clinical research on inflammation after intracerebral hemorrhage," *Progress in Neurobiology*, vol. 92, no. 4, pp. 463–477, 2010.

[32] C. Iadecola and J. Anrather, "The immunology of stroke: from mechanisms to translation," *Nature Medicine*, vol. 17, no. 7, pp. 796–808, 2011.

[33] R. Macrez, C. Ali, O. Toutirais et al., "Stroke and the immune system: from pathophysiology to new therapeutic strategies," *The Lancet Neurology*, vol. 10, no. 5, pp. 471–480, 2011.

[34] Á. Chamorro, A. Meisel, A. M. Planas, X. Urra, D. van de Beek, and R. Veltkamp, "The immunology of acute stroke," *Nature Reviews Neurology*, vol. 8, no. 7, pp. 401–410, 2012.

[35] K. Yaffe, A. Kanaya, K. Lindquist et al., "The metabolic syndrome, inflammation, and risk of cognitive decline," *JAMA*, vol. 292, no. 18, pp. 2237–2242, 2004.

[36] K. Arfanakis, D. A. Fleischman, G. Grisot et al., "Systemic inflammation in non-demented elderly human subjects: brain microstructure and cognition," *PloS One*, vol. 8, no. 8, article e73107, 2013.

[37] S. W. Seto, D. Chang, W. Ko et al., "Sailuotong prevents hydrogen peroxide (H_2O_2)-induced injury in EA.hy926 cells," *International Journal of Molecular Sciences*, vol. 18, no. 1, p. 95, 2017.

[38] F. Mennicken, R. Maki, E. B. de Souza, and R. Quirion, "Chemokines and chemokine receptors in the CNS: a possible role in neuroinflammation and patterning," *Trends in Pharmacological Sciences*, vol. 20, no. 2, pp. 73–78, 1999.

[39] S. M. Allan and N. J. Rothwell, "Cytokines and acute neurodegeneration," *Nature Reviews Neuroscience*, vol. 2, no. 10, pp. 734–744, 2001.

[40] C. M. Mastroianni, L. Lancella, F. Mengoni et al., "Chemokine profiles in the cerebrospinal fluid (CSF) during the course of pyogenic and tuberculous meningitis," *Clinical and Experimental Immunology*, vol. 114, no. 2, pp. 210–214, 1998.

[41] S. Gyoneva and R. M. Ransohoff, "Inflammatory reaction after traumatic brain injury: therapeutic potential of targeting cell-cell communication by chemokines," *Trends in Pharmacological Sciences*, vol. 36, no. 7, pp. 471–480, 2015.

[42] A. A. Sosunov, X. Wu, N. M. Tsankova, E. Guilfoyle, G. M. McKhann, and J. E. Goldman, "Phenotypic heterogeneity and plasticity of isocortical and hippocampal astrocytes in the human brain," *Journal of Neuroscience*, vol. 34, no. 6, pp. 2285–2298, 2014.

[43] P. J. W. Naudé, C. Nyakas, L. E. Eiden et al., "Lipocalin 2: novel component of proinflammatory signaling in Alzheimer's disease," *The FASEB Journal*, vol. 26, no. 7, pp. 2811–2823, 2012.

[44] F. Bi, C. Huang, J. Tong et al., "Reactive astrocytes secrete lcn2 to promote neuron death," *Proceedings of the National Academy of Sciences of the United States of America*, vol. 110, no. 10, pp. 4069–4074, 2013.

[45] K. Suk, "Lipocalin-2 as a therapeutic target for brain injury: an astrocentric perspective," *Progress in Neurobiology*, vol. 144, pp. 158–172, 2016.

[46] S. Lee, J. Y. Park, W. H. Lee et al., "Lipocalin-2 is an autocrine mediator of reactive astrocytosis," *Journal of Neuroscience*, vol. 29, no. 1, pp. 234–249, 2009.

[47] T. Kisseleva, S. Bhattacharya, J. Braunstein, and C. W. Schindler, "Signaling through the JAK/STAT pathway, recent advances and future challenges," *Gene*, vol. 285, no. 1-2, pp. 1–24, 2002.

[48] L. B. Ivashkiv, "Jak-STAT signaling pathways in cells of the immune system," *Reviews in Immunogenetics*, vol. 2, no. 2, pp. 220–230, 2000.

[49] C. W. Schindler, "Series introduction: JAK-STAT signaling in human disease," *Journal of Clinical Investigation*, vol. 109, no. 9, pp. 1133–1137, 2002.

[50] Y. J. Na, J. K. Jin, J. I. Kim, E. K. Choi, R. I. Carp, and Y. S. Kim, "JAK-STAT signaling pathway mediates astrogliosis in brains of scrapie-infected mice," *Journal of Neurochemistry*, vol. 103, no. 2, pp. 637–649, 2007.

[51] S. Lee, J. H. Kim, J. H. Kim et al., "Lipocalin-2 is a chemokine inducer in the central nervous system: role of chemokine ligand 10 (CXCL10) in lipocalin-2-induced cell migration," *Journal of Biological Chemistry*, vol. 286, no. 51, pp. 43855–43870, 2011.

Hindawi
Oxidative Medicine and Cellular Longevity
Volume 2019, Article ID 8549727, 9 pages
https://doi.org/10.1155/2019/8549727

Research Article

Effect of Zinc on the Oxidative Stress Biomarkers in the Brain of Nickel-Treated Mice

Jurgita Šulinskienė,[1] Rasa Bernotienė,[1] Dalė Baranauskienė,[1] Rima Naginienė,[1] Inga Stanevičienė,[2] Artūras Kašauskas,[2] and Leonid Ivanov[2]

[1]*Neuroscience Institute, Lithuanian University of Health Sciences, Kaunas LT-50161, Lithuania*
[2]*Faculty of Medicine, Medical Academy, Lithuanian University of Health Sciences, Kaunas LT-50161, Lithuania*

Correspondence should be addressed to Jurgita Šulinskienė; jurgita.sulinskiene@lsmuni.lt

Received 21 May 2019; Accepted 20 August 2019; Published 2 September 2019

Guest Editor: João C. M. Barreira

The overexposure to nickel due to the extensive use of it in modern technology remains a major public health concern. The mechanisms of pathological effects of this metal remain elusive. The present study was devoted to evaluate the effect of nickel on the oxidative state of the brain cells of mice and to assess whether zinc as redox state modulator could efficiently protect cells against nickel's neurotoxicity. As oxidative stress biomarkers in the present study, we have measured the concentrations of reduced glutathione, metallothioneins, and malondialdehyde and the activity of the enzyme δ-aminolevulinate dehydratase. For the single metal exposure, mice were i.p. injected once with solutions of $NiCl_2$ and/or $ZnSO_4$; repeated exposure was performed i.p. injecting metal salt solutions for 14 days (once a day). The control mice received i.p. injections of saline. Results of our study demonstrate that single and 14 days of Ni^{2+} exposure decreased reduced glutathione and increased malondialdehyde contents in the brain of mice. Repeated Ni^{2+} administration significantly inhibited δ-aminolevulinate dehydratase while increasing brain metallothionein concentration at both exposure periods. Zinc exhibited a protective effect against nickel-induced glutathione and lipid peroxidation in brain cells of mice at both intervals of time, while repeated exposure to this metal significantly raised the brain metallothionein content. Repeated Zn^{2+} pretreatment protected δ-aminolevulinate dehydratase from Ni^{2+}-induced inhibition and significantly increased metallothionein concentration at both investigated time intervals.

1. Introduction

Nickel is a transition metal found in the Earth's crust in combination most usually with iron, sulphur, oxygen, or arsenic. Ni compounds and metallic form of this metal are used in a wide variety of industrial and commercial applications [1, 2]. In combination with some other metals, Ni is used to form alloys, to produce coins, ceramics, steel, jewellery, battery, medical devices, electroplating, orthodontic appliances, and many others [3, 4]. Extensive use and high consumption of Ni-containing products inevitably lead to a high level of contamination and the environmental pollution by Ni and its derivatives [5]. Pollution increases human exposure to Ni primarily via inhalation and ingestion; however, wearing the jewellery may also result in cutaneous absorption of Ni [6].

Ni has been added to the list of essential trace elements quite recently; however, by now, there exists a substantial list of Ni-required enzymes [2, 7, 8]. It was considered as an essential element based on reports of Ni necessity for plants and deficiency in some animal species; however, the functional importance of Ni and its physiological relevance in humans yet remain unclear, and deficiency was never reported either [2, 3, 9]. Although healthy human body contains up to 10 mg of Ni and some data suggest that it might be involved primarily in the regulation of liver function, related to normal growth, Fe homeostasis, and red blood cell production, the exact role of Ni is still unclear [10, 11].

Toxicity of Ni depends on the route of the exposure as well as solubility of Ni compound and has a number of possible mechanisms, including disruption of trace elements and iron homeostasis, interaction with macromolecules,

Table 1: Metal exposure groups and doses of metal solutions.

	Ni	Zn	Zn+Ni
Acute single metal exposure	96 μmol Ni^{2+}/1 kg b.w.	24 μmol Zn^{2+}/1 kg b.w.	24 μmol Zn^{2+}/1 kg b.w. and 96 μmol Ni^{2+}/1 kg b.w.
Acute repeated metal exposure	19 μmol Ni^{2+}/1 kg b.w.	24 μmol Zn^{2+}/1 kg b.w.	24 μmol Zn^{2+}/1 kg b.w. and 19 μmol Ni^{2+}/1 kg b.w.

disturbance of development and energy metabolism, and induction of oxidative stress [6, 11, 12]. Since inhaled Ni is mainly accumulated in the cerebral cortex and whole brain, the nervous system is widely considered as a major target of Ni toxicity [6, 7]. Some studies with animals showed neurobehavioral changes, degeneration of neurons in the hippocampus and cerebral histopathological changes, and alteration of cognitive and locomotor behaviors in rats; however, current knowledge of Ni's neurotoxicity mechanisms still remain limited [3, 7].

Zinc is the second most abundant biometal after iron; it is the most commonly utilized metal cofactor, required for about 16% of all enzymes [13, 14]. Nearly 10 percent of the proteins, encoded in human genome require Zn for their proper structure and function [14]. Zn acts as antioxidant, which protects from the oxidation sulfhydryl groups of enzymes and other proteins, thus stabilizing these biomolecules [15]. The precise mechanism of antioxidant action of Zn is not completely understood; however, there are suggestions that being redox stable, Zn replaces redox active metals at critical cellular or extracellular sites and/or induces synthesis of cysteine-rich protein metallothioneins [15, 16].

Reduced glutathione (GSH) is the most abundant water-soluble tripeptide within the cell. The thiol group from cysteine provides GSH great reducing power, while high intracellular concentration makes it one of the major components of the cellular antioxidant system [17]. GSH deficiency is considered to be one of the earliest biochemical indicators of neuronal oxidative damage, degeneration in aging or certain mental disorders [17, 18].

δ-Aminolevulinate dehydratase (δ-ALAD) is a Zn-dependent metalloenzyme, rich in thiol groups, and therefore, sensitive to all chemical agents that are inclined to interact with them. Proximity between thiol groups renders δ-ALAD extremely sensitive to inhibition by heavy metals that displace Zn and/or oxidize the sulfhydryl groups [19]. Recent studies propose this enzyme as one of the most sensitive to cellular levels of Zn and a marker protein of oxidative stress [19, 20].

Metallothioneins (MTs) are cysteine-rich low molecular weight, metal-binding proteins, which are involved in many physiological and pathophysiological processes [21, 22]. They have been proposed to protect cells against metal toxicity, regulate homeostasis of trace elements, and provide a shield against reactive oxygen species (ROS) and are considered as one of the most important markers to monitor environmental metal contamination [21–23].

The excess ROS exposure is known to cause oxidative damage to cellular components involving polyunsaturated fatty acid residues of phospholipids, which are extremely sensitive to oxidation [24, 25]. As malondialdehyde (MDA) is a major endogenous product of lipid peroxidation (LPO), its content in membranes is one of the most usable indicators of this process [26, 27].

Our previous studies performed with mice liver and blood, as well as few studies accomplished by other scientists, proposed the existence of some kind of competition between Ni^{2+} and Zn^{2+} [15, 28–30] as well as a possible protective role of Zn against oxidative stress. However, detailed studies of the mechanisms of the interaction of these metals in the brain are almost nonexistent while research on the ability of Zn to protect the brain from Ni is very scarce.

Thus, the aim of this study was to investigate the effect of Ni^{2+} on oxidative stress markers of the brain cells of mice and to evaluate whether Zn^{2+} as redox state modulator could efficiently protect cells against Ni's neurotoxicity. Therefore, the responses of four biomarkers, i.e., contents of GSH, MDA, and MT and activity of δ-ALAD, were examined.

2. Materials and Methods

4–6-week-old out-bred white laboratory mice, each weighing from 20 to 25 g were used in these experiments. All experiments were performed according to the Republic of Lithuania Law on the Care, Keeping and Use of Animals (License of State Veterinary Service for Working with Laboratory Animals No. 0200). Mice were randomly assigned into 3 metal exposure groups plus a control group which received i.p. injections of saline. Mice of Ni and Zn exposure groups received an i.p injections of corresponding amounts of $NiCl_2$ and $ZnSO_4$ dissolved in saline as shown in Table 1. Mice of the Zn+Ni exposure group were i.p. injected with $ZnSO_4$ and after 20 min with $NiCl_2$ solutions in corresponding doses (see Table 1). There were two models chosen with a different duration of mouse exposure to the metals. For the acute single metal exposure, the exposure time was set at 24 hours and mice were injected once. For the acute repeated exposure, mice were i.p. injected for 14 days (once a day) with metal salt solutions (see Table 1).

All the animals of each group were anesthetized and terminated 24 h after the last dosing, according to the rules defined by the European Convention for the Protection of Vertebrate Animals Used for Experimental and Other Purposes. The brain was removed, washed, weighed, and cooled on ice.

Brain tissues were homogenized with 6 volumes w/v of 5% trichloroacetic acid. The homogenate was centrifuged at 10,000×g for 7 min.; obtained supernatant was further used to asses GSH concentration. The content of GSH of a brain tissue was measured by reaction with 5,5′-Dithiobis-(2-Nitrobenzoic Acid) (DTNB), known as Ellman's Reagent, to give a yellow colored compound that absorbs at a wavelength of 412 nm. [15]. Every single sample contained 0.6 mM DTNB in 0.2 M sodium phosphate (pH 8.0),

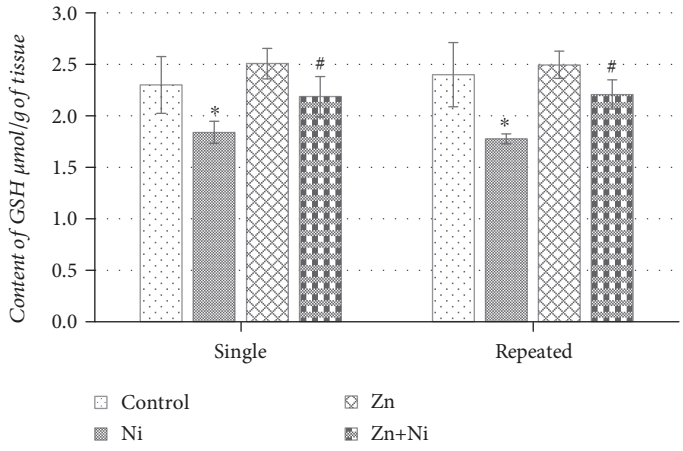

Figure 1: Content of GSH in the brain of mice after single and repeated (14 days) Ni^{2+} and/or Zn^{2+} exposure. Data represents results of 8–12 separate experiments. $^{*}p < 0.05$ vs. the control group of mice; $^{\#}p < 0.05$ vs. the group of Ni^{2+}-treated mice.

supernatant fraction, and 0.2 M phosphate buffer [15]. GSH content was expressed as μmol/g of the wet weight of the tissue.

The activity of δ-ALAD was examined by a method of Berlin and Schaller modified by Sassa [31, 32]. Brain tissues were homogenized with 7 volumes w/v 0.15 M NaCl (pH 7.4). The brain homogenate was centrifuged at 15,000×g for 15 min.; obtained supernatant was further used to asses δ-ALAD activity. For the determination of reaction product porphobilinogen, Ehrlich's reagent was used [31, 32]. Absorbance was measured at the wavelength of 555 nm. Activity of δ-ALAD was expressed in nmol/h/mg of protein.

Metallothioneins were assayed in mouse brain according to the method proposed by the United Nations Environment Program [33]. Tissues were homogenized with 3 volumes w/v sucrose-TRIS buffer (pH 8.6), resulting homogenate was centrifuged at 30,000×g for 20 min. High molecular weight proteins precipitated using cold (-20° C) absolute ethanol and chloroform and centrifuged again at 6,000×g for 10 min. The obtained supernatant (after elimination of low molecular weight soluble thiols) was further used to determine MT concentration by evaluating the –SH residue content by a spectrophotometric method, using Ellman's reagent. The absorbance of the supernatant was evaluated at wavelength 412 nm. GSH was used as a standard for quantification of MT in the sample, taking into account that GSH contains one cysteine per molecule [33].

To determine the extent of LPO, the content of MDA was measured. MDA is known to form adduct with 2 thiobarbituric acid (TBA) molecules to produce a pink colored pigment [34]. Tissues of a brain were homogenized with 9 volumes w/v of cold 1.15% KCl. Resulting homogenate was added to 1% H_3PO_4 and 0.6% TBA aqueous solution. The reaction mixture was heated for 45 min in a boiling water bath, then cooled, added n-butanol, and mixed thoroughly. The butanol phase was used to determine light absorbance at 535 and 520 nm. [34]. The results are expressed as nmol/g of the wet weight of the tissue.

Statistical analysis was performed using a statistical software package (Statistica 6.0). Statistical analysis of the obtained data is expressed as the mean (M) ± standard error of mean (SE). To determine the existence of statistically significant differences between the means of groups, Student's t-test was performed. p value less than 0.05 was considered statistically significant.

3. Results

According to the results, represented in Figure 1, a single dose of $NiCl_2$ caused a statistically significant decrease of GSH content in the mouse brain as compared to the control. Mouse treatment with $ZnSO_4$ solution did not have any effect on the content of GSH; however, pretreatment with $ZnSO_4$ 20 min before $NiCl_2$ injections attenuated the effects of Ni^{2+} and returned GSH content in the cells of the brain to the control level (Figure 1). Continuous 14-day exposure to Ni^{2+} reduced brain GSH concentration even further than the single $NiCl_2$ administration and as compared to the control group of mice ($p < 0.05$) (Figure 1). Repeated $ZnSO_4$ administration did not provide any effect on the brain GSH level; however, repeated pretreatment with Zn^{2+} before $NiCl_2$ injections seemed to have an appreciable protective effect against Ni^{2+}-induced GSH oxidation, returning its content to the level of the control mouse group (Figure 1).

According to the data presented in Figure 2, neither single $NiCl_2$ nor $ZnSO_4$ or both metal coadministration had an appreciable impact on δ-ALAD activity in the brain of mice. Repeated administration of Ni salt (Figure 2) seemed to significantly suppress brain enzyme activity as compared to the control group of mice. Repeated $ZnSO_4$ administration, just as the single one, had no tangible effect on the activity of δ-ALAD; meanwhile, repeated mouse pretreatment with Zn^{2+} before $NiCl_2$ injections seemed to attenuate a suppressing effect of Ni^{2+} and returned brain enzyme activity back to the control level (Figure 2).

The data of Figure 3 shows that brain MT content significantly increased in animals once treated with Ni^{2+} however remained at the control level after single $ZnSO_4$ administration. In the brain of animals once administered by both metals, the content of MT was significantly higher as

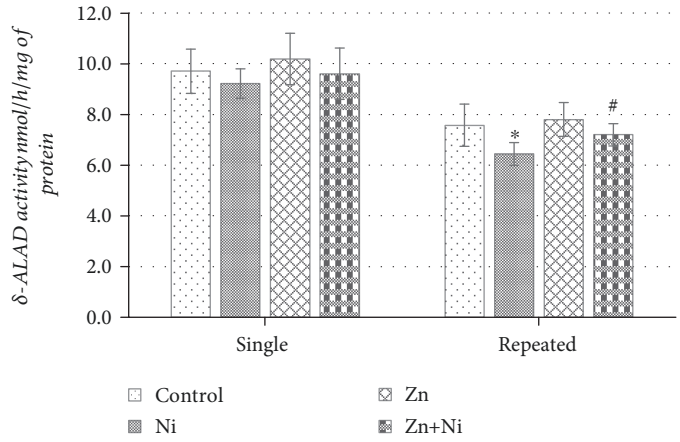

Figure 2: δ-ALAD activity in the brains of mice after single and repeated (14 days) Ni^{2+} and/or Zn^{2+} exposure. Data represents results of 8–12 separate experiments. $^{*}p < 0.05$ vs. the control group of mice; $^{\#}p < 0.05$ vs. the group of Ni^{2+}-treated mice.

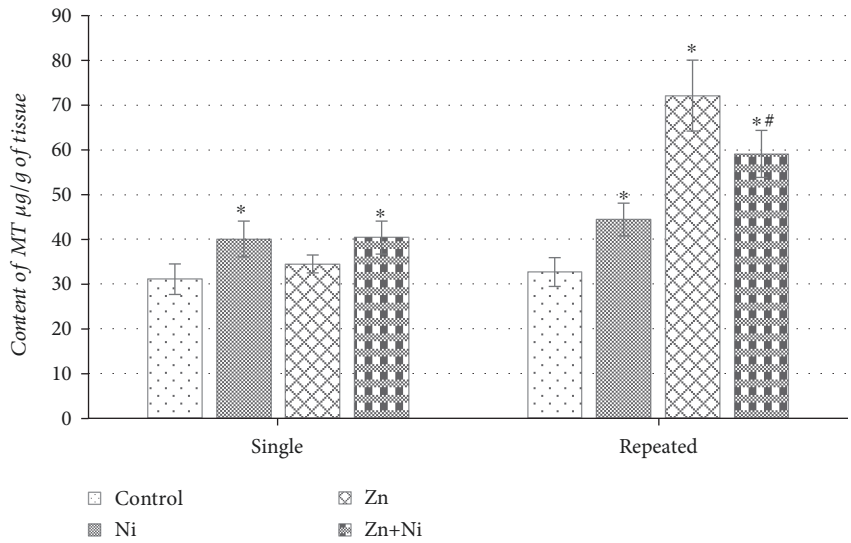

Figure 3: Content of MT in the brain of mice after single and repeated (14 days) Ni^{2+} and/or Zn^{2+} exposure. Data represents results of 8–12 separate experiments. $^{*}p < 0.05$ vs. the control group of mice; $^{\#}p < 0.05$ vs. the group of Ni^{2+}-treated mice.

compared to the control group of mice ($p < 0.05$). Further results (Figure 3) shows that 14 days of $NiCl_2$ treatment, even more than a single Ni^{2+} administration increased the metallothionein content in the brain of mice ($p < 0.05$). Though a single dose of Zn^{2+} did not seem to have any significant effect on MT quantity, repeated exposure to this metal apparently increased the brain MT content in comparison to control ($p < 0.05$). The same tendency was observed in the $ZnSO_4$ pretreated animal group; repeated exposure to both metals significantly increased MT concentration as well (Figure 3).

Results represented in Figure 4 indicate that a single dose of Ni^{2+} significantly increased the MDA content in the brain of mice, as compared to the control ($p < 0.05$). Although single $ZnSO_4$ administration seemed to induce some LPO increasing brain MDA content ($p < 0.05$), single Zn^{2+} pretreatment before $NiCl_2$ injection subdued LPO ($p < 0.05$) comparing with the Ni^{2+} group, though could not restore it to the control level (Figure 4). Repeated injections of $NiCl_2$ just like a single, this metal exposure increased MDA amount in the brain in comparison to control ($p < 0.05$) (Figure 4). Continuous administration of $ZnSO_4$ had a very similar effect to that of a single dose; Zn^{2+} tended to slightly activate LPO ($p < 0.05$). However, repeated Zn^{2+} pretreatment before $NiCl_2$ injections partially protected against Ni^{2+} induced brain lipid oxidation reducing the MDA content as compared to the nickel-affected group of mice ($p < 0.05$).

4. Discussion

Our attention in Zn/Ni interaction was drawn due to the fact that environmental Ni contamination is a widespread phenomenon in recent times. The possible impact and effects of Ni on physiologically essential metal-dependent biological systems and its metabolic pathways in the brain are not yet fully understood.

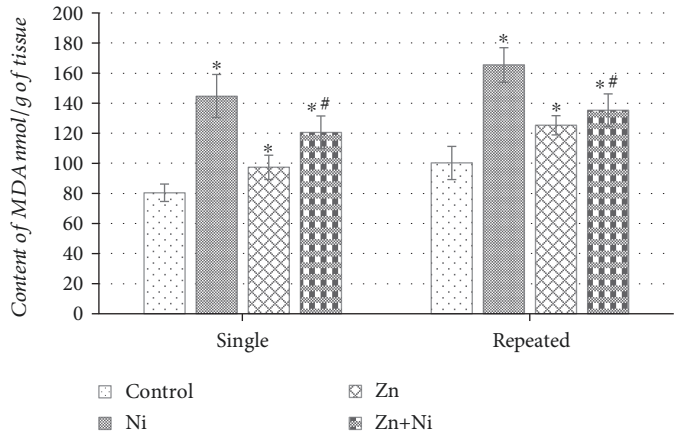

Figure 4: Content of MDA in the brain of mice after single and repeated (14 days) Ni^{2+} and/or Zn^{2+} exposure. Data represents results of 8–12 separate experiments. $^{*}p < 0.05$ vs. the control group of mice; $^{\#}p < 0.05$ vs. the group of Ni^{2+}-treated mice.

In order to assess the antioxidant status of the brain, we have evaluated the alterations of GSH, MDA, and MT contents as well as the activity of ALAD as reliable oxidative stress biomarkers, since these parameters are closely related and interdependent [26, 35–38].

There are several reasons that makes the brain especially prone to oxidative stress. Although the mass of the brain is relatively small compared to the rest of the body, it consumes up to one-fifth of the total oxygen consumed by the body [39]. Although the O_2 is absolutely essential for the brain, it also is considered as potentially toxic mutagenic gas, since it is able to give rise to free radical and nonradical species, such as superoxide anion ($O_2^{\cdot-}$), hydrogen peroxide (H_2O_2), and hydroxyl radical [38, 39]. In the healthy brain, where the redox balance is maintained, the resulting ROS are beneficial and even necessary; however, redox balance disturbance causes a condition known as oxidative stress, which is closely related to neurodegeneration [39, 40]. High O_2 exposure, considerable levels of polyunsaturated n-3 fatty acids, generous Fe and Cu stores, and a quite weak antioxidant system with low levels of the antioxidant enzymes make the brain very susceptible to oxidative stress [39, 40]. It has been shown that heavy metals penetrate across the blood brain barrier causing oxidative stress and alterations in the metabolism of some proteins involved in neurodegeneration [22].

It has been suggested that transition metal Ni disturbs the homeostasis of Fe, leading to iron accumulation, which activates free radical generation through Haber-Weiss and Fenton chemistry [5, 41]. By substituting for Fe, Ni supposedly inhibits many Fe-containing enzymes; it has been shown to suppress the activities of several tricarboxylic acid cycle and electron transfer chain oxidoreductases, thus generating free radicals due to disrupted mitochondrial respiration [6, 28]. Data suggest possible Ni's inhibition of Zn metalloenzymes—several Zn-metallopeptidases had shown susceptibility to micromolar amounts of Ni [28]. By linking with cysteine, histidine, or glutamate residues, Ni seems to have the ability to inhibit a wide range of enzymes that do not require a metal for their catalytic activity [28]. Despite ROS formation, disturbed electron transfer in mitochondria is followed by inhibition of oxidative phosphorylation, thus forcing cells to turn anaerobic glycolysis on. Restricted production of ATP in nerve cells is known to cause brain tissue dysfunction and neurological disorders [5, 6]. Studies suggest that beside some respiratory chain enzyme inhibition, Ni is able to suppress the gene expression of them thereby exacerbating the damage to the mitochondria even further [41]. Since mitochondria are the prime target for Ni exposure, oxidative damage done to it is considered as one of the key causes of Ni toxicity [3, 6].

Glutathione is a water-soluble tripeptide of vital importance in millimolar concentrations found in cells of various tissues and body fluids [42]. It is the most abundant intracellular antioxidant molecule, containing a sulfhydryl group which is critical for the biological activity of GSH [43]. GSH has been suggested as the primary defence against metal cation toxicity, while it has many different functions including heavy metal and xenobiotic detoxification, reduction of sulfhydryl groups of thiols, neutralization of ROS, and regeneration of other essential antioxidants [44]. Depending on the redox status of the cell, the tripeptide exists in a reduced or oxidized form (GSSG). The relative amounts of each form (ratio of GSH/GSSG) reflect the cellular oxidative index and serve as measurable biomarkers of redox status of the cell or whole body [42, 43].

The intracellular level of GSH is an important factor in the process of cellular resistance to Ni^{2+} [44]. Our previous study demonstrated a statistically significant decrease (by 20%) of GSH content in the liver as well as the blood of mice after 24 hours of $NiCl_2$ exposure. Recent studies accomplished by other scientists report a considerable GSH depletion even after single Ni^{2+} exposure [15].

It was observed that electroplate workers with exposure to high levels of Ni^{2+} had significantly lower levels of GSH than the others [27]. Consequently, a significant brain GSH content decrease after single as well as repeated exposure to Ni observed in our present study is likely to evidence the oxidative damage to the brain induced by this metal. Thus, the results of our study are corroborating the conclusions of scientists who claim intracellular GSH depletion as the result of

Ni-induced toxicity [5]. Some researchers, however, have showed that Ni does not diminish but even increases GSH levels in the cell. Topal et al. found that 21-day oral $NiCl_2$ treatment significantly increased GSH levels in brain tissues of rainbow trout [6, 7]. This GSH content increase could be the outcome of the adaptive mechanism, when synthesis of this tripeptide-antioxidant increases as a response to cell oxidative damage caused by toxicity of metals [7]. To the control level, restored concentration of GSH in the brain of the Zn-pretreated mouse group, observed in our present study, might be the outcome of both—Zn's ability to compete with Ni or its importance in the regulation of GSH synthesis, due to the increased expression of glutamate-cysteine ligase which is the rate-limiting enzyme of glutathione de novo synthesis [36, 37, 45].

Since thiol groups have been proposed to be the first and primary targets of heavy metal exposure and it has also been shown that some of the zinc-dependent enzymes are vulnerable to micromolar amounts of Ni, next object of our study was investigation of the possible damage caused by Ni to Zn-dependent enzymes such as δ-ALAD [35, 40].

δ-ALAD is a metalloenzyme with 3 adjacent sulfhydryl groups in its active site that requires Zn for its activity, therefore might be sensitive to the substances that compete with Zn or to those that oxidize -SH groups [20]. It is a widely distributed enzyme in nature that plays a primary role in most aerobic organisms since it catalyses condensation of two molecules of δ-aminolevulinic acid (δ-ALA) to form porphobilinogen in the heme biosynthesis pathway [26]. Recent studies have indicated that due to its high sensitivity to prooxidant situations, δ-ALAD can be a reliable universal biomarker of oxidative stress—various observations evidence a negative correlation between enzyme activity and level of oxidative stress [20, 26]. δ-ALAD inhibition due to thiol group oxidation leads to δ-ALA autoxidation, further δ-ALAD inhibition, additional $O_2^{\cdot-}$ generation, and antioxidant system depletion [26, 46]. Excess δ-ALA in the brain disrupts γ-aminobutyric acid/glutamate system causing neurotoxicity and cell death [19, 46] while decreased heme biosynthesis is known to cause neuronal cell dysfunction, since heme is critical for neuronal cell growth, differentiation, and survival [47]. Literature data show that Ni is especially prone to bind to amino acids like cysteine and histidine, small peptides like glutathione, and amine-containing compounds thus accelerating the rate of oxidative damage [28]. In our previous research [30], we ascertained that single exposure to $NiCl_2$ suppressed the activity of δ-ALAD in the liver and the blood of mice, while Zn-pretreatment diminished this effect of Ni. Repeated $NiCl_2$ administration decreased δ-ALAD's activity in the liver of mice, though Zn did not protect enzyme from Ni-induced inhibition [30]. Other studies suggest that some heavy and transition metals cause inhibition of the δ-ALAD activity [19, 20] that supports the inhibitory effect of Ni on the enzyme activity after 14 days of $NiCl_2$ treatment observed in our study. The fact that the single $NiCl_2$ exposure did not induce any appreciable effect on δ-ALAD activity might be associated with the decreased levels of GSH found in the brain of mice after single Ni^{2+} treatment or with compensatory mechanisms of other antioxidant system components such as ascorbic acid or antioxidant enzymes [27, 48]. Literature suggests that due to antioxidant capacity, GSH is able to attenuate free radical generation as well as LPO, reduce oxidant burden, and partially restore enzymatic δ-ALAD activity, suppressed by different prooxidants [19, 20, 26].

The structure of δ-ALAD is characterised by vicinal cysteine residues in its active site, which are involved in the coordination of cofactor Zn^{2+} [20]. Literature suggests that close spatial arrangement of thiol groups determines the specific sensitivity of the enzyme to oxidation. Since Zn is involved in sulfhydryl group stabilization, its removal or replacement is known to accelerate enzyme autooxidation [19]. The protective effect of Zn^{2+} on the activity of the enzyme after fourteen days of metal exposure determined in our study confirms the findings of other scientists who claim Zn's ability to protect δ-ALAD from the inhibition, which indicates that enzyme activity suppression occurs not only by thiol group oxidation but also by Zn displacement [20].

Well-known antioxidants and heavy metal contamination biomarkers, cysteine-rich protein MTs, are also involved in maintaining some biologically essential metal ion homeostasis [22, 49]. Scientific data indicate that MTs act as antioxidant by scavenging ROS; they are capable of reducing oxidative tissue damage and helping the cells to withstand heavy metal toxicity [50, 51]. There was an established direct correlation between intracellular heavy metal and MT concentration in organs such as the liver, kidneys, and gills of aquatic animals [22, 49]. Other scientific sources show the ability of Ni to induce MTs' synthesis in various organisms and in cultured cells [52]. However, there is a sparse data on the ability of MT to reduce heavy metal-induced oxidative nerve tissue damage.

Although MTs have a particular affinity for Zn^{2+}, in excess of some transition or heavy metals, Zn^{2+} can be easily displaced by them. Up to eighteen different metals are known to have the ability to associate with MTs [51]. Zn^{2+} from the Zn-MT complex can be ejected not only by certain metals; it is known by now that Zn might be displaced from MT's as a response to the exposure to ROS. Literature indicates that MT's ability to couple or release Zn^{2+} depends very much on the redox state of the cell [23]. The free Zn^{2+} merges with the six Zn fingers of metal response element-binding transcription factor-1 (MTF-1), thus activating it and inducing the expression of MT genes, thereby increasing their concentration in the cell [51]. That could explain the same trends in the increase of MT concentrations observed in our study after the repeated Zn^{2+} treatment as well as after acute and prolonged exposure to both metals on the brain of mice. It is interesting to note that an apparent increase in the content of MT determined in the brains of Zn+Ni-treated mouse group correlates with the restored content of GSH and regained enzyme δ-ALAD activity, which supports the idea of Zn's and MT's ability to suppress toxicity of Ni^{2+}.

Since Zn excess, just as the deficiency is damaging to the cells—the cellular Zn^{2+} concentration must be precisely regulated. Scientific data affirm that this balance is supported mainly by MT and MTF-1 and might be disturbed as a response to the stress of the cell, caused by different stressors, like prooxidants and heavy metal ions [51]. It has been

shown that MTF-1 regulates the MT gene expression as a response not only to changes in Zn but also to changes in other heavy metal, such as Ni concentrations [2, 51]. It was also demonstrated that exposure to $NiSO_4$ activates protein phosphatase 2A, which induces MTF-1 dephosphorylation that is required for transcription factor translocation to nucleus to induce the expression of MT [2]. Increase in brain MT content, obtained in our study after single and repeated Ni^{2+} exposure, seems to be consistent with other researchers' data confirming Ni's ability to induce MT synthesis not only in the liver or kidneys but obviously in the brain as well.

The brains are enriched by redox active transition metals, like Fe^{2+} and Cu^{2+}, consume lots of O_2, and basically are composed of easily oxidizable polyunsaturated fatty acids. Neurons possess around 50 percent lower cytosolic GSH levels; as compared to cells of other tissue, enzymatic GSH-dependent antioxidant system in the brain is modest which determines nerve tissue vulnerability to oxidative stress-induced LPO [39]. Although Ni, compared with other metals such as Fe, is not very effective in Fenton chemistry, its reactivity seems to be enhanced when it is chelated by oligopeptides or histidine [12]. Ni is known to strongly interfere with Fe homeostasis, leading to Fe^{2+} accumulation which in turn induces oxidative stress through Fenton and Haber-Weiss reactions and initiates LPO [39, 48]. Topal et al. showed that after three weeks of daily treatment, Ni in a dose-dependent manner significantly increased rainbow trout brain LPO, which caused demyelination and necrotic changes in some brain areas [7]. Other researchers notice that beside LPO, Ni depletes the intracellular antioxidants and significantly increases the activity of antioxidant enzymes like glutathione reductase and catalase [3, 12]. Lipid peroxides formed due to LPO are converted to their corresponding alcohols by the glutathione peroxidases, which convert GSH into oxidized glutathione disulphide [27]. Our observed overlap of MDA content elevation with expend of GSH, after single and continuous Ni^{2+} exposure, appears consistent with other researchers' findings confirming Ni's ability to induce oxidative damage, which significantly promote LPO and antioxidant system depletion not only in other organs but also in the brain [6, 7, 12].

According the data of our experiments, Zn^{2+} pretreatment before Ni^{2+} injections seemed to significantly reduce brain LPO as compared to the $NiCl_2$-treated group of mice. A decrease in MDA might involve Zn's ability to induce synthesis of glutathione, which is a coenzyme of glutathione peroxidase, thus increasing antioxidant enzyme activity [36]. Zn's ability to compete with Fe and Cu for the binding sites in the cell membranes could be another explanation of brain lipid protection, since both Fe and Cu are able to induce the formation of free radicals from lipid peroxides. In this case, the replacement of Fe or Cu with redox stable Zn could prevent cell from free radical formation [36]. Zn acts a cofactor for another antioxidant metalloenzyme superoxide dismutase (SOD) which promotes two $O_2^{\cdot-}$ radical conversion to H_2O_2 and O_2, thus reducing toxicity of ROS [36]. An increase in SOD activity might appear as a result of Ni^{2+}/Zn^{2+} competition for enzyme binding or to Zn's ability to activate SOD synthesis at a transcriptional level [28, 53]. A number of pathologies like neurodegeneration and myocardial injury were observed in SOD-deficient mice, since the enzyme is indispensable in protection against oxidative damage [48].

5. Conclusions

Single and repeated exposure to Ni^{2+} resulted in an expended resource of GSH as well as enhanced LPO in mouse brain. Single i.p. injection of $NiCl_2$ did not affect enzyme δ-ALAD activity; however, single as well as repeated Ni^{2+} administration significantly inhibited enzyme and increased the content of MT. Zn^{2+} provided the protective effect against Ni^{2+}-induced GSH depletion and LPO at both exposure periods. After continuous pretreatment, Zn^{2+} managed to return Ni-suppressed δ-ALAD activity back to the level of control; MT content after prolonged both metal administration remained increased.

In summary, Zn definitely has shown some protective mechanisms against toxicity of Ni; however, further studies on the Ni-Zn interaction, including the response of brain antioxidant enzymes, would potentially help to further understand the effects of these metals on the redox state of the brain.

Data Availability

The data supporting the findings of our study are available within the article.

Conflicts of Interest

The authors declare that they have no conflicts of interest.

References

[1] A. Mudipalli and J. T. Zelikoff, *Essential and Non-essential Metals. Molecular and Integrative Toxicology*, Humana Press, 2017.

[2] B. Zambelli, V. N. Uversky, and S. Ciurli, "Nickel impact on human health: an intrinsic disorder perspective," *Biochimica et Biophysica Acta (BBA) - Proteins and Proteomics*, vol. 1864, no. 12, pp. 1714–1731, 2016.

[3] O. M. Ijomone, S. Y. Olatunji, J. O. Owolabi, T. Naicker, and M. Aschner, "Nickel-induced neurodegeneration in the hippocampus, striatum and cortex; an ultrastructural insight, and the role of caspase-3 and α-synuclein," *Journal of Trace Elements in Medicine and Biology*, vol. 50, pp. 16–23, 2018.

[4] D. Keinan, E. Mass, and U. Zilberman, "Absorption of nickel, chromium, and iron by the root surface of primary molars covered with stainless steel crowns," *International Journal of Dentistry*, vol. 2010, Article ID 326124, 4 pages, 2010.

[5] S. Xu, M. He, M. Zhong et al., "The neuroprotective effects of taurine against nickel by reducing oxidative stress and maintaining mitochondrial function in cortical neurons," *Neuroscience Letters*, vol. 590, pp. 52–57, 2015.

[6] X. Song, S. S. Fiati Kenston, L. Kong, and J. Zhao, "Molecular mechanisms of nickel induced neurotoxicity and chemoprevention," *Toxicology*, vol. 392, pp. 47–54, 2017.

[7] A. Topal, M. Atamanalp, E. Oruc et al., "Neurotoxic effects of nickel chloride in the rainbow trout brain: assessment of c-Fos

activity, antioxidant responses, acetylcholinesterase activity, and histopathological changes," *Fish Physiology and Biochemistry*, vol. 41, no. 3, pp. 625–634, 2015.

[8] D. B. Zamble, "Nickel in biology," *Metallomics*, vol. 7, no. 4, pp. 588-589, 2015.

[9] US Department of Health and Human Services, *Public Health Service Agency for Toxic Substances and Disease Registry. Toxicological profile for Ni*, Agency for Toxic Substances and Disease Registry, 2005.

[10] G. Bánfalvi, *Cellular Effects of Heavy Metals*, Springer, Dordrecht, Netherlands, 2011.

[11] K. K. Das, S. N. Das, and S. A. Dhundasi, "Nickel its adverse health effects & oxidative stress," *The Indian Journal of Medical Research*, vol. 128, pp. 412–425, 2008.

[12] K. V. Brix, C. E. Schlekat, and E. R. Garman, "The mechanisms of nickel toxicity in aquatic environments: an adverse outcome pathway analysis," *Environmental Toxicology and Chemistry*, vol. 36, no. 5, pp. 1128–1137, 2017.

[13] A. W. Foster, D. Osman, and N. J. Robinson, "Metal preferences and metallation," *Journal of Biological Chemistry*, vol. 289, no. 41, pp. 28095–28103, 2014.

[14] J. E. Cummings and J. P. Kovacic, "The ubiquitous role of zinc in health and disease," *Journal of Veterinary Emergency and Critical Care*, vol. 19, no. 3, pp. 215–240, 2009.

[15] J. Sulinskiene, I. Sadauskiene, and L. Ivanov, "Effect of zinc ions on the level of reduced glutathione and lipid peroxidation in nickel treated mice," *Trace Elements and Electrolytes*, vol. 30, no. 4, pp. 46–50, 2013.

[16] J. Guynn and E. A. W. Chan, "Zinc and zinc-dependent proteins in cancer and chemotherapeutics," in *Essential and Non-essential Metals*, pp. 69–94, Humana Press, 2017.

[17] M. Farina and M. Aschner, "Glutathione antioxidant system and methylmercury-induced neurotoxicity: an intriguing interplay," *Biochimica et Biophysica Acta (BBA) - General Subjects*, no. article 129285, 2019.

[18] S. Fernandez-Fernandez, V. Bobo-Jimenez, R. Requejo-Aguilar et al., "Hippocampal neurons require a large pool of glutathione to sustain dendrite integrity and cognitive function," *Redox Biology*, vol. 19, pp. 52–61, 2018.

[19] J. B. T. Rocha, R. A. Saraiva, S. C. Garcia, F. S. Gravina, and C. W. Nogueira, "Aminolevulinate dehydratase (δ-ALA-D) as marker protein of intoxication with metals and other prooxidant situations," *Toxicology Research*, vol. 1, no. 2, p. 85, 2012.

[20] E. Sauer, A. Moro, N. Brucker et al., "Liver δ-aminolevulinate dehydratase activity is inhibited by neonicotinoids and restored by antioxidant agents," *International Journal of Environmental Research and Public Health*, vol. 11, no. 11, pp. 11676–11690, 2014.

[21] A. Bizon and H. Milnerowicz, "Participation of metallothionein and superoxide dismutase in the blood of smoking smelters," *International Journal of Occupational Medicine and Environmental Health*, vol. 27, no. 2, pp. 326–334, 2014.

[22] J. H. Kim and J. C. Kang, "Oxidative stress, neurotoxicity, and metallothionein (MT) gene expression in juvenile rock fish *Sebastes schlegelii* under the different levels of dietary chromium (Cr^{6+}) exposure," *Ecotoxicology and Environmental Safety*, vol. 125, pp. 78–84, 2016.

[23] S. J. Lee, "A different role of metallothionein-3 (Mt3) in oxidative stress and neurodegeneration of brain," *Journal of Neuroinfectious Diseases*, vol. 7, no. 2, p. 221, 2016.

[24] N. Bozan, H. Demir, T. Gursoy et al., "Alterations in oxidative stress markers in laryngeal carcinoma patients," *Journal of the Chinese Medical Association*, vol. 81, no. 9, pp. 811–815, 2018.

[25] Z. Liu, Z. Zhu, J. Zhao et al., "Malondialdehyde: a novel predictive biomarker for post-stroke depression," *Journal of Affective Disorders*, vol. 220, pp. 95–101, 2017.

[26] L. de Lucca, F. Rodrigues, L. B. Jantsch et al., "Delta-aminolevulinate dehydratase activity and oxidative stress markers in preeclampsia," *Biomedicine & Pharmacotherapy*, vol. 84, pp. 224–229, 2016.

[27] Y.-C. Tsao, P.-W. Gu, S.-H. Liu, I.-S. Tzeng, J.-Y. Chen, and J.-C. J. Luo, "Nickel exposure and plasma levels of biomarkers for assessing oxidative stress in nickel electroplating workers," *Biomarkers*, vol. 22, no. 5, pp. 455–460, 2017.

[28] L. Macomber and R. P. Hausinger, "Mechanisms of nickel toxicity in microorganisms," *Metallomics*, vol. 3, no. 11, pp. 1153–1162, 2011.

[29] G. Nunez-Nogueira, C. Mouneyrac, A. Muntz, and L. Fernandez-Bringas, "Metallothionein-like proteins and energy reserve levels after Ni and Pb exposure in the Pacific white prawn *Penaeus vannamei*," *Journal of Toxicology*, vol. 2010, Article ID 407360, 9 pages, 2010.

[30] J. Sulinskiene, D. BaranauskienÄ, R. Naginiene, and L. Ivanov, "Protective effect of zinc ions against lead and nickel induced inhibition of δ-aminolevulinic acid dehydratase activity in mice liver," *Trace Elements and Electrolytes*, vol. 32, no. 04, pp. 91–96, 2015.

[31] A. Berlin and K. H. Schaller, "European standardized moethod for the determination of delta-aminolevulinic acid dehydratase activity in blood," *Zeitschrift fur klinische Chemie und klinische Biochemie*, vol. 12, pp. 389-390, 1974.

[32] S. Sassa, "Delta-aminolevulinic acid dehydratase assay," *Enzyme*, vol. 28, no. 2-3, pp. 133–145, 1982.

[33] UNEP/RAMOGE, *Manual on the Biomarkers Recommended for the MED POL Biomonitoring Programme*, United Nations Environment Programme, Athens, Greece, 1999.

[34] T. P. Devasagayam, K. K. Boloor, and T. Ramasarma, "Methods for estimating lipid peroxidation: an analysis of merits and demerits," *Indian Journal of Biochemistry & Biophysics*, vol. 40, no. 5, pp. 300–308, 2003.

[35] E. Ho, K. Karimi Galougahi, C. C. Liu, R. Bhindi, and G. A. Figtree, "Biological markers of oxidative stress: applications to cardiovascular research and practice," *Redox Biology*, vol. 1, no. 1, pp. 483–491, 2013.

[36] D. Marreiro, K. Cruz, J. Morais, J. Beserra, J. Severo, and A. de Oliveira, "Zinc and oxidative stress: current mechanisms," *Antioxidants*, vol. 6, no. 2, p. 24, 2017.

[37] B. Ruttkay-Nedecky, L. Nejdl, J. Gumulec et al., "The role of metallothionein in oxidative stress," *International Journal of Molecular Sciences*, vol. 14, no. 3, pp. 6044–6066, 2013.

[38] L. A. Sena and N. S. Chandel, "Physiological roles of mitochondrial reactive oxygen species," *Mollecular Cell*, vol. 48, no. 2, pp. 158–167, 2012.

[39] J. N. Cobley, M. L. Fiorello, and D. M. Bailey, "13 reasons why the brain is susceptible to oxidative stress," *Redox Biology*, vol. 15, pp. 490–503, 2018.

[40] J. M. Samet and P. A. Wages, "Oxidative stress from environmental exposures," *Current Opinion in Toxicology*, vol. 7, pp. 60–66, 2018.

[41] S. C. Xu, M. D. He, M. Zhong et al., "Melatonin protects against nickel-induced neurotoxicity in vitro by reducing

oxidative stress and maintaining mitochondrial function," *Journal of Pineal Research*, vol. 49, pp. 86–94, 2010.

[42] C. Vacchi-Suzzi, L. Viens, J. M. Harrington, K. Levine, R. Karimi, and J. R. Meliker, "Low levels of lead and glutathione markers of redox status in human blood," *Environ Geochem Health*, vol. 40, no. 4, pp. 1175–1185, 2018.

[43] B. Schmitt, M. Vicenzi, C. Garrel, and F. M. Denis, "Effects of N-acetylcysteine, oral glutathione (GSH) and a novel sublingual form of GSH on oxidative stress markers: a comparative crossover study," *Redox Biology*, vol. 6, pp. 198–205, 2015.

[44] J. Liu, H. Liu, Y. Li, and H. Wang, "Probing the coordination properties of glutathione with transition metal ions (Cr^{2+}, Mn^{2+}, Fe^{2+}, Co^{2+}, Ni^{2+}, Cu^{2+}, Zn^{2+}, Cd^{2+}, Hg^{2+}) by density functional theory," *Journal of Biological Physics*, vol. 40, no. 4, pp. 313–323, 2014.

[45] M. Martiniaková, R. Omelka, B. Grosskopf, H. Chovancová, P. Massányi, and P. Chrenek, "Effects of dietary supplementation of nickel and nickel-zinc on femoral bone structure in rabbits," *Acta Veterinaria Scandinavica*, vol. 51, no. 1, pp. 52–58, 2009.

[46] M. M. Taha, O. A. E. A. Gaber, N. A. Sabbah, and A. A. S. A. Elazem, "Association between δ-aminolevulinate dehydratase G177C polymorphism and blood lead levels in brain tumor patients," *Molecular and Clinical Oncology*, vol. 3, no. 5, pp. 995–1000, 2015.

[47] H. A. Bergonia, M. R. Franklin, J. P. Kushner, and J. D. Phillips, "A method for determining δ-aminolevulinic acid synthase activity in homogenized cells and tissues," *Clinical Biochemistry*, vol. 48, no. 12, pp. 788–795, 2015.

[48] O. M. Ighodaro and O. A. Akinloye, "First line defence antioxidants-superoxide dismutase (SOD), catalase (CAT) and glutathione peroxidase (GPX): their fundamental role in the entire antioxidant defence grid," *Alexandria Journal of Medicine*, vol. 54, no. 4, pp. 287–293, 2018.

[49] C. Vanparys, T. Dauwe, K. van Campenhout et al., "Metallothioneins (MTs) and δ-aminolevulinic acid dehydratase (ALAd) as biomarkers of metal pollution in great tits (*Parus major*) along a pollution gradient," *Science of The Total Environment*, vol. 401, no. 1-3, pp. 184–193, 2008.

[50] M. U. Beg, N. Al-Jandal, S. Al-Subiai et al., "Metallothionein, oxidative stress and trace metals in gills and liver of demersal and pelagic fish species from Kuwaits' marine area," *Marine Pollution Bulletin*, vol. 100, no. 2, pp. 662–672, 2015.

[51] G. Dong, H. Chen, M. Qi, Y. Dou, and Q. Wang, "Balance between metallothionein and metal response element binding transcription factor 1 is mediated by zinc ions (Review)," *Molecular Medicine Reports*, vol. 11, no. 3, pp. 1582–1586, 2015.

[52] M. P. Waalkes, J. Liu, K. S. Kasprzak, and B. A. Diwan, "Minimal influence of metallothionein over-expression on nickel carcinogenesis in mice," *Toxicology Letters*, vol. 153, no. 3, pp. 357–364, 2004.

[53] C. Tarhan, M. Pekmez, S. Karaer, N. Arda, and A. T. Sarikaya, "The effect of superoxide dismutase deficiency on zinc toxicity in *Schizosaccharomyces pombe*," *Journal of Basic Microbiology*, vol. 47, no. 6, pp. 506–512, 2007.

Hindawi
Oxidative Medicine and Cellular Longevity
Volume 2019, Article ID 3614960, 16 pages
https://doi.org/10.1155/2019/3614960

Research Article

Antidepressant and Antiaging Effects of Açaí (*Euterpe oleracea* Mart.) in Mice

José Rogério Souza-Monteiro,[1] Gabriela P. F. Arrifano,[1,2] Ana Isabelle D. G. Queiroz,[3] Bruna S. F. Mello,[3] Charllyany S. Custódio,[3] Danielle S. Macêdo,[3] Moisés Hamoy,[4] Ricardo S. O. Paraense,[1] Leonardo O. Bittencourt,[5] Rafael R. Lima,[5] Rommel R. Burbano,[6] Hervé Rogez,[7] Cristiane F. Maia,[8] Barbarella M. Macchi,[9] José Luiz M. do Nascimento,[9] and Maria Elena Crespo-López[1]

[1]*Laboratory of Molecular Pharmacology, Institute of Biological Sciences, Federal University of Pará, Belém, Brazil*
[2]*Laboratory of Experimental Neuropathology, Department of Pharmacology, University of Oxford, Oxford OX1 3QT, UK*
[3]*Laboratory of Neuropharmacology, Department of Physiology and Pharmacology, Federal University of Ceará, Fortaleza, Brazil*
[4]*Laboratory of Pharmacology and Toxicology of Natural Products, Institute of Biological Sciences, Federal University of Pará, Belém, Brazil*
[5]*Laboratory of Structural and Functional Biology, Institute of Biological Sciences, Federal University of Pará, Belém, Brazil*
[6]*Laboratory of Molecular Biology, Ophir Loyola Hospital, Belém, Pará, Brazil*
[7]*Centre for Valorisation of Amazonian Bioactive Compounds (CVACBA) and Federal University of Pará, Belém, Brazil*
[8]*Laboratory of Pharmacology of Inflammation and Behavior, Institute of Health Sciences, Federal University of Pará, Belém, PA, Brazil*
[9]*Laboratory of Molecular and Cellular Neurochemistry, Institute of Biological Sciences, Federal University of Pará, Belém, Brazil*

Correspondence should be addressed to Maria Elena Crespo-López; maria.elena.crespo.lopez@gmail.com

Received 1 March 2019; Revised 10 May 2019; Accepted 19 May 2019; Published 24 July 2019

Guest Editor: Rosane M. Peralta

Depression is a mental disorder that affects 300 million people of all ages worldwide, but fewer than half of those with the condition receive adequate treatment. In addition, the high pharmacological refractoriness (affecting 30%-50% of patients) and toxicity of some classical antidepressants support the pursuit of new therapies. People with this condition show depressed mood, loss of pleasure, high levels of oxidative stress, and accelerated biological aging (decreased telomere length and expression of the telomerase reverse transcriptase (TERT), the enzyme responsible for telomere maintenance). Because of the close relationship between depression and oxidative stress, nutraceuticals with antioxidant properties are excellent candidates for therapy. This study represents the first investigation of the possible antidepressant and antiaging effects of commercial samples of clarified açaí (*Euterpe oleracea*) juice (EO). This fruit is rich in antioxidants and widely consumed. In this study, mice were treated with saline or EO (10 μL/g, oral) for 4 days and then with saline or lipopolysaccharide (0.5 mg/kg, i.p.) to induce depressive-like behavior. Only four doses of EO were enough to abolish the despair-like and anhedonia behaviors and alterations observed in electromyographic measurements. The antidepression effect of EO was similar to that of imipramine and associated with antioxidant and antiaging effects (preventing lipid peroxidation and increasing TERT mRNA expression, respectively) in three major brain regions involved in depression (hippocampus, striatum, and prefrontal cortex). Additionally, EO significantly protected hippocampal cells, preventing neuronal loss associated with the depressive-like state and nitrite level increases (an indirect marker of nitric oxide production). Moreover, EO alone significantly increased TERT mRNA expression, revealing for the first time a potent antiaging action in the brain that suggests neuroprotection against long-term age-related consequences.

1. Introduction

Depression is a mental disorder that represents an important and growing problem in public health, with an estimated 300 million people of all ages affected worldwide [1]. Although the pharmacological arsenal for depression includes selective serotonin reuptake inhibitors (SSRIs), such as fluoxetine, or tricyclic antidepressants, such as imipramine, the World Health Organization estimates that less than half of the patients receive adequate treatment [1]. In some countries, that rate is less than 10% [1]. In addition to difficulties with adequate access to health care, a main problem in the treatment of depression is pharmacological refractoriness, which affects 30%-50% of people with the condition [2]. Side effects of some classical antidepressants make it urgent to seek new therapies that could serve as adjuvants or less-toxic alternatives.

Depression is characterized by symptoms such as depressed mood, loss of interest or pleasure, feelings of guilt or low self-esteem, and sleep or appetite disorders, creating a significant impact on quality of life [1]. Accelerated aging also has been demonstrated in patients with depression characterized by a significant decrease in telomere length and expression of telomerase reverse transcriptase (TERT), the enzyme responsible for telomere maintenance [3–6]. This effect may especially affect the brain increasing its susceptibility to age-related disorders.

Many areas of the brain are involved in mood regulation [7–10] and thus relevant to the neurobiology of major depressive disorder (MDD) and depressive-like symptoms [11]. Among the main symptoms present in people with MDD, learning and memory problems are related to hippocampal damage, and reward and emotional behaviors are associated with alterations in the prefrontal cortex and striatum [11].

Clinical and preclinical studies have confirmed the close relationship between MDD and the imbalance of increased oxidative stress and decreased antioxidant defenses [12–15]. Oxidative and nitrosative stress play a crucial role in the pathophysiology of unipolar and bipolar depression [16]. In parallel to oxidative stress, immunoinflammatory mechanisms of depression have been described [17]. Based on the inflammatory/oxidative stress component of depression, a mouse model of depressive-like behavior induced by lipopolysaccharide (LPS) has been developed. After 24 hours of a single low exposure to LPS, the animals show depressive-like alterations such as anhedonia and despair-like behavior [18]. This model has translational validity based on recent findings that depressed patients have higher plasma LPS levels [19].

Although analysis of isolated compounds from natural sources for the development of new antidepressant drugs is important, the study of nutraceuticals (a food, part of a food, vitamin, mineral, or herb that provides health benefits) is also essential to uncover potential nutritional strategies. A key reason is that these products can be realistic alternatives and adjunctive therapies for depression in isolated populations or people living in developing and low-income countries.

In this context, Amazonia biodiversity provides a special opportunity. Açaí is a fruit (of a very common palm in the Amazon basin, *Euterpe oleracea* Martius, family Arecaceae) commonly consumed in the Amazon and largely available on the international market [20, 21]. This fruit, or the drink made from it, is a well-recognized functional food. Called a "superfruit" because of its antioxidant properties, açaí has attracted increasing attention from the global nutraceutical market [21, 22]. Its biological activities, such as antiparasitic, anticarcinogenic, or metabolic action have been described [23–25]. Moreover, recent preclinical data support a potent neuroprotective effect of açaí [26]. In the latter study, consumption of commercial samples of clarified açaí juice significantly reduced tonic-clonic seizures and their consequences [26], probably because of the action on the gabaergic system [27].

Despite this pronounced neuroprotective effect, *in vivo* studies with açaí are scarce, especially those related to neuropsychiatric disorders. In the last decade, however, some phytochemical compounds such as ellagic acid and apigenin have shown efficacy in preventing depressive-like behaviors [28–30], and many of them are found in açaí.

The aim of this study was to investigate for the first time the possible antidepressant-like and antiaging effects of commercial samples of clarified açaí juice (EO).

2. Materials and Methods

2.1. Animals and Ethical Aspects. Male Swiss mice (20-30 g) were maintained in standard environmental conditions ($22 \pm 1^{\circ}$C, humidity $60 \pm 5\%$, and 12 h light-dark cycle) with food and water *ad libitum*. All experimental procedures were approved by the Committee for Ethics in Experimental Research with Animals of the Federal University of Pará (license number 89-15) and followed the guidelines of the NIH Guide for the Care and Use of Laboratory Animals.

2.2. Clarified Açaí (Euterpe oleracea Mart.) Juice (EO). Samples of EO were kindly provided by Amazon Dreams (Belém, Pará, Brazil) and produced by a patented process (PI 1003060-3). Briefly, clarified açaí was prepared from fresh fruits of *E. oleracea* Martius (Arecaceae). After cleaning the fruits, pulping was performed with the addition of 0.5 L of water per kilogram of fruits. The juice was subsequently microfiltered (Souza-Monteiro et al., 2005; [27]). EO is a thin, translucent, wine-colored liquid with no lipids, proteins, or fibers but rich in phenolic compounds (>1400 mg gallic acid equivalents/L). The major phenolic compounds of EO were previously analyzed using two UHPLC-DAD methods and found to be cyanidin 3-rutinoside (450 mg/L), orientin (380 mg/L), taxifolin deoxyhexose (310 mg/L), homoorientin (250 mg/L), and cyanidin 3-glucoside (180 mg/L) [27].

2.3. Treatments. The animals were orally treated with clarified açaí or saline (10 μL/g body weight) daily for 4 days (Figure 1). Thirty minutes after the last dose, a set of animals received also imipramine (5 or 10 mg/kg, i.p.). At 24 hours following this dose, animals were treated with a single dose

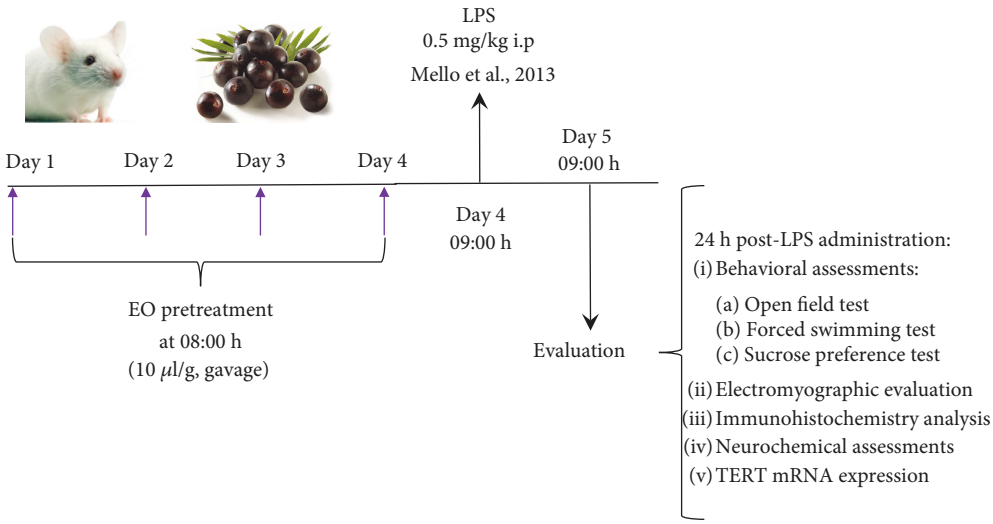

Figure 1: Experimental design of the study. EO, clarified juice of *Euterpe oleracea*; i.p., intraperitoneal; LPS, lipopolysaccharide.

of saline or LPS at 0.5 mg/kg, i.p. to induce by 24 hours the depressive-like behavior that has been described previously [18]. All reagents were obtained from Sigma-Aldrich Corp., St. Louis, USA.

One set of animals was used for the analysis of spontaneous locomotor activity, despair-like behavior, neurochemical evaluations, and mRNA expression. After behavior assessments, all animals were sacrificed by cervical dislocation, and the prefrontal cortices, hippocampi, and striata were stored at -20°C (part of the tissue was previously frozen in liquid nitrogen and the other part maintained in RNA-later solution; Thermo Fisher Scientific, São Paulo, Brazil), until analysis.

Electromyographical analysis, immunohistochemical evaluations, and the study of anhedonia-like behavior were performed separately in different sets of animals as described below.

2.4. Behavioral Evaluations. Twenty-four hours after the administration of LPS, behavioral evaluations (mobility in open-field and forced swimming or sucrose preference test) were performed.

2.4.1. Assessment of Spontaneous Locomotor Activity (Open-Field Test). The animals were placed into an open-field arena (30 × 30 × 15 cm) with white walls and a black floor, divided into nine squares of equal areas. Spontaneous locomotor activity was observed for 5 minutes, and the number of crossed quadrants (crossings), total distance, rearings, and groomings were recorded [31].

2.4.2. Assessment of Despair-Like Behavior (Forced Swim Test). After the open-field test, the animals were placed in an acrylic transparent cylinder (25 cm height and 10 cm diameter) containing water at 22-24°C. After 1 minute of habituation, immobility time (in seconds) was recorded for a period of 5 minutes. Immobility was defined as an absence of active behaviors such as swimming, jumping, rearing, or diving [32, 33]. Animals presenting difficulties keeping their heads above water were removed and excluded.

2.4.3. Assessment of Anhedonia Behavior (Sucrose Preference Test). The presence of anhedonia behavior was tested in a different set of animals as described by Mao et al. [34]. At 48 hours before LPS administration (concomitant with pretreatment with EO or saline), animals were habituated to the consumption of 1% (*w*/*v*) sucrose solution for 24 hours. Then, the sucrose solution was replaced by water for an additional 24 hours. Animals were deprived of water and food before LPS administration. Twenty-four hours later, they were individually housed in cages with free access to two bottles, one containing water and the other containing 1% sucrose solution. Volumes consumed of each bottle were recorded after 1 hour, and the sucrose preference was calculated as follows:

$$\text{Sucrose preference} = \frac{\text{sucrose consumption}}{\text{water consuption} + \text{sucrose consuption}} \times 100\%. \quad (1)$$

2.5. Electromyographic Evaluations. For additional evaluation of the despair/scape-like behavior, we performed electromyographic measurements. After the treatments, stainless-steel-conjugated electrodes were implanted in the semitendinosus muscle of the limbs of a subgroup of animals to acquire electromyographic records, with a recording time of 5 minutes for each animal. Electrodes were connected to a high-impedance amplifier (Grass Technologies, P511), monitored by an oscilloscope (Protek, 6510). The entire analysis was performed inside a Faraday cage. Data were continuously scanned at a rate of 1 kHz by a computer equipped with a data acquisition board (National Instruments, Austin, TX) and processed through specialized software (LabVIEW express).

The amplitude graphs show the potential difference between the reference and the electrode. A total of 1000 samples per second were observed. The spectrograms were calculated using a Hamming window with 256 points (256/1000 s), and each frame was generated with an overlap of 128 points per window. For each frame, the spectral power density (SPD) was calculated by the Welch average periodogram method. The frequency histogram was generated by the first PSD calculation of the signal using the Hamming window with 256 points, without overlap, with the PSD, resulting in a histogram constructed with boxes of 1 Hz.

2.6. Neurochemical Assessments

2.6.1. Evaluation of Lipid Peroxidation. Lipid peroxidation was assayed by evaluating thiobarbituric acid-reactive substances [35]. Briefly, samples were slowly thawed and homogenized in Tris-HCl solution. Aliquots of these homogenates were mixed with 10% trichloroacetic acid and 0.67% thiobarbituric acid. They were then heated in a boiling water bath for 15 minutes and immediately placed in ice. Absorbance at 532 nm was recorded and compared to that of standard solutions of malonaldehyde (MDA). Lipid peroxidation was expressed as micromoles of MDA/g tissue.

2.6.2. Assay of Nitrite Levels. The production of nitric oxide was indirectly evaluated by the nitrite levels in the tissue as described by Green [36]. Aliquots of the homogenates were incubated at room temperature for 10 minutes with equal volumes of the Griess solution (1% sulfanilamide in 1% H_3PO_4 : 0.1% N-(1-naphthyl)-thylenediamine dihydrochloride : distilled water; 1 : 1 : 1) at room temperature for 10 minutes. The absorbance was recorded at 560 nm and compared to those of standard solutions of sodium nitrite. Nitrite levels were expressed as micromoles of nitrites per milligram of tissue.

2.7. TERT mRNA Expression.

TERT mRNA expression was determined by two-step quantitative reverse transcription PCR (RT-qPCR) using the TaqMan Gene Expression Assay, as described by Silva et al. [37]. Briefly, total RNA was extracted with the Tri Reagent (Applied Biosystems, USA) following the manufacturer's instructions. A NanoDrop spectrophotometer (Kisker, Germany) was used to evaluate the RNA concentration and quality along with 1% agarose gels. The synthesis of complementary DNA was performed using the High-Capacity cDNA Reverse Transcription Kit (Applied Biosystems, Poland).

RT-qPCR was performed using StepOnePlus equipment (Applied Biosystems, Brazil) with TaqMan® Universal PCR Master Mix and TaqMan probes (Applied Biosystems, Brazil). The GAPDH gene was selected as an internal control for RNA input and reverse transcription efficiency. All qRT-PCR reactions were run in triplicate with a final volume of 10 μL for the target gene (TERT: Hs00972656_m1) and the internal control (GAPDH: NM_002046.3), for 40 cycles, using the standard cycling conditions of the machine.

Relative quantification of the gene expression was calculated by the $\Delta\Delta$Ct method and expressed as the fold change proposed by Livak and Schmittgen [38]. In the present study, the control group was designated as the calibrator.

2.8. Immunohistochemistry Analysis for Hippocampal Mature Neurons. Animals were deeply anesthetized by intraperitoneal injection of ketamine and xylazine solution for subsequent transcardiac perfusion. First, saline solution (pH 7.4) heparinized 0.9% and then paraformaldehyde (Sigma-Aldrich, USA) 4% were used in the perfusion system for fixation of the brains. Then, the brains were removed and postfixed for 4 hours in Bouin's solution with dehydration and clarification in hydroalcoholic solutions with increasing concentrations and xylol. The specimens were subsequently embedded in Paraplast® (McCormick Scientific, USA). The coronal sections of the anterior hippocampus were sliced on a microtome at 5 μm of thickness. For immunohistochemical assays, the slides were pretreated with poly-D-lysine (Sigma-Aldrich) prior to the placement of sections.

Sections were immunolabeled for mature neurons (anti-NeuN: 1 : 100, Millipore). For this purpose, tissue antigen sites were recovered by heating at 60°C in citrate buffer for 20 minutes and cooled naturally. For the inhibition of the endogenous peroxidase, slides were treated with hydrogen peroxide solution in methanol for 20 minutes. After three consecutive 10-minute washes in phosphate-buffered saline- (PBS-) Tween (Sigma-Aldrich), the sections were incubated in 10% normal horse serum in PBS for 2 hours. Sections were then incubated with the primary antibody diluted in PBS previously coated overnight, with subsequent washes in PBS-Tween, and incubated with the biotinylated secondary antibody, diluted in PBS for 2 hours. They were washed again in PBS-Tween to be incubated with an avidin-biotin-peroxidase complex (ABC Kit, Vector Laboratories, USA) for 1 hour. Sections were then exposed in DAB for 40 seconds, dehydrated in alcohol and xylol, and coverslipped. Some slides were counterstained with hematoxylin for histological delimitations. More details about this protocol have been described previously [39–41].

The photomicrographs were taken with a Moticam system coupled to a Nikon Eclipse 50i optic photomicroscope. For quantification of positive cells for anti-NeuN, we used the light optical microscope Nikon Eclipse E2000 with a 1 mm^2 grid in the eyepiece, under 40x objective magnification. In the dorsal hippocampus, three fields from each region (CA1, CA3, and dentate gyrus) were counted, as described elsewhere [39–41].

2.9. Statistical Analyses.

Statistical analyses were performed using GraphPad Prism (version 5.0). The normality and homoscedasticity of the data were verified using the D'Agostino-Pearson test and the Bartlett test, respectively. Data are presented as mean and standard deviation (SD) and were analyzed using one-way analysis of variance followed by Tukey's post hoc test, when appropriate. $P < 0.05$ was considered significant for all analyses.

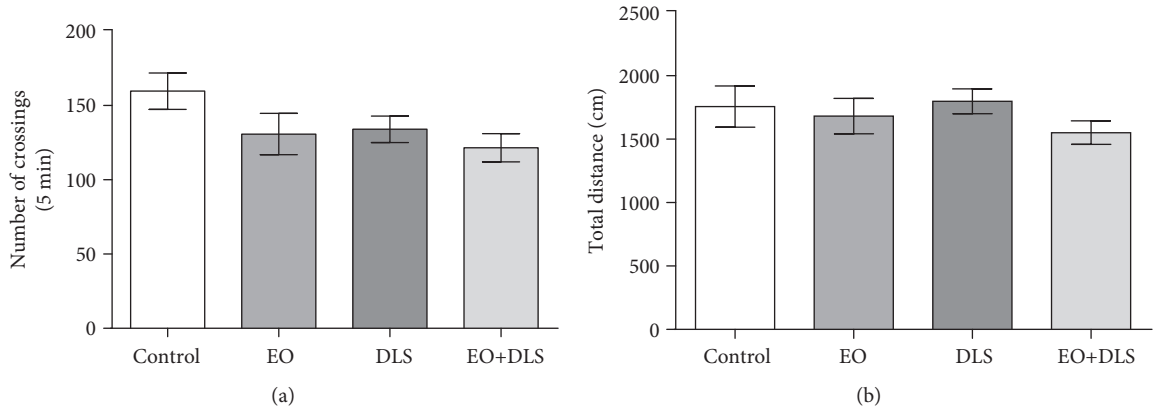

Figure 2: Spontaneous locomotor activity of mice in a depressive-like state (DLS) and/or treated with clarified açaí (EO): number of crossings in 5 min (a) and total distance covered (b). Data are presented as mean ± SD ($n = 10$). No significant difference was detected.

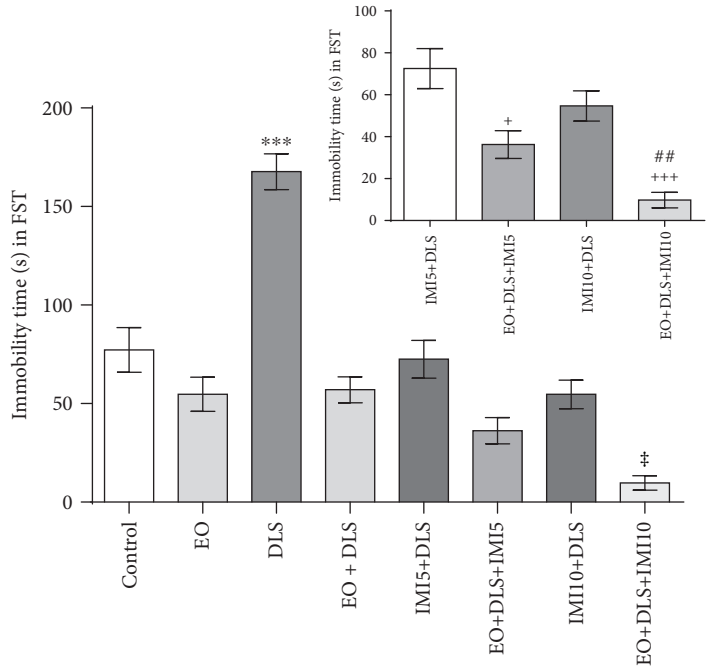

Figure 3: Despair-like behavior (immobility time) in the forced swim test of mice in a depressive-like state (DLS) and/or treated with clarified açaí (EO) and/or imipramine (5 or 10 mg/kg, IMI5 or IMI10, respectively). The inset shows the statistical analysis when only four groups were considered. Data are presented as mean ± SD ($n = 5$). $^{***}P < 0.001$ vs. all groups, $^{‡}P < 0.05$ vs. control, $^{+}P < 0.05$ and $^{+++}P < 0.001$ vs. IMI5 + DLS, and $^{\#\#}P < 0.01$ vs. IMI10+LPS.

3. Results

EO treatment did not interfere with the spontaneous locomotor activity, as demonstrated by the number of crossings and the total distance traveled in the open-field test (Figure 2).

As expected, 24 hours after LPS exposure the immobility time in the forced swim test increased significantly, indicating a depressive-like state (DLS) (Figure 3), which EO treatment reduced to control levels. Moreover, when groups treated with imipramine (given as IMI in the graphs) were compared separately (Figure 3, inset), significant differences between the therapeutic treatment with imipramine (the IMI5+DLS and IMI10+DLS groups) and the treatments with both EO and IMI (the EO+DLS+IMI5 and EO+DLS+IMI10 groups) were detected. Although additional experiments are necessary, this fact may point to a certain degree of synergism between EO and imipramine. Despite this possible synergism, the antidespair effect of EO treatment alone was as effective as that of imipramine.

In the sucrose preference test, animals showed a significant decrease in sucrose consumption (anhedonia behavior) caused by LPS administration, corroborating the depression-like state of the animals (Figure 4). Again, EO treatment completely

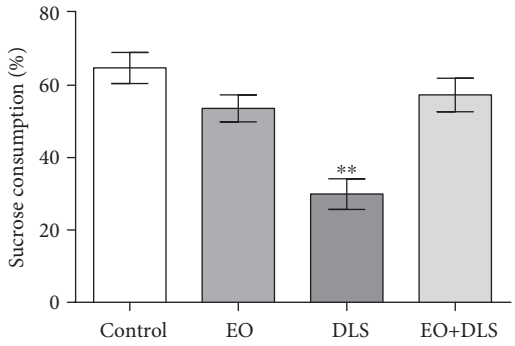

Figure 4: Anhedonia behavior (reduced sucrose consumption) of mice in a depressive-like state (DLS) and/or treated with clarified açaí (EO). Data are presented as mean ± SD ($n = 13$). $^{**}P < 0.01$ vs. all groups.

prevented the anhedonia-like state induced by LPS, supporting the potent antidepressant effect of this treatment.

As an additional approach to assessing the despair/scape-like behavior, we performed electromyographic measurements with 5-minute recordings of the muscular responses to stimulus from the electrode implantation. Control and EO-treated animals showed energy levels up to 50 Hz (Figure 5) corresponding to normal muscle activity. However, LPS administration caused a significant decrease in muscle activity that was entirely prevented by EO. In fact, the muscular activity of the animals that received both LPS and EO treatments was similar to that of control animals.

The results of the forced swim test and electromyography together show that EO prevented immobility or the absence of response to stimulus, representing a significant improvement in one of the more characteristic symptoms of depressive-like behavior.

The animals with depressive-like behavior (as confirmed by the behavioral tests) presented a significant decrease (as low as 49%) of the expression of TERT in these three areas that was completely reversed by EO treatment (Figure 6). Of interest, EO alone significantly increased the expression of TERT mRNA in the three brain areas evaluated (Figure 6).

When thiobarbituric acid-reactive substances were analyzed to evaluate oxidative stress burden, mice with depressive-like behavior (as confirmed by the behavioral tests) presented high levels of lipid peroxidation in the three examined brain areas (Figure 7). The hippocampus was the most affected, with about two times the levels of lipid peroxidation when compared to control values. Despite this pronounced prooxidant state of the hippocampus, EO treatment totally reverted this scenario, eliminating the presence of lipid peroxidation products (Figure 7).

The hippocampus was the area most affected by the lipid peroxidation; oxidative stress is a known inducer of telomere shortening and aging, and the presence of TERT was reduced, and it is essential to protect against this deleterious effect. Given these findings, we analyzed their association with neuronal death, one of the most serious cellular consequences of oxidative stress and a probable cause, at least in part, for the depressive-like behavior.

Immunochemical studies in the hippocampus revealed a significant decrease in NeuN-positive cells in CA1 (Figure 8), CA3 (Figure 9), and dentate gyrus (Figure 10) of the animals presenting the depressive-like behavior. In all the three regions, EO protected the hippocampal cells, preventing the neuronal death associated with the DLS.

To confirm the important role of oxidative stress in the neuronal death detected in the hippocampus, we also measured nitrite levels as indirect markers of the production of one of the major free radicals, nitric oxide (Figure 11). Significantly high levels of nitrites were detected in animals with depressive-like behavior, pointing to an exacerbated nitric oxide production. This increase in products of this free radical was not observed in animals that received EO, demonstrating the potent antioxidant property of this fruit.

4. Discussion

This study is the first to demonstrate that EO juice for human consumption prevents the depressive-like behavior in an *in vivo* model. The potent antidepressant influence of EO was associated with antioxidant and antiaging effects in three major brain regions involved in mood regulation. Additionally, treatment with EO significantly protected hippocampal neurons and reduced the nitrite levels (an indirect marker of nitric oxide production).

Açaí juice is frequently consumed by Amazonian populations, and the clarified juice is available in the international market as a base for soft drinks [20]. In 2015, the State of Pará in Brazil alone consumed more than one million tons of açaí and exported more than 6 million tons of a mixture (açaí+banana+guaraná) to the United States and Japan [42]. The EO dose used in this work (equivalent to 750 mL for an adult of 70 kg, approximately) reproduces the daily intake of human populations in the northern region of Brazil (usually 300-1000 mL daily) [20]. This work tested for the first time commercial samples of EO (of known composition) in a model of depression, which guaranteed reproducibility of the preparation and relevance for human intake. Additionally, EO by gavage, not by free access to food, ensured that all animals received the same treatment.

In this study, we used a model of depressive-like behavior induced by the administration of a low dose of LPS (less than 20 times the dose used for endotoxemia models) [43]. The behavioral alterations in this model mimic some characteristics of clinical depression in humans [33, 44] and meet all the criteria (apparent, constructive and predictive validity) necessary for an animal model [45], being widely used for the screening of potential antidepressant drugs with good specificity and sensitivity [46]. Indeed, LPS exposure mimics a situation of increased plasma bacterial translocation. In line with this evidence, a recent study revealed that patients with depression present increased gut permeability and increased plasma levels of LPS when compared to unaffected people [19]. The presence of higher LPS plasma levels in patients with depression may trigger peripheral inflammatory and oxidative alterations by the activation of the Toll-like receptor 4. These cytokines may reach the brain, causing

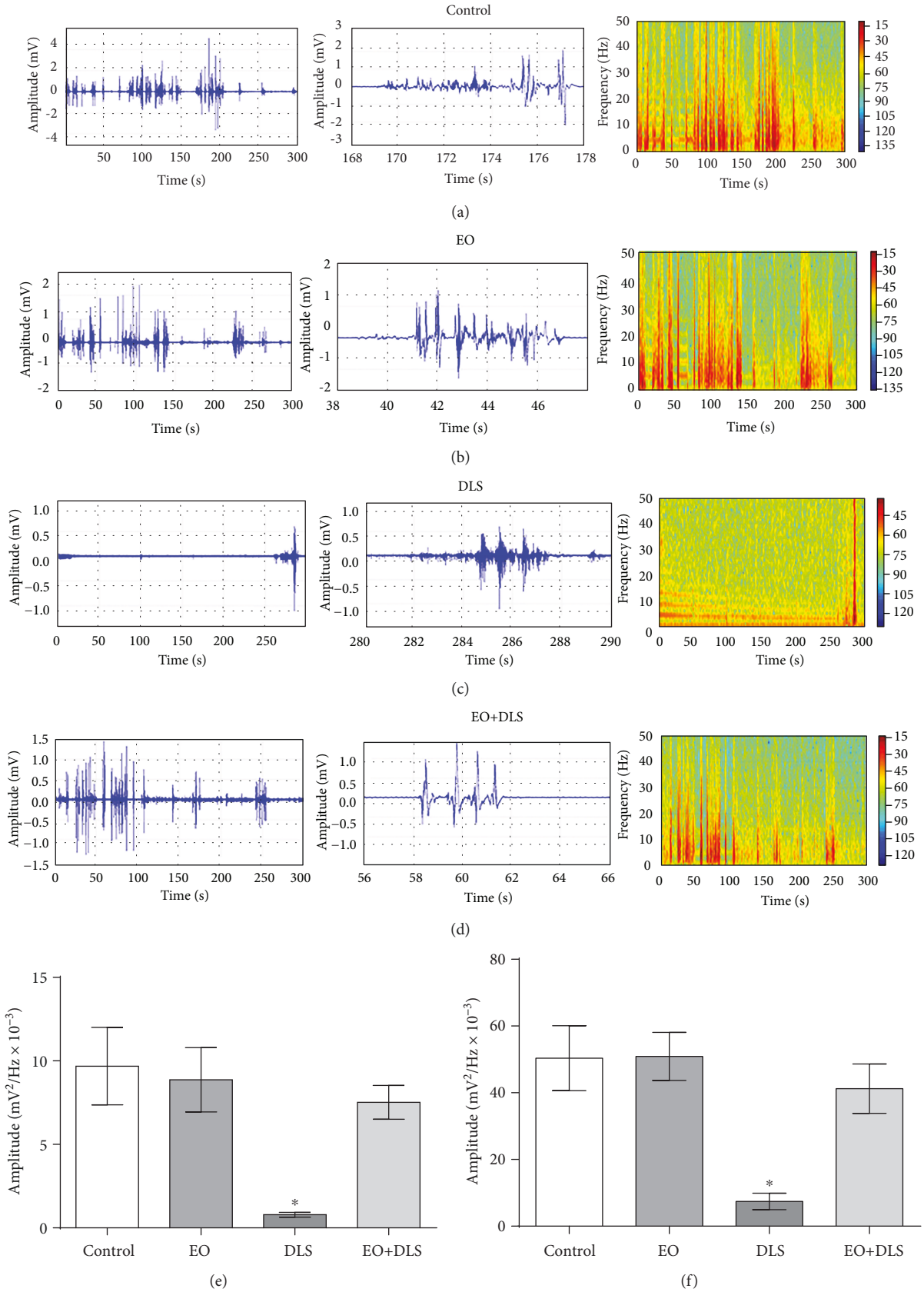

Figure 5: Electromyographic recordings and energy distributions (a-d), amplitude distributions (e), and amplitudes of the maximum muscular activity (f) of the frequencies up to 50 Hz recorded for 5 min in mice in a depressive-like state (DLS) and/or treated with clarified açaí (EO). Data in (e) and (f) are presented as mean ± SD ($n = 5$). $^*P < 0.05$ vs. all groups.

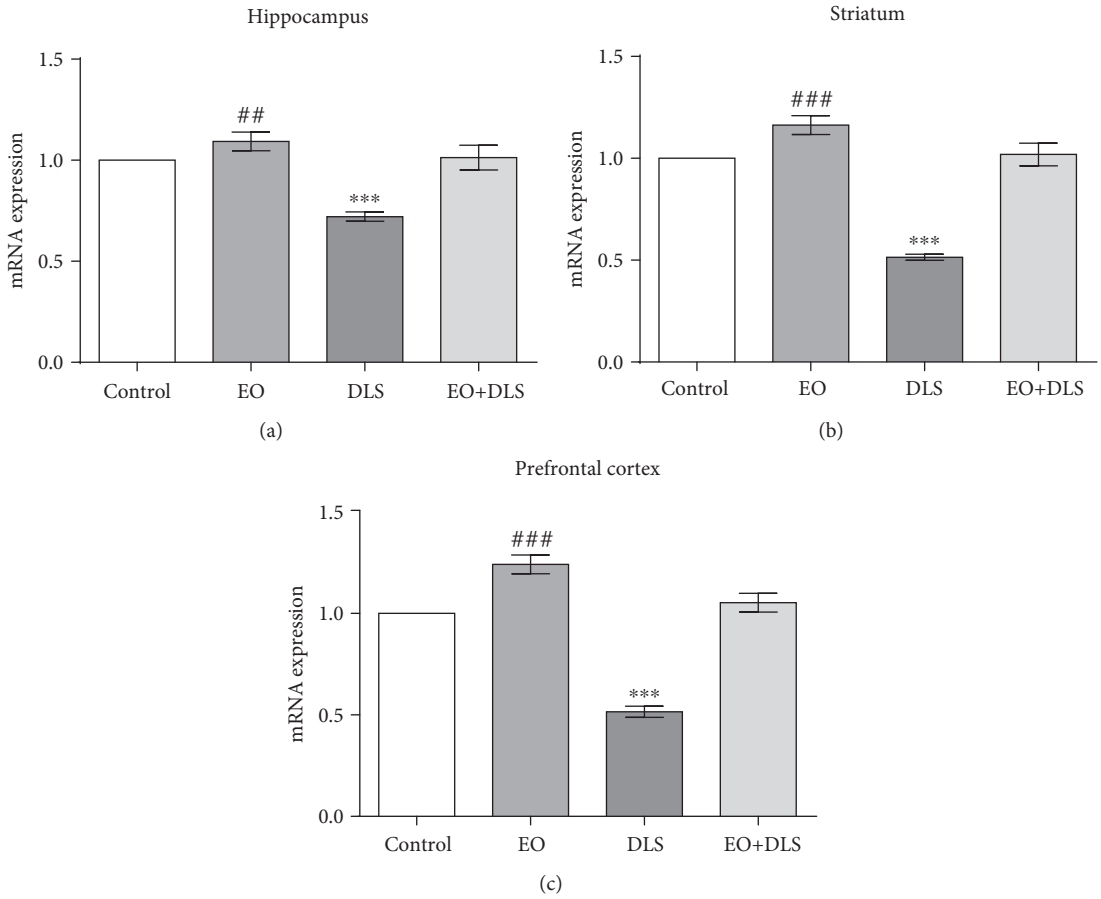

Figure 6: Relative expression of telomerase reverse transcriptase (TERT) mRNA in the hippocampus (a), striatum (b), and prefrontal cortex (c) of mice in a depressive-like state (DLS) and/or treated with clarified açaí (EO). Data are presented as mean ± SD (n = 5-6). $^{***}P < 0.001$ vs. all groups and $^{###}P < 0.001$ and $^{##}P < 0.01$ vs. control.

neuroinflammatory alterations and compromising neurotransmission mechanisms [47].

In this model, it is important to demonstrate the establishment of the depressive-like behavior with no symptom of sickness behavior (such as alterations in locomotor activity), because factors such as sex can influence the outcomes [48]. Our results demonstrated no alterations in the number of crossings and total distance covered in the open-field test, supporting the absence of sickness behavior in the LPS-treated animals (Figure 2). EO treatment alone did not change body weight (data not shown) or spontaneous locomotor activity (Figure 2), and it did not cause anhedonia/despair-like behaviors (Figures 3 and 4), confirming previous results regarding a lack of behavioral toxicity of the fruit [26].

Animals treated with LPS, however, presented much longer immobility in the forced swim test and consumed significantly less sucrose in the sucrose preference test (Figures 3 and 4). The latter tests are gold-standard methods for evaluating the depressive-like phenotype in rodents, especially to demonstrate the presence of despair-like and anhedonia behaviors [44, 49]. In our study, the increased immobility time and reduced sucrose consumption support the presence of a depressive-like phenotype in the animals. This study also applied reliable electromyographic measurements to confirm the DLS in the animals, an innovative method which may be more sensitive than behavioral testing alone (Figure 5).

Despite evident DLS in LPS-treated animals, the regular consumption of EO for 4 days was enough to eliminate all of these changes (Figures 3–5). Of interest, in the forced swim test, this protection was similar to that conferred by imipramine (Figure 3), pointing to a probable synergistic effect of EO and this drug (Figure 3, inset). Imipramine is a classical tricyclic antidepressant that blocks transport of monoamines, increasing serotonin and norepinephrine levels in the synaptic cleft. In addition to the modulation of the monoaminergic system, imipramine exerts antidepressant effects through its antioxidant activity [18]. In a similar way, the antidepressant effect of EO could be attributable to the inhibition of the monoaminergic system, in addition to potent antioxidant properties of the fruit. This hypothesis is supported by the modulatory effects that some açaí compounds (such as ellagic acid, ferulic acid, gallic acid, apigenin, rutin, and resveratrol) exert on the monoaminergic system [28, 29, 50–52]. Similar effects on the same targets could explain the apparent synergism observed in our work.

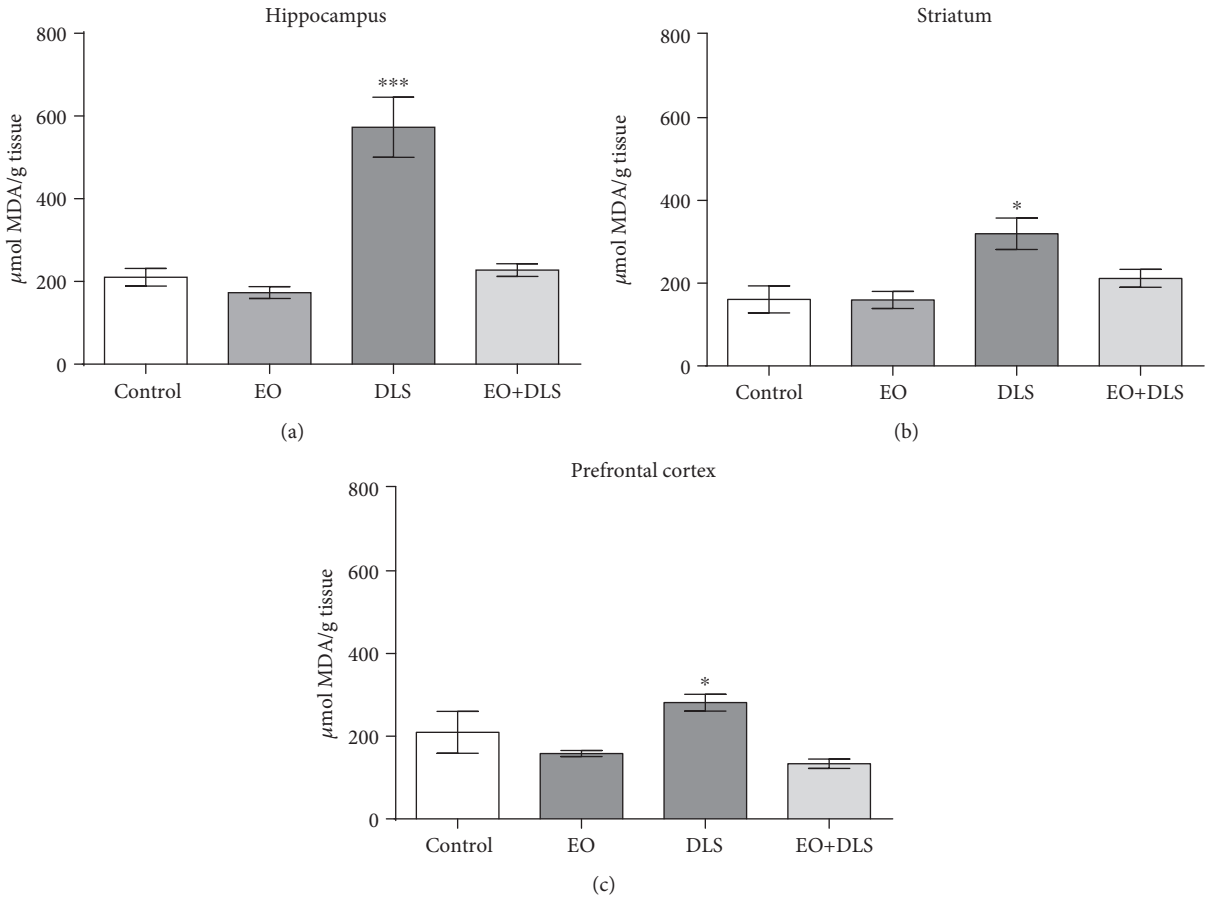

Figure 7: Lipid peroxidation in the hippocampus (a), striatum (b), and prefrontal cortex (c) of mice in a depressive-like state (DLS) and/or treated with clarified açaí (EO). Data are presented as mean ± SD of μmol of malonaldehyde (MDA)/g tissue ($n = 6$-10). $^{*}P < 0.05$ and $^{***}P < 0.001$ vs. all groups.

Although additional studies are necessary to confirm this possible synergism and their molecular mechanisms, our results are already promising for the treatment of depression because supplementation with EO may eventually allow for reduced doses of drugs with high toxicity, such as tricyclic antidepressants. Moreover, based on preclinical data, the protective effect of EO would be at least as potent as that of classical drugs used in depression, such as the SSRIs (fluoxetine and paroxetine), the serotonin-norepinephrine reuptake inhibitors (venlafaxine), or the tricyclic antidepressants (imipramine), as demonstrated by our results and those in the literature involving the same model [53, 54]. Although decreased serotoninergic and adrenergic actions were considered for many years to be the main explanation for depression and targets for drug development, other phenomena such as neuroinflammation, neurotrophism, or oxidative stress also play a major role and are targets for the development of new antidepressant therapies.

Among the most recent phenomena associated with MDD, an accelerated biological aging process has been related to clinical depression in epidemiological studies [3, 5, 6]. In these studies, aging was characterized by a significant decrease in telomere length and TERT expression in human peripheral and central nervous system cells [3–6]. Moreover, preclinical data demonstrated that inhibition of hippocampal TERT activity abolishes the behavioral effects of antidepressant drugs such as fluoxetine, supporting a close relationship between TERT activity and antidepressant effects [55].

In animal models of depressive-like behavior, reduced TERT expression has been reported in tissues such as the liver and hippocampus [55–57], but this study is the first to show a significant decrease in three major brain regions (the hippocampus, striatum, and prefrontal cortex) involved in depression (Figure 6). This pronounced decrease (between 25% to 50%) of the de novo synthesis of TERT may be partially responsible for the long-term deleterious consequences associated with depression, such as accelerated brain aging and increased susceptibility to age-related disorders. In our work, four doses of EO were enough to completely restore the expression of the enzyme (Figure 6), an effect similar to that described for treatments with classical antidepressants such as fluoxetine (10 mg/kg per day, for 28 days) [55]. This fact confirms the important role of TERT in the treatment of depression and the potency of the antidepressant effect of the fruit.

An interesting result was that EO alone could significantly increase TERT mRNA expression in these three brain

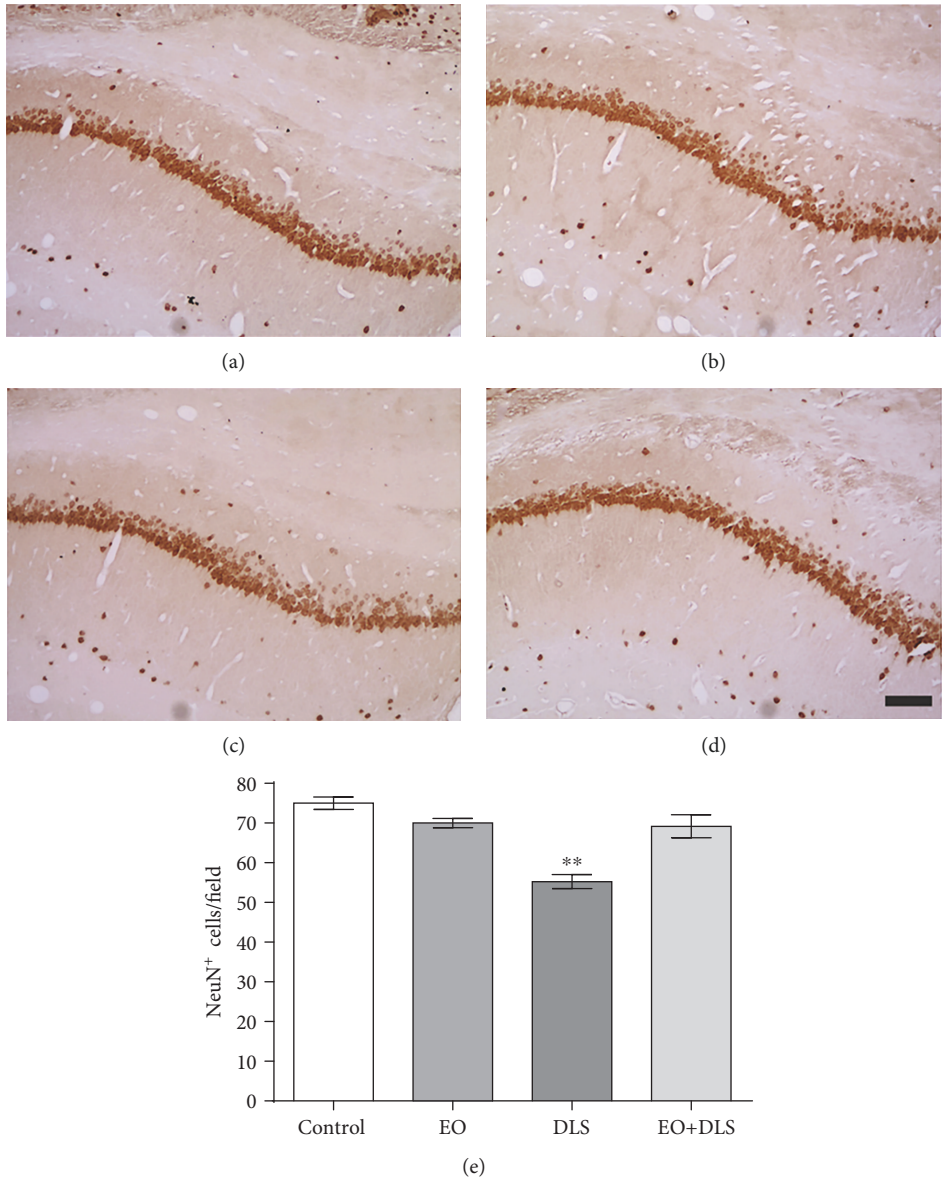

Figure 8: NeuN-positive cells in the CA1 region of the hippocampus of mice in a depressive-like state (DLS) and/or treated with clarified açaí (EO). Representative microphotographs of control (a), EO (b), DLS (c), and DLS+EO (d) samples and quantitation of NeuN-positive cells (e). Data are presented as mean and SD ($n = 4$-5). $^{**}P < 0.01$ vs. all groups. Scale bar: μm.

areas, revealing a potent antiaging action of the fruit (Figure 6). The brain is especially susceptible to aging and age-related disorders, with serious effects on the quality of life of patients and their families. Additional studies will permit a better understanding of the antiaging effect of EO that we report here.

The presence of TERT is essential, especially in conditions of exacerbated oxidative stress, a known inducer of telomere shortening [58–60]. The oxidative profile of this model is largely known in the literature, with characteristics such as increased lipid peroxidation and decreased antioxidant defenses, especially involving glutathione ([18]; Tanaguti et al., 2019; Tanaguti et al., 2018). In fact, lipid peroxidation (evaluated using MDA levels) is frequently used in this model as the main hallmark of the consequences of oxidative stress on macromolecules ([18]; Domingues et al., 2018; Tanaguti et al., 2019; Tanaguti et al., 2018). In our work, animals in a DLS had significantly high levels of lipid peroxidation in the three studied brain areas (the hippocampus, striatum, and prefrontal cortex) (Figure 7), confirming earlier findings. Lipid peroxidation is frequently increased in both patients with depression [61] and in animals in a DLS ([33]; and this study).

The treatment with EO completely reversed this scenario, maintaining the levels of lipid peroxidation as low as those detected in the control group (Figure 7). This result is not surprising considering that an EO dilution of 1 : 100 has stronger scavenger properties than 800 μM Trolox (a soluble analogue of vitamin E) [26]. This potent antioxidant activity of açaí is mainly exerted by anthocyanins, proanthocyanidins,

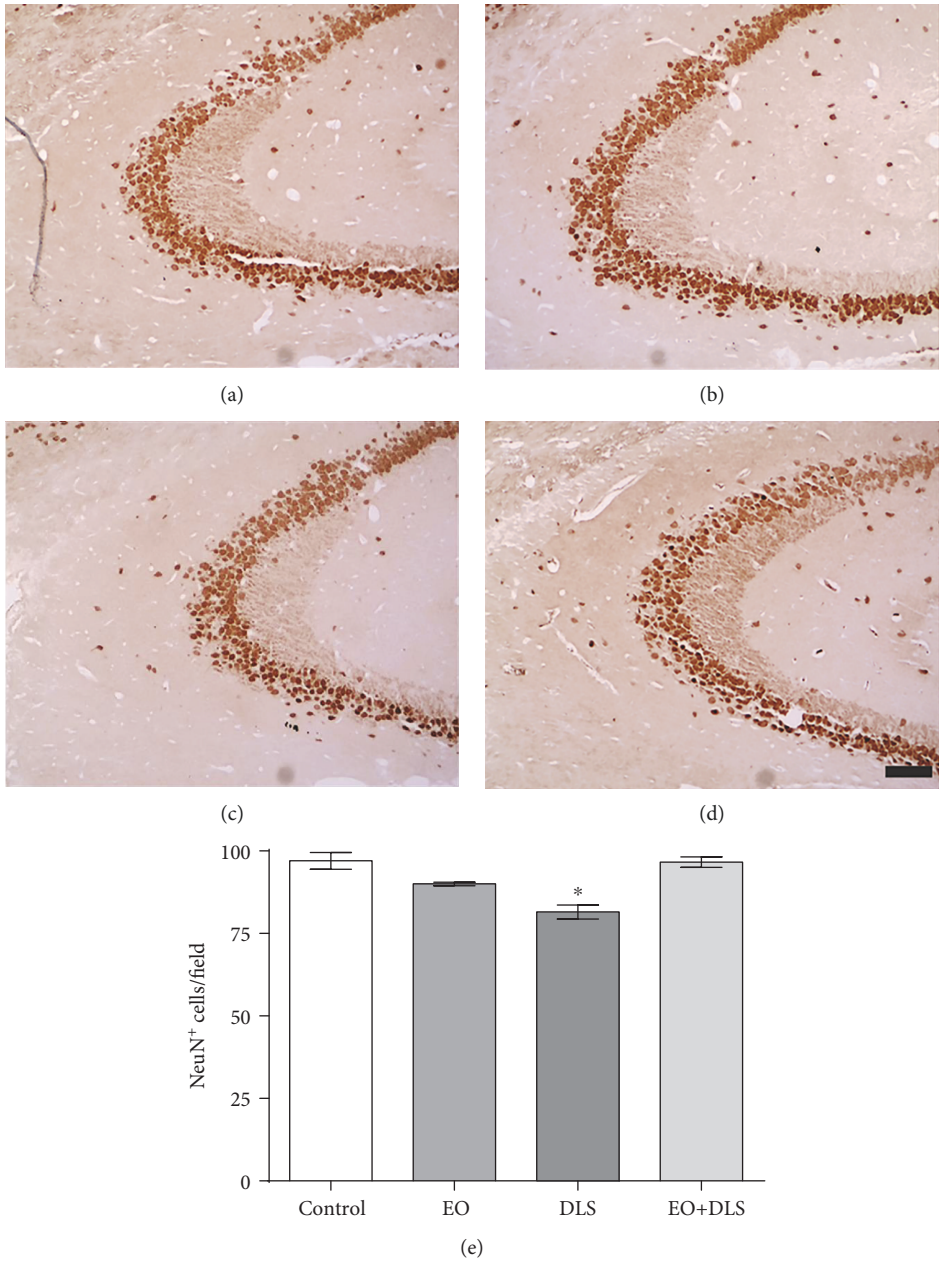

Figure 9: NeuN-positive cells in the CA3 region of the hippocampus of mice in a depressive-like state (DLS) and/or treated with clarified açaí (EO). Representative microphotographs of control (a), EO (b), DLS (c), and DLS+EO (d) groups and quantitation of NeuN-positive cells (e). Data are presented as mean and SD ($n = 4$-5). $^*P < 0.05$ vs. all groups. Scale bar: μm.

flavonoids, and liganins [62], many of which have shown antidepressant properties singly in animal models [63–65]. Recent evidences demonstrated that phenolic compounds, such as anthocyanins, anthocyanidins, and orientin, improves depressive-like behavior [66, 67].

Considering the high potency of the antidepressant effect of the EO treatment observed in this work and the multiple targets that can be influenced by EO, such as GABAergic receptors and transporters [27], free radicals [26], or TERT expression (this study), it seems unlikely that the protective effect we have detected is related to only one compound. Probably, an association of several bioactive components contributes to this effect.

It is noteworthy that the oxidative stress especially affected the hippocampus, which presented about twice the levels of lipid peroxidation when compared to the other areas (Figure 7). This fact, in addition to the decreased TERT mRNA expression (Figure 6), suggests a specifically deleterious scenario for this area. TERT exerts a protective effect in the hippocampus, and hippocampal neurons lacking TERT have increased susceptibility to oxidative stress [68]. To study the possible hippocampal neuronal death in our model and the potential neuroprotection provided by EO, we carried out immunohistochemical analysis in three areas of the hippocampus (CA1, CA3, and dentate gyrus). In addition, the increased oxidative stress was

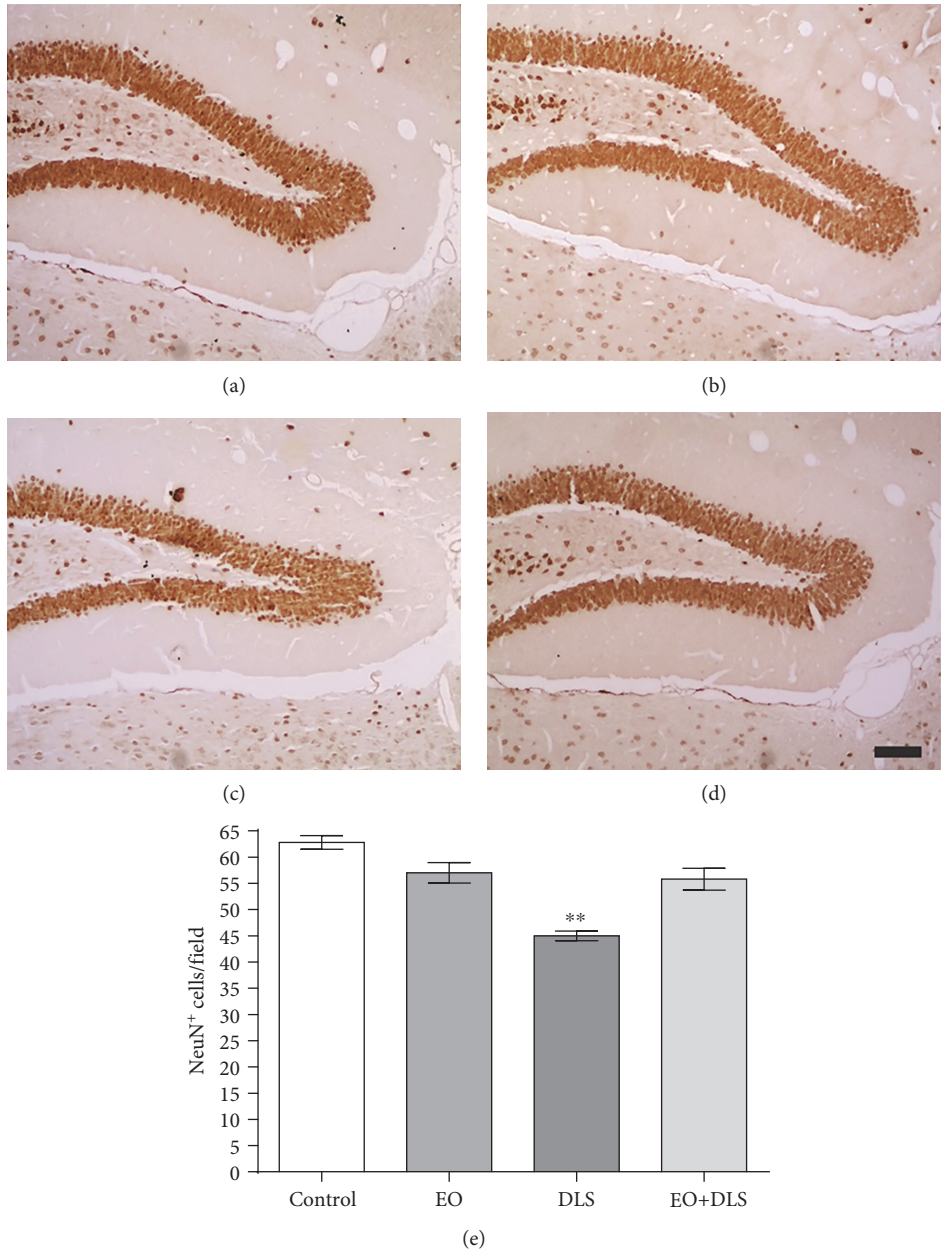

Figure 10: NeuN-positive cells in the dentate gyrus of mice in a depressive-like state (DLS) and/or treated with clarified açaí (EO). Representative microphotographs of control (a), EO (b), DLS (c), and DLS+EO (d) groups and quantitation of NeuN-positive cells (e). Data are presented as mean ± SD (n = 4-5). $^{**}P < 0.01$ vs. all groups. Scale bar: μm.

confirmed by quantifying levels of nitrites, an indirect marker of nitric oxide production.

Our results showed that animals in a DLS had significantly decreased NeuN-positive cells in all three regions (Figures 8–10) and increased hippocampal levels of nitrites (Figure 11). Our data are in agreement with previous studies suggesting a prominent role of nitric oxide and the nitrergic pathway in the pathophysiology of depression and in the modulation of the behavioral and neurochemical changes observed in this model [33, 69].

The evident neuronal death detected in the hippocampus confirms the deleterious consequences of simultaneously increasing oxidative stress and decreasing TERT expression. The neuronal loss of the hippocampal regions (as high as 30.2%) would be in agreement with the reduced hippocampal volume observed in patients with depression [70, 71], apparently specific to the *cornu ammonis* and dentate gyrus areas [70], and responsible for some well-documented cognitive deficits (especially related to learning and memory) that accompany major depression [70, 71].

The potent neuronal protection observed with the EO treatment that completely abolished the hippocampal neuronal loss (Figures 8–10) suggests a general, if not universal, effect of EO for the brain. The treatment used in this work has already been suggested to protect neurons against other severe conditions, such as generalized seizures [26].

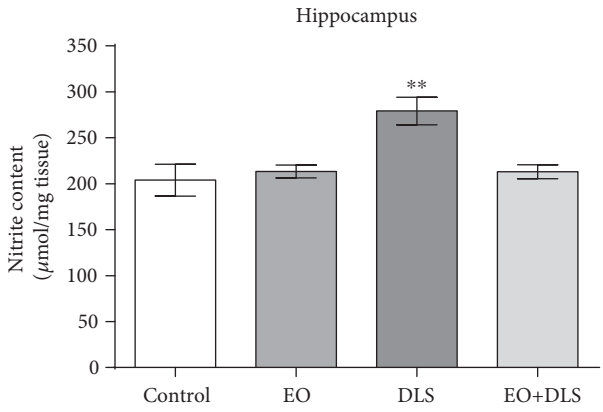

FIGURE 11: Nitrite levels in the hippocampus of mice in a depressive-like state (DLS) and/or treated with clarified açaí (EO). Data are presented as mean ± SD ($n = 10$). $^{**}P < 0.01$ vs. all groups.

In summary, our results demonstrated an antidepressant effect of EO at different levels of analysis (behavioral, cellular, biochemical, and molecular). This potent effect (apparently, as potent as imipramine) was observed with only four doses of EO, similar in content to typical human consumption. Moreover, EO appeared to improve the effects of antidepressant drugs, such as imipramine, on depressive conditions. Our results, in addition to the absence of toxic effects for humans who consume similar amounts of the clarified juice [72], support the use of this fruit as an important protection for the brain against the development of depressive-like disorders. Moreover, for the first time, we describe an antiaging effect of EO that suggests neuroprotection against long-term age-related consequences.

Abbreviations

EO: Clarified juice of *Euterpe oleracea*
DM: Dry matter
LPS: Lipopolysaccharide
TBARS: Thiobarbituric acid-reactive substance
MDA: Malondialdehyde.

Data Availability

The data used to support the findings of this study are available from the corresponding author upon request.

Disclosure

The funders had no role in study design, data collection and analysis, decision to publish, or preparation of the manuscript.

Conflicts of Interest

Authors declare that no conflicts of interest exist. The donations from Amazon Dreams or Instituto Evandro Chagas do not imply any competing interests and they do not alter the authors' adherence to the policies of Oxidative Medicine and Cellular Longevity journal.

Acknowledgments

We thank Instituto Evandro Chagas (IEC, Brazil), Amazon Dreams (Pará, Brazil), and Federal University of Ceara (UFC, Brazil) for kindly providing the animals and the samples of clarified açaí juice for this study. This work was supported by Conselho Nacional de Desenvolvimento Científico e Tecnológico (CNPq, Brazil; grant numbers 427784/2018-2, 467143/2014-5, and 307564/2017-7) and Pró-Reitoria de Pesquisa da UFPA (PROPESP, UFPA, Brazil). J.L.M. do Nascimento, R.R. Burbano, H. Rogez, and M.E. Crespo-López thank CNPq for their researcher awards. Also, J.R. Souza-Monteiro, and G.P.F. Arrifano thank Coordenação de Aperfeiçoamento de Pessoal de Nivel Superior (CAPES, Brazil) for their PhD and post-doctoral fellowships, respectively.

References

[1] WHO, "Depression," 2018, February 2019, https://www.who.int/en/news-room/fact-sheets/detail/depression.

[2] G. E. Hodes, V. Kana, C. Menard, M. Merad, and S. J. Russo, "Neuroimmune mechanisms of depression," *Nature Neuroscience*, vol. 18, no. 10, pp. 1386–1393, 2015.

[3] P. Y. Lin, Y. C. Huang, and C. F. Hung, "Shortened telomere length in patients with depression: a meta-analytic study," *Journal of Psychiatric Research*, vol. 76, pp. 84–93, 2016.

[4] A. Szebeni, K. Szebeni, T. DiPeri et al., "Shortened telomere length in white matter oligodendrocytes in major depression: potential role of oxidative stress," *The International Journal of Neuropsychopharmacology*, vol. 17, no. 10, pp. 1579–1589, 2014.

[5] M. C. Vance, E. Bui, S. S. Hoeppner et al., "Prospective association between major depressive disorder and leukocyte telomere length over two years," *Psychoneuroendocrinology*, vol. 90, pp. 157–164, 2018.

[6] J. E. Verhoeven, D. Révész, E. S. Epel, J. Lin, O. M. Wolkowitz, and B. W. J. H. Penninx, "Major depressive disorder and accelerated cellular aging: results from a large psychiatric cohort study," *Molecular Psychiatry*, vol. 19, no. 8, pp. 895–901, 2014.

[7] R. Admon, L. M. Holsen, H. Aizley et al., "Striatal hypersensitivity during stress in remitted individuals with recurrent depression," *Biological Psychiatry*, vol. 78, no. 1, pp. 67–76, 2015.

[8] J. Jin and S. Maren, "Prefrontal-hippocampal interactions in memory and emotion," *Frontiers in Systems Neuroscience*, vol. 9, p. 170, 2015.

[9] V. Maletic, M. Robinson, T. Oakes, S. Iyengar, S. G. Ball, and J. Russell, "Neurobiology of depression: an integrated view of key findings," *International Journal of Clinical Practice*, vol. 61, no. 12, pp. 2030–2040, 2007.

[10] V. Reinhart, S. E. Bove, D. Volfson, D. A. Lewis, R. J. Kleiman, and T. A. Lanz, "Evaluation of TrkB and BDNF transcripts in prefrontal cortex, hippocampus, and striatum from subjects with schizophrenia, bipolar disorder, and major depressive disorder," *Neurobiology of Disease*, vol. 77, pp. 220–227, 2015.

[11] M. Pandya, M. Altinay, D. A. Malone Jr., and A. Anand, "Where in the brain is depression?," *Current Psychiatry Reports*, vol. 14, no. 6, pp. 634–642, 2012.

[12] C. N. Black, M. Bot, P. G. Scheffer, P. Cuijpers, and B. W. J. H. Penninx, "Is depression associated with increased oxidative stress? A systematic review and meta-analysis," *Psychoneuroendocrinology*, vol. 51, pp. 164–175, 2015.

[13] S. Y. Lee, S. J. Lee, C. Han, A. A. Patkar, P. S. Masand, and C. U. Pae, "Oxidative/nitrosative stress and antidepressants: targets for novel antidepressants," *Progress in Neuro-Psychopharmacology & Biological Psychiatry*, vol. 46, pp. 224–235, 2013.

[14] M. Maes, P. Galecki, Y. S. Chang, and M. Berk, "A review on the oxidative and nitrosative stress (O&NS) pathways in major depression and their possible contribution to the (neuro)degenerative processes in that illness," *Progress in Neuro-Psychopharmacology & Biological Psychiatry*, vol. 35, no. 3, pp. 676–692, 2011.

[15] P. Palta, L. J. Samuel, E. R. Miller III, and S. L. Szanton, "Depression and oxidative stress: results from a meta-analysis of observational studies," *Psychosomatic Medicine*, vol. 76, no. 1, pp. 12–19, 2014.

[16] S. Moylan, M. Berk, O. M. Dean et al., "Oxidative & nitrosative stress in depression: why so much stress?," *Neuroscience & Biobehavioral Reviews*, vol. 45, pp. 46–62, 2014.

[17] M. Maes, W. Stevens, L. DeClerck et al., "Immune disorders in depression: higher T helper/T suppressor-cytotoxic cell ratio," *Acta Psychiatrica Scandinavica*, vol. 86, no. 6, pp. 423–431, 1992.

[18] B. S. Ferreira Mello, A. S. Monte, R. S. McIntyre et al., "Effects of doxycycline on depressive-like behavior in mice after lipopolysaccharide (LPS) administration," *Journal of Psychiatric Research*, vol. 47, no. 10, pp. 1521–1529, 2013.

[19] B. R. Stevens, R. Goel, K. Seungbum et al., "Increased human intestinal barrier permeability plasma biomarkers zonulin and FABP2 correlated with plasma LPS and altered gut microbiome in anxiety or depression," *Gut*, vol. 67, no. 8, pp. 1555–1557, 2018.

[20] C. M. G. Bichara and H. Rogez, "Açaí (*Euterpe oleracea*)," in *Postharvest Biology and Technology of Tropical and Subtropical Fruits Vol 2: Açaí to Citrus*, E. Yahia, Ed., vol. 2, Woodhead Publishing, 2011.

[21] K. K. de Lima Yamaguchi, L. F. R. Pereira, C. V. Lamarão, E. S. Lima, and V. F. da Veiga-Junior, "Amazon acai: chemistry and biological activities: a review," *Food Chemistry*, vol. 179, pp. 137–151, 2015.

[22] S. K. Chang, C. Alasalvar, and F. Shahidi, "Superfruits: phytochemicals, antioxidant efficacies, and health effects – a comprehensive review," *Critical Reviews in Food Science and Nutrition*, vol. 59, no. 10, pp. 1580–1604, 2019.

[23] B. J. M. Da Silva, J. R. Souza-Monteiro, H. Rogez, M. E. Crespo-López, J. L. M. Do Nascimento, and E. O. Silva, "Selective effects of *Euterpe oleracea* (açai) on *Leishmania* (*Leishmania*) *amazonensis* and *Leishmania infantum*," *Biomedicine & Pharmacotherapy*, vol. 97, pp. 1613–1621, 2018.

[24] V. da Silva Cristino Cordeiro, G. F. de Bem, C. A. da Costa et al., "*Euterpe oleracea* Mart. seed extract protects against renal injury in diabetic and spontaneously hypertensive rats: role of inflammation and oxidative stress," *European Journal of Nutrition*, vol. 57, no. 2, pp. 817–832, 2018.

[25] G. R. Romualdo, M. F. Fragoso, R. G. Borguini, M. C. P. de Araújo Santiago, A. A. H. Fernandes, and L. F. Barbisan, "Protective effects of spray-dried açaí (*Euterpe oleracea* Mart) fruit pulp against initiation step of colon carcinogenesis," *Food Research International*, vol. 77, Part 3, pp. 432–440, 2015.

[26] J. R. Souza-Monteiro, M. Hamoy, D. Santana-Coelho et al., "Anticonvulsant properties of *Euterpe oleracea* in mice," *Neurochemistry International*, vol. 90, pp. 20–27, 2015.

[27] G. P. F. Arrifano, M. P. Lichtenstein, J. R. Souza-Monteiro et al., "Clarified Açaí (*Euterpe oleracea*) juice as an anticonvulsant Agent: *in vitro* mechanistic study of GABAergic targets," *Oxidative Medicine and Cellular Longevity*, vol. 2018, Article ID 2678089, 6 pages, 2018.

[28] D. Dhingra and R. Chhillar, "Antidepressant-like activity of ellagic acid in unstressed and acute immobilization-induced stressed mice," *Pharmacological Reports*, vol. 64, no. 4, pp. 796–807, 2012.

[29] C. Girish, V. Raj, J. Arya, and S. Balakrishnan, "Evidence for the involvement of the monoaminergic system, but not the opioid system in the antidepressant-like activity of ellagic acid in mice," *European Journal of Pharmacology*, vol. 682, no. 1-3, pp. 118–125, 2012.

[30] R. Li, D. Zhao, R. Qu, Q. Fu, and S. Ma, "The effects of apigenin on lipopolysaccharide-induced depressive-like behavior in mice," *Neuroscience Letters*, vol. 594, pp. 17–22, 2015.

[31] J. Archer, "Tests for emotionality in rats and mice: a review," *Animal Behaviour*, vol. 21, no. 2, pp. 205–235, 1973.

[32] R. D. Porsolt, "Animal model of depression," *Biomedicine*, vol. 30, no. 3, pp. 139-140, 1979.

[33] V. S. Tomaz, R. C. Cordeiro, A. M. N. Costa et al., "Antidepressant-like effect of nitric oxide synthase inhibitors and sildenafil against lipopolysaccharide-induced depressive-like behavior in mice," *Neuroscience*, vol. 268, pp. 236–246, 2014.

[34] Q. Q. Mao, Z. Huang, X. M. Zhong, Y. F. Xian, and S. P. Ip, "Brain-derived neurotrophic factor signalling mediates the antidepressant-like effect of piperine in chronically stressed mice," *Behavioural Brain Research*, vol. 261, pp. 140–145, 2014.

[35] H. H. Draper, E. J. Squires, H. Mahmoodi, J. Wu, S. Agarwal, and M. Hadley, "A comparative evaluation of thiobarbituric acid methods for the determination of malondialdehyde in biological materials," *Free Radical Biology & Medicine*, vol. 15, no. 4, pp. 353–363, 1993.

[36] L. C. Green, D. A. Wagner, J. Glogowski, P. L. Skipper, J. S. Wishnok, and S. R. Tannenbaum, "Analysis of nitrate, nitrite, and [^{15}N]nitrate in biological fluids," *Analytical Biochemistry*, vol. 126, no. 1, pp. 131–138, 1982.

[37] T. C. R. Silva, M. F. Leal, D. Q. Calcagno et al., "*hTERT*, *MYC* and *TP53* deregulation in gastric preneoplastic lesions," *BMC Gastroenterology*, vol. 12, no. 1, p. 85, 2012.

[38] A. Arocho, B. Chen, M. Ladanyi, and Q. Pan, "Validation of the 2-$\Delta\Delta$Ct calculation as an alternate method of data analysis for quantitative PCR of BCR-ABL P210 transcripts," *Diagnostic Molecular Pathology*, vol. 15, no. 1, pp. 56–61, 2006.

[39] R. R. Lima, L. N. S. Santana, R. M. Fernandes et al., "Neurodegeneration and glial response after acute striatal stroke: histological basis for neuroprotective studies," *Oxidative Medicine and Cellular Longevity*, vol. 2016, Article ID 3173564, 15 pages, 2016.

[40] A. C. A. Oliveira, M. C. S. Pereira, L. da Silva Santana et al., "Chronic ethanol exposure during adolescence through early adulthood in female rats induces emotional and memory deficits associated with morphological and molecular alterations in hippocampus," *Journal of Psychopharmacology*, vol. 29, no. 6, pp. 712–724, 2015.

[41] F. B. Teixeira, L. N. . S. Santana, F. R. Bezerra et al., "Chronic ethanol exposure during adolescence in rats induces motor impairments and cerebral cortex damage associated with oxidative stress," *PLoS One*, vol. 9, no. 6, article e101074, 2014.

[42] Ministério de Agricultura and Pecuária e Abastecimento, "Açaí, o sabor da Amazônia que se espalha pelo mundo," 2016, February 2019, http://www.agricultura.gov.br/noticias/acai-o-sabor-da-amazonia-que-se-espalha-pelo-mundo.

[43] E. Crespo, M. Macias, D. Pozo et al., "Melatonin inhibits expression of the inducible NO synthase II in liver and lung and prevents endotoxemia in lipopolysaccharide-induced multiple organ dysfunction syndrome in rats," *The FASEB Journal*, vol. 13, no. 12, pp. 1537–1546, 1999.

[44] R. Dantzer, J. C. O'Connor, G. G. Freund, R. W. Johnson, and K. W. Kelley, "From inflammation to sickness and depression: when the immune system subjugates the brain," *Nature Reviews Neuroscience*, vol. 9, no. 1, pp. 46–56, 2008.

[45] G. R. Fries and P. V. da Silva Magalhães, "A pesquisa básica na Revista de Psiquiatria do Rio Grande do Sul," *Revista de Psiquiatria do Rio Grande do Sul*, vol. 32, no. 2, pp. 33-34, 2010.

[46] R. Dantzer, J. C. O'Connor, M. A. Lawson, and K. W. Kelley, "Inflammation-associated depression: from serotonin to kynurenine," *Psychoneuroendocrinology*, vol. 36, no. 3, pp. 426–436, 2011.

[47] J. Steiner, M. Walter, T. Gos et al., "Severe depression is associated with increased microglial quinolinic acid in subregions of the anterior cingulate gyrus: evidence for an immune-modulated glutamatergic neurotransmission?," *Journal of Neuroinflammation*, vol. 8, no. 1, p. 94, 2011.

[48] C. E. Millett, B. E. Phillips, and E. F. H. Saunders, "The sex-specific effects of LPS on depressive-like behavior and oxidative stress in the hippocampus of the mouse," *Neuroscience*, vol. 399, pp. 77–88, 2019.

[49] J. C. O'Connor, M. A. Lawson, C. Andre et al., "Lipopolysaccharide-induced depressive-like behavior is mediated by indoleamine 2,3-dioxygenase activation in mice," *Molecular Psychiatry*, vol. 14, no. 5, pp. 511–522, 2009.

[50] D. G. Machado, L. E. B. Bettio, M. P. Cunha et al., "Antidepressant-like effect of rutin isolated from the ethanolic extract from *Schinus molle* L. in mice: evidence for the involvement of the serotonergic and noradrenergic systems," *European Journal of Pharmacology*, vol. 587, no. 1-3, pp. 163–168, 2008.

[51] Y. Yu, R. Wang, C. Chen et al., "Antidepressant-like effect of *trans*-resveratrol in chronic stress model: behavioral and neurochemical evidences," *Journal of Psychiatric Research*, vol. 47, no. 3, pp. 315–322, 2013.

[52] A. L. B. Zeni, A. D. E. Zomkowski, M. Maraschin, A. L. S. Rodrigues, and C. I. Tasca, "Ferulic acid exerts antidepressant-like effect in the tail suspension test in mice: evidence for the involvement of the serotonergic system," *European Journal of Pharmacology*, vol. 679, no. 1-3, pp. 68–74, 2012.

[53] Y. Ohgi, T. Futamura, T. Kikuchi, and K. Hashimoto, "Effects of antidepressants on alternations in serum cytokines and depressive-like behavior in mice after lipopolysaccharide administration," *Pharmacology, Biochemistry, and Behavior*, vol. 103, no. 4, pp. 853–859, 2013.

[54] Z. Ren, P. Yan, L. Zhu et al., "Dihydromyricetin exerts a rapid antidepressant-like effect in association with enhancement of BDNF expression and inhibition of neuroinflammation," *Psychopharmacology*, vol. 235, no. 1, pp. 233–244, 2018.

[55] Q. G. Zhou, Y. Hu, D. L. Wu et al., "Hippocampal telomerase is involved in the modulation of depressive behaviors," *The Journal of Neuroscience*, vol. 31, no. 34, pp. 12258–12269, 2011.

[56] X. Xie, Y. Chen, L. Ma et al., "Major depressive disorder mediates accelerated aging in rats subjected to chronic mild stress," *Behavioural Brain Research*, vol. 329, pp. 96–103, 2017.

[57] X. Xie, Y. Chen, Q. Wang et al., "Desipramine rescues age-related phenotypes in depression-like rats induced by chronic mild stress," *Life Sciences*, vol. 188, pp. 96–100, 2017.

[58] Y. Gonzalez-Giraldo, D. A. Forero, V. Echeverria et al., "Neuroprotective effects of the catalytic subunit of telomerase: a potential therapeutic target in the central nervous system," *Ageing Research Reviews*, vol. 28, pp. 37–45, 2016.

[59] D. Lindqvist, E. S. Epel, S. H. Mellon et al., "Psychiatric disorders and leukocyte telomere length: underlying mechanisms linking mental illness with cellular aging," *Neuroscience and Biobehavioral Reviews*, vol. 55, pp. 333–364, 2015.

[60] A. Manoliu, O. G. Bosch, J. Brakowski, A. B. Bruhl, and E. Seifritz, "The potential impact of biochemical mediators on telomere attrition in major depressive disorder and implications for future study designs: a narrative review," *Journal of Affective Disorders*, vol. 225, pp. 630–646, 2018.

[61] P. Galecki, J. Kedziora, A. Florkowski, and E. Galecka, "Lipid peroxidation and copper-zinc superoxide dismutase activity in patients treated with fluoxetine during the first episode of depression," *Psychiatria Polska*, vol. 41, no. 5, pp. 615–624, 2007.

[62] J. Kang, C. Xie, Z. Li et al., "Flavonoids from acai (*Euterpe oleracea* Mart.) pulp and their antioxidant and anti-inflammatory activities," *Food Chemistry*, vol. 128, no. 1, pp. 152–157, 2011.

[63] R. Bahramsoltani, M. H. Farzaei, M. S. Farahani, and R. Rahimi, "Phytochemical constituents as future antidepressants: a comprehensive review," *Reviews in the Neurosciences*, vol. 26, no. 6, pp. 699–719, 2015.

[64] X. Jiang, J. Liu, Q. Lin et al., "Proanthocyanidin prevents lipopolysaccharide-induced depressive-like behavior in mice via neuroinflammatory pathway," *Brain Research Bulletin*, vol. 135, pp. 40–46, 2017.

[65] H. Khan, S. Perviz, A. Sureda, S. M. Nabavi, and S. Tejada, "Current standing of plant derived flavonoids as an antidepressant," *Food and Chemical Toxicology*, vol. 119, pp. 176–188, 2018.

[66] Y. Liu, N. Lan, J. Ren et al., "Orientin improves depression-like behavior and BDNF in chronic stressed mice," *Molecular Nutrition & Food Research*, vol. 59, no. 6, pp. 1130–1142, 2015.

[67] P. B. Shewale, Y. A. Hiray, and R. A. Patil, "Antidepressant-like activity of anthocyanidins from *Hibiscus rosa-sinensis* flowers in tail suspension test and forced swim test," *Indian Journal of Pharmacology*, vol. 44, no. 4, pp. 454–457, 2012.

[68] A. Spilsbury, S. Miwa, J. Attems, and G. Saretzki, "The role of telomerase protein TERT in Alzheimer's disease and in tau-related pathology in vitro," *The Journal of Neuroscience*, vol. 35, no. 4, pp. 1659–1674, 2015.

[69] A. Dhir and S. K. Kulkarni, "Involvement of L-arginine-nitric oxide-cyclic guanosine monophosphate pathway in the antidepressant-like effect of venlafaxine in mice," *Progress in Neuro-Psychopharmacology & Biological Psychiatry*, vol. 31, no. 4, pp. 921–925, 2007.

[70] N. V. Malykhin and N. J. Coupland, "Hippocampal neuroplasticity in major depressive disorder," *Neuroscience*, vol. 309, pp. 200–213, 2015.

[71] D. W. Roddy, C. Farrell, K. Doolin et al., "The hippocampus in depression: more than the sum of its parts? Advanced hippocampal substructure segmentation in depression," *Biological Psychiatry*, vol. 85, no. 6, pp. 487–497, 2019.

[72] S. U. Mertens-Talcott, J. Rios, P. Jilma-Stohlawetz et al., "Pharmacokinetics of anthocyanins and antioxidant effects after the consumption of anthocyanin-rich acai juice and pulp (*Euterpe oleracea* Mart.) in human healthy volunteers," *Journal of Agricultural and Food Chemistry*, vol. 56, no. 17, pp. 7796–7802, 2008.

Hindawi
Oxidative Medicine and Cellular Longevity
Volume 2019, Article ID 7849876, 15 pages
https://doi.org/10.1155/2019/7849876

Research Article

Chronic Alcohol Exposure Induced Neuroapoptosis: Diminishing Effect of Ethyl Acetate Fraction from *Aralia elata*

Bong Seok Kwon,[1] Jong Min Kim,[1] Seon Kyeong Park,[1] Jin Yong Kang,[1] Jeong Eun Kang,[1] Chang Jun Lee,[1] Sang Hyun Park,[1] Su Bin Park,[1] Seul Ki Yoo,[1] Uk Lee,[2] Dae-Ok Kim,[3] and Ho Jin Heo[1]

[1]*Division of Applied Life Science (BK21 Plus), Institute of Agriculture and Life Science, Gyeongsang National University, Jinju 52828, Republic of Korea*
[2]*Division of Special Purpose Tree, National Institute of Forest Science, Suwon 16631, Republic of Korea*
[3]*Department of Food Science and Biotechnology, Kyung Hee University, Yongin 17104, Republic of Korea*

Correspondence should be addressed to Ho Jin Heo; hjher@gnu.ac.kr

Received 21 January 2019; Revised 15 April 2019; Accepted 22 April 2019; Published 9 May 2019

Guest Editor: João C. M. Barreira

An ethyl acetate fraction from *Aralia elata* (AEEF) was investigated to confirm its neuronal cell protective effect on ethanol-induced cytotoxicity in MC-IXC cells and its ameliorating effect on neurodegeneration in chronic alcohol-induced mice. The neuroprotective effect was examined by methylthiazolyldiphenyl-tetrazolium bromide (MTT) and 2′,7′-dichlorodihydrofluorescein diacetate (DCF-DA) assays. As a result, AEEF reduced alcohol-induced cytotoxicity and oxidative stress. To evaluate the improvement of learning, memory ability, and spatial cognition, Y-maze, passive avoidance, and Morris water maze tests were conducted. The AEEF groups showed an alleviation of the decrease in cognitive function in alcohol-treated mice. Then, malondialdehyde (MDA) levels and the superoxide dismutase (SOD) content were measured to evaluate the antioxidant effect of AEEF in the brain tissue. Treatment with AEEF showed a considerable ameliorating effect on biomarkers such as SOD and MDA content in alcohol-induced mice. To assess the cerebral cholinergic system involved in neuronal signaling, acetylcholinesterase (AChE) activity and acetylcholine (ACh) content were measured. The AEEF groups showed increased ACh levels and decreased AChE activities. In addition, AEEF prevented alcohol-induced neuronal apoptosis *via* improvement of mitochondrial activity, including reactive oxygen species levels, mitochondrial membrane potential, and adenosine triphosphate content. AEEF inhibited apoptotic signals by regulating phosphorylated c-Jun N-terminal kinases (*p*-JNK), phosphorylated protein kinase B (*p*-Akt), Bcl-2-associated X protein (BAX), and phosphorylated Tau (*p*-Tau). Finally, the bioactive compounds of AEEF were identified as caffeoylquinic acid (CQA), 3,5-dicaffeoylquinic acid (3,5-diCQA), and chikusetsusaponin IVa using the UPLC-Q-TOF-MS system.

1. Introduction

Alcohol has been reported to cause various diseases such as fatty liver, liver cirrhosis, cardiovascular disease, cancer of various organs, and especially damage to the brain tissue [1, 2]. In addition, alcohol can cause various neurological diseases such as Alzheimer's disease, stroke, and Korsakoff's syndrome related to thiamine deficiency [3]. For the mechanism of alcoholic neurodegeneration, it was reported that alcohol has a direct toxic effect on the brain [4]. Alcohol is dehydrogenated to acetaldehyde, which is also toxic in the central nervous system, by alcohol dehydrogenase. This acetaldehyde is then decomposed to acetate by acetaldehyde dehydrogenase [5]. Although the body has an oxidative stress defense system such as superoxide dismutase (SOD), not only does the metabolic process of alcohol produce excessive reactive oxygen species (ROS) but also chronic alcohol consumption causes an imbalance in the oxidative stress defense system [6]. As a result, oxidative stress causes secondary problems such as lipid peroxidation and

mitochondria dysfunction, which lead to neuronal apoptosis in chronic alcohol-induced cognitive disorder [7]. In addition, alcohol leads to inflammatory reaction. The consumption of alcohol induces bacterial overgrowth and increases the serum concentration of the lipopolysaccharide (LPS) derived from the cell walls of intestinal gram negative-bacteria [8]. Increased LPS in the blood induces inflammatory cytokines from Kupffer cells located in the liver [9]. The inflammatory cytokines activate microglial cells in the brain that are responsible for brain immunity, intensifying the inflammatory response. Continuous stimulation of the microglia leads to neuronal inflammation, which ultimately leads to the apoptosis of brain cells [10].

Aralia elata grows in the wild in tropical areas, and its stems and root bark are widely used for various diseases, such as diabetes, hypotension, and hepatitis, as folk medicine in East Asia [11]. *A. elata* contains various saponins such as stipuleanosides, elatoside, and chikusetsusaponin IVa [12]. Several previous investigations reported that *A. elata* has various bioactivities, such as an anti-inflammatory effect, antioxidant activity, and anti-fatty liver effect [13–15]. However, there are few studies about the inhibitory effects on alcohol-induced neurodegeneration and cognitive deficit. Therefore, our research was designed to study the use of *A. elata* for the improvement of ethanol-induced cognitive dysfunction and neurodegeneration, and the major bioactive compounds with ameliorating effects were identified.

2. Materials and Methods

2.1. Materials. Minimum essential medium (MEM) media and fetal bovine serum (FBS) were purchased from Gibco-BRL Co. (Grand Island, NY, USA). Penicillin, streptomycin, methylthiazolyldiphenyl-tetrazolium bromide (MTT), 2′,7′-dichlorodihydrofluorescein diacetate (DCF-DA), vitamin C, H_2O_2, ethanol, acetylthiocholine, 5,5′-dithiobis (2-nitrobenzoic acid) (DTNB), trichloroacetic acid, thiobarbituric acid, bovine serum albumin, dimethyl sulfoxide (DMSO), egtazic acid (EGTA), and 5,5′,6,6′-tetrachloro-1,1′,3,3′-tetraethylbenzimidazolocarbocyanine iodide (JC-1) were purchased from Sigma-Aldrich Chemical Co. (St. Louis, MO, USA). An ENLITEN adenosine triphosphate (ATP) assay system was purchased from Promega Corp. (Madison, WI, USA). ProtinEX Animal cell/tissue, a tissue lysis buffer, was purchased from GeneAll Biotechnology (Seoul, Korea). Phosphorylated c-Jun N-terminal kinases (*p*-JNK), phosphorylated Tau (*p*-Tau), and *β*-actin were purchased from Santa Cruz Biotechnology (Dallas, TX, USA) and phosphorylated protein kinase B (*p*-Akt) and Bcl-2-associated X protein (BAX) were purchased from Cell Signaling Technology (Danvers, MA, USA).

2.2. Sample Preparation. A. elata was purchased from Changnyeong in Korea, and washed *A. elata* was lyophilized using a freeze-drying apparatus (OPERON, Gimpo, Korea) and ground into powder form. This sample was stored at -20°C until use. The sample was extracted with 80% ethanol at 40°C for 2 h. The extract was filtered using filter paper (Whatman International Limited, Kent, UK), and the extractive solvent was completely removed using a vacuum evaporator (N-N series, EYELA Co., Tokyo, Japan). Then, the sample was mixed with distilled water, and it was fractionated using *n*-hexane, chloroform, and ethyl acetate of the same volume, continuously. Fractionates were lyophilized, and the ultimate ethyl acetate fraction of *A. elata* (AEEF) was used as a sample in the preliminary study.

2.3. Measurement of Oxidative Stress Levels and Cell Viability in MC-IXC Cells

2.3.1. Cell Culture. MC-IXC cells, a neuronal cell line (CRL-2270, American Type Culture Collection, Rockville, MD, USA) were cultured in MEM media containing 10% FBS, 50 unit/mL penicillin, and 100 μg/mL streptomycin. The cells were incubated in an incubator maintained at 5% CO_2 and 37°C.

2.3.2. Reactive Oxygen Species (ROS). The level of ROS was determined by the DCF-DA method [16]. Cells seeded as 1×10^4 cells/well ($n = 5$) in a 96-well black plate were incubated for 24 h. Vitamin C as a positive control or different concentrations of AEEF were treated to stabilize the seeded cells for 24 h. To confirm the protective effect against H_2O_2, every well except for the control was treated with 200 μM H_2O_2 for 3 h. Also, to investigate the protective effect against ethanol, every well except for the control was provided with 500 mM ethanol for 24 h after sample treatment for 3 h. Finally, 50 μM DCF-DA in phosphate buffered saline (PBS) was treated in every well for 50 min to measure intracellular oxidative stress. The level of ROS was measured using a fluorescence microplate reader (Infinite 200, Tecan Co., Zurich, Switzerland) at 485 nm excitation and 530 nm emission filters.

2.3.3. Cell Viability. Cell viability was measured by the MTT method [16]. Cells were seeded and pretreated with EFAE or vitamin C in the same manner as the DCF-DA method in a 96-well plate. As a final step, MTT reagent was treated in every well for 3 h, and the formed formazan was dissolved by DMSO. Then, cell viability was measured using a microplate reader (Epoch 2, BioTek Instruments Inc., Winooski, VT, USA) with a wavelength of 570 nm (reference wavelength of 690 nm).

2.4. Animal Experimental Design. C57BL/6 mice (male, 4 weeks) were purchased from Samtako (Osan, Korea). These mice were housed under standard laboratory conditions and were acclimatized to conditions for one week. The experimental groups were divided as follows: a control group administered water (orally, $n = 13$), alcohol group administered ethanol (orally, 25% *v*/*v*; 5 g/kg of body weight, $n = 13$), AEEF 50 group administered ethanol and AEEF 50 mg/kg of body weight (orally, $n = 13$), and AEEF 100 group administered ethanol and AEEF 100 mg/kg of body weight (orally, $n = 13$) for 8 weeks (Figure 1) [17–19]. All animal experiments complied with the guidelines of the Ethical Committee of the Ministry of Health and Welfare, Korea, and experimental protocols were approved by the institutional Animal Care and Use Committee (IACUC) of

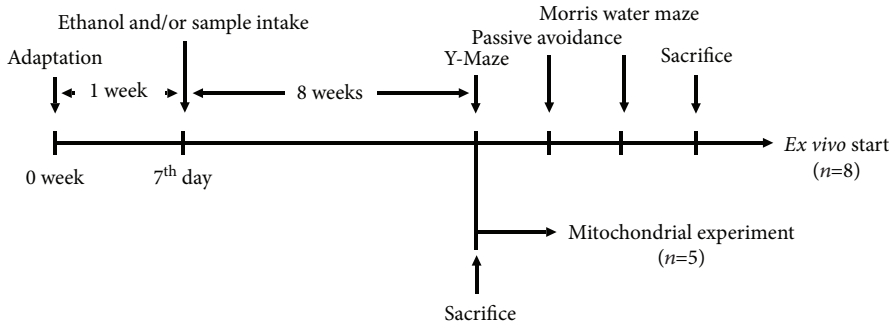

Figure 1: Experimental design of the *in vivo* test for alcohol-induced learning and memory impairment in mice.

Gyeongsang National University (certificate: GNU-150226-M0004). After the administration of alcohol and sample was completed, the experiment was divided into two groups. One group performed cognitive *in vivo* tests and sacrificed for *ex vivo* experiments ($n = 8$). The other group was immediately sacrificed for mitochondrial-related experiments after administration of alcohol and sample ($n = 5$).

2.5. Behavioral Tests

2.5.1. Y-Maze Tests. Space perception ability was assessed using a Y-maze test. The Y-maze consists of three equal angle arms 33 cm long, 10 cm wide, and 15 cm high. Each mouse was allowed to freely move in the Y-maze for 8 min, and the movement was recorded and analyzed using Smart 3.0 software (Panlab, Barcelona, Spain). Alternation behavior was calculated using the following equation: alternation behavior (%) = number of spontaneous alternation/(total arm entries − 2) × 100 [20].

2.5.2. Passive Avoidance Tests. Learning ability and short-term memory were confirmed using a passive avoidance test [20]. The experimental apparatus for passive avoidance was composed in two areas with adjustable brightness separated by a door. Mice were identically placed in the bright area. When the mouse stepped into the dark area, the door closed. Then, a 0.5 mA electric shock was immediately applied to the mouse for 3 sec through steel rods. After 24 h, the mice were placed in the bright area again, and the time they remained in the bright area was recorded up to 300 sec.

2.5.3. Morris Water Maze Tests. To evaluate cognitive memory and spatial learning ability, a Morris water maze test was conducted [21]. The Morris water maze consists of a round pool (120 cm in diameter and 50 cm in height) filled with water mixed with milk powder, at 20-22°C. The pool was divided into four quadrants, W, E, S, and N zones. A white platform was located in the N zone. During learning trials for 4 days, mice freely swam for 60 sec to find the hidden platform. The mice that found the platform on their own remained for 10 sec. When the mice failed to find it, they were moved to the platform and stayed for 20 sec. The movement to search for the platform was recorded using Smart 3.0 software (Panlab). After the training period, each mouse freely swam in the pool for 90 sec without the platform as a probe test and the retention time in the N zone was recorded to confirm long-term memory and learning ability.

2.6. Preprocessing of the Brain Tissue for Biochemical Assays. After the *in vivo* tests, the mice were fasted for 12 h and sacrificed for *ex vivo* experiments. Brains were collected and kept at -70°C until use. To investigate the biomarkers, the brains were homogenized with 10-fold PBS using a bullet blender (Next Advance Inc., Averill Park, NY, USA) at ice-cold temperatures. Then, homogenates were centrifuged in the appropriate conditions for each experiment.

2.7. Determination of the Antioxidant System

2.7.1. Determination of Malondialdehyde (MDA) Content. The homogenized brain tissue was centrifuged at 2,450 g for 10 min at 4°C. The obtained supernatants were mixed with 1% phosphoric acid and 0.67% thiobarbituric acid. The mixture was boiled for 1 h at 95°C and was measured by spectrophotometer (Libra S32PC, Biochrom Ltd., Cambridge, UK) at 532 nm. The absorbance values were substituted into the MDA standard curve to calculate MDA content, and the MDA content was expressed as MDA content per protein level measured by the Bradford method [22].

2.7.2. Determination of Superoxide Dismutase (SOD) Content. The homogenized brain tissue was centrifuged at 400 g for 10 min at 4°C, The obtained pellets were mixed with extractive buffer (10x SOD buffer solution of assay kit, 20% (*v*/*v*) Triton x-100, and 200 mM phenylmethanesulfonyl fluoride) and resuspended. After 30 min, the mixtures were centrifuged at 10,000 g for 10 min and the supernatants were finally obtained for a SOD assay. The SOD assay was conducted according to the manufacturer's process and measured using a microplate spectrophotometer (Epoch 2) at 450 nm. The absorbance values were substituted into the SOD standard curve to calculate SOD content.

2.8. Cholinergic System Evaluation

2.8.1. Determination of Acetylcholine (ACh) Content. To evaluate AChE activity and ACh content, the homogenate was centrifuged at 14,000 g for 30 min at 4°C. To assess ACh content, alkaline hydroxylamine reagent was added to the obtained supernatants, which consisted of 2 M hydroxylammonium chloride and 3.5 M sodium hydroxide at the

same volume. Then, 0.5 N HCl and 0.37 M $FeCl_3 \cdot 6H_2O$ were reacted, and the mixture was measured using a microplate spectrophotometer (Epoch 2) at 540 nm. The absorbance values were substituted into the ACh standard curve, which was drawn using acetylcholine chloride in 1 mM sodium acetate trihydrate (pH 4.5).

2.8.2. Determination of Acetylcholinesterase (AChE) Activity. To assess AChE activity, 50 mM of sodium phosphate buffer (pH 8.0) was added to the obtained supernatants and this mixture was incubated for 15 min at 37°C. Then, 500 μM substrate solution (500 μM acetylthiocholine and 1 mM DTNB in buffer) was added, and absorbance was measured using a microplate spectrophotometer (Epoch 2) at 405 nm.

2.9. Mitochondrial Activities

2.9.1. Isolation of Mitochondria. The brain tissue was homogenized with a 10-fold isolation buffer (215 mM mannitol, 75 mM sucrose, 0.1% BSA, 20 mM HEPES sodium salt, and 1 mM EGTA; pH 7.2) using a bullet blender (Next Advance Inc.). The homogenates were centrifuged at 1,300 g for 10 min to remove the unbroken cells. Then, the supernatant was centrifuged again at 13,000 g for 10 min, and the supernatants were removed to obtain a pellet. The obtained pellet was resuspended in the isolation buffer with 0.1% digitonin. After 5 min, the mixture was centrifuged at 13,000 g for 15 min. Then, buffer was added to the pellet without EGTA and as a final step spun down again at 10,000 g for 10 min to obtain mitochondria. The mitochondrial pellet was reacted with buffer without EGTA and used for each experiment [23].

2.9.2. ROS Measurement. Mitochondrial ROS was determined using the DCF-DA method [16]. The isolated mitochondria were reacted with 25 μM DCF-DA for 25 min. Fluorescence was measured using a fluorescence microplate reader (Infinite 200).

2.9.3. MMP Measurement. To measure mitochondrial membrane potential (MMP), the isolated mitochondria was diluted to the same protein concentration using the buffer without EGTA and 5 mM pyruvate, 5 mM malate, and 1 μM JC-1 were added to the buffer. The mixture was incubated for 20 min and measured with a fluorescence microplate reader (Infinite 200) at 530 nm (excitation filters) and 590 nm (emission filters).

2.9.4. ATP Measurement. The measurement of the ATP content of isolated mitochondria was conducted with an ATP bioluminescence assay kit in accordance with the manufacturer's process and measured using a luminescence microplate reader (GloMax-Multi+ Detection System, Promega Corp., Madison, WI, USA). The ATP content was calculated using a standard curve.

2.10. Western Blot Analysis. The brain tissue of the experimental animals ($n = 3$) was homogenized to extract protein using a bullet blender (Next Advance Inc.) with ProtinEX Animal cell/tissue containing a 1% protease inhibitor cocktail (PPI-1015, Quartett, Berlin, Germany). This homogenized brain tissue was centrifuged at 13,000 g for 15 min. The protein samples were loaded with the same concentration of protein and separated by SDS-PAGE gel. Then, the protein was transferred to a polyvinylidene difluoride membrane. The membrane was blocked with 5% skim milk in TBST buffer (20 mM Tris-HCl, 137 mM sodium chloride, and 0.1% Tween 20; pH 7.6) for 1 h. The blocked membrane was reacted in diluted (1 : 1,000) primary antibodies including *p*-JNK, *p*-Akt, BAX, *p*-Tau, and β-actin and gently shaken overnight. Then, the membrane was washed using TBST and soaked in a secondary antibody for 1 h. The membrane was then completely washed with TBST. Finally, the level of protein was detected using TMB solution (Thermo Scientific, Rockford, IL, USA). Band images were obtained using an Epson scanner (L655 series, Epson, Suwa, Japan), and the image was analyzed using ImageJ (National Institutes of Health, Bethesda, MD, USA).

2.11. Analysis of Bioactive Compounds. The main bioactive compounds of AEEF were analyzed using ultraperformance liquid chromatography/quadrupole time-of-flight tandem mass spectrometry (UPLC-Q-TOF-MS, Vion, Waters Corp., Milford, MA, USA). The AEEF dissolved in methanol was eluted by linear gradient of acetonitrile for 8 min and dwindled acetonitrile for 8-10 min with a flow rate of 0.4 mL/min using a C_{18} column (100 × 2.1 mm, 1.7 μm, Waters Corp.). The physiological compounds were analyzed by negative electrospray ion (ESI) mode to gain MS data. The conditions used for the ESI source were as follows: ramp collision energy, 20–45 V; oven temperature, 40°C; capillary voltage, 3 kV; and mass range, 50–1200 m/z.

2.12. Statistical Analysis. Result expression was presented as mean and standard deviation (SD). The statistical relation of groups was verified by one-way analysis of variance with Duncan's new multiple-range test ($p < 0.05$) with SAS 9.4 (SAS Institute Inc., Cary, NC, USA).

3. Results

3.1. Neuronal Cell Protective Effect. DCF-DA and MTT assays were conducted to measure cellular oxidative stress and cell viability against ethanol and H_2O_2, respectively. The DCF-DA results (Figures 2(a) and 2(b)) indicated that the ROS content was increased by ethanol (129.28%) and H_2O_2 (115.25%) compared to the control group (100.00%), whereas AEEF treatment showed a remarkable reduction in oxidative stress induced by both ethanol and H_2O_2 at all concentrations. As the AEEF concentration was increased, the intracellular ROS content induced by both ethanol and H_2O_2 was decreased. Treatment with 50 μg/mL (49.46 and 55.15%, respectively) and 100 μg/mL (45.76 and 51.08%, respectively) of AEEF led to a decreased cellular ROS compared to vitamin C (62.97 and 60.36%, respectively).

The results of cell viability to ethanol and H_2O_2 are shown in Figures 2(c) and 2(d). The cell viability of the ethanol group (86.49%) and H_2O_2 group (22.67%) decreased significantly relative to the control group (100.00%). However, all AEEF groups showed improved cell viability compared

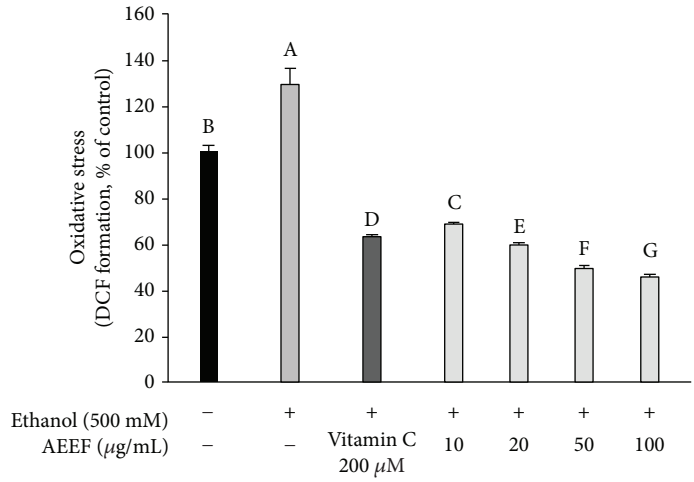

(a)

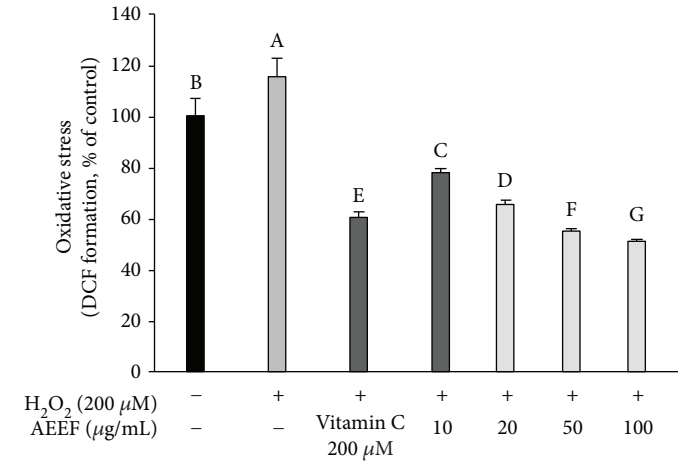

(b)

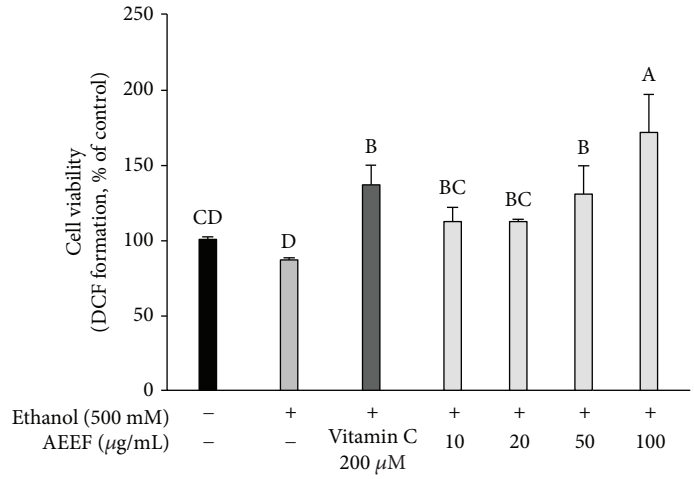

(c)

Figure 2: Continued.

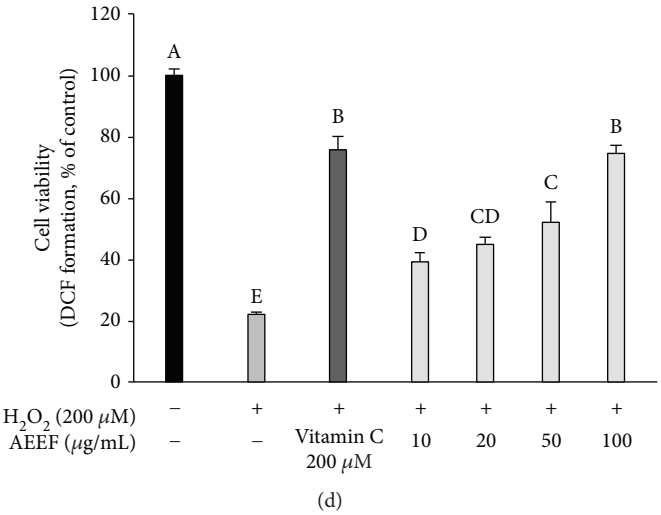

Figure 2: Neuronal cell protective effect of the ethyl acetate fraction from *Aralia elata* (AEEF) in MC-IXC cells. Intracellular ROS content induced by ethanol (a) and H_2O_2 (b) and the cell viability against toxicity induced by ethanol (c) and H_2O_2 (d). Result expressions are mean and standard deviation ($n = 5$). Statistical differences of data were verified at $p < 0.05$ and, in consequence, indicated as different capital letters in the graph.

to the negative groups. In particular, the 100 μg/mL concentration of AEEF showed similar or higher cell viability (170.95% and 74.48%, ethanol and H_2O_2, respectively) compared to the vitamin C group (136.49% and 75.86%, ethanol and H_2O_2, respectively).

3.2. Effect of AEEF on Behavioral Tests. In Figure 3(a), the results of the Y-maze test showed that the alcohol group (56.19%) had decreased space perceptual ability compared to the control group (68.94%). However, the AEEF 50 (63.43%) and AEEF 100 (64.22%) groups showed statistically similar alternation behaviors as the control group. The number of arm entries was not statistically different among all groups (approximately 22.77 times). In the path tracing results (Figure 3(b)), the alcohol group mainly entered one arm, while the control and AEEF groups showed relatively equal entry into the three arms. To confirm the ameliorating effect on short-term memory impairment, a passive avoidance test was conducted (Figure 3(c)). The step-through latency time of the alcohol group (42.60 sec) was markedly decreased relative to the control group (300.00 sec), whereas the AEEF 50 and 100 groups recovered to 105.40 and 138.40 sec, respectively. A Morris water maze test was conducted to validate learning ability and long-term memory. During the training period, the escape latency time of all groups gradually decreased as the training progressed (Figure 3(d)). Nonetheless, the alcohol group (respective decrease, 30.82%) was significantly different from the other groups (respective decrease: control: 72.15%, AEEF 50: 60.10%, and AEEF 100: 68.65%) in the last training. A probe test was conducted by recording the swimming route of mice without a platform, and the results of recorded path tracing established the cognitive function of the mice through movement. The alcohol group exhibited movement in the whole area (Figure 3(e)) and less retention time (18.11%) in the platform zone (the N zone) compared to the control group (54.76%) (Figure 3(f)). In contrast, there was a considerable improvement of cognitive function from alcohol-induced impairment in the AEEF 50 (58.13%) and AEEF 100 (49.65%) groups.

3.3. Ameliorating Effect of AEEF in MDA and SOD Content. MDA content was used as a definitive marker of lipid peroxidation. The MDA content of the alcohol group (4.16 nmole/mg of protein) significantly increased compared to that of the control group (3.72 nmole/mg of protein), whereas the AEEF groups (AEEF 50 group, 3.75 nmole/mg of protein) remarkably reduced MDA production in the brain tissue (Figure 4(a)). In particular, the AEEF 100 (3.56 nmole/mg of protein) group effectively inhibited lipid peroxidation compared to the control group. Also, the SOD content of the alcohol group showed decrease (2.77 U/mg of protein) compared with that of the control group (3.71 U/mg of protein) (Figure 4(b)). However, AEEF treatment showed a statistically small increase (AEEF 50 group: 3.33, AEEF 100 group: 3.25 U/mg of protein).

3.4. Ameliorating Effect of AEEF in Cholinergic System. To confirm the ameliorating effect of AEEF in the cholinergic system, the content of ACh and activity of AChE were measured (Figure 5). The alcohol group showed excessive AChE activity (126.99%) and lower ACh content (0.26 mmole/mg of protein) in the brain tissue compared to the control group (100.00% and 0.32 mmole/mg of protein, respectively). However, both AEEF treatment groups showed an ameliorated cholinergic system, resulting in similar levels of both AChE activity (104.93 and 102.70%) and ACh content (both 0.30 mmole/mg of protein) compared to the control group.

3.5. Effect of AEEF on Mitochondrial Activity. Mitochondrial activity was evaluated through the ROS level, MMP level, and ATP content to confirm the ameliorating effect of AEEF on alcohol-induced mitochondrial dysfunction. In Figure 6(a),

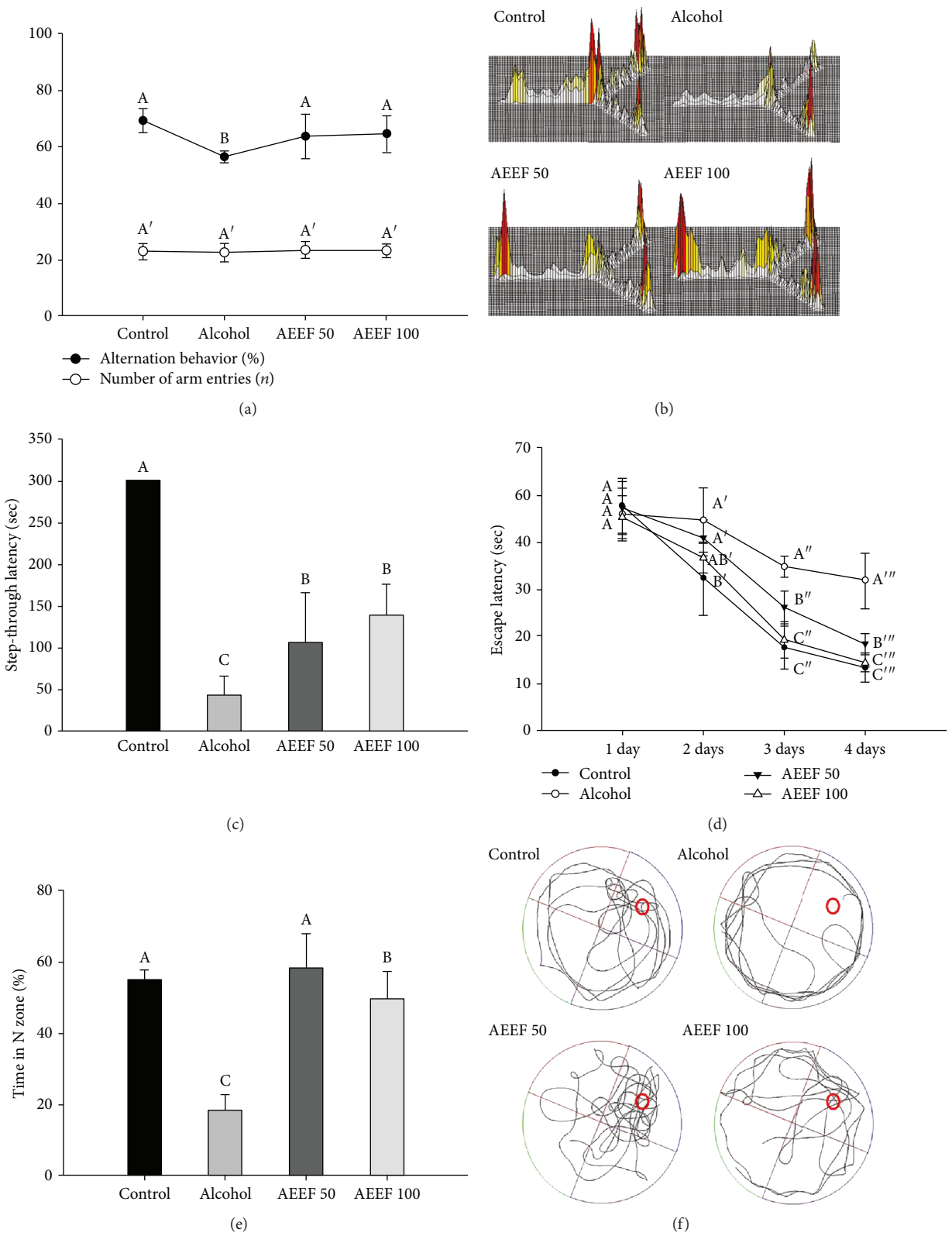

FIGURE 3: Effect of the ethyl acetate fraction from *Aralia elata* (AEEF) on cognitive function in alcohol-treated mice. Alternation behavior and number of arm entries (a) and path tracing of each group (b) in the Y-maze test; the step-through latency (c) in the passive avoidance test; and escape latency in the training trials (d), time in the N zone of the probe trial (e), and path tracing of the probe trial (f) in the Morris water maze test. Result expressions are mean and standard deviation ($n = 8$). Statistical differences of data were verified at $p < 0.05$ and, in consequence, indicated as different capital letters in the graph.

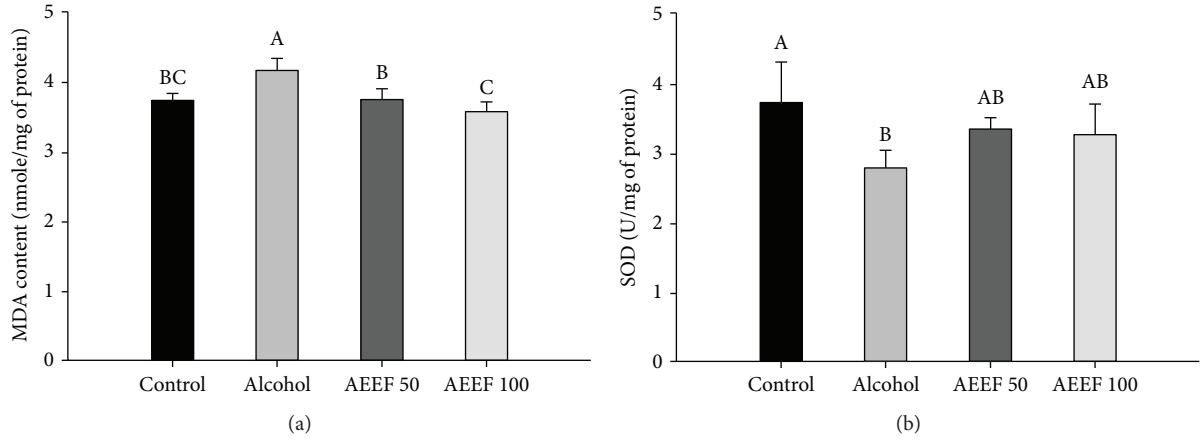

Figure 4: Ameliorating effect of the ethyl acetate fraction from *Aralia elata* (AEEF) on biomarkers. Malondialdehyde (MDA) (a) and superoxide dismutase (SOD) (b) content in the brain homogenate of chronic alcohol-treated mice. Result expressions are mean and standard deviation ($n = 8$). Statistical differences of data were verified at $p < 0.05$ and, in consequence, indicated as different capital letters in the graph.

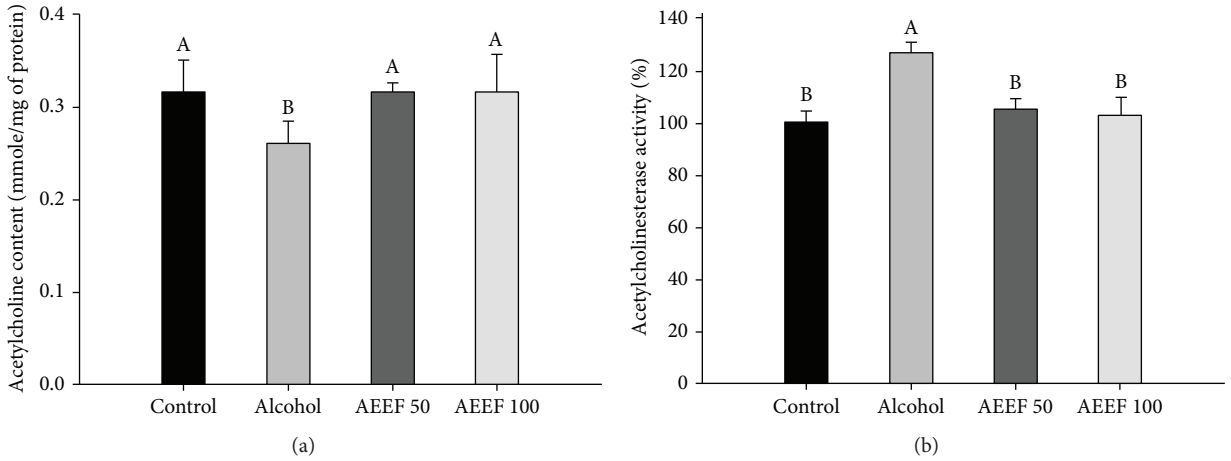

Figure 5: Ameliorating effect of the ethyl acetate fraction from *Aralia elata* (AEEF) on the cholinergic system. Acetylcholinesterase (AChE) activities (a) and acetylcholine (ACh) content (b) in the brain homogenate of chronic alcohol-treated mice. Result expressions are mean and standard deviation ($n = 8$). Statistical differences of data were verified at $p < 0.05$ and, in consequence, indicated as different capital letters in the graph.

the ROS levels in mitochondria isolated from the brain tissue of the alcohol group (196.65%) had significantly increased, approximately two times more than the control group (100.00%). However, both AEEF groups (141.28 and 139.25%, AEEF 50 and AEEF 100, respectively) showed a substantial decrease in ROS production compared to the alcohol group. The MMP level and ATP content were reduced in the alcohol group (74.75% and 98.89 pmole/mg of protein, respectively) relative to the control group (100.00% and 165.64 pmole/mg of protein, respectively) (Figures 6(b) and 6(c)). Although administration of AEEF 50 (79.06 %) did not significantly improve the MMP levels in alcohol-induced mitochondrial dysfunction, both AEEF groups exhibited elevated ATP content (139.17 and 165.47 pmole/mg of protein, AEEF 50 and AEEF 100, respectively) that was statistically similar to that of the control.

3.6. Effect of AEEF on the Apoptotic Signaling Pathway. To confirm the protective effect of AEEF against alcoholic apoptosis, the expression of proteins associated with neuronal cell apoptosis, such as phosphorylated *p*-JNK, *p*-Akt, BAX, and *p*-Tau, was evaluated by western blot analysis. The expression of *p*-JNK as proapoptotic proteins increased 21.52% compared to that of the control group (Figure 7(b)). The AEEF 100 group showed the suppression of *p*-JNK (85.39% compared to the alcohol group). In contrast, the *p*-Akt expression level of the alcohol group was reduced (a decrease of 21.21%) compared with that of the control group (Figure 7(c)). The AEEF 100 group showed the enhancement of *p*-Akt (169.15% compared to the alcohol group). In common with the results of *p*-JNK, the expressions of BAX (an increase of 34.66% compared to the control group) and *p*-Tau (an increase of 55.92% compared to the control group) were significantly upregulated compared to

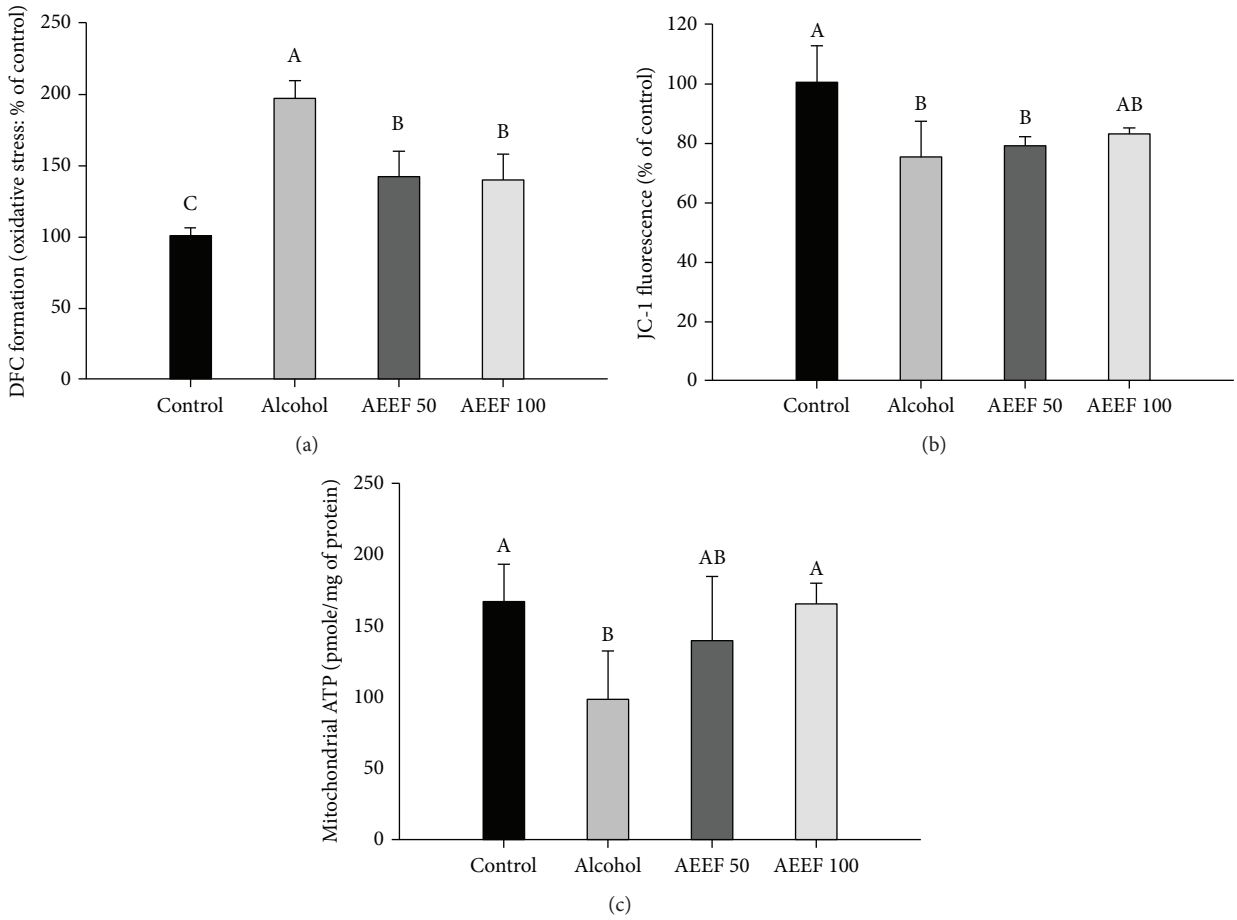

Figure 6: Effect of the ethyl acetate fraction from *Aralia elata* (AEEF) on mitochondrial activity. Mitochondrial reactive oxygen species (ROS) levels (a), mitochondrial membrane potential (MMP) (b), and adenosine triphosphate (ATP) content (c) in isolated mitochondria from the brain homogenate of chronic alcohol-treated mice. Result expressions are mean and standard deviation ($n = 5$). Statistical differences of data were verified at $p < 0.05$ and, in consequence, indicated as different capital letters in the graph.

that of the control group (Figures 7(d) and 7(e)). However, the AEEF 100 group showed the suppression of BAX (89.21% compared to the alcohol group) and *p*-Tau (80.50% compared to the alcohol group).

3.7. Analysis of Physiological Compounds with UPLC-Q-TOF-MS. The major compounds in AEEF were identified using a UPLC-Q-TOF-MS system (Figure 8 and Table 1). The base peaks of main compounds were obtained at 353.09 *m*/*z* (compound A, RT: 2.01 min), 515.12 *m*/*z* (compound B, RT: 2.76 min), and 793.44 *m*/*z* (compound C, RT: 4.16 min) in the negative ion mode. The MS fragmentation ions in the 40-60 eV region showed compound A (191.06 *m*/*z*), compound B (191.06 and 353.09 *m*/*z*), and compound C (631.38 and 569.38 *m*/*z*). The main compounds A, B, and C were identified as 1-caffeoylquinic acid (CQA), 3,5-dicaffeoylquinic acid (3,5-diCQA), and chikusetsusaponin IVa, respectively [24–26].

4. Discussion

Alcohol directly causes neurodegeneration and indirectly damages neuronal cells through several pathways such as the production of ROS [4]. ROS is produced in various alcoholic metabolic processes such as catalase and the CYP2E1 system [27]. As with the results of the DCF-DA assay, ROS was increased by treatment with ethanol (Figure 2(a)). Excessive ROS production compared to the antioxidant system which cannot be eradicated in the body leads to lipid peroxidation and mitochondrial dysfunction [7]. Eventually, mitochondria lose the cell survival function, which leads to the apoptosis of neuronal cells. *A. elata* contains various bioactive components, including triterpenoid saponin and the glycosidic form of flavonoids [28]. *Dipsacus asper*, which contains a large amount of triterpene saponin, decreased cytotoxicity in PC12 cells [29]. Also, Ishige et al. reported several protective mechanisms of flavonoid protection against oxidative stress in hippocampal cells [30]. Flavonoids may increase the level of glutathione by removing ROS and inhibiting Ca^{2+} influx. Hence, the above results, namely, the reduction of ROS and increase in cell viability, are also considered to be due to the biological components of *A. elata*.

Previous studies commonly used rodent models fed alcohol for various periods to confirm the harmful effects of chronic alcohol consumption [31, 32]. According to Raghavendra and Kulkarni, Balb/C mice fed ethanol (15%,

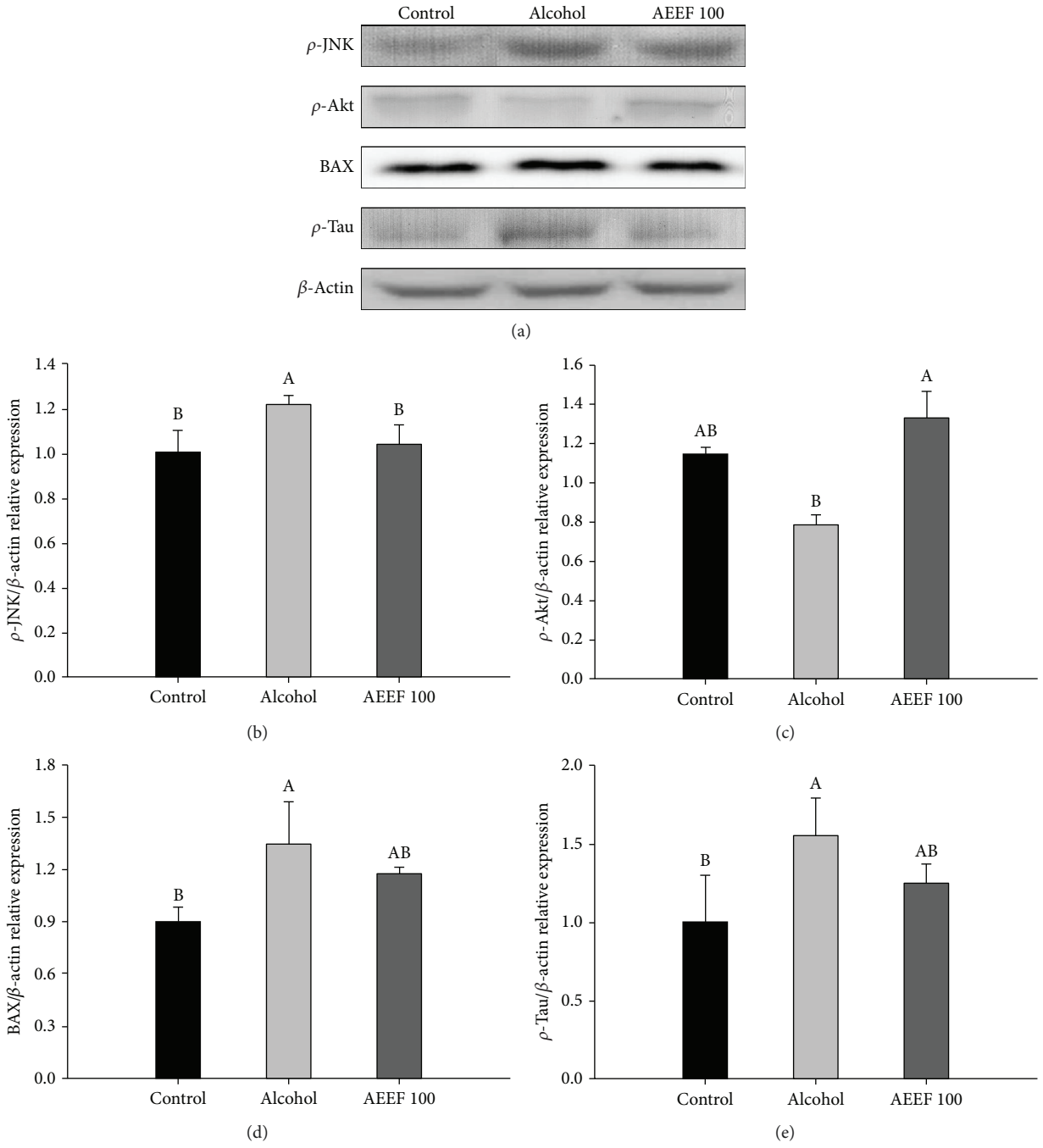

Figure 7: Regulating effect of the ethyl acetate fraction from *Aralia elata* (AEEF) on apoptotic signaling in the brain homogenate of chronic alcohol-treated mice. Relative expression of *p*-JNK (b), *p*-Akt (c), BAX (d), and *p*-Tau (e). Result expressions are mean and standard deviation ($n = 3$). Statistical differences of data were verified at $p < 0.05$ and, in consequence, indicated as different capital letters in the graph.

2 g/kg) for 24 days showed cognitive deficits and memory impairment [33]. In the mice model of the current study, the behavioral experiment results also showed impairment of cognitive function. Alcohol consumption causes declined judgment and impaired memory. One of the reasons for these defects is the reduction of the brain-derived neurotrophic factor (BDNF), which is a growth factor for neuronal cells. Repeated exposure to alcohol induces a decline in BDNF and inhibition of neurogenesis, which causes difficulties in memory formation [34]. In addition, alcohol damages the hippocampus, which plays an important role in memory formation [35]. This damage induces the loss of hippocampal CA1 and CA3 pyramidal neurons and transient changes in the granule cell number in the DG [36]. Therefore, impairment of the hippocampus leads to trouble in learning ability and space perceptual ability. Also, alcohol causes difficulty in neurotransmission with the diminishment of the acetylcholine level, a neurotransmitter in the cholinergic system [37]. Therefore, in the above behavioral findings, the reduction of cognitive function such as learning ability,

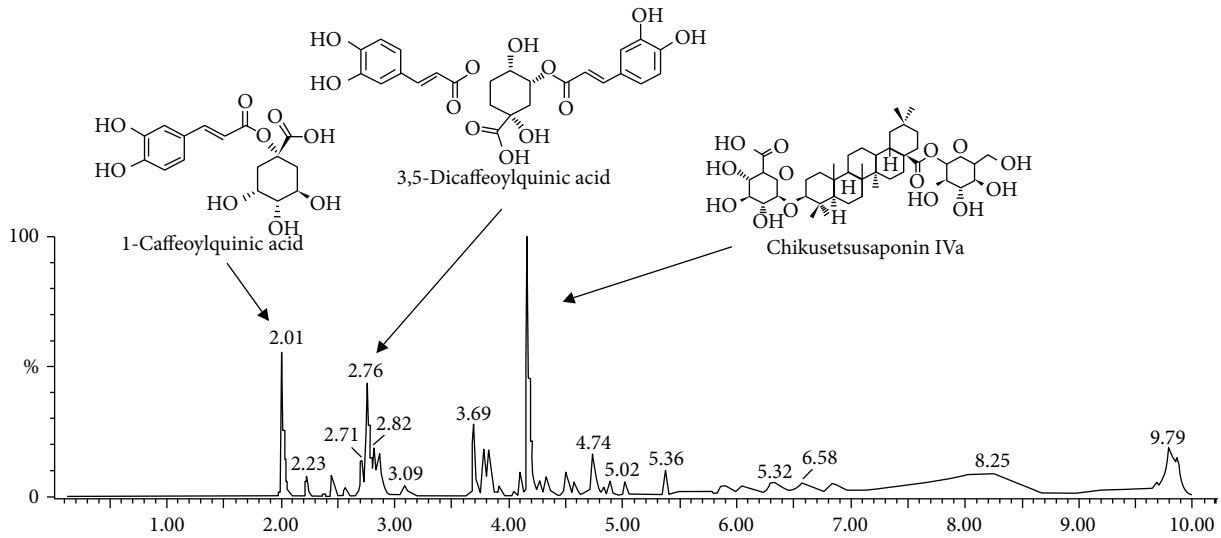

Figure 8: MS^E chromatography in the negative ion mode of the ethyl acetate fraction from *Aralia elata* (AEEF) using the UPLC-Q-TOF-MS system.

Table 1: Compounds identified from the ethyl acetate fraction from *Aralia elata* (AEEF).

No.	RT (min)	Parent ion (m/z)[a]	MS^E ions (m/z)[b]	Compound
1	2.01	353	**191**	1-Caffeoylquinic acid (CQA)
2	2.76	515	353, **191**	3,5-Dicaffeoylquinic acid (3,5-diCQA)
3	4.16	793	**631**, 569, 455	Chikusetsusaponin IVa

[a]Ions are presented in m/z $[M\text{-}H]^-$. [b]Bold indicates the main fragment of MS^E ions of each compound.

space perceptual ability, and memory ability is considered due to the alcohol intake, whereas phenolic compound and saponin activate the survival pathways and expression of BDNF, and they have protective effects in the cognitive function with the protection of the neuronal membrane [38]. Moreover, Socci et al. reported that the administration of antioxidants improves impaired cognitive function [39]. Considering that *A. elata* contains various saponins and phenolic compounds, the administration of AEEF protects the neuronal cell and ameliorates the alcohol-induced impairment of cognitive function.

The process of energy generation occurs naturally in the production of oxidative stress, and it is eliminated by the antioxidant system such as glutathione, catalase, and SOD. SOD reduces oxidative stress by converting superoxide to oxygen or hydrogen peroxide by using the metal ions they have. This property effectively blocks the cascade of cellular oxidation [40]. However, chronic alcohol intake causes damage to antioxidant systems that eradicate these oxidative stresses in the brain tissue [6]. Also, the brain contains rich polyunsaturated fatty acids which are vulnerable to lipid peroxidation by ROS. However, alcohol-induced lipid peroxidation induces the death of neuronal cells and ultimately induces cognitive decline. Therefore, inhibition of lipid peroxidation contributes to cognitive function, and the status of antioxidants is also involved in it [41], whereas AEEF upregulates SOD activity and the inhibition of MDA production in the cerebral tissue. According to Chung and Jung, the ethanol extract of *A. elata* has considerable antioxidant properties and enhances the SOD activity in Sprague Dawley rats treated with benzo(α)pyrene [14]. On the other hand, alcohol increases the overgrowth of intestinal gram negative bacteria that produce LPS. This increased LPS produced by intestinal microorganisms stimulates Kupffer cells to produce tumor necrosis factor-alpha (TNF-α) [8]. TNF-α can enter the blood-brain barrier (BBB) and increase the immune response in the brain. Also, TNF-α upregulates the expression of inducible nitric oxide synthase, which creates nitric oxide and various cytokines [23]. However, a previous study showed that the saponins of *A. elata* reduce oxidative stress *via* downregulation of inflammatory signaling such as interleukin- (IL-) 6, IL-1β, and TNF-α eNOS and iNOS [42]. Consequentially, although alcohol-induced oxidative stress caused neuronal inflammation and damage, cognitive dysfunction could be protected by administrating AEEF containing the various physiologic compounds.

ACh plays an important role in the cholinergic system in cognitive function as a neurotransmitter [43]. ACh is synthesized from acetyl CoA and choline by acetylcholine transferase. The ACh released from synapses stimulates receptors for neurotransmission and opens the ion channels of postsynaptic nerve cells. After the function of the neurotransmitter is completed, ACh is decomposed to acetate and choline by AChE [44]. However, overactivated AChE makes neurotransmission difficult due to the excessive decomposition of ACh [45]. Chronic alcohol consumption causes changes in

the cholinergic system [46]. Arendt et al. reported that a decrease in the activity of the cholinergic system was seen over time in Sprague Dawley rats fed 20% (*v*/*v*) ethanol for different periods of time [19]. In particular, significant differences were seen when those rats were treated for 8 weeks. Chronic alcohol consumption showed decreased ACh content and increased AChE activity in almost the whole brain [46]. Also, alcohol promotes lipid peroxidation in the brain tissue. AChE, which has a cell membrane-bound structure, is reported to be more active due to lipid peroxidation [47]. However, it is known that such disorders of the cholinergic system are ameliorated by polyphenolic compounds. The deterpenoids contained in *Aralia cordata*, which belongs to the same family (*Araliaceae*) as *A. elata*, have an inhibitory effect on AChE and a cognitive function improvement effect [48]. In addition, dicaffeoylquinic acids (diCQAs) such as 1,5-diCQA, 3,5-diCQA, and 4,5-diCQA have been reported to help improve the cholinergic system and inhibit the activity of AChE [49]. Although the precise mechanism between the AChE structure and CQA derivatives is unknown, the above results suggest that AEEF helps improve the cholinergic system and improve cognitive function.

Mitochondria which perform a critical role in energy production are an important factor in the apoptosis pathway. Excessive alcohol-induced ROS impairs mitochondrial membrane function through mitochondrial lipid peroxidation and the alteration of mitochondrial membrane properties [7]. These changes include the reduction of MMP in the electron transport chain and decline of energy generation [50]. Moreover, chronic alcohol intake increases not only mitochondrial ROS but also nitric oxide, which is produced by alcohol-induced nitric oxide synthase. This oxidative stress inhibits mitochondrial function by combining with mitochondrial respiratory chain enzymes, and modulates mitochondrial ion channels [51]. Continuous mitochondrial dysfunction becomes the cause of apoptosis progress, and cytochrome c located in mitochondria is released to the cytosol. On the other hands, various phenolic compounds, which act as antioxidants, can reduce mitochondrial oxidative stress [52]. The phenolic compounds protect cells from alcohol-induced cytotoxicity by inhibiting inappropriate changes that can trigger mitochondrial permeability transition and blocking apoptotic pathways [50]. Also, in the results of Zhang et al., the polysaccharide of *A. elata* protects the mitochondria from H_2O_2 and inhibits the release of cytochrome c in H9c2 cells [53]. Also, manganese SOD, one of the SOD species, is mainly located in the mitochondrial matrix [40]. Manganese SOD also removes the mitochondrial superoxide, and the mitochondrial ROS result is considered to be associated with previous results and improvement of the SOD level by AEEF (Figure 4(b)). Therefore, these results suggest that AEEF attenuates abnormal energy metabolism through the protection of the mitochondrial function in chronic alcohol-induced neurodegeneration.

Apoptosis is programmed cell death, which is associated with changes to several proteins. The prominent apoptotic route is known as the phosphorylated c-Jun N-terminal kinase (JNK) pathway. JNK is phosphorylated by various stresses, such as UV radiation, inflammatory stimuli, and ROS [54]. Several studies suggest that phosphorylated JNK (*p*-JNK) phosphorylates proapoptotic proteins such as the Bim protein, which activates BAX through the inactivation of Bcl-2 in the mitochondrial apoptosis pathway [55]. Following the cell death signal, BAX translocates to the mitochondria and permeabilizes the mitochondrial membrane by inducing the opening of the mitochondrial voltage-dependent anion channel which reduces the MMP and releases cytochrome c to the cytosol [50]. Released cytochrome c initiates activation of the caspases which induce the apoptosis in the cells. Moreover, phosphorylation of JNK stimulates the phosphorylation of the Tau protein which leads to the death of neuronal cells *via* disintegration of the microtubules and formation of Neurofibrillary tangles [55]. Contrary to this mechanism, activated Akt eliminates the proapoptotic feature of the Bcl-2/BAX complex by inactivating BAD, which is the Bcl-2 associated with the death promoter [56]. As a result of apoptotic signaling, AEEF reduced the expression of *p*-JNK, BAX, and *p*-Tau which cause apoptosis and increased the expression of p-Akt, as an antiapoptotic factor. Similar to these results, Luo et al. reported that saponins of *A. elata* suppress the increased phosphorylation of JNK and inflammatory cytokines in ApoE knockout mice [57]. Also, 3,5-diCQA lowered the ratio of BAX/Bcl in neurons, reducing neuronal cytotoxicity and reducing the release of Ca^{2+} from the cells [58]. Taken together, administration of AEEF prevents apoptosis of neuronal cells with the upregulation of Akt and inhibition of *p*-JNK, which phosphorylates the Tau protein in chronic alcohol-induced neurodegeneration (Figure 7).

CQA and 3,5-diCQA, the main physiologic compounds of AEEH, are known as phenolic compounds commonly found in plants and perform antioxidant and anti-inflammatory activities [59]. In particular, 3,5-diCQA, derived from a (-)-quinic acid and a transcaffeic acid, stimulates the overexpression of phosphoglycerate kinase 1 (PGK1) involved in glycolysis as a glycolytic enzyme that catalyzes the conversion of 1,3-diphosphoglycerate to 3-phosphoglycerate and increases ATP levels in SH-SY5Y neuronal cells [60]. Moreover, 3,5-diCQA has a neuroprotective effect in SH-SY5Y cells and also improves spatial learning and memory in SAMP8 (senescence-accelerated) mice. Also, chikusetsusaponin IVa, an oleanolic acid saponin, is mainly isolated from ginseng and *A. elata* [57]. Moreover, these saponins have been reported to have neuroprotective effects, such as the inhibition of cognitive dysfunction and improvement of the cholinergic system [61]. Chikusetsusaponin IVa also protects neuronal cells against H_2O_2-induced oxidative stress *via* activation of SOD and glutathione and upregulates the Sirt1/Foxo3a/Mn-SOD pathway [62]. Therefore, various physiological activities such as the neuroprotective effect and improvement of cognitive function of AEEF have been attributed to its various physiologically active compounds. However, in order to confirm which of these compounds has a high contribution to the physiological activity of AEEF, individual experiments of each compound should be conducted in the future.

5. Conclusion

This study suggests that AEEF ameliorates chronic alcohol-induced neurodegeneration with the improvement of cognitive function and protection of brain tissue. Chronic alcohol intake causes oxidative stress and neurodegeneration. However, AEEF exerts a protective effect on neuronal cell survival and significantly improves cognitive functions, such as spatial cognition, memory, and learning ability in ethanol-administrated mice. These ameliorating effects are considered to be due to improvement of the cholinergic and antioxidant system and the reduction of oxidative stress in the brain tissue. In addition, AEEF enhances mitochondrial activity through the inhibition of *p*-JNK expression and oxidative stress and downregulates the apoptotic pathway in neuronal cells. CQA, 3,5-diCQA, and chikusetsusaponin Iva, the main compounds identified in AEEF, may be considered the bioactive components of *A. elata*, and the physiological activity of AEEF is presumed to be due to these compounds. Therefore, *A. elata* has significant potential as a natural agent to ameliorate alcohol-induced neurodegeneration.

Data Availability

The data used to support the findings of this study are available from the corresponding author upon request.

Conflicts of Interest

The authors have no relevant conflicts of interest.

Authors' Contributions

Bong Seok Kwon and Jong Min Kim have contributed equally to this work and are co-first authors.

Acknowledgments

This work was financially supported by the Basic Science Research Program through the National Research Foundation of Korea (certificate: 2018043398).

References

[1] C. S. Lieber, "Alcohol and the liver: metabolism of alcohol and its role in hepatic and extrahepatic diseases," *Mount Sinai Journal of Medicine*, vol. 67, no. 1, pp. 84–94, 2000.

[2] F. T. Crews, T. Buckley, P. R. Dodd et al., "Alcoholic neurobiology: changes in dependence and recovery," *Alcoholism: Clinical & Experimental Research*, vol. 29, no. 8, pp. 1504–1513, 2005.

[3] N. Butters, "Alcoholic Korsakoff's syndrome: some unresolved issues concerning etiology, neuropathology, and cognitive deficits," *Journal of Clinical and Experimental Neuropsychology*, vol. 7, no. 2, pp. 181–210, 1985.

[4] J. Haorah, S. H. Ramirez, N. Floreani, S. Gorantla, B. Morsey, and Y. Persidsky, "Mechanism of alcohol-induced oxidative stress and neuronal injury," *Free Radical Biology & Medicine*, vol. 45, no. 11, pp. 1542–1550, 2008.

[5] H. Sprince, C. M. Parker, G. G. Smith, and L. J. Gonzales, "Protective action of ascorbic acid and sulfur compounds against acetaldehyde toxicity: implications in alcoholism and smoking," *Agents and Actions*, vol. 5, no. 2, pp. 164–173, 1975.

[6] C. S. Lieber, "Ethanol metabolism, cirrhosis and alcoholism," *Clinica Chimica Acta*, vol. 257, no. 1, pp. 59–84, 1997.

[7] V. D. Reddy, P. Padmavathi, G. Kavitha, B. Saradamma, and N. Varadacharyulu, "Alcohol-induced oxidative/nitrosative stress alters brain mitochondrial membrane properties," *Molecular and Cellular Biochemistry*, vol. 375, no. 1-2, pp. 39–47, 2013.

[8] C. Bode and J. Christian Bode, "Effect of alcohol consumption on the gut," *Best Practice & Research Clinical Gastroenterology*, vol. 17, no. 4, pp. 575–592, 2003.

[9] J. Petrasek, P. Mandrekar, and G. Szabo, "Toll-like receptors in the pathogenesis of alcoholic liver disease," *Gastroenterology Research and Practice*, vol. 2010, Article ID 710381, 12 pages, 2010.

[10] V. Tiwari and K. Chopra, "Protective effect of curcumin against chronic alcohol-induced cognitive deficits and neuroinflammation in the adult rat brain," *Neuroscience*, vol. 244, pp. 147–158, 2013.

[11] N. X. Nhiem, H. Y. Lim, P. V. Kiem et al., "Oleanane-type triterpene saponins from the bark of *Aralia elata* and their NF-κB inhibition and PPAR activation signal pathway," *Bioorganic & Medicinal Chemistry Letters*, vol. 21, no. 20, pp. 6143–6147, 2011.

[12] M. Yoshikawa, T. Murakami, E. Harada, N. Murakami, J. Yamahara, and H. Matsuda, "Bioactive saponins and glycosides. VII. On the hypoglycemic principles from the root cortex of *Aralia elata* Seem. : structure related hypoglycemic activity of oleanolic acid oligoglycoside," *Chemical & Pharmaceutical Bulletin*, vol. 44, no. 10, pp. 1923–1927, 1996.

[13] Y. Chen, Z. Zhao, H. Chen, T. Yi, M. Qin, and Z. Liang, "Chemical differentiation and quality evaluation of commercial Asian and American ginsengs based on a UHPLC-QTOF/MS/MS metabolomics approach," *Phytochemical Analysis*, vol. 26, no. 2, pp. 145–160, 2015.

[14] C.-K. Chung and M.-E. Jung, "Ethanol fraction of *Aralia elata Seemann* enhances antioxidant activity and lowers serum lipids in rats when administered with benzo(α)pyrene," *Biological & Pharmaceutical Bulletin*, vol. 26, no. 10, pp. 1502–1504, 2003.

[15] K. A. Hwang, Y. J. Hwang, G. R. Kim, and J. S. Choe, "Extracts from *Aralia elata (Miq)* Seem alleviate hepatosteatosis *via* improving hepatic insulin sensitivity," *BMC Complementary and Alternative Medicine*, vol. 15, no. 1, pp. 347–356, 2015.

[16] J. Kim, S. Park, J. Kang et al., "Ethyl acetate fraction from persimmon (*Diospyros kaki*) ameliorates cerebral neuronal loss and cognitive deficit *via* the JNK/Akt pathway in TMT-induced mice," *International Journal of Molecular Sciences*, vol. 19, no. 5, p. 1499, 2018.

[17] A. Bahi, V. Tolle, J. A. Fehrentz et al., "Ghrelin knockout mice show decreased voluntary alcohol consumption and reduced ethanol-induced conditioned place preference," *Peptides*, vol. 43, pp. 48–55, 2013.

[18] Y. N. Zhao, F. Wang, Y. X. Fan, G. F. Ping, J. Y. Yang, and C. F. Wu, "Activated microglia are implicated in cognitive deficits, neuronal death, and successful recovery following intermittent ethanol exposure," *Behavioural Brain Research*, vol. 236, no. 1, pp. 270–282, 2013.

[19] T. Arendt, Y. Allen, R. M. Marchbanks et al., "Cholinergic system and memory in the rat: effects of chronic ethanol, embryonic basal forebrain brain transplants and excitotoxic lesions of cholinergic basal forebrain projection system," *Neuroscience*, vol. 33, no. 3, pp. 435–462, 1989.

[20] J. M. Kim, S. K. Park, T. J. Guo et al., "Anti-amnesic effect of *Dendropanax morbifera via* JNK signaling pathway on cognitive dysfunction in high-fat diet-induced diabetic mice," *Behavioural Brain Research*, vol. 312, pp. 39–54, 2016.

[21] R. Morris, "Developments of a water-maze procedure for studying spatial learning in the rat," *Journal of Neuroscience Methods*, vol. 11, no. 1, pp. 47–60, 1984.

[22] M. M. Bradford, "A rapid and sensitive method for the quantitation of microgram quantities of protein utilizing the principle of protein-dye binding," *Analytical Biochemistry*, vol. 72, no. 1-2, pp. 248–254, 1976.

[23] M. R. Brown, J. W. Geddes, and P. G. Sullivan, "Brain region-specific, age-related, alterations in mitochondrial responses to elevated calcium," *Journal of Bioenergetics and Biomembranes*, vol. 36, no. 4, pp. 401–406, 2004.

[24] M. N. Clifford, S. Knight, and N. Kuhnert, "Discriminating between the six isomers of dicaffeoylquinic acid by LC-MS^n," *Journal of Agricultural and Food Chemistry*, vol. 53, no. 10, pp. 3821–3832, 2005.

[25] G. M. Weisz, D. R. Kammerer, and R. Carle, "Identification and quantification of phenolic compounds from sunflower (*Helianthus annuus* L.) kernels and shells by HPLC-DAD/ESI-MS^n," *Food Chemistry*, vol. 115, no. 2, pp. 758–765, 2009.

[26] Y. Cao, C. Gu, F. Zhao et al., "Therapeutic effects of *Cyathula officinalis* Kuan and its active fraction on acute blood stasis rat model and identification constituents by HPLC-QTOF/MS/MS," *Pharmacognosy Magazine*, vol. 13, no. 52, pp. 693–701, 2017.

[27] D. R. Koop, "Alcohol metabolism's damaging effects on the cell: a focus on reactive oxygen generation by the enzyme cytochrome P450 2E1," *Alcohol Research & Health*, vol. 29, no. 4, pp. 274–280, 2006.

[28] Q.-H. Wang, J. Zhang, X. Ma et al., "A new triterpenoid saponin from the leaves of *Aralia elata*," *Chinese Journal of Natural Medicines*, vol. 9, no. 1, pp. 17–21, 2011.

[29] D. Ji, Y. Wu, B. Zhang, C. F. Zhang, and Z. L. Yang, "Triterpene saponins from the roots of *Dipsacus asper* and their protective effects against the Aβ_{25-35} induced cytotoxicity in PC12 cells," *Fitoterapia*, vol. 83, no. 5, pp. 843–848, 2012.

[30] K. Ishige, D. Schubert, and Y. Sagara, "Flavonoids protect neuronal cells from oxidative stress by three distinct mechanisms," *Free Radical Biology & Medicine*, vol. 30, no. 4, pp. 433–446, 2001.

[31] A. K. Singh, Y. Jiang, S. Gupta, and E. Benlhabib, "Effects of chronic ethanol drinking on the blood–brain barrier and ensuing neuronal toxicity in alcohol-preferring rats subjected to intraperitoneal LPS injection," *Alcohol and Alcoholism*, vol. 42, no. 5, pp. 385–399, 2007.

[32] Z. Zhou, L. Wang, Z. Song, J. T. Saari, C. J. McClain, and Y. J. Kang, "Zinc supplementation prevents alcoholic liver injury in mice through attenuation of oxidative stress," *The American Journal of Pathology*, vol. 166, no. 6, pp. 1681–1690, 2005.

[33] V. Raghavendra and S. K. Kulkarni, "Possible antioxidant mechanism in melatonin reversal of aging and chronic ethanol-induced amnesia in plus-maze and passive avoidance memory tasks," *Free Radical Biology & Medicine*, vol. 30, no. 6, pp. 595–602, 2001.

[34] J. Hellmann, H. Rommelspacher, and C. Wernicke, "Long-term ethanol exposure impairs neuronal differentiation of human neuroblastoma cells involving neurotrophin-mediated intracellular signaling and in particular protein kinase c," *Alcoholism: Clinical and Experimental Research*, vol. 33, no. 3, pp. 538–550, 2009.

[35] A. M. White and H. S. Swartzwelder, "Hippocampal function during adolescence: a unique target of ethanol effects," *Annals of the New York Academy of Sciences*, vol. 1021, no. 1, pp. 206–220, 2004.

[36] M. P. Puglia and C. F. Valenzuela, "Repeated third trimester-equivalent ethanol exposure inhibits long-term potentiation in the hippocampal CA1 region of neonatal rats," *Alcohol*, vol. 44, no. 3, pp. 283–290, 2010.

[37] R. P. Vetreno, J. M. Hall, and L. M. Savage, "Alcohol-related amnesia and dementia: animal models have revealed the contributions of different etiological factors on neuropathology, neurochemical dysfunction and cognitive impairment," *Neurobiology of Learning and Memory*, vol. 96, no. 4, pp. 596–608, 2011.

[38] B. Jiang, Z. Xiong, J. Yang et al., "Antidepressant-like effects of ginsenoside Rg1 are due to activation of the BDNF signalling pathway and neurogenesis in the hippocampus," *British Journal of Pharmacology*, vol. 166, no. 6, pp. 1872–1887, 2012.

[39] D. J. Socci, B. M. Crandall, and G. W. Arendash, "Chronic antioxidant treatment improves the cognitive performance of aged rats," *Brain Research*, vol. 693, no. 1-2, pp. 88–94, 1995.

[40] R. M. Lebovitz, H. Zhang, H. Vogel et al., "Neurodegeneration, myocardial injury, and perinatal death in mitochondrial superoxide dismutase-deficient mice," *Proceedings of the National Academy of Sciences of the United States of America*, vol. 93, no. 18, pp. 9782–9787, 1996.

[41] M. A. Lovell, C. Xie, and W. R. Markesbery, "Acrolein is increased in Alzheimer's disease brain and is toxic to primary hippocampal cultures," *Neurobiology of Aging*, vol. 22, no. 2, pp. 187–194, 2001.

[42] R.-C. Chen, J. Wang, Y.-L. Yu, G.-B. Sun, and X.-B. Sun, "Protective effect of total saponins of *Aralia elata* (Miq) Seem on lipopolysaccharide-induced cardiac dysfunction *via* down-regulation of inflammatory signaling in mice," *RSC Advances*, vol. 5, no. 29, pp. 22560–22569, 2015.

[43] B. D. Drever, G. Riedel, and B. Platt, "The cholinergic system and hippocampal plasticity," *Behavioural Brain Research*, vol. 221, no. 2, pp. 505–514, 2011.

[44] R. S. Jope, "High affinity choline transport and acetylCoA production in brain and their roles in the regulation of acetylcholine synthesis," *Brain Research Reviews*, vol. 1, no. 3, pp. 313–344, 1979.

[45] K. Y. Yoo and S. Y. Park, "Terpenoids as potential anti-Alzheimer's disease therapeutics," *Molecules*, vol. 17, no. 3, pp. 3524–3538, 2012.

[46] D. Ehrlich, M. Pirchl, and C. Humpel, "Effects of long-term moderate ethanol and cholesterol on cognition, cholinergic neurons, inflammation, and vascular impairment in rats," *Neuroscience*, vol. 205, pp. 154–166, 2012.

[47] M. Lasner, L. G. Roth, and C. H. Chen, "Structure-functional effects of a series of alcohols on acetylcholinesterase-

associated membrane-vesicles - elucidation of factors contributing to the alcohol action," *Archives of Biochemistry and Biophysics*, vol. 317, no. 2, pp. 391–396, 1995.

[48] H. A. Jung, E. J. Lee, J. S. Kim et al., "Cholinesterase and BACE1 inhibitory diterpenoids from *Aralia cordata*," *Archives of Pharmacal Research*, vol. 32, no. 10, pp. 1399–1408, 2009.

[49] J. Deng, X. L. Qi, Z. Z. Guan, X. M. Yan, Y. Huang, and Y. L. Wang, "Pretreatment of SH-SY5Y cells with dicaffeoylquinic acids attenuates the reduced expression of nicotinic receptors, elevated level of oxidative stress and enhanced apoptosis caused by β-amyloid peptide," *Journal of Pharmacy and Pharmacology*, vol. 65, no. 12, pp. 1736–1744, 2013.

[50] J. B. Hoek, A. Cahill, and J. G. Pastorino, "Alcohol and mitochondria: a dysfunctional relationship," *Gastroenterology*, vol. 122, no. 7, pp. 2049–2063, 2002.

[51] Z. Lacza, A. V. Kozlov, E. Pankotai et al., "Mitochondria produce reactive nitrogen species *via* an arginine-independent pathway," *Free Radical Research*, vol. 40, no. 4, pp. 369–378, 2006.

[52] H. Haraguchi, N. Yoshida, H. Ishikawa, Y. Tamura, K. Mizutani, and T. Kinoshita, "Protection of mitochondrial functions against oxidative stresses by isoflavans from *Glycyrrhiza glabra*," *Journal of Pharmacy and Pharmacology*, vol. 52, no. 2, pp. 219–223, 2000.

[53] J. Zhang, H. Wang, Y. Xue, and Q. Zheng, "Cardioprotective and antioxidant activities of a polysaccharide from the root bark of *Aralia elata* (Miq.) Seem," *Carbohydrate Polymers*, vol. 93, no. 2, pp. 442–448, 2013.

[54] D. N. Dhanasekaran and E. P. Reddy, "JNK signaling in apoptosis," *Oncogene*, vol. 27, no. 48, pp. 6245–6251, 2008.

[55] K. Lei and R. J. Davis, "JNK phosphorylation of Bim-related members of the Bcl2 family induces Bax-dependent apoptosis," *Proceedings of the National Academy of Sciences of the United States of America*, vol. 100, no. 5, pp. 2432–2437, 2003.

[56] S. Mehan, H. Meena, D. Sharma, and R. Sankhla, "JNK: a stress-activated protein kinase therapeutic strategies and involvement in Alzheimer's and various neurodegenerative abnormalities," *Journal of Molecular Neuroscience*, vol. 43, no. 3, pp. 376–390, 2011.

[57] Y. Luo, X. Dong, Y. Yu, G. Sun, and X. Sun, "Total aralosides of *Aralia elata* (Miq) Seem (TASAES) ameliorate nonalcoholic steatohepatitis by modulating IRE1α-mediated JNK and NF-κB pathways in ApoE–/– mice," *Journal of Ethnopharmacology*, vol. 163, pp. 241–250, 2015.

[58] J. Y. Kim, H. K. Lee, B. Y. Hwang, S. Kim, J. K. Yoo, and Y. H. Seong, "Neuroprotection of *Ilex latifolia* and caffeoylquinic acid derivatives against excitotoxic and hypoxic damage of cultured rat cortical neurons," *Archives of Pharmacal Research*, vol. 35, no. 6, pp. 1115–1122, 2012.

[59] S. G. Lee, H. Lee, T. G. Nam et al., "Neuroprotective effect of caffeoylquinic acids from *Artemisia princeps* Pampanini against oxidative stress-induced toxicity in PC-12 cells," *Journal of Food Science*, vol. 76, no. 2, pp. C250–C256, 2011.

[60] J. Han, Y. Miyamae, H. Shigemori, and H. Isoda, "Neuroprotective effect of 3,5-di-O-caffeoylquinic acid on SH-SY5Y cells and senescence-accelerated-prone mice 8 through the upregulation of phosphoglycerate kinase-1," *Neuroscience*, vol. 169, no. 3, pp. 1039–1045, 2010.

[61] H. Ma, J. Han, and Q. Dong, "Neuroprotective effect of *Annona glabra* extract against ethanol-induced apoptotic neurodegeneration in neonatal rats," *Journal of Photochemistry and Photobiology B: Biology*, vol. 181, pp. 106–114, 2018.

[62] J. Wan, L. Deng, C. Zhang et al., "Chikusetsu saponin V attenuates H_2O_2-induced oxidative stress in human neuroblastoma SH-SY5Y cells through Sirt1/PGC-1α/Mn-SOD signaling pathways," *Canadian Journal of Physiology and Pharmacology*, vol. 94, no. 9, pp. 919–928, 2016.